

**FOR REFERENCE ONLY**

Enos ✓  
2/2/10

0 4 FEB 2008 428329

40 0785526 6



ProQuest Number: 10183209

All rights reserved

INFORMATION TO ALL USERS

The quality of this reproduction is dependent upon the quality of the copy submitted.

In the unlikely event that the author did not send a complete manuscript and there are missing pages, these will be noted. Also, if material had to be removed, a note will indicate the deletion.



ProQuest 10183209

Published by ProQuest LLC (2017). Copyright of the Dissertation is held by the Author.

All rights reserved.

This work is protected against unauthorized copying under Title 17, United States Code  
Microform Edition © ProQuest LLC.

ProQuest LLC.  
789 East Eisenhower Parkway  
P.O. Box 1346  
Ann Arbor, MI 48106 – 1346

Investigation of a  
Digital FEM Height Reference Surface  
as  
Vertical Reference System

Sascha Schneid

A thesis submitted in partial fulfilment of the requirements of The Nottingham Trent  
University for the degree of Doctor of Philosophy

August 2007

## Abstract

### **Investigation of the Digital FEM Height Reference Surface (DFHRS) as Vertical Reference System**

In recent years, the number of precise online DGNSS (Differential Global Navigation Satellite System) applications has significantly increased. Precise DGNSS correction services have been created that enable an online positioning with accuracy in the centimetre region. In contrast to the co-ordinates found by DGNSS, the measured height needs to be transformed. This is because national height systems refer to a physically defined Height Reference Surface, HRS, that approximates the mean sea level, while the height derived from DGNSS positioning is the height above the WGS84 (World Geodetic System 1984), a mathematical model of the earth and is therefore called "ellipsoidal height". So for the application of precise DGNSS services and for the generation of transformation messages, such as RTCM 3.0, there is an urgent need for a HRS, in a unified datum with appropriate accuracy.

This thesis deals with the concept of the Digital FEM (Finite Element Method) Height Reference Surface, DFHRS. This concept enables the rigorous least squares adjustment of any HRS related observation. The HRS is modelled as continuous surface by a local Taylor-series expansion in a grid of FEM-meshes. With this, areas of any size may be computed. The theory of the DFHRS and further development of the mathematical model, especially the incorporation of observed gravity accelerations, are the main parts of this thesis.

As the applied Taylor-series expansion of the DFHRS concept only holds for a two-dimensional approximation, Spherical Cap Harmonics, SCH, had to be introduced as auxiliary parameter, to give a complete representation of the local gravity field. Spherical Cap Harmonics, SCH, may be interpreted as the general case of Spherical Harmonics, SH, that have been applied in geodetic applications for decades. The goal of the SCH coefficients, in contrast to the SH coefficients is that they may be applied over areas with limited extent. Due to numerical reasons, the combined least squares estimation of the DFHRS and the SCH coefficients in practical computations had to be done applying a sequential procedure.

In practical examples, different HRS representations with centimetre accuracy were computed by combining GNSS/Levelling points and precise gravimetric geoid models according to the DFHRS concept.

In a further example, gravity acceleration observations and a global geopotential model have been introduced into a combined least squares estimation of SCH coefficients. It could be shown that the introduction of the gravity accelerations leads to a significant improvement of the representation of the local gravity field. To perform a two step adjustment, height anomalies were derived from the determined SCH coefficients and introduced together with GNSS/Levelling points into a second adjustment according to the DFHRS concept. By comparison with a reference model, the resulting accuracy of the HRS representation was estimated to be 0.025m.

*Keywords:* GNSS based levelling. Geoid. Height Reference Surface. Spherical Cap Harmonics.

## **Acknowledgements**

The author wishes to acknowledge the following for their support.

The project supervisors Dr. Mark Breach, Prof. Peter Thomas and Prof. Dr.-Ing. Reiner Jäger, who is also the leader of the DHFRS project at Karlsruhe – University of applied sciences.

Helmut Meichle from Landesvermessungsamt Baden-Württemberg for providing the GNSS/Levelling points as well as the gravity observations used in this study.

His wife Ruth for her tolerance and understanding.

# Table of Contents

		<b>Page</b>
	<b>Abstract</b>	<b>ii</b>
	List of figures	<b>vii</b>
	List of tables	<b>x</b>
	List of abbreviations	<b>xii</b>
	List of symbols	<b>xiv</b>
<b>1</b>	<b>Introduction</b>	<b>1</b>
	1.1 Objectives	3
<b>2</b>	<b>Earth's Gravity Field</b>	<b>4</b>
	2.1 Introduction	4
	2.2 Fundamentals	4
	2.3 The geodetic boundary value problem	8
	2.4 Parameterisation of the Gravity field	20
	2.4.1 Spherical harmonics	20
	2.4.2 Point mass models	25
<b>3</b>	<b>Heights and Height Systems</b>	<b>28</b>
	3.1 Introduction	28
	3.2 Ellipsoidal heights	28
	3.3 Physically defined heights	29
	3.3.1 Dynamic heights	30
	3.3.2 Orthometric heights	31
	3.3.3 Normal heights	32
	3.4 Height systems	34
<b>4</b>	<b>Determination and application of HRS-models</b>	
	4.1 Methods of HRS determination	36
	4.1.1 GNSS/Levelling points	37
	4.2.1 Astrogeodetic geoid determination	37
	4.2.2 Gravimetric geoid determination	39

4.3	Height determination using GPS and HRS models	42
4.4	Discussion of methods	46
<b>5</b>	<b>The Concept of the Digital FEM Height Reference Surface DFHRS</b>	<b>49</b>
5.1	The system of observation equations	51
5.1.1	Identical points (h, H)	52
5.1.2	Existing (quasi-) geoid models alone and in combination	53
5.1.3	Deflections from the vertical ( $\xi, \eta$ )	54
5.1.4	Gravity disturbances $\delta g$	55
5.2	Derivation of continuity conditions	57
5.3	Least squares estimation of the DFHRS parameters	61
5.4	Computation design and elimination of long-wave and systematic errors	63
5.4.1	FEM-meshing and geoid patching for a precise representation of the HRS	64
5.4.2	Generation and application of synthetic covariance matrices	66
5.5	Block algorithms for the inversion of huge matrices	70
5.6	Computation examples	75
5.6.1	The DFHRS of Germany	75
5.6.2	The DFHRS of Europe	78
<b>6</b>	<b>Spherical Cap Harmonics – SCH</b>	<b>82</b>
6.1	Introduction	82
6.2	Definition and geo-referencing of the spherical cap	83
6.3	Validation of the SCH concept	84
6.4	Computing the associated Legendre functions of real degree	91
6.5	Finding the roots of the associated Legendre functions	93
6.6	Rotation of the gravity vector	95
6.7	Modification of the spherical cap	96
6.8	Regularisation of the linear equation system	98
<b>7</b>	<b>Computation examples</b>	<b>100</b>
7.1	Example 1: Representation of a spherical harmonic	100

	geopotential model	
7.2	Example 2: Combination of GNSS/levelling points and a geopotential model	102
7.3	Example 3: Combination of GNSS/levelling points and the GCG2005 – Quasigeoid	103
7.4	Implementation of terrestrial gravity disturbances, $\delta g$	104
7.5	Application of the DFHRS patching concept to reduce systematic errors	118
7.6	Discussion	121
<b>8.</b>	<b>Conclusions</b>	<b>124</b>
	References	129
	Publications	139

## List of Figures

	<b>Page</b>
2.1	Geocentric earth-fixed Cartesian co-ordinates, $x, y, z$ . 5
2.2	Natural co-ordinates: astronomic latitude, $\Phi$ , and longitude, $\Lambda$ , and the potential, $W$ 9
2.3	Geodetic co-ordinate system: Geodetic latitude, $\phi$ , and longitude, $\lambda$ and ellipsoidal height, $h$ . 13
2.4	The GBVP according to Stokes 14
2.5	The GBVP according to Molodensky 15
2.6	<b>left:</b> Spherical geocentric co-ordinates. <b>right:</b> Spherical polar triangle 19
2.7	Planar ellipsoidal geodetic co-ordinate system. 27
3.1	Ellipsoidal height, $h$ , versus standard height, $H$ , with respect to a Height Reference Surface (HRS) 29
3.2	Definition of the orthometric height $H^O$ 32
3.3	Definition of the normal height $H^N$ 34
5.1	Sketch of a DFHRS FEM meshing. The whole area of interest, here Germany with its federal states, is subdivided into FEM meshes. 51
5.2	Scheme of two neighbouring meshes, I and II, where a continuous transition at the common border straight line AE has to be forced 57
5.3	To determine a complete continuous surface, conditions to 8 neighbouring meshes have to be modelled 61
5.4	Positions of the 46 GPS/levelling points. In a second project, 11 points from the inner zone (red) have been removed. 70
5.5	FEM meshing of the DFHRS-Germany with 102 geoid-patches. 76
5.6	Visualisation of the Digital FEM Height Reference Surface for Germany 77
5.7	The Digital FEM Height Reference Surface for Europe, computed from the EVRF200 (triangles) and the EGG97. 79
6.1	Definition and georeferencing of the spherical cap 83
	<b>Left:</b> The Legendre functions, $P_2, P_4$ and $P_6$ . <b>Right:</b> The Legendre functions, $P_{n(2)}, P_{n(4)}$ and $P_{n(6)}$ 94
6.2	Modification of the spherical cap according to the TOSCA concept 97

7.1	34 points (triangles) are used to estimate correction parameters in 4 patches	101
7.2	The test area contains 15 GNSS/levelling points (triangles) and 1066 gravity observations (blue circles). The HRS is computed for the area within the blue lines and compared within the investigation.	106
7.3	The surface of differences between the GCG2005 and the SCH-Model, estimated using the GNSS/Levelling points and the GPM98CR model.	107
7.4	The surface of differences between the GCG2005 and the SCH-Model, estimated using the GNSS/Levelling points and the EIGEN04 model.	109
7.5	The surface of differences between the GCG2005 and the SCH representation up to $k_{\text{Max}}=90$	111
7.6	The square roots of the degree variances for the height anomaly, $\zeta$ , for the SCH representation up to degree 90	112
7.7	The square roots of the degree variances for the gravity disturbances, $\delta g$ , for the SCH representation up to degree 90. The degrees less than $k=14$ are not displayed to ensure clarity. The maximum was reached at $k=3$ with 2830 mGal	112
7.8	The surface of differences between the GCG2005 and the SCH representation up to $k_{\text{Max}}=10$	114
7.9	The square roots of the degree variances for the height anomaly, $\zeta$ , for the SCH representation up to degree 100. The degrees less than $k=14$ are not displayed for clarity	114
7.10	The degree variances for the gravity disturbances, $\delta g$ , for the SCH representation up to degree 100. The degrees less than $k=14$ are not displayed for clarity. The maximum degree variance was reached at $k=3$ with $1900^2\text{mGal}^2$	115
7.11	Degree variances for the height anomaly, $\zeta$ , for the SCH representation over the smaller cap up to degree 90	116
7.12	Degree variances for the height anomaly, $\zeta$ , for the SCH representation over the smaller cap up to degree 90. The degrees less than $k=14$ are not displayed for clarity. The maximum degree variance was reached at $k=3$ with 20.8 mGal	116

7.13	The surface of differences between the GCG2005 and the SCH representation of the smaller cap up to $k_{\text{Max}}=90$	117
7.14	FEM meshes and GNSS/levelling points over the area of the test project	119
7.15	The surface of differences between the DFHRS of this example and the GCG2005.	120

## List of Tables

	<b>Page</b>
2.1	Approximation error of a geopotential model according to the degree variance model of Tscherning and Rapp (Wenzel, 1999): 25
5.1	The $C_1$ -continuity condition at a common border of neighbouring meshes is reached by differentiating the parametric expression of the border straight line in the x- and y- directions. 59
5.2	Different output qualities with different mesh sizes 65
5.3	The mesh size of the FEM meshes is the most important design parameter needed to produce a Digital FEM Height Reference Surface of a required quality 66
5.4	Another important design parameter to achieve the desired quality is the size of the geoid patches 66
5.5	Comparison of the results, when applying different covariance functions. 69
5.6	Comparison of the results from re-computing the points that had been removed, when applying different covariance functions 69
5.7	Compilation of the results for different countries where independent GNSS/Levelling points were computed 75
7.1	Statistical result from the adjustment of EIGEN04 height anomalies and gravity disturbances 101
7.2	Differences between a computed grid derived from the EIGEN04 and a grid derived from the SCH-representation 101
7.3	Result from the combined adjustment of GNSS/levelling points and the EIGEN04 103
7.4	Result from the combined adjustment of GNSS/levelling points and the GCG2005 104
7.5	Omission error for gravity disturbances according to Tscherning and Rapp (1974) 105
7.6	Result from the combined adjustment of GNSS/levelling points the GPM98CR, and terrestrial gravity disturbances. 110
7.7	Results from the combined adjustment of GNSS/levelling points, GPM98CR, and terrestrial gravity anomalies over the smaller cap 115

7.8	Residuals from the combined adjustment of the GPM98CR, and terrestrial gravity disturbances	119
7.9	Residuals from the combined adjustment	120

## List of Abbreviations

BKG	Bundesamt für Kartographie und Geodäsie
BVP	Boundary Value Problem
CHAMP	Challenging Mini-Satellite Payload for Geophysical Research and Application
DFHRS	Digital Finite Element Height Reference Surface
DGNSS	Differential Global Navigation Satellite System
DTM	Digital Terrain Model
EGG97	European Gravimetric Quasi-Geoid 1997
EGM96	Earth's Gravitational Model
ETRS89	European Terrestrial Reference System 1989
EUPOS	European Positioning System
EVRS	European Vertical Reference System
FEM	Finite Element Method
GBVP	Geodetic Boundary Value Problem
GCG2005	German Combined Quasi-Geoid 2005
GNSS	Global Navigation Satellite System
GOCE	Gravity Field and Steady-State Ocean Circular Explorer
GPM	Gravitational Potential Model
GPS	Global Positioning System
GRACE	Gravity Recovery and Climate Experiment
GRS80	Geodetic Reference System 1980
HRS	Height Reference Surface
MSL	Mean Sea Level
NAP	Normal Amsterdam's Peil
RMS	Root Means Square
RRT	Remove Restore Technique
RTCM	Radio Technical Commission for Maritime Services
RTM	Residual Terrain Model
SAPOS	Satellite Positioning System
SCH	Spherical Cap Harmonics
SH	Spherical Harmonics
TOSCA	Translated Origin Spherical Cap Harmonic Analysis

UENL  
WGS84

Unified European Levelling Network  
World Geodetic System 1984

## List of Symbols

$\nabla$	Laplace operator
<b>A</b>	Design matrix or Set of harmonic coefficients; see context
<b>B</b>	Set of harmonic coefficients
<b>C</b>	Geopotential number or Co-variance matrix or set of continuity conditions; see context
$C_{n,m}, S_{n,m}$	Spherical harmonic coefficients, of degree $n$ and order $m$
<b>d</b>	Set of trend parameters
<b>G</b>	Newton's gravitational constant
<b>g</b>	Gravity vector
<b>h</b>	Ellipsoidal height
$H^N$	Normal Height
$H^O$	Orthometric Height
$H_{obs}$	Observed standard height
<b>M</b>	Radius of Meridian curvature
<b>N</b>	Matrix of normal equations
<b>N</b>	Geoid height or radius of normal curvature, see context
<b>p</b>	Set of FEM parameters
<b>r</b>	Part of redundancy or radial distance; see context
<b>T</b>	Anomalous gravity potential
<b>U</b>	Normal potential
$U_0$	Normal potential of the reference ellipsoid
<b>V</b>	Gravitational potential
<b>v</b>	Residual
$V^N$	Normal gravitational potential
<b>W</b>	Gravity potential
$W_0$	Vertical datum
$X, Y, Z$	Geocentric co-ordinates
$x^c, y^c, z^c$	Cartesian co-ordinates referred to the pole of a spherical cap
<b>z</b>	Vector of centrifugal acceleration
$\Delta C_{n,m}, \Delta S_{n,m}$	Reduced spherical harmonic coefficients, of degree $n$ and order $m$
$\Delta g$	Gravity anomaly
$\Delta m$	Scale term

$\Delta T$	Systematic error of the anomalous gravity potential
$\Delta T_{\eta}$	Systematic error of the anomalous gravity potential, in the direction of $\eta$
$\Delta T_{\xi}$	Systematic error of the anomalous gravity potential, in the direction of $\xi$
$\Delta T_{\zeta}$	Systematic error of the anomalous gravity potential, in the direction of $\zeta$
$\Phi$	Astronomical Latitude
$\vartheta^c, \alpha^c$	Spherical co-ordinates in the local system of a spherical cap
$\Lambda$	Astronomical Longitude
$\beta$	Correlation length
$\delta g$	Gravity disturbance
$\delta \mathbf{g}$	Gravity disturbance vector
$\gamma$	Normal gravity
$\boldsymbol{\gamma}$	Normal gravity vector
$\gamma_0$	Normal gravity of the reference ellipsoid
$\eta$	Deflection from the vertical, in direction of longitude
$\eta_{\text{astro}}$	Deflection from the vertical, in direction of longitude, observed
$\eta_{\text{grav}}$	Deflection from the vertical, in direction of longitude, derived from a gravimetric model
$\varphi$	Geodetic Latitude
$\lambda$	Geodetic Longitude
$\theta, \lambda, r$	Spherical co-ordinates
$\theta_0, \lambda_0, r_0$	Spherical co-ordinates at the pole of a spherical cap
$\sigma_0$	a-priori standard deviation
$\xi$	Deflection from the vertical, in direction of latitude
$\xi_{\text{astro}}$	Deflection from the vertical, in direction of latitude, observed
$\xi_{\text{grav}}$	Deflection from the vertical, in direction of latitude, derived from a gravimetric model
$\zeta$	Height anomaly
$\zeta_{\text{DFHRS}}$	Height anomaly, provided by the DFHRS database
$\zeta_{\text{FEM}}$	Height anomaly, represented by a FEM

$\zeta_{\text{grav}}$

Height anomaly, derived from a gravimetric model

# Chapter 1

## Introduction

In recent years, the number of precise online DGNSS (Differential Global Navigation Satellite System) applications has significantly increased. Precise online DGNSS correction services, such as SAPOS (AdV, 2007), ASCOS (Eon-Ruhrgas, 2007) or EUPOS (EUPOS, 2007) have been created. Within these services, networks of active DGNSS reference stations determine correction parameters that are transmitted to the DGNSS user for precise online positioning. The latest version of the transmission message, RTCM 3.0 (RTCM, 2007), also contains transformation parameters for vertical, as well as for horizontal positioning. The DGNSS is now able to determine the position not only in global co-ordinate systems, but also in national, regional and local co-ordinate systems, depending on the relation of the transformation parameters in the RTCM 3.0 message. The accuracy of the position determined by means of such applications may reach centimetre level, depending on the time of the observations.

In contrast to the transformation of the plan co-ordinates the transformation of the height component is more difficult, because national height systems are physically defined while the height derived from DGNSS positioning is the height above the WGS84 (World Geodetic System 1984), a mathematical model of the earth and is therefore called “ellipsoidal height”. So for the application of precise DGNSS services and for the generation of transformation messages, such as RTCM 3.0, there is an urgent need for a Height Reference Surface, HRS, in a unified datum with appropriate accuracy.

In Europe, the first steps have been taken by installing the European Vertical Reference System, EVRS (BKG 2003). The EVRS is represented by the unification of the European vertical datum, the Unified European Levelling Network, UELN95/98, and the European Terrestrial Reference System, ETRS89. This point-wise realisation of a European HRS is now to be taken as a reference for any surface covering model that is derived from related terrestrial observations. These are of gravity magnitude,  $g$ , and deflections from the vertical from the normal to the ellipsoid in the north-south and the east-west directions,  $\xi$  and  $\eta$ .

The determination of the HRS, by a combination of gravity, vertical deflections and GNSS/levelling points, provided by the respective terrestrial reference networks, is a current and important task of geodetic research.

The approach that has been applied for HRS determination over decades is the so-called “Remove-Restore-Technique” (RRT) (Hofmann-Wellenhof and Moritz, 2005). The HRS models, computed by means of this technique are reaching centimetre level in the short-wave parts. The long-wave parts show systematic errors up to the decimetre level, resulting mainly from the applied geopotential models. Other sources are for example, approximations in the applied mathematical models. In addition, the information from some observation types, such as deflections from the vertical or points with known ellipsoidal and standard heights, remains unused.

To eliminate the long-wave errors, additional measurements on control points with known heights and also, more or less complicated mathematical operations are necessary to determine the standard height to an adequate accuracy. In consequence, the precise standard height determination by means of DGNSS techniques is still very uneconomical. To make complete use of the benefits of modern online DGNSS correction services, such as SAPOS, ASCOS and EUPOS, and to generate an applicable transformation message like RTCM 3.0, the application of a mathematical concept has to be derived that enables the determination of a HRS in a closed model, which fits the national height systems. Further, the mathematical model should enable the combined evaluation of HRS related observations.

A concept that enables the rigorous least squares adjustment of any HRS related observation is the concept of the Digital FEM (Finite Element Method) Height Reference Surface, DFHRS. In this concept the “actual” HRS, with all its uncertainties resulting from systematic errors in levelling and in the gravimetric observation is modelled as continuous surface by local Taylor-series expansion in a grid of FEM-meshes. With this, areas of any size may be computed. Applying the DFHRS approach, HRS models have been computed for many countries in Europe, Africa and the US (Jäger and Schneid, 2000-2007), and the concept has become standard for online DGNSS based height determination. The theory of the Digital FEM Height Reference Surface, DFHRS, and further development of the mathematical model are the main parts of this thesis.

The thesis starts with the basics of the Earth’s Gravity field in chapter 2. The properties of the gravity potential and the geodetic boundary value problem are explained and the different coordinate systems used in geodetic applications are explained. Finally two parameterisations of the gravity field are introduced.

In chapter 3, the different types of heights and the relation to the gravity field of the Earth are explained. Chapter 4 is concerned with the determination and the application of HRS models. The different methods of HRS determination are explained and the advantages and

disadvantages are discussed briefly. The concept of the DFHRS is the topic of chapter 6. The mathematical model is completely derived and example computations are presented. The focus is set on the combination of GNSS/levelling points and existing gravimetric HRS models, by a rigorous two-step adjustment. A strategy to eliminate the long-wave errors in such models is derived and discussed. It is further shown, that the application of covariance matrices, generated by appropriate correlation functions, leads to a further increase of the resulting accuracy.

As the Taylor series, that are used to represent the HRS within the DFHRS concept, are not able to hold the gravity information, the adjustment of the gravity observation has to be situated in the first step of the two-step adjustment in the DFHRS concept. A parametric model that enables the complete representation of the gravity field over areas of limited extent is presented in chapter 6. Spherical Cap Harmonics, SCH, may be interpreted as the general case of Spherical Harmonics, SH. These have been applied in geodetic applications for decades. The mathematical model of the SCH is completely derived and the mathematical strictness is proved. The determination of SCH coefficients is to be seen as the first step in the sequential adjustment. In this step the gravity observations are combined with geopotential models. In the second step, the SCH coefficients, or derived height anomalies, respectively, are introduced into a least squares adjustment following the DFHRS concept.

In chapter 7, several examples for the determination of SCH parameters are presented and discussed.

## 1.1 Objectives

The aim and objectives of this project are

- To develop a method to determine standard heights from Global Navigation Satellite System (GNSS) positioning in an online mode
- to develop the application of mathematical techniques for the derivation of covariance matrices of HRS models and
- to investigate their properties to increase the rigorousness and accuracy of adjustments of DFHRS databases
- to develop further a mathematical model to accommodate deflections from the vertical
- to develop further a mathematical model to introduce gravity observations into the sequential least squares estimation of the DFHRS parameters.

## Chapter 2

### Earth's Gravity Field

“The problem of geodesy is to determine the figure and external gravity field of the earth and of other celestial bodies as a function of time, from observations on and exterior to the surfaces of these bodies”

[Torge, 2001]

#### 2.1 Introduction

This chapter starts with a brief introduction to the fundamentals of the gravity field of the earth and its approximation by a mathematical earth model. The relation between the actual potential and the model potential is explained. This will be necessary to understand the relation between the gravity potential and the standard height systems in chapter 3. Afterwards, the geodetic boundary value problem and the solutions according to Stokes and Molodensky are introduced. Finally, the spherical harmonic expansion of the earth's gravity field is explained.

#### 2.2 Fundamentals

The gravity potential,  $W$ , of the earth may be split into two parts: The gravitational potential,  $V$ , and the centrifugal potential,  $Z$ .

$$W = W(x, y, z) = V(x, y, z) + Z(x, y, z) \quad (2-1)$$

The quantities  $x, y, z$  denote the geocentric earth-fixed co-ordinates (Fig. 2.1).

The gravitational potential,  $V$ , is completely generated by the attracting masses of the earth and may be written as:

$$V = V(x, y, z) = G \cdot \iiint_{\text{Earth}} \frac{dM}{l}, \quad \lim_{l \rightarrow \infty} V = 0. \quad (2-2)$$

In (2-2), the quantity,  $G$ , denotes Newton's gravitational constant,  $M$  is the mass of the earth and  $l$  means the distance between the mass element  $dM$  and the actual computational point  $(x, y, z)$ . The mass element,  $dM$  maybe expressed by the volume density,  $\rho$ , and the volume element  $dv$  :

$$dM = \rho \cdot dv \tag{2-2a}$$

The centrifugal potential,  $Z$ , is completely determined with the co-ordinate components  $(x, y)$  of the computational point and the angular velocity of the earth,  $\omega$ . This reads:

$$Z = Z(x, y, z) = \frac{1}{2} \omega^2 \cdot (x^2 + y^2). \tag{2-3}$$

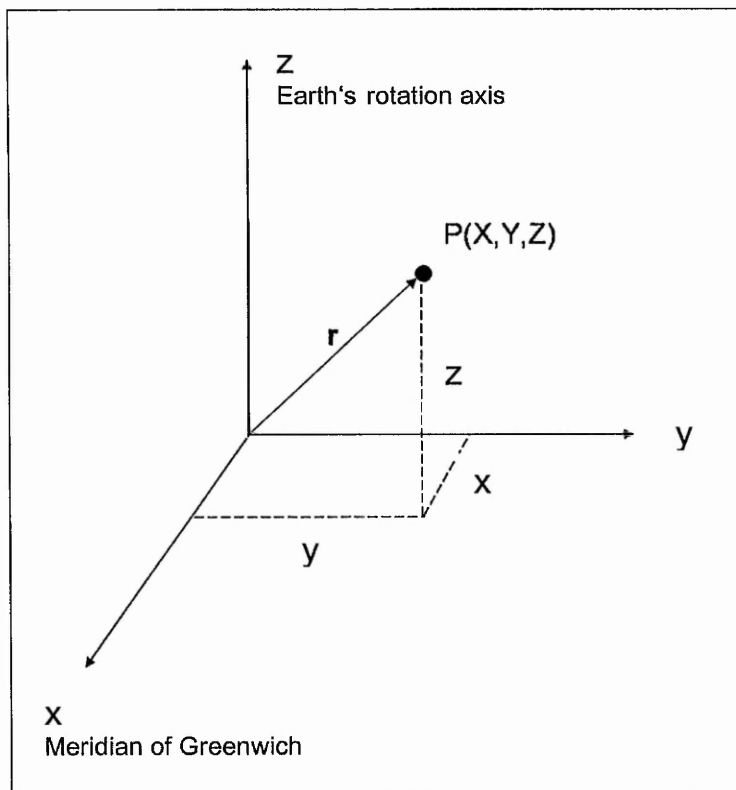


**Fig. 2.1:** Geocentric earth-fixed Cartesian co-ordinates,  $x, y, z$ .

Accordingly, we find with (2-1), (2-2) and (2-3), the expression for the gravity potential,  $W$ :

$$W = G \iiint_{\text{Earth}} \frac{dM}{l} + \frac{1}{2} \omega^2 (x^2 + y^2). \quad (2-4)$$

Differentiating (2-4), we find

$$\nabla W \equiv \frac{\partial W^2}{\partial x^2} + \frac{\partial W^2}{\partial y^2} + \frac{\partial W^2}{\partial z^2} \quad (2-5a)$$

$$= \nabla V + \nabla Z \quad (2-5b)$$

$$= \left( \frac{\partial V^2}{\partial x^2} + \frac{\partial V^2}{\partial y^2} + \frac{\partial V^2}{\partial z^2} \right) + \left( \frac{\partial Z^2}{\partial x^2} + \frac{\partial Z^2}{\partial y^2} + \frac{\partial Z^2}{\partial z^2} \right) \quad (2-5c)$$

$$= (-4\pi \cdot G \cdot \rho) + (2\omega^2). \quad (2-5d)$$

Equation (2-5d) is called the “generalised Poisson equation” for the gravity potential. The quantity,  $\rho$ , denotes the mass density. As can be seen from (2-5d), the discontinuities of the gravity potential,  $W$ , are the discontinuities of the gravitational potential,  $V$ . They only depend on the mass density,  $\rho$ . Outside the attracting masses, where  $\rho = 0$ , the first term of (2-5d) becomes zero. This special case is called “Laplace’s equation” (Blakely, 1995)

$$\nabla V = \left( \frac{\partial V^2}{\partial x^2} + \frac{\partial V^2}{\partial y^2} + \frac{\partial V^2}{\partial z^2} \right) = 0. \quad (2-6)$$

From (2-6) follows that the gravitational potential,  $V$ , is a continuous function exterior the earth surface, where space is not occupied by mass.

A surface with the constant gravity potential

$$W(x, y, z) = \text{constant} \quad (2-7)$$

is called an equipotential surface. The special equipotential surface that approximates to mean sea level (MSL) is called the geoid and is defined with the equation

$$W = W_0 = W_{MSL} = \text{constant} . \quad (2-8)$$

The geoid plays an important role in the definition of standard height systems and geodetic height determination. The determination of the gravity field of the earth automatically contains the determination of the geoid, as a representable equipotential surface (Torge, 2003; Hofmann-Wellenhof and Moritz, 2005).

The gravity vector,  $\mathbf{g}$ , is related to the gravity potential,  $W$ , by

$$\begin{aligned} \mathbf{g} &= \text{grad } W \equiv \left[ \frac{\partial W}{\partial x}, \frac{\partial W}{\partial y}, \frac{\partial W}{\partial z} \right] \\ &= -g \cdot \begin{bmatrix} \cos \Phi \cos \Lambda \\ \cos \Phi \sin \Lambda \\ \sin \Phi \end{bmatrix} \end{aligned} \quad (2-9)$$

The magnitude,  $g$ , of the gravity vector,  $\mathbf{g}$ , is called gravity or gravity acceleration. The direction of  $\mathbf{g}$  is the direction of the plumb line, given with the components  $\Phi$  and  $\Lambda$ . These components may be observed with astronomic methods and are therefore called the astronomic Latitude,  $\Phi$ , and Longitude,  $\Lambda$ .  $\Phi$ ,  $\Lambda$  and  $W$  are called natural co-ordinates (fig. 2.2).

The gravity vector,  $\mathbf{g}$ , is the sum of the gravitational acceleration vector,  $\mathbf{b}$ , and the centrifugal acceleration vector,  $\mathbf{z}$ :

$$\mathbf{g} = \mathbf{b} + \mathbf{z} \quad (2-10)$$

The vectors,  $\mathbf{b}$  and  $\mathbf{z}$ , are defined as the gradient of the gravitational potential,  $V$ , and the centrifugal potential,  $Z$ , respectively:

$$\mathbf{b} = \text{grad}(V) \quad (2-11)$$

$$\mathbf{z} = \text{grad}(Z) \quad (2-12)$$

The gravity potential,  $V$ , at a point,  $P$ , indicates the work, that must be done by gravitation in order to move a unit mass from infinity, where  $V = 0$ , to  $P$ . The units of potential are  $m^2 s^{-2}$ .

The gravity,  $g$ , has the dimensions of an acceleration and is measured in Gal (1 Gal =  $0.01m/s^2$ ). The numerical value of  $g$  is about 978 Gal at the equator, and 983 Gal at the poles (Torge, 2003; Hofmann-Wellenhof and Moritz, 2005).

To summarise the above, the following theorems may be stated (Blakely, 1995):

1. The gravitational potential,  $V$ , and the acceleration of gravity exist and are continuous throughout space if caused by a bounded distribution of piecewise-continuous density.
2. The potential,  $V$ , is everywhere differentiable, so equation  $\mathbf{b} = \text{grad}(V)$  is true throughout space.
3. Poisson's equation  $\nabla^2 V = -4\pi \cdot G \cdot \rho$  describes the relationship between mass and potential throughout space. Laplace's equation  $\nabla^2 V = 0$  is a special case of Poisson's equation, valid in regions of space not occupied by mass.

### 2.3 The geodetic boundary value problem

If the density,  $\rho = \rho(x, y, z)$ , was known all over the earth, the gravitational potential,  $V$ , could be calculated as function of the position,  $(x, y, z)$ , easily by means of (2-2). Unfortunately, detailed density information of the earth is only available for the upper layers.

The gravity potential,  $W$ , and the gravitational potential,  $V$ , cannot be measured directly. Only potential differences  $\Delta W$  and derivatives of the potential can be found by geodetic levelling or respective geodetic applications (chapter 3).

Therefore, these gravity-field observations, taken on the earth's surface, have to be used in order to determine the exterior gravity-field.

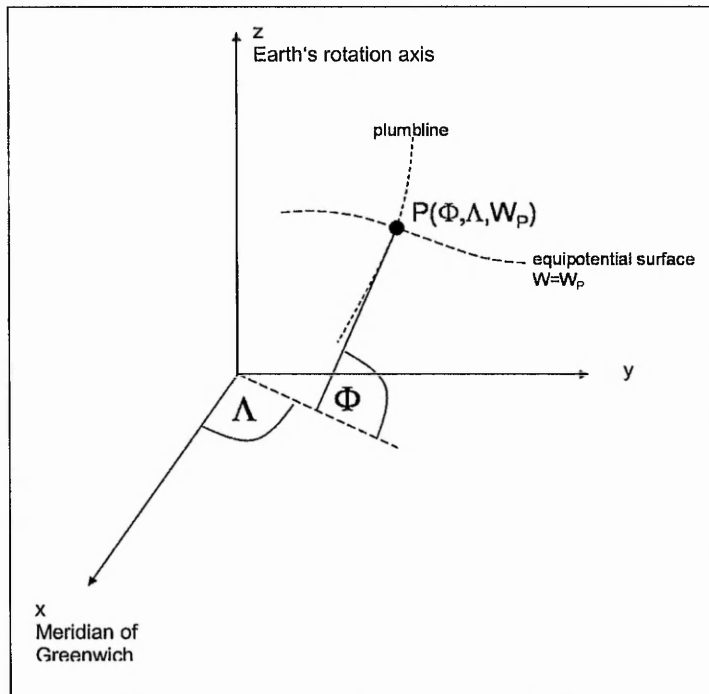


**Fig 2.2:** Natural co-ordinates: astronomic latitude,  $\Phi$ , and longitude,  $\Lambda$ , and the potential,  $W$

The determination of the gravitational potential,  $V$ , from such measurements is called the “geodetic boundary-value problem” (GBVP).

In principle, three different boundary-value problems exist in potential theory:

1. Dirichlet’s boundary-value problem: The potential,  $V$ , on a surface has specified values,
2. Neumann’s boundary-value problem: The derivative of the potential,  $V$ , with respect to the normal of a surface has specified values,
3. Mixed boundary-value problem: The linear combination of the potential,  $V$ , and the derivative with respect to the normal of a surface has specified values.

The above boundary-value problems (BVP) of potential theory usually require a knowledge of the boundary surface  $S$ . For the GBVP, this surface is usually unknown. In case of geoid

determination, the boundary surface  $S$  is actually the object to be determined. This problem is then called "free GBVP".

To solve the free GBVP an approximate gravity field or normal gravity field,  $U$ , respectively an approximate boundary surface  $S_0$  is introduced. The earth is for example well approximated by a flattened ellipsoid of revolution of the same mass, where the minor axis coincidences the average rotation axis of the earth. If this reference ellipsoid rotates with the same angular velocity  $\omega$  of the earth, it creates a normal gravity potential,  $U$ , that may be written in analogy to (2-1) as:

$$U = V^N + Z \quad (2-13)$$

The normal potential,  $U$ , is resulting from the summation of the normal gravitational potential,  $V^N$ , and the centrifugal potential,  $Z$  (2-3). In analogy to (2-6) the  $V^N$  follows Laplace's equation

$$\nabla V^N = 0. \quad (2-14)$$

Generally the normal gravity potential,  $U$ , is chosen in a way, that the reference ellipsoid is an equipotential surface for  $U$ :

$$U(x, y, z) = U_0 = \text{constant} \quad (2-15)$$

Such an ellipsoid that is usually applied in geodetic applications is the GRS80 (Geodetic Reference System 1980). The normal potential,  $U$ , of a point  $P(x, y, z)$  may be computed easily with the fundamental parameters of the respective reference ellipsoid (Moritz, 1990). For the constant potential  $U_0$ , for example, we have:

$$U_0 = \frac{GM}{\epsilon} \arctan \frac{\epsilon}{b} + \frac{\omega^2}{3} a^2, \quad (2-16)$$

with the product of Newton's gravitational constant and Earth's mass,  $GM$ , the semi-major and the semi-minor axes of the reference ellipsoid,  $a$  and  $b$ , the linear eccentricity,  $\epsilon$ , and the rate of Earth's rotation,  $\omega$ .

According to the actual gravity vector,  $\mathbf{g}$  (2-9), the normal gravity vector,  $\boldsymbol{\gamma}$ , is defined as gradient of the normal gravity potential:

$$\begin{aligned}\boldsymbol{\gamma} &= \text{grad } U \equiv \left[ \frac{\partial U}{\partial x}, \frac{\partial U}{\partial y}, \frac{\partial U}{\partial z} \right] \\ &= -\gamma \cdot \begin{bmatrix} \cos \varphi \cos \lambda \\ \cos \varphi \sin \lambda \\ \sin \varphi \end{bmatrix}\end{aligned}\tag{2-17}$$

The co-ordinate components  $\varphi$  and  $\lambda$  give the direction of the normal. They may be determined by geodetic positioning methods, such as GPS, and are called geodetic latitude,  $\varphi$  and longitude,  $\lambda$  (fig. 2.3).

In analogy to the normal gravity potential,  $U$ , the normal gravity,  $\gamma$ , may be computed easily from the fundamental parameters of the normal gravity field. The normal gravity on the surface of the reference ellipsoid,  $\gamma_0$ , is found by means of

$$\gamma_0 = \gamma_a \frac{1 + k \sin^2 \varphi}{\sqrt{1 - e^2 \sin^2 \varphi}}, \text{ with } k = \frac{b\gamma_b}{a\gamma_a} - 1,\tag{2-18}$$

where  $\gamma_a$  and  $\gamma_c$  mean the normal gravity at equator and pole respectively (Moritz, 1990).

The normal gravity,  $\gamma$ , at a point that is not situated on the reference ellipsoid, is usually expanded as Taylor series with respect to the ellipsoidal height,  $h$  (Wenzel, 1989):

$$\gamma = \gamma_0 + \left( \frac{\partial \gamma}{\partial h} \right)_0 \cdot h + \frac{1}{2} \left( \frac{\partial \gamma}{\partial h} \right)_0^2 \cdot h^2\tag{2-19}$$

In most applications the approximate

$$\gamma = \gamma_0 \left( 1 - \frac{2}{a} (1 + f + m - 2f \sin^2 \varphi) \cdot h + \frac{3}{a^2} h^2 \right)\tag{2-20}$$

is used. In accordance, the normal gravity potential,  $U$ , at a point not situated on the reference ellipsoid could be computed by Taylor series expansion on the ellipsoid.

With

$$\gamma_0 = -\frac{\partial U_0}{\partial h} \quad (2-21)$$

the respective series reads to a first order approximation

$$U = U_0 + \left(\frac{\partial U}{\partial h}\right)_0 \cdot h \quad (2-22a)$$

$$= U_0 - \gamma_0 \cdot h. \quad (2-22b)$$

For practical computations, either closed formulas in ellipsoidal co-ordinates, or a spherical harmonic expansion (2-46a) may be used.

The difference between the actual gravity potential,  $W$ , and the normal gravity potential,  $U$ , is called anomalous gravity potential or disturbing gravity potential,  $T$ . The equation for  $T$  reads:

$$T(x, y, z) = T = W - U \quad (2-23)$$

The main objective of the GBVP is to derive the anomalous gravity potential,  $T$ , at a position  $\varphi, \lambda, h$ .

In the classical theory of Stokes (fig. 2.4), the geoid,  $W_0$ , serves as boundary surface. The unknown to determine, the height anomaly vector,  $\zeta$ , is in this case called the geoid height,  $N$ . The normal potential on the ellipsoid,  $U=U_0$ , should be the same than the actual potential,  $W_0=\text{constant}$ , on the geoid (chapter 3).

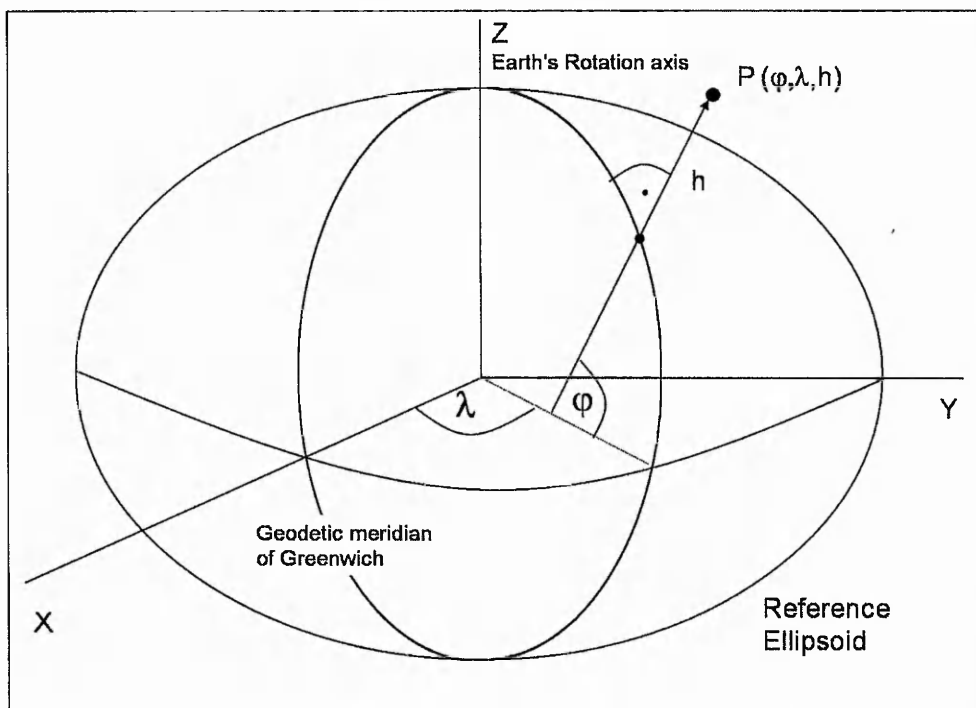


**Fig. 2.3:** Geodetic co-ordinate system: Geodetic latitude,  $\phi$ , and longitude,  $\lambda$  and ellipsoidal height,  $h$ .

The anomalous potential,  $T$ , is finally derived by a Taylor series expansion, similar to (2-22) and the geoid height or geoid undulation,  $N$ , is then found by the famous Bruns formula

$$N = \frac{T}{\gamma_0}, \quad (2-24)$$

where  $\gamma_0$  denotes the normal gravity acceleration on the reference ellipsoid (e.g. Torge, 2001)

The theory of Stokes contains however some assumptions, that do not hold in reality. As the geoid serves as the boundary surface in the GBVP, it is assumed, that this surface includes all masses. As the geoid is approximated to a first order by the mean sea level, it is obvious, that this assumption fails. Hence, it is necessary, to reduce these masses mathematically. In addition, the geodetic observations refer to the earth surface rather than to the boundary surface, the geoid. Consequently, they have to be reduced to the geoid, which is the actual object to be determined.

The calculation of quantities based on these assumptions is not sufficient from a theoretical point of view. In addition, the computation is very time expensive and uneconomical.

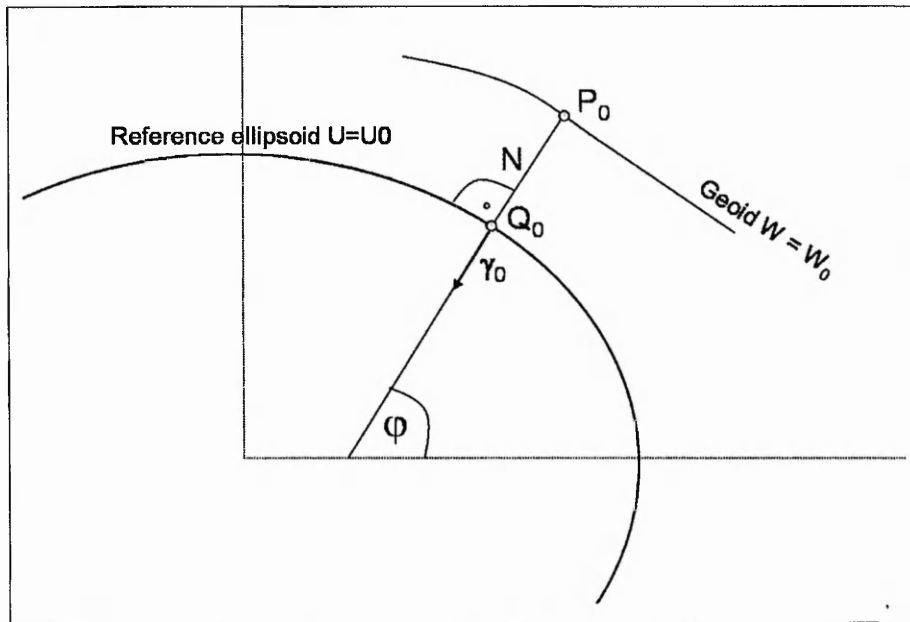


Fig. 2.4: The GBVP according to Stokes

An alternative to the classical theory of Stokes, a method that avoids the above mentioned assumptions was presented by Molodensky (fig. 2.5). In contrast to the Stokes problem this modern theory uses the earth surface as boundary surface  $S$ . Any point,  $P(x, y, z)$ , at the earth's surface,  $S$ , is linked to the normal gravity field of the reference ellipsoid by the condition.

$$W_P = U_Q. \quad (2-25)$$

The surface,  $S_0$ , that results from the points  $Q \in S_0$  in (2-19), serves as an approximate boundary surface and is called the telluroid. In contrast to the geoid, the telluroid is not an equipotential surface and has no other physical meaning.

The main objective of Molodensky's theory is, in analogy to Stokes' theory, the determination of the metric distance of the anomaly,  $\zeta$ , between the points,  $P$  and  $Q$ , on the earth's surface and the telluroid respectively.

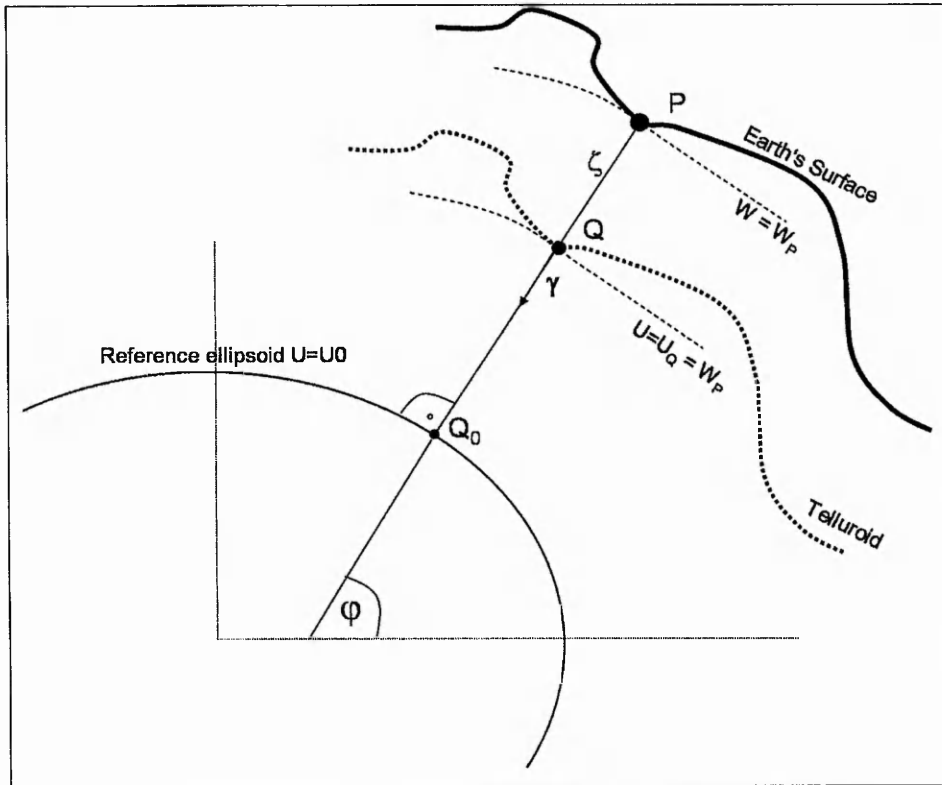


Fig. 2.5: The GBVP according to Molodensky

The anomaly,  $\zeta$ , again is found by means of Bruns' equation, but, in contrast to (2-24), the anomalous gravity potential,  $T$ , is determined at the point,  $P$ , on the earth's surface:

$$\zeta = \frac{T_P}{\gamma_Q} \quad (2-26)$$

The anomaly,  $\zeta$ , from (2-26) is now determined without any assumptions. The geodetic observations, measured at the earth's surface, do not need to be reduced, and no masses need to be eliminated mathematically.

The difference between the actual gravity vector,  $\mathbf{g}$ , and the normal gravity vector,  $\boldsymbol{\gamma}$ , at a point,  $P$ , on the earth's surface, is called gravity disturbance vector,  $\delta\mathbf{g}$ .

$$\delta\mathbf{g} = \mathbf{g}_P - \boldsymbol{\gamma}_P \quad (2-27)$$

The magnitude of the vector,  $\delta\mathbf{g}$ , is the difference between the actual and normal gravity acceleration,  $g$  and  $\gamma$ , and is called the gravity disturbance,  $\delta g$ . The difference in direction is

called the deflection of the vertical. It has a north-south component,  $\xi$ , and an east-west component,  $\eta$ . Both components might be found from the following relationship between the astronomical co-ordinates,  $\Phi$  and  $\Lambda$ , and the geodetic co-ordinates,  $\varphi$  and  $\lambda$ :

$$\xi = \Phi - \varphi \quad (2-28a)$$

and

$$\eta = (\Lambda - \lambda) \cdot \cos \varphi. \quad (2-28b)$$

In recent decades, the gravity anomaly,  $\Delta g$ , defined as the difference between the vectors,  $g$  and  $\gamma$ , calculated at the point,  $Q$ , on the approximate boundary surface  $S_0$ , was used to solve the GBVP. The equation for  $\Delta g$  reads:

$$\Delta g = g_p - \gamma_Q. \quad (2-29)$$

Using traditional geodetic observation techniques, such as levelling, it was not possible to determine the ellipsoidal height,  $h$ . Modern positioning techniques, such as GPS, enable the precise observation of the ellipsoidal height,  $h$ , in a very economic way. So the calculation of the gravity anomalies,  $\Delta g$ , will become less and less important.

From (2-9) and (2-17) it follows that

$$\delta g = \text{grad}(T), \quad (2-30)$$

and if the deflections of the vertical (2-28a, b) are neglected:

$$\delta g = -\frac{\partial T}{\partial h}, \quad (2-31a)$$

In analogy the gravity anomaly is written

$$\Delta g = -\frac{\partial T}{\partial h} + \frac{1}{\gamma} \frac{\partial \gamma}{\partial h} T. \quad (2-31b)$$

Because of the historical importance of the gravity anomaly,  $\Delta g$ , (2-31b) is called “the fundamental equation of physical geodesy” (Torge, 2003). In future it will be replaced by (2-31a) as the positioning of the gravity measurements will take place by GNSS providing the ellipsoidal height,  $h$ . Hence, in the following of this thesis, the focus will be on the disturbances,  $\delta g$ .

The anomalous Potential,  $T$ , in the sense of Stokes' theory, is finally found from the gravity disturbances,  $\delta g$ , by means of

$$T(\theta, \lambda) = \frac{R}{4\pi} \iint_{\sigma} K(\psi) \delta g \cdot d\sigma. \quad (2-32)$$

Equation (2-32) results from a spherical approximation. The mean radius  $R$  is defined as the radius of a sphere with the same volume as the reference ellipsoid.  $\sigma$  denotes a unit sphere.  $K(\psi)$  denotes the Hotine-Koch function (Hoffman-Wellenhof and Moritz, 2005)

$$K(\psi) = \frac{1}{\sin(\psi/2)} - \ln \left( 1 + \frac{1}{\sin(\psi/2)} \right). \quad (2-33)$$

The quantity,  $\psi$ , is called the spherical distance, between the actual point of computation,  $P$ , and the surface element  $d\sigma$ . The spherical distance,  $\psi$ , is one component of the spherical polar co-ordinates. As required by the theory of Stokes,  $\delta g$  or  $\Delta g$ , respectively, have to be reduced to the geoid.

The geoid height,  $N$ , is found by inserting Koch's formula (2-32) into Bruns' equation (2-24). This leads to Koch's formula

$$N(\theta, \lambda) = \frac{R}{4\pi\gamma_0} \iint_{\sigma} K(\psi) \delta g \cdot d\sigma. \quad (2-34)$$

For the theory of Molodensky, the respective equations are more complicated. As the disturbances,  $\delta g$ , are not reduced, the approximation  $r = R$ , as used in the Stokes approach above, is not allowed. To solve this problem, so-called Molodensky corrections are derived in the sense of a Taylor series expansion up to a specified degree  $n$  (e.g. Hofmann-Wellenhof and Moritz, 2005).

$$\zeta = \zeta_0 + \zeta_1 + \zeta_2 + \dots + \zeta_n \quad (2-35)$$

A first order approximation, for example, reads as:

$$\zeta = \frac{R}{4\pi\gamma_0} \iint_{\sigma} K(\psi) \left( \delta g - \frac{\partial \delta g}{\partial h} (h - h_p) \right) \cdot d\sigma. \quad (2-36)$$

The computation of the geoid undulation,  $N$ , or the height anomaly,  $\zeta$ , by means integral formulas such as (2-34) and (2-36), from gravity observations is one application of this formula and may be the most important from a geodetic point of view.

There are other applications, for example the computation of the deflections from the vertical,  $\xi$  and  $\eta$ , from gravity disturbances,  $\delta g$ .

The deflections may be interpreted as slope of the geoid,  $W_0$ , in the directions of the latitude,  $\varphi$ , and the longitude,  $\lambda$ . Using a spherical approximation, with  $r = R$ , this reads as (Torge, 2005):

$$\xi_0 = -\frac{\partial N}{\partial S_{North}} = -\frac{\partial N}{M_0(\varphi) \cdot \partial \varphi} \approx -\frac{1}{r} \frac{\partial N}{\partial \varphi} \quad (2-37)$$

$$\eta_0 = -\frac{\partial N}{\partial S_{East}} = -\frac{\partial N}{N_0(\varphi) \cdot \cos \varphi \cdot \partial \lambda} \approx -\frac{1}{r} \frac{\partial N}{\cos(\varphi) \partial \lambda} \quad (2-38)$$

If equation (2-28) is inserted into (2-31) and (2-32), the formulas of Vening-Meinesz are achieved:

$$\xi_0 = \frac{1}{4\pi\gamma_0} \iint_{\sigma} \Delta g \frac{dS(\psi)}{d\psi} \cos(\alpha) \cdot d\sigma \quad (2-39)$$

$$\eta_0 = \frac{1}{4\pi\gamma_0} \iint_{\sigma} \Delta g \frac{dS(\psi)}{d\psi} \sin(\alpha) \cdot d\sigma, \quad (2-40)$$

where  $\alpha$  is the azimuth, one component of the spherical polar co-ordinates (Torge, 2003).

The respective expressions for Molodensky's theory again contain correction terms similar to (2-36). This reads with a first order approximation for the case of disturbances

$$\xi = \frac{1}{4\pi\gamma_0} \iint_{\sigma} \left( \delta g - \frac{\partial \delta g}{\partial h} h \right) \frac{dK(\psi)}{d\psi} \cos(\alpha) \cdot d\sigma \quad (2-41)$$

$$\eta = \frac{1}{4\pi\gamma_0} \iint_{\sigma} \left( \delta g - \frac{\partial \delta g}{\partial h} h \right) \frac{dS(\psi)}{d\psi} \sin(\alpha) \cdot d\sigma, \quad (2-42)$$

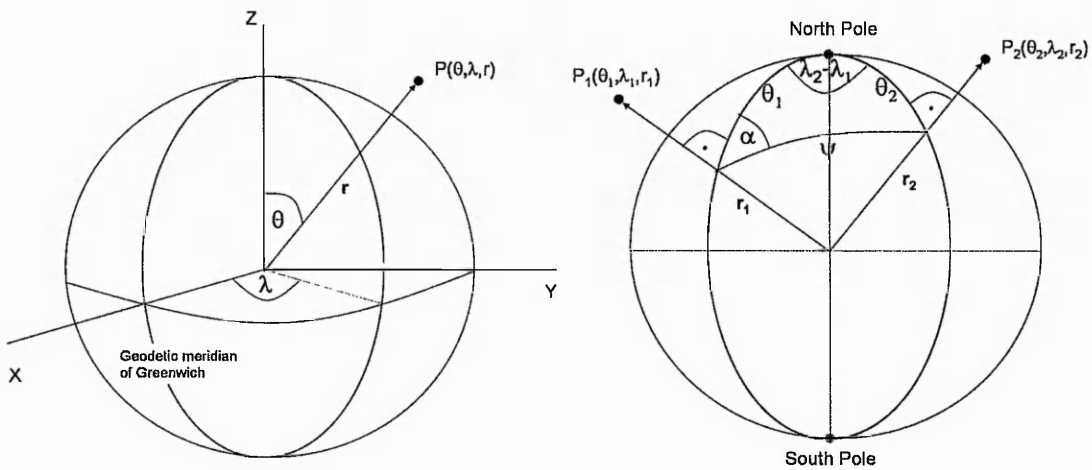


**Fig. 2.6: left:** Spherical geocentric co-ordinates. **right:** Spherical polar triangle

In practical applications, the computation of integral Formulae have to be approximated by summation. This summation has to be done all over the earth, in theory. Unfortunately, precise terrestrial observations are only available for limited areas. In practice, gravity data for remote areas are therefore taken from a global spherical harmonic model [chapter. 2.3.1].

In recent decades, the so-called “Remove-Restore-Technique”, RRT, has been derived and applied in many projects of precise local and regional geoid determination. The principle of this application is briefly explained and discussed in chapter 4.

Within the application of integral equations it is not possible to combine different geodetic observation types. In contrast, a parametric model would allow a least squares adjustment of all relevant terrestrial observations, such as gravity disturbances,  $\delta g$ , deflections from the vertical,  $\xi$  and  $\eta$ , and of course directly “observed” geoid heights,  $N$ , in points with known

ellipsoidal heights,  $h$ , and standard heights,  $H$ . The different types of standard height systems and their relation to the geoid are explained in chapter 3. In the following section, different parametric models, which may be applied for the approximation of the gravity potential, are introduced.

## 2.4 Parameterisation of the Gravity field

In most geodetic applications, a parametric model is preferred, rather than integral formulas, such as (2-34) or (2-36), to model the potential or the anomalous potential,  $W$  or  $T$ , respectively. The coefficients of such a model may then be determined by means of a least-squares adjustment of the geodetic observations, on or exterior to the earth's surface. Different harmonic base functions have been applied for the parameterisation of the gravity field, for example spherical harmonics (e.g. Lemoine et. al 1996; Wenzel, 1998); point mass models (e.g. Barthelmes, 1986; Lehmann, 1994) or multipoles (e.g. Marchenko, 1998).

The most important of these for further investigation in this thesis are the spherical harmonic models and the point mass models. They are therefore introduced in the following sections.

### 2.4.1 Spherical harmonics

Since the gravitational potential,  $V$ , follows Laplace's equation (2-6), it may be written in terms of spherical harmonics (Hobson, 1960):

$$V = \frac{GM}{a} \sum_{n=0}^{\infty} \sum_{m=0}^n \left( \frac{a}{r} \right)^{n+1} (\bar{C}_{n,m} \cos(m \cdot \lambda) + \bar{S}_{n,m} \sin(m \cdot \lambda)) \bar{P}_{n,m}(\cos \theta) \quad (2-43)$$

In (2-43), the quantity,  $a$ , denotes is the major axis of the reference ellipsoid.  $\bar{C}_{n,m}$  and  $\bar{S}_{n,m}$  are the fully normalised spherical harmonic coefficients. The quantity  $r$  denotes the length of the space vector,  $\mathbf{r}$ , from the origin of the co-ordinate system to the actual computational point. The direction of  $r$  is given by spherical geocentric co-ordinates,  $\theta$  and  $\lambda$ . The function  $\bar{P}_{n,m}(\cos(\theta))$  is the fully normalised Legendre function of degree,  $n$ , and order,  $m$ , at the polar distance,  $\theta$ .

In practice, it is assumed that the infinite series (2-43) converges, and therefore the series truncated at a specified degree  $n_{\max}$  so that the omission error  $\varepsilon_{n_{\max}}$  is negligible. The description of the gravitational potential,  $V$ , reads:

$$V = \frac{GM}{a} \sum_{n=0}^{n_{\max}} \left(\frac{a}{r}\right)^{n+1} \sum_{m=0}^n (\bar{C}_{n,m} \cos(m \cdot \lambda) + \bar{S}_{n,m} \sin(m \cdot \lambda)) \bar{P}_{n,m}(\cos \theta) + \varepsilon_{n_{\max}} \quad (2-44)$$

$$= \sum_{n=0}^{n_{\max}} \left(\frac{a}{r}\right)^{n+1} \sum_{m=0}^n V_n(\theta, \lambda, r) + \varepsilon_{n_{\max}} \quad (2-44a)$$

$$= \sum_{n=0}^{n_{\max}} \sum_{m=0}^n V_{n,m}(\theta, \lambda, r) + \varepsilon_{n_{\max}} \quad (2-44b)$$

In the following sections of this thesis, the omission error,  $\varepsilon_{n_{\max}}$ , will be neglected.

The normal gravitational potential,  $V^N$ , may also be expanded with a spherical harmonic series. This reads:

$$V^N = \frac{GM}{a} \sum_{n=0}^{n_{\max}} \left(\frac{a}{r}\right)^{n+1} \sum_{m=0}^n (\bar{C}^N_{n,m} \cos(m \cdot \lambda) + \bar{S}^N_{n,m} \sin(m \cdot \lambda)) \bar{P}_{n,m}(\cos \theta) \quad (2-45)$$

Since the normal gravitational potential,  $V_N$ , results from an ellipsoid of revolution, only the zonal components,  $\bar{C}^N_n$ , with an even degree,  $n$ , are needed, and expression (2-45) may be reduced to:

$$V^N = \frac{GM}{a} \sum_{n=0(2)}^{n_{\max}} \left(\frac{a}{r}\right)^{n+1} \bar{C}^N_n \cdot \bar{P}_n(\cos \theta). \quad (2-46)$$

The normal potential,  $U$ , may now be written as:

$$U = \frac{GM}{a} \sum_{n=0(2)}^{n_{\max}} \left(\frac{a}{r}\right)^{n+1} \bar{C}^N_n \cdot \bar{P}_n(\cos \theta) + \frac{\omega^2}{2} r^2 \sin^2 \theta. \quad (2-46a)$$

Finally the anomalous potential, T, in terms of spherical harmonics, is found by introducing (2-44) and (2-46) into (2-23):

$$T = \frac{GM}{a} \sum_{n=0}^{n_{\max}} \left(\frac{a}{r}\right)^{n+1} \sum_{m=0}^n (\Delta\bar{C}_{n,m} \cos(m \cdot \lambda) + \Delta\bar{S}_{n,m} \sin(m \cdot \lambda)) \bar{P}_{n,m}(\cos\theta) \quad (2-47)$$

The geoid height, N, and the height anomaly,  $\zeta$ , are:

$$N = \frac{GM}{a \cdot \gamma_0} \sum_{n=0}^{n_{\max}} \left(\frac{a}{r}\right)^{n+1} \sum_{m=0}^n (\Delta\bar{C}_{n,m} \cos(m \cdot \lambda) + \Delta\bar{S}_{n,m} \sin(m \cdot \lambda)) \bar{P}_{n,m}(\cos\theta), \quad (2-48)$$

or

$$\zeta = \frac{GM}{a \cdot \gamma} \sum_{n=0}^{n_{\max}} \left(\frac{a}{r}\right)^{n+1} \sum_{m=0}^n (\Delta\bar{C}_{n,m} \cos(m \cdot \lambda) + \Delta\bar{S}_{n,m} \sin(m \cdot \lambda)) \bar{P}_{n,m}(\cos\theta) \quad (2-49)$$

respectively.

The derivatives of the anomalous gravity potential, T, may now be found by inserting the respective operator (2-31a, 2-31b, 2-37, 2-38) into (2-47).

For the gravity disturbance,  $\delta g$ , we have:

$$\delta g = -\frac{\partial T}{\partial h} \approx -\frac{\partial T}{\partial r} \quad (2-50)$$

$$= \frac{GM}{a} \sum_{n=0}^{n_{\max}} \left(\frac{a}{r}\right)^{n+1} (n+1) \sum_{m=0}^n (\Delta\bar{C}_{n,m} \cos(m \cdot \lambda) + \Delta\bar{S}_{n,m} \sin(m \cdot \lambda)) \bar{P}_{n,m}(\cos\theta) \quad (2-51)$$

and for the deflections from the vertical,  $\xi$  and  $\eta$ :

$$\xi = -\frac{GM}{a \cdot r \cdot \gamma} \sum_{n=0}^{n_{\max}} \left(\frac{a}{r}\right)^{n+1} \sum_{m=0}^n (\Delta \bar{C}_{n,m} \cos(m \cdot \lambda) + \Delta \bar{S}_{n,m} \sin(m \cdot \lambda)) \frac{d\bar{P}_{n,m}(\cos \theta)}{d\theta} \quad (2-52)$$

$$\eta = -\frac{GM}{a \cdot r \cdot \sin(\theta) \cdot \gamma} \sum_{n=0}^{n_{\max}} \left(\frac{a}{r}\right)^{n+1} \sum_{m=0}^n (-m \cdot \Delta \bar{C}_{n,m} \sin(m \cdot \lambda) + m \cdot \Delta \bar{S}_{n,m} \cos(m \cdot \lambda)) \bar{P}_{n,m}(\cos \theta) \quad (2-53)$$

The equations (2-51, 2-52 and 2-53) are spherical approximations. For precise computations several ellipsoidal corrections are necessary, due to the flattening of the reference ellipsoid and the normal gravity field (e.g. Gruber, 2000; Wenzel, 1985).

In principle, the spherical harmonic coefficients  $\Delta \bar{C}_{n,m}$  and  $\Delta \bar{S}_{n,m}$  could now be determined by means of a least squares adjustment of the respective terrestrial observations,  $N$  or  $\zeta$ ,  $\xi$  and  $\eta$ ,  $\delta g$ , with the observation equations (2-48 or 2-49, 2-51, 2-52 and 2-53). In practice, however, the coefficients are usually determined by means of integral equations (e.g. Gruber, 2000; Wenzel, 1985; Wenzel, 1998):

$$\begin{Bmatrix} \Delta \bar{C}_{n,m} \\ \Delta \bar{S}_{n,m} \end{Bmatrix} = \frac{1}{4\pi GM} \iint_{\sigma} r \gamma \left(\frac{r}{a}\right)^l \bar{N} \cdot \bar{P}_{n,m} \cos(\theta) \begin{Bmatrix} \cos(m\lambda) \\ \sin(m\lambda) \end{Bmatrix} d\sigma \quad (2-54)$$

$$\begin{Bmatrix} \Delta \bar{C}_{n,m} \\ \Delta \bar{S}_{n,m} \end{Bmatrix} = \frac{1}{4\pi GM} \iint_{\sigma} \frac{r^2}{l+1} \left(\frac{r}{a}\right)^l \delta \bar{g} \cdot \bar{P}_{n,m} \cos(\theta) \begin{Bmatrix} \cos(m\lambda) \\ \sin(m\lambda) \end{Bmatrix} d\sigma \quad (2-55)$$

The integration is done over the unit sphere,  $\sigma$ . The quantities,  $\bar{N}$  and  $\delta \bar{g}$ , denote the mean geoid height or gravity disturbance, of the surface increment,  $d\sigma$ .

As most of the earth's surface is occupied by water, it is not possible to collect precise terrestrial observations all over the earth. Hence, most of the observations are incorporated from space methods, for example satellite gravity missions. The measurement methods are mainly satellite altimetry, satellite-to-satellite tracking and satellite gravity gradiometry (Hofmann-Wellenhof and Moritz, 2005; Hofmann-Wellenhof et. al. 2001; Seeber, 2003)

Since the beginning of geopotential modelling applying spherical harmonics in the sixties, several geopotential models have been derived using satellite observations or combinations with terrestrial gravity observations. Gruber (2000) lists all models starting from 1966 to 1999, separating long-wave gravity field models and high resolution gravity field models. Later models, especially those resulting from the latest satellite missions may be found for example at (GFZ, 2006).

Recent investigations show that the accuracy of such model reaches the level of 0.2 – 0.4 m (e.g. Amos and Featherstone). Long-wave errors result mainly from approximations made in the computation and missing gravity observations at the Earth surface. The integrations, (2-54) and (2-55), of course have to be approximated by summation. Depending on the density of the available observations, the surface elements cannot be kept small to ensure good accuracy.

To improve especially the long-wave accuracy of global gravitational models, several satellite missions have been started, namely CHAMP (Challenging Mini-Satellite Payload for Geophysical Research and Application), GRACE (Gravity Recovery and Climate Experiment) and GOCE (Gravity Field and Steady-State Ocean Circulation Explorer). These missions are still running, but some spherical harmonic models have already been derived from CHAMP and GRACE data (GFZ, 2006). The EIGEN04 model will be subject of some computations later in this thesis.

The short-wave accuracy comes from the resolution of the spherical harmonic coefficients. The resolution may be expressed by the minimum wave-length of the SH (Spherical Harmonics) coefficients. Table 2.1 shows the approximation error of SH-Coefficients, derived from the formula of Tscherning and Rapp (1974); c.f. Wenzel (1999).

Applying integral equations, (Wenzel, 1998) computed spherical harmonic coefficients up to degree and order 1800, to reach an approximate error of 3 cm for the height anomaly. This approximate error would be acceptable for many GNSS applications. In contrast, the approximate error of 12.68 mGal for the gravity anomalies and 1.89'' for the deflections from the vertical is still not enough for many geodetic applications. In addition, Wenzel reports anticipated numerical problems, when computing the associated Legendre functions for degree's >2200. This problem is also discussed in Holmes and Featherstone (2002) where

modified algorithms were used to compute the Legendre functions up to degree and order 2700 with an appropriate precision.

In contrast, spherical harmonic models give a good representation of the long-wave gravity field components. They are therefore used as global model within geoid determination by means of the remove restore technique [chapter 4].

**Table 2.1:** Approximation error of a geopotential model according to the degree variance model of Tscherning and Rapp (Wenzel, 1999):

Max. degree	Resolution [km]	Height anomaly [m]	Gravity anomaly [mGal]	Deflection from the vertical (arc sec)
360	55.0	0.228	25.27	3.76
720	27.5	0.103	20.12	3.00
1440	13.8	0.042	14.54	2.16
1800	11.0	0.030	12.68	1.89
3600	5.5	0.010	7.12	1.06
5400	3.7	0.004	4.34	0.65
7200	2.8	0.002	2.74	0.41

### 2.4.2 Point mass models

The concept of the point mass models is based on the application of Newton's law of gravitation. The anomalous potential,  $T$ , may be approximated by superposition of several parts of the anomalous potential,  $T_i$ , which are created by a collection of disturbing masses  $m_i$ . The equation for the potential part,  $T_i$ , reads:

$$T_i = G \frac{m_i}{l_i}, \tag{2-56}$$

where  $l_i$  is the distance between the actual computational point,  $P$ , and the disturbing mass element  $m_i$ . The total anomalous gravitational potential may now be written as:

$$T = G \sum_{i=1}^{i_{\max}} \frac{m_i}{l_i} \tag{2-57}$$

In a local geodetic vertical co-ordinate system (fig 2.7), with the northern direction,  $x$ , the eastern direction,  $y$ , and the upper direction,  $h$ , the distance,  $l$ , between the computational point,  $P$ , and the point mass,  $i$ , is given by

$$l = \sqrt{(x_p - x_i)^2 + (y_p - y_i)^2 + (h_p - h_i)^2} \quad (2-58)$$

According to the definition of such a planar ellipsoidal co-ordinate system, the direction of the upward co-ordinate,  $h$ , is given along the normal to the respective reference ellipsoid. Therefore, the gravity disturbance,  $\delta g$ , in the point mass concept, is now found by inserting (2-31a) into (2-57):

$$\delta g = -\frac{\partial}{\partial h} G \sum_{i=1}^{i_{\max}} \frac{m_i}{l_i} \quad (2-59)$$

$$= G \sum_{i=1}^{i_{\max}} \frac{m_i (h_p - h_i)}{l_i^3} \quad (2-60)$$

The unknown disturbing masses,  $m_i$ , may now be estimated by means of a least-squares adjustment of respective observations,  $\delta g$  (2-60), or the “observed” anomalous potential in identical points (2-57).

Point mass models for the approximation of the gravitational potential of the earth have been investigated in the 1980's by Barthelmes (Barthelmes, 1986). Since then, two different applications of this method have been derived (Lehmann, 1994, Liebsch et. al. 2006):

1. Fixed-position point-mass modelling.

Here, a regular grid of masses is used to generate the gravity field.

The advantage is the very simple mathematical model and the numerical behaviour, because only the magnitudes of the masses have to be determined. The disadvantage is the unrealistic behaviour (oscillation effects) of the determined gravity field, if the point masses are placed in a wrong manner.

## 2. Free-position point mass modelling.

Here both, the magnitude and the position of the point masses are unknowns and simultaneously determined by a least squares adjustment. The advantage is that the oscillation effects are eliminated, because the positions of the point masses are estimated as well. The disadvantage is, that this presents a non-linear problem, which must be solved iteratively.

The point-mass method has also been used in discrete gravity field approximation, such as integrated network adjustments (Müller, 1990; Klein 1995);

Within the application of precise geoid determination, the point mass concept is usually applied together with the Remove-Restore-Technique, see chapter 4. This has the big advantage that only residual quantities have to be determined.

The point mass method is subject of further discussions, in chapter 4, where the Remove-Restore-Technique is briefly explained and discussed. In the following chapter, the different standard height definitions and their relationship to the gravity potential of the earth are introduced.

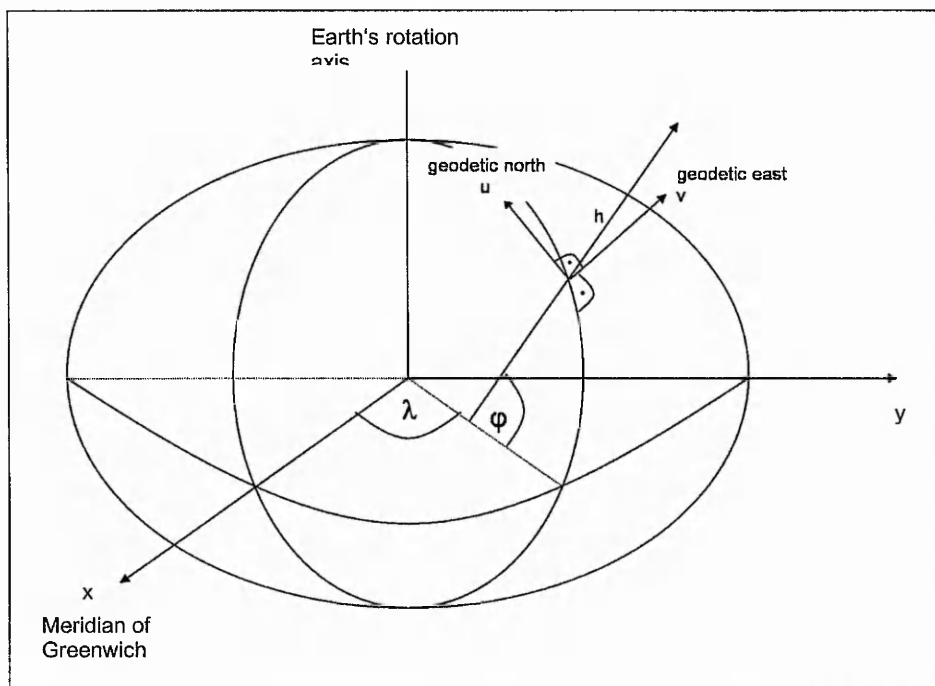


**Fig. 2.7.:** Local geodetic vertical co-ordinate system.

## Chapter 3

# Heights and Height Systems

### 3.1 Introduction

In chapter 2 the gravity potential,  $W$ , of the earth and its gradient, the gravity vector,  $\mathbf{g}$ , have been introduced. It has been shown, that the normal potential,  $U$ , of a reference ellipsoid of revolution is used create an approximate boundary surface to solve the geodetic boundary value problem, GBVP.

The next step is to introduce different standard height types and examine their relation to the potential,  $W$ , and their determination by means of geodetic observations.

### 3.2 Ellipsoidal heights

A point,  $P$ , on the Earth's surface is usually described with three coordinates, latitude, a longitude and a height. The latitude and longitude refer to an ellipsoid of revolution, and are more precisely called geodetic latitude and longitude,  $\phi$  and  $\lambda$ . In the case of a GNSS (Global Navigation Satellite System), for example GPS based coordinates,  $\phi$  and  $\lambda$ , this ellipsoid is the WGS84 (World Geodetic System 1984), a mathematically defined figure that was chosen to approximate the mean sea level globally. Its centre is assumed to be the Earth's centre of mass and the minor axis is aligned with the Earth's reference pole.

The height  $h$  of a GNSS based position at a point,  $P$ , would refer to the surface of this ellipsoid. It gives a measure of the distance from the ellipsoid to the point,  $P$ , along the normal to the ellipsoid. It is called the ellipsoidal height,  $h_P$ .

In most surveying applications, the height above the ellipsoid,  $h$ , is not of any direct interest. Usually the national standard height system is referred to a so called "vertical datum", a well defined Height Reference Surface (HRS), close to mean sea level that is accessible at, at least one point, called the point of origin,  $P_0$ .

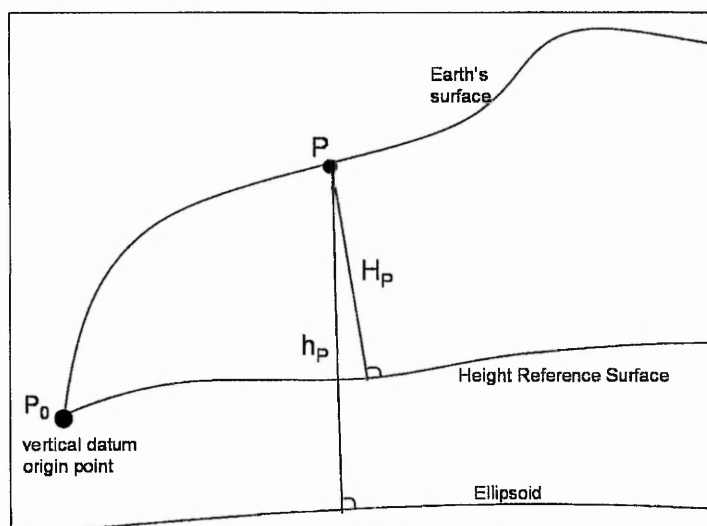


**Fig 3.1:** Ellipsoidal height,  $h$ , versus standard height,  $H$ , with respect to a Height Reference Surface (HRS)

The ellipsoid may be defined as the Height Reference Surface for ellipsoidal heights. In this case the accessibility is achieved indirectly, because the ellipsoid is realised in a coordinate frame, determined by GNSS positioning, that provides the three dimensional coordinates of a point, for example the ETRS89 (European Terrestrial Reference System 1989) (BKG 2003).

For physical reasons, an ellipsoid height system cannot be used as the standard height system. The definition of physical heights and related height systems is the topic of the next sections.

### 3.3 Physically defined heights

The fundamental idea of a physical height definition is, that a surface, that is assumed to be level, should have a constant potential at each point. At the same time, water should not flow between two points of the same potential. According to this principle, the direction that water flow, determines, what is up and what is down. With this, points of the same potential are situated on an equipotential surface of the Earth's gravity field.

The difference between the actual geopotential,  $W_P$ , at a point,  $P$ , and at an equipotential reference surface, or in a geodetic sense, a vertical datum,  $W_0$ , is called the geopotential number  $C_P$ :

$$C_P = W_0 - W_P. \quad (3-1)$$

Theoretically, geopotential numbers,  $C$ , could be used to give numerical values for height, as they are in case of the UELN (Unified European Levelling Network). Starting at a point,  $P_0$ , with a known geopotential,  $W_0$ , the geopotential number,  $C_P$ , of a point,  $P$ , is found from:

$$C_P = W_0 - W_P = \int_{P_0}^P g \cdot dn, \quad (3-2)$$

where  $dn$  is the levelled height increment and  $g$  the average magnitude of the gravity vector along the levelling line from  $P_0$  to  $P$ .

Geopotential numbers are used as the basic quantity for the definition and adjustment of 1<sup>st</sup> and 2<sup>nd</sup> order height networks. Apart from this, they are used mostly for scientific purposes; this is because the unit is not metric. The unit 1 GPU (geopotential unit) =  $10\text{m}^2\text{s}^{-2}$  is used instead.

To find a metric unit for the standard height,  $H$ , the geopotential number,  $C$ , is divided by a gravity value,  $g$ , which may be found in different ways, reading as:

$$H = \frac{C}{g}. \quad (3-3)$$

A well-defined Height Reference Surface (HRS) can define a vertical datum geometrically, in a way that  $H_P$  is the metric length of the plumb line from a point,  $P$ , on the Earth's surface, to the HRS. It may be found by extending downwards  $H_i$  from any point,  $P_i$ , on the Earth's surface.

Depending on the definition of the gravity value,  $g$ , there are three different types of physically defined heights. The dynamic height, the orthometric height and the normal height.

### 3.3.1 Dynamic heights

Geopotential numbers,  $C$ , may be divided by an arbitrarily chosen gravity value  $\gamma_0$ . With this, the dynamic height  $H^D$  is found:

$$H^D = \frac{C}{\gamma_0}. \quad (3-4)$$

The dynamic height,  $H^D$ , has the same advantages as the geopotential number,  $C$ . For example the direction of flowing water depends on the dynamic height. The reason is that points, situated on an equipotential surface of the gravity potential with a constant  $W$ , get the same dynamic height. On the other hand the same reason leads to the main disadvantage of a dynamic height system. The constant potential difference,  $\Delta W$ , of two equipotential surfaces would lead to a constant dynamic height difference,  $\Delta H^D$ . This conflicts with reality. Equipotential surfaces do not run parallel to each other because of the uneven distribution of masses in the Earth. This means, that a unified geometric reference surface for dynamic heights is not possible and dynamic heights do not have any geometrical meaning.

### 3.3.2 Orthometric heights

The orthometric height,  $H^O$ , of a point,  $P$ , is defined as the metric length of the plumb line to an equipotential reference surface with  $W=W_0$ , the geoid (see section 2.2).

$H^O$  may be found by dividing the geopotential number,  $C$ , by a mean gravity along the plumb line,  $\bar{g}$ .

$$H^O = \frac{C}{\bar{g}} = \frac{W_0 - W}{\bar{g}} \quad (3-5)$$

The orthometric height has a geometrical meaning, in contrast to the dynamic height, which does not. But because of the non parallelism of the equipotential surfaces of the gravity potential, points situated on an equipotential surface do not necessary have the same orthometric height. With this, the requirement to have static water between points of the same height is not theoretically fulfilled.

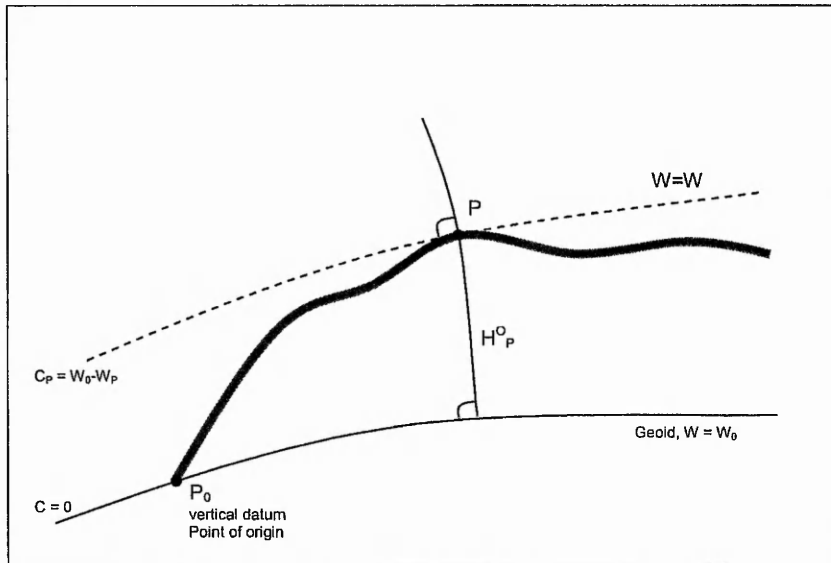


**Fig.3.2:** Definition of the orthometric height  $H^O$

To find the orthometric height with (3-5) the mean gravity,  $\bar{g}$ , along the plumb line is needed. Usually, this value cannot be measured or computed directly, because this would require complete knowledge of the mass density of the Earth's crust. Therefore, the orthometric height cannot be determined exactly, and practical computations depend on some density hypothesis (Jekeli 2000).

The separation between the reference ellipsoid with  $U = U_0$  and the HRS of the orthometric heights, the geoid, is called geoid undulation, or geoid height,  $N$ .

$$N = h - H^O \tag{3-6}$$

Orthometric height systems are realised in many European countries, for example Spain, Switzerland, Austria, France, Portugal, Denmark and the United Kingdom.

### 3.3.3 Normal heights

The normal height is a physically defined, geometrically interpretable height that avoids the need for a density hypothesis for the Earth's crust. Therefore, the Earth's gravity field is approximated by a normal gravity field,  $U$ , generated by an Earth-fitting reference ellipsoid of revolution, for example the GRS80 (Geodetic Reference System 1980). The reference

ellipsoid contains the Earth's mass and its surface is an equipotential surface,  $U_0$ , of the normal gravity potential,  $U$ , that it creates.

To find the normal height,  $H^N$ , of a point,  $P$ , a second point,  $Q$ , is created artificially.  $Q$  is situated on the normal plumb line extended downwards from  $P$ . In addition,  $Q$  fulfils the condition (2-25). The geopotential number,  $C$ , may now be expressed, using terms of the normal gravity field. With a mean normal gravity value  $\bar{\gamma}$ , we obtain:

$$H^N = \frac{W_0 - W}{\bar{\gamma}} = \frac{U_0 - U}{\bar{\gamma}} = \frac{C}{\bar{\gamma}}. \quad (3-7)$$

The mean normal gravity,  $\bar{\gamma}$ , depends on the height,  $h$  (2-20), (Torge, 2001). If the ellipsoidal height,  $h$ , is known, for example from GPS measurements, it may be used. Otherwise, some iteration is necessary:

$$H^N = \frac{C}{\gamma_0(\varphi)} \left( 1 + (1 + f + m - 2f \sin^2 \varphi) \frac{C}{a\gamma_0(\varphi)} + \left( \frac{C}{a\gamma_0(\varphi)} \right)^2 \right). \quad (3-8)$$

The normal height,  $H^N$ , now is the metric distance between  $Q$  and the reference ellipsoid  $U_0$ . (see fig.3.3). The surface that is defined by all points  $Q$  with (2-25) is called the telluroid. The metric distance between  $Q$  and  $P$  is called height anomaly,  $\zeta$ . The equation for the anomaly,  $\zeta$ , is from (3-6):

$$\zeta = h - H^N \quad (3-9)$$

If the normal heights are extended downwards from all points,  $P$ , the quasigeoid is created. It may be interpreted as the geometrical height reference surface for the normal heights. The physical height reference surface is still the geoid, with the vertical datum, where  $W=W_0$  (fig. 3.3).

Normal heights have a geometrical meaning, but the requirement for static water between points of the same metric height value,  $H^N$ , is not fulfilled theoretically. However, in contrast to the orthometric heights, no hypothesis concerning the mass density of the Earth's crust is necessary.



Some countries in Europe are using normal orthometric heights  $H^{NO}$ , as standard heights. This may be interpreted as a preliminary stage of computing the normal height. To find the normal orthometric height, the geopotential numbers,  $C$ , are approximated by the so called “normal geopotential numbers”,  $C$ , using the normal gravity. Normal orthometric heights were introduced, to avoid uneconomical gravity measurements, but because of several disadvantages, they will be replaced by physically defined height systems soon (Marti and Schlatter, 2002, Schneid and Meichle, 2005).

The new European Vertical Reference System, EVRS, is defined as a physical height system, using normal heights as metric height values. The vertical datum, of the EVRS, is taken from the MSL of the North Sea at Amsterdam (Normal Amsterdam’s Peil, NAP) and was realised in the UELN95/98.

The EVRS is geo-referenced to the ETRS89, by the co-ordinates determined in the EUVN97 (European Vertical Reference Network 1997). It is described by the UELN95/98 and the EUVN97, and is called the EVRF2000 (European Vertical Reference Frame 2000). With this, the EVRS is accessible for use with modern and economical GNSS techniques. To use GNSS for precise standard height determination – GNSS-levelling – the respective vertical datum has to be known at any point of interest. So the determination of a precise model of the vertical datum, or the HRS, is a current problem of geodesy. A precise model of the HRS would make the determination and continuation of national height networks very economical, because the traditional and currently applied methods, levelling combined with gravity measurements (3-2) is very expensive.

The following chapters of this thesis introduce the different methods of HRS determination, which have been developed and applied in recent decades. The advantages and disadvantages are discussed and an alternative concept, the Digital FEM Height Reference (DFHRS) is introduced.

## Chapter 4

### Determination and application of HRS-models

In the previous chapter, the different physically defined height types and the associated gravity field of the earth have been introduced. All these different heights refer to a well defined vertical datum, or Height Reference Surface, HRS, which at least approximately coincides with the Mean Sea Level, MSL. To find a mathematical model of the HRS would make 3-dimensional GNSS-positioning methods, such as GPS or Galileo, a very economic tool for standard height determination and the continuation of height networks.

In this chapter, different methods for computing HRS models are derived and discussed. The advantages and disadvantages of each method are described and methods to combine and to refine such models are introduced.

#### 4.1 Methods of HRS determination

The following discussion gives an overview of the most important concepts that have been applied for precise HRS determination in recent decades. The focus is on methods that use terrestrial observation data, such as gravity disturbances,  $\delta g$ , deflections from the vertical,  $\xi$  and  $\eta$ , and GNSS/Levelling points with known standard heights,  $H$ , and ellipsoidal heights,  $h$ . There are of course many other methods to determine the gravity field, for example based on space methods (e.g. Seeber, 2003), which are not subject of this thesis.

The discussion starts with methods that only use one observation type. The basics of these methods are given in short. After the introduction of these methods, two different methods of combined HRS determination are described and discussed. Finally, a new combination concept, the “Digital FEM Height Reference Surface” (DFHRS) is developed.

In the following, the separation between the HRS and the reference ellipsoid is referred to as the general anomaly,  $\zeta$ . In the case of geoid determination,  $W_0$ , the height anomaly,  $\zeta$  is identical to the geoid height,  $N$ . The standard height, is the quantity,  $H$ ,

### 4.1.1 GNSS/Levelling points

Local modelling of the HRS by means of GNSS/Levelling points is often used in practice, for example in engineering projects. This approach has the advantage, that local disturbances in the height system such as those resulting from systematic errors in the measurements, are modelled as well.

The height anomaly,  $\zeta$ , may be approximated by a local surface, for example with a second order polynomial. This reads:

$$\zeta = a_0 + a_1 \cdot x + a_2 \cdot y + a_3 \cdot x^2 + a_4 \cdot x \cdot y + a_5 \cdot y^2 \quad (4-1)$$

The unknown parameters may now be estimated by means of a least-squares adjustment of “observed” anomalies,  $\zeta$ . In some applications of this concept, an additional scale difference,  $\Delta m$ , is introduced as an additional approximation parameter.

$$\zeta = (h - H) = (a_0 + a_1 \cdot x + a_2 \cdot y + a_3 \cdot x^2 + a_4 \cdot x \cdot y + a_5 \cdot y^2) + \Delta m \cdot h. \quad (4-2)$$

The quantities,  $x$ ,  $y$  and  $h$ , in (4-1 and 4-2) are the co-ordinates of a planar ellipsoidal geodetic system (fig. 2.7).

Depending on the density and quality of the identical points, and the extension of the area of interest, for example to less than 20km x 20km the resulting accuracy of the HRS may reach centimetre level (Dinter et al. 1996).

### 4.2.1 Astrogeodetic geoid determination

Astrogeodetic geoid determination is based on astrogeodetic levelling (e.g. Heck, 2003). It uses deflections from the vertical  $\xi$  and  $\eta$  as terrestrial observations. The deflections are found with the difference between an astronomical position,  $(\Phi, \Lambda)$  and a GNSS-based position  $(\varphi, \lambda)$ , (2-28a and b).

The observed  $\xi$  and  $\eta$  may be interpreted as the difference between the actual plumb line, related to the respective equipotential surface  $W_P$ , and the normal to the level ellipsoid  $U_0$ . To

use the observed deflections of the vertical for geoid determination, they have to be reduced to the geoid level, as defined by Pizetti (Torge, 2003).

The astrogeodetic approach provides relative HRS information, or differences,  $\Delta\zeta$ . The geoid height difference between two points,  $P_1$  and  $P_2$ , may be found from

$$\Delta\zeta_{P_2,P_1} = \zeta_{P_2} - \zeta_{P_1} = \int_{P_1}^{P_2} d\zeta = - \int_{P_1}^{P_2} (\xi \cdot \cos \alpha + \eta \cdot \sin \alpha) \cdot dS = - \int_{P_1}^{P_2} \varepsilon \cdot dS, \quad (4-3)$$

where  $\alpha$  is the azimuth of  $P_2$  from  $P_1$  (fig. 2.6).

The application of astrogeodetic levelling to profiles in different directions enables the determination of local sections of the geoid, by modelling  $\Delta\zeta$  from (4-3) with a 2-dimensional function  $\Delta\zeta = \Delta\zeta(\varphi, \lambda)$ . To get the final geoid height, the resulting surface,  $\Delta\zeta(\varphi, \lambda)$ , has to be referenced, for example to a known reference point,  $P_0$ , with  $\zeta = \zeta_0$ . We finally reach:

$$\zeta(\varphi, \lambda) = \Delta\zeta(\varphi, \lambda) + \zeta_0. \quad (4-4)$$

In practical applications in areas of small extensions, (4-4) is often expanded within a planar geodetic co-ordinate system, according to (4-1). The principle relation between the deflections from the vertical and the height anomaly, (2-41 and 2-42) is then approximated by:

$$\xi = -\frac{\partial N}{\partial S_{North}} = -\frac{\partial N}{M_0(\varphi) \cdot \partial \varphi} \approx -\frac{\partial N}{\partial x} \quad (4-5)$$

$$\eta = -\frac{\partial N}{\partial S_{East}} = \frac{\partial N}{N_0(\varphi) \cdot \cos \varphi \cdot \partial \lambda} \approx -\frac{\partial N}{\partial y} \quad (4-6)$$

$M_0$  is the radius of the meridian curvature and  $N_0$  is the radius of the transverse curvature (e.g. Heck, 2003). The resulting equations, for  $\xi$  and  $\eta$ , which may be applied in a least-squares adjustment, are found by inserting (4-5 and 4-6) into (4-1)

$$\xi \approx -a_1 - 2a_3x - a_4y \quad (4-7)$$

$$\eta \approx -a_2 - a_4x - 2a_5y \quad (4-8)$$

It is of course possible to use a more complex function, for example a spherical harmonic expansion of the anomalous gravity potential, rather than a second order polynomial. The principle however stays the same.

Astrogeodetic HRS determination is becoming more important in recent years. The advent of modern automated observation techniques that make use of methods from digital image processing, has made this method more economic (Hirt and Bürki, 2002).

#### 4.2.2 Gravimetric geoid determination

The gravimetric method is the most important method for national, regional or continental HRS computation. This is because the density of GNSS/Levelling points or astrogeodetic points is very sparse. And the densification of the existing networks to reach the necessary accuracy of HRS models derived from such points, would last decades and also is very uneconomic.

On the other hand, gravity measurements are very simple to handle, and the geo-referencing of such measurement may easily be done by GNSS-techniques in an appropriate accuracy. The first order height network of Baden-Württemberg, a federal state in Southern Germany, for example, contains 131 points precise GNSS/Levelling. In contrast, the gravity network contains more than 10000 points. On the other hand, the information about the geoid, contained in one single gravity observation, is nearly zero.

However, the methods of (quasi-)geoid determination, which have been developed and applied in recent decades, are obviously good enough, to derive HRS models with relative accuracies reaching centimetre level.

The computational method that has been applied within any project of precise geoid determination in the last years is the so-called "Remove-Restore-Technique", RRT. Fundamental literature concerning this topic is given for example with (Denker et. al.1986; Denker, 1994; Torge, 2003; Hofmann-Wellenhof and Moritz, 2005).

The computation of the height anomaly,  $\zeta$ , from gravity disturbances,  $\delta g$ , by means of integral equations (2-38), theoretically requires observations all over the earth. In most applications, gravity data are only available over limited areas. To keep the integration radius small, the anomalies,  $\zeta$ , are therefore computed with respect to a global potential model, GPM, usually represented by spherical harmonic coefficients. Such models are for example the EGM96 (Lemoine et. al., 1996), the GPM98CR (Wenzel, 1999) or the EIGEN04 (GFZ, 2007).

For the computation, the observed gravity disturbances  $\delta g$  are reduced from the long-waved parts by subtracting computed gravity anomaly from a GPM,  $\delta g_{GPM}$  (2-50c). Short-waved gravity anomaly reduction are made using data from a high resolution residual terrain model  $\delta g_{RTM}$

$$\delta g_{res} = \delta g - \delta g_{GPM} - \delta g_{RTM} . \quad (4-9)$$

In practical computations, planar approximations are accepted and the equation for  $\delta g_{RTM}$  reduces to

$$\delta g_{RTM} = 2\pi G\rho(h - h_{DTM}) - c_Q \quad (4-10)$$

The height  $h_{DTM}$  may be taken from a smooth global digital terrain model, and the quantity  $c_Q$  is the terrain correction (Moritz, 1980; Hofmann-Wellenhof and Moritz, 2005).

The method of point mass modelling also makes use of the heights of identical points,  $h$  and  $H$ . The difference between ellipsoidal height,  $h$  and the orthometric height,  $H$  is then treated as a direct observation,  $\zeta$ , for the height anomaly and is also reduced

$$\zeta_{res} = \zeta_G - \zeta_{GPM} - \zeta_{RTM} . \quad (4-11)$$

$\zeta_{GPM}$  contains the long-wave information from the applied global gravity potential model. It is found from (2-49).  $\zeta_{RTM}$  contains the short-wave information derived from a high resolution residual terrain model. The equation for  $\zeta_{RTM}$  for a planar approximation is:

$$\zeta_{RTM} = \frac{\rho}{\gamma} \iint_{-\infty-\infty}^{\infty} \frac{(h - h_{DTM})}{D} dx dy \quad (4-12)$$

Besides terrestrial observations of gravity, additional data sources related to the gravity field are necessary for the determination of regional geoid models. These data sources may be airborne gravimetry, marine gravimetry, satellite altimetry, satellite to satellite tracking (SST) and satellite gravity gradiometry. (Seeber, 2003)

In the next step, the resulting residual gravity disturbances,  $\delta g_{res}$ , are transformed into residual geoid heights. In a first step, the residual anomalous gravity potential  $T_{res}$ , has to be determined. The height anomaly,  $\zeta$ , is then found by the application of Bruns' formula (2-26). The different methods for gravimetric (quasi)geoid determination applying the RRT mainly differ in the way that the residual anomalous gravity potential,  $T_{res}$ , is modelled. Over the years, several modifications of Stokes', or Hotine-Koch's formula, respectively, have been derived and applied. Comparisons of some methods are given in (Omang and Forsberg, 2002; Agren, 2004).

After the computation of residual height anomalies,  $\zeta_{res}$ , from the residual gravity disturbances,  $\delta g_{res}$ , and the complete height anomaly is found from the following summation.

$$\zeta = \zeta_{GPM} + \zeta_{res} + \zeta_{RTM} \quad (4-13)$$

For the concepts based on the solution of the boundary value problem the estimator for the height anomaly becomes

$$\zeta = \frac{R}{4\pi\gamma} \iint_{\sigma} K(\psi) \cdot (\delta g - \delta g_{GPM} + c_Q - 2\pi G\rho(h - h_{DTM})) d\sigma + \zeta_{GPM} + \zeta_{RTM} \quad (4-14)$$

(Sjöberg, 2005). There are several kinds to apply the RRT. The method described above is called the "RTM-method". It is definitely the most used concept in Europe, as it is compatible with the system of normal heights. The other concept that may be applied, is "Helmert's second condensation approach" (Hofmann-Wellenhof and Moritz, 2005; Torge 2003; Sjöberg, 2005)

As mentioned before, the method of point mass modelling enables the application of least squares techniques (chapter 2.3.2). The reduced observations from (4-9) and (4-11) may be set up into a common adjustment with the following observation equations:

$$\zeta_{res} + v = \frac{G}{\gamma} \sum_{k=1}^{k_{Max}} \frac{m_k}{l_k} \quad (4-15)$$

$$\delta g_{res} + v = G \sum_{ki=1}^{k_{Max}} \frac{m_k (h_p - h_k)}{l_k^3} \quad (4-16)$$

The final height anomaly,  $\zeta$ , is in analogy to the BVP concept (4-13) found by summation.

Gravimetric (quasi)geoid models, derived by the RTM method (4-14), such as the EGG97 (European Gravimetric Quasigeoid 1997) (Denker and Torge, 1997), are reaching centimetre-accuracy in their short-waved parts. To give a representation of the respective HRS and to reduce long-waved errors, the model is usually fitted to a number of points where  $h$  and  $H$  are known. Such long-wave effects result from two sources. First the GPM that is used in the RRT described above. Older models, like the EGM96 (Lemoine et. al. 1996) suffer from long-wave errors, resulting from a sparse distribution of observations. It is expected, that the results of current satellite missions, like CHAMP and GRACE, both SST missions, or upcoming satellite gravity gradiometry missions, for example GOCE, will improve the global models and with this their long-wave accuracy will increase (Torge, 2003). Additional effects are caused by so-called weak-shapes (Jäger, 1988), which are the sum of the principal long-waved stochastical parts, which in return are related to the maximum eigenvectors of the covariance matrix as carrier functions, in extended networks where one or several dominant eigenvalues  $\lambda_i$  occur. There are two types of effect, the natural weak shapes and the effect arising because of neglected correlations in the stochastical model. These error sources will remain, even after incorporating data from new satellite missions.

### 4.3 Height determination using GPS and HRS models

In the past, several HRS, mostly gravimetrical geoid models, with a relative accuracy better than 1-5 cm, for example the EGG97 (Denker and Torge 1997) and OSGM02 (Forsberg et. al. 2002) have been computed. These models give the height of the HRS,  $\zeta$ , as a function of a position  $\zeta = \zeta(\varphi, \lambda)$ , to get the standard height  $H$ .

In practice, however, the well known formula (Torge, 2003)

$$H = h - \zeta(\varphi, \lambda) \quad (4-17)$$

does not hold (Fig. 3.2). The main reason for this is that gravity field models suffer from long-waved systematic errors,  $\Delta T$ .

Error sources in such geoid models maybe listed as (Torge and Denker 1999)

- Long-waved errors in the global model, such as EGM96, used in the RRT
- Errors in the terrestrial gravity observations,  $g$ , as sum of errors in the gravity measurement and the gravity reduction
- Errors in the anomalies, found by transforming observations from satellite altimetry,
- Errors in digital terrain models used in the RRT
- Errors in the reduction to unified reference systems
- Approximations in the algorithms used.

These errors appear as “local datum effects” in the derivatives, for example in the height anomaly, as a systematic error  $\Delta T_\zeta$ .

These effects can only be modelled with identical points of known height,  $h$  and  $H$ , by changing (3-26) into:

$$H = h - \zeta'(\varphi, \lambda) + \Delta T_\zeta(\mathbf{d}) . \quad (4-18)$$

There will be numerical problems when modelling in small areas because only heights can be used for the estimation of  $\Delta T_\zeta(\mathbf{d})$ , for example, when modelling three translations ( $u, v, w$ ) as:

$$\Delta T_\zeta(\mathbf{d}) = \cos(\varphi) \cdot \cos(\lambda) \cdot u + \cos(\varphi) \cdot \sin(\lambda) \cdot v + \sin(\varphi) \cdot w, \quad (4-19)$$

with

$$\mathbf{d} = [u \quad v \quad w]$$

For areas with small extensions, a simple offset  $c$  and two rotations  $e_x$  and  $e_y$  are modelled

$$\begin{aligned} \Delta T_\zeta(\mathbf{d}) = c + [e^2 \cdot N(\varphi) \cdot \sin(\varphi) \cdot \cos(\varphi) \cdot \sin(\lambda)] \cdot \varepsilon_x \\ + [-e^2 \cdot N(\varphi) \cdot \sin(\varphi) \cdot \cos(\varphi) \cdot \cos(\lambda)] \cdot \varepsilon_y, \end{aligned} \quad (4-20)$$

where

$$\mathbf{d} = [c \quad \varepsilon_x \quad \varepsilon_y]$$

The approach (4-18), with  $\Delta T_\zeta(\mathbf{d})$  modelled by (4-20), holds, if height anomalies,  $\zeta$ , from a suitable geoid model, are available. The resulting accuracy may reach centimetre level in areas less than 20 km across and with a suitable number of identical points.

In larger areas, and if a suitable number of identical points are available, this additional information may be used to model geoid “refinements”. The area of interest may be subdivided into a number of meshes in which, in addition to the transition parameters  $\Delta T_\zeta(\mathbf{d})$ , a so-called “geoid-refinement”  $R_{FEM}(\mathbf{p})$  may be modelled. The refinement may be modelled as a difference surface, using coefficients,  $\mathbf{p}$ , of a bivariate polynomial

$$R_{FEM}(\mathbf{p}) = a_{00} + a_{10}x + a_{01}y + a_{20}x^2 + a_{11}xy + a_{02}y^2. \quad (4-21)$$

The system of observation equations for the geoid-refinement approach is:

$$H + v = H \quad (4-22a)$$

$$h + v = H + \Delta m \cdot h + \zeta(\varphi, \lambda) \quad (4-22b)$$

$$\zeta'(\varphi, \lambda) + v = \zeta(\varphi, \lambda) + R_{FEM}(\mathbf{p}) + \Delta T_\zeta(\mathbf{d}) \quad (4-22c)$$

$$0 + v = C(\mathbf{p}). \quad (4-22d)$$

In (4-22c) the height anomaly  $\zeta'(\varphi, \lambda)$  from a gravimetric geoid model is used as an observation. With (4-22d) a set of continuous conditions  $C(\mathbf{p})$  at the common border of two neighbouring meshes may be introduced. The “geoid-refinement” approach is often used in practice, for example the software package HEIDI2©Dinter/Ilner/Jäger (Dinter et al. 1996). The results show centimetre-accuracies or better, even in areas greater than 100 km across (Dinter et al. 1996).

Besides the method described above, which is based on Finite Element Modelling (FEM), least squares collocation has successfully been used to adapt a gravimetrical geoid model at identical points (Grote 1996, Forsberg 1998, Smith and Roman, 2001). In this concept, the error  $\Delta T_\zeta(\varphi, \lambda)$  at a position,  $(\varphi, \lambda)$ , is split into three components: a trend,  $t$ , a signal,  $s$  and a remaining noise,  $n$ . This reads as:

$$\begin{aligned}\Delta T_{\zeta}(\varphi, \lambda) &= \Delta T_{\zeta} \\ &= t + s + n\end{aligned}\tag{4-23}$$

Methods that are based on a stochastic process, such as collocation, may only be applied to residual quantities. Therefore, in a first step, the trend component,  $t$ , is removed by a parametric model, such as (4-19).

$$\Delta T_r = \Delta T_{\zeta} - t\tag{4-24a}$$

$$= \Delta T_{\zeta} - (\cos(\varphi) \cdot \cos(\lambda) \cdot u + \cos(\varphi) \cdot \sin(\lambda) \cdot v + \sin(\varphi) \cdot z)\tag{4-24b}$$

The respective coefficients,  $(u, v, z)$ , may be found by least-squares estimation.

In the second step a signal,  $s$ , at a position  $(\phi, \lambda)$  may be estimated from the vector of remaining residuals,  $\Delta \mathbf{T}_r$ , at the identical points. This reads as:

$$s = \mathbf{c}_{sr}^T (\mathbf{C}_{\Delta T_{\zeta}} + \mathbf{C}_{\Delta T_r})^{-1} \Delta \mathbf{T}_r.\tag{4-25}$$

The vector  $\mathbf{c}_{sr}$  contains the correlation between the points used and the computational point  $(\phi, \lambda)$ . The matrices  $\mathbf{C}_{\Delta T_{\zeta}}$  and  $\mathbf{C}_{\Delta T_r}$  are the covariance matrices of  $\Delta \mathbf{T}_{\zeta}$  and  $\Delta \mathbf{T}_r$ , respectively. As the correlations  $\mathbf{c}_{sr}$  are never known, they are estimated from an appropriate covariance function, for example a second order Markov model.

$$c(d) = \sigma_0 \left( 1 + \frac{d}{\alpha} \right) \cdot e^{-\frac{d}{\alpha}},\tag{4-26}$$

where the quantity,  $d$ , denotes the distance and the quantity,  $\alpha$ , is the correlation length. In contrast to a parametric model, such as the aforementioned geoid-refinement approach, the collocation method is not unbiased with respect to the stochastic model. The choice of the covariance function (4-26) affects the result systematically. However, collocation has been applied in many projects, and several investigations have shown, the these effects are rather small (e.g. Marti, 1998)

#### 4.4 Discussion of methods

The gravimetric (quasi)geoid determination based on the solution of the GBVP requires, theoretically, the fulfilment of three conditions:

1. Origin, orientation of the axes, mass and potential of geoid and level ellipsoid are all the same
2. The whole mass of the earth is situated within the geoid
3. The gravity potential is known all over the earth's surface.

In practice only the first condition is fulfilled. Several approximations in the algorithms are accepted to make the classical approach (3-14) accessible to modern and fast techniques of computation. Gravity information for remote areas is usually taken from global gravity potential models, such as the EGM96 (Lemoine et.al., 1998) or the GPM98CR (Wenzel, 1999).

For practical applications, the terrestrial gravimetric observations are easy to manage. The height information about a measured gravity point is not necessary for centimetre accuracy solutions so may be taken from less accurate digital terrain models (DTM). On the other hand the algorithms for reducing the gravity observations and processing the data for a gravimetric geoid model are rather complex.

Gravimetric geoid determination is usually applied where a national a continental geoid model is required and significant gravity data exists. Modern gravimetric geoid models such as the EGG97 show relative short-wave accuracy down to centimetre-level. On the other hand, systematic errors in the long-wave domain occur because of errors in the remote gravity data and appear as errors due to the so-called "weak-forms" described above. Such systematic errors may be eliminated either by means of parametric models (Fotopolous, 2003; Fotopolous et. al. 2002; Dinter et. al. 1996) or by means of collocation (Smith and Roman, 2001; Denker et. al. 2000).

Geoid models derived from point mass modelling (Claessens et. al. 2001; Antunes et. al. 2003 and Liebsch et. al. 2006) are reaching better accuracy in their long-waved parts. The use of identical points makes this approach less dependent on gravity information from remote areas. However, the short-waved quality of those geoid models depends on the number of modelled point masses. If the masses are placed too close to the earth's surface, the resulting geoid model will suffer from unrealistic oscillation effects.

The latest geoid for Germany, the German Combined QuasiGeoid 2005, GCG05, is a combination of both approaches (Liebsch et. al. 2006). Two independent solutions have been determined, both based on RRT. One solution was computed at the Bundesamt für Kartographie und Geodäsie, BKG, in Frankfurt. It is based on the point mass concept. The second solution was computed at the Institute für Erdmessung, IfE, at the University of Hannover. It is based on integration and collocation. The solutions agreed with a standard deviation of 5mm. The maximum difference of 6 centimetres is situated in the Alps. The final model was found by averaging both solutions.

In contrast to the gravimetric method described above, one advantage of astrogeodetic geoid determination is that there is no need to have data from remote locations. Height information related to observed points is only necessary for the reduction for the plumb line curvature, and therefore may be taken from a DTM. On the other hand, the density of existing astrogeodetic measurements is usually very sparse, because of the time it takes to make each observation. Only for a small number of regions in Europe will there be an average distance between the stations of less than 10-20 km.

The resulting accuracy of the computed astrogeodetic geoid model depends on the density of measurements of vertical deflections, on the quality of the interpolation of the vertical deflections and the reductions used in the computations.

In closed areas, especially in mountainous regions, astrogeodetic deflections of the vertical define the local geoid better than local gravity observations, because vertical deflections may be observed directly.

Therefore, for local applications, astrogeodetic geoid determination will lead to precise solutions in a more economical way than the gravimetric solution.

The GPS/levelling point method is by far the simplest method of deriving a local geoid model, but it depends on the quality of the known heights and the density of the identical points. If the resulting accuracy of a standard height,  $H$ , reaches the order of one centimetre,

levelling becomes a very time-consuming process. The determination of GNSS-based ellipsoidal height,  $h$ , with a compatible accuracy would require a measurement period of greater than 12 hours and a rigorous computation, for example with the Bernese GPS-Software. If this effort is acceptable, or if good height data are available, the GPS/levelling point method is an economical way to compute a local model of the HRS such as GPS based height determination.

The actual methods of combining geoid models with GPS measurements are concerned with fitting an existing geoid model, gravimetric or astrogeodetic, to identical points, where the HRS is known, using the relationship between  $h$  and  $H$  (4-17). Long-waved systematic errors are eliminated by means of modelling a trend function  $\Delta T_{\zeta}(\mathbf{d})$  either by least-squares collocation or by FEM techniques.

Each of the above approaches is sufficient for a specific application, and therefore each one is justified. However, none of them are sufficient for application in GNSS-based online height determination, which we wish to use to replace the uneconomical traditional methods of standard height determination by levelling.

The reason for this is that the methods of combining GPS height with geoid models are typically in post-processing applications. The estimated trend or datum parameters,  $\Delta T_{\zeta}(\mathbf{d})$ , are only valid in the area close to the identical points. Datum or trend extrapolation would lead to significant discrepancies in the resulting computed standard heights. Only the direct conversion of ellipsoidal heights to standard heights, without loss of accuracy, would make GNSS-techniques an economical way to determine heights other than by levelling.

In the following chapter, a new method for the combined adjustment of HRS related observations, GNSS/Levelling points,  $h$  and  $H$ , deflections from the vertical,  $\xi$  and  $\eta$ , gravity observations,  $g$ , and existing HRS-models,  $\zeta$ , is introduced. It is based on the mathematical concept of finite element modelling, FEM, and therefore called the Digital FEM Height Reference Surface.

## Chapter 5

### The Concept of the Digital FEM Height Reference Surface DFHRS

In chapter 4, different methods used to compute a HRS were presented. The mentioned methods to combine a model with GNSS/Levelling points, as in section 3.5, are all based on an existing, mostly gravimetric (quasi-) geoid model. By means of different algorithms, like least squares collocation or FEM-techniques, a kind of “refinement” or “fitting” is determined, which is added to the existing model. In (Fotopolous, G. et al. 2003; Fotopolous, G. 2003) a corrector surface is estimated by means of least squares techniques in a similar way. Several parametric models, based on the parameterisation of a similarity transformation as well as polynomial surfaces are generated to correct a gravimetric geoid model to fit to a number of reference points with heights,  $h$  and  $H$ .

The aforementioned approaches are definitely suitable to eliminate long-waved errors in regional or local (quasi-) geoid determination. But nevertheless, approaches which combine all different information of the HRS in one unique model of the HRS are to be preferred.

In the following chapter, the concept of the Digital FEM Height Reference Surface, DFHRS, is presented. The DFHRS concept dates back to Jäger (1998, 1999). The DFHRS-research project at the University of Technology in Karlsruhe was funded from 2000-2002 by the Bundesministerium für Bildung und Forschung (BMBF).

The DFHRS concept enables the common adjustment of all HRS-related observations in a continuous HRS.

According to the concept of the FEM, (Finite Element Method), the area over which a HRS is to be computed is subdivided into a grid of meshes (fig.5.1). In this way, the HRS is modelled meshwise as a continuous surface over the whole area by a FEM, a potential series for each single mesh. The meshwise representation follows the idea of representing the height anomaly or geoid-height at a position,  $\zeta(\phi, \lambda)$ , as a 2D-Taylor series with respect to the centre,  $P(\phi_0, \lambda_0)$ , of each mesh. This reads as:

$$\zeta(\varphi, \lambda) = \left( \sum_{i=0}^{\infty} \left( \frac{\partial}{\partial X} x + \frac{\partial}{\partial Y} y \right)^i \cdot \frac{\zeta(X, Y)}{i!} \right)_{X_0, Y_0} \quad (5-1)$$

Where  $x = X - X_0$ ;  $y = Y - Y_0$

X and Y are the plan co-ordinates in an arbitrary cartesian projection, for example the Lambert-projection.  $X = X(\varphi, \lambda)$ ;  $Y = Y(\varphi, \lambda)$ .

By transformation of the Taylor-series, we find:

$$\begin{aligned} \zeta(X, Y) &= a_{00} + a_{10}x + a_{01}y + a_{20}x^2 + a_{11}xy + a_{02}y^2 + \dots \\ &= \sum_{i=0}^{\infty} \sum_{j=0}^{\infty} a_{i,j} x^i y^j. \end{aligned} \quad (5-2)$$

A derivation up to degree n leads to the bivariate polynomial:

$$\zeta_{FEM}(X, Y | \mathbf{p}) = \sum_{i=0}^n \sum_{j=0}^{n-i} a_{i,j} x^i y^j = \mathbf{f}^T \cdot \mathbf{p}. \quad (5-3)$$

With

$$\begin{aligned} \mathbf{f}^T &= [1 \quad y \quad x \quad y^2 \quad xy \quad x^2 \dots] \text{ and} \\ \mathbf{p}^T &= [a_{00} \quad a_{01} \quad a_{10} \dots]. \end{aligned}$$

Potential series converge absolutely in their area of application and are differentiable arbitrarily often. So the HRS in a single FEM-mesh is described by a bivariate polynomial of n-th degree, and with that, it is differentiable n-times in each mesh. For an HRS to be continuous it has to be, that its representation as an FEM-surface is differentiable at all points.

## 5.1 The system of observation equations

With equation (5-3) an expression for the HRS, which is accessible for the methods of a least squares adjustment is found. Any HRS related information/observation might be introduced.

These are:

- Points with known heights in the standard system,  $H$ , and ellipsoidal heights,  $h$
- Gravimetric (Quasi-)geoid heights,  $\zeta_{\text{grav}}$
- Deflections from the Vertical ( $\xi, \eta$ )
- Gravity anomalies,  $\Delta g$ , and/or gravity disturbances,  $\delta g$ , respectively.

In the following the derivation of the listed observation equations are derived.

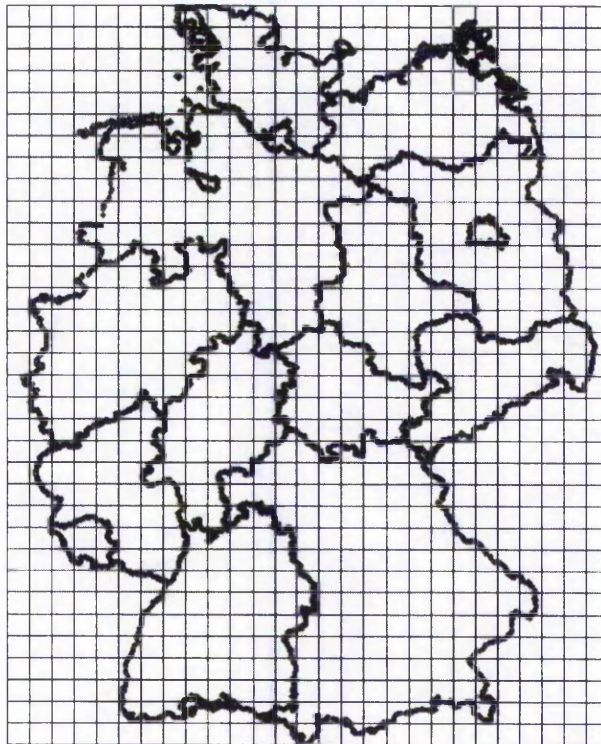


**Fig. 5.1:** Sketch of a DFHRS FEM meshing. The whole area of interest, here Germany with its federal states, is subdivided into FEM meshes.

### 5.1.1 Identical points (h, H)

In chapter 4 the method of geoid determination using GNSS/levelling points is described. The difference between a GNSS-based height,  $h$ , and a standard height,  $H$ , is treated as a discrete observation of the height anomaly,  $\zeta_P = h_P - H_P$ , at a point,  $P$ . The accuracy of the anomaly,  $\zeta_P$ , depends on the quality of the GNSS height,  $h_P$ , and of the standard height,  $H_P$ . If centimetre accuracy is strived for, especially the determination of the standard height will become a very time expensive procedure.

In practice the adjustment of a levelling network is the first step required to create a height reference system. A recent example is the European Vertical Reference Frame 2000 (EVRF2000). At all EVRF2000 points  $P$ , 3-dimensional co-ordinates, related to the ETRS89, were derived. In addition the geopotential numbers  $C_P$  and the normal heights,  $H_P^N$ , are provided. (BKG, 2003). The EVRF2000 was endorsed as realisation of the EVRS by the IAG-Subcommision for Europe (EUREF). A new European quasigeoid model, or in general, a Height Reference Surface, HRS, has to be consistent with the EVRS.

Hence, the points from the EVRF2000, as one group of observations, are the reference for any additional observation group and for modelling the long-waved systematic errors and the weak-form in gravimetric geoid models.

$$H_{obs} + v = \hat{H} \quad (5-4)$$

$$h^j + v = \hat{H} + \Delta m^j \cdot h + \zeta_{FEM}(\varphi, \lambda | \mathbf{p}) \quad (5-5)$$

The superscript  $j$  designates a certain observation group of ellipsoidal heights,  $h$ , used to determine the respective scale correction,  $\Delta m$ . This correction may be interpreted as a topography-based correction of the HRS.

As  $\Delta m$  can differ from area to area, a number of scale corrections  $\Delta m$  may be estimated.  $\Delta m$  may also be modelled as a function

$$\begin{aligned} \Delta m &= \Delta m(\varphi, \lambda) \\ &= \Delta m_0 + \Delta m_1 \cdot \varphi + \Delta m_2 \cdot \frac{\lambda}{\cos(\varphi)} \end{aligned} \quad (5-5a)$$

### 5.1.2 Existing (quasi-) geoid models alone and in combination

Using complete (quasi)geoid models instead of the original gravity observations has practical benefits and leads to the same results. The use of gravimetric height anomalies  $\zeta_{\text{grav}}$  is to be interpreted as the second step of a 2-step adjustment (Jäger, 2002; Jäger and Schneid, 2002). In step one, the processing of the gravity disturbances  $\delta g$  is undertaken, e.g. by means of the Hotine-Koch formula (2-36):

$$\zeta = \frac{R}{4\pi\gamma_0} \iint_{\sigma} K(\psi) \left( \delta g - \frac{\partial \delta g}{\partial h} (h - h_p) \right) \cdot d\sigma. \quad (5-6)$$

This classical problem of the determination of gravimetric height anomalies,  $\zeta_{\text{grav}}$ , may be written in for the cases of the minimum number of observations and more than the minimum number of observations as:

$$E\{\zeta_{\text{grav}}\} = \mathbf{A}_{\text{grav}} \cdot \Delta g. \quad (5-7)$$

The least squares result reads

$$\zeta_{\text{grav}} = (\mathbf{A}_{\text{grav}}^T \cdot \mathbf{C}_{\Delta g}^{-1} \cdot \mathbf{A}_{\text{grav}})^{-1} \cdot \mathbf{A}_{\text{grav}}^T \cdot \mathbf{C}_{\Delta g}^{-1} \Delta g \quad (5-8)$$

with the stochastic model

$$\mathbf{C}_{\zeta_{\text{grav}}} = (\mathbf{A}_{\text{grav}}^T \cdot \mathbf{C}_{\Delta g}^{-1} \cdot \mathbf{A}_{\text{grav}})^{-1} \quad (5-9)$$

with  $\mathbf{A}_{\text{grav}}$  and  $\mathbf{C}_{\Delta g}$  as the respective design and covariance matrices are introduced.

In step two, the resulting gravimetric height anomalies,  $\zeta_{\text{grav}}$ , are introduced into the DFHRS computation as discrete observation,  $\zeta(\phi, \lambda)$ , as follows:

$$\zeta_{\text{grav}}(\varphi, \lambda)^j + v = \zeta_{\text{FEM}}(\varphi, \lambda | \mathbf{p}) + \Delta T_{\zeta}(\mathbf{d})^j. \quad (5-10)$$

To reduce the effect of the long-wave and systematic errors of the gravimetric geoid models as well as those of the standard height system (Dinter et. al., 1997), the mathematical model of the DFHRS concept allows subdividing any geoid model that is used into a number of so-called “geoid-patches”.

The good short-wave quality of applied gravimetric geoid models allows the introduction of the models “by the piece”. To provide the optimum height anomaly,  $\zeta(\phi, \lambda)$ , the surface of the computed model has to be identical to the reference surface of the respective standard height system. A correction  $\Delta T_{\zeta}(\mathbf{d})$  may be found using (4-19, 4-20).

### 5.1.3 Deflections from the vertical ( $\eta, \xi$ )

The observation of astronomical deflections from the vertical was very time consuming and therefore expensive in the past, but in recent years several approaches to get the deflections by means of procedures from image processing have been developed (Breach 2002, Hirt and Bürki, 2002). Astronomical deflections are an additional observation group, independent from gravimetric geoid models and gravity observations. The observation equation in the DFHRS adjustment reads (cf. 3-22)

$$\xi^j = -\frac{\partial \zeta_{FEM}(\varphi, \lambda | \mathbf{p})}{M(\varphi) \cdot \partial \varphi} + \Delta T_{\xi}(\mathbf{d})^j \quad (5-11)$$

and (5-12)

$$\eta^j = -\frac{\partial \zeta_{FEM}(\varphi, \lambda | \mathbf{p})}{N(\varphi) \cdot \cos \varphi \cdot \partial \lambda} + \Delta T_{\eta}(\mathbf{d})^j$$

$M(\phi)$  and  $N(\phi)$  denote the radius of meridian and normal curvature at the latitude,  $\varphi$ , respectively. With  $\Delta T_{\xi}(\mathbf{d})$  and  $\Delta T_{\eta}(\mathbf{d})$  a set of datum parameters is introduced, to model either a datum transition for deflections that refer to another geodetic datum, or local effects that come from systematic error sources, for example if the deflections were derived from a gravity potential model. A parametric model for the local datum-shift, that is compatible with (4-19), for the deflections from the vertical,  $\Delta T_{\xi}$  and  $\Delta T_{\eta}$ , may be found by consideration of the definition of  $\xi$  and  $\eta$ , (5-11 and 5-12) with

$$\Delta T_{\xi}(\mathbf{d})^j = -\frac{1}{M(\varphi)} \cdot \frac{\partial \Delta T_{\xi}(\mathbf{d})^j}{\partial \varphi} \quad (5-13a)$$

and

$$\Delta T_{\eta}(\mathbf{d})^j = -\frac{1}{N(\varphi)} \cdot \frac{\partial \Delta T_{\xi}(\mathbf{d})^j}{\cos \varphi \cdot \partial \lambda} \quad (5-13b)$$

By introducing (5-13a and b) into (4-19), we obtain

$$\Delta T_{\xi}(\mathbf{d})^j = \begin{bmatrix} \frac{-\cos(\lambda) \cdot \sin(\varphi)}{M(\varphi)} & \frac{-\sin(\lambda) \cdot \sin(\varphi)}{M(\varphi)} & \frac{-\cos(\varphi)}{M(\varphi)} \end{bmatrix} \cdot \mathbf{d} \quad (5-14a)$$

And

$$\Delta T_{\eta}(\mathbf{d})^j = \begin{bmatrix} \frac{-\sin(\lambda)}{N(\varphi)} & \frac{-\cos(\lambda)}{N(\varphi)} & \mathbf{0} \end{bmatrix} \cdot \mathbf{d} \quad (5-14b)$$

The parameterisation of  $\Delta T_{\xi}$  and  $\Delta T_{\eta}$  for a 6-parameter datum transition is described in (5-2 and 5-3). With  $N(\varphi)$  and  $M(\varphi)$  the radius of normal curvature and the radius of meridian curvature are introduced,  $W = \frac{a}{N(\varphi)}$ , and  $\mathbf{d}^T = [u \quad v \quad w]$ . The index,  $j$ , points to different observation groups.

#### 5.1.4 Gravity disturbances $\delta g$

The use of a correlated (quasi-)geoid model leads a strict two step adjustment (Jäger 2002; Jäger and Schneid 2002). So the use of gravity disturbances,  $\delta g$ , is only necessary, if those observations were not used in the determination of the applied (quasi)geoid model.

But as gravity observations,  $g$ , are carrying most of the medium- and short-waved information of the earths' gravity field and the concept of the Finite Elements allows us to introduce any HRS-related observation, it is one more possible observation group in the common least squares adjustment.

The anomalous gravity potential,  $T$ , may be represented by the coefficients,  $\mathbf{A}$  and  $\mathbf{B}$ , of a harmonic function,  $f$ . This reads as:

$$T = f(\mathbf{A}, \mathbf{B}) \quad (5-15)$$

In analogy, the gravity disturbances,  $\delta g$ , may be represented by the same set of coefficients,  $\mathbf{A}$  and  $\mathbf{B}$ , applying the harmonic function,  $g$ . This reads as:

$$\delta g = g(\mathbf{A}, \mathbf{B}) \quad (5-16a)$$

The equations (5-15 and 5-16a) only hold, if the function,  $g$ , is related to the function,  $f$ , by

$$g(\mathbf{A}, \mathbf{B}) = -\frac{\partial}{\partial h} f(\mathbf{A}, \mathbf{B}), \quad (5-16b)$$

see (2-31a). The coefficients,  $\mathbf{A}$  and  $\mathbf{B}$ , are to be treated as auxiliary parameters in the least-squares estimation of the actual DFHRS-parameters,  $\mathbf{p}$ . Therefore, they could be eliminated in a later step.

To link the harmonic coefficients  $\mathbf{A}$  and  $\mathbf{B}$ , to the DFHRS parameters,  $\mathbf{p}$ , one set of condition equations has to be introduced. For the gravity disturbances we have the final observation equation

$$\delta g + v = g(\mathbf{A}, \mathbf{B}). \quad (5-17a)$$

The condition equation is found by applying Bruns' theorem (2-24)

$$0 + v = \zeta_{FEM}(\varphi, \lambda | \mathbf{p}) - \frac{1}{\gamma} f(\mathbf{A}, \mathbf{B}) \quad (5-17b)$$

The coefficients,  $\mathbf{A}$  and  $\mathbf{B}$ , may be the coefficients of any harmonic function, such as Fourier series or spherical harmonic series [chapter 2]. In the frame of this research, coefficients have been applied, that may represent a harmonic function over the area of a spherical cap. This approach has been introduced by (Haines, 1985) and successfully been applied in several geophysical projects (Korte, 1999; Amm and Viljanen, 1999; Amm, 1998; Kotze, 2001; Hwang and Chen 1997) and already in a geodetic project (Jiancheng et al. 1995). The theory of such "Spherical Cap Harmonics, SCH" is the topic of chapter 6.

## 5.2 Derivation of continuity conditions

To make sure, that the resulting FEM-surface of  $n$ -th degree is differentiable  $n$ -times at any point of the surface, additional continuity conditions need to be introduced at common borders of neighbouring meshes (Dinter et. a. 1996).

The approximate quality of the resulting FEM surface should be in the order of better than 1 cm. The continuity at a common border of neighbouring meshes should be of a compatible quality.

The modelling of strict continuous conditions requires the dimensions of the matrix of normal equations to be increased. Forcing complete continuity on a FEM grid of  $n$ -meshes carried by polynomials would have the same effect as representing the whole area by only one polynomial. Because of the reasons mentioned, the continuity is modelled by introducing pseudo-observations into the common least squares adjustment in chapter 4.1.

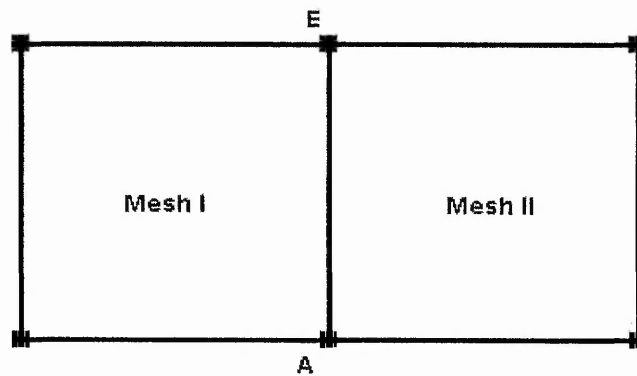


**Fig. 5.2:** Scheme of two neighbouring meshes, I and II, where a continuous transition at the common border straight line AE has to be forced

The modelling of the continuity conditions for  $C_0$ -continuity forces the same functional value at the common border straight line and is described in the following.

With  $x^I$  and  $x^{II}$  we denote two independent point positions, situated on a HRS, on the common border of two neighbouring meshes, mesh I and in mesh II. This reads:

$$x^I = \begin{bmatrix} x \\ y \\ \zeta^I(x,y) \end{bmatrix} = \begin{bmatrix} x \\ y \\ \sum_{i=0}^n \sum_{k=0}^{n-i} a_{i,k}^I \cdot x^i y^k \end{bmatrix} \quad \text{and} \quad x^{II} = \begin{bmatrix} x \\ y \\ \zeta^{II}(x,y) \end{bmatrix} = \begin{bmatrix} x \\ y \\ \sum_{i=0}^n \sum_{k=0}^{n-i} a_{i,k}^{II} \cdot x^i y^k \end{bmatrix} \quad (5-18)$$

According to the DFHRS concept the "z-component" is replaced by the polynomial function  $\zeta(x,y)$  of the bivariate polynomial  $a_{ik}$  as a function of the plan position  $(x,y)$ . Both independent surface points are introduced by (5-18) are now restricted to run along the common border straight line AE (fig. 5.2) of both meshes.

For this reason, the next step requires a description of the straight line, AE, in its parametric expression for both meshes I and II and we get (Dinter et. a. 1996):

$$x^I = \begin{bmatrix} x_a + t(x_e - x_a) \\ y_a + t(y_e - y_a) \\ \sum_{i=0}^n \sum_{k=0}^{n-i} a_{i,k}^I \cdot (x_a + t(x_e - x_a))^i (y_a + t(y_e - y_a))^k \end{bmatrix} \quad (5-19a)$$

and

$$x^{II} = \begin{bmatrix} x_a + t(x_e - x_a) \\ y_a + t(y_e - y_a) \\ \sum_{i=0}^n \sum_{k=0}^{n-i} a_{i,k}^{II} \cdot (x_a + t(x_e - x_a))^i (y_a + t(y_e - y_a))^k \end{bmatrix} \quad (5-19b)$$

with

$x_e, y_e$  = plan coordinates of point E,

$x_a, y_a$  = plan coordinates of point A

$t \in (0,1)$  = parameter of straight line position within AE.

It is obvious, that the vectors  $x^I$  and  $x^{II}$  can only differ with respect to the position and degrees of freedom, determined by the number of the two sets of different polynomial coefficients  $a_{ik}^I$  and  $a_{ik}^{II}$  respectively. So both surfaces are  $C_0$  – continuous only if the functions  $\zeta^I(x,y,a_{ik}^I)$  and  $\zeta^{II}(x,y,a_{ik}^{II})$  are restricted to the same values along the border AE, meaning that the function's difference is zero. With the abbreviations

$$da_{ik} = a_{ik}^I - a_{ik}^{II}, \quad dx = x_e - x_a, \quad dy = y_e - y_a \quad (5-20a)$$

we obtain for the difference vector

$$\Delta x_I'' = \begin{bmatrix} 0 \\ 0 \\ \Delta \zeta(t) \end{bmatrix} = \begin{bmatrix} 0 \\ 0 \\ \sum_{i=0}^n \sum_{k=0}^{n-i} da_{i,k} \cdot (x_a + t(dx))^i (y_a + t(dy))^k \end{bmatrix} \equiv \begin{bmatrix} 0 \\ 0 \\ 0 \end{bmatrix}. \quad (5-20b)$$

By differentiating  $\Delta \zeta(t)$  in (5-20b) in x- and y- direction respectively, we reach  $C_1$ -continuity, meaning the same tangential plan at the common border straight line (Table 5.1) is also the same

**Table 5.1:** The  $C_1$ -continuity condition at a common border of neighbouring meshes is reached by differentiating the parametric expression of the border straight line in the x- and y- directions.

$$\Delta \zeta(t) = \sum_{i=0}^n \sum_{k=0}^{n-i} da_{i,k} \cdot (x_a + t(dx))^i (y_a + t(dy))^k \equiv 0 \quad C_0\text{-continuity}$$

$$\left( \frac{\partial}{\partial x} \right) \cdot \Delta \zeta(t) = \left( \frac{\partial}{\partial x} \right) \sum_{i=0}^n \sum_{k=0}^{n-i} da_{i,k} \cdot (x_a + t(dx))^i (y_a + t(dy))^k \equiv 0 \quad C_1\text{-continuity}$$

$$\left( \frac{\partial}{\partial y} \right) \cdot \Delta \zeta(t) = \left( \frac{\partial}{\partial y} \right) \sum_{i=0}^n \sum_{k=0}^{n-i} da_{i,k} \cdot (x_a + t(dx))^i (y_a + t(dy))^k \equiv 0$$

While the difference in the plan position components (x,y) automatically becomes zero by the restriction to the common straight line, AE, the difference

$$\Delta \zeta(t) = \zeta^I(x, y, a_{ik}^I, t) - \zeta^{II}(x, y, a_{ik}^{II}, t) \quad (5-21)$$

leads to an univariate polynomial in t, of  $n^{\text{th}}$  degree. Requiring the difference,  $\Delta \zeta(t)$ , to become zero is equivalent of Forcing a so called  $C_0$ -continuity. In FEM terminology, this means there are the same DFHRS functional values along the common border.

With  $n=2$ , as an example, and setting the corresponding difference,  $\Delta \zeta(t)$  (5-21b), to zero, we obtain a polynomial in t, of  $2^{\text{nd}}$  degree. After a separation with respect to the different powers

of the free parameter,  $t$ , we get the following structure and coefficients A, B, C for the polynomial in  $t$ :

$$A(a_{ik}^I, a_{ik}^{II}, x_e, x_a, y_e, y_a) \cdot t^2 + B(a_{ik}^I, a_{ik}^{II}, x_e, x_a, y_e, y_a) \cdot t^1 + C(a_{ik}^I, a_{ik}^{II}, x_e, x_a, y_e, y_a) \cdot t^0 \equiv 0 \quad (5-22)$$

The constant coefficients A, B and C depend on the polynomial coefficients and the nodal point position, A and E. As (5-22) has to be valid for all  $t \in (0,1)$  to force  $C_0$ -continuity, we require

$$A(a_{ik}^I, a_{ik}^{II}, x_e, x_a, y_e, y_a) \equiv 0 \quad (5-23a)$$

$$B(a_{ik}^I, a_{ik}^{II}, x_e, x_a, y_e, y_a) \equiv 0. \quad (5-23b)$$

$$C(a_{ik}^I, a_{ik}^{II}, x_e, x_a, y_e, y_a) \equiv 0 \quad (5-23c)$$

Upon evaluation for  $n=2$  the following  $C_0$ -continuity restrictions are found

$$A = da_{0,2} dy^2 + da_{1,1} dx dy + da_{2,0} dx^2 = 0 \quad (5-24a)$$

$$B = da_{0,1} dy + 2da_{0,2} y_a dy + da_{1,0} dx + da_{1,1} x_a dy + da_{1,1} dx y_a + 2da_{2,0} x_a dx = 0 \quad (5-24b)$$

$$C = da_{0,0} + da_{0,1} y_a + da_{0,1} y_a^2 + da_{1,0} x_a + da_{1,1} x_a y_a + da_{2,0} x_a^2 = 0, \quad (5-24c)$$

which are used in the practical DFHRS adjustments with respect to each common border line, AE, of the mesh grid (fig.4.3) as pseudo-observations  $C(\mathbf{p})$

$$\mathbf{0} + \mathbf{v} = C(\mathbf{p}). \quad (5-25)$$

Up to now continuity with neighbouring meshes at common border lines has been required. In addition to this, the diagonal neighbouring meshes have to be treated at one common point (Fig. 5.3). To force  $C_0$ -continuity, the difference at a common point of two diagonal neighbouring meshes is modelled as the pseudo-observation

$$\mathbf{0} + \mathbf{v} = \left( a_{00} + a_{01}y + a_{10}x + a_{20}y^2 + a_{11}xy + a_{02}x^2 \right)_I - \left( a_{00} + a_{01}y + a_{01}x + a_{20}y^2 + a_{11}xy + a_{02}x^2 \right)_{II} \quad (5-26)$$

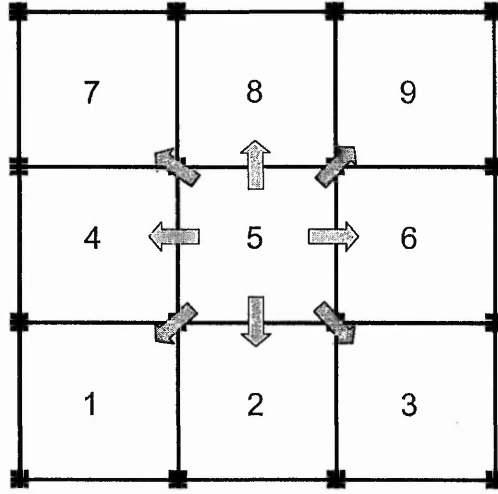


**Fig. 5.3:** To determine a complete continuous surface, conditions to 8 neighbouring meshes have to be modelled

To force  $C_1$  continuity, (5-26) has to be differentiated in  $x$ - and  $y$ - directions. The resulting observation equations read:

$$\begin{aligned} \theta + v &= \frac{\partial}{\partial x} \left( \sum_{i=0}^2 \sum_{j=0}^{2-j} a_{i,j} x^i y^j \right) - \frac{\partial}{\partial x} \left( \sum_{i=0}^2 \sum_{j=0}^{2-j} a_{i,j} x^i y^j \right) & (5-27) \\ &= a_{10} + a_{11}y + 2 \cdot a_{20}x \end{aligned}$$

$$\begin{aligned} \theta + v &= \frac{\partial}{\partial y} \left( \sum_{i=0}^2 \sum_{j=0}^{2-j} a_{i,j} x^i y^j \right) - \frac{\partial}{\partial y} \left( \sum_{i=0}^2 \sum_{j=0}^{2-j} a_{i,j} x^i y^j \right) & (5-28) \\ &= a_{01} + a_{11}x + 2 \cdot a_{02}y. \end{aligned}$$

Practical computations show, that an introduction of the  $C_1$ -continuity is necessary only with a small weight. As the HRS has to be determined better than 1cm, the weight of the condition equations needs to be set accordingly.

### 5.3 Least squares estimation of the DFHRS parameters

The observation equations derived in sections 5.1 and 5.2 of this chapter, are set up in a statistically controlled least squares adjustment. For reasons of clarity, the equations are listed again

$$H_{obs} + v = H \quad (5-4)$$

$$h^i + v = H - h \cdot \Delta \mathbf{m}^i + \zeta_{FEM}(\varphi, \lambda | \mathbf{p}) \quad (5-5)$$

$$\zeta_{grav}(\varphi, \lambda)^j + v = \zeta_{FEM}(\varphi, \lambda | \mathbf{p}) + \Delta T_{\zeta}(\mathbf{d}^j) \quad (5-10)$$

$$\begin{Bmatrix} \xi \\ \eta \end{Bmatrix}^k + v = \begin{Bmatrix} -\mathbf{f}_{\varphi} / M(\varphi) \\ -\mathbf{f}_{\lambda} / N(\varphi) / \cos(\varphi) \end{Bmatrix} \cdot \mathbf{p} + \begin{Bmatrix} \Delta T_{\xi}(\mathbf{d}^k) \\ \Delta T_{\eta}(\mathbf{d}^k) \end{Bmatrix} \quad (5-29a)$$

$$\delta g + v = g(\mathbf{A}, \mathbf{B}) \quad (5-17a)$$

$$0 + v = \zeta_{FEM}(\varphi, \lambda | \mathbf{p}) - \frac{1}{\gamma} f(\mathbf{A}, \mathbf{B}) \quad (5-17b)$$

$$0 + v = C(\mathbf{p}). \quad (5-25)$$

with

$$\mathbf{f}_{\varphi} = \frac{\partial}{\partial \varphi} \zeta_{FEM}(\varphi, \lambda) = \frac{\partial}{\partial \varphi} \mathbf{f}^T(X(\varphi, \lambda), Y(\varphi, \lambda))$$

$$\mathbf{f}_{\lambda} = \frac{\partial}{\partial \lambda} \zeta_{FEM}(\varphi, \lambda) = \frac{\partial}{\partial \lambda} \mathbf{f}^T(X(\varphi, \lambda), Y(\varphi, \lambda))$$

$M(\varphi)$  and  $N(\varphi)$  mean the radius of meridian and normal curvature respectively. The indices  $i$ ,  $j$  and  $k$  designate the respective groups of observations for the modelling of the correction parameters  $\mathbf{d}$ .

The unknown parameters  $\mathbf{H}$ ,  $\Delta \mathbf{m}$ ,  $\mathbf{p}$ ,  $\mathbf{d}$ ,  $\mathbf{A}$  and  $\mathbf{B}$  are contained within  $\mathbf{x}$  and estimated in the Gauss-Markov model as follows

$$\hat{\mathbf{x}} = (\mathbf{A}^T \mathbf{C}_1^{-1} \mathbf{A})^{-1} \mathbf{A}^T \mathbf{C}_1^{-1} \mathbf{l} \quad (5-30)$$

$$\mathbf{C}_{\hat{\mathbf{x}}} = (\mathbf{A}^T \mathbf{C}_1^{-1} \mathbf{A})^{-1} \quad (5-31)$$

where

$$\mathbf{A}^T = \left[ \mathbf{A}_H \quad \mathbf{A}_h \quad \mathbf{A}_{\zeta_{grav}} \quad \mathbf{A}_{\xi, \eta} \quad \mathbf{A}_{\delta g} \quad \mathbf{A}_{C1} \quad \mathbf{A}_{C2} \right] \text{ the design matrix of the observations}$$

$$\mathbf{l}^T = \left[ \mathbf{H} \quad h \quad \zeta_{grav} \quad (\xi, \eta) \quad \delta g \quad 0 \quad 0 \right] \text{ the vector of observations,}$$



available, the area of interest again may be divided into a number of patches. Within each patch, a number of appropriate parameters are used to model a correction to the height anomalies within the respective gravimetric model. The resulting quality depends mainly on the size of these patches and also the density of the points.

In areas, where the identical points are sparse, correlation functions, such as (4-26), may be used, to give a better approximation of the stochastic model and with this realise a strict two steps adjustment (Jäger, 2002; Jäger and Schneid, 2002).

In the following section, the sizes of FEM meshes, patches and the effect of correlation functions are investigated.

#### **5.4.1 FEM-meshing and geoid patching for a precise representation of the HRS**

The first part of a DFHRS-computation is the generation of appropriate FEM-meshes. The size of the FEM meshes and the degree of the polynomials representing it are essential design parameters needed to control the resulting quality of the HRS representation.

To represent the HRS by a FEM, it is necessary to make sure that the HRS may be approximated to each single mesh in an acceptable quality. In the DFHRS-concept, a geoid model, which is available, may be interpreted as “direct observation” of the HRS. So in this first step if useful results are to be obtained, the polynomial in each mesh must be suitable to approximate the geoid model used to the desired accuracy.

The EGG97 (Denker and Torge, 1997) is a continental quasigeoid model with a local accuracy in the centimetre range. So in the case of a DFHRS computation for Europe it can give a potential group of “direct observations” of quasigeoid heights,  $\zeta$ .

To estimate the approximate quality of bivariate polynomials of 3<sup>rd</sup> degree, a FEM representation of the EGG97 was computed for a representative area. An area of about 140km x 140km, situated in southern Germany and Switzerland, was subdivided into meshes with 30km, 10km and 5km border lengths. The area was selected, because the geoid is known to be very rough in this area.

In addition to the height anomaly  $\zeta_{\text{grav}}$ , the EGG97 may also provide the vertical deflections ( $\xi, \eta$ ) at any point of the area covered. Both may be functions of the disturbing gravity potential  $T$ .

To get a strict HRS representation, the geoid height information together with its real covariance matrix would be sufficient to estimate the FEM parameters. But as long as no stochastic

information is available both geoid heights as well as vertical deflections, set up as uncorrelated observation groups in a least squares adjustment, guarantee an unbiased estimation of the HRS (5-18).

The 3 examples with differently sized FEM meshes (30km, 10km, 5km) were computed with the same a-priori parameters, as there are:

- 25 height anomalies,  $\zeta$ , distributed regular in each mesh, with  $\sigma_{\zeta}=0.03\text{m}$
- 25 vertical deflection points  $(\xi, \eta)$ , distributed regularly in each mesh, with  $\sigma_{(\xi, \eta)}=2''$

The maximum and average residuals of the adjusted observations of the different adjustments are listed in Table 5.2.

**Table 5.2:** Different output qualities with different mesh sizes

	30 km	10km	5km
maximum residual $\zeta$ / RMS	0.203m / 0.040m	0.053m / 0.005m	0.017 m / 0.001m
maximum residual $\xi$ / RMS	20.78'' / 2.60''	10.15'' / 0.73''	4.86'' / 0.29''
maximum residual $\eta$ / RMS	14.81'' / 2.23''	9.61'' / 0.68''	4.03'' / 0.26''

The results of the three examples as well as investigations in other areas (Ludwig, 2002) concerning the approximation quality with different mesh sizes, show that the border length of the FEM meshes is correlated with the resulting accuracy. A border length of 5 km will be sufficient for a precise HRS representation with a quality of better than 1cm. With 10km x 10km mesh size the resulting quality will be compatible with the positioning qualities in DGNS networks like the German SAPOS or ASCOS services. To get the 10 cm quality of that is strived for by the EUREF-TWG for the new European Height Reference Surface, a mesh size of not bigger than 30 km will be sufficient (Table 5.3).

Comparable investigations took place concerning the size of the geoid-patches. In contrast to the size of the FEM meshes, the size of the geoid-patches may not be chosen arbitrarily. They depend on the density of the points with known heights  $h$  and  $H$ . So the density of

GNSS/levelling points as well becomes an important design parameter needed to produce a DFHRS of high quality (Jäger, 1988).

**Table 5.3:** The mesh size of the FEM meshes is the most important design parameter needed to produce a Digital FEM Height Reference Surface of a required quality

Approximation Quality	Mesh-size
1 cm	5 km
1 - 3 cm	10 km
5 - 10 cm	$\leq 30$ km

The number of estimated parameters in a single geoid patch, e.g. 3 if  $\Delta T_{\zeta}(\mathbf{d})$  is modelled according to (4-19) or (4-20), in combination with the density and quality of the identical points is also decisive for the size of a patch.

Table 5.4 shows the HRS representation quality which depends on the patch size. The quantities are estimated using experience that was gained in several DFHRS computation projects (Ludwig, 2002; Streifeneder, 2003; Schneid, 2003; Jäger and Schneid, 2005). They give a “rule of thumb”, for a computational design with an average number of 5 points with  $\sigma_h = \sigma_H = 1.0$  cm in each patch and modelling  $\Delta T_N$  according to (4-20).

**Table 5.4:** Another important design parameter to achieve the desired quality is the size of the geoid patches

Representation quality	Patch size
1 cm	(30 – 50) km
1-3 cm	(50 – 100) km
5-10 cm	(100 – 300) km

### 5.4.2 Generation and application of synthetic covariance matrices

The weak-forms, mentioned in the context of significant long-wave errors in gravimetric HRS models see chapter 4, as a stochastic source for  $\Delta T_{\zeta}$ ,  $\Delta T_{\xi}$  and  $\Delta T_{\eta}$ , would be significantly

less, if the true co-variance matrix,  $C_{\zeta\zeta}$ , for the geoid heights and  $C_{\xi\xi}/C_{\eta\eta}$ , for the deflections of the vertical, as well as the co-variance matrices,  $C_{\zeta\xi}$ ,  $C_{\zeta\eta}$  and  $C_{\xi\eta}$ , were available. Unfortunately, the stochastic model resulting from the determination of a gravity field model is never available. As a substitute, synthetic co-variance matrices may be generated for the geoid heights  $\zeta_{\text{grav}}$ , by means of an appropriate co-variance function. A suitable co-variance function is for example given with (4-26) or with (Dinter et. al. 1997):

$$C_{\zeta_i, \zeta_j} = \sigma_0 \cdot e^{-\frac{\ln(0.5) \cdot S_{i,j}}{\beta}} \quad (5-32)$$

In the expression above,  $S_{i,j}$  denotes the distance between two points,  $i$  and  $j$ . The quantity,  $\beta$ , is the correlation length. According to Moritz (1980), p. 108 the remaining co-variances may be found with

$$C_{\zeta_i, \xi_j} = \frac{\partial C_{N_i, N_j}}{M(\varphi) \cdot \partial \varphi_j} \quad (5-33a)$$

$$C_{\zeta_i, \eta_j} = \frac{\partial C_{N_i, N_j}}{N(\varphi_j) \cos \varphi_j \cdot \partial \lambda_j} \quad (5-33b)$$

$$C_{\xi_i, \xi_j} = \frac{\partial^2 C_{N_i, N_j}}{M(\varphi_i) M(\varphi_j) \partial \varphi_i \partial \varphi_j} \quad (5-33c)$$

$$C_{\eta_i, \eta_j} = \frac{\partial^2 C_{N_i, N_j}}{N(\varphi_i) N(\varphi_j) \cos \varphi_i \cos \varphi_j \cdot \partial \lambda_i \partial \lambda_j} \quad (5-33d)$$

$$C_{\xi_i, \eta_j} = \frac{\partial C^2_{N_i, N_j}}{M(\varphi_i) N(\varphi_j) \cos \varphi_j \cdot \partial \varphi_i \partial \lambda_j} \quad (5-33e)$$

As is known from the theory of least-squares adjustment, the estimation is unbiased with respect to the stochastic model (Jäger et. al. 2004). Therefore, the estimated FEM parameters,  $\mathbf{p}$ , and the HRS are unbiased, even if the stochastic model in (5-33a – 5-33e) was approximated, for example as:

$$\tilde{C}_{\zeta\zeta} = \sigma_{0,\zeta}^2 \cdot \mathbf{I} \quad (5-34a)$$

$$\tilde{\mathbf{C}}_{\xi\xi} = \sigma_{0,\xi}^2 \cdot \mathbf{I} \quad (5-34b)$$

$$\tilde{\mathbf{C}}_{\eta\eta} = \sigma_{0,\eta}^2 \cdot \mathbf{I} \quad (5-34c)$$

and

$$\tilde{\mathbf{C}}_{N\xi} = \tilde{\mathbf{C}}_{N\eta} = \tilde{\mathbf{C}}_{\xi\eta} = 0 \quad (5-34d)$$

However the most accurate FEM-representation of the HRS comes from the use of a proper stochastic model (Jäger et. al., 2005). So the accuracy of the HRS increases with the quality of the approximation of the co-variance matrices (5-32 and 5-33a-e).

In recent years, several DFHRS databases have been computed, to support GNSS-based height determination. Due to the different possible applications of a HRS, there are different types of DFHRS databases. “High-end products”, with a statistically controlled accuracy of less than one centimetre were computed for six state land service departments in Germany (Baden-Württemberg, Bayern, Hessen, Nordrhein-Westfalen, Rheinland-Pfalz and Saarland) (Jäger and Schneid, 2000-2007).

The DFHRS for Germany was designed to support an online GNSS-height determination in combination with the DGNSS-correction services ASCOS and SAPOS, with a quality of less than three centimetres. (Schneid, 2003; Seiler, 2004).

The investigations show, that a model for a HRS may be computed with an average accuracy of one centimetre if the concept of the DFHRS is applied. The main design parameters to be considered for the desired resulting quality of the FEM representation of a HRS are the size of the FEM meshes and the size of the “geoid-patches”. If the distribution of the used GNSS/Levelling points is sparse, the number of possible “geoid-patches” is limited. The quality of the HRS representation then may be improved by using a co-variance function, such as 5-30 and 5-31a-e to generate an a priori co-variance matrix,  $\mathbf{C}_1$ .

In a test project, a significant increase in the computed accuracy was demonstrated. The HRS was approximated by FEM meshes of 10 km border length (fig. 5.4). 46 GNSS/levelling points were introduced and a 3-parameter datum shift, containing one constant offset and two rotations, was modelled to reduce long-wave errors in the applied gravimetric geoid model, here the EGG97.

In a first computation, the a-priori covariance matrix,  $C_{\zeta_{\text{grav}}}$ , of the geoid heights used,  $\zeta_{\text{grav}}$ , was simply approximated using (5-32a). The resulting standard deviation,  $\sigma_{\text{DFHRS}}$ , of the estimated DFHRS, was  $\pm 1.9$  cm, and was found by the re-computation of known points.

In a second and third computation, two different covariance functions were used to generate a better approximation for  $C_{\zeta\zeta}$ . A correlation length,  $\beta$ , of 100 km was used. A compilation of the results is given in table 5.5.

The reliability of this result was demonstrated in a second investigation. 11 GNSS/levelling points from the inner zone of the project area were removed and not used for the adjustment of the DFHRS (Fig. 5.5). The re-computation using the 11 points removed had a standard deviation,  $\sigma_{\text{DFHRS}}$ , of  $\pm 0,82$ cm. The complete results are compiled in table 5.6.

The accuracy of other projects may be significantly increased using a similar FEM design. The use of an appropriate covariance function for the stochastic model of gravimetric geoid heights increases the accuracy of the HRS, even in areas where the density of GNSS/levelling points is sparse.

**Table 5.5:** Comparison of the results, when applying different covariance functions.

Covariance function for $\zeta_{\text{grav}}$	RMS [cm]	maximum $\Delta H$ [cm]	Minimum $\Delta H$ [cm]
Uncorrelated	1.92	4.4	-3.1
$\sigma_0 \cdot e^{-\ln(0.5) \cdot \frac{S}{\beta}}$	0.86	2.1	-2.1
$\sigma_0 \cdot \frac{\beta}{\beta + S}$	0.86	2.1	-2.0

**Table 5.6:** Comparison of the results from re-computing the points that had been removed, when applying different covariance functions

Covariance function for $\zeta_{\text{grav}}$	RMS [cm]	maximum $\Delta H$ [cm]	minimum $\Delta H$ [cm]
Uncorrelated	1.53	0.6	-2.7
$\sigma_0 \cdot e^{-\ln(0.5) \cdot \frac{S}{\beta}}$	0.82	0.3	-1.4
$\sigma_0 \cdot \frac{\beta}{\beta + S}$	0.84	0.3	-1.4

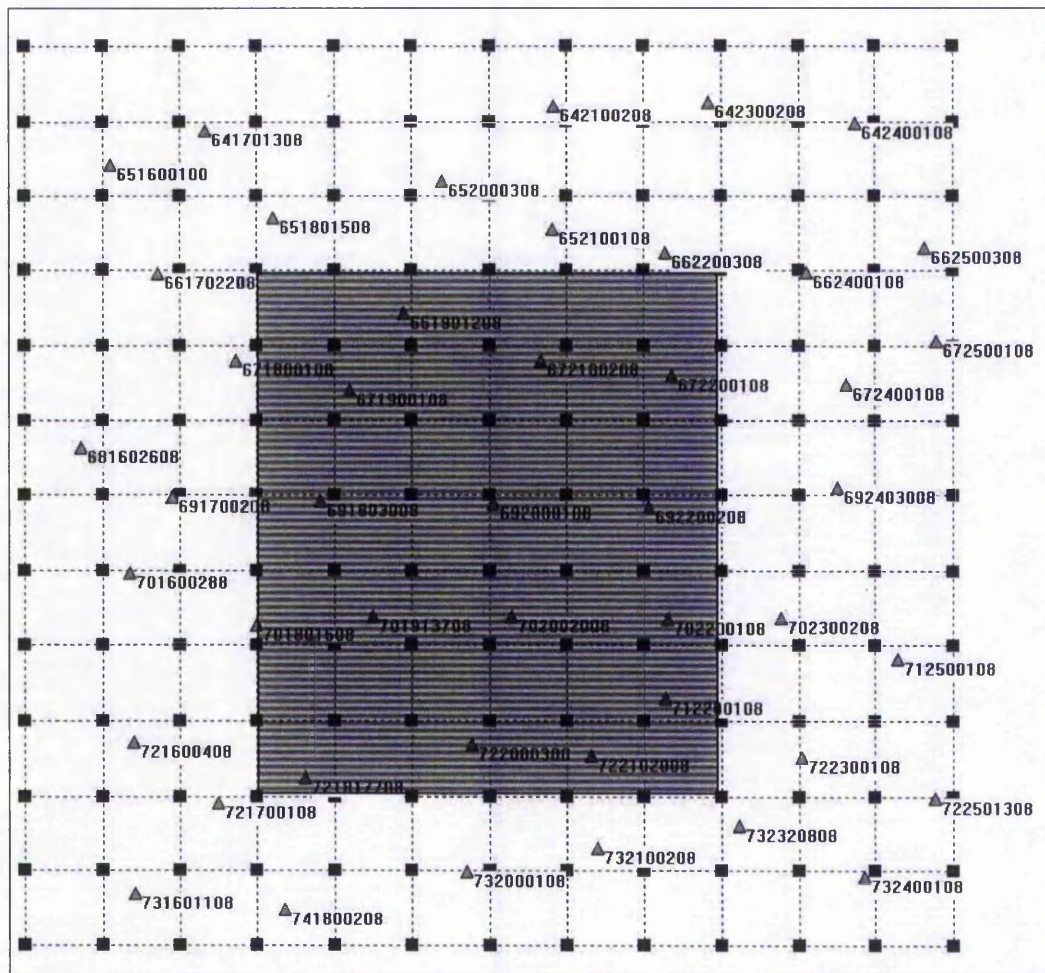


**Fig.5.4:** Positions of the 46 GNSS/levelling points. In a second project, 11 points from the inner zone (red) have been removed.

## 5.5 Block algorithms for the inversion of huge matrices

To provide a software tool that can be used to compute DFHRS databases of any size and any quality, it is necessary to develop special algorithms for the solution of linear equation systems. As the quality of DFHRS databases mainly depends on the size of the FEM meshes, it is obvious that the number of unknowns increases with a better FEM representation. For the computation of the DFHRS for Germany, for example, a number of 51719 unknowns had to be solved for. It is obvious that this cannot be done with standard algorithms. For implementation in software, for example, algorithms based on block-matrices may be programmed to solve the linear equation system of the least-squares estimation. Two possible

solutions are given in the following. The linear equation system of a least squares estimation reads:

$$\mathbf{p} = (\mathbf{A}^T \cdot \mathbf{C}_{II}^{-1} \cdot \mathbf{A})^{-1} \cdot \mathbf{A}^T \cdot \mathbf{C}_{II}^{-1} \cdot \mathbf{l} \quad (5-35a)$$

$$= \mathbf{N}^{-1} \cdot \mathbf{n} \quad (5-35b)$$

In the equations above,  $\mathbf{p}$  means the vector of the unknown DFHRS parameters.  $\mathbf{A}$  denotes the design matrix of the DFHRS observations,  $\mathbf{l}$ , and  $\mathbf{C}_{II}$  is the co-variance matrix of the observations. If the matrix of normal equations,  $\mathbf{N}$ , may be subdivided into  $n \times n$  sub-matrices, (5-35b) may be written as:

$$\begin{bmatrix} \mathbf{p}_1 \\ \mathbf{p}_2 \\ \mathbf{p}_3 \\ \dots \\ \mathbf{p}_n \end{bmatrix} = \begin{bmatrix} \mathbf{N}_{1,1} & \mathbf{N}_{2,1}^T & \mathbf{N}_{3,1}^T & \dots & \mathbf{N}_{n,1}^T \\ \mathbf{N}_{2,1} & \mathbf{N}_{2,2} & \mathbf{N}_{3,2}^T & \dots & \dots \\ \mathbf{N}_{3,1} & \mathbf{N}_{3,2} & \mathbf{N}_{3,3} & \dots & \dots \\ \dots & \dots & \dots & \dots & \dots \\ \mathbf{N}_{n,1} & \dots & \dots & \mathbf{N}_{n,n-1} & \mathbf{N}_{n,n} \end{bmatrix}^{-1} \cdot \begin{bmatrix} \mathbf{n}_1 \\ \mathbf{n}_2 \\ \mathbf{n}_3 \\ \dots \\ \mathbf{n}_n \end{bmatrix} \quad (5-36)$$

The symmetric and positive definite matrix,  $\mathbf{N}$ , may be written as the product of a normalised lower triangle matrix,  $\mathbf{L}$ , and a diagonal matrix,  $\mathbf{D}$ , such as:

$$\mathbf{N} = \mathbf{L} \cdot \mathbf{D} \cdot \mathbf{L}^T \quad (5-37a)$$

$$= \begin{bmatrix} \mathbf{D}_{1,1} & \mathbf{D}_{1,1} \mathbf{L}_{2,1}^T & \mathbf{D}_{1,1} \mathbf{L}_{3,1}^T \\ \mathbf{L}_{2,1} \mathbf{D}_{1,1} & \mathbf{L}_{2,1} \mathbf{D}_{1,1} \mathbf{L}_{2,1}^T + \mathbf{D}_{2,2} & \mathbf{L}_{2,1} \mathbf{D}_{1,1} \mathbf{L}_{3,1}^T + \mathbf{D}_{2,2} \mathbf{L}_{3,2}^T \\ \mathbf{L}_{3,1} \mathbf{D}_{1,1} & \mathbf{L}_{3,1} \mathbf{D}_{1,1} \mathbf{L}_{2,1}^T + \mathbf{L}_{3,2} \mathbf{D}_{2,2} & \mathbf{L}_{3,1} \mathbf{D}_{1,1} \mathbf{L}_{3,1}^T + \mathbf{L}_{3,2} \mathbf{D}_{2,2} \mathbf{L}_{3,2}^T + \mathbf{D}_{3,3} \end{bmatrix} \quad (5-37b)$$

$$= \mathbf{L} \cdot (\mathbf{D} \cdot \mathbf{L}^T) = \mathbf{L} \cdot \mathbf{U} \quad (5-37c)$$

$$= \begin{bmatrix} \mathbf{U}_{1,1} & \mathbf{U}_{1,2} & \mathbf{U}_{1,3} \\ \mathbf{L}_{2,1} \mathbf{U}_{1,1} & \mathbf{L}_{2,1} \mathbf{U}_{1,2} + \mathbf{U}_{2,2} & \mathbf{L}_{2,1} \mathbf{U}_{1,3} + \mathbf{U}_{2,3} \\ \mathbf{L}_{3,1} \mathbf{U}_{1,1} & \mathbf{L}_{3,1} \mathbf{U}_{1,2} + \mathbf{L}_{3,2} \mathbf{U}_{2,2} & \mathbf{L}_{3,1} \mathbf{U}_{1,3} + \mathbf{L}_{3,2} \mathbf{U}_{2,3} + \mathbf{U}_{3,3} \end{bmatrix} \quad (5-37d)$$

The sub-matrices,  $\mathbf{L}_{i,j}$  and  $\mathbf{D}_{i,i}$  of the matrix of normal equations are computed, and stored in a file in a compressed mode. This so-called "LDL-Decomposition" (Bjorck and Dahlquist,

2002) may be interpreted as a special case of the LU-decomposition, (5-37c), (Press et. al. 2002), for symmetrical matrices.

The single blocks, or sub-matrices are solved using algorithm (A-5.1) below. The LDL-decomposition has the benefit that only the disk space required for the lower triangle of the matrix of normal equations is used for the storage. The LU-decomposition needs less computations, as the matrix  $U = D \cdot L^T$ , does not have to be computed. On the other hand, it needs almost double the hard disk space.

The linear equation system (5-36) may be solved as follows:

$$L \cdot (D \cdot L^T \cdot p) = n \quad (5-38a)$$

$$L \cdot y = n \quad (5-38b)$$

$$y = L^{-1} \cdot n \quad (5-38c)$$

$$L^T \cdot p = D^{-1} \cdot y \quad (5-38d)$$

for k=1 to maxColumn-1	
begin	
$ID_{k,k} = D_{k,k}^{-1}$	1. Inversion of the first block
for i=k+1 to maxRow	
begin	
$L_{i,k} = L_{i,k} \cdot ID_{k,k}$	2. k-th column, $L_{i,k}$ , is computed
end	
for j=k+1 to maxColumn	
begin	
for j=j to maxRow	
begin	
$L_{i,j} = L_{i,j} - L_{i,k} \cdot L_{j,k}$	3. the remaining blocks are reduced from the products with the blocks of the k-th column
end	
$ID_{k,k} = D_{k,k}^{-1}$	4. Inversion of the final diagonal block

**Algorithm A-5.1:** Solving the single sub-matrices of the matrix of normal equations

Usually, the computation of a DFHRS - project takes three to five iterations, until the best settings are found, for example the best fitting parametric model for the local datum correction of the applied geoid model. So usually (5-38a-b) are used to solve the unknown parameters (Algorithm A-5.2), as the inversion of the matrix of normal equations takes a lot of computation time.

To accomplish complete statistical quality control, the inverse matrix  $\mathbf{Q}_{pp} = \mathbf{N}^{-1}$ , has to be computed.  $\mathbf{Q}_{pp}$  may easily be found with:

$$\mathbf{Q}_{pp} = \mathbf{L}^{\text{T}-1} \cdot \mathbf{D}^{-1} \cdot \mathbf{L}^{-1} \quad (5-39)$$

```

p = n
for i=1 to maxRow
begin
  for j=1 to i-1
  begin
    pi = pi - Li,j · nj
  end
end
for i=maxRow down to 1
begin
  sum = pi
  for j=i+1 to maxRow
  begin
    sum = sum - Li,j · pj
  end
  pi = IDi,i · sum
end
End

```

**Algorithm A-5.2:** Solving unknown parameters, **p**, after LDL-decomposition

As  $\mathbf{L}$  is a normalised lower triangle matrix it may easily be inverted. If the matrix  $\mathbf{N}$  was subdivided into  $n \times n$  sub-matrices, then we obtain for  $\mathbf{L}$ :

$$\mathbf{L} = \mathbf{L}_{(1)} \cdot \mathbf{L}_{(2)} \cdot \dots \cdot \mathbf{L}_{(n)} \quad (5-40)$$

and for  $\mathbf{L}^{-1}$ :

$$\mathbf{L}^{-1} = \mathbf{L}_{(n)}^{-1} \cdot \mathbf{L}_{(n-1)}^{-1} \cdot \dots \cdot \mathbf{L}_{(1)}^{-1} \quad (5-41)$$

In (5-38), we have for example for  $n=4$ :

$$\mathbf{L} = \begin{bmatrix} \mathbf{I} & & & \\ \mathbf{L}_{2,1} & \mathbf{I} & & \\ \mathbf{L}_{3,1} & \mathbf{L}_{3,2} & \mathbf{I} & \\ \mathbf{L}_{4,1} & \mathbf{L}_{4,2} & \mathbf{L}_{4,3} & \mathbf{I} \end{bmatrix}$$

and

$$\mathbf{L}_{(1)} = \begin{bmatrix} \mathbf{I} & & & \\ \mathbf{L}_{2,1} & \mathbf{I} & & \\ \mathbf{L}_{3,1} & \mathbf{0} & \mathbf{I} & \\ \mathbf{L}_{4,1} & \mathbf{0} & \mathbf{0} & \mathbf{I} \end{bmatrix}; \mathbf{L}_{(2)} = \begin{bmatrix} \mathbf{I} & & & \\ \mathbf{0} & \mathbf{I} & & \\ \mathbf{0} & \mathbf{L}_{3,2} & \mathbf{I} & \\ \mathbf{0} & \mathbf{L}_{4,2} & \mathbf{0} & \mathbf{I} \end{bmatrix}; \mathbf{L}_{(3)} = \begin{bmatrix} \mathbf{I} & & & \\ \mathbf{0} & \mathbf{I} & & \\ \mathbf{0} & \mathbf{0} & \mathbf{I} & \\ \mathbf{0} & \mathbf{0} & \mathbf{L}_{4,3} & \mathbf{I} \end{bmatrix}$$

and in (5-41) we have for  $n=4$ :

$$\mathbf{L}_{(1)}^{-1} = \begin{bmatrix} \mathbf{I} & & & \\ -\mathbf{L}_{2,1} & \mathbf{I} & & \\ -\mathbf{L}_{3,1} & \mathbf{0} & \mathbf{I} & \\ -\mathbf{L}_{4,1} & \mathbf{0} & \mathbf{0} & \mathbf{I} \end{bmatrix}; \mathbf{L}_{(2)}^{-1} = \begin{bmatrix} \mathbf{I} & & & \\ \mathbf{0} & \mathbf{I} & & \\ \mathbf{0} & -\mathbf{L}_{3,2} & \mathbf{I} & \\ \mathbf{0} & -\mathbf{L}_{4,2} & \mathbf{0} & \mathbf{I} \end{bmatrix}; \mathbf{L}_{(3)}^{-1} = \begin{bmatrix} \mathbf{I} & & & \\ \mathbf{0} & \mathbf{I} & & \\ \mathbf{0} & \mathbf{0} & \mathbf{I} & \\ \mathbf{0} & \mathbf{0} & -\mathbf{L}_{4,3} & \mathbf{I} \end{bmatrix}$$

So the computation of  $\mathbf{L}^{-1}$  is done by matrix multiplication of the column matrices  $\mathbf{L}_{(n)}^{-1}$  with the opposite direction of that of (5-40).

The above algorithms have been implemented in software. The application is then able to solve linear equation systems and with this, to compute DFHRS databases of any size. The only restriction is the hard disk space of the computer used.

## 5.6 Computation examples

### 5.6.1 The DFHRS of Germany

The DFHRS for Germany was designed to have an accuracy of less than three centimetres. (Schneid, 2003). This accuracy is appropriate for online positioning in Online GNSS-Networks.

In the first step, the whole area was subdivided into a grid of regular FEM-meshes with 10km x 10km mesh-size. To reduce the long- and medium-wave systematic errors 102 geoid patches were introduced each with its own set of local datum parameters (Fig. 5.5).

For the DFHRS of Germany 51933 unknowns in total had to be solved in a least-squares adjustment. These were:

- 822 standard heights  $H$  (from identical points) with 1cm uncertainty
- 1 scale correction  $\Delta m$  between the heights  $h$  and  $H$
- 520 datum parameters (3 Translations, 2 Rotations) in 102 patches
- 50590 FEM – parameters (10 for each mesh)

The DFHRS computation included statistical quality controls. Besides the standard methods of data-snooping to detect gross errors and variance component estimation, another very simple, but effective control is the computation of the so-called reproduction-value or “repro-value” of each identical point  $i$

$$\nabla H_i = H_{i,known} - H_{i,DFHRS} \quad (5-42)$$

$$= -\frac{v_i}{r_i} \quad (5-43)$$

where  $v_i$  and  $r_i$  are the residual and the part of redundancy respectively.

This value  $\nabla H_i$  gives a measure of the change in the resulting DFHRS if the point  $H_{i,known}$  would not have been used in the adjustment. In the case of a non-significant test statistic, a big repro-value  $\nabla H_i$  with a big part of redundancy ( $r_i > 30\%$ ) indicates either inaccurate identical points or wrong modelling of the DFHRS (i.e. mesh-size too big). In the case of a

non-significant test statistic, a big repro-value  $\nabla H_i$ , together with a small part of redundancy ( $r_i < 30\%$ ) suggests too few GNSS/Levelling points in this area. The target in the computation of the DFHRS Germany was to keep the “repro-value” less than about 5cm.

In addition to the height anomaly  $\zeta_{DFHRS}$ , its standard-deviation  $\sigma_{DFHRS(\varphi, \lambda, h) C\Delta m, p}$  is provided by the co-variance matrix of the parameters for further analysis.

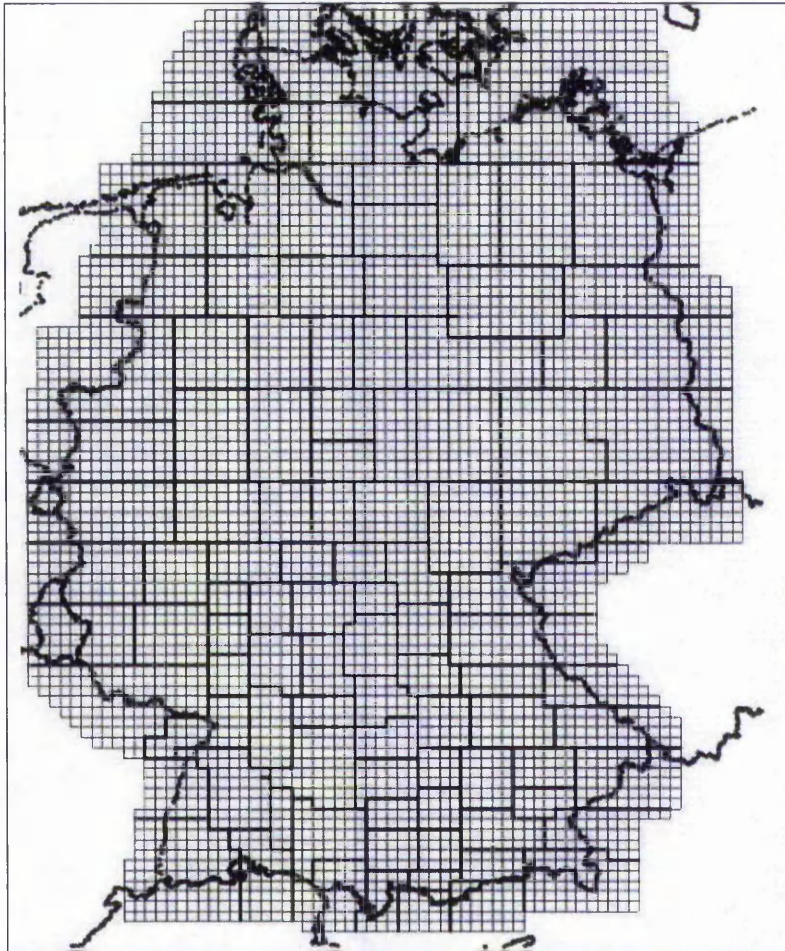


**Fig.5.5:** FEM meshing of the DFHRS-Germany with 102 geoid-patches.

The best and most independent quality control of a database comes from measurements at points within the area of investigation. To simulate this, some places or regions in southwestern Germany were used. Points in the database of the University of Applied Sciences Karlsruhe were used to test the external quality of the computed databases. These points were not used in the computation of the database. They had a quality of 3 cm. Only at 16 points of 3243 (maximum standard deviation  $\sigma_H = 3\text{cm}$ ), or about 0.5 %, showed a difference of more than 5 cm.

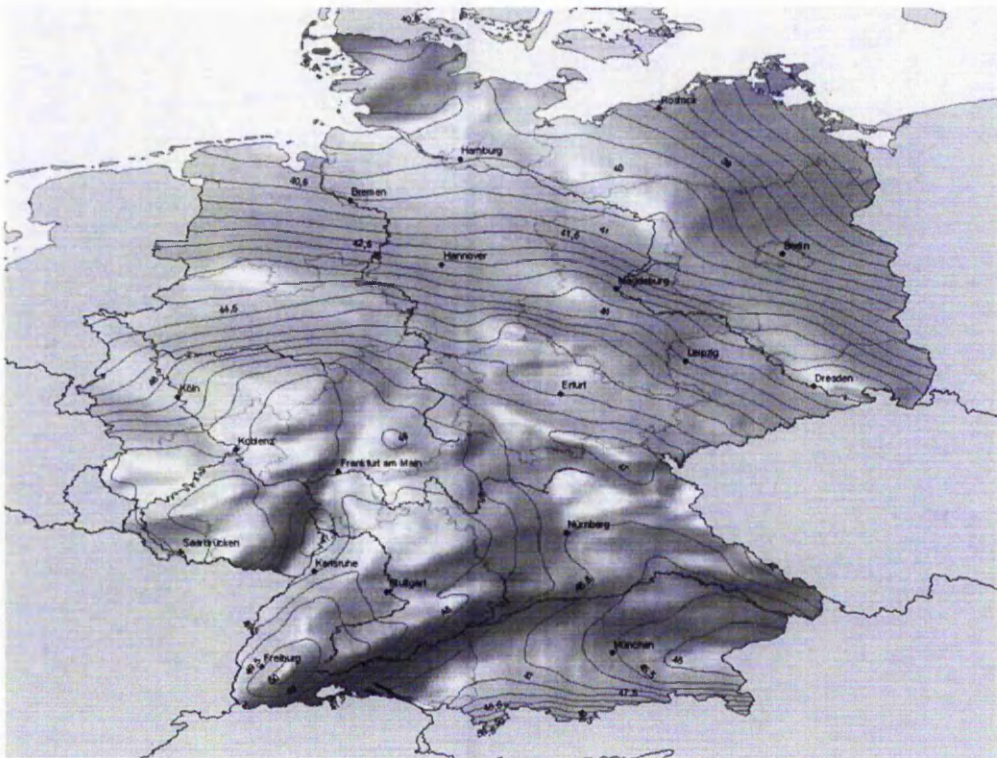


**Fig.5.6:** Visualisation of the Digital FEM Height Reference Surface for Germany

The differences (5-42) between the known height  $H$  and the heights  $H_{DFHRS}$  transformed by means of the DFHRS are given by

$$\nabla H_i = H_{i,known} - (h_i - \zeta_{DFHRS}) \quad (5-44)$$

From (5-42) a standard deviation of  $\sigma_{H,DFHRS} = 1.8$  cm can be evaluated using the 3243 control points. This value represents the accuracy of the computed heights  $H_{DFHRS}$ . Hence the standard deviation of the height anomaly derived from the DFHRS  $\sigma_{DFHRS} < 1.8$ cm and can be approximated with

$$\sigma_{DFHRS} = \sqrt{\sigma_{H,DFHRS}^2 + \sigma_{H,known}^2 + \sigma_h^2} \quad (5-45)$$

The estimated co-variance matrix  $C_{DFHRS}$  of Germany shows an accuracy of  $< 2.0$  cm in the heights of most parts of the surface. This is in accordance with the estimation (5-43) applied to the control points.

The quality control of the DFHRS Germany showed that the principle aim of the project, to compute a database with an uncertainty of less than three centimetres has been achieved and has been surpassed. With this accuracy the database is a well balanced tool for online height determination in GNSS networks. It can be improved by updating the computation when new observations, i.e. GNSS/Levelling points,  $h$  and  $H$ , are available.

### 5.6.2 The DFHRS of Europe

Using the DFHRS concept, the area of Europe was subdivided into of 7035 FEM meshes (Jäger and Schneid, 2004). As can be seen from figure 5.7, some of the European states are not involved in this computation. This is because these states are not connected to the European Vertical Reference Frame (EVRF), the European height datum.

The size of the meshes was chosen to be with 30km border length to compute the EVRF with an accuracy of less than one decimetre. To reduce the long-wave biases in the gravimetric model used, in this case the EGG97 (Denker and Torge, 1997), 34 patches were created, to eliminate the long-wave errors. Due to the sparse distribution of the GNSS/Levelling points, the patch size varies from 100km to 800km in border length.

The height anomalies,  $\zeta$ , as well as the deflections from the vertical,  $\xi$  and  $\eta$ , derived from the EGG97 were introduced as observations in the combined adjustment (5-4, 5-5, 5-10, 5-17, 5-29a - c). The GNSS/Levelling points from the EVRF2000 (BKG, 2003) were used as an observation group ( $h$  and  $H$ ). Additional points from national densification were available in Estonia, Germany, Latvia, Lithuania and Switzerland. In total, 355 points with ellipsoidal and sea level heights were used.

Besides the standard procedures like data-snooping for blunders, the computation of  $\sim 200$  independent control points with known heights,  $h$  and  $H$ , was used part of the quality control. These points are situated in Austria, Germany, Estonia, Latvia, Lithuania and Switzerland. The results show, that the resulting quality of the DFHRS for Europe is better than 10 centimetres (table 5.7).

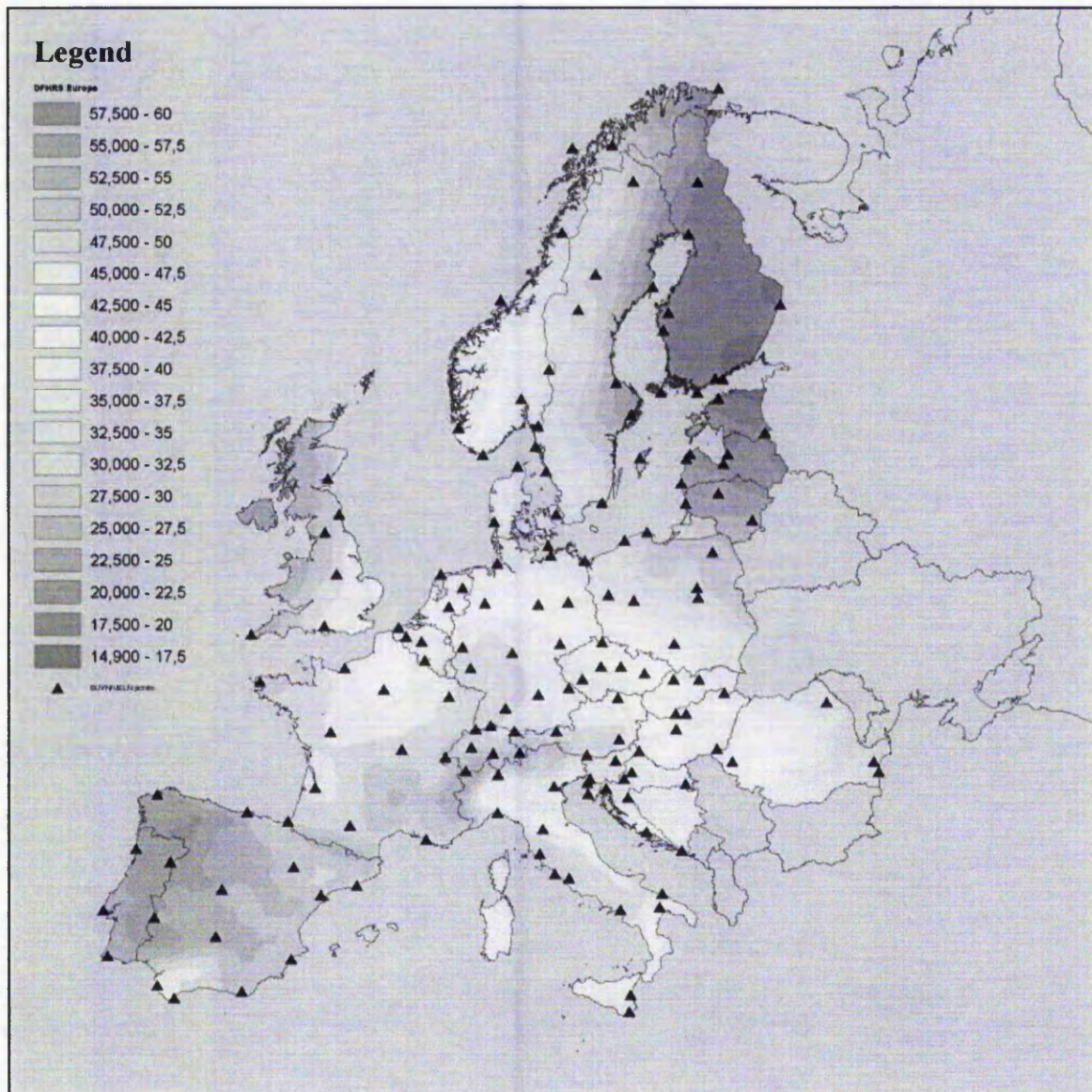


**Fig. 5.7:** The Digital FEM Height Reference Surface for Europe, computed from the EVRF200 (triangles) and the EGG97.

**Table 5.7:** Compilation of the results for different countries where independent GNSS/Levelling points were computed

	Austria	Germany	Estonia	Latvia	Lithuania	Switzerland
No. of control points	9	95	21	25	46	13
Std.Dev. [cm]	7.5	4.2	8.8	9.2	6.8	7.0

The re-computation of known points indicates that the external accuracy of less than 10 centimetres for the DFHRS Europe has been achieved in each country where control points were available. This quality may be improved by introducing more GNSS/Levelling points, for example, from national densification. A higher number of such fitting points would enable the creation of more geoid patches and hence lead to a better representation of the EVRS (Jäger, R. and S. Schneid (2004)).

The quality of a DFHRS depends only on the design parameters. These are the size of the FEM meshes (Table 5.3) and the size of the patches (Table 5.4). The size and the number of the patches mainly depend on the number of the GNSS/Levelling points that are available over the area of interest. It may be expected that with the points from the national densifications of the EVRS, a DFHRS with a quality of approximately three centimetres could be computed, in analogy with the DFHRS from Germany, [chapter 5.7.1], where 10 km meshes were used.

With the concept of the DFHRS, a mathematical model has been found that enables the optimal adjustment of HRS related geodetic observations. The FEM concept further enables the production of HRS databases in a designed quality. By varying the mesh sizes as well as the number and size of geoid patches, any accuracy may be reached in theory. In practical applications, the number, the density and the quality of the available geodetic observations is the third design parameter.

A rigorous two-step adjustment is reached, if proper correlation functions are applied for approximating the stochastic model of gravimetric geoid databases. The investigations that are discussed in section 5.4.2 show the effect of a significantly increased accuracy when applying such functions. In addition, so-called geoid patches may be introduced to eliminate long-wave systematic effects in gravimetric (quasi)geoid models. The parameters,  $\mathbf{d}$ , that are modelled for carrying this refinement, may be applied for height anomalies,  $\zeta$ , or geoid heights,  $N$ , respectively, together with the gravimetric deflections from the vertical,  $\xi$  and  $\eta$ , if this information was derived from the same potential model. In any other case, they may still be applied for observation groups of the same kind.

In (Jäger 2002; Jäger and Schneid 2002) the mathematical equivalence of the two-step adjustment and the direct use of gravity observation was presented. However, there could be cases, where the use of gravity information was required.

The traditional way of gravimetric HRS determination is based on integral equations, see chapter 4. In recent years, point mass models have been applied in some projects. So the first steps towards least squares approaches were made. On the other hand, the point mass models have been applied using the RRT concept, so the quality of the computed models also depends on the geopotential model used and the mathematical techniques that were applied within the RRT, for example, for deriving a grid of the gravity anomalies. In theory, the gravity may be applied directly, without any reduction or grid interpolation. So a concept that incorporates gravity information into the adjustment using the DFHRS concept would be a goal, because for the first time a statistically controlled processing of such data would be enabled.

A concept that is an upcoming tool in geophysical applications is called the “Spherical Cap Harmonic analysis”, SCH. It may be seen as a generalised spherical harmonic analysis, because it may be applied in areas of limited extension.

The theory and the application of SCH is the topic of the following chapter in this thesis. The respective observation equations for a least squares adjustment are derived, and numerical examples are presented.

## Chapter 6

### Spherical Cap Harmonics - SCH

#### 6.1 Introduction

In the previous chapter, concepts for the determination of the HRS have been described and the advantages and disadvantages have been stated. In recent years, two different methods used to combine different observations types in one model have been derived. One approach, which has been applied in several projects for precise HRS determination, is based on a combined least squares adjustment of gravity observations and height anomalies, the point mass method e.g. Liebsch et. al. (2005). Although the concept of point mass modelling should be appropriate for direct application, it is usually applied together with the Remove-Restore-Technique. This approach gives a mathematically correct solution.

In 1985, Haines introduced a new method, the so-called “Spherical Cap Harmonic Analysis”, SCH for approximating potential fields (Haines, 1985). Since then, this method has successfully been applied in geophysics (Kotzè, 2001; Amm, 1998; Amm and Viljanen, 1999; Korte, 1999) and in geodesy (Jiangchen et al., 1995; De Santis and Falcone, 1995; Jäger and Schneid, 2006a; Jäger and Schneid, 2006b). From Haines’ papers as well as from De Santis and Torta (1997) it is possible to see that the origins from SCH-analysis are older (e.g. Smythe 1939; Kelvin and Tait, 1896).

The goal of the SCH-concept, in contrast to that of “ordinary” Spherical Harmonics, SH, is that it is to represent completely the potential in limited areas.

In the following subsections, the adaptation of the SCH-concept for the combined adjustment of height anomalies,  $\zeta$ , gravity disturbances,  $\delta g$ , and deflections from the vertical,  $\xi$  and  $\eta$ , is derived. The definition of the spherical cap and the boundary conditions are explained and the observation equations for the estimation of the SCH-coefficients are described. In addition, practical examples are computed and the results of these applications are discussed.

## 6.2 Definition and geo-referencing of the spherical cap

The spherical cap is determined by an earth-fixed, geocentric, spherical cone (fig. 6.1). The size of the cap is given with the half angle  $\mathcal{G}_0^c$ , and the cap-pole is geo-referenced with global spherical geocentric co-ordinates,  $\theta_0$ ,  $\lambda_0$ , and  $r_0$  (fig. 2.6).

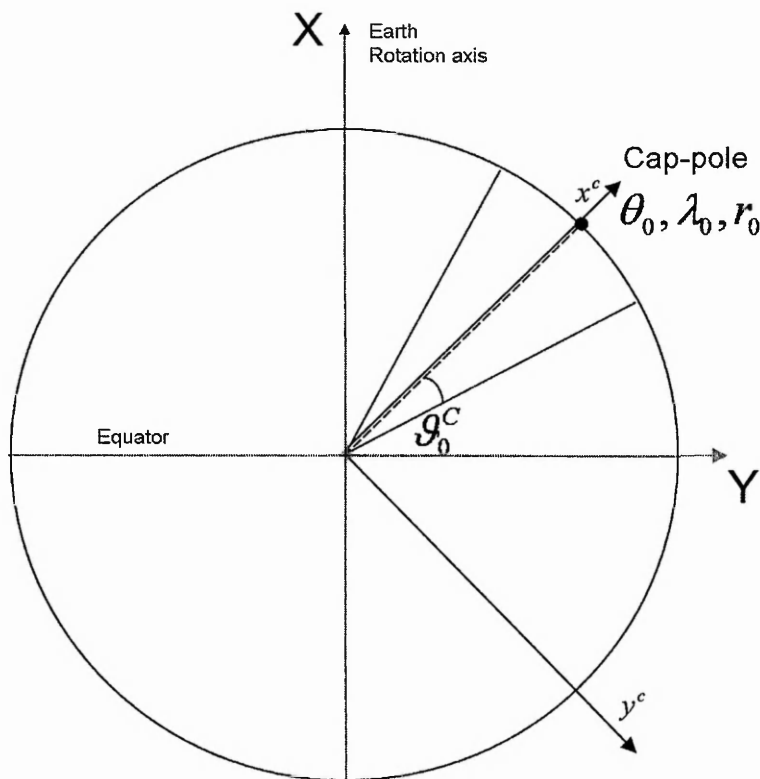


**Fig. 6.1:** Definition and georeferencing of the spherical cap

The radius,  $r_0$ , may be chosen to be identical to the major axis of the reference ellipsoid. We will see later that there are numerical advantages in choosing the radius to suit the location. The centre of the cap is the pole of a local spherical polar co-ordinate system. The local co-ordinates of a point, P, referred to the cap-pole, may now be found by means of the following computations.

First, the geocentric cartesian co-ordinates,  $x$ ,  $y$  and  $z$ , are rotated into the local cartesian system of the cap,  $x^c$ ,  $y^c$ ,  $z^c$ :

$$\begin{bmatrix} x^c \\ y^c \\ z^c \end{bmatrix} = \begin{bmatrix} -\cos \theta_0 \cos \lambda_0 & -\cos \theta_0 \sin \lambda_0 & \sin \theta_0 \\ -\sin \lambda_0 & \cos \lambda_0 & 0 \\ \sin \theta_0 \cos \lambda & \sin \theta_0 \sin \lambda & \cos \theta_0 \end{bmatrix} \cdot \begin{bmatrix} x \\ y \\ z \end{bmatrix} \quad (6-1)$$

The local co-ordinates,  $\varrho^c, \alpha^c, r^c$  in the system of the spherical cap (fig. 6.1) may now be expressed by the following relationships

$$r^c = \sqrt{x^c \cdot x^c + y^c \cdot y^c + z^c \cdot z^c} \quad (6-2a)$$

$$\cos \varrho^c = \frac{z^c}{r^c} \quad (6-2b)$$

$$\sin \varrho^c = \frac{\sqrt{x^c \cdot x^c + y^c \cdot y^c}}{r^c} \quad (6-2c)$$

$$\sin \alpha^c = \frac{y^c}{\sqrt{x^c \cdot x^c + y^c \cdot y^c}} \quad (6-2d)$$

$$\cos \alpha^c = \frac{x^c}{\sqrt{x_c^2 + y_c^2}} \quad (6-2e)$$

### 6.3 Validation of the SCH concept

Global gravitational potential models are usually expanded in SH coefficients. For local applications, the method is suboptimal. The base functions of this application do not form an orthogonal base over arbitrary areas. In contrast to “ordinary” SH, spherical cap harmonics are suitable for approximation of the potential field over a limited area, the spherical cap. This is due to the fact, that orthogonal base functions may be generated over the area of the cap (Haines, 1985).

For the following validation of the SCH-concept, we must first go back to equation (2-47). The anomalous potential,  $T$ , may be written as a truncated series of SH-coefficients

$$T = \sum_{n=0}^{\infty} \sum_{m=0}^n T_{n,m}(\theta, \lambda, r) \quad (6-3a)$$

with

$$T_{n,m} = \frac{GM}{a} \left( \frac{a}{r} \right)^{n+1} (C_{n,m} \cos(m\lambda) + S_{n,m} \sin(m\lambda)) \cdot P_{n,m} \cos \theta \quad (6-3b)$$

Equation (6-3a) is a solution of Laplace's equation, in spherical co-ordinates. It is found by separating the variables and solving the individual eigenvalue problems (e.g. Kautzleben, 1965). The eigenvalues,  $m$  and  $n$ , are determined by boundary conditions.

The main requirement of the actual problem is that a differentiable function,  $T$ , is to be represented over the area of a spherical cap in terms of functions of the form given with (6-3b).

The eigenvalues,  $n(n+1)$  and  $m$ , have to be computed in a way, that the terms containing  $\theta$  and  $\lambda$  in the functions  $T_{n,m}$  (6-3b) can be summed or integrated to give a representation of  $T$  (6-3a). This may again be done by considering boundary conditions

For the longitude  $\lambda$ , over a cap, where  $\lambda$  may reach any numerical value the following equations must hold:

$$T_{n,m}(\theta, \lambda, r) = T_{n,m}(\theta, \lambda + 2\pi, r) \quad (6-4a)$$

$$\frac{\partial T_{n,m}(\theta, \lambda, r)}{\partial \lambda} = \frac{\partial T_{n,m}(\theta, \lambda + 2\pi, r)}{\partial \lambda}. \quad (6-4b)$$

These conditions force  $m$  to be real and integer. In addition, all coefficients  $S_{n,0}$  have to be zero. The solution for the conditions (6-4a, b) is the harmonic oscillator in  $\lambda$  (6-3b), well known from the Fourier series expansion, which holds for both, the representation by ordinary SH as well as for harmonics over a spherical cap. In the local co-ordinate system of the cap, this reads as:

$$T_{n,m}(\vartheta^c, \alpha^c, r^c) = T_{n,m}(\vartheta^c, \alpha^c + 2\pi, r^c) \quad (6-5a)$$

$$\frac{\partial T_{n,m}(\vartheta^c, \alpha^c, r^c)}{\partial \alpha^c} = \frac{\partial T_{n,m}(\vartheta^c, \alpha^c + 2\pi, r^c)}{\partial \alpha^c}. \quad (6-5b)$$

The boundary condition in the co-latitude,  $\theta$ , is that at  $\theta = 0$ :

$$\frac{\partial T_{n,m}(\theta, \lambda, r)}{\partial \theta} = 0 \quad \text{for } m = 0 \quad (6-6a)$$

$$T_{n,m}(\theta, \lambda, r) = 0 \quad \text{for } m \neq 0. \quad (6-6b)$$

The meaning of this condition is, that the potential at the pole, where  $\theta = 0$ , is independent from the longitude,  $\lambda$ . The condition is satisfied by Legendre functions of the first kind (e.g. Kautzleben, 1965). Again, this condition is similar to the case of a representation over a spherical cap:

$$\frac{\partial T_{n,m}(\vartheta^c, \alpha^c, r^c)}{\partial \vartheta^c} = 0 \quad \text{for } m = 0 \quad (6-7a)$$

$$T_{n,m}(\vartheta^c, \alpha^c, r^c) = 0 \quad \text{for } m \neq 0. \quad (6-7b)$$

The boundary condition on  $\theta$  at  $\theta = \theta_0$  is the same in the case of ordinary SH, where  $\theta = \pi$ :

$$\frac{\partial T_{n,m}(\theta_0 = \pi, \lambda, r)}{\partial \theta} = 0 \quad \text{for } m = 0 \quad (6-8a)$$

$$T_{n,m}(\theta_0 = \pi, \lambda, r) = 0 \quad \text{for } m \neq 0. \quad (6-8b)$$

This condition forces  $n$  to be an integer and real and the Legendre functions reduce to the (associated) Legendre Polynomials,  $P_{n,m} \cos(\theta)$  in equation (6-3b).

For a spherical cap with the half-angle  $\vartheta_0 \neq \pi$ , the potential as well as the derivative with respect to the latitude,  $\vartheta$ , must be functions of the position,  $\vartheta^c, \alpha^c, r^c$ :

$$T(\vartheta_0^c, \alpha^c, r^c) = f(\alpha^c, r^c) \quad (6-9a)$$

$$\frac{\partial T(\vartheta_0^c, \alpha^c, r^c)}{\partial \vartheta^c} = g(\alpha^c, r^c) \quad (6-9b)$$

The functions, f and g, of course have to satisfy the same conditions with respect to  $r^c$  and  $\alpha^c$  as T and  $\partial T/\partial \mathcal{G}$ , respectively. Haines (1985) showed that the conditions (6-9a, b) hold if the values for n are chosen in a way that :

$$\frac{\partial T_{n,m}(\mathcal{G}^c, \lambda, r)}{\partial \mathcal{G}^c} = 0 \quad (6-10a)$$

$$T_{n,m}(\mathcal{G}^c, \lambda^c, r^c) = 0. \quad (6-10b)$$

These conditions are fulfilled by the associated Legendre functions of the first kind, with real, but not necessarily integer degree, n. Since  $T_{n,m}$  and  $\partial T_{n,m}/\partial \mathcal{G}$  cannot simultaneously be zero, Haines showed, that (6-10a) enables (6-9a) to hold, while (6-10b) enables (6-9b) to hold (Haines, 1985). The different real values of the degrees, n, that satisfy the conditions, depend separately on m. They are therefore denoted by  $n_k(m)$ , where the subscript, k, is chosen to order the various roots, n, in a way like the integer values of the degrees, n, in ordinary SH.

The function, now denoted as  $T_{n_k(m),m}$ , is divided into two infinite sets of base functions, one where (k-m) is even and one with (k-m) is odd, such that the functions in each set are mutually orthogonal over the spherical cap. The  $n_k(m)$  for which (k-m) is even are the roots of (6-10a) and the  $n_k(m)$  for which (k-m) is odd are the roots of (6-10b), if the respective equation is considered to be a function of n.

The boundary condition for the radial distance, r, is the same for both, the SH and the SCH representation. For SH we have:

$$\lim_{r \rightarrow \infty} T_{n,m}(\theta, \lambda, r) = 0 \quad (6-11a)$$

and for SCH:

$$\lim_{r^c \rightarrow \infty} T_{n_k(m),m}(\mathcal{G}^c, \alpha^c, r^c) = 0. \quad (6-11b)$$

In geodetic literature, for instance Hofmann-Wellenhof and Moritz (2005), it is usually stated, that this condition requires n to be not less than zero. Haines remarks, that there is also a

harmonic of order  $m=0$  and degree  $n=-1$ . It is simply a constant term that cannot be determined, if only derivatives of the potential may be observed. However, the existence of this harmonic will not be discussed in this thesis, as in many practical applications, SH representations of the gravitational potential have been computed without modelling this constant.

Without loss of generality, the anomalous gravity potential,  $T$ , represented by harmonic coefficients over a spherical cap may finally be written as:

$$T = \frac{GM}{r_0^c} \sum_{k=0}^{\infty} \sum_{m=0}^k \left( \frac{r_0^c}{r^c} \right)^{n_k(m)+1} (C_{k,m}^c \cos(m\alpha^c) + S_{k,m}^c \sin(m\alpha^c)) P_{n_k(m),m}(\cos \vartheta^c) \quad (6-12)$$

In the harmonic coefficients,  $C_{k,m}^c$  and  $S_{k,m}^c$ , are dimensionless. If the coefficients are determined by means of least-squares estimation, there are some numerical advantages when estimating the harmonic coefficients in a way that they have the same dimension as the potential.

Equation (6-12) is therefore rewritten:

$$T = \sum_{k=0}^{\infty} \sum_{m=0}^k \left( \frac{r_0^c}{r^c} \right)^{n_k(m)+1} (A_{k,m}^c \cos(m\alpha^c) + B_{k,m}^c \sin(m\alpha^c)) P_{n_k(m),m}(\cos \vartheta^c) \quad (6-13)$$

The coefficients are further annotated with the integer  $k$ , and the coefficients  $B_{k,0}^c$  are zero.

The height anomaly,  $\zeta$ , derived from the spherical cap harmonics  $A_{k,m}^c$  and  $B_{k,m}^c$  reads as:

$$\zeta = \frac{1}{\gamma} \sum_{k=0}^{\infty} \sum_{m=0}^k \left( \frac{r_0^c}{r^c} \right)^{n_k(m)+1} (A_{k,m}^c \cos(m\alpha^c) + B_{k,m}^c \sin(m\alpha^c)) P_{n_k(m),m}(\cos \vartheta^c), \quad (6-13a)$$

where the normal gravity,  $\gamma$ , is still related to the reference ellipsoid.

The derivatives of  $T$ , the radial gravity disturbance,  $\delta g_r^c$ , and the disturbances in the direction of  $\vartheta$  and  $\alpha$ , in the co-ordinate system of the local cap, are now:

$$\delta g_r^c = \frac{1}{r^c} \sum_{k=0}^{\infty} \sum_{m=0}^k \left( \frac{r_0^c}{r^c} \right)^{n_k(m)+1} (n_k(m)+1) (A_{k,m}^c \cos(m\alpha^c) + B_{k,m}^c \sin(m\alpha^c)) P_{n_k(m),m}(\cos \vartheta^c) \quad (6-14)$$

$$\delta g_{\theta}^c = \frac{1}{r^c} \sum_{k=0}^{\infty} \sum_{m=0}^k \left( \frac{r_0^c}{r^c} \right)^{n_k(m)+1} (A_{k,m}^c \cos(m\alpha^c) + B_{k,m}^c \sin(m\alpha^c)) \frac{dP_{n_k(m),m}(\cos \theta^c)}{d\theta^c} \quad (6-15a)$$

$$\delta g_{\lambda}^c = -\frac{1}{r^c \sin \theta^c} \sum_{k=0}^{\infty} \sum_{m=0}^k \left( \frac{r_0^c}{r^c} \right)^{n_k(m)+1} (-A_{k,m}^c \sin(m\alpha^c) + B_{k,m}^c \cos(m\alpha^c)) \cdot m \cdot P_{n_k(m),m}(\cos \theta^c) \quad (6-15b)$$

In the case of ordinary SH representation, it can be shown, that the degree, n, is restricted to being an integer. This follows from the orthogonality relationships of the eigenfunction solution of the co-latitude  $\theta$ . This is the associated Legendre Polynomial,  $P_{n,m}(\cos \theta)$  (Kautzleben, 1965, p.39f). In the case of a SCH representation there are two eigenvalue problems in the co-latitude,  $\theta^c$ , one with the boundary conditions (6-7a, b and 6-10a) and the other with (6-7a, b and 6-10b). The  $T_{n_k(m)}(\theta^c, \alpha^c, r^c)$  may thus be divided into two infinite sets of base functions, one where (k-m) is even and one where (k-m) is odd, so that each function is orthogonal over the spherical cap. This can easily be proved by computing

$$\int_0^{\theta_0} P_{n_j(m)}(\cos \theta) P_{n_k(m)}(\cos \theta) \sin \theta \cdot d\theta; \quad j \neq k, \quad (6-16)$$

where (j-m) and (k-m) are either both odd or are both even.

Finally, it can be shown that equations (6-9a, b) follow from (6-10a, b). Therefore, the summation terms are re-ordered. This is correct, because of the property of the Legendre functions (Kautzleben, 1965),

$$P_{n,m}(\cos \theta) = 0; \quad \text{for } m > n \quad (6-17)$$

In a first step, the expression (6-10b), which is satisfied when (k-m) is odd, is substituted into (6-10a). This gives

$$T(\theta_0^c, \alpha^c, r^c) = \sum_{m=0}^{\infty} \sum_{\substack{k=m \\ k-m=\text{even}}}^{\infty} \left( \frac{r_0^c}{r^c} \right)^{n_k(m)+1} (A_{k,m}^c \cos(m\alpha^c) + B_{k,m}^c \sin(m\alpha^c)) P_{n_k(m),m}(\cos \theta_0^c) \quad (6-18a)$$

Rewriting the SCH-coefficients, in this way

$$a_m = \sum_{\substack{k=m \\ k-m=\text{even}}}^{\infty} \left( \frac{r_0^c}{r^c} \right)^{n_k(m)+1} A_{k,m}^c \cos(m\lambda) P_{n_k(m),m}(\cos \mathcal{G}_0^c) \quad (6-18b)$$

and

$$b_m = \sum_{\substack{k=m \\ k-m=\text{even}}}^{\infty} \left( \frac{r_0^c}{r^c} \right)^{n_k(m)+1} B_{k,m}^c \sin(m\lambda) P_{n_k(m),m}(\cos \mathcal{G}_0^c) \quad (6-18c)$$

we finally obtain

$$T(\mathcal{G}_0^c, \alpha^c, r^c) = f(\alpha^c, r^c) = \sum_{m=0}^{\infty} (a_m \cos(m\alpha^c) + b_m \sin(m\alpha^c)) \quad (6-18d)$$

This is the proof that  $T(\mathcal{G}^c, \alpha^c, r^c)$  can be equated to function  $f(\alpha^c, r^c)$ , with the same condition applied to  $r$  and  $\alpha$  as in the function,  $T$ . The coefficients,  $a_m$  and  $b_m$ , must be Fourier coefficients of the orthogonal eigenfunction expansion of  $\alpha$  in the function  $f(\alpha^c, r^c)$ . (c.f. Haines, 1985).

In a similar way, it can be shown that

$$\frac{dT(\mathcal{G}_0^c, \alpha^c, r^c)}{d\mathcal{G}^c} = \sum_{m=0}^{\infty} \left( \frac{r_0^c}{r^c} \right)^{n_k(m)+1} \sum_{\substack{k=m \\ k-m=\text{even}}}^{\infty} (A_{k,m}^c \cos(m\alpha^c) + B_{k,m}^c \sin(m\alpha^c)) \frac{dP_{n_k(m),m}(\cos \mathcal{G}_0^c)}{d\mathcal{G}^c} \quad (6-19a)$$

$$\frac{dT(\mathcal{G}_0^c, \alpha^c, r^c)}{d\mathcal{G}^c} = g(\alpha^c, r^c) = \sum_{k=0}^{\infty} (c_m \cos(m\alpha^c) + d_m \sin(m\alpha^c)) \quad (6-19b)$$

where

$$(6-19c)$$

$$c_m = \sum_{k=m+1}^{\infty} \left( \frac{r_0^c}{r^c} \right)^{n_k(m)+1} \frac{dP_{n_k(m),m} \cos(\mathcal{G}^c)}{d\mathcal{G}} A_{k,m} \quad (6-19d)$$

and

$$d_m = \sum_{k=m+1}^{\infty} \left( \frac{r_0^c}{r^c} \right)^{n_k(m)+1} \frac{dP_{n_k(m),m} \cos(\mathcal{G}^c)}{d\mathcal{G}} B_{k,m}$$

The harmonic coefficients,  $A_{k,m}^C$  and  $B_{k,m}^c$ , could now be determined by means of a least-squares estimation, applying the respective observation equations (6-13, 6-14 and 6-15a, b). However, before the system of normal equation can be set up, the roots,  $n$ , of the functions (6-10a, b) have to be found.

From (6-3b) it follows, that  $T_{n(k),m}(\mathcal{G}^c, \lambda^c, r^c)$  and  $\partial T_{n,m}(\mathcal{G}^c, \lambda^c, r^c) / \partial \mathcal{G}$  can only be zero if

$$P_{n_k(m)}(\cos \mathcal{G}^c) = 0; \quad \text{for } (k - m) \text{ is odd} \quad (6-20a)$$

$$\frac{dP_{n_k(m)}(\cos \mathcal{G}^c)}{d\mathcal{G}} = 0; \quad \text{for } (k - m) \text{ is even} \quad (6-20b)$$

The real degrees,  $n_k(m)$ , that satisfy the conditions (6-10a, b) are the roots of the associated Legendre functions (6-20a) and the derivatives with respect to co-latitude (6-20b), respectively, if the respective expressions are considered to be functions of  $n_k(m)$ . Before the roots can be solved a way to compute the Legendre functions of real degree has to be found first.

#### 6.4 Computing the associated Legendre functions of real degree

The Legendre function  $P_{n,m}(t)$  is the solutions of the Laplace differential equation in the co-latitude direction. It is defined by

$$P_{n,m}(t) = \frac{1}{2^n n!} (1-t^2)^{\frac{m}{2}} \frac{d^{n+m}}{dt^{n+m}} (t^2-1)^n. \quad (6-21)$$

For  $m=0$  the function reduces to the Legendre polynomials:

$$P_{n,0}(t) = P_n(t) = \frac{1}{2^n n!} \frac{d^n}{dt^n} (t^2 - 1)^n, \quad (6-22)$$

where the quantity,  $t$ , is a substitute for  $\cos \theta$ .

Because of the factorial function in the equations (6-21 and 6-22) there are numerical problems when applying such formulae for the computation of  $P_{n,m}$ . The numerical computation becomes more effective, if the Legendre polynomials are normalised by some means. In geodetic applications they are usually “fully” normalised (Hofmann-Wellenhof and Moritz, 2005). This reads:

$$\bar{P}_{n,m}(t) = \sqrt{k(2n+1) \frac{\Gamma(n-m+1)}{\Gamma(n+m+1)}} P_{n,m}(t) \quad (6-23)$$

With given starting values, for the degrees 0, 1 and 2, the fully normalised associated Legendre Polynomials may be computed very effectively by means of the recursion formula: (e.g. Wenzel, 1985)

$$\begin{aligned} \bar{P}_{n,m}(\cos \theta) = & \sqrt{\frac{(2n+1)(2n-1)}{(n+m)(n-m)}} \cos \theta \cdot \bar{P}_{n-1,m}(\cos \theta) \\ & - \sqrt{\frac{(2n+1)(n+m-1)(n-m-1)}{(2n-3)(n+m)(n-m)}} \cdot \bar{P}_{n-2,m}(\cos \theta). \end{aligned} \quad (6-24)$$

Wenzel investigated the above formula and found unacceptable errors for degrees  $n > 2200$ . In some applications, the Clenshaw summation is used to compute the associated Legendre functions (e.g. Tscherning and Pöder, 1982). Recent research concerning this topic was published by Holmes and Featherstone (2000). A modified recursion was introduced to enable computation of the associated Legendre functions up to degree and order 2700. The problems with such high degrees are only of a numerical kind, and appear as underflows or overflows in the numerical capacity of the personal computers used.

For a SCH representation of the gravitational potential, the above recursion formulae may also be used, as they hold for real  $n$  as well. However, starting values have to be computed directly, so a method to compute the  $P_{n,m}(t)$  with real degree,  $n$ , has to be found first.

It is well known, e.g. Hobson (1965), and Kautzleben (1965) that the Legendre functions  $P_n(t)$  may be represented by the Gauss hypergeometric function

$$P_n(t) = F\left(-n, n+1; 1; \frac{1-t}{2}\right) \quad (6-25)$$

With the definition of the associated Legendre functions (6-21) and the following property of the hypergeometric function

$$\frac{d}{dz} F(a, b; c; z) = \frac{ab}{c} F(a+1, b+1; c+1; z), \quad (6-26)$$

a representation of the associated Legendre functions can be found that enables computation with a real degree,  $n$  (Hwang and Chen, 1997):

$$P_{n,m}(t) = \frac{1}{2^m m!} \frac{\Gamma(n+m+1)}{\Gamma(n-m+1)} (1-t^2)^{\frac{m}{2}} \cdot F\left(m-n, m+n+1; m+1; \frac{1-t}{2}\right) \quad (6-27)$$

This formula could now be applied to create a system of normal equations for the estimation of the SCH coefficients by a least-squares adjustment of related geodetic observations. Actually, it can be applied, but again numerical underflows and overflows occur, resulting from the numerical precision of the personal computer.

An algorithm that avoids numerical under- or overflows was published by Olver, Smith and Lozier, (1981) and Olver and Smith (1983). Within their research extended range arithmetic was developed and published, that enables the computation of extremely high degree Legendre functions with  $n > 10000$ . The algorithm has already been used for the SCH-representation of geomagnetic fields (Thebault et al. 2004), where an accuracy of 15 digits was reached for a real  $n > 9000$ , with half-angle  $\mathcal{G}_0 = 5^\circ$ .

## 6.5 Finding the roots of the associated Legendre functions

The computation of the roots of the associated Legendre functions and the hypergeometric function, respectively, has been the topic of many mathematical investigations (e.g. Pal

1919a, 1920b; Hobson, 1965). It is therefore proposed to make use of numerical methods, for example bracketing and bisection (Press, et al., 2002).

The Legendre function,  $P_{n,m}(\cos\theta)$  has  $(n - m)$  roots in the range of  $0 \leq \theta \leq \frac{\pi}{2}$ . To provide the same base function for the SCH representation as for SH representation, the roots  $n_k(m)$  have to be computed in such a way that  $P_{n_k(m),m}(\cos\theta^c)$  has  $(k-m)$  roots in the ranges  $0 \leq \theta^c \leq \theta_0^c$  (fig. 6.2).

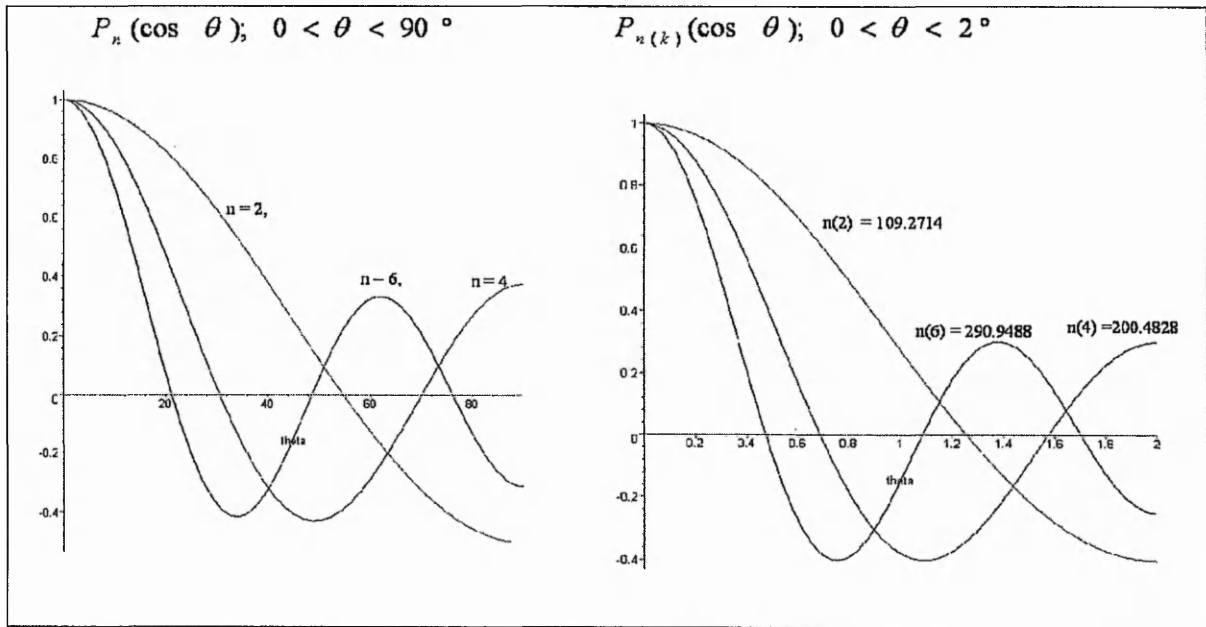


**Fig. 6.2:** Left: The Legendre functions,  $P_2, P_4$  and  $P_6$ . Right: The Legendre functions,  $P_{n(2)}, P_{n(4)}$  and  $P_{n(6)}$ ,

The degree  $n_k(m)$  is approximately given by

$$n_k(m) \approx \frac{\pi}{2\theta_0^c} \left( k + \frac{1}{2} \right) - \frac{1}{2} \tag{6-28}$$

The respective wavelength,  $\omega$ , of the SCH is

$$\omega = \frac{2\pi \cdot r_0}{n_k(m)} \tag{6-29}$$

The well known SH-Model, EGM96, (Lemoine et. al, 1997.) was computed with a maximum degree  $n=360$ . The maximum index  $k_{\max}$ , which is the respective quantity for a SCH-Model, for a cap with the half angle  $\vartheta_0^c = 2^\circ$  may be found approximately by

$$\begin{aligned} k_{\max} &\approx \frac{\vartheta_0^c}{90^\circ} \left( \frac{360^\circ}{\omega_{\min}} + \frac{1}{2} \right) - \frac{1}{2} \\ &\approx \frac{\vartheta_0^c}{90^\circ} \left( n(k) + \frac{1}{2} \right) - \frac{1}{2} \end{aligned} \quad (6-30)$$

with  $\vartheta_0^c$  in degree.

## 6.6 Rotation of the gravity vector

For the least squares adjustment of the observed gravity data, two rotations have to be calculated, to find the gravity disturbance,  $\delta g^c$ , referred to the system of the spherical cap. If the deflections from the vertical,  $\xi$  and  $\eta$ , are known, the astronomical co-ordinates,  $\Phi$  and  $\Lambda$ , are found from the relationships (2-28a, b). If the deflections are not known, the gravity vector is approximated.

$$\mathbf{g} = -g \begin{bmatrix} \cos(\Phi) \cos(\Lambda) \\ \cos(\Phi) \sin(\Lambda) \\ \sin(\Phi) \end{bmatrix} \approx -g \begin{bmatrix} \cos(\varphi) \cos(\lambda) \\ \cos(\varphi) \sin(\lambda) \\ \sin(\varphi) \end{bmatrix} \quad (6-31)$$

The gravity disturbance vector is obtained by subtracting the normal gravity vector from the actual gravity vector. This reads as:

$$\delta \mathbf{g}_P = \mathbf{g}_P - \gamma_P. \quad (6-32)$$

In a first step, the gravity vector is rotated from the geodetic ellipsoidal co-ordinate system into the geocentric earth fixed Cartesian co-ordinate system:

$$\begin{aligned}
 \begin{bmatrix} \delta g_x \\ \delta g_y \\ \delta g_z \end{bmatrix} &= \begin{bmatrix} -\sin(\Phi)\cos(\Lambda) & -\sin(\Lambda) & \cos(\Phi)\cos(\Lambda) \\ -\sin(\Phi)\sin(\Lambda) & \cos(\Lambda) & \cos(\Phi)\sin(\Lambda) \\ \cos(\Phi) & 0 & \sin(\Phi) \end{bmatrix} \cdot \delta g \cdot \begin{bmatrix} \cos(\varphi)\cos(\Lambda) \\ \cos(\varphi)\sin(\Lambda) \\ \sin(\varphi) \end{bmatrix} \\
 &\approx \begin{bmatrix} -\sin(\varphi)\cos(\lambda) & -\sin(\lambda) & \cos(\varphi)\cos(\lambda) \\ -\sin(\varphi)\sin(\lambda) & \cos(\lambda) & \cos(\varphi)\sin(\lambda) \\ \cos(\varphi) & 0 & \sin(\varphi) \end{bmatrix} \cdot \delta g \cdot \begin{bmatrix} \cos(\varphi)\cos(\lambda) \\ \cos(\varphi)\sin(\lambda) \\ \sin(\varphi) \end{bmatrix}
 \end{aligned} \tag{6-33}$$

The second rotation relates the cartesian gravity vector,  $\delta g$ , resulting from (6-33) to the pole of the local spherical cap:

$$\begin{bmatrix} \delta g_x^c \\ \delta g_y^c \\ \delta g_z^c \end{bmatrix} = \begin{bmatrix} -\cos(\theta_0)\cos(\lambda_0) & -\cos(\theta_0)\sin(\lambda_0) & \sin(\theta_0) \\ -\sin(\lambda_0) & \cos(\lambda_0) & 0 \\ \sin(\theta_0)\cos(\lambda) & \sin(\theta_0)\sin(\lambda_0) & \cos(\theta_0) \end{bmatrix} \cdot \begin{bmatrix} \delta g_x \\ \delta g_y \\ \delta g_z \end{bmatrix} \tag{6-34}$$

Finally, the disturbing gravity vector, in the system of the spherical co-ordinates of the local cap is found by a third rotation:

$$\begin{bmatrix} \delta g_\vartheta^c \\ \delta g_\alpha^c \\ \delta g_r^c \end{bmatrix} = \begin{bmatrix} -\cos(\vartheta^c)\cos(\alpha^c) & -\cos(\vartheta^c)\sin(\alpha^c) & \sin(\vartheta^c) \\ -\sin(\alpha^c) & \cos(\alpha^c) & 0 \\ \sin(\vartheta^c)\cos(\alpha^c) & \sin(\vartheta^c)\sin(\alpha^c) & \cos(\vartheta^c) \end{bmatrix} \cdot \begin{bmatrix} \delta g_x^c \\ \delta g_y^c \\ \delta g_z^c \end{bmatrix} \tag{6-35}$$

With the observation equations (6-14, 6-15a, b) and the gravity disturbance vector in the system of the local cap (6-35), the spherical cap harmonic coefficients  $A_{k,m}^c$  and  $B_{k,m}^c$  may now be estimated by means of least squares techniques.

## 6.7 Modification of the spherical cap

In 1991, De Santis published a modification of the SCH concept called ‘‘Translated origin spherical cap harmonic analysis – TOSCA’’ (De Santis, 1991). The concept of TOSCA enables the approximation of a potential field by means of SCH coefficients related to a new reference system with a vertical translated origin, along the radius from the centre of the Earth (fig. 6.3). The co-ordinates  $\bar{\vartheta}^c, \alpha^c, \bar{r}^c$  of a point, related to the translated origin, are found by changing (6-2a, b and c) into

$$\bar{r}^c = \sqrt{x^c \cdot x^c + y^c \cdot y^c + \bar{z}^c \cdot \bar{z}^c} \quad (6-36a)$$

$$\cos \bar{\vartheta}^c = \frac{\bar{z}^c}{\bar{r}^c} \quad (6-36b)$$

$$\sin \bar{\vartheta}^c = \frac{\sqrt{x^c \cdot x^c + y^c \cdot y^c}}{\bar{r}^c} \quad (6-36c)$$

with

$$\bar{z}^c = z^c - \Delta r$$

and  $\Delta r$  is the translation of the origin in the vertical direction (fig 6.3).

The application of the TOSCA concept reduces the computational effort required to reach a spatial resolution.

As the new latitude  $\bar{\vartheta}^c$  always has a larger numerical value than  $\vartheta^c$  it is obvious that the numerical value of the maximum degree  $n_k(m)$ , found by means of (6-28), reduces, if the potential is represented over a cap with a translated origin, while the minimum wavelength  $\omega$ , (6-29) stays the same.

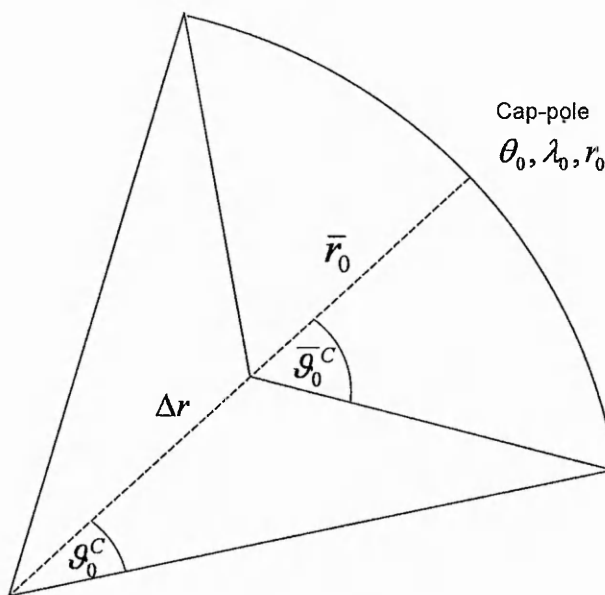


**Fig. 6.3:** Modification of the spherical cap according to the TOSCA concept

A numerically smaller degree  $n_k(m)$  also reduces the computation time dramatically, as the algorithm of Olver and Smith (1983) uses recurrence relations. The new Legendre functions are computed in the same way as in SCH, but in the new reference system. Obviously they are still solutions of Laplace's equation, because the latter does not change for any translation of the co-ordinate system.

### 6.8 Regularisation of the linear equation system

When computing the SCH coefficients by means of a least squares estimation, the same well known numerical difficulties as in computation of ordinary SH coefficients appear. The system of the normal equations becomes numerically unstable. In a number of test computations the condition number reached values of  $10^{30}$ . A linear equation system with such a condition may not be solved by inverting the matrix of normal equations,  $\mathbf{N}$  (5-35a, b), because of the limits in the numerical precision of a standard computer.

In geodetic applications a singular equation system is usually regularised by computing the Pseudo-Inverse, or Moore-Penrose-Inverse,  $\mathbf{N}^+$ , (Jäger et. al., 2006). In test computations, this method failed, because of numerical reasons. The eigenvalues of  $\mathbf{N}$  could not be determined in an acceptable accuracy. Also, some of the computed eigenvalues were negative.

In theory the most accurate method to solve an ill-conditioned linear equation system is the Singular Value Decomposition, SVD, (Press et. al. 2002). Unfortunately, this method may not be applied, as the SVD is dealing with the design matrix,  $\mathbf{A}$ , instead of the normal equation matrix,  $\mathbf{N}$ . In the current case of least squares estimation of SCH coefficients, the matrix  $\mathbf{A}$  reaches the dimensions of the introduced terrestrial observations,  $n$ , and the estimated unknowns,  $u$ . Therefore, it may be used only for areas with a very small extension.

Korte and Holme (2003) present a method for the regularisation of spherical cap harmonics, using the linear inversion method (Whaler and Gubbins, 1981, Gubbins, 1983). This method is comparable with a method that is used in geodetic applications.

In many projects used to determine SH coefficients to approximate the global potential, stochastic regularisation (Kaschenz, 2006) is applied. The linear equation system is regularised by adding the inverse of a covariance matrix  $\mathbf{C}_R$ , derived from a signal degree variance model to the matrix of normal equations (e.g. Wenzel 1985).

If this concept is applied for the determination of the SCH coefficients, the least-squares estimator reads as:

$$\mathbf{p} = \left( \mathbf{A}^T \cdot \mathbf{C}_{\parallel}^{-1} \cdot \mathbf{A} + \sigma^2 \cdot \mathbf{C}_{\mathbf{R}}^{-1} \right)^{-1} \cdot \mathbf{A}^T \cdot \mathbf{C}_{\parallel}^{-1} \cdot \mathbf{l} \quad (6-37)$$

In (6-37) the vector,  $\mathbf{p}$ , contains the SCH coefficients.  $\mathbf{C}_{\parallel}$  denotes the covariance matrix of the gravity field observations,  $\mathbf{l}$ , and  $\mathbf{A}$  is the design matrix. The matrix,  $\mathbf{C}_{\mathbf{R}}$ , is the introduced regularisation matrix with the signal degree variances on the diagonal, derived from an appropriate model, e.g. Tscherning and Rapp (6-38), and  $\sigma$  is introduced as a weight for  $\mathbf{C}_{\mathbf{R}}$ .

According to the signal degree variance model of Tscherning and Rapp, the variance  $\sigma_n^2$  for a degree,  $n$ , reads as:

$$\sigma_n^2 = \frac{A \cdot (n-1)}{(n-2) \cdot (n+B)} \cdot s^{n+2} \quad (6-38)$$

with

$$A = 425.28 \text{ mGal}^2$$

$$B = 25$$

$$s = 0.999617$$

It is obvious that the spherical cap harmonic coefficients, estimated by means of (6-38) are biased with respect to  $\sigma$  and  $\mathbf{C}_{\mathbf{R}}$ . Therefore, the generation of the regularisation matrix has to be done very carefully. It is possible to change the defining parameters  $A$ ,  $B$ , and  $s$  in (6-38) to get a matrix  $\mathbf{R}$ , which enables a numerically stable solution of the equation system, and gives a realistic degree variance model for the approximated gravity field in the local area of the spherical cap. The evaluation of the results may be done for example by means of variance component estimation.

The concept of the spherical cap harmonic analysis has been applied in a project in Baden-Württemberg, Southern Germany, for the approximation of local gravity fields and the derivation of height reference surfaces. The results of the different test computations are shown and discussed in the following chapter.

# Chapter 7

## Computation examples

### 7.1 Example 1: Representation of a spherical harmonic geopotential model

For the first computation example, the height anomalies,  $\zeta$ , as well as the gravity disturbances,  $\delta g$ , over an area in Baden-Württemberg were introduced into a combined least squares adjustment, for the estimation of spherical cap harmonic coefficients,  $\mathbf{A}_{k,m}^c$  and  $\mathbf{B}_{k,m}^c$ . The anomalies,  $\zeta$ , and the disturbances,  $\delta g$ , were derived from the EIGEN04 model (GFZ, 2007). The height anomalies,  $\zeta$ , vary in this area approximately from 48.8m to 50.4m and the gravity disturbances approximately from 18.0mGal to 70.0mGal. In total 1572 height anomalies and 1572 gravity disturbances were used in a common least squares adjustment, with the observation equations (6-13a, 6-14). The observations were introduced in two layers, at 100m and at 1000m altitude. The height anomalies were introduced with a-priori accuracy of  $\pm 0.2$  m and the gravity anomalies with  $\pm 10$  mGal. The half-angle of the spherical cap is  $0.6427^\circ$  and the radius is 6366285.95m. A maximum degree for the harmonic coefficients,  $\mathbf{A}_{k,m}^c$  and  $\mathbf{B}_{k,m}^c$ , of  $k=15$  was used to represent the EIGEN04 model. The maximum residuals as well as the computed RMS are listed in table 7.1.

In the next step, a grid of height anomalies,  $\zeta$ , and gravity disturbances,  $\delta g$ , at an altitude of 500m was computed from the estimated SCH-coefficients and compared with the same grid, computed from the EIGEN04 spherical harmonic model. The residuals as well as the RMS of the comparison are compiled in table 7.2.

As consequence of this investigation we can summarise, that the derivatives of a spherical harmonic geopotential model may be represented by harmonic coefficients over a spherical cap. The goal of the SCH-representation is to reduce to a very small number of unknowns that are required. This contrasts to the large number of unknowns that are required for ordinary spherical harmonic representations. In this example it is 225.

**Table 7.1:** Statistical result from the adjustment of EIGEN04 height anomalies and gravity disturbances

	$\zeta$ [m]	$\delta g$ [mGal]
Max residual	0.001	0.03
Min residual	-0.002	-0.034
RMS	$\sim 0.00045$	$\sim 0.007$

**Table 7.2:** Differences between a computed grid derived from the EIGEN04 and a grid derived from the SCH-representation

	$\zeta$ [m]	$\delta g$ [mGal]
Max residual	0.0025	0.013
Min residual	-0.0015	-0.024
RMS	$\sim 0.0005$	$\sim 0.004$

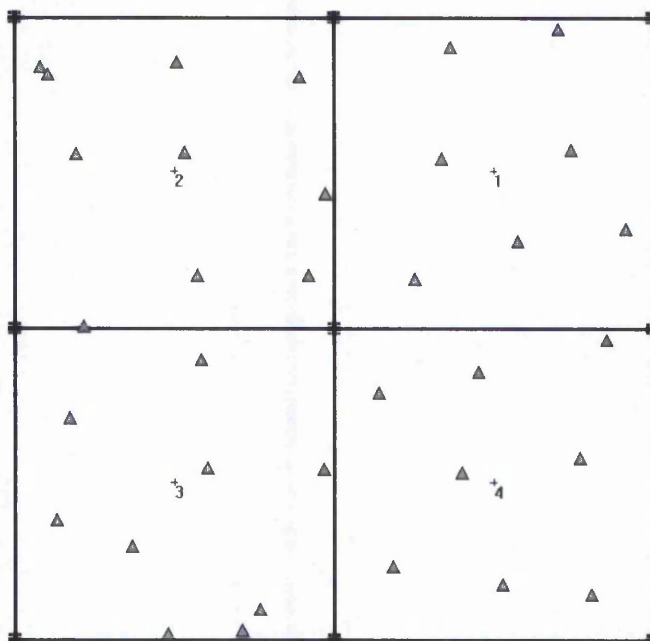


**Fig.7.1:** 34 points (triangles) are used to estimate correction parameters in 4 patches

## 7.2 Example 2: Combination of GNSS/levelling points and a geopotential model

The next computation example is concerned with the combination of GNSS/levelling points and a geopotential model. In an area of approximately 100km x 100km, 34 GNSS/levelling points as well as the EIGEN04 geopotential model were used to represent the HRS by SCH-coefficients. The GNSS/levelling points were made available from the state land service department of Baden-Württemberg.

In accordance to the DFHRS concept, four patches have been used, to eliminate systematic errors,  $\Delta T_{\zeta}$  and  $\Delta T_{\delta g}$ , in the EIGEN04 and to ensure a good fit to the HRS (fig.7.1). To apply the technique of geoid patching, a compatible parameterisation for the gravity disturbances has to be found. Therefore, the parameterisation for  $\Delta T_{\zeta}$  (4-19) is rewritten in spherical coordinates in the local system of the spherical cap.

$$\Delta T_{\zeta}(\mathbf{d}) = \sin(\vartheta^c) \cdot \cos(\alpha^c) \cdot u + \sin(\vartheta^c) \cdot \sin(\alpha^c) \cdot v + \cos(\vartheta^c) \cdot z \quad (7-1)$$

Using the relationship between spherical and Cartesian co-ordinates we now can write

$$\Delta T_{\zeta}(\mathbf{d}) = \frac{x^c}{r^c} \cdot u + \frac{y^c}{r^c} \cdot v + \frac{z^c}{r^c} \cdot z. \quad (7-2)$$

With the approximation c.f. (2-31a)

$$\delta g \approx -\frac{\partial T}{\partial r} \quad (7-3)$$

and applying Bruns' theorem (2-26) we finally obtain

$$\Delta T_g(\mathbf{d}) = \frac{x^c \gamma}{r^c \cdot r^c} \cdot u + \frac{y^c \gamma}{r^c \cdot r^c} \cdot v + \frac{z^c \gamma}{r^c \cdot r^c} \cdot z \quad (7-4)$$

Obviously, more complicated parametric models may be applied, for example with additional rotations.

The parametric models (7-2, 7-4) have been applied in a combined adjustment of 34 GNSS/levelling points (fig. 7.1) and the EIGEN04 geopotential model. The a-priori accuracy

of the height anomalies, measured in the GNSS/levelling points was 0.007m. The results of this computation are listed in table 7.3.

Summarising the results of this investigation it can be stated that SCH coefficients are generally suitable for parameterisation of the HRS in combination with GNSS/levelling points and geopotential models. The estimated SCH-coefficients may be used in geodetic applications, for example GNSS Levelling. Additionally, the SCH coefficients give a representation of the gravity field. Therefore, they may also be used in applications of physical geodesy, such as the computation of free-air gravity anomalies.

**Table 7.3:** Result from the combined adjustment of GNSS/levelling points and the EIGEN04

	$\zeta$ [m] (GNSS/Levelling)	$\zeta$ [m] ( EIGEN04)	$\delta g$ [mGal] (EIGEN04)
Max residual	0.013	0.268	16.203
Min residual	-0.023	-0.297	-12.133
RMS	0.007	0.073	2.711

To evaluate the SCH representation of the HRS, a grid of points at an altitude of 500 m was used to find the difference from the GCG2005 (Liebsch et al., 2006). The maximum difference was 0.29 m and the minimum was -0.33 m with a RMS of  $\pm 0.05$  m

In a later computation, additional observed gravity disturbances were introduced into the adjustment. In theory, this should lead to smaller differences between the SCH-representation and the GCG2005. However, before this computation was done, a test for the resolution of the local degree  $k=15$  was computed.

### 7.3 Example 3: Combination of GNSS/levelling points and the GCG2005 – Quasigeoid

This computation example was designed to test the resolution of the SCH coefficients, derived to a degree  $k=15$ . The maximum root  $n(k=15)$  is 2028.38 (Appendix 1), so according to table 2.1, the representation quality of the SCH coefficients should be better than 0.03 m.

The height anomalies,  $\zeta$ , derived from the GCG2005 again were introduced in two layers, at 100m and 1000m. The a-priori accuracy for this data was assumed to be 0.01 m. To make

sure that the design of the previous computation gives a 1 cm representation, four patches were introduced, each with the parameterisation (6-37). The results are listed in table 7.4.

From the results it can be seen, that the local degree  $k=15$  is sufficient to give a representation of the HRS with an accuracy better than 1 cm. The estimated RMS of 0.006 m for the GNSS/levelling points and 0.005 m for the GCG2005 height anomalies indicates a good representation quality.

**Table 7.4:** Result from the combined adjustment of GNSS/levelling points and the GCG2005

	$\zeta$ [m] (GNSS/Levelling)	$\zeta$ [m] (GCG2005)
Max residual	0.015	0.022
Min residual	-0.012	-0.018
RMS	0.006	0.005

#### 7.4 Implementation of terrestrial gravity disturbances, $\delta g$

At the beginning of this section, the necessary degree of expansion of the spherical cap harmonic coefficients series is discussed. This is very important, because to reach an optimum estimation from a least squares adjustment, each observation has to be introduced and represented in its observation accuracy.

Using modern gravimeter equipment, the observation error of a single gravity observation is in a region of 0.01 mGal (Torge, 2003). As the national gravity networks were observed over decades, this accuracy does not hold for the complete network. For example, the average accuracy for a gravity point of the German gravity network DHSN96 (Deutsches Hauptschwerenetz 1996), is quoted as 0.05 mGal (Torge, 2003).

The decisive quantity for the representation quality of SCH coefficients and of course for SH coefficients is the wavelength,  $\omega$ , and, as a consequence from (6-30), the maximum degree  $k_{\max}$ , where the infinite series expansion (6-14) is truncated. This truncation leads to the so-called “truncation error“, or “omission error”. To compute the omission error for a series expansion of SH coefficients, usually the well-known formula of Tscherning and Rapp (6-38)

is used. If the degree variances  $\sigma_n^2$  are added for all omitted degrees  $n > n_{\max}$  and so the omission error  $\sigma_{O(n)}$  is obtained:

$$\sigma_{O(n)} = \sqrt{\sum_{d=n+1}^{\infty} \sigma_d^2} \tag{7-5}$$

Table 2.1 shows the truncation errors according to (6-38) for a SH geopotential model. As can be seen, the error  $\sigma_{\zeta}$  for the height anomaly of 0.002 m is negligible for a degree  $n = 7200$ . So for this observation group, the omission error is less than the observation error.

In contrast to the height anomalies, gravity values still has an omission error of 2.74 mGal at degree 7200. This is worse than the accuracy of a gravity observation. In Table 7.5 the omission error  $\sigma_{O(n)}$  for the gravity observations is listed, stepwise for different degrees  $n$ , until  $\sigma_{O(n)}$  is less than the observation accuracy of 0.01 mGal.

**Table 7.5:** Omission error for gravity disturbances according to Tscherning and Rapp (1974)

max. degree n	7200	10000	20000	30000	35000	40000
Resolution [km]	2.8	2.0	1.0	0.6	0.57	0.5
$\sigma_{O(n)}$	2.74	1.40	0.15	0.02	0.007	0.002

As can be seen from table 7.5, a maximum degree of  $n \sim 25000$ , or a respective resolution of  $\sim 800\text{m}$ , would be necessary to reach an omission error for the gravity representation that is compatible with the observation accuracy.

Following the “rule of thumb” (6-30), a local degree  $k = 180$  would be necessary for the design of the test project, with  $\vartheta_0^c = 0.6427^\circ$ , to reach this representation quality. A spherical harmonic expansion up to degree 180 contains more than 32000 unknowns. This means that, according to the degree-variance model (6-38), 32000 SCH coefficients would be necessary for a representation quality of 0.02mGal for the gravity disturbances,  $\delta g$ . In contrast to this, the height anomaly,  $\zeta$ , is already represented by an accuracy of better than 1 centimetre, by SCH coefficients using a maximum local degree of  $k = 15$ , containing 256 unknowns.

This already shows one of the big difficulties in gravity field approximation: To achieve high accuracies a huge number of unknowns are necessary and the equation systems to solve them are not sparse. So the solution for such equation systems becomes the main problem at all.

In section 5.6 an algorithm was presented, that enables inversion of arbitrarily large matrices, by using block matrices. This algorithm might be applied here as well. But, in contrast to the estimation of FEM parameters in DFHRS computation, the matrix of normal equations in the case of SCH coefficient estimation is not sparse. Therefore the generation of the normal equations matrix takes a lot of computation time. In practice it uses so much time that the computation examples in this thesis have to be kept small, because a standard laptop was used for the computations.

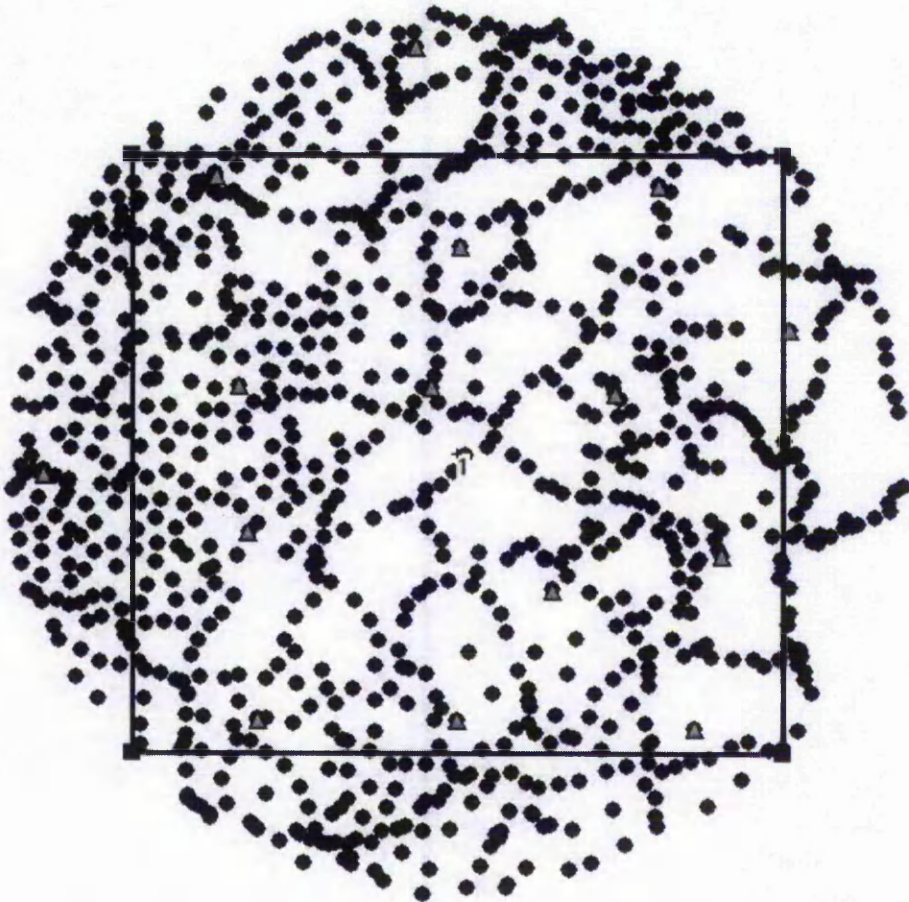


**Fig. 7.2:** The test area contains 15 GNSS/levelling points (triangles) and 1066 gravity observations (blue circles). The HRS is computed for the area within the blue lines and compared within the investigation.

For the combined adjustment of GNSS/levelling points,  $\zeta$ , a geopotential model,  $\zeta$  and  $\delta g$ , and terrestrial gravity observations,  $\delta g$ , an area of approximately  $(60 * 60)$  km<sup>2</sup> that contains 1066 gravity observations was chosen (fig. 6.5). To reach the required spatial resolution, for the complete representation of the observed gravity disturbances,  $\delta g$ , a maximum degree  $k_{MAX}=90$  was chosen. This degree enables a resolution of  $\sim 700$ m and therefore the necessary approximation quality of the SCH coefficients (Table 6.5). In this computation, the TOSCA concept (section 6.7) was applied, to reduce the computation time as well as to achieve a better numerical behaviour of the linear equation system.

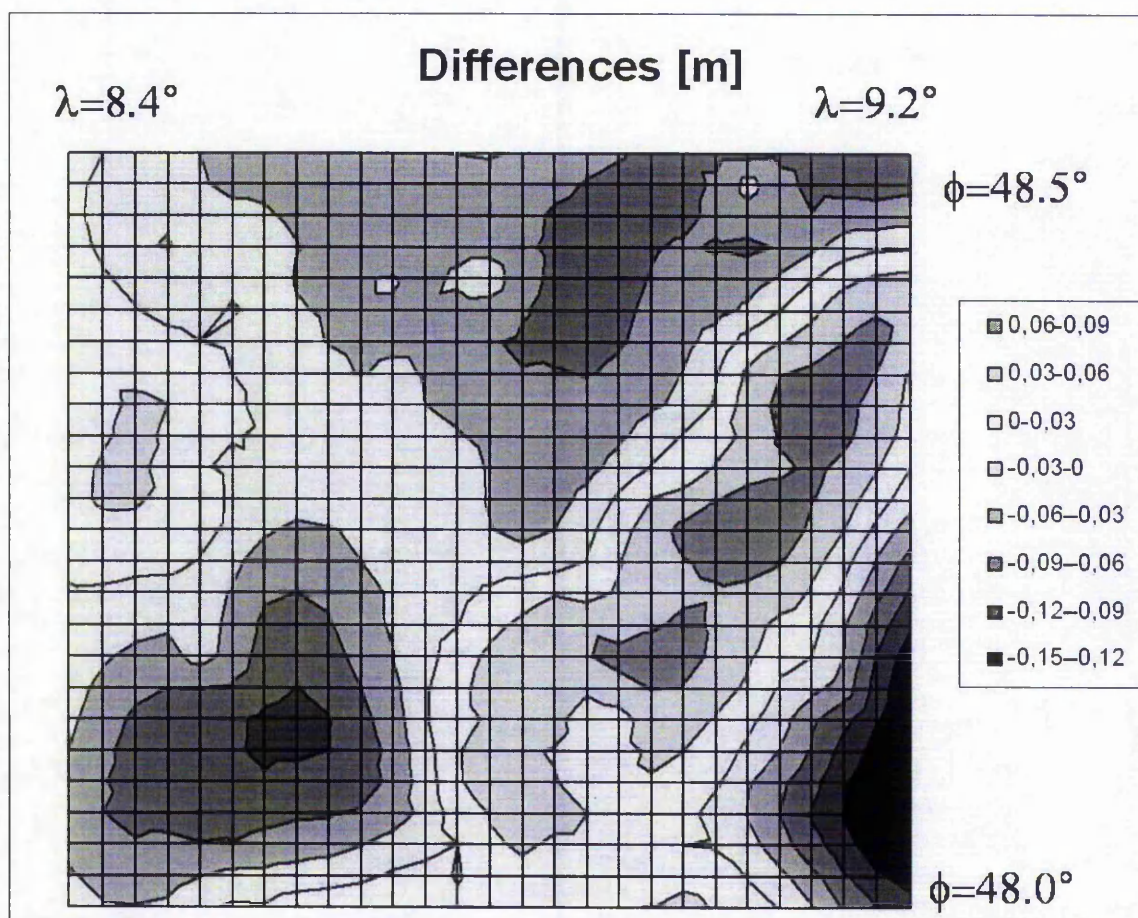


**Fig. 7.3:** The surface of differences between the GCG2005 and the SCH-Model, estimated using the GNSS/Levelling points and the GPM98CR model.

To evaluate the quality of the HRS derived from the computed SCH coefficients, a reference surface is needed. The test area is situated in Baden-Württemberg, Southern Germany. For this federal state a precise DFHRS is available with an accuracy of one centimetre (Jäger,

2007). As the theory of the DFHRS is also topic of this thesis, the results were compared with the GCG2005 (Liebsch et. a., 2005).

For the regularisation of the matrix of normal equations, the degree variance model of Tscherning and Rapp (6-38) was used. Several test computations showed that in this area the best results are found when the parameter  $s$  is set to  $s=0.996$ .

To evaluate the influence of the introduced gravity disturbances,  $\delta g$ , the example project was first computed without introducing terrestrial gravity, using only GNSS/Levelling and the GPM98CR. A surface of differences between the derived HRS and the GCG2005 was generated. It is shown in fig. 7.3. The differences with an absolute value of more than 0.1m in the south-eastern part of the area may be treated as boundary effects. The remaining differences vary from 0.09m to -0.09m with a standard deviation of 0.045m.

For comparison, the computation of the SCH coefficients was done a second time. This time the GPM98CR was replaced by the EIGEN04 model. The generated surface of differences is shown in fig. 7.4. The differences show, in general, the systematic effects as the surface generated from the SCH coefficients estimated from the GPM98CR model, but with less detail. Starting in the north western part and ending in the south eastern part of the computed area, the differences change their sign three times. This is because the EIGEN04 model is derived with SH coefficients up to a global degree of  $l=360$ . Therefore, it only gives a long-wave representation of the gravity field.

The GPM98CR model used in this thesis is applied up to a degree of  $l=760$ . So it gives a more detailed representation of the gravity field. Therefore, all the following investigations and test computations were made using the GPM98CR geopotential model.

For the next computation the terrestrial gravity disturbances,  $\delta g$ , were introduced and the combined adjustment was computed, together with the GPM98CR and the GNSS/Levelling points. The a-priori standard deviation of the gravity disturbances was introduced with  $\sigma_{\delta g}=0.02\text{mGal}$ . The height anomalies,  $\zeta_{\text{GPM}}$ , and the gravity disturbances,  $\delta g$ , derived from the GPM98CR model were introduced with an a-priori standard deviation of  $\sigma_{\zeta}=0.15\text{m}$  and  $\sigma_{\delta g}=35\text{mGal}$ , respectively. The height anomalies,  $\zeta$ , derived from the GNSS/Levelling points were introduced with an a-priori accuracy of  $\sigma_{\zeta}=0.01\text{m}$ .

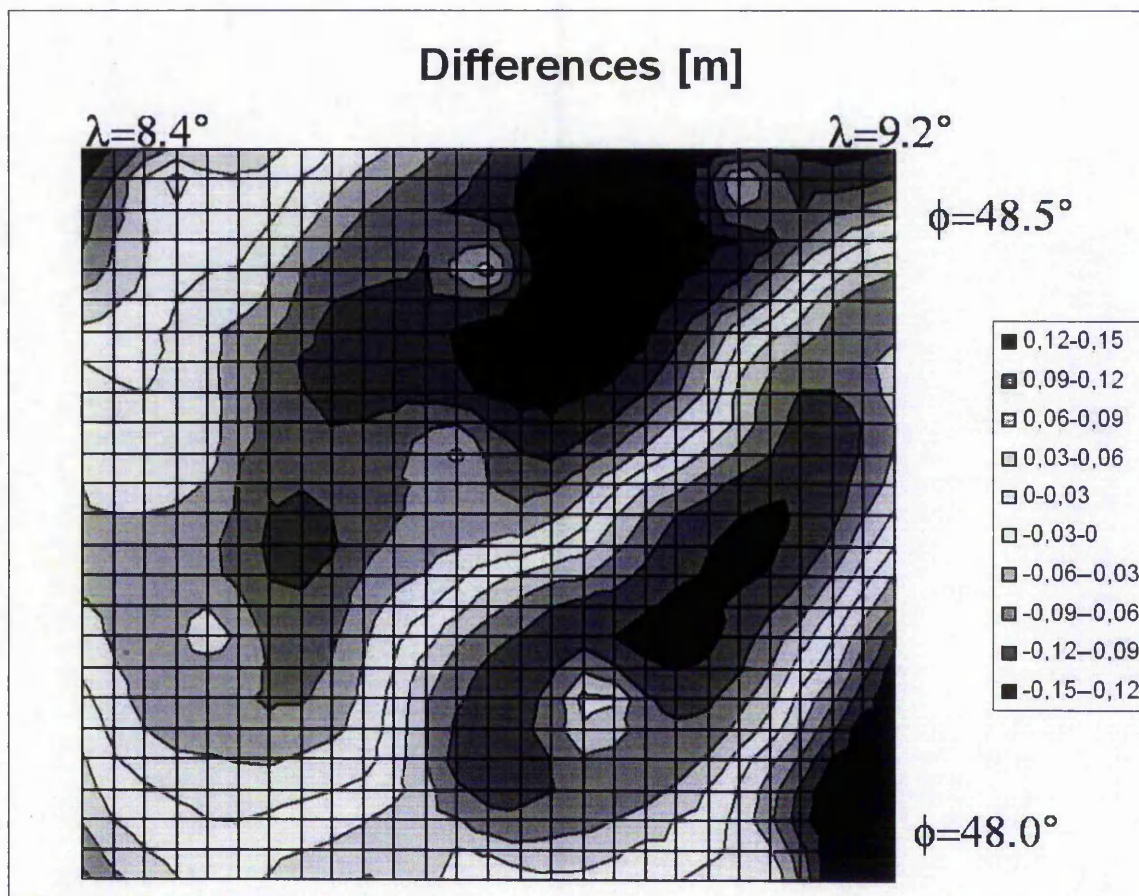


**Fig. 7.4:** The surface of differences between the GCG2005 and the SCH-Model, estimated using the GNSS/Levelling points and the EIGEN04 model.

To reduce systematic effects in the observations, additional correction parameters have been estimated, using the parametric model (7-2) and (7-4), for the observations derived from the GPM98CR as well as for the terrestrial observations  $\delta g$ .

The estimated residuals, as well as the derived RMS for each observation group are listed in Table 7.6. The observations,  $\zeta_{\text{GPM}}$  and  $\delta g_{\text{GPM}}$ , derived from the GPM98CR as well as the terrestrial gravity disturbances,  $\delta g$ , are correctly represented with their accuracy. The residuals of the terrestrial disturbances,  $\delta g$ , vary from  $-0.065\text{mGal}$  up to  $0.079\text{mGal}$ , with a RMS of  $0.0057\text{mGal}$ . So the spatial resolution of the SCH coefficients up to a maximum local degree of  $k_{\text{MAX}}=90$  enables the representation of the introduced terrestrial gravity disturbances,  $\delta g$ , within the least-squares adjustment.

The residuals of the height anomalies,  $\zeta$ , derived from the GNSS/Levelling points vary from  $-0.024\text{m}$  to  $0.026\text{m}$ , with a RMS of  $0.0165\text{m}$ .

To evaluate the quality of the SCH representation of the HRS, a grid of points with altitudes derived from the GTOPO30 model was used to find the difference from the GCG2005 quasigeoid. The maximum difference was 0.138 m and the minimum was 0.069 m with a RMS of 0.035 m. So the introduction of gravity disturbances improved the accuracy of the HRS representation by 0.01 m.

**Table 7.6:** Result from the combined adjustment of GNSS/levelling points the GPM98CR, and terrestrial gravity disturbances.

	$\zeta$ [m] (GNSS/Levelling)	$\zeta$ [m] ( GPM98Cr)	$\delta g$ [mGal] (GPM98CR)	$\delta g$ [mGal] (terrestrial)
Max residual	0.026	0.177	88.72	0.079
Min residual	-0.024	-0.079	-81.73	-0.065
RMS	0.0165	0.024	11.25	0.0057

Figure 7.5 shows the differences between the HRS derived from the SCH representation and the GCG2005. The differences which are bigger than  $\pm 0.1$ m, are situated in the south eastern part of the area. They may be treated as boundary effects. It can also be seen that there are regions, which are not close to the boundary, with a difference of more than  $\pm 0.05$  cm. On a first view, it seems that those errors are not of a short-wave nature, but may result from the long-wave errors of the applied geopotential model, GPM98CR.

To make sure, that this is not a problem of resolution, the anomaly degree variances (i.e. Torge, 2003) have been computed for the height anomalies as well as for the gravity disturbances.

The anomaly degree variances of the SCH coefficients, estimated by means of the equation observations (6-13, 6-14) read as

$$\sigma(\zeta)_k^2 = \frac{1}{\gamma} \sum_{m=0}^k \left( (\mathbf{A}_{k,m}^c)^2 + (\mathbf{B}_{k,m}^c)^2 \right) \tag{7-6a}$$

and

$$\sigma(\delta g)_k^2 = \frac{(k+1)^2}{r_0^2} \sum_{m=0}^k \left( (\mathbf{A}_{k,m}^c)^2 + (\mathbf{B}_{k,m}^c)^2 \right). \tag{7-6b}$$

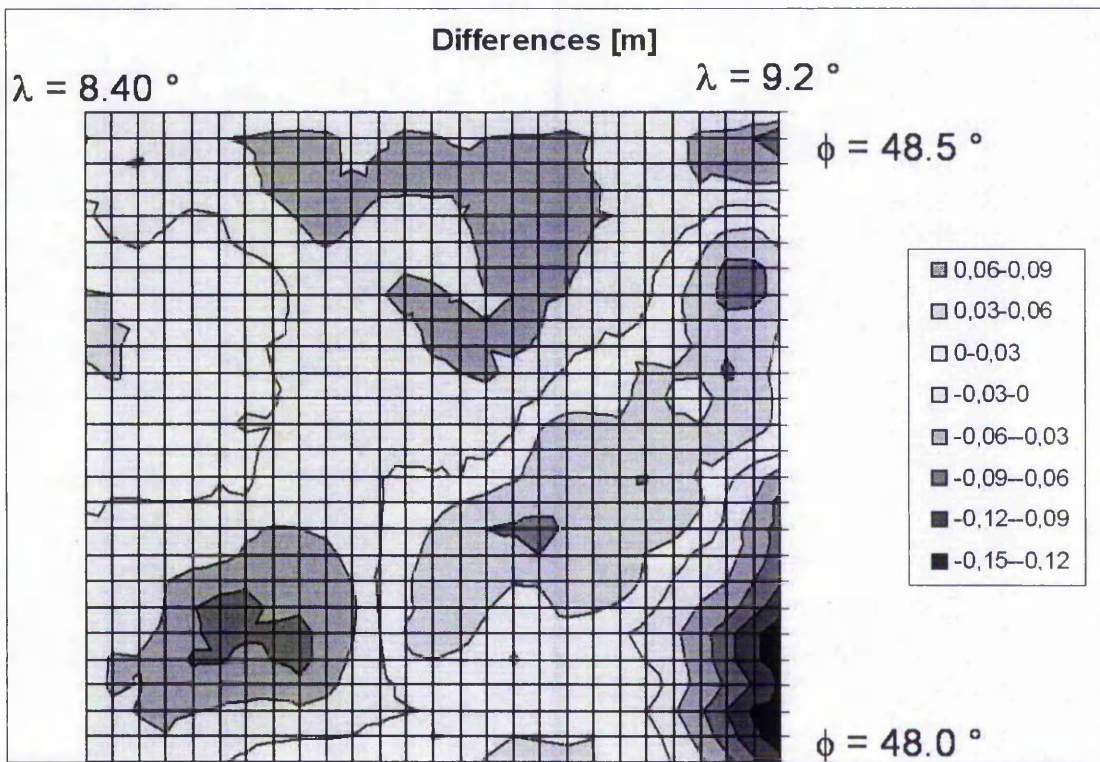


**Fig 7.5:** The surface of differences between the GCG2005 and the SCH representation up to  $k_{\text{Max}}=90$

As the graph of the square root of the degree variances (Fig 7.6) shows, the height anomaly,  $\zeta$ , is already represented in the range of 0.001m by the SCH coefficients up to a degree of  $k \sim 50$ . The square root of the degree variance for the height anomaly,  $\zeta$ , for the maximum degree  $k_{\text{MAX}}=90$  was calculated with a variance 0.0002 m. The degree variances of the gravity disturbances also show convergence in the higher degrees (Fig 7.7). For the maximum degree,  $k_{\text{MAX}}=90$ , the square root of the degree variance was 0.16mGal.

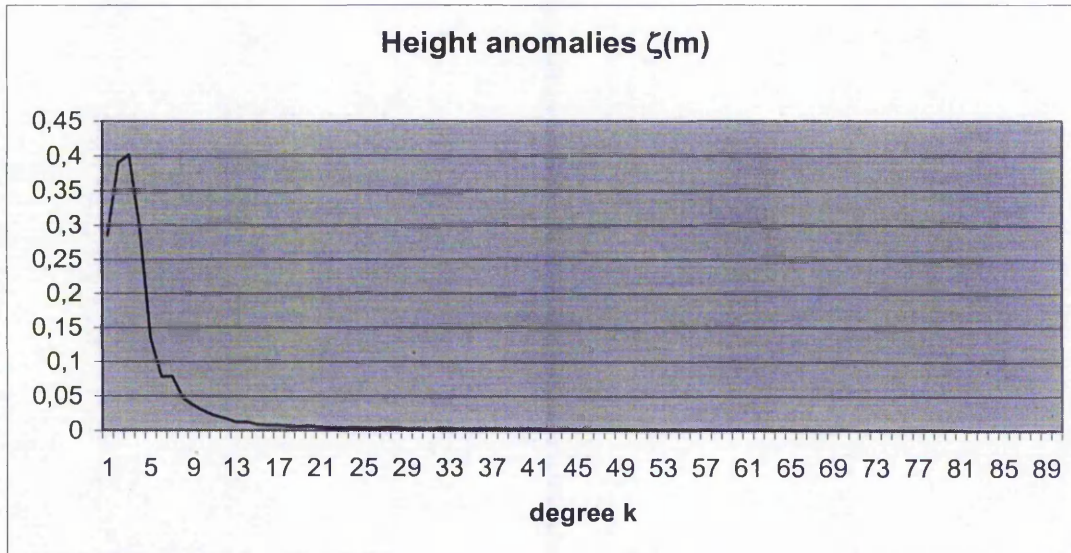


**Fig. 7.6:** The square roots of the degree variances for the height anomaly,  $\zeta$ , for the SCH representation up to degree 90

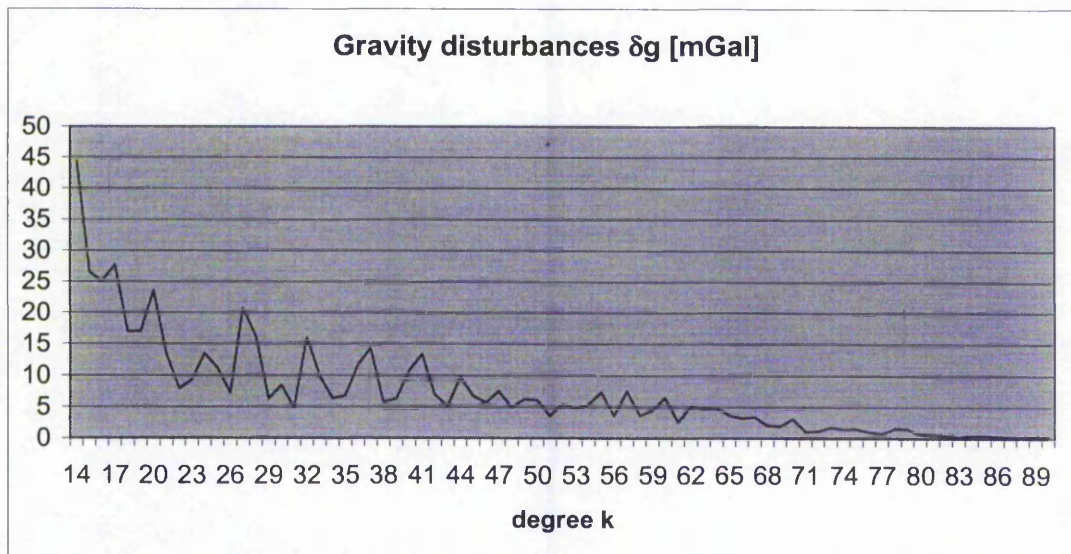


**Fig. 7.7:** The square roots of the degree variances for the gravity disturbances,  $\delta g$ , for the SCH representation up to degree 90. The degrees less than  $k=14$  are not displayed to ensure clarity. The maximum was reached at  $k=3$  with 2830 mGal

It may be expected that especially for the height anomalies, there is nothing neglected in the higher degrees. As a proof, the area was computed again, this time with a local degree up to  $k_{MAX}=100$ . The increased maximum degree applied on the same spherical cap provides a spatial resolution of  $\sim 500m$ . But, the degree  $k_{MAX}=100$  already leads to 10201 unknowns.

So to solve this equation system, the block algorithms of section 5.6 had to be applied. In contrast to the estimation of the FEM parameters in the DFHRS approach, the linear equation system that is generated when estimating SCH-coefficients is not sparse. In addition, the computation of the Legendre functions of non-integer degree takes a lot of time. Both effects make the application of the SCH concept very uneconomic.

The generated differences are shown in fig 7.8. They show the same systematic effects as in previous the computation (fig. 7.3, 7.4 and 7.5). So it can be stated that the quality of the representation has not increased, nor has it changed significantly, by increasing the local degree of the SCH coefficient expansion.

The degree variances, computed for the height anomalies,  $\zeta$ , and the gravity disturbances,  $\delta g$ , show convergence in the higher degrees. The degree variances for the gravity disturbances,  $\delta g$ , show a peak at the degrees  $k = 75-80$  (Fig. 7.10). This could be a result of over-parameterisation. For this computation the series expansion was increased from the degree  $k=90$  up to the degree  $k=100$ . This means 1920 additional unknowns without introducing additional observations. It is possible that the unknown parameters are not determined by the observations, but only by the regularisation (6-37).

In section 7.1 a set of SCH coefficients up to a local degree of  $k=15$  was used to completely represent the geopotential model over an area that was more than twice as big as in the current example. When computing the current example, the expansion up to a local degree of  $k=90$  already shows convergence. The spatial resolution of the unknown parameters now is increased without introducing new observations into the linear equation system.

The surface of differences in this example, with  $k_{MAX}=100$  is more rough than in the example before with a maximum local degree  $k_{MAX}=90$  (fig. 7.8). The RMS of the difference was estimated as 0.037m. So there is no significant difference to the example above, where the standard deviation was estimated with  $\pm 0.035m$ .

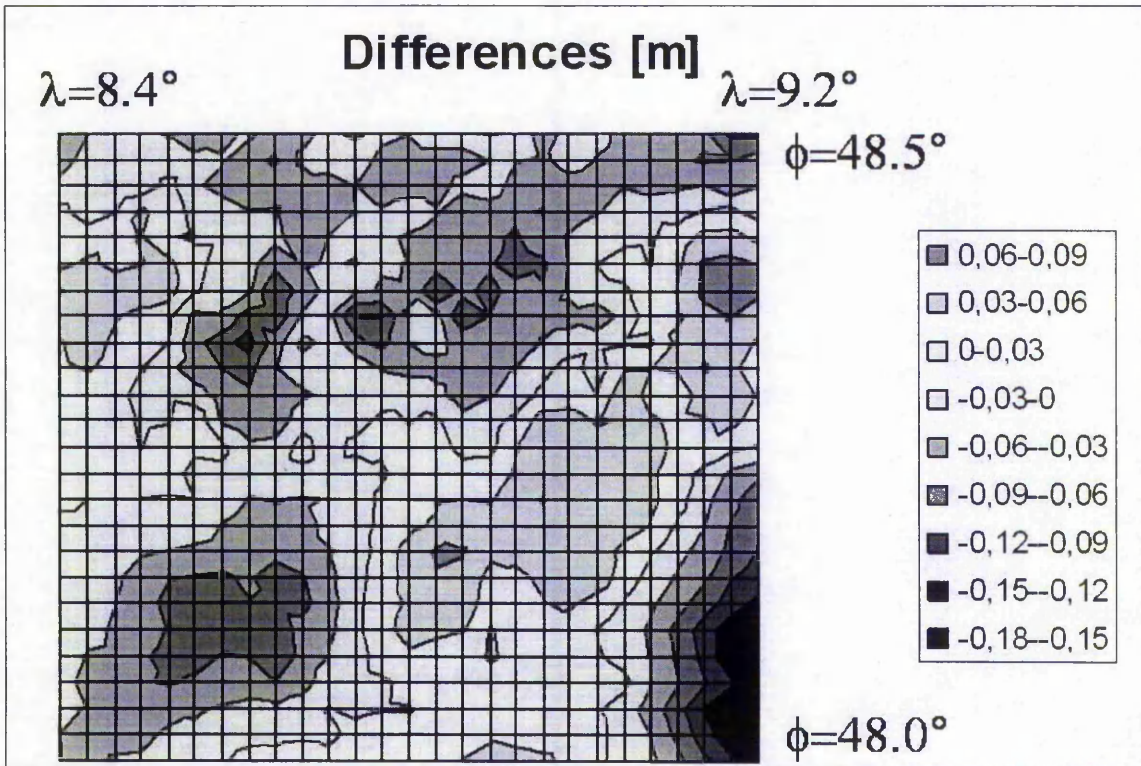


**Fig 7.8:** The surface of differences between the GCG2005 and the SCH representation up to  $k_{Max}=100$

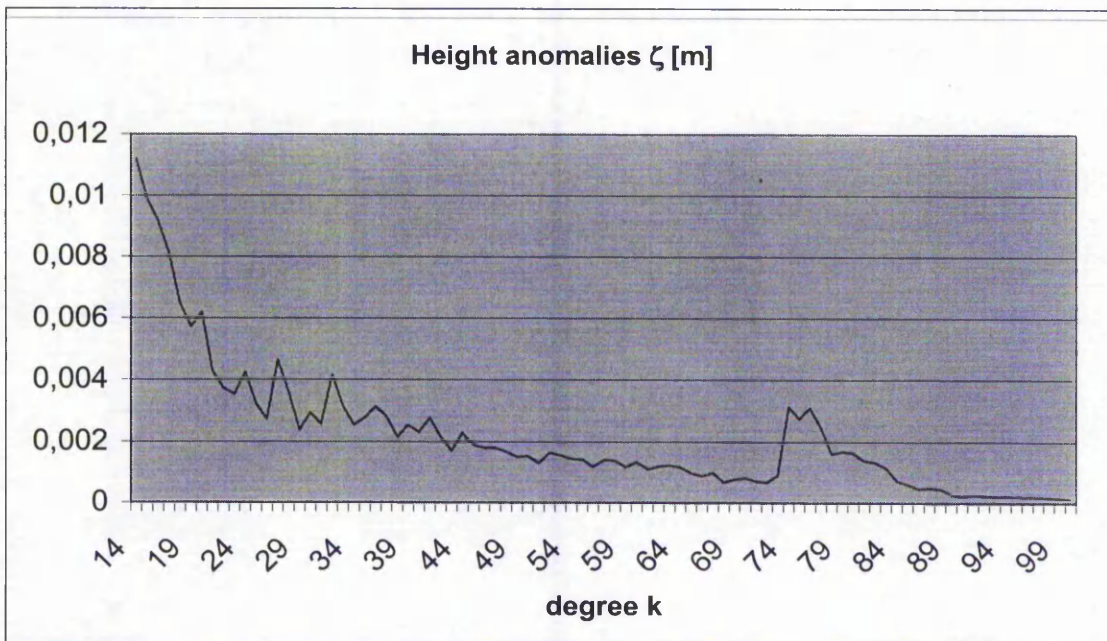


**Fig. 7.9:** The square roots of the degree variances for the height anomaly,  $\zeta$ , for the SCH representation up to degree 100. The degrees less than  $k=14$  are not displayed for clarity.

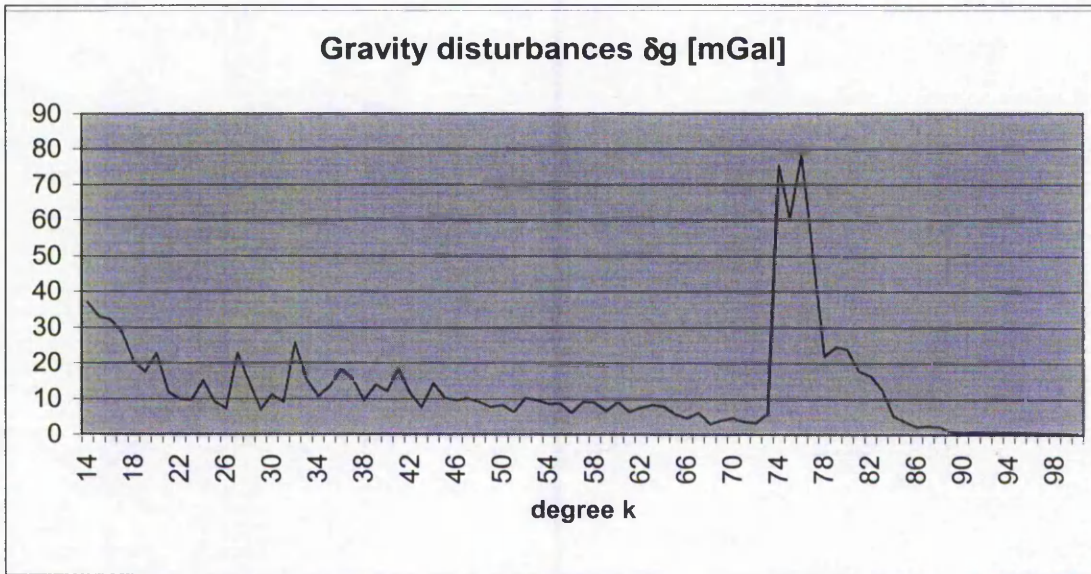


**Fig. 7.10:** The degree variances for the gravity disturbances,  $\delta g$ , for the SCH representation up to degree 100. The degrees less than  $k=14$  are not displayed for clarity. The maximum degree variance was reached at  $k=3$  with  $1900^2 \text{mGal}^2$

The spatial resolution may also be increased by applying the maximum degree,  $k_{\text{MAX}}=90$ , of the SCH coefficient expansion, to a spherical cap of smaller extent. To demonstrate this, the size of the area in the example has been further reduced to a size of  $\sim 45 * 45 \text{ km}^2$ . So a spatial resolution of  $\sim 500\text{m}$  was reached.

The spherical cap has the centre point at  $\lambda=8.7^\circ$  and  $\varphi=48.15^\circ$ . This is close to a “critical area”, where the difference between the HRS derived from the SCH representations, with  $k_{\text{MAX}}=90$  and  $k_{\text{MAX}}=100$ , of the current example and the GCG2005 varies from  $-0.06\text{m}$  to  $0.09\text{m}$  (Fig. 7.5 and 7.8). The estimated residuals the derived RMS are shown in table 7.7.

**Table 7.7:** Results from the combined adjustment of GNSS/levelling points, GPM98CR, and terrestrial gravity anomalies over the smaller cap

	$\zeta$ [m] (GNSS/Levelling)	$\zeta$ [m] ( GPM98CR)	$\delta g$ [mGal] (GPM98CR)	$\delta g$ [mGal] (terrestrial)
Max residual	0.0015	0.050	41.09	0.010
Min residual	-0.0028	-0.071	-47.05	-0.013
RMS	0.0014	0.0136	8.16	0.001

The anomaly degree variances show convergence for the height anomaly,  $\zeta$ , as well as for the gravity disturbance,  $dg$  (Fig. 7.11, 7.12).

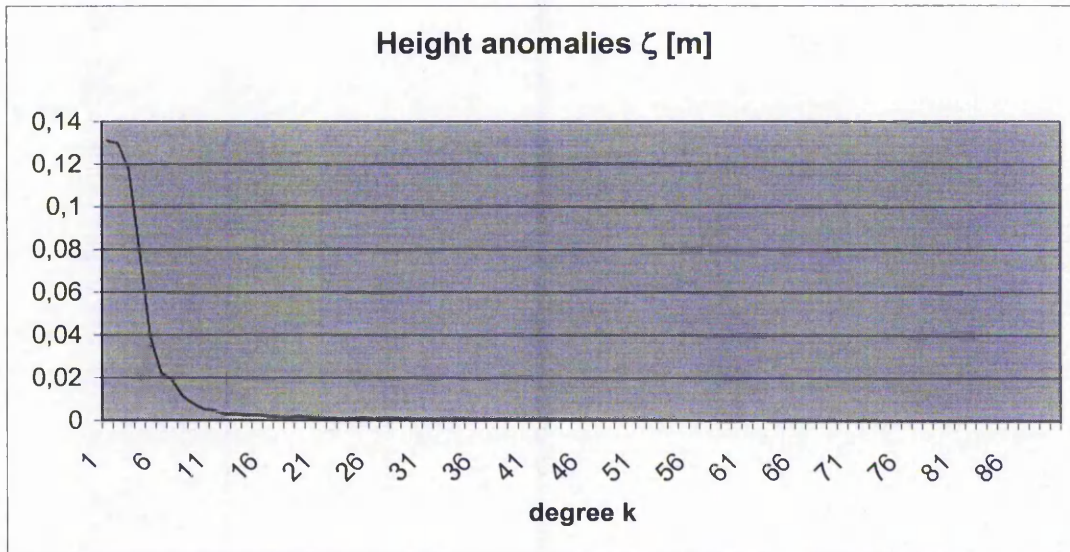


**Fig. 7.11:** Degree variances for the height anomaly,  $\zeta$ , for the SCH representation over the smaller cap up to degree 90

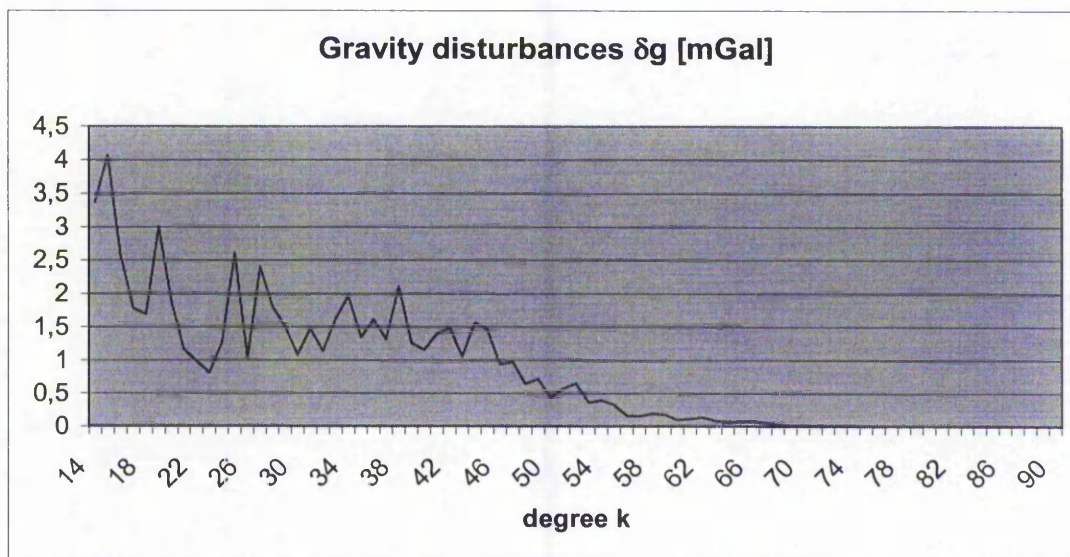


**Fig. 7.12:** Degree variances for the height anomaly,  $\zeta$ , for the SCH representation over the smaller cap up to degree 90. The degrees less than  $k=14$  are not displayed for clarity. The maximum degree variance was reached at  $k=3$  with 20.8 mGal

The differences between the HRS, derived from the SCH representation and the GCG2005 is shown in fig. 7.13.

As can be seen, the differences have not changed significantly, compared to fig. 7.8 and fig. 7.5. They still vary from -0.09m to 0.06m in this area. The RMS of the difference was

estimated with 0.037m. So again, there is no significant change to the SCH representation with  $k_{MAX}=90$ , where the RMS was estimated with 0.035m, and the SCH representation with  $k_{MAX}=100$ , where the RMS was estimated with 0.037m.

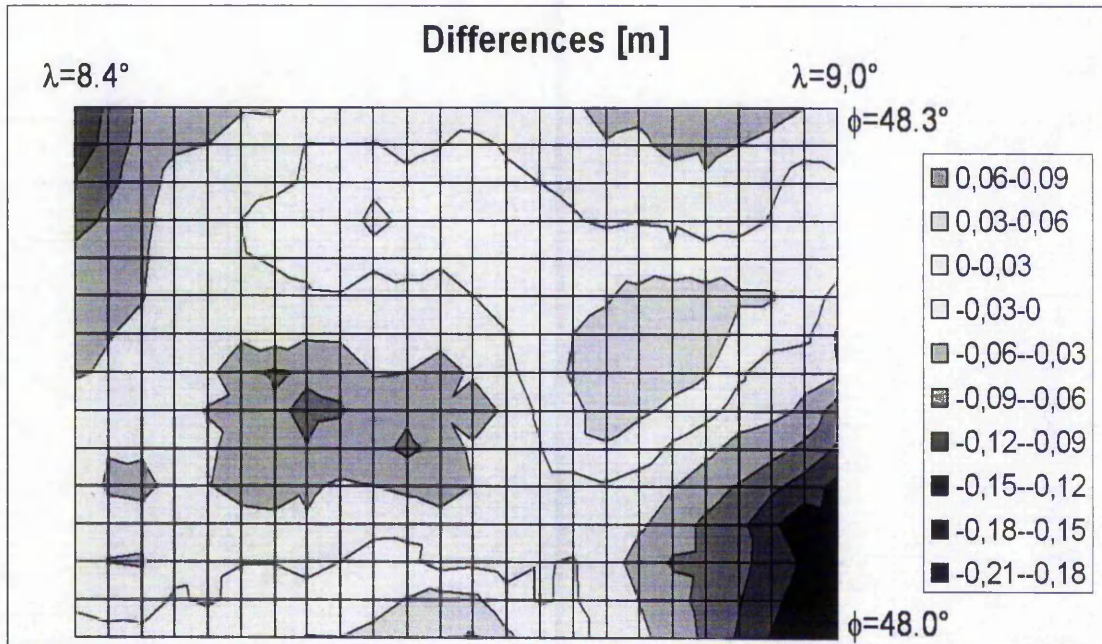


**Fig 7.13:** The surface of differences between the GCG2005 and the SCH representation of the smaller cap up to  $k_{Max}=90$

To summarise the results of this investigation, it can be stated, that the differences in the “critical area” could not be reduced by increasing the resolution of the SCH-coefficients. Neither the series expansion up to local degree  $k_{MAX}=100$  nor reduction of the extent of the investigated area, led to a significant change of the representation quality. This may result from the density of the gravity network and corresponding to this, the number of gravity observations situated within the spherical cap.

The density of the gravity network may be too sparse for a complete representation of the local gravity field given the observation accuracy of 0.02mGal. A discrete observation maybe recomputed by means of the estimated SCH-coefficients. But the representation quality in the gaps between the observed points is not known. This can be seen from the parts of redundancies, estimated for each observation. The average part of redundancy for a single gravity disturbance is less than 0.01. This means, that the group of gravity disturbance observations is not controlled in a statistical sense. In other words, the observation fully provide to the determination of the unknowns. They are not adjusted.

Related research was published by (Flury, 2002), whose investigations were concerned with the accuracy of modern methods for the representation of gravity disturbances. Flury reports a representation quality better than 1 mGal, if the average distances between the measured point gravity values is less than 1 km and modern digital terrain models are applied.

The gravity disturbances,  $\delta g$ , could be controlled within the least-squares estimation if they were available at a density that corresponds with the applied resolution of the expansion of the SCH coefficients. In the current example the resolution is  $\sim 600\text{m}$ . This corresponds with the investigation published by Flury (2002). Unfortunately, the national gravity networks of European states do not provide such densities.

The differences, or at least parts of the differences between the height anomalies,  $\zeta$ , derived from the SCH coefficients and from the GCG2005 respectively may also result from a less than optimum fit to the GNSS/Levelling points.

In the example computations of this section, the geopotential model was introduced at several layers of different heights. The gravity disturbances,  $\delta g$ , as well as the height anomalies,  $\zeta$ , from the GNSS/levelling points are observed on the earth's surface. The question, as to whether the three dimensional gravity field may be fitted to a surface, by means of a parametric model, such as (7-2, 7-4) is not answered yet and also not discussed in this thesis.

In the chapter 5, the DFHRS approach has been successfully used, to reduce long-wave systematic errors of a gravimetric model, by introducing so-called "geoid-patches" as well as generating artificial co-variance matrices for the gravimetric height anomalies,  $\zeta_{\text{grav}}$ . The use of such a co-variance model enables a strict two-step adjustment, see section 5.1.2 and also (Jäger, 2002; Jäger and Schneid, 2002). So the next computation example is an application of the DFHRS concept.

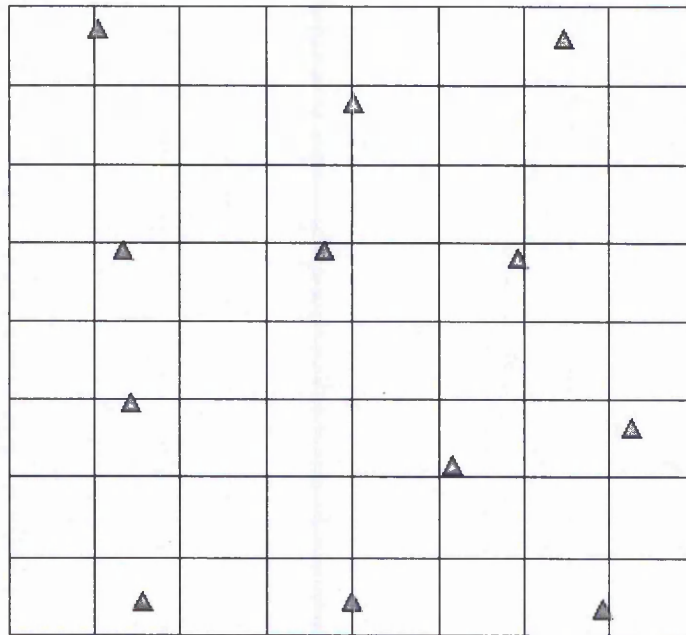
## **7.5 Application of the DFHRS patching concept to reduce systematic errors**

The first step of the following 2-step adjustment is the combination of the GPM98CR with the terrestrial gravity disturbances,  $\delta g$ , applying the SCH concept. Therefore, the SCH-coefficients of the test area, fig. 7.2 have been estimated up to a maximum local degree of  $k_{\text{MAX}}=90$ . The residuals and the derived RMS of each observation group are listed in table 7.8

**Table 7.8:** Residuals from the combined adjustment of the GPM98CR, and terrestrial gravity disturbances

	$\zeta$ [m] (GPM98CR)	$\delta g$ [mGal] (GPM98CR)	$\delta g$ [mGal] (terrestrial)
Max residual	0.175	105.29	0.074
Min residual	-0.073	-93.83	-0.062
RMS	0.019	11.69	0.005

In the second step, the area was subdivided into a number of 64 FEM meshes (fig 7.14) for the representation of the HRS by the DFHRS parameters.

**Fig. 7.14:** FEM meshes and GNSS/levelling points over the area of the test project

A synthetic co-variance matrix has been generated for a grid of height anomalies,  $\zeta$ , derived from the SCH coefficients estimated in the first step, using the co-variance function:

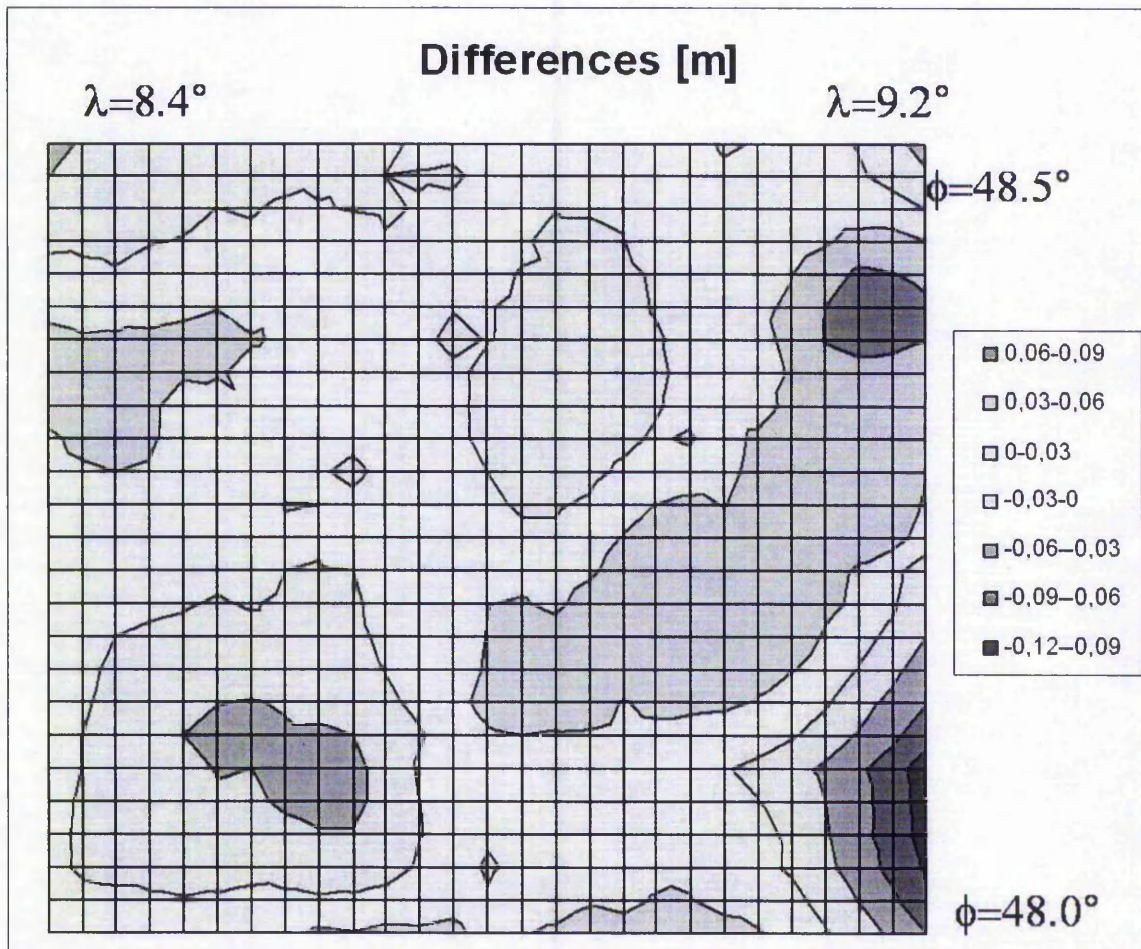
$$\sigma_0 \cdot e^{-\ln(0.5) \frac{S}{\beta}} \quad (7-7)$$

The resulting residuals of the combined adjustment of the height anomalies,  $\zeta$ , derived from the GNSS/Levelling points and from the SCH coefficients, respectively, are listed in table 7.9.

**Table 7.9:** Residuals from the combined adjustment

	$\zeta$ [m] (GNSS/Levelling)	$\zeta$ [m] (SCH)
Max residual	0.008	0.057
Min residual	-0.012	-0.0145
RMS	0.006	0.008

For comparison with the HRS derived from the examples computed in the previous section, the surface of differences between the DFHRS computed above and the GCG2005 was generated and visualised in fig. 7.15.

**Fig. 7.15:** The surface of differences between the DFHRS of this example and the GCG2005.

It can be seen that the differences in the south western area have been reduced to an absolute value of  $<0.06\text{m}$ . This shows the effect of introducing a co-variance matrix for the gravimetric height anomalies,  $\zeta_{\text{grav}}$ , derived from the SCH coefficients.

The DFHRS parameters now give a good representation of the local HRS. The RMS of the difference to the GCG2005 model again reduced to  $0.025\text{m}$ .

## 7.6 Discussion

In this chapter, several examples have been computed, to demonstrate the potential of the concept of spherical harmonic analysis. The SCH expansion is a strict mathematical solution of Laplace's equation (2-6) and therefore, SCH coefficients may be used to represent a local gravity field. The representation of the gravity field by SCH coefficients is very economic, because in contrast to global spherical harmonic models, the SCH coefficients may be applied, to give a detailed short-wave representation of areas of limited extent.

With the computed examples, it could be shown, that the SCH concept may be used to combine terrestrial gravity disturbances,  $\delta g$ , with a global spherical harmonic model and GNSS/Levelling points, in a rigorous least squares adjustment.

The HRS that was derived from the SCH coefficients computed in this example was compared with another, independent HRS model. For the area of Baden-Württemberg a precise DFHRS is available with a proofed accuracy of one centimetre (Jäger, 2007). As the theory of the DFHRS is also topic of this thesis, the results were compared with the GCG2005 (Liebsch et. a., 2005).

The quality of the HRS representation could be increased from a standard deviation of  $0.045\text{m}$ , for the GNSS/Levelling and GPM98CR solution, down to  $0.035\text{m}$ , for the combined solution with terrestrial gravity.

Applying the SCH concept, a high short-wave resolution could be reached that enabled the representation of newly introduced discrete point gravity disturbances,  $\delta g$ , with an observational accuracy of  $0.02\text{mGal}$ , (Table 7.7, 7.8 and 7.9).

Remaining systematic effects from the geopotential model could not be reduced in the combined estimation of the SCH coefficients. The spatial resolution was further increased by increasing the maximum degree of the spherical cap harmonic expansion, as well as applying the same degree over a spherical cap of smaller extent. In this way, it could be shown, that

the differences of 0.09m between the computed height anomalies and the GCG2005 are not a problem of resolution, but more likely a problem of the density of the gravity observations.

In the next example, additional parameters and an improved stochastic model were introduced in a 2-step adjustment. First the combination of terrestrial gravity disturbances,  $\delta g$ , and the GPM98CR was computed by applying the SCH concept. In the second step, the height anomalies,  $\zeta$ , were derived from the SCH coefficients and a co-variance matrix was generated. Applying the DFHRS concept, with additional parameters and an improved stochastic model, the systematic errors were reduced further and finally a RMS of 0.025m was achieved (fig 2.15). So the introduction of gravity disturbances,  $\delta g$ , and the application of a rigorous least squares estimation, following the DFHRS concept, improved the quality of the local gravity field representation by  $\sim 50\%$ .

The main difficulties in the application of the SCH concept are the computation of the Legendre functions and the resulting numerical problems. The Legendre functions (section 6.4) are the solution of Laplace's equation, so they may not be replaced. For the use of global spherical harmonic analysis, they may be computed easily by means of recurrence relations (Wenzel, 1985). If the Legendre functions are applied over a spherical cap, they have to be computed for non-integer degrees. In addition, to provide a good short-wave resolution, the Legendre functions have to be computed for very high degrees. In this thesis an algorithm was applied that makes use of an extended range arithmetic (Olver and Smith, 1983), because the standard arithmetic of a personal computer does not provide the necessary numerical precision. Legendre functions may be computed for very high degrees, using extended arithmetic, but the computation time becomes unacceptable for practical applications.

Applying the TOSCA concept (De Santis, 1991), the SCH-coefficients may be determined in the same resolution, but, by varying the cap size, this resolution may be provided without the need to compute the Legendre function of very high degrees (section 6.7).

Another difficulty is the enormous numerical problems that occur when generating the matrix of normal equations. When determine SCH coefficients by least-squares estimation, the matrix reaches condition numbers up to  $10^{30}$ . Such numerical problems are well known from gravity field approximation by means of ordinary spherical harmonics (e.g. Wenzel, 1985). The problems are usually solved by means of a regularisation of the matrix of normal equations. In recent years several numerical techniques have been investigated (Colombo, 1981, Wenzel, 1985, Kaschenz, 2006) and applied (Wenzel, 1999; Gruber, 2000; Pail et. al.

2006). In this thesis, regularisation matrices have been generated by means of the degree variance model of Tscherning and Rapp (1974) and added to the matrix of normal equations, to avoid this problem (section 6.8).

When estimating SCH coefficients, the matrix of normal equations is not sparse. Therefore the inversion as well as the generation takes a lot of computational time. For the estimation of ordinary spherical harmonics, the matrix may be reduced to block diagonal structure if the observations are introduced as a grid (Colombo, 1981; Gruber, 2000). It may be expected that this has the same effect in case of spherical cap harmonics. The aim of this project was to introduce each observation without any reduction or interpolation. Therefore the introduction of a grid of gravity disturbances was not investigated.

A further improvement could be achieved by introducing additional information, for example digital terrain models and density models. Modern concepts of gravity prediction enable the use of such models to generate grids of terrestrial gravity disturbances (e.g. Marti, 2001). In this way, very dense grids may be generated that give a representation of the gravity disturbances in an accuracy of  $\sim 0.3\text{mGal}$  (Flury, 2002).

The use of a grid could also be a method to introduce gravity observations from remote area, not situated within the border of the spherical cap. In the presented computation examples, only the global geopotential model contains information from remote area. The gravity observations from remote areas, as well as the GNSS/Levelling points are not used. If the spherical cap size is increased, to incorporate such observations, the maximum degree of the series expansion has to be increased as well, to provide the same spatial resolution. This means that a more of unknown coefficients have to be determined. So there still is a lack of information.

The introduction of a grid of gravity disturbances that was generated from all available gravity observations within a distance up to, for example, 200 km to the spherical cap could be interpreted as an additional sequential adjustment step.

It can be expected, that the introduction of a dense grid of gravity disturbances into the combined least squares adjustment will give a further improvement to the quality of the estimated SCH coefficients. Related investigations are still outstanding.

## Chapter 8

### Conclusions

The application of precise GNSS based levelling requires knowledge of the Height Reference Surface, HRS, in an appropriate accuracy. With the advent of online GNSS correction data services, such as SAPOS (ADV, 2007), ASCOS (EON-Ruhrgas, 2007), there is an urgent need for techniques, that enables the computation of the HRS with an accuracy in the centimetre regions, as this is the accuracy that may be reached when measuring in such networks. For decades, the standard application for HRS determination was the Remove Restore Technique, RRT (e.g. Hofmann-Wellenhof and Moritz, 2005). When applying this concept, the height anomaly may be found with accuracies in the centimetre region. Recent HRS determination projects were published for example by Gerlach (2003), Erker et al. (2003), Marti and Schlatter (2005) and Liebsch et al. (2005).

Sjöberg (2005) points out several approximations made in the practical application of this technique.

In theory, the most precise results are achieved when estimating the HRS by means of a combined least squares adjustment of any HRS related geodetic observation, such as GNSS/Levelling points, deflections from the vertical, gravity accelerations and geopotential models. A combined least adjustment enables statistical quality control of the introduced observations and also guarantees the estimation of unbiased coefficients. In this thesis a concept is presented, that for the first time enables a rigorous least squares adjustment of HRS-related observations, in a two step procedure.

The concept of the Digital FEM Height Reference Surface, DFHRS, which was introduced in chapter 5, has already been successfully used to compute precise HRS solutions in several countries (Jäger and Schneid, 2000-2007).

Different observation types may be introduced into a combined and statistically controlled least squares adjustment. These observation types are GNSS/Levelling points,  $\zeta$ , deflections from the vertical,  $\xi$  and  $\eta$ , and height anomalies,  $\zeta_{\text{grav}}$ , derived from a gravimetric (quasi-)geoid model. The mathematical foundation of the concept has been explained and the observation equations have been derived.

The concept is based on the representation of HRS by a local Taylor series expansion within a regular or irregular grid of meshes. The FEM parameters are determined by means of least squares estimation. To provide a continuous transition between the FEM meshes, a set of continuity conditions is introduced as additional, highly weighted observations. By varying the size of the FEM-meshes and the degree of the Taylor-series expansion, the HRS may be approximated with chosen accuracy.

Existing long-wave errors in the applied gravimetric (quasi-) geoid models may be eliminated by means of a process called “geoid-patching”. Here, the applied (quasi-) geoid model is introduced patch-wise. For each patch, the parameters of a local trend function are estimated to eliminate the systematic errors of the respective model. Following this process, several (quasi-) geoid models may be introduced simultaneously into the adjustment. Possible datum inconsistencies between the applied geoid models may be eliminated. If trend functions are chosen, that enables a rigorous datum transition.

To perform a rigorous two step adjustment, the co-variance matrix of the applied (quasi-) geoid model would be required, but, unfortunately, it is usually not known. Therefore, it has to be approximated by means of mathematical methods. In the computation examples, it could be shown, that appropriate correlation functions may be used to approximate the co-variance matrix of a gravimetric model. If they are introduced in the stochastic model, such matrices lead to a further improvement of the accuracy of the HRS, represented by the estimated FEM coefficients (Table 5.5, 5.6).

If the size of the FEM meshes is chosen too small, the number of unknowns that have to be solved in the procedure will become very large and therefore the linear equation system may not be solved by inverting the matrix of normal equations using standard routines. An algorithm was derived and programmed, that enables the rigorous inversion of symmetric, positive definite matrices of any size by means of subdividing the matrix into block matrices.

Finally, two examples of DFHRS computations were presented.

The DFHRS of Germany was designed with 10 km border lengths of the FEM meshes and an average patch size of 60 km by 60 km (Schneid, 2002). The observation groups that were introduced were GNSS/Levelling points and height anomalies as well as deflections from the vertical, derived from the EGG97 quasigeoid (Denker and Torge, 1997). According to the

specification above, the accuracy could reach the centimetre level. By means of computing more than 3000 control points, a standard deviation of 1.8 cm was found.

The DFHRS Europe was designed with a border length of 30km for the FEM meshes, in order to reach an accuracy at the decimetre level (Jäger and Schneid, 2004). Introducing the GNSS/Levelling points from the EVRF2000 (BKG, 2003) 34 geoid patches were introduced to eliminate long-wave systematic errors in the applied gravimetric quasigeoid, the EGG97. By computing control points that were available in Austria, Germany, Estonia, Latvia, Lithuania and Switzerland it could be shown that the accuracy at least in these countries is better than one decimetre.

The adjustment using the DFHRS concept is to be seen as the second step of a two step adjustment. It makes use of a gravimetric (quasi-) geoid model that is introduced into a least squares adjustment as one observation group.

The determination of the gravimetric model is situated in the first step and was also a topic of this thesis. As the applied Taylor-series expansion of the DFHRS concept only holds for a two-dimensional approximation, a parametric model had to be found that is able to carry the whole information of a potential field.

The gravity field of the Earth may be represented by a truncated series expansion of spherical harmonic coefficients (Hoffman-Wellenhof and Moritz, 2005), because spherical harmonics, SH, are the solution of Laplace's equation. In geophysical projects, the representation of potential fields by means of more general spherical cap harmonics, SCH, has become a standard application, since Haines (1985) introduced this method.

While SH coefficients are of global nature, the SCH coefficients may be applied for the representation of local potential fields. By varying the cap angle, the SCH concept may be applied in areas of any size and by varying the maximum degree of expansion, the spatial resolution may be designed arbitrarily. The mathematical rigorousness of the approach was shown and the observation equations for height anomalies,  $\zeta$ , and gravity disturbances,  $\delta g$ , were derived.

The SCH coefficients may be estimated with a least squares adjustment. Therefore, it is also possible to determine the FEM parameters of the DFHRS representation and the SCH coefficients in one closed estimation step. The SCH coefficients would then be linked to the FEM parameters by means of condition equations (5-17b).

For the generation of the normal equations and for the computation of the gravity potential and its derivatives from the SCH coefficients, the Legendre-functions need to be computed

for non-integer degrees. In this thesis, the algorithm of Olver and Smith (1983) was applied. It makes use of extended range arithmetic to avoid numerical overflow and computes the Legendre-functions to an acceptable accuracy (Thebault et. al, 2004).

In several computation examples, the suitability and the flexibility of the SCH concept for local gravity field approximation was shown.

One goal of the SCH concept is that in contrast to the ordinary SH concept, the number of unknown is rather small. The spatial resolution of the coefficients may be increased by expanding the series up to a maximum degree that provides the complete representation of the observations introduced into the adjustment. In this way, the gravity observations may be introduced with their original observational accuracy.

Numerical instabilities in the matrix of normal equations were resolved by adding a regularisation matrix that was generated by applying the degree variance model of Tscherning and Rapp (1974).

In a computation example the GPM98CR geopotential model (Wenzel, 1999) was introduced into a combined least squares adjustment together with terrestrial gravity disturbances. The local gravity field was approximated over a cap with an approximate diameter of 80 km. The quality of the HRS representation provided by the GPM98CR in this area was estimated to be 4.5 cm by comparison to a reference model. The quality of the HRS representation provided by the estimated SCH coefficients was estimated to be 3.5 cm. So a significant improvement was reached by combining the GPM98CR with terrestrial gravity data. By visualising the differences with respect to the reference model as a surface, it was shown that the remaining errors are of a long wave nature.

In the final computation, the second step of the sequential adjustment concept was performed. The estimated SCH coefficients were introduced into a second adjustment using GNSS/Levelling points and applying the DFHRS concept. Additional trend parameters were estimated using the patching concept and an adequate correlation function has been used to approximate the co-variance model of the height anomalies that were derived from the SCH coefficients. The quality of the HRS representation, provided by the determined FEM parameters was estimated to be 2.5 cm. It is obvious that the further improvement in the second adjustment only results from the application of the DFHRS patching concept.

To summarise the results it can be stated that the adjustment concept presented enables the rigorous combination of geopotential models, terrestrial gravity data and GNSS/Levelling points. In practical applications, the number of the unknown FEM parameters and SCH

coefficients may become very large. Therefore the concept may be performed as sequential adjustment.

Further work could be undertaken to improve the process as follows. It can be expected that the incorporation of further information provided by additional observation groups, namely gravity from remote areas, will lead to a further improvement of the approximation quality. This leads to a third step in the sequential least squares adjustment.

The complete sequential adjustment would then contain the following steps

1. Prediction of a grid of gravity disturbances, for example by means of collocation techniques, using the observed gravity data, digital terrain models and density models.
2. Estimation of SCH coefficients by means of a combined adjustment of the gridded gravity data and a geopotential model.
3. Estimation of the FEM parameters by means of a combined adjustment of height anomalies, derived from the SCH coefficients determined in step 2, GNSS/Levelling points and, if available deflections from the vertical.

The introduction of the gravity data as a grid contrasts with the geodetic tradition of using the original observations in a least squares adjustment. Therefore, if the resulting HRS representation should achieve accuracy in centimetre the region, the applied adjustment concept should contain the above mentioned three steps.

## References

- Agren, J. (2004): Regional Geoid Determination Methods for the Era of Satellite Gravimetry. Royal Institute of Technology (KTH), Stockholm, Sweden, 2004. ISBN 91-7323-097-9
- Amm, O. (1998): Method of characteristics in spherical geometry applied to a Harang-discontinuity situation, *Annales Geophysicae* 16, pp. 413-424, ECS-Springer-Verlag 1998.
- Amm, O. and A. Viljanen (1999): Ionospheric disturbance magnetic field continuation from the ground to the ionosphere using spherical elementary current systems, *Earth Planets Space*, 561, pp. 431-440, 1999
- Antunes, C., R. Pail and J. Catalão (2003). Point mass method applied to the regional gravimetric determination of the geoid. *Studia Geophysica & Geodaetica*, Vol. 47, July, p. 495-509, Prague, Czech Republic.
- Barthelmes, F. (1986): Untersuchungen zur Approximation des äußeren Schwerefeldes der Erde durch Punktmassen mit optimierten Positionen. Veröffentlichung Zentralinstitut für Physik der Erde Nr. 92, Potsdam, 19786
- Bjorck and Dahlquist, (2002): Numerical Mathematics and Scientific Computing. Vol. I-III, <http://www.mai.liu.se/~akbio/NMbook.html>
- Breach, M.C., (2002): An automated approach to astrogeodetic levelling. Ph.D. thesis, Nottingham Trent University
- BKG (2003): European Vertical Reference System EVRS, Homepage <http://evrs.leipzig.ifag.de/>, Bundesamt für Kartographie und Geodäsie, Frankfurt.
- Blakely, R.J., (1995): Potential theory in gravity and magnetic applications, Cambridge University Press 1995. ISBN 0-521-41508-X

- Claessens, S.J., Featherstone, W.E. and F. Barthelmes (2001): Experiences with free positioned point-mass geoid modelling in the Perth region of Western Australia, *Geomatics Research Australasia* 75, p. 53-86.
- Colombo, O.L.(1981): Numerical methods for harmonic analysis on the sphere, Technical Report 310, The Ohio State University, Columbus, Ohio 1981
- De Santis, A. (1991): Translated origin spherical cap harmonic analysis, *Geophysical Journal International* (1991) 106, pp. 253-263.
- De Santis, A. and C. Falcone (1995) Spherical cap models of Laplacian potentials and general fields, in: *Geodetic Theory Today*, pp.141-150, Springer, New York
- De Santis, A. and J.M. Torta (1997): Spherical cap harmonic analysis : a comment on its proper use for local gravity field representation. *Journal of Geodesy* 71, p526-532
- De Santis, A., J.M. Torta and C. Falcone (1999), Spherical cap harmonics revisited and their relationship to ordinary spherical harmonics, *Phys. Chem. Earth*, 24(11-12), pp.935-941.
- Denker, H., D. Lelgemann, W. Torge, G. Weber, H.-G. Wenzel: Strategies and Requirements for a new European Geoid Determination. *Proceed. Intern Symp. On the Definition of the Geoid*, Vol. 1, 207-222, 1st Geogr. Mil. Ital. Florenz, 1986
- Denker, H. (1994): Großräumige Höhenbestimmung mit GPS- und Schwerefelddaten, in: *GPS-Leistungsbilanz '94*, Schriftenreihe des DVW, Band 18, Verlag Konrad Wittwer GmbH, Stuttgart 1995
- Denker, H. and W. Torge (1997): The European Gravimetric Quasigeoid EGG97 – An IAG supported continental enterprise. In: *Geodesy on the Move – Gravity Geoid, Geodynamics, and Antarctica*. R. Forsberg, M. Feissel, R. Dietrich (eds.) IAG Symposium Proceedings Vol. 119, Springer, Berlin Heidelberg New York: 249-254.
- Denker, H.; Torge, W.; Wenzel, G. and J. Ihde (2000): Investigation of different methods for the combination of gravity and GPS/levelling data. In: K.P. Schwarz (ed.): *Geodesy*

- Beyond 2000 – The Challenges of the First Decade, IAG Symposia, Vol. 121, S.137-142, Springer Verlag Berlin-Heidelberg, 2000
- Dinter, G.; Illner, M. and R. Jäger (1996): A synergetic approach for the integration of GPS heights into standard height systems and for the quality control and refinement of geoid models. In: Veröffentlichungen der Internationalen Erdmessung der Bayerischen Akademie der Wissenschaften (57). IAG Subcommittee for Europe Symposium EUREF, Ankara 1996. Beck'sche Verlagsbuchhandlung, München.
- Erker, E., Höggerl, N., Imrek, E., Hofmann-Wellenhof, B. and N Kühtreiber (2003): The Austrian Geoid – Recent Steps to a New Solution. Österreichische Zeitschrift für Vermessung und Geoinformation, 91. Jahrgang 2003, Heft 1/2003, p 4-13.
- Flury, J. (2002): Schwerefunktionale im Gebirge. Modellierungsgenauigkeit, Messpunktdichte und Darstellungsfehler am Beispiel des Testnetzes Estergebirge. Bayer. Akademie d. Wissenschaften, Deutsche Geodätische Kommission (DGK), Reihe C, Nr.557
- Forsberg R. and C.C. Tscherning (1981): The use of height data in gravity field approximation by collocation. J. Geophys. Res., 86, No. B9, p7843-7854.
- Forsberg R, G Stykowsky, J C Iliffe, M Ziebart, P A Cross, C C Tscherning, P Cruddace, K Stewart, C Bray and O Finch (2003): OSGM02, A New Geoid Model of the British Isles. Proceedings of the Third Meeting of the International Gravity and Geoid Commission, GG2002, Aug. 26 - 30, 2002, Thessaloniki, I. Tziavos (ed.), Editions Ziti, p132-137.
- Fotopolous, G. , Featherstone, W.E., and M.G. Sideris (2002): Fitting a Gravimetric Geoid Model to the Australien Height Datum via GPS Data. Proceed. of the 3rd Meeting of the International Gravity and Geoid Commission of the International Association of Geodesy, Thessaloniki, Greece. <http://olimpia.topo.auth.gr/GG2002/>
- Fotopolous, G. (2003): An Analysis on the Optimal Combination of Geoid, Orthometric and Ellipsoidal Height Data. Department of Geomatics Engineering, University of Calgary, Canada <http://www.geomatics.ucalgary.ca/Papers/Thesis/MGS/03.20185.GFotopoulos.pdf>

- Gerlach, Ch. (2003): Zur Höhenumstellung und Geoidberechnung in Bayern. Bayer. Akademie d. Wissenschaften, Deutsche Geodätische Kommission (DGK), Reihe C, Nr.571
- GFZ (2007): Combined Gravity Field Model EIGEN-GL04C, Geoforschungszentrum Potsdam (GFZ), Sektion Gravitationsfeld und Erdmodelle  
[http://www.gfz-potsdam.de/pb1/pg3/index\\_S13d.html](http://www.gfz-potsdam.de/pb1/pg3/index_S13d.html)
- Grote, Th. (1996): Regionale Quasigeoidmodellierung aus heterogenen Daten mit cm-Genauigkeit. Wiss. Arb. Univ. Hannover 212:
- Gruber, Th. (2000): Hochauflösende Schwerefeldbestimmung aus Kombination von terrestrischen Messungen und Satellitendaten über Kugelfunktionen; Scientific Technical Report STR00/16, GFZ Potsdam, 2000.
- Gubbins, D., 1983: Geomagnetic field analysis – I. Stochastic inversion, Geophys. J. R. astr. Soc., 73, p641-652
- Haines, G.V. (1985): Spherical cap harmonic analysis, Journal of Geophysical Research, Vol.90, No. B3, pp2583-2591, 1985
- Haines, G.V. (1988): Computer programs for Spherical cap harmonic analysis and general fields, Computers & Geosciences, Vol 14, No. 4, pp. 413-447, 1988.
- Heck, B.: Rechenverfahren und Auswertemodelle der Landesvermessung - Klassische und moderne Methoden. H. Wichmann, Heidelberg 2003. ISBN: 3-87907-347-3
- Heck, B. and Seitz, K (2002) : " Geschlossene" Lösungen des Geodätischen Randwertproblems für eine ellipsoidische Randfläche. Geodätische Woche Frankfurt 2002, Session 3, 15.10.2002.
- Heiskanen WA and Moritz H (1967): Physical Geodesy, W.H. Freeman and Company, San Francisco.
- Hirt, C. und Bürki, B. (2002): The Digital Zenith Camera - A New High-Precision and Economic Astrogeodetic Observation System for Real-Time Measurement of Vertical

- Deflections, Proceed. of the 3rd Meeting of the International Gravity and Geoid Commission of the International Association of Geodesy, Thessaloniki, Greece. <http://olimpia.topo.auth.gr/GG2002/>
- Hobson, E.W. (1965): The theory of Spherical and Ellispoidal Harmonics, 2<sup>nd</sup> reprint ed. Chelsea, New York
- Hoffman-Wellenhof, B. and H. Moritz (2005): Physical Geodesy, Springer-Verlag Wien, 2005. ISBN 3-211-23584-1
- Holmes, S.A. and W.E. Featherstone (2002) A unified approach to the Clenshaw summation and the recursive computation of very high degree and order normalised associated Legendre Functions. Journal of Geodesy 76, 279-299
- Hwang, C. and S. K. Chen (1997): Fully normalized spherical cap harmonics: application to the analysis of sea-level data from TOPEX/POSEIDON and ERS-1, Geophysical Journal International (1997) 129, pp.450-460.
- Jäger, R (1988): Analyse und Optimierung geodätischer Netze nach spektralen Kriterien und mechanische Analogien, Deutsche Geodätische Kommission bei der Bayerischen Akademie der Wissenschaften, Reihe C, Dissertationen ; H. Nr. 342, ISBN 3-7696-9390-6
- Jäger, R. (1998): Ein Konzept zur selektiven Höhenbestimmung für SAPOS. Beitrag zum 1. SAPOS-Symposium. Hamburg 11./12. Mai 1998. Arbeitsgemeinschaft der Vermessungsverwaltungen der Länder der Bundesrepublik Deutschland (Hrsg.), Amt für Geoinformation und Vermessung, Hamburg. S. 131-142.
- Jäger, R. (1999): State of the art and present developments of a general approach for GPS-based height determination. In (M. Lilje ed.): Proceedings of the Symposium Geodesy and Surveying in the Future – The importance of Heights, March 15-17,1999. Gävle/Sweden. Reports in Geodesy and Geographical Information Systems. LMV-Rapport 1999:3. Gävle Sweden. ISDN 0280-5731. p. 161-174.

Jäger, R. und S. Kälber (2000): Konzepte und Softwareentwicklungen für aktuelle Aufgabenstellungen für GPS und Landesvermessung. DVW Mitteilungen, Landesverein Baden-Württemberg. 10/2000. ISSN 0940-2942.

Jäger, R. and S. Schneid (2001): Online and Postprocessed GPS-heighting based on the Concept of a Digital Height Reference Surface (DFHRS). Report on the Symposium of the IAG subcommission for Europe (EUREF) held in Dubrovnik, May 2001. Veröffentlichungen der bayerischen Kommission für die internationale Erdmessung der Bayerischen Akademie der Wissenschaften.

Jäger, R. (2002): Online and Postprocessed GPS-heighting based on the Concept of a Digital Finite Element Height Reference Surface. In: J. Kaminskis and R. Jäger (Eds.): 1st Common Baltic Symposium, GPS-Heighting based on the Concept of a Digital Height Reference Surface (DFHRS) and Related Topics - GPS-Heighting and Nationwide Permanent GPS Reference Systems Riga, June 11, 2001. ISBN 9984-9507-7-5

Jäger, R. and S. Schneid (2002): Online and Postprocessed GPS-Heighting based on the Concept of a Digital Height Reference Surface. In : IAG International Symposium 'Vertical Reference Systems', H. Drewes, A. Dodson, L.P.S. Fortes, L. Sanchez, P. Sandoval (EDS), Vol. 124, Springer Berlin, Heidelberg New York, pp 203-208.

Jäger, R. and Schneid (2002): Passpunktfreie direkte Höhenbestimmung mittels DFHBF – ein Konzept für Positionierungsdienste wie SAPOS. Landesvermessung und Geobasisinformation Niedersachsen (LGN) (Editor). Hannover. p. 149-166.

Jäger, R. and S. Kälber (2004): Precise Vertical Reference Surface Representation and Precise Transformation of Classical Networks to ETRS89 / ITRF - General Concepts and Realisation of Databases for GIS, GNSS and Navigation Applications in and outside Europe. In: 2<sup>nd</sup> Common Baltic Symposium, GPS-Heighting based on the Concept of a Digital Height Reference Surface (DFHRS) and Related Topics - GPS-Heighting and Nationwide Permanent GPS Reference Systems. Riga, 2003. in press.

Jäger, R. and S. Schneid (2004): A Decimetre Height Reference Surface (HRS) for the European Vertical Reference System (EVRS) based on the DFHRS Concept. Contribution

- in IAG Subcommittee for Europe Symposium EUREF 2004, Bratislava, Slovakia.  
EUREF-Mitteilungen. Bundesamt für Kartographie und Geodäsie (BKG), Heft 14,  
Frankfurt. ISBN 3-89888-795-2. S. 194-202.
- Jäger, R. and S. Schneid (2006a): Extension of the DFHRS approach for gravity observations  
and computation design for a 1cm fitted DFHRS of Europe. Proceedings EUREF  
Symposium 2005, 14-17 June 2005 Vienna.
- Jäger, R. and S. Schneid (2006b): DFHRS (Digital FEM Height Reference Surface) – A  
Rigorous Approach for the Integrated Adjustment and Fitting of Height Reference Surfaces  
EUREF Symposium 2006, 14-17 June 2006, Riga.
- Jäger, R. and S. Schneid (2000-2007): Homepage of the DFHRS-project, [www.dfhbf.de](http://www.dfhbf.de)
- Jekeli, C. (2000): "Heights, the Geopotential, and Vertical Datums," Technical Report 459,  
Ohio Sea Grant Development Program, NOAA, Grant No. NA86RG0053 (R/CE-7-PD),  
[http://www.ceegs.ohio-state.edu/greports/reports/report\\_459.pdf](http://www.ceegs.ohio-state.edu/greports/reports/report_459.pdf)
- Jiangchen, L., Ch. Dingbo and N. Jinsheng (1995): Spherical cap harmonic expansion for  
local gravity field representation. Manuscripta geodaetica 20, p265-277
- Kaschenz, J.(2006): Regularisierung unter Berücksichtigung von Residuentoleranzen.  
Technische Universität Berlin, D-83, Berlin 2006
- Kaula, W.M. (1966): Theory of Satallity Geodesy. Blaisdell Publ. London
- Kautzleben, H. (1965): Kugelfunktionen, Geomagnetismus und Aeronomie Band 1, B.G.  
Teubner Verlagsgesellschaft Leipzig, 1965
- Klein, U. (1997): Analyse und Vergleich unterschiedlicher Modelle der dreidimensionalen  
Geodäsie. Bayer. Akademie d. Wissenschaften, Deutsche Geodätische Kommission  
(DGK), Reihe C, Nr.479

- Korte, M. (1999): Kombination regionaler magnetischer Vermessungen Europas zwischen 1955 und 1995, Scientific Technical Report STR99/11, GFZ Potsdam, 1999.
- Korte, M. and Holme, R.T.(2003): Regularization of spherical cap harmonics, *Geophysical Journal International*, 153, 1, pp. 253-262.
- Kotze, P. B. (2001): Spherical cap modelling of Orsted magnetic field vectors over South Africa, *Earth Planets Space* 53, pp. 357-361, 2001
- Lehmann, R. (1994): Zur Bestimmung des Erdschwerefeldes unter Verwendung des Maximum-Entropie-Prinzipes, Bayer. Akademie d. Wissenschaften, Deutsche Geodätische Kommission (DGK), Reihe C, Nr.425
- Lemoine, F.; S. Kenyon; J. Factor; R. Trimmer, N. Pavlis; D. Chinn; M. Cox; S. Klosko; S. Luthcke; M. Torrence; Y. Wang; R. Williamson; E. Pavlis; R. Rapp and T. Olson (1998): The development of the Joint NASA GSFC and NIMA Geopotential Model EGM96. NASA Goddard Space Flight Center, Greenbelt, Maryland, 20771, USA.
- Liebsch G., U. Schirmer, J. Ihde, H. Denker, J. Müller (2006): Quasigeoidbestimmung für Deutschland. DVW-Schriftenreihe, No. 49, 127-146, 2006.
- Marchenko, A.N. (1998): Parameterization of the Earth's gravity field. Point and line singularities. Lviv Astronomical and Geodetic Society, 1998
- Marti, U.(1998): The new geoid CHGEO97 of Switzerland. Finnish Geodetic Institute Report 98:4, pp. 281-287. Proceedings of the 2nd Continental Workshop on the Geoid in Europe, Budapest, March 10-14, 1998.
- Marti, U and A. Schlatter (2003): Höhenreferenzsysteme und –rahmen. *Vermessung, Photogrammetrie, Kulturtechnik*. 1/2002 p. 8-12.
- Marti, U and A. Schlatter (2005): Festlegung des Höhenbezugsrahmens LHN95 und Berechnung des Geoidmodells CHGeo2004. *GEOMATIK SCHWEIZ, JAHR 103; HEFT 8*, pages 445-449

- Moritz, H. (1980): On the computation of a Global Covariance Model. Rep. 255, Dept. Geod. Sci. Ohio State University, Columbus
- Moritz, H. (1980): Advanced Physical Geodesy, Wichmann Verlag, Karlsruhe, 1980. ISBN 3-87907-106-3
- Moritz, H. (1990): The figure of the earth: theoretical geodesy and the earth's interior, Wichmann Verlag, Karlsruhe 1990, ISBN 3-87907-220-5
- Müller, T (1990) : Integrierte Ausgleichung geodätischer Netze im Massenpunktmodell. München, Bayer. Akademie d. Wissenschaften, Deutsche Geodätische Kommission (DGK), Reihe C, Nr.362
- NGS, National Geodetic Survey (2003) : The NGS GEOID Page  
<http://www.ngs.noaa.gov/GEOID/>
- Olver, F. & Smith, J. (1983): Associated Legendre functions on the cut. Journal of Computational Physics, 51, pp. 502-518.
- Omang, O.C.D. and R. Forsberg (2002) The northern European geoid: a case study on long-wavelength geoid errors, Journal of Geodesy (2002) 76, pp. 369-380, Springer Verlag, 2002
- Pail, R., Metzler, B., Preimesberger, T., Goiginger, H., Mayrhofer, R., Höck, E., Schuh, W.-D., Alkathib, H., Boxhammer, Ch., Siemes, Ch. And M. Wermuth (2007): GOCE-Schwerefeldprozessierung: Software-Architektur und Simulationsergebnisse, Zeitschrift für Vermessungswesen 1/2007. vol 132. p 16-25.
- Pal, B. (1919): On the numerical calculation of the roots of the equations  $P_{nm}(\mu) = 0$  and  $(d/d\mu)P_{nm}(\mu) = 0$  regarded as equations in  $n$ , Bull. Calcutta Math. Soc. Vol.9 (1917-1918) pp. 85-95, 1919.
- Pal, B. (1919): On the numerical calculation of the roots of the equations  $P_{nm}(\mu) = 0$  and  $(d/d\mu)P_{nm}(\mu) = 0$  regarded as equations in  $n$ , Bull. Calcutta Math. Soc. Vol.10 (1917-1919) pp. 187-194, 1920.

- Press, W H, Teukolski, S A, Vetterling, W T and B P Flannery (2002): Numerical Recipes in C++, Cambridge : Cambridge University Press, 2002. ISBN 0-521-75033-4
- Seeber, G. (2003): Satellite Geodesy, de Gruyter, Berlin New York, 2003. ISBN 3-11-017549-5
- Schneid, S. (2002): Software Development and DFHRS computations for several countries. J. Kaminskis and R. Jäger (Eds.): 1<sup>st</sup> Common Baltic Symposium, GPS-Heighting based on the Concept of a Digital Height Reference Surface (DFHRS) and Related Topics - GPS-Heighting and Nation-wide Permanent GPS Reference Systems Riga, June 11, 2001. ISBN 9984-9507-7-5
- Schneid, S.(2003): The Digital FEM-Height Reference Surface DFHRS of Germany. In: Proc. of the 2<sup>nd</sup> Common Baltic Symposium, GPS-Heighting based on the Concept of a Digital Height Reference Surface (DFHRS) and Related Topics - GPS-Heighting and Nationwide Permanent GPS Reference Systems. Riga, June 11, 2003.
- Schneid, S. and H. Meichle (2005): Normalhöhen in Baden-Württemberg, Arbeiten zur Einführung von Höhen im System des Deutschen Haupthöhennetzes 1992. DVW-Landesverein Baden-Württemberg, Mitteilungen 2/2005. ISSN 0940-2942
- Schwarzer, F. (2000): Entwicklung graphikfähiger C-Software zur Berechnung Digitaler Finite Element Höhenbezugsflächen (DFHBF) und DFHBF-Implementierung in GPS-Kommunikationssoftware. Diploma-thesis, Studiengang Vermessung und Geomatik, FH Karlsruhe, unpublished
- Sjöberg, L.E. (2005): A discussion on the approximations made in the practical implementation of the remove-compute-restore technique in regional geoid modelling. Journal of Geodesy 78, p. 645-653,
- Smith, D.A. and D.R. Roman (2001): GEOID99 and G99SSS: 1-arc-minute geoid models for the United States, Journal of Geodesy 75, p. 469-490
- Thebault, E., Schott, J.J. and M. Manda (2006): Revised spherical cap harmonic analysis (R-SCHA): Validation and properties., Journal of Geophysical, Research, Vol. 111, 2006

- Thebault, E., Schott, J.J., Manda, M. and J.P.Hoffbeck (2004): A new proposal for spherical cap harmonic modelling, *Geophysical Journal International* (2004) 159, pp. 83-103.
- Torge, W., H. Denker (1999): Zur Verwendung des Europäischen Gravimetrischen Quasigeoids EGG97 in Deutschland. *Z.f.Verm.wesen* 124, 154-166, 1999.
- Torge, W. (2003): *Geodesy*. 3<sup>rd</sup> Edition, de Gruyter, Berlin New York, 2001. ISBN 3-11-017072-8
- Tscherning, C.C. and H. Rapp (1974) Closed covariance expressions for gravity anomalies, geoid undulations and deflections of the vertical implied by anomaly degree variance models. OSU Rep. 208, Columbus, Ohio.
- Wenzel, H-G. (1981): Zur Geoidbestimmung durch Kombination von Schwereanomalien und einem Kugelfunktionsmodell mit Hilfe von Integralformeln. *Zeitschrift für Vermessungswesen*, vol. 106, 102-111, Stuttgart 1981.
- Wenzel, H-G. (1985): Hochauflösende Kugelfunktionsmodelle für das Gravitationspotential der Erde. *Wiss. Arb. Univ. Hannover* 137.
- Wenzel, H-G. (1989): On the definition and numerical computation of free air gravity anomalies. *Bureau Gravimetrie International, Bulletin d'Information*, vol. 64, 23-40, Toulouse 1989.
- Wenzel, H-G. (1999): Schwerefeldmodellierung durch ultra-hochauflösende Kugelfunktionsmodelle. *Zeitschrift für Vermessungswesen*, vol. 126, 144-154, Stuttgart 1999.
- Whaler, K.A. and D. Gubbins (1981): Spherical harmonic analysis of the geomagnetic field: an example of a linear inverse problem, *Geophys. J.R. astr. Soc.*, 65, p 645-693.

## **Publications**

Jäger, R. and S. Schneid (2006a):

Extension of the DFHRS approach for gravity observations and computation design for a 1cm fitted DFHRS of Europe. Proceedings EUREF Symposium 2005, 14-17 June 2005 Vienna.

# Extension of the DFHRS approach for gravity observations and computation design for a 1cm fitted DFHRS of Europe<sup>1</sup>

Prof. Dr.-Ing. Reiner Jäger and Dipl.-Ing. (FH) Sascha Schneid

Hochschule Karlsruhe für Technik und Wirtschaft – University of Applied Sciences  
Fakultät für Geoinformationswesen, Institut für Angewandte Forschung (IAF)  
Moltkestrasse 30, D-76133 Karlsruhe  
Email: [reiner.jaeger@web.de](mailto:reiner.jaeger@web.de)

## Abstract

The Digital FEM Height Reference Surface - DFHRS - is modelled as a continuous surface in arbitrary large areas by bivariate polynomials  $\mathbf{p}$  over a grid of Finite Element meshes (FEM). Up to now geoid heights  $N$ , deflections of the vertical  $(\xi, \eta)$  and identical points  $(h, H)$ , were used as observation groups in a common a least squares computation of the DFHRS parameters  $\mathbf{p}$ . Geoid models and sets of deflections of the vertical may be parted into different "patches" with individual datum-parameters to reduce the effect of existing medium- and long-waved systematic errors. The resulting DFHRS parameters  $\mathbf{p}$  uniquely represent the Height Reference Surface HRS. The DFHRS database (DFHRS\_DB) provides the separation  $DFHRS(\mathbf{p}|B,L,h) = h - H$ , to transform ellipsoidal GNSS heights  $h$  into physical standard heights  $H$  directly. One part of this "DFHRS-correction" consists of the FEM representation of the HRS ("geoid-part") as function of the position  $(B, L)$ , related to  $\mathbf{p}$ . In case of significance, an additional "scale part" is introduced as a function of  $h$ .

Introductionary the presentation gives a general overview about the state of the art of the concept of the Digital Finite Element Height Reference Surface (DFHRS), its standardization in GNSS services and industry, and DFHRS databases computed in different European states.

The second part of the presentation is dealing with the further development of the DFHRS approach with respect to the rigorous mathematical approach of an introduction of gravity observations, based on spherical Cap Harmonics Analysis (SCHA). Computation results of the present evaluation of the 1\_cm gravity data based DFHRS of Saarland and Baden-Württemberg are presented, as well as the present version of the DFHRS-software. Based on the computation results for Saarland and Baden-Württemberg, and following the presentation of a one decimeter DFHRS for Europe on EUREF 2004, the last part of the presentation deals with the computation design for a one centimeter HRS-Europe based on the extended DFHRS approach.

## 1 FEM representation of a Height Reference Surface (DFHRS)

The finite element representation  $NFEM(\mathbf{p}|x,y)$  is carried by bivariate polynomials of degree  $n$ , which are set up in regular or irregular meshes ([4], [8], [10], [11], [12], [15], [16], [21], [43]). If we describe with  $\mathbf{p}^i$  the polynomial coefficients  $(a_{00}, a_{10}, a_{01}, a_{20}, a_{11}, a_{02}, \dots)^T$  of the  $i$ -th of  $n$  meshes in total, we have for the height  $NFEM(\mathbf{p}^i|x,y)$  of the HRS over the ellipsoid:

$$NFEM(\mathbf{p}^i | x, y) = \mathbf{f}(x, y)^T \cdot \mathbf{p}^i \quad (1a)$$

$$\mathbf{p}^i = [a_{jk}^i]^T; j=0, n; k=0, n \text{ and } \mathbf{f}(x, y)^T = (1, x, y, x^2, xy, y^2, \dots) \quad (1b), (1c)$$

The plan position  $(x, y)$  in (1a,c) is due to metric ellipsoidal coordinates,  $y(B,L)$ ="East" and  $x(B,L)$ ="North", introduced e.g. as Mercator or Lambert coordinates, which are in any case functions

---

<sup>1</sup> Jäger, R. and S. Schneid (2007): Extension of the DFHRS Approach for Gravity Observations and Computation design for a 1cm fitted DFHRS of Europe. Proceedings IAG Subcommission for Europe Symposium EUREF 2005, Vienna. EUREF-Mittellungen. Bundesamt für Kartographie und Geodäsie (BKG), Heft 15, Frankfurt. S. 308 ff.

of the ellipsoidal geographical coordinates (B, L). The vector  $\mathbf{f}$  means the Vandermond vector and contains the different powers of the coordinates (x, y) according to the polynomial degree n.

To imply a continuous surface representation NFEM( $\mathbf{p}|x,y$ ), one set of continuity conditions of different type  $C_{0,1,2}$  has to be set up for the computation of  $\mathbf{p}$  for each couple of neighbouring meshes (fig. 3.4). The continuity type  $C_0$  implies the same functional values, the continuity type  $C_1$  implies the same tangential planes and the continuity type  $C_2$  the same curvature along common mesh borders of the DFHRS representation NFEM( $\mathbf{p}|x,y$ ) (1a). The continuity conditions occur as additional observation equations  $C(\mathbf{p})=0$  related to the polynomial sets of the coefficients  $(a_{jk})^m$  and  $(a_{jk})^n$  of each couple of neighbouring meshes m and n. To force e.g.  $C_0$ -continuity, the difference  $\Delta N_{m,n}$  in the geoid height  $N_G$  of any point S at the common border SA–SE of two meshes m and n (see fig. 8) has to become zero. So the basic condition equation for a polynomial representation of  $n^{\text{th}}$  degree reads [16]:

$$\Delta N_{m,n} = \sum_{j=0}^n \sum_{k=0}^{n-j} (a_{jk,n} - a_{jk,m}) \cdot (y_{SA} + t \cdot (y_{SA} - y_{SE}))^j \cdot (x_{SA} + t \cdot (x_{SA} - x_{SE}))^k = 0 \quad (1d)$$

With  $(y_{SA}, x_{SA}, y_{SE}, x_{SE})$  we introduce the plan metric coordinates of the nodal points SA and SE of a mesh borderline. Equation (1d) represents a polynomial of n-th degree parametrized in the border line parameter t with  $t \in [0,1]$ . The subset of (n+1)  $C_0$ -continuity condition equations  $C(\mathbf{p})=0$  for the border between mesh m and n results in case of  $C_0$ -continuity from (1d) by setting all (n+1) coefficients related to t to zero ([16]).

The mesh size and mesh shape for the computation of the NFEM( $\mathbf{p}|x,y$ ) - representing the so called HRS or "geoid" part (3.3a) of the DFHRS correction and database (DB) content - may be chosen arbitrarily. The best approximation of a HRS by NFEM( $\mathbf{p}|x,y$ ) results of course by introducing small meshes, e.g. in a range of  $(5 \text{ km})^2$  to keep a 5 mm precision for any HRS shape approximation by a polynomial degree up to  $n=3$ . A special advantage and characteristic of the NFEM( $\mathbf{p}|x,y$ ) representation consists in the fact, that the nodal points of the FEM grid are totally independent from the location of the geodetic observations and the geoid data points. In principle any type of HRS and height related observation data can be used for the determination of the parameter vector  $\mathbf{p}$  of NFEM( $\mathbf{p}|x,y$ ), namely height observations  $(h, H, \Delta h, \Delta h)$ , the geoid-model heights  $N_G(B, L)$ , deflections of the vertical  $(\xi, \eta)$  and - in the extended DFHRS approach presented in that paper - also gravity observations g (see chap. 3).

## 2 Digital FEM Height Reference Surface (DFHRS) – State of the Art

### 2.1 Mathematical Adjustment Model

The mathematical model of the so-called "DFHRS database production step" reads in the system of observation equations (functional model) and the corresponding stochastic models of a least squares adjustment as follows ([6], [43], [12], [14], [15], [16]):

**Table 1:** The mathematical model of the DFHRS production step

Functional Model	Observation Types and Stochastic Models	
$h + v = H + h \cdot \Delta m + \text{NFEM}(\mathbf{p}   x, y),$ with $\text{NFEM}(\mathbf{p}   x, y) =: \mathbf{f}(x, y) \cdot \mathbf{p}$	Uncorrelated observations of ellipsoidal heights h. Covariance matrix $\mathbf{C}_h = \text{diag}(\sigma_{h_i}^2)$ .	(2a)
$N_G(B, L)^j + v = \mathbf{f}(x, y)^T \cdot \mathbf{p} + \partial N_G(\mathbf{d}^j)$	Correlated geoid height observations. With a given real covariance matrix $\mathbf{C}_{N_G}$ or a $\mathbf{C}_{N_G}$ evaluated from an synthetic covariance function.	(2b)
$\xi + v = -\mathbf{f}_B^T / M(B) \cdot \mathbf{p} + \partial \xi(\mathbf{d}_{\xi, \eta})$	Observations of deflections from the vertical $(\eta, \xi)$ . Pair wise correlated or uncorrelated in case of astronomical observations. Correlated if derived from a gravity potential model.	(2c)
$\eta + v = -\mathbf{f}_L^T / (N(B) \cdot \cos(B)) \cdot \mathbf{p} + \partial \eta(\mathbf{d}_{\xi, \eta})$		(2d)

$H + v = H$	Uncorrelated standard height $H$ observations with covariance matrix $C_H = \text{diag}(\sigma_{H_i}^2)$ .	(2e)
$C + v = C(\mathbf{p})$	Continuity condition equations (1d) introduced as uncorrelated so-called pseudo observations with accordingly small variances and high weights.	(2f)

With  $\mathbf{f}_B$  and  $\mathbf{f}_L$  we introduce the partial derivatives of the Vandermond's vector  $\mathbf{f}(x,y)$  (2c) with respect to the geographical coordinates  $B$  and  $L$ .  $M(B)$  and  $N(B)$  mean the radius of meridian and normal curvature at a latitude  $B$  respectively.

The continuity of the resulting HRS representation  $\text{NFEM}(\mathbf{p}|x,y) = \mathbf{f}(x,y)^T \cdot \mathbf{p}$  is automatically provided by the continuity equations  $C(\mathbf{p})$  (2f).

A number of identical points ( $h, H$ ) are introduced by the observation equations (2a) and (2e).

In the practice of DFHRS data base evaluation, one or a number of different geopotential models, such as the EGG97 [7], may be used as additional observations to produce DFHRS\_DB in the least squares estimation (2a-f).

To reduce the effect of medium- or long-wave systematic shape deflections, namely the natural and stochastic "weak-shape" ([2], [3], [4], [5], [9], [26]) in such models, they are subdivided to into a number of so-called "geoid-patches", each represented by the vector of geoid height observations  $N_G(B, L)^j$  (2b) within the respective meshes. Each patch is related to a set of individual parameters  $\mathbf{d}^j$ , which are introduced in the datum parametrization  $\partial N_G(\mathbf{d}^j)$  (2b). In this way, it is of course possible to introduce any number of different geoid-, quasigeoid- or geopotential models in the same area. In case of already fitted models the datum-parametrization  $\partial N_G(\mathbf{d}^j)$  is neglected.

The deflections of the vertical,  $\xi$  and  $\eta$ , are introduced in their classical meaning as slope of  $N_G$  in the direction of the latitude  $B$  and the longitude  $L$ . With the polynomial representation  $\text{NFEM}(\mathbf{p}|x,y)$  we get :

$$\xi = -\partial N / \partial s_B = -\partial \text{NFEM} / \partial B \cdot \partial B / \partial s_B = -\mathbf{f}(x,y)_B \cdot \mathbf{p} \cdot \partial B / \partial s_B, \quad (2g)$$

$$\eta = -\partial N / \partial s_L = -\partial \text{NFEM} / \partial L \cdot \partial L / \partial s_L = -\mathbf{f}(x,y)_L \cdot \mathbf{p} \cdot \partial L / \partial s_L. \quad (2h)$$

For  $\partial B / \partial s_B$  and  $\partial L / \partial s_L$  we have the curvature of the meridian  $\partial B / \partial s_B = M(B)$  and the normal curvature  $\partial L / \partial s_L = N(B) \cdot \cos(B)$ , respectively.

With  $\partial \xi(\mathbf{d}_{\xi,\eta})$  and  $\partial \eta(\mathbf{d}_{\xi,\eta})$  we describe the datum parametrization of the observation type of deflections of the vertical  $\xi = (\varphi_{\text{astr}} - B)$  and  $\eta = (\lambda_{\text{astr}} - L) \cdot \cos B$  respectively. In case of gravimetric deflections of the vertical ( $\xi, \eta$ ), derived from the same potential model as the geoidheights  $N_G$ , the parameters  $\mathbf{d}$  are also expected to be the same. Therefore it holds  $\mathbf{d}(2b) = \mathbf{d}_{\xi,\eta}(2c) = \mathbf{d}_{\xi,\eta}(2d)$ . In any other case or for sets of astronomically observed vertical deflections, different groups of datum parameters  $\mathbf{d}$  have to be introduced.

The so-called "DFHRS-correction"  $\text{DFHRS}(\mathbf{p}, \Delta m | B, L, h)$  results from equation (2a). It enables the conversion of a GNSS-heights  $h$  at a GNSS-position  $(B, L, h)$  to the physical height  $H$  and reads ([6],[15]):

$$\begin{aligned} H &= h - N = h - \text{DFHRS}(\mathbf{p}, \Delta m | B, L, h) \\ &= h - (\text{NFEM}(\mathbf{p} | x(B, L), y(B, L)) + h \cdot \Delta m) = h - \mathbf{f}(x, y) \cdot \mathbf{p} - h \cdot \Delta m \end{aligned} \quad (2i)$$

The first part  $NFEM(\mathbf{p} | x, y)$  is called "geoid (or quasigeoid) surface part". The second part  $h \cdot \Delta m$  is called the "scale part". The scale part may be relevant as well as significant in older height systems like e.g. the German NN-height system.

## 2.2 DFHRS Software and Quality Control in DFHRS\_DB Computation

The DFHRS approach has been realized in the software DFHBF©Jäger/Schneid/Schwarzer, version 4.0. There the mathematical model of the DFHRS approach (Table 1) is embedded in the quality control standards of a priori and a posteriori variance related tests (data snooping) and variance component estimations. The covariance matrix of the resulting parameters  $(\mathbf{p}, \Delta m)$  can be used to compute and visualize the accuracy of the HRS as provided by the DFHRS\_DB using formula (3b). An additional and valuable way to prove the external accuracy of the DFHRS\_DB is to compute a so-called "reproduction quality" and point-wise "reproduction values" [16], [17], [18]. The "reproduction quality" and a number of  $n$  resulting "reproduction values  $\nabla H_i$ " - all over the DFHRS area - are simply defined by the values of differences. For this quality proof no explicit "control measurements" are needed. We just have to compute successively the "DFHRS-height"  $H_{DFHRS,i}$  of each point  $i$  of the  $n$  identical points applying (2i). This is done using the individual parameters  $\mathbf{p}_i$ , where  $H_i$  was excluded from the respective DFHRS\_DB production (2a-f), which was then evaluated with the remaining  $(n-1)$  points. The "reproduction values"  $\nabla H_i$  are much more objective and informative than the pure least squares residuals  $v_i$  (2e). The reproduction values  $\nabla H_i$  are to be computed in the unique DFHRS production step (2a-k) of the DFHRS adjustment. The respective formula reads ([6], [10],[11]):

$$\nabla H_i = - \frac{v_{H_i}}{r_{H_i}} \quad (3a)$$

With  $v_{H_i}$  and  $r_{H_i}$  we describe the residual and the redundancy part of  $H_i$  in equation (2e). The above reproduction values (3a) are however only directly interpretable as a quality measure, if they are applied to the part of the high accurate identical points  $(h, H)$ . A general measure for the precision of a DFHRS\_DB is based on the local variance  $\sigma^2_{DFHRS}(B, L, h)$  of the position-dependent DFHRS-correction (2i). It can be computed based on the covariance matrix of the parameters  $\mathbf{p}$  and  $\Delta m$  of the DFHRS-correction (2i) reading:

$$\sigma^2_{DFHRS}(B, L, h) = \begin{bmatrix} \mathbf{f}(B, L)^T \\ h \end{bmatrix} \cdot \begin{bmatrix} C_{p,p} & C_{p,\Delta m} \\ C_{\Delta m,p} & C_{\Delta m,\Delta m} \end{bmatrix} \cdot \begin{bmatrix} \mathbf{f}(B, L) \\ h \end{bmatrix}^T \quad (3b)$$

From (3b) a so-called "surface of precision" can be evaluated by gridding (3b) with the approximative height  $h$  resulting from a rough digital terrain and geoid-model.

## 2.2 DFHRS\_DB Contents and DFHRS\_DB Access Software

The essential adjustment unknowns of the mathematical model (2a-f) and parameters of resulting DFHRS\_DB are  $\mathbf{p}$  and  $\Delta m$ . These represent the continuous model  $NFEM(\mathbf{p}|x,y)$  of the HRS and enable an additional scale correction  $\Delta m \cdot h$ . So these parameters provide the DFHRS correction  $DFHRS(\mathbf{p}, \Delta m | x, y, h)$  (2i) for an online or post-processed GNSS heighting.

Besides the header (version name etc.), a DFHRS\_DB contains a second block with the mesh design (coordinates of the mesh nodal points, mesh number and topological description) and finally the block with the mesh-wise parameter sets  $\mathbf{p}$  and  $\Delta m$ .

## 2.3 European HRS as part of the European Vertical Reference System (EVRS)

An essential and very precious characteristic of the embedded FEM principle is, that any DFHRS\_DB and its quality (3a,b) respectively, which are to be achieved by using the DFHRS approach (2a-f) in a small area, is to be achieved - without loss of accuracy - in a corresponding large area scene. Only

provided that the density of the identical points (H,h) and the quality of the geoid information  $N_G$  are kept. Fig. 1 gives an overview about the DFHRS\_DB computations in Europe. Following the proposal in [14] and the IAG Subcommission for Europe (EUREF) conclusions in 2001, a continuous “<\_10\_cm European HRS” for normal heights was computed using the DFHRS approach in 2004 (fig. 1, green), meaning an essential improvement with respect to the EGG97, which shows long-waved “weak-shape deflections” [5] much larger than 10 cm [25]. A <1 cm DFHRS DB was also computed for the orthometric height system of Albania [27].

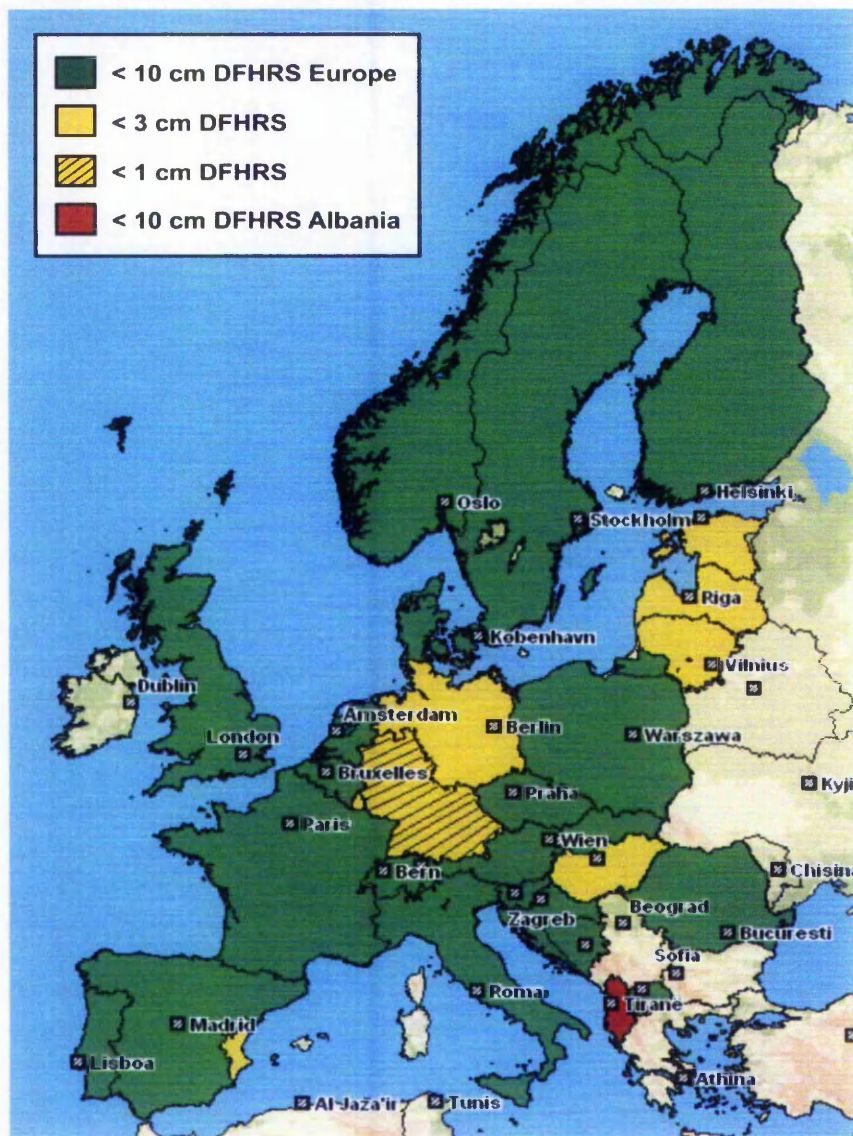


**Fig. 1:**

**Overview on DFHRS\_DB computed all over Europe**

The present 1<sup>st</sup> class and high end however, are so-called “<1cm DFHRS\_DB”, which are defined by a mean reproduction value  $\sqrt{H_i} \leq 1$  cm (3a) and an accuracy surface (3b)  $\leq 1$  cm. They are in any size and scale to be computed with a mesh size of (5 km)<sup>2</sup>, a fitting-point density of about 50 identical points (H, h) per (100 km x 100 km) and a (30 - 40) km geoid-model “patch” size. Different “<1cm DFHRS\_DB”, which represent the present “high end” quality type, have been computed in Germany (fig.1, hatched yellow) and for the Tallinn area. In Germany these 1\_cm DFHRS\_DB are available as

official geo-data products at different state land service departments and used in SAPOS® ([8], [13], [21], [22]).

The 2<sup>nd</sup> quality class of “< 3cm DFHRS\_DB” is defined by an average reproduction value  $VH_i \leq 3$  cm (3a) and an accuracy surface (3b) less than 3 cm. That type was first computed for the district of Valencia, Spain in 2003/4 (see, [24]). A closed “<3 cm DFHRS\_DB Germany” (fig. 1. hatched and non-hatched yellow area together) for the new normal heights was evaluated in 2005/2006 with a density of 10 identical points (H, h) per (100 km x 100 km) area, a mesh size of 10 km, and a polynomial degree  $n=3$ .

A closed and continuous solution of a “(1-3) cm DFHRS\_DB Baltic States” (fig. 1) was computed for the Baltic States Estonia, Latvia and Lithuania in the frame of a cooperation with the State Land Service of Latvia, Riga ([25],[32]). In 2005 a “<(1-2) cm DFHRS\_DB Hungary” was computed in the frame of a master thesis and in a cooperation with FÖMI ([34], [35]).

Outside of Europe a “<30 cm DFHRS\_DB Namibia” and the “(2-3) cm DFHRS\_DB Windhoek” were computed for the state of Namibia and for the district of Windhoek respectively [18], [19], [42] based on the EGM96 and fitting points.

In the USA a “<5 cm DFHRS\_DB Florida” was evaluated in 2005 in the frame of a master-thesis at the Karlsruhe University of Applied Sciences (fig. 2) [33]. For further information about existing DFHRS databases and project it is referred to the DFHRS homepage [www.dfhbf.de](http://www.dfhbf.de) [21] and [22].

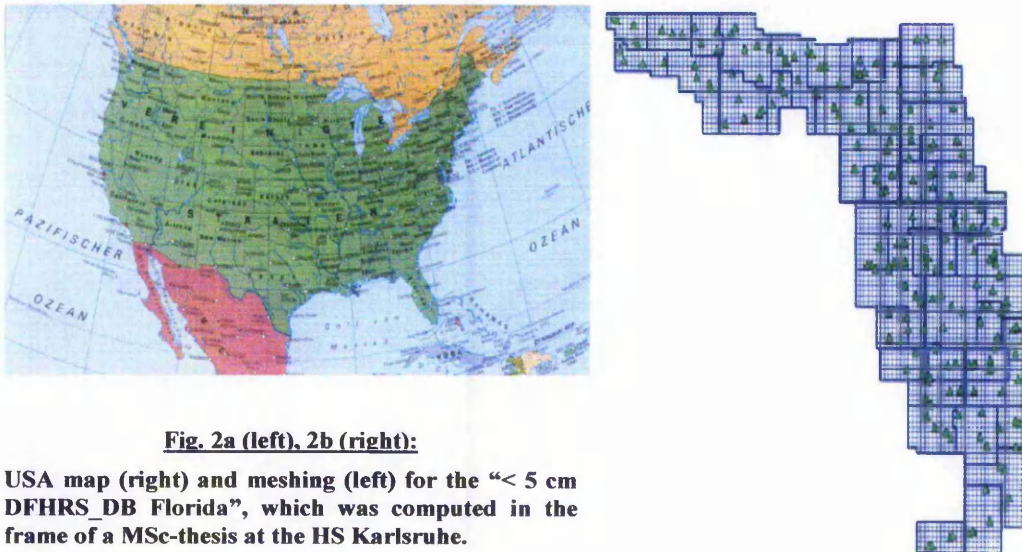


**Fig. 2a (left), 2b (right):**

**USA map (right) and meshing (left) for the “< 5 cm DFHRS\_DB Florida”, which was computed in the frame of a MSc-thesis at the HS Karlsruhe.**

## 2.4 Standardisation and use of DFHRS Databases

### 2.4.1 Direct and Grid-based Access used in GNSS-Controllers

For the implementation of DFHRS databases and also DFLBF/CoPaG databases respectively into existing software packages the access software have been realized as DLL (Dynamics Link Library) ([43], [21], [29]).



**GPS System 500 V4.0** just nach mehr Möglichkeiten!

**Referenzliste und Verwaltung**  
 - Nutzung von GAPS- und ASCII-Daten  
 - Verarbeiten von Feld- und Bürodaten  
 - Verwaltung von AD/Netz- und PUNKT

**Aktuelle und logische Anwendung**  
 - Mitteilungsliste absolut oder gewichtet  
 - Reaktionsfähigkeit im Feld  
 - Höhenmodell „DFHRS“  
 - Identifikation des nächstgelegenen Punktes

**Technik**  
 - Permanent Integrity Monitoring der RTK-Corrig.  
 - RTK-Zuverlässigkeit basierend auf 99,99%  
 - Kompatibilität zu weiteren Formaten (MAGNETIC)  
 - Koordinatenkonverter an Zonen, RECSN, Geoidhöhe = x  
 - Integrierte Höhenplanung für Grenzübertragung  
 - Und viele weitere neue Features und Verbesserungen...  
 - Mit der neuen Firmware V4.0 ist das System 500 ausstärker  
 - für jede Anwendung!

**Leica Geosystems**

**Fig. 3.**

**DFLBF/CoPaG and DFHRS access realized in Trimble Survey Manager Software (left; [www.trimble.com](http://www.trimble.com)) and in the controller of Leica-geosystems (right; [www.leica-geosystems.com](http://www.leica-geosystems.com)).**

The DLL is also running in the so-called “grid-factories” of different GNSS-companies. (DFLBF/CoPaG databases are designed for transformation between horizontal positions of classical reference network and modern ITRF-based ones). The growing acceptance and the different implementations of the DFLBF/CoPaG and DFHRS database standard into different GNSS equipments and software packages of the GNSS industry are shown in fig. 3 and fig. 4. That list of DFLBF/DFHBF database access-DLL implementation can be continued with respect to a number of companies, that develop own surveying-software with GNSS- and totalstations-interfaces for electronic field-books, e.g. GeoSamos ([www.breining.de](http://www.breining.de)), Gart2000 ([www.allsat.de](http://www.allsat.de)) (see, [22]).



**Fig. 4:**

**DFLBF/CoPaG and DFHRS access realized in the GNSS controller-software TopSURV of TOPCON ([www.topcon.de](http://www.topcon.de)) and by Thales Navigation ([www.thales-navigation.com](http://www.thales-navigation.com)).**

Besides the GNSS domain, the DFHRS\_DB access software is used and implemented into different GIS software packages. For details it is referred to [21], [22] and [29].

#### 2.4.2 RTCM 3.0 Conversion

The DFHRS\_DB and DFLBF\_DB can be converted consistently and directly into the new RTCM 3.0 transformation messages 1022-1028.

### 3 Extension of the DFHRS approach for gravity observations

#### 3.1 Strict sequential solution

Observations from gravimetric geoid models  $N_G$  (2b) are to be introduced instead of the original gravity observations  $g$ , which had already been introduced for the computation of  $N_G$ . In this case the correlated geoid models observations  $N_G$  (2b) and original gravity observations (gravity anomalies  $\Delta g$ , gravity disturbances  $dg$  or absolute gravity values  $g$ ) lead to identical results for the HRS represented by the parameters  $p$ . This follows from the theory of sequential least squares adjustment, and it was proofed in the context with the DFHRS approach explicitly in [12]. So the use of the type  $N_G$  (2b) implies the same result as the original gravity observations, as soon as the original covariance matrix  $C_{NG}$  is known or approximated by a proper covariance function.

Functional Model	Observation Types and Stochastic Model
$N_G + v = f(x, y) \cdot p$ $= NFEM(p   x, y)$	"Gravity based" observation group, for example (quasi)geoid heights from a gravimetric model. Original covariance matrix $C_{NG}$ from the computation of $N_G$ or artificial covariance matrix $C_{NG}$ from an appropriate covariance function. (4)

#### 3.2 Extension of the approach to explicit gravity observations

##### 3.2.1 Explicit gravity observations versus sequential concept – general discussion

Following the concept of a strict sequential least squares adjustment the incorporation of explicit gravity observations  $g$  (gravity anomalies  $\Delta g$ , gravity disturbances  $\delta g$  may be introduced alternatively) would principally be needed, only if they occur as additional observations, which have so far not been used for the determination of the "gravity based" model introduced with (2b), (4).

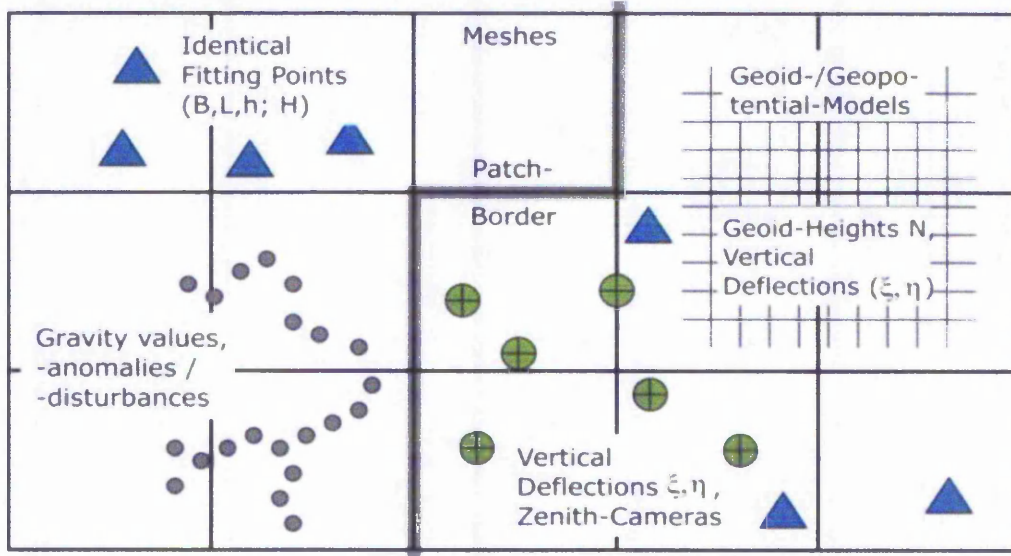


**Fig. 5:**  
**Observation types of the extended DFHRS-approach**  
**realised in the DFHRS software version 5.0**

The lack of a correct covariance matrix  $C_{NG}$  (4) leads to more or less small discrepancies (so-called "latent week shapes" [26]) with respect the strictness of a sequential adjustment solution realized in the DFHRS approach by (4). Above this, the big dimension of the matrix  $C_{NG}$  disables presently its

practical use for large areas. At last it holds, that GPS and non-fitted gravimetric geoid models  $N_G$  not only suffer from long-waved weak shapes (correct treatment and optimal reduction on using the DFHRS concept (2a-f) with the original covariance matrix in (2b)), but they also suffer from insufficiencies in the mathematical model, approximations in the reduction of gravity values and possible gross errors in the gravity observations. All these facts imply a hidden deterministic bias  $\nabla N_G$  in the resulting HRS. This suggested the extension of the DFHRS approach to direct use of the original physical observations. In that way all HRS contributing original observation groups, as shown in fig. 5, can be used. The so-called "extended DFHRS approach" was realized in the DFHRS-software version 5.0 ©Jäger/Schwarzer/Schneid and enables an over-determined controlled HRS computation with any type of observation.

### 3.2.2 Extension of the DFHRS concept using spherical cap harmonics (SCH)

#### 3.2.2.1 Introduction and basic concept

This chapter deals with the extension of the DFHRS approach to physical observations, following Molodenski's theory ([36], [38]). As "physical observations" we call the scalar or vector-like observation types  $l$ , which are as  $l=l(W)$  related to an appropriate parametrization of the gravity potential  $W_P(x, y, z)$  of the earth or by  $l=l(T)$  to its anomalous potential  $T_P = (W - W_{ref})_P$  (see [36], [38], [39], [40], [41]). With  $W_{ref}$  we describe the potential of the reference gravity field, which is presently defined by the GRS80 ([37], [38]). With  $g_P = \text{grad}(W)$  the classical measured components  $l_i = g_{P,i}$  of the gravity vector  $g_P$ , as well as respective difference observations  $\Delta l_{i,j} = g_{P,j} - g_{P,i}$  between points  $P_i$  and  $P_j$  belong to the type  $l=l(W)$ . Gravity disturbance observations  $l = \delta g_P = g_P - \gamma_P = \text{grad}(T)$  and components  $l_i = \delta g_{P,i}$  of  $\delta g_P = g_P - \gamma_P = \text{grad}(T)$  belong to the type  $l=l(T)$  of physical observations. With  $\gamma_P = \text{grad}(W_{ref})$  these observations require in the parametrization gravity reference field functionals, both on the left and the right hand side, of the respective observation equations. The gravity potential  $W$  may be written as sum of gravitational potential  $V$  and the centrifugal potential  $Z$ . If we write  $V$  in terms of a truncated spherical harmonic series, this reads: ([36], [38], [39]):

$$W(r, \lambda, \theta) = V + Z = \frac{GM}{a} \sum_{n=0}^{n_{MAX}} \left(\frac{a}{r}\right)^{n+1} \sum_{m=0}^n (C_{n,m} \cdot \cos m\lambda + S_{n,m} \cdot \sin m\lambda) \cdot P_{n,m}(\cos \theta) + \frac{\omega^2}{2} r^2 \sin^2 \theta \quad (5a)$$

In the expression above  $GM$  denotes the geocentric gravitational constant,  $C_{n,m}$  and  $S_{n,m}$  are spherical harmonic coefficients.  $P_{n,m}$  are the associated Legendre functions and  $(r, \lambda, \theta)$  are the spherical coordinates of a point position  $P(r, \lambda, \theta)$  in regard.

If we introduce reference gravitational field as  $V_{ref} = V_{ref}(C_{n,m}^{GRS80})$  the anomalous gravitational potential  $T$  may in analogy to (5a) also be written in terms of a truncated spherical harmonic series

$$T(r, \lambda, \theta) = (V + Z) - (V_{ref} + Z_{ref}) = V - V_{ref,GRS80} = \frac{GM}{a} \sum_{n=0}^{n_{MAX}} \left(\frac{a}{r}\right)^{n+1} \cdot \sum_{m=0}^n (C_{n,m} \cdot \cos m\lambda + S_{n,m} \cdot \sin m\lambda) \cdot P_{n,m}(\cos \theta) - V_{ref,GRS80} \quad (5b)$$

(5c)

$$T(r, \lambda, \theta) = \frac{GM}{a} \sum_{n=0}^{\infty} \sum_{m=0}^n \left(\frac{a}{r}\right)^{n+1} \cdot (\Delta C_{nm} \cdot \cos m\lambda + S_{nm} \cdot \sin m\lambda) \cdot P_{n,m}(\cos \theta)$$

In 1985 Haines [30] introduced a new method, the so-called "spherical cap harmonic analysis (SCHA)" for the presentation of geomagnetic fields of the earth. Since then, this method has successfully been applied in geophysics and partly also in geodesy. In contrast to the ordinary spherical harmonic representation (5a) the SCHA is suitable for the parametrization of the gravity field over a limited area. In the following we assume that the reference ellipsoid and the reference sphere for the cap are concentric. Other mutual georeferencing designs between the ITRF and the SCHA cap are regarded in [31]. The limited "cap" area in SCHA is in the concentric case to be characterized by the cap pole situated at the earth surface position  $P_0(x, y, z)$  or  $P_0(r, \lambda, \theta)$ , e.g. at the centre of the area in regard. This enable a direct georeferencing in the spherical cap coordinates  $P(r, \lambda', \theta')$ , a local azimuthal co-ordinate system with the pole of the cap  $P_0(r, \lambda_0, \theta_0) = P_0(r, \lambda_0 = 0, \theta_0 = 0)$  as origin.

The total area extension of the cap is to be expressed by the spherical cap half-angle  $\alpha = \theta'_{\max}$ , with e.g.  $\alpha = 1^\circ$  for a cap area radius of 110 km. Using the georeferencing  $P(r, \lambda', \theta')$  the SCHA-parametrization for  $V$  is to be set up in analogy to the SHA case, except that the occurring non-integer degrees  $n = n(k)$  have to be determined as the zeros of the generalised associated Legendre functions  $P_{n(k),m}(\cos \theta')$  with respect to  $k$  ([30],[31]). So we have in analogy to the classical SHA (5a):

$$V(r, \lambda', \theta') = \frac{G \cdot M}{a} \sum_{k=0}^{\max} \left(\frac{a}{r}\right)^{n(k)+1} \sum_{m=0}^k (C'_{n(k),m} \cdot \cos m\lambda' + S'_{n(k),m} \cdot \sin m\lambda') \cdot P_{n(k),m}(\cos \theta') \quad (6a)$$

On rescaling the SCHA-coefficients (6a) by GM we arrive at:

$$V(r, \lambda', \theta') = \sum_{k=0}^{\max} \left(\frac{a}{r}\right)^{n(k)+1} \sum_{m=0}^k (\bar{C}'_{n(k),m} \cdot \cos m\lambda' + \bar{S}'_{n(k),m} \cdot \sin m\lambda') \cdot P'_{n(k),m}(\cos \theta') \quad (6b)$$

for the SCHA gravitational potential  $V$ . For the SCHA anomalous potential  $T$  we get

$$T(r, \lambda', \theta') = \sum_{k=0}^{\max} \left(\frac{a}{r}\right)^{n(k)+1} \sum_{m=0}^k (\bar{C}'_{n(k),m} \cdot \cos m\lambda' + \bar{S}'_{n(k),m} \cdot \sin m\lambda') \cdot P'_{n(k),m}(\cos \theta') - V_{\text{ref};\text{GRS80}} \quad (7a)$$

and

$$T(r, \lambda', \theta') = \sum_{k=0}^{\max} \left(\frac{a}{r}\right)^{n(k)+1} \sum_{m=0}^k (\Delta \bar{C}'_{n(k),m} \cdot \cos m\lambda' + \Delta \bar{S}'_{n(k),m} \cdot \sin m\lambda') \cdot P'_{n(k),m}(\cos \theta') \quad (7b)$$

The transition (7a) to (7b) does not only imply differences in some coefficients of low degree (like in SHA (5c)), but in all SCHA-coefficients.  $V_{\text{ref};\text{GRS80}}$  can be introduced explicitly by (7a), while by (7b)  $V_{\text{ref};\text{GRS80}}$  is contained and estimated as part of the SCHA coefficients.

With respect to the same level of a resolution of the SHA and the SCHA representation, the following relation between the respective maximum degrees holds as function of the area size parameter  $\alpha$  [31]:

$$n_{\text{SHA}} = n(k) \approx \frac{90^\circ}{\alpha} \cdot (k + 0.5) - 0.5. \quad (8)$$

So for a resolution of 2 mm and 2.7 mgal in the quasi-geoid height  $N_{\text{QG}}$  and for the a gravity observation  $g_{P,i}$  respectively, we need a degree of  $n_{\text{max}} = 7200$  [39]. We need however only a degree

of  $n_{\max} = 80$  for the same resolution for cap with area size  $\alpha = 1^\circ$  (111 km radius round the cap pole). The principle (8) reduces essentially the number of parameters and unknowns  $u$ , in the example from  $u=51.840.000$  in case of SHA to  $u'=640$  in case of SCHA. So SCHA is the key to enable the computation of high resolution HRS in integrated over-determined HRS-computation approaches, such as DFHRS.

Finally, we find the (quasi)geoid height  $N_{QG}$  by inserting (7a), (7b) into the Bruns' equation:

$$N(r, \lambda', \theta') = N(\bar{C}_{n(k),m}, \bar{S}_{n(k),m}) = \frac{1}{\gamma_Q} \cdot \left( \sum_{k=0}^{k_{\max}} \left( \frac{a}{r} \right)^{n(k)+1} \sum_{m=0}^k (\bar{C}'_{n(k),m} \cdot \cos m\lambda' + \bar{S}'_{n(k),m} \cdot \sin m\lambda') \cdot P'_{n(k),m}(\cos \theta') \right) - V_{\text{ref};GRS80} \quad (9a)$$

and

$$N(r, \lambda', \theta') = N(\Delta \bar{C}'_{l(n'),m'}, \Delta \bar{S}'_{l(n'),m'}) = \frac{1}{\gamma_Q} \cdot \sum_{k=0}^{k_{\max}} \left( \frac{a}{r} \right)^{n(k)+1} \sum_{m=0}^k (\Delta \bar{C}'_{n(k),m} \cdot \cos m\lambda' + \Delta \bar{S}'_{n(k),m} \cdot \sin m\lambda') \cdot P_{n(k),m}(\cos \theta') \quad (9b)$$

The SCHA-parameters within the DFHRS-concept (2a-2h) are however regarded as auxiliary unknowns to parametrize the geopotential model information (EGM96, EIGEN) as well as the groups of the physical observation like  $g$ , while the NFEM-parameters  $\mathbf{p}$  are the main unknowns for the HRS surface representation. By the condition equations (10) – introduced as pseudo observations with a high weight - the SCHA-parameters  $(\bar{C}'_{n(k),m}, \bar{S}'_{n(k),m})$  used in (9a,b) and in (11d) are related back again to the NFEM polynomial parameters  $\mathbf{p}$  of the existing DFHRS-approach. The condition equation reads:

Functional Model	Observation Types and Stochastic Model	
$0 + v_{\Delta N} = N(\bar{C}_{n(k),m}, \bar{S}_{n(k),m}) - (\mathbf{f}^T \cdot \mathbf{p} + \Delta \mathbf{m} \cdot \mathbf{h})$	Condition equations "HRS from N(SCHA) = NFEM(p)" as uncorrelated pseudo observations with small variances and high weights.	(10)

### 3.2.2.2 Extension of the DFHRS approach to gravity observations

The original gravity observation  $g_p$  is referring to the local astronomical vertical system (LAV) and represented there as

$$\mathbf{g}^{\text{LAV}} = [0, 0, -g_p]^T \text{ - Original gravity observation and vector} \quad (11a)$$

The astronomical vertical  $(\Phi = B + \xi, \Lambda = L + \eta / \cos(B))$  is set up by the ellipsoidal vertical  $(B, L)$  and the deflections from the vertical  $(\xi, \eta)$ . The original vector  $\mathbf{g}^{\text{LAV}}$  is first rotated to the earth-centred earth fixed system (ECEF) using  $(\Phi, \Lambda)$ . The centrifugal parts are removed. In that way the original observation (11a) is strictly reduced with respect to the vertical deflections ("topography") and to centrifugal accelerations. Afterwards it further rotated to the local geodetic vertical system (LGV) of the cap sphere, and we have

$$\mathbf{g}_{\text{red}}^{\text{LGV}} = [g_N, g_E, g_r]^T \text{ - Reduced gravity observation vector} \quad (11b)$$

In the parametric space we have together with the SCHA representation of  $V$  (7a) for the observation vector  $\mathbf{g}_{red}^{LAV}$  (11b) above ([40], [41]):

$$\mathbf{g}_{grav}^{LGV} = \left[ \frac{1}{r} \cdot \frac{\partial V}{\partial \theta'}, \frac{1}{r \cdot \sin \theta'} \cdot \frac{\partial V}{\partial \lambda}, \frac{\partial V}{\partial r} \right]^T - \text{Hypothesis free and strict parametrization of (11b)} \quad (11c)$$

The "vertical" and principal component of the reduced gravity observation  $\mathbf{g}_{red}^{LAV}$  (11b) is referring to  $\mathbf{g}_{grav,r}^{LGV} = -\frac{\partial V}{\partial r}$ . So the main contribution of the "vertical" component  $\mathbf{g}_r$  can now be used for setting up the observation equation for gravity-meter observation. In the DFHRS approach the observation equation reads:

$$\mathbf{g}_{grav,r}^{LGV} + v = \sum_{k=0}^{\infty} \left( \frac{a}{r} \right)^{n(k)+1} \frac{(n(k)+1)}{r} \sum_{m=0}^k (\bar{C}'_{n(k),m} \cdot \cos m\lambda' + \bar{S}'_{n(k),m} \cdot \sin m\lambda') \cdot P_{n(k),m}(\cos \theta') \quad (11d)$$

The consideration of additional datum parameters in the observation equation (11d) is possible, and is presently investigated in the frame of the real-data projects reported in chap. 4. The additional prior information of geopotential models (GPM), such as e.g. EGM96 or EIGEN, may be introduced with respect to the quasi-geoid height as:

$$\begin{aligned} N_{GPM}^j + v &= N(\bar{C}'_{n(k),m}, \bar{S}'_{n(k),m}) + \partial N(\mathbf{d}^j) \\ &= \frac{1}{\gamma_Q} \left( \sum_{k=0}^{\infty} \left( \frac{a}{r} \right)^{n(k)+1} \sum_{m=0}^k (\bar{C}'_{n(k),m} \cdot \cos m\lambda' + \bar{S}'_{n(k),m} \cdot \sin m\lambda') \cdot P_{n(k),m}(\cos \theta') \right. \\ &\quad \left. - V_{ref,GRS80} \right) + \partial N(\mathbf{d}^j) \end{aligned} \quad (12)$$

The prior GPM information (12) is corresponding to the alternative kind of GPM introduction, namely by "remove-restore" in the classical HRS computation approaches. In order to avoid the influence of long-waved deflections, the introduced GPM (12) may again be parted into a number of "patches" by the introduction of datum parts  $\partial N(\mathbf{d}^j)$  like in (2b), (2c), (2d).

## 4 Examples and Conclusions

The extended DFHRS approach is described by the basic observation type and equations (2a)-(2f), (10), (12d) and (13) is open for all geometrical and physical observation types. It means a new and complete method, both for the over-determined fixed boundary value problem, especially for the (quasi-)geoid determination, as well as for the solution of a direct and online GNSS-heighting by the use of DFHRS databases and the respective DFHRS correction (2i).

The first application of the extended DFHRS approach was the computation of the new "1\_cm DFHRS\_DB Saarland" for the Federal State Saarland, Germany in 2005. The fig. 7 shows a screenshot of the DFHRS computation for Saarland with the DFHRS software version 5.0, namely with the GUI, menu and the toolbar, and in the graphics window the meshes (blue), the identical points (green triangles) and the positions of gravity observations (blue dots).

As second project the DFHRS computation of the "1\_cm DFHRS\_BD Baden-Württemberg" for the Federal State Baden-Württemberg, Germany is about to be finished. For computation design see fig. 7. Fig. 8 shows a part of the list of adjusted gravity disturbance observations.

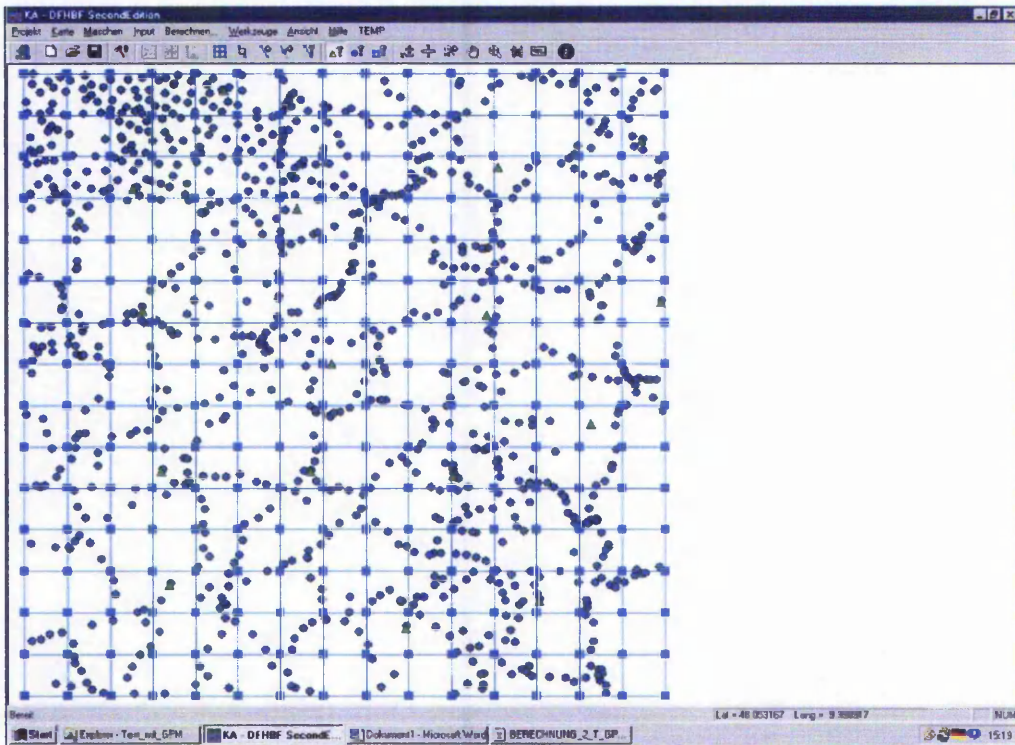


**Fig. 6:**

Computation Design of the normal-height based "1\_cm DFHRS\_DB" for the federal state of Saarland, Germany. Meshes (blue), gravity observations (blue dots) and fitting points (blue dots)

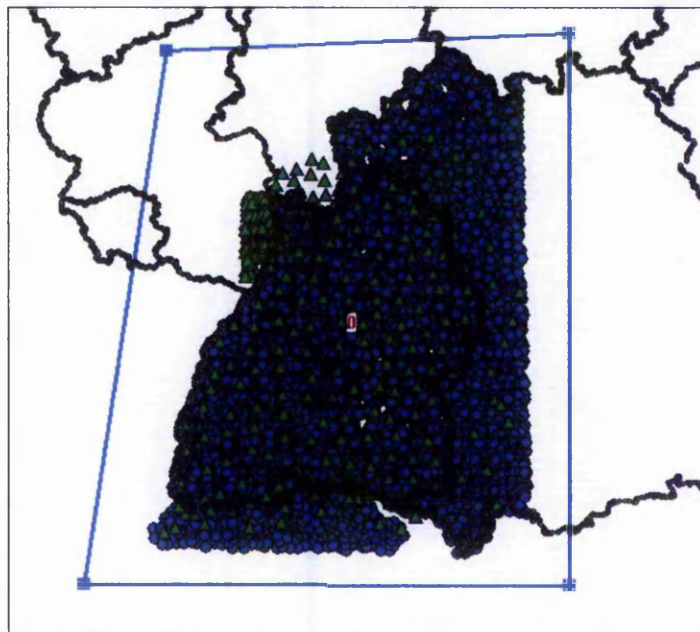


**Fig. 7:**

Computation Design of the normal-height based "1\_cm DFHRS\_DB" for the federal state of Baden-Württemberg, Germany with some overlapping to the neighbouring countries (except France). Gravity observations (blue), fitting points (green), country borders (black).

Number	B [°]	L [°]	dg [mgal]	v [mgal]
6221803000	49.744402	9.325176	17.27052630	0.016
6221803100	49.754800	9.320541	18.29553958	0.004
6221810000	49.731079	9.322965	48.72880615	-0.002
6221810100	49.767690	9.323488	16.90448271	-0.009
6221810200	49.739588	9.295846	16.90117365	-0.005
:	:	:	:	:
6222803100	49.787317	9.482121	25.19440159	-0.006
6222803800	49.730625	9.411164	35.48699735	0.012
6222803900	49.748882	9.486150	46.45989551	-0.019
6222804000	49.735388	9.450240	45.58427649	-0.022
6222804104	49.717601	9.439384	46.62347815	-0.018
6222804204	49.702843	9.456634	55.15177619	-0.029
6222810000	49.699664	9.417770	47.55625221	-0.003
:	:	:	:	:

**Fig. 8**

**DFHRS-software report for the gravity disturbances dg with the list of corrections v**

The maximum degree  $k$  for the SCHA representation for the Saarland computation (area 100 km x 100 km) was  $k=20$ . For Baden-Württemberg  $k$  will be in the maximum order of  $80 < k < 100$ . Assuming a cap half-angle  $\alpha = 25^\circ$  the maximum  $k$  to represent the a "1\_cm DFHRS\_EB Europe" would be  $k=2000$  with regard to (8) and a 2 mm resolution for the SCHA-based HRS (9a) in case of including the original gravity observations  $g$  (gravity disturbances or anomalies alternatively) of the different countries in the extended DFHRS approach.

As concerns the further DFHRS design parameters - namely the fitting point density and the mesh and patch-design of the "1\_cm DFHRS\_DB Europe" - it is referred to the EUREF contribution [25].

**References**

[1] Denker, H. and W. Torge (1997): The European Gravimetric Quasigeoid EGG97 – An IAG supported continental enterprise. In: Geodesy on the Move – Gravity Geoid, Geodynamics, and Antarctica. R. Forsberg, M. Feissel, R. Dietrich (eds.). IAG Symposium Proceedings Vol. 119, Springer, Berlin Heidelberg New York: 249-254.

[2] Jäger, R. (1990): Spectral Analysis of Relative and Supported Geodetic Levelling Networks due to Random and Systematic Errors. 'Precise Vertical Positioning'. Invited Paper to the Hannover Workshop of October 08-12, 1990.

[3] Jäger, R. and H. Kaltenbach (1990): Spectral analysis and optimization of geodetic networks based on eigenvalues and eigenfunctions. Manuscripta Geodetica (15), Springer Verlag. S. 302-311.

[4] Jäger, R. und S. Kälber (2000): Konzepte und Softwareentwicklungen für aktuelle Aufgabenstellungen für GPS und Landesvermessung. DVW Mitteilungen, Landesverein Baden-Württemberg. 10/2000. ISSN 0940-2942.

[5] Jäger, R. and S. Leinen (1992): Spectral Analysis of GPS-Networks and Processing Strategies due to Random and Systematic Errors. In: Defense Mapping Agency and Ohio State University (Eds.) Proceedings of the Sixth International Symposium on Satellite Positioning, Columbus/Ohio (USA), 16-20 March. Vol. (2), p. 530-539.

[6] Jäger, R. and S. Schneid (2001): GPS-Höhenbestimmung mittels Digitaler Finite-Elemente Höhenbezugsfläche (DFHBF) - das Online-Konzept für DGPS-Positionierungsdienste. XI. Internationale Geodätische Woche in Oberegurgl/Österreich, Februar 2001. Institutsmittellungen, Heft Nr. 19, Institut für Geodäsie der Universität Innsbruck: 195-200.

[7] Lemoine, F.; S. Kenyon; J. Factor; R. Trimmer; N. Pavlis; D. Chinn; M. Cox; S. Klosko; S. Luthcke; M. Torrence; Y. Wang; R. Williamson; E. Pavlis; R. Rapp and T. Olson (1998): The development of the Joint NASA GSFC and NIMA Geopotential Model EGM96. NASA Goddard Space Flight Center, Greenbelt, Maryland, 20771, USA.

[8] Meichle, H. (2001): Digitale Finite Element Höhenbezugsfläche (DFHBF) für Baden-Württemberg. DVW Mitteilungen, Heft 2. DVW Landesverein Baden-Württemberg. ISSN 0940-2942. S. 23-31.

- [9] Schmitt, G. (1997): Spectral Analysis and Optimization of two dimensional networks. Geomatics Research Australasia (67): 47-64.
- [10] Schneid, S. (2002): Software Development and DFHRS computations for several countries. J. Kaminskis and R. Jäger (Eds.): Proceedings of the 1st Common Baltic Symposium, GPS-Heighting based on the Concept of a Digital Height Reference Surface (DFHRS) and Related Topics - GPS-Heighting and Nationwide Permanent GPS Reference Systems. Riga, June 11, 2001; Riga, Latvia.
- [11] Jäger, R. (2002): Online and Postprocessed GPS-heighting based on the Concept of a Digital Finite Element Height Reference Surface (DFHRS). J. Kaminskis and R. Jäger (Eds.): Proceedings of the 1st Common Baltic Symposium, GPS-Heighting based on the Concept of a Digital Height Reference Surface (DFHRS) and Related Topics - GPS-Heighting and Nationwide Permanent GPS Reference Systems. Riga, June 11, 2001; Riga, Latvia.
- [12] Jäger, R. and S. Schneid (2002): Passpunktfreie direkte Höhenbestimmung – ein Konzept für Positionierungsdienste wie SAPOS®. Proceedings 4. SAPOS® Symposium, 21.-23. Mai 2002. Landesvermessung und Geobasisinformation Niedersachsen (LGN) (Hrsg.). LGN, Hannover. S. 149-166.
- [13] Wirtschaftsministerium Baden-Württemberg (2002): Neue Projekte und Produkte mit Kunden- und Praxisbezug im Landesbetrieb Vermessung. Festschrift „50 Jahre Baden-Württemberg – 50 Jahre Hightech-Vermessungsland. 150 Jahre Badische Katastervermessung“. Wirtschaftsministerium Baden-Württemberg (Hrsg.). S. 39-50.
- [14] Ihde, J. and W. Augath (2000): European Vertical Reference System (EVRS). In: Veröffentlichungen der Internationalen Erdmessung der Bayerischen Akademie der Wissenschaften (61). IAG Subcommission for Europe Symposium EUREF, Tromsø 2000. Beck'sche Verlagsbuchhandlung, München. S. 101 ff.
- [15] Jäger, R. (1998): Ein Konzept zur selektiven Höhenbestimmung für SAPOS. Beitrag zum 1. SAPOS-Symposium. Hamburg 11./12. Mai 1998. Arbeitsgemeinschaft der Vermessungsverwaltungen der Länder der Bundesrepublik Deutschland (Hrsg.). Amt für Geoinformation und Vermessung, Hamburg. S. 131-142.
- [16] Jäger, R. and S. Schneid (2002): Online and Postprocessed GPS-Heighting based on the Concept of a Digital Height Reference Surface. Contribution to IAG International Symposium on Vertical Reference Systems, February 2001, Cartagena, Columbia. In: H. Drewes, A.H. Dodson, L. P. Fortes, L. Sanches, P. Sandoval (Eds.). International Association of Geodesy Symposia. Symposium No. 124: 'Vertical Reference Systems', Cartagena, Colombia, February 20-23, 2001. Springer Verlag, Berlin, Heidelberg, New York. ISBN 3-540-43011-3. S. 203-208.
- [17] Jäger, R. und S. Schneid (2002): GNSS Online Heighting based on the Concept of a Digital Finite Element Height Reference Surface (DFHRS) and the Evaluation of the European HRS. Proceedings, GNSS 2002 Symposium. CD-ROM Publication The Nordic Institute of Navigation, Kopenhagen.
- [18] Jäger, R.; Volkmann, W.E.; Niethammer, S.; Christmann, I. and A. Schick (1999): NAM97-Report – Calculation of a Zero Order ITRF based Reference Network for Namibia. Republic of Namibia, Ministry of Lands, Resettlement and Rehabilitation, Directorate of Survey and Mapping (ed.). 26 pages.
- [19] Jäger, R. (2003): Realisierung eines dreidimensionalen hochgenauen ITRF-Referenzsystems zur satellitengestützten GNSS-Positionierung in Namibia. (Fachhochschule Karlsruhe, Hrsg.): Forschungsbericht der Fachhochschule Karlsruhe – University of Applied Sciences.
- [20] Jäger, R., Kälber, S., Schneid, S. und S. Seiler (2003): Konzepte und Realisierungen von Datenbanken zur hochgenauen Transformation zwischen klassischen Landessystemen und ITRF/ETRS89 im aktuellen GIS- und GNSS-Anwendungsprofil. (Chesi/Weinold, Hrsg.): 12. Internationale Geodätische Woche Oberurg, 2003 Wichmann Verlag, Heidelberg. ISBN 3-87907-401-1. S. 207-211.
- [21] Jäger, R. and S. Schneid (2002-2006): [www.dfhbf.de](http://www.dfhbf.de). DFHBF Website.
- [22] Seiler, S. (2000-2006): [www.ib-seiler.de](http://www.ib-seiler.de). IBS-Website.
- [23] Lace, L. and J. Kaminskis (2003): DGPS service / DGPS – heighting in Latvia and all Baltic States based on DFHRS. Paper presented to 2<sup>nd</sup> Common Baltic Symposium “GPS-Heighting based on the Concept of a Digital Height Reference Surface (DFHRS) and Related Topics - GPS Heighting and National-wide Permanent GPS Reference Systems”, Riga 12-13 June 2003. State Land Service of Latvia, Riga.
- [24] Jäger, R., Schneid, S., Garcia Villa Major, L., Garrigues Talens, P. and L. Pascual Llorens (2003): Precise Plan Representation of Classical National Networks to ITRF/ETRS89 and Precise Vertical Reference Surface Transformation by Digital FEM Height Reference Surfaces (DFHRS) - Concepts, Databases, Present Developments and Realisation of a 5 cm DFHRS-Database District of Valencia, Spain. Symposium, IAG Subcommission for Europe, Toledo, June 2003. EUREF Publication No. 12. Verlag des Bundesamtes für

Kartographie und Geodäsie. Frankfurt am Main.

- [25] Jäger, R. and S. Schneid (2004): A Decimetre Height Reference Surface (HRS) for the European Vertical Reference System (EVRS) based on the DFHRS Concept. Contribution to IAG Subcommission for Europe Symposium EUREF 2004, Bratislava, Slovakia. EUREF-Mitteilungen. Bundesamt für Kartographie und Geodäsie (BKG), Heft 14, Frankfurt. In Press.
- [26] Jäger, R.; Müller, T.; Saler, H. und R. Schwäble (2005): Klassische und robuste Ausgleichungsverfahren - Ein Leitfaden für Ausbildung und Praxis von Geodäten und Geoinformatikern. Wichmann-Verlag, Heidelberg. ISBN 3-87907-370-8.
- [27] Jäger, R.; Kälber, S.; Schneid, S.; Oeleshi, G.; Nurce, B. and Cekrezi, I. (2006): Realization of CoPaG/DF-LBF and DFHRS Databases for Albania. Buletini i Shkencave Gjeologjike (2), 2004. Redaksia e Buletinit te Shkencave Gjeologjike. Tirana, Albania.
- [28] Jäger, R., Kälber, S. (2006): Precise Transformation of Classical Networks to ITRF by CoPaG and Precise Vertical Reference Surface Representation by DFHRS - General Concepts and Realisation of Databases for GIS, GNSS and Navigation Applications. Proceedings to GeoSiberia 2006. Volume 1. S. 3-31. Novosibirsk, Russia.. ISBN 5-87693-199-3
- [29] Jäger, R. and S. Kälber (2003-2006): [www.geozilla.de](http://www.geozilla.de). GeoZilla Website.
- [30] Haines, G.V (1985): Spherical Cap Harmonic Analysis. Journal Geophysics Research (90). P. 2593-2598.
- [31] A. De Sanits (1991): Translated origin spherical cap harmonic analysis . Geophys. J. Int (106). P. 253-263.
- [32] L. Lace (2004): Computation of a Precise Height Reference Surface for Latvia and the Baltic States using the DFHRS concept and software. Co-tutelle de thèse MSc thesis between Hochschule Karlsruhe – Technik und Wirtschaft, TU Jelgava, Latvia and State Land Service Department (SLS) Riga, Latvia. Unpublished.
- [33] B. S. Okrah (2004): Computation of a DFHRS Database for Florida (USA) and Implementation of a Blockmatrix Inversion as a C++ based DLL into the DFHRS Software. MSc thesis. Hochschule Karlsruhe – Technik und Wirtschaft. Unpublished.
- [34] R. Gvenes (2005): Height Reference Surface Modelling and Computation. MSc thesis. Hochschule Karlsruhe – Technik und Wirtschaft. Unpublished.
- [35] R. Gvenes (2005): Height Reference Surface Modelling and Computation. Poster Presentation at 66. DVW-Seminar "GPS und GALILEO", February 2006. TU Darmstadt, Darmstadt, Germany.
- [36] Marchenko, A. (1998): Parametrization of the Earth's gravity field – Point and line singularities. Lviv Astronomical and Geodetic Society, Lviv. Ukraine.
- [37] Moritz H. (2000): Geodetic Reference System 1980. The Geodesist's Handbook, Journal of Geodesy. 74: 128-133.
- [38] Hofmann-Wellenhof, B. and H. Moritz (2005): Physical Geodesy. Springer, Wien.
- [39] Torge, W. (2001): Geodesy. Walter de Gruyter, Berlin-New York.
- [40] Chatfield, A.B. (1997): Fundamentals of High Accuracy Inertial Navigation. Progress in Astronautics and Aeronautics (174). American Institute of Astronautics and Aeronautics. Virginia, USA.
- [41] Jekeli, C. (2001): Inertial Navigation Systems with Geodetic Applications. Walter de Gruyter, Berlin, New York.
- [42] Hofmann, A. und S. Tepper (2002): Planung, Berechnung und Qualitätsanalyse der DFHBF\_DB Namibia und Windhoek unter Einbindung zusätzlicher GPS-Messungen als Kooperationsprojekt zwischen African Geomatics und der University of Applied Sciences (FH) Karlsruhe sowie begleitende C++ Softwareentwicklungen. Diplomarbeit an der Hochschule Karlsruhe – Technik und Wirtschaft. Unveröffentlicht.
- [43] Schwarzer, F. (2000): Entwicklung von C++-Software zur grafikunterstützten Berechnung Digitaler Finite Elemente Modell Höhenbezugsflächen (DFHBF) und DFHBF-Implementierung in GPS-Kommunikationssoftware. Diplomarbeit an der Hochschule Karlsruhe – Technik und Wirtschaft. Unpublished.

Jäger R., Schneid, S., Kälber, S. and Seiler, S. (2006):

Precise Transformation of Classical Networks to ITRF by CoPaG and Precise Vertical Reference Surface Representation by DFHRS – General Concepts and Realisation of Databases for GIS, GNSS and Navigation Applications. 1st International Fair of Geodesy, Cartography, Navigation and Geoinformatics. Prague, Czech Republic. 16.03.2006 - 18.03.2006. Milan Tallich (Eds.): Conference Proceedings. ISBN 80-85881-25-X.

# Precise Transformation of Classical Networks to ITRF by CoPaG and Precise Vertical Reference Surface Representation by DFHRS - General Concepts and Realisation of Databases for GIS, GNSS and Navigation Applications

<sup>1)</sup> Prof. Dr.-Ing. Reiner Jäger, <sup>1)</sup> Dipl. Ing. (FH) Sascha Schneid,  
<sup>2)</sup> Dipl.-Ing. (FH) Simone Kälber and <sup>3)</sup> Dipl. Ing. (FH) Stephan Seiler

<sup>1)</sup> Fachhochschule Karlsruhe - University of Applied Sciences  
Studiengang Vermessung und Geomatik and  
International Department and Programme Geomatics (MSc)  
Moltkestrasse 30, D-76133 Karlsruhe

Email: reiner.jaeger@hs-karlsruhe.de, sascha.schneid@hs-karlsruhe.de URL: [www.dfhbf.de](http://www.dfhbf.de)

<sup>2)</sup> Lamprechtstrasse 13, D-76227 Karlsruhe, Email: [simone.kaelber@web.de](mailto:simone.kaelber@web.de).

<sup>3)</sup> Ingenieurbüro Seiler (IBS), Hauptstrasse 45, D-77886 Lauf,  
Email: [stephan.seiler@ib-seiler.de](mailto:stephan.seiler@ib-seiler.de), URL: [www.ib-seiler.de](http://www.ib-seiler.de).

## 1 Introduction

As concerns the georeferencing of position data in modern data bases, the availability of GNSS (GPS/GLONASS/GALILEO) related code- and phase-measurement DGNSS-correction data, which are provided in different ways by different positioning services in and outside Europe leads to the replacement of the classical geodetic reference systems by GNSS-consistent ITRS-based reference systems. So the transformation of the old plan position data  $(N,E)_{class}$  related to the classical reference systems to the ITRS/ETRS89 datum  $(N,E)_{ITRS}$  becomes urgently necessary. A sophisticated and general solution of this transformation problem has to include a respective data base concept for the provision of the corresponding transformation parameters for GIS, GNSS and Navigation purposes. Further the capacity of a one-cm-positioning by GNSS services, such as e.g. SAPOS® and ascos® in Germany, is also appropriate for a GNSS related heighting. The GNSS-based determination of sea-level (orthometric, normal) heights  $H$  requires however the transformation of the ellipsoidal GNSS heights  $h_{ITRS}$  to the respective physically defined height reference surface (HRS). The first part of the contribution is dealing with the concept of a homogenizing precise and continuous transformation of plan positions  $(N,E)_{class}$  to the ITRS/ETRS89 datum  $(N,E)_{ITRS}$ . From the theoretical point of view a respective transformation can not renounce completely on height information. The presented so-called CoPaG (Continuously Patched Geoferencing) concept however, has the advantage that the point height information is needed only on a poor accuracy level. Further basic considerations and a respective problem solution for the plan datum transition are due to the occurrence and the mathematical treatment of so-called 'weak-shapes. These are long-waved deflections of the network shape of the classical networks, reaching a range of several meters in the nation-wide scale, e.g. for the size of Germany. This requires the partition of the total network area into a set of different "patches". The introduction of continuity conditions along the patch borders implies restrictions between the transformation parameters  $d$  of neighbouring patches. Because of its mathematical strictness and general validity the CoPaG concept has (like the DFHRS approach

below) a broad and far-reaching application profile in the context with the big amount of similar datum transition problems occurring world-wide in the upcoming GNSS-age. The realisation of a software system for the statistically controlled set up of a transformation parameter  $\mathbf{d}$  data base for the transformation of positions  $(N,E)_{\text{class}}$  to the ITRS datum  $(N,E)_{\text{ITRS}}$  and vice versa is presented at different examples.

The second part of the contribution is dedicated to the DFHRS (Digital-Finite-Element-Height-Reference-Surface) concept, which allows a GNSS height positioning (GPS/GLONASS/GALILEO etc.) by a direct online conversion of ellipsoidal heights  $h$  into standard heights  $H$  referring to the height reference surface (HRS). The DFHRS is modelled as a continuous HRS with parameters  $\mathbf{p}$  in arbitrary large areas by bivariate polynomials over a grid of Finite Element meshes (FEM). Geoid heights  $N$ , vertical deflections  $(\xi,\eta)$ , gravity disturbances and anomalies  $\Delta g$  and identical points  $(h, H)$  can be used as observations in a least squares computation to derive the DFHRS-parameters  $\mathbf{p}$ . Any number of geoid models may be introduced simultaneously and geoid models may be parted into different "patches" with individual datum-parameters in order to reduce the effect of existing medium- and long-waved systematic errors. So the resulting DFHRS parameters  $\mathbf{p}$ , set up as a DRHRS data-base, provide a three-dimensional correction  $\text{DFHRS}(\mathbf{p}|B,L,h)$  to transform by  $H=h-\text{DFHRS}(\mathbf{p}|B,L,h)$  ellipsoidal GNSS heights  $h$  into standard heights  $H$ . The mathematical model of DFHRS computation and the software are pointed out. The authors present the results of DFHRS\_DB computations for the GNSS online heighting in the cm-accuracy range for different countries and nations in and outside of Europe.

Above the theoretical concepts the implementation and use of DFLBF\_DB and DFHRS\_DB in GNSS-equipment for real-time positioning in GNSS-services (e.g. *SAPOS*® and *ascos*®) is shown, as well as the setting up the RTCM.3.0 transformation messages based on the above databases.

## **2 GNSS Plan Positioning – Data Bases to transform between ETRS89/ITRS and Classical Datum Systems**

### **2.1 Continuous Patched Georeferencing (CoPaG) Concept**

This part of the contribution deals with the homogenisation, cm-accurate and neighbourhood consistent transformation of plan coordinates between classical national reference-systems  $(N,E)_{\text{Class}}$  and the unique ITRF/ETRS89-datum  $(N,E)_{\text{ITRF}}$ .

The so-called CoPaG (Continuously Patched Georeferencing) transformation concept [26] implies the improvement and homogenisation of the geometrical quality of existing classical networks (such as e.g. the German DHDN network and datum, fig. 2.1; fig. 2.2) by the developed method of an ITRF/ETRS89 related georeferencing. So the qualification of the old position data for a future utilization and the continuation of existing databases are provided. Therefore also a high economic benefit as well as signals for further innovative developments in the GIS-, GNSS- and LBS-sector is set by the CoPaG concept of transforming the old classical data to the GNSS consistent ITRF/ETRS89 datum.

The CoPaG concept is based on a strict three-dimensional similarity transformation between the two concerned reference-systems. The equations of this transformation are linearized under the realistic assumption of small rotation angles and the linearization point of the geographical coordinates  $(B,L,h)_1$ . This leads to the resulting part for the plan component  $(B,L)$  of the three-dimensional similarity transformation in geographical coordinates  $(B,L,h)$  reading [8], [9], [26]:

$$B_2 + v = B_1 + \partial B_1(d) = B_1 + \partial B_1(u, v, w, \varepsilon_x, \varepsilon_y, \varepsilon_z, \Delta m, \Delta a, \Delta f) \quad (2.1a)$$

$$= B_1 + \left[ \frac{-\cos(L) \cdot \sin(B)}{M+h} \right]_1 \cdot u + \left[ \frac{-\sin(L) \cdot \sin(B)}{M+h} \right]_1 \cdot v + \left[ \frac{\cos(B)}{M+h} \right]_1 \cdot w +$$

$$\left[ \frac{-\sin(L) \cdot \frac{a \cdot W+h}{M+h}}{M+h} \right]_1 \cdot \varepsilon_x + \left[ \frac{\cos(L) \cdot \frac{a \cdot W+h}{M+h}}{M+h} \right]_1 \cdot \varepsilon_y + [0] \cdot \varepsilon_z +$$

$$\left[ \frac{-\sin(B) \cdot \cos(B) \cdot N \cdot e^2}{M+h} \right]_1 \cdot \Delta m + \Delta B(a_1, a_2, b_1, b_2)$$

$$L_2 + v = L_1 + \partial L_1(d) = L_1 + \partial L_1(u, v, w, \varepsilon_x, \varepsilon_y, \varepsilon_z, \Delta m, \Delta a, \Delta f) \quad (2.1b)$$

$$= L_1 + \left[ \frac{-\sin(L)}{(N+h) \cdot \cos(B)} \right]_1 \cdot u + \left[ \frac{\cos(L)}{(N+h) \cdot \cos(B)} \right]_1 \cdot v + [0] \cdot w +$$

$$\left[ \frac{\cos(L) \cdot \sin(B) \cdot (N \cdot (1-e^2) + h)}{(N+h) \cdot \cos(B)} \right]_1 \cdot \varepsilon_x + \left[ \frac{\sin(L) \cdot \sin(B) \cdot (N \cdot (1-e^2) + h)}{(N+h) \cdot \cos(B)} \right]_1 \cdot \varepsilon_y +$$

$$-[1] \cdot \varepsilon_z + [0] \cdot \Delta m + \Delta L(a_1, a_2, b_1, b_2)$$

In the above formulas the following abbreviations were introduced:

$$\Delta B(a_1, b_1, a_2, b_2) = B(a_1, b_1) - B(a_2, b_2), \quad (2.1c,d)$$

$$\Delta L(a_1, b_1, a_2, b_2) = L(a_1, b_1) - L(a_2, b_2) = 0 \quad \text{and}$$

$$N = \frac{a^2}{b \cdot \sqrt{1+e^2 \cdot \cos^2 B}}; \quad M = \frac{a^2}{b \cdot \left( \sqrt{1+e^2 \cdot \cos^2 B} \right)^3}; \quad W = \frac{a}{N}; \quad e^2 = \frac{a^2 - b^2}{a^2} \quad (2.1e,f,g,h)$$

As transformation parameters  $\mathbf{d}$  (2.1a,b) three translations ( $u, v, w$ ), three rotations ( $\varepsilon_x, \varepsilon_y, \varepsilon_z$ ) and a scale difference  $\Delta m$  between the two reference systems occur in the observation equations (2a,b). The corrections  $\Delta B$  and  $\Delta L$  (2.1c,d) are due to the known changes ( $\Delta a, \Delta f$ ) in the ellipsoid dimensions  $a$  and  $f$  at the transition from reference system 1 (e.g. DHDN in Germany) to reference system 2 (e.g. ETRS89). As the transformation is concerning the plan component ( $B, L$ ), and in general no heights for the respective identical points, nor for the points to be transformed (e.g. cadastral points, buildings etc.) are available in the different databases, the height component  $h$  – taken as third observation equation – is only needed for a small number of three dimensional identical points (e.g. points of a 1<sup>st</sup> order networks). The transformation equation for the height component  $h$  reads

$$h_2 + v = h_1 + \partial h_1(d) = h_1 + \partial h_1(u, v, w, \varepsilon_x, \varepsilon_y, \varepsilon_z, \Delta m, \Delta a, \Delta f) \quad (2.1h)$$

$$= h_1 + [\cos(B) \cdot \cos(L)]_1 \cdot u + [\cos(B) \cdot \sin(L)]_1 \cdot v + [\sin(B)]_1 \cdot w +$$

$$\left[ -e^2 \cdot N \cdot \sin(B) \cdot \cos(B) \cdot \sin(L) \right]_1 \cdot \varepsilon_x + \left[ e^2 \cdot N \cdot \sin(B) \cdot \cos(B) \cdot \cos(L) \right]_1 \cdot \varepsilon_y$$

$$+ [0] \cdot \varepsilon_z + [h + a \cdot W]_1 \cdot \Delta m + \Delta h(a_1, a_2, b_1, b_2),$$

accordingly with  $\Delta h(a_1, a_2, b_1, b_2) = h(a_1, b_1) - h(a_2, b_2)$ . An advantage of the approach (2.1a-

h) is that the ellipsoidal heights  $h_1$  (which are due to all classical network datum close to the standard heights  $H$ ) are only needed with a subordinate accuracy. Due to the fact, that for the classical national datum systems the ellipsoid's surface and the height reference surface were adapted to each other, the ellipsoidal height  $h_1$  in the coefficients (2.1a) and (2.1b) can be replaced in different cases by the national standard heights  $H_2$ . For the same, reason the height information  $h_1$  can in case of a classical system be taken from free available databases (e.g. the digital terrain model databases ETOPO5 or ETOPO30).

The formulas (2.1a-h) are based on a linearization, so that in case of large datum parameters  $d$  (e.g. for the translations  $u, v, w$  between two systems 1 and 2) a corresponding pre-transformation between system 1 and 2 with approximate parameters has to be performed before the application of (2.1a-h) [9].

## 2.2 CoPaG and DFLBF Data Bases (DB) for Germany

Besides some solutions for different German states and city areas in Germany, two nationwide databases for Germany were computed with the CoPaG software, namely the "(3-5)\_cm\_CoPaG\_DB Germany" (Fig. 2.2a) and the "(3-5)\_cm\_DFLBF\_DB Germany" (fig. 2.2b) [28].

As the ETRS89 frame has one cm precision, e.g. all over Germany and the 1<sup>st</sup> order ITRF/ETRS89 of other states all over the world, the residuals shown in fig. 2.1 left mean the deflection of the classical plan DHDN network coordinates  $\hat{x}=(B,L)_1$  from its true shape  $\tilde{x}$ . The residuals of the DHDN network of Germany West (fig. 2.1, left) reach the range of  $\pm 2.5$  m.

The shape and amount of the deflections  $\nabla x = \tilde{x} - \hat{x}$  are to be explained by the theory of so-called "natural weak-forms" [4], [5], [6], [15] and eventually a second part of so-called "stochastic weak-forms" [10]. The "natural weak-forms" of classical geodetic networks are related to the eigenvalue-problem

$$[C_{\hat{x}} - \mu_i \cdot I] \cdot m_i = 0 . \quad (2.2a)$$

of the covariance matrix  $C_{\hat{x}}$  of the adjusted network coordinates  $\hat{x}$ .

The eigenvalue problem (2.2a) is part of the theory and concepts of spectral analysis and optimization of geodetic networks [4], [7]. It is shown in [4], [5], [7], [15] and [9] that the spectral components  $\nabla_i$

$$\nabla_i = \sqrt{\mu_i} \cdot m_i . \quad (2.2b)$$

are the key for the prediction (comparing e.g. the 1989 prediction results for Baden-Württemberg [6] with the real deflections for Baden-Württemberg presented 2000 in [9]) and theoretical understanding of deflections  $\nabla \hat{x}$  of large networks from their true shape  $\tilde{x}$ .

In case of an occurring shape deflection  $\nabla \hat{x}$  - like shown for the plan German DHDN network in fig. 2.1, left - the spectral components  $\nabla_i$  (2.2b), which are carried by the eigenvectors  $m_i$  (2.2a) and scaled by the square roots of the corresponding eigenvalues  $\mu_i$  (2.2a) give - in the descending order of the eigenvalue size  $\mu_i$  - the probability and amount of respective geometric deflection parts, which span up the total deflection shape  $\nabla \hat{x}$  (fig. 2.1, left). As large geodetic networks tend to have a number of high dominant eigenvalues, the maximum spectral components (2.2b) (especially the maximum component  $\nabla_{\max} = \sqrt{\mu_{\max}} \cdot m_{\max}$ ) point out the

quasi systematic shape deflection  $\nabla \hat{x}$ . In case that the covariance matrix  $C_{\hat{x}}$  is regarded with respect to the assumed stochastic model of normal distributed observations, and the spectral analysis is accordingly based on (2.2a,b), the essential main spectral components  $\nabla_i = \sqrt{\mu_i} \cdot m_i$  are called the “natural weak-forms” of a geodetic network [4], [15].

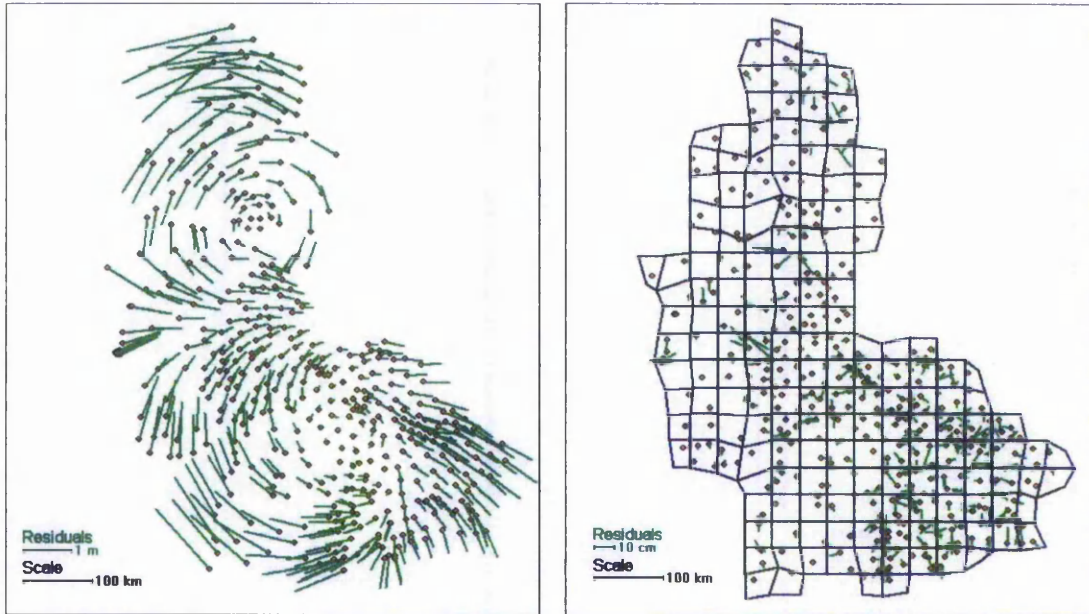


**Fig. 2.1. left:**

**Residuals up to 2.5 m for the transformation of the German DHDN plan coordinates to ETRS89 with only one nationwide set of transformation parameters  $d$ .**

**Fig. 2.1. right:**

**Strict transformation with continuity conditions of the transformation parameters of the coordinates from German DHDN to ITRF (ETRS89) under partition in 177 patches. This leads to a drastic reduction of the residuals to less than 0.02 m in average.**

Another type and an additional amount of weak-form deflections  $\nabla \hat{x}$  - namely the so-called “stochastic weak forms”  $\nabla_{i, \text{stoch}} = \sqrt{\mu_{i, \text{stoch}}} \cdot m_{i, \text{stoch}}$  already mentioned above – occur due to neglects in the stochastic model of the observations of a geodetic network adjustment [5], or a non over-determined parameter-computation  $\hat{x}$  from a respective observation set. The spectral components  $\nabla_i = \sqrt{\mu_i} \cdot m_i$  of the “stochastic weak forms” are then related to a general eigenvalue problem, which is regarded in [10].

To manage the weak-form problem with respect to the plan transformation (2.1a,b), the transformation area has to be divided into so-called patches (fig. 2.1b) with individual datum parameter sets  $d^j$  (accordingly the term CoPaG = Continuously Patched Georeferencing). In the example of applying the CoPaG concept to the plan German DHDN network, the average residual was reduced from 0.33 m (only one patch and datum set  $d$  for the whole area of Germany, fig. 2.1, left) to a range of less than 0.02 m by the division of the transformation area into 177 patches with individual datum parameters  $d^j$  (fig. 2.1, right).

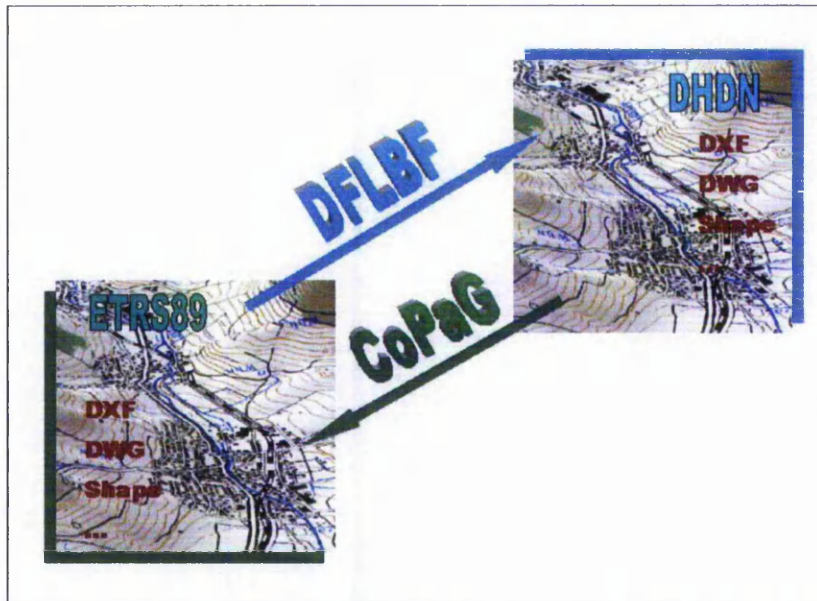


**Fig. 2.2a, b:**

**Left: DFLBF\_DB for the transformation from ETRS89 to a classical plan reference system.  
 Right: CoPaG\_DB for the transformation from a classical plan reference system to ETRS89.**

To achieve a continuous and homogenising transformation, appropriate continuity conditions  $C(\mathbf{d}^j, \mathbf{d}^{j+1})$  - in analogy to these of the DFHRS concept (3.6f) - along the borders of neighbouring patches  $j$  and  $(j+1)$  have to be set up as additional condition equations concerning neighbouring parameter sets  $\mathbf{d}^j$  and  $\mathbf{d}^{j+1}$ , in order to complete the CoPaG adjustment approach (2.1a,b,h) [26].

The present CoPaG\_DB and the DFLBF\_DB (Digital Finite Element Plan Reference System Transformation, in analogy to the term DFHBF, chap. 3) allow the strict and neighbourhood consistent transformation from/to the classical German reference-systems (e.g. DHDN in Western Germany presented in fig. 2.1 and RD83 in Eastern Germany) to/from ETRS89 with a reproduction quality of (3-5) cm.

### 2.3 CoPaG Software and CoPaG/DFLBF\_DB Access Software

The CoPaG approach (2.1a-h) was realized in the CoPaG-Software ©Jäger/Kälber. The CoPaG software (fig. 2.3) allows the computation of transformation parameters  $\mathbf{d}^j$  on dividing the whole transformation area into an arbitrary number of irregular patches (fig. 2.1b, fig. 2.3).

Additionally continuity conditions  $C(\mathbf{d}^j, \mathbf{d}^{j+1})$  have to be introduced to achieve the continuity of the total set of parameters and the homogenisation of the transformed configuration.

Fig. 2.3 shows a screen-shot of the CoPaG-Software at the example of the view on the CoPaG Software at the example of the project “(1-2)\_cm DFLBF\_DB and CoPaG\_DB Rheinland-Pfalz”. Whereas in fig. 2.3 the mean mesh size is 15 km, the final mesh size for (1-2) cm databases was 7 km.

The quality control is – in addition to standards of statistical testing – performed by regarding the

quality measure of reproduction values. The two-dimensional test statistics and the so-called reproduction values are evaluated in the CoPaG concept and software in analogy to these of the quality control concept of DFHRS computation (see chapter 3.3.2). Besides this a so-called accuracy surface (Fig. 2.4) can be computed from the covariance-matrix in function of position.

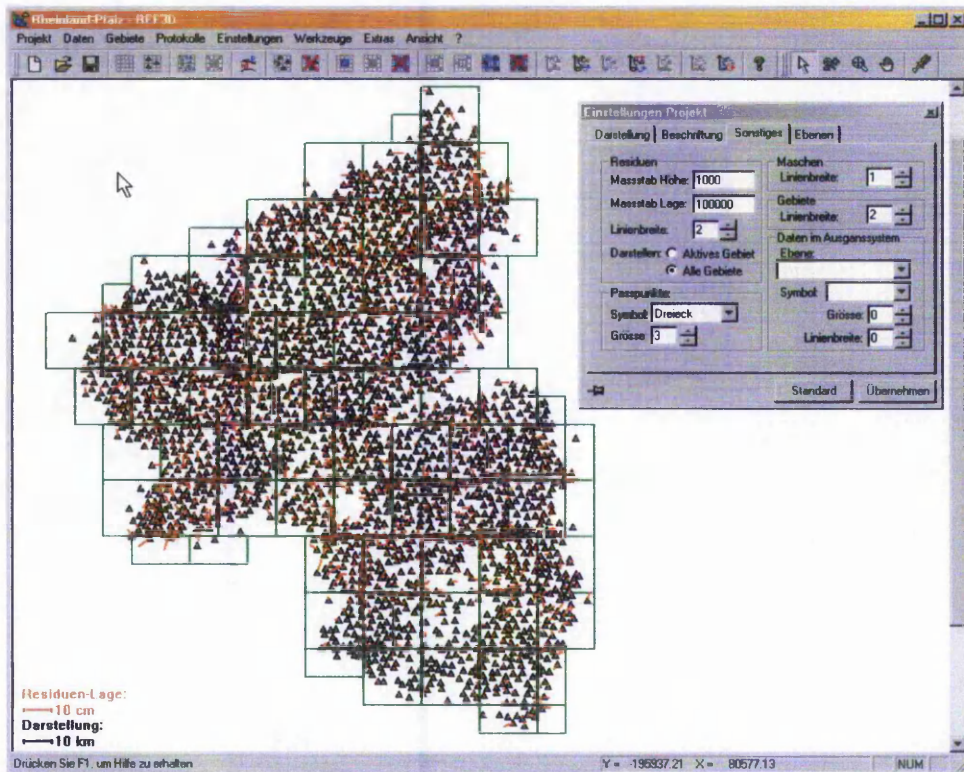
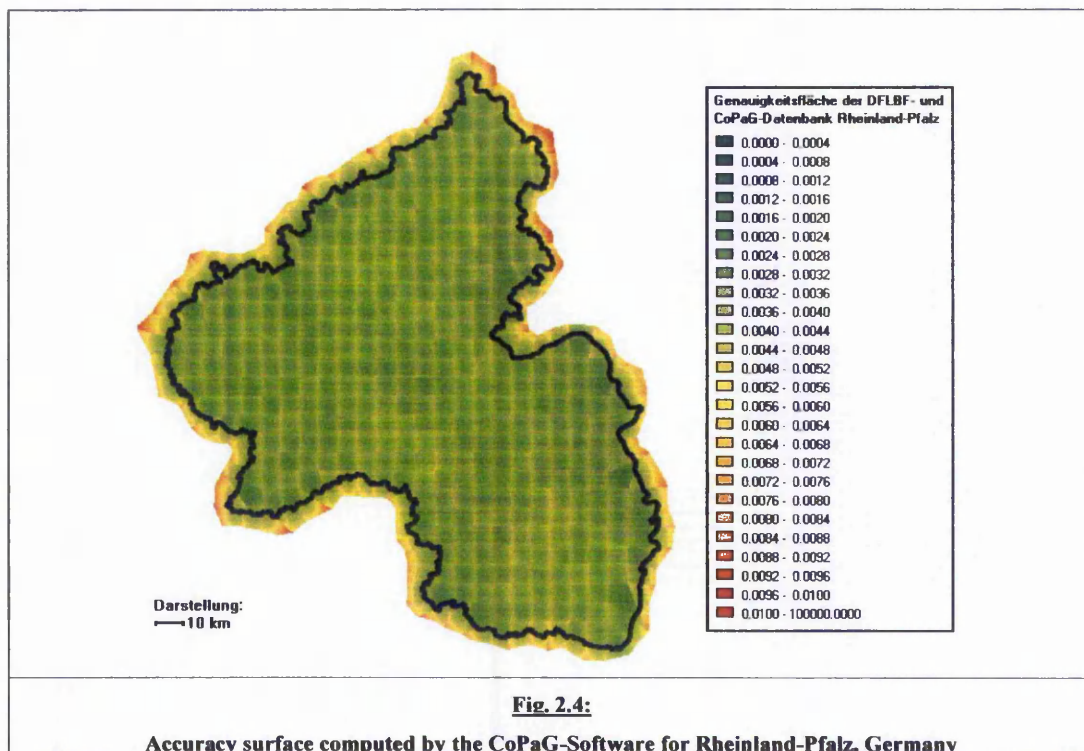


**Fig. 2.3:**

**View on the CoPaG Software at the example of the project “(1-2)cm DFLBF\_BD and CoPaG\_DB Rheinland-Pfalz”**

After finishing computation and quality control the parameter sets for all patches and also the residuals of the identical points are stored in a well-defined format in the so-called DFLBF\_DB and CoPaG\_DB files and can be used by any software providing a DFLBF/CoPaG Access.

The direct access is realized by a DLL, which can be implemented into any GNSS or GIS software. Many GNSS and GIS companies meanwhile use a direct access. As concerns the alternative way of converting DFLBF\_DB to gridfiles for a use in GNSS positioning in the so-called gridfactory philosophy and technology, e.g. within the Leica-Geosystem SKI\_PRO software and the Trimble TSO software, it is referred to [28] and to the homepages of these companies respectively.



## 2.4 Outlook to the CoPaG Concept and CoPaG/DFLBF\_DB

The CoPaG\_DB provide the direct transformation (no identical points) of the classical plan networks and related DB positions to the ETRS89 datum (fig. 2.2b), and the DFLBF\_DB (fig. 2.2a) are used vice-verse for the direct transformation (no identical points) of ETRS89 related GNSS positions in SAPOS®- and ascos® GNSS positioning to the classical plan datum systems.

The further development of the (3-5)\_cm data bases, which is directed to the computation of a “1\_cm\_CoPaG\_DB/DFLBF\_DB for Germany” is merely a question of the number and density of further identical points. This is to be concluded from successful test computations for the area of Rheinland-Pfalz, Germany, where a number of 2535 identical points was used to evaluate the respective continuous transformation parameters sets  $\mathbf{d} = (d^1, \dots, d^j, \dots, d^n)$  enabling a mean reproduction quality of the coordinates of 1\_cm.

The weak-form problem (fig. 2.1, left) is of general nature, and it concerns all classical networks all over Europe and the whole world respectively. So the CoPaG concept can be applied generally to solve the related transformation problems and to evaluate precise and economic CoPaG\_DB and DFLBF\_DB worldwide.

For further information it is referred to [www.geozilla.de](http://www.geozilla.de) [36].

### 3 GNSS-Heighting - Precise Vertical Height Reference Surface Representation by the Digital FEM Height Reference Surface Concept (DFHRS) and DFHRS Data Bases

#### 3.1 Motivation and Situation

Standard heights  $H$  are referring to different types of height reference surfaces (HRS). The common root of all three relevant HRS-types is the idea, that the HRS should be that equipotential surface of the earth's gravity field with a potential  $W_0$ , which coincides with the normal potential  $U_0$  and the mean sea-level surface  $H=0$  (fig. 3.1, fig. 3.2)<sup>1</sup> and continues it outside the oceans. The datum of a height system is fixed by at least one point with an assigned value  $W_0$  and  $H=0$ . The height  $H_P$  of any point  $P$  on the earth's surface (ES) is then defined as the curved distance between  $P$  and the respective HRS (fig. 3.1; fig. 3.2).

The two modern standard HRS-types are the geoid and the so called quasi-geoid. The geoid HRS type realizes exactly the equipotential surface concept. The related so-called orthometric heights  $H_{\text{orth}} = (W_0 - W_P) / \bar{g}$  or  $H_{\text{orth}} = C_P / \bar{g}$  respectively are found, by dividing the geopotential number  $C_P$  (difference between  $W_0$  and the point  $P$  potential  $W_P$ ) by the mean gravity value  $\bar{g}$  between  $P$  and the HRS. A disadvantage of a HRS type of a geoid and a related orthometric height system  $H_{\text{orth}}$  is however due to the fact, that the density assumptions for the area of  $P$  are needed to evaluate  $\bar{g}$ . The quasi-geoid HRS and the respective so-called normal heights  $H_{\text{normal}} = C_P / \bar{\gamma}$ , as an alternative HRS and height system  $H$ , are found by dividing the geopotential number  $C_P$  by the mean gravity value  $\bar{\gamma}$  taken from the normal potential between  $P$  and the HRS. In this case the modern standard for the normal potential and  $\bar{\gamma}$  is related to the Global Reference System 80 (GRS80). The value  $\bar{\gamma}(B,h)$  is free from any density hypothesis. Therefore the decision for the new HRS and height type  $H$  for the European reference system EUREF was met for the quasi-geoid and normal height type  $H$  respectively (EUREF symposium, Ankara 1996, resolution No. 10, see [3]).

The most precise way to determine the standard height of a point  $H_P$  of the earth's surface (ES) is still based on levelling, or better levelling and gravity measurements in higher order networks, meaning by the realization of the geopotential number  $C_P$  as  $C_P = \sum g_i \cdot \Delta n_i$ .

The recent adjustment of the normal height  $H$  related European Vertical Network - as part of new European Vertical Reference System (EVRS) - was based on  $C_P$  and is ready on the continental level [20]. The accuracy as e.g. predicted to be 5 cm on continental level [5] is kept. The short-wave precision of the adjusted height differences  $\Delta H$  of neighbouring points in the different European national networks of lower order is of course better and represented in the low sub-cm range [20].

The GNSS-based determination of standard heights  $H$  on any accuracy level however requires principally the transition of the ellipsoidal GNSS height  $h$  to the standard height  $H$ . So a GNSS-based determination of standard height  $H$  makes it necessary to subtract the height  $N_G$  of the height reference surface (HRS) from the ellipsoidal GNSS height  $h$  (fig. 3.1; fig. 3.2). Therefore

<sup>1</sup> For the new Europe normal height system presently the Normaal Amsterdams Peils (NAP) [20]

the HRS must be represented relative to the ellipsoid surface in terms of a two-dimensional HRS model  $N_G(B,L)$ . The old term “geoid” and “geoid height” for the HRS model and  $N_G(B,L)$  (fig. 3.1) are getting properly replaced by “HRS” and “height of the HRS (fig. 3.2, DFHRS)”, which is more convenient with respect to the above mentioned different standard HRS and height types<sup>2</sup>.

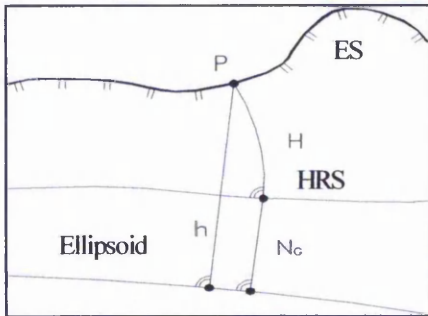
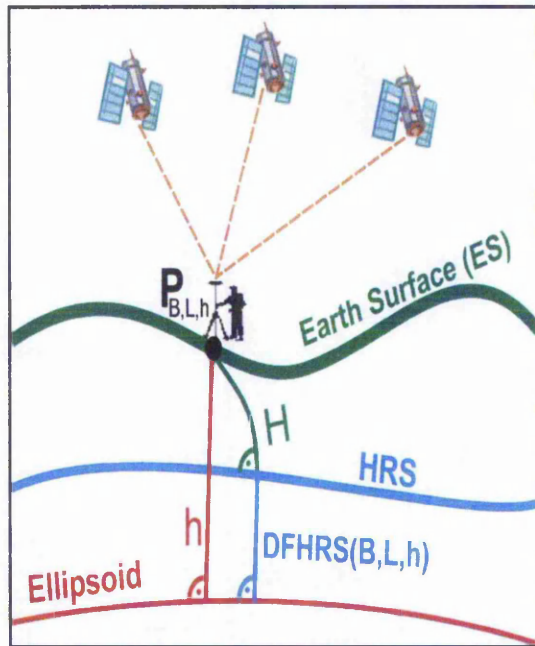


**Fig. 3.1 (above):**

Formula ideal (1a): earth surface (ES) at position  $P(B,L)$ , ellipsoidal GPS/GNSS height  $h$ , standard height  $H$  and a two-dimensional HRS model  $N_G$ .

**Fig. 3.2 (right):**

In real world GNSS-positioning the extended formulas (1b,c) and a three-dimensional HRS model  $N_G(B,L,h)$  however have to be taken into account.



The classical gravity related geoid or quasi-geoid models  $N_G(B,L)$ , such as EGG97 [1], EGM96 [13] ) and the large number of local and regional geoid models are not fitted to the HRS. This is for the reason, that the geometrical information of the identical points ( $h,H$ ) is in general not taken into account as part of a “geoid-computation” approach. A quasi-geoid for example is computed based on the Stokes formula as

$$N_G(B,L) = \frac{a}{4\pi \cdot \gamma(B)} \iint_{\sigma} \Delta g \cdot S(\psi) \cdot d\sigma \quad (3.1a)$$

In practice of course (3.1a) is submitted to the so-called remove restore technique and algorithm [1], whereas the global gravity reference EGM96 [13] is used as geopotential reference.

The precise geometric information for the HRS

$$N_G(B,L) = (h - H)_{B,L} \quad (3.1b)$$

remains however unused as additional information in the state of the art of most gravity based geoid computation approaches. So the ideal formula

$$H = h - N_G(B,L) \quad (3.2)$$

<sup>2</sup> For historical reasons even some types more exist, such as e.g. the NN-type of HRS and the respective spheroidal normal heights (“NN-heights”) as precursor of the normal heights.

fig. 3.1 does not hold for the use of standard HRS in terms of “geoid-model” in GNSS-based heighting. In spite of a however sufficient HRS shape representation in the short wave range, HRS models represented by standard geoid models (3.1a) suffer from medium and long waved systematic shape deflections. The reasons are again a big amount of both types of “weak forms” (chap. 2). Also for locally and short waved precise geoid models, e.g. the EGG97 [1], the “weak-form” deflections reach a “meter range” over large areas e.g. for Europe (fig. 3.3).

Of course the HRS represented by the standard height system  $H$  and  $h$  (3.1b) is also subjected to “weak-forms” in  $H$  and  $h$ , but their amount is much smaller. For  $H$  they reach only in a “cm” range or a “few cm” range respectively in large areas [5], [15]. For Europe and the EVRS we have a range of 5 cm, see [5]. Consequently “levelled heights”  $H$ , which were evaluated from geopotential numbers (levelling and gravity) and the respective precise ellipsoidal heights  $h$  are representing by (3.1b) the precise and discrete control points for the long and short-wave domain of the HRS shape, while geoid-models of standard type  $N_G(B,L)$  (3.1a) (fig. 3.3) can be used only as observations concerning the HRS shape in the local short wave domain.

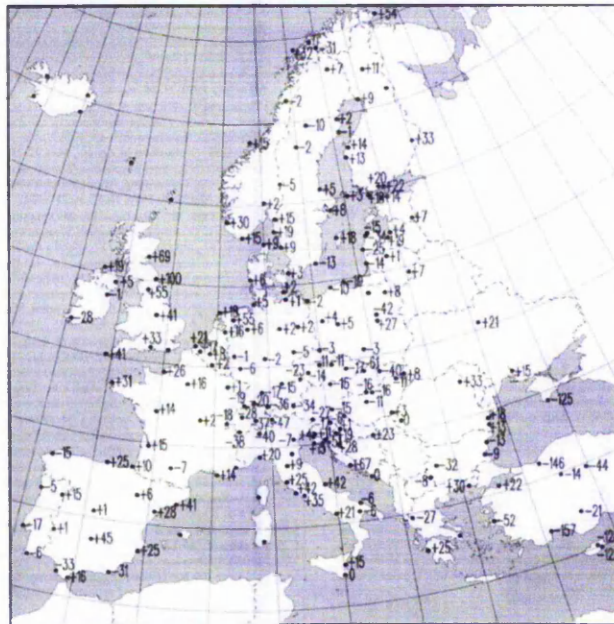


**Fig. 3.3.:**

**Long-waved deflections, to be declared as natural and stochastic “weak-forms” (chap.1), in the (dm – meter) range of the EGG97, which has above these long-waved distortions a cm-accuracy concerning the local shape quality (published in different EUREF series, [20])**

An additional reason why (3.2) is not valid, is because of a scale difference  $\Delta m$  occurring between the GPS/GNSS-heights  $h$  and the heights  $H$  of the standard height system ([2], [3], [18], [19]). One reason for scale inconsistency  $\Delta m$  is, that most existing standard height systems  $H$  were not evaluated by the GRS80 normal gravity field  $\gamma(B,h)$ . Other proved sources for scale effects  $\Delta m$  are occurring due to neglected (hidden) observation correlations and related stochastic weak-forms [5] and different systematic error types in levelling ([5], [10]). All these systematics tend to imply a scale error  $\Delta m$ . So, all in all, the above formula ideal (3.2) has to be modified with respect to “real world conditions”. In classical approaches ([2], [3]) and software

packages like HEIDI2©Dinter/Illner/Jäger [3], which use explicitly geoid models  $N_G(B,L)$  (3.1a), the relation between GNSS heights  $h$  and standards heights  $H$  reads:

$$H = h - \frac{(N_G(B,L) + \partial N(\mathbf{d}_{local}) + NFEM(\mathbf{p}|B,L)) - \Delta m_{regional}}{\text{Uncontinuous "3 component" HRS}} \cdot H \quad (3.3a)$$

The formula (3.3a) represents the so-called “geoid-refinement approach” [3], [11], [14]. Here the geoid model heights  $N_G(B,L)$  are used both as observations and as unknowns. So the geoid-model heights  $N_G(B,L)$  become part of the HRS together with additional local datum parts  $\partial N(\mathbf{d}_{local})$ ,  $\mathbf{d}_{local}^T = [u, v, w, \varepsilon_x, \varepsilon_y, \Delta m_G]$  and an additional refinement  $NFEM(\mathbf{p}|B,L)$  component.

The refinement part  $NFEM(\mathbf{p}|B,L)$ , which is described theoretically in chap. 3.2, is based on the same mathematical concept of a surface representation as in the DFHRS concept. But it has a quite different meaning in the DFHRS concept than in the above classical geoid-refinement approach (3.3a). With respect to the determination of new points in the geoid-refinement approach (3.3a), the final HRS is to be considered as a compound of 3 components – the original and unimproved geoid-model  $N_G(B,L)$ , the local datum-parts  $\partial N(\mathbf{d}_{local})$  and the refinement  $NFEM(\mathbf{p}|B,L)$ . The compound of a three component HRS would be a badly portable and heterogeneous concept for a data base in online GNSS heighting. Therefore the geoid refinement approach (3.3a) is in practice a post-processing solution. Above this, the effect of the local datum-parts  $\partial N(\mathbf{d}_{local})$  of the geoid-model(s) (3.3a) introduced in the total area (3.3a), reading explicitly

$$\begin{aligned} \partial N_G(\mathbf{d}) = & [\cos(L) \cdot \cos(B)] \cdot u + [\cos(B) \cdot \sin(L)] \cdot v + [\sin(B)] \cdot w \\ & + [e^2 \cdot N(B) \cdot \sin(B) \cdot \cos(B) \cdot \sin(L)] \cdot \varepsilon_x + [-e^2 \cdot N(B) \cdot \sin(B) \cdot \cos(B) \cdot \cos(L)] \cdot \varepsilon_y \\ & + [-N_G] \cdot \Delta m_G \end{aligned} \quad (3.3b)$$

is not controlled with respect to the continuity of the three-component HRS model at the borders of the local areas. These are some decisive disadvantages of the “geoid refinement” approach (3.3a). The datum part (3.3b), which is also used in (3.6a), is – except the simplified scale part  $[-N_G] \cdot \Delta m_G$  of the geoid model  $N_G$  – identical with (2.1h).

In the DFHRS approach [11], [16], [17], [18], [21], [22], [23] and the computation of DFHRS\_DB [14], [26], [27], [28] for GNSS-based heighting, which are further treated as main subject of chap. 3, however the role of the former three-component HRS model (3.3a) is completely taken over by the one-component HRS model of a Digital Finite Element Height Reference Surface (DFHRS).

In DFHRS modelling the HRS is described continuously by the surface  $NFEM(\mathbf{p}|B,L)$ .

The two-dimensional Finite Element Model (FEM)  $NFEM(\mathbf{p}|B,L)$  (3.5a) of the HRS takes over the role of the HRS (fig. 3.1; fig. 3.2), and is represented in a continuous way by mesh-wise sets of polynomial parameters  $\mathbf{p}$  (3.5b). So we have for the DFHRS concept the following basic relation between the ellipsoidal GNSS height  $h$  and the standard height  $H$  (fig. 3.1; fig. 3.2):

$$H = h - \frac{\text{NFEM}(\mathbf{p} | B, L)}{\text{Continuous "one-component" HRS}} - \Delta m_{\text{regional}} \cdot H \quad (3.4a)$$

In this way the continuous Finite Element Model NFEM( $\mathbf{p}|B,L$ ) of the HRS is a two-dimensional function of the plan position ( $B,L$ ), and is accordingly called the "geoid-part" of the so-called three-dimensional DFHRS correction. The part  $\Delta m \cdot h$  is accordingly called the "scale part" of the DFHRS correction.

So three-dimensional DFHRS correction DFHRS( $B,L,h$ ) (fig. 3.2), which has to be subtracted from the GNSS height  $h$  in order to receive the standard height  $H$ , reads in total:

$$H = h - \text{DFHRS}(\mathbf{p}, \Delta m | B, L, h) = h - (\text{NFEM}(\mathbf{p} | B, L) - \Delta m \cdot H) \quad (3.4b)$$

The respective DFHRS data bases (DB) contain - as essential parts for HRS representation and the scale parametrisation - the "DFHRS\_DB parameters"  $\mathbf{p}$  and  $\Delta m$ .

### 3.2 FEM representation of a Height Reference Surface (DFHRS)

The finite element representation NFEM( $\mathbf{p}|x,y$ ) is carried by the base functions of bivariate polynomials of degree  $n$ , which are set up in regular or irregular meshes. If we describe with  $\mathbf{p}^i$  the polynomial coefficients ( $a_{00}, a_{10}, a_{01}, a_{20}, a_{11}, a_{02}, \dots$ ) <sup>$i$</sup>  of the  $i$ -th mesh, we have for the height NFEM( $\mathbf{p}^i|x,y$ ) of the HRS over the ellipsoid (fig. 3.1; fig. 3.2) in the  $i$ -th mesh:

$$\text{NFEM}(\mathbf{p}^i | x, y) = \mathbf{f}(x(B, L), y(B, L)) \cdot \mathbf{p}^i ; i = 1, m; \text{ with} \quad (3.5a)$$

$$\mathbf{p}^i = (a_{00}, a_{10}, a_{01}, \dots)^i \text{ and } \mathbf{f}(x(B, L), y(B, L)) = (1, x, y, x^2, xy, y^2, \dots) \quad (3.5b), (3.5c)$$

The vector  $\mathbf{f}$  means the so called Vandermond vector and contains the different powers of the coordinates ( $x,y$ ) according to the polynomial degree  $n$ . The total parameter vector  $\mathbf{p}$  consists of the coefficient sets  $\mathbf{p}^i = (a_{j,k})^i$ , ( $j=0,n; k=0,n$ ) of all  $m$  meshes. The plan position in (3.5a,c) is due to metric ellipsoidal coordinates ( $y(B,L)$ ="East" and  $x(B,L)$ ="North") introduced e.g. as Mercator or Lambert coordinates, which are in any case functions of the geographical coordinates ( $B,L$ ).

To imply a continuous surface NFEM( $\mathbf{p}|x,y$ ), one set of continuity conditions of different type  $C_{0,1,2}$  has to be set up for the computation of NFEM( $\mathbf{p}|x,y$ ) for each couple of neighbouring meshes (fig. 3.4). The continuity type  $C_0$  implies the same functional values, the continuity type  $C_1$  implies the same tangential planes and the continuity type  $C_2$  the same curvature along common mesh borders of the DFHRS as represented by NFEM( $\mathbf{p}|x,y$ ) (3.5a). The continuity conditions occur as additional observation equations  $C(\mathbf{p})=0$  to be added to the parametrization of NFEM( $\mathbf{p}|x,y$ ). The condition equations  $C(\mathbf{p})=0$  are related to the polynomial sets of the coefficients ( $a_{j,k})^m$  and ( $a_{j,k})^n$  of each couple of neighbouring meshes  $m$  and  $n$ . To force e.g.  $C_0$ -continuity, the difference  $\Delta N_{m,n}$  in the geoid height  $N_G$  of any point  $S$  at the common border  $SA-SE$  of two meshes  $m$  and  $n$  (see fig. 3.4; fig. 3.8) has to become zero. So the basic condition equation for a polynomial representation of  $n^{\text{th}}$  degree reads [22]:

$$\Delta N_{m,n} = \sum_{j=0}^n \sum_{k=0}^{n-j} (a_{j,k,n} - a_{j,k,m}) \cdot (y_{SA} + t \cdot (y_{SA} - y_{SE}))^j \cdot (x_{SA} + t \cdot (x_{SA} - x_{SE}))^k = 0 \quad (3.5d)$$

With ( $y_{SA}, x_{SA}, y_{SE}, x_{SE}$ ) we introduce the plan metric coordinates of the nodal points  $SA$  and  $SE$  of a mesh borderline. Equation (3.5d) represents a polynomial of  $n$ -th degree parametrized in the border line parameter  $t$  with  $t \in [0,1]$ . The subset of  $(n+1)$   $C_0$ -continuity condition equations

$C(\mathbf{p})=0$  for the border between mesh  $m$  and  $n$  results in case of  $C_0$ -continuity from (3.5d) by setting all  $(n+1)$  coefficients related to  $t$  to zero ([22]).

The mesh size and mesh shape for the computation of the NFEM( $\mathbf{p}|x,y$ ) - representing the so called HRS or "geoid" part (3.3a) of the DFHRS correction and DB content - may be chosen with an arbitrary shape. The best approximation of a HRS by NFEM( $\mathbf{p}|x,y$ ) results of course by introducing small meshes, e.g. in a range of 5 km to keep a 5 mm range for any HRS shape approximation by a polynomial degree up to  $n=3$ .

A special advantage and characteristic of the NFEM( $\mathbf{p}|x(B,L), y(B,L)$ ) representation consists in the fact, that the nodal points of the FEM grid are totally independent of the location of the geodetic observations and the geoid data points. In principle any type of HRS and height related observation data can be used for the determination of the parameter vector  $\mathbf{p}$  of NFEM( $\mathbf{p}|x,y$ ), namely height observations  $(h,H,\Delta H,\Delta h)$ , the geoid-model heights  $N_G(B,L)$ , deflections of the vertical  $(\xi,\eta)$  and gravity anomalies  $\Delta g$  (see chap. 3.3).

### 3.3 Digital FEM Height Reference Surface (DFHRS) Approach and Computation

#### 3.3.1 Mathematical Adjustment Model

The mathematical model of the so-called DFHRS data base production step reads in the system of observation equations (functional model) and the corresponding stochastic models of a least squares adjustment as follows:

<u>Functional Model</u>	<u>Observation Types and Stochastic Models</u>	
$h + v = H + h \cdot \Delta m + \mathbf{f}(x, y) \cdot \mathbf{p},$ <p style="margin-left: 40px;">with NFEM(<math>\mathbf{p} x,y</math>) = <math>\mathbf{f}(x(B,L), y(B,L)) \cdot \mathbf{p}</math></p>	Uncorrelated observations of ellipsoidal heights $h$ Covariance matrix $\mathbf{C}_h = \text{diag}(\sigma_{h_i}^2).$	(3.6a)
$N_G(B,L)^j + v = \mathbf{f}(x, y) \cdot \mathbf{p} + \partial N_G(\mathbf{d}^j)$	Correlated geoid height observations. With a given real covariance matrix $\mathbf{C}_{N,G}$ or a $\mathbf{C}_{N,G}$ evaluated from an artificial covariance function.	(3.6b)
$\xi + v = -\mathbf{f}_B / M(B) \cdot \mathbf{p} + \partial B(\mathbf{d}_{\xi,\eta})$	Observations of vertical deflections $(\eta, \xi)$ . Pair wise correlated or uncorrelated among each other in case of astronomical observations. Correlated in $(\eta, \xi)$ . Pair wise correlated or uncorrelated among each other in case of astronomical model.	(3.6c)
$\eta + v = -\mathbf{f}_L / (N(B) \cdot \cos(B)) \cdot \mathbf{p} + \partial L(\mathbf{d}_{\xi,\eta})$		(3.6d)
$\eta + v = -\mathbf{f}_L / (N(B) \cdot \cos(B)) \cdot \mathbf{p} + \partial L(\mathbf{d}_{\xi,\eta})$		(3.6e)
$H + v = H$	Uncorrelated standard height $H$ observations with covariance matrix $\mathbf{C}_H = \text{diag}(\sigma_{H_i}^2).$	(3.6e)
$C + v = C(\mathbf{p})$	Continuity condition equations (3.5d) introduced as uncorrelated so-called pseudo observations with accordingly small variances and high weights.	(3.6f)

With  $\mathbf{f}_B$  and  $\mathbf{f}_L$  we introduce the partial derivatives of the Vandermond's vector  $\mathbf{f}(x(B,L), y(B,L))$  (3.6c) with respect to the geographical coordinates  $B$  and  $L$ .  $M(B)$  and  $N(B)$  mean the radius of

meridian and normal curvature at a position P(B,L) respectively. The continuity of the resulting HRS  $NFEM(\mathbf{p}|x,y)=\mathbf{f}(x,y)\cdot\mathbf{p}$  is automatically provided by the continuity equations C(p) (3.6f).

A number of identical points (h, H) (3.1b) are introduced by the observation equations (3.6a) and (3.6e). In the practice of DFHRS data base evaluation, also one or a number of several geoid models  $N_G(B,L)^j$  are used as additional observations to produce DFHRS\_DB in the least squares estimation (3.6a-k). To reduce the effect of medium or long waved systematic shape deflections, namely the natural and stochastic "weak-forms" (chap. 2) of geoid models  $N_G$  (3.6b) (fig. 3.3), the geoid model heights observations  $N_G$  (3.6b) are parted to into a number of so-called "geoid-patches"  $N_G(B,L)^j$  (3.6b) (see fig. 3.8). Each patch is set up, with individual datum-parameters  $\mathbf{d}^j$ , which are introduced by the datum part  $\partial N_G(\mathbf{d}^j)$  (3.3b) into (3.6b). It is of course also possible to introduce by  $N_G(B,L)^j$  - and a respective parameterization  $\partial N_G(\mathbf{d}^j)$  - (3.6b) several patched or unpatched geoid models in the same area, and of course also geoid models of a different type than the classical ones (3.1a) may be used.

With the classical relations  $\xi = -\partial N/\partial s_B$  and  $\eta = -\partial N/\partial s_L$  between vertical deflections and the 1<sup>st</sup> derivatives of the HRS in northern and eastern direction and the NFEM- polynomial representation as a product (see (3.5a-c) and (3.6a)) of Vandermond's vector  $\mathbf{f}$  and the polynomial parameters  $\mathbf{p}$  we get :

$$\xi = -\partial N/\partial s_B = -\partial NFEM/\partial B \cdot \partial B/\partial s_B = -\mathbf{f}(x(B,L),y(B,L))_B \cdot \mathbf{p} \cdot \partial B/\partial s_B, \quad (3-6g)$$

$$\eta = -\partial N/\partial s_L = -\partial NFEM/\partial L \cdot \partial L/\partial s_L = -\mathbf{f}(x(B,L),y(B,L))_L \cdot \mathbf{p} \cdot \partial L/\partial s_L. \quad (3-6h)$$

For  $\partial B/\partial s_B$  and  $\partial L/\partial s_L$  we have the classical relations  $\partial B/\partial s_B=M(B)$  and  $\partial L/\partial s_L=N\cdot\cos(B)$ . With  $\partial B(\mathbf{d}_{\xi,\eta})$  and  $\partial L(\mathbf{d}_{\xi,\eta})$  we describe the datum parts of the type deflections of the vertical  $\xi = (\varphi_{astr} - B)$  and  $\eta = (\lambda_{astr} - L) \cdot \cos B$  respectively. According to these definitions we receive the datum-parts  $\partial B(\mathbf{d}_{\xi,\eta})$  and  $\partial L(\mathbf{d}_{\xi,\eta})$  by introducing (2.1a) and (2.1b). So it holds that  $\partial B(\mathbf{d}_{\xi,\eta}) \equiv -\partial B_1(\mathbf{d})$  (2.1a) and  $\partial L(\mathbf{d}_{\xi,\eta}) \equiv -\partial L_1(\mathbf{d}) \cdot \cos B$ .

Using the vertical deflections  $(\xi, \eta)$ , which were derived from the same geopotential model as the geoid-model  $N_G$ , the datum parameter  $\mathbf{d}$  are also expected to be the same, and it holds  $\mathbf{d}(3.6b) = \mathbf{d}_{\xi,\eta}(3.6c) = \mathbf{d}_{\xi,\eta}(3.6d)$ . Otherwise, e.g. for sets of astronomically observed vertical deflections, different groups of datum parameters  $\mathbf{d}$  have to be introduced.

Observations from classical geoid models  $N_G$  (3.6b) are to be introduced instead of the original gravity observations  $\Delta g$ , which had been introduced for the computation of  $N_G$ . In this case the correlated geoid models observations  $N_G$  (3.6b) and original gravity observations  $\Delta g$  lead to identical results for the HRS by the parameters  $\mathbf{p}$  ([22], [23]). So the use of observation type  $N_G$  (3.6b) allows a more elegant and easier data treatment than by the use of the original gravity anomalies  $\Delta g$  (3.6i). Consequently observation equations for gravity observations  $\Delta g$  need to be set up in the DFHRS approach (3.6a-k), only if additional gravity observations  $\Delta g$  occur, which have not yet been used for the former computation of a geoid model  $N_G$  (3.6b).

### Functional Model

$$\frac{a}{4\pi \cdot \gamma(B)} \iint_{\sigma} \Delta g \cdot S(\psi) \cdot d\sigma + v = \mathbf{f}(x,y) \cdot \mathbf{p} \\ = NFEM(\mathbf{p} | x, y)$$

### Observation Types and Stochastic Model

Vector of reduced gravity anomalies  $\Delta g$  introduced with covariance matrix  $C_g$  into Stokes (3.6i) formula. The gravity anomalies  $\Delta g$  in this way determine the DFHRS with parameters  $\mathbf{p}$  at position  $(x(B,L),y(B,L))$ .

The integration of gravity observations  $g$  is done by the functional model (3.6j). The gravity observation  $g$  is represented in the local astronomical vertical system by the vector  $g^{LAV} = [0, 0, -g]^T$ . It is reduced due to vertical deflections ("topography") and then rotated to the system referring to the pole  $(\varphi_0, \lambda_0)$  of a local spherical cap harmonics (SCH) representation ([34], [35]).

**Functional Model**

$$g + v_g = g(\bar{C}_{nm}, \bar{S}_{nm} | \lambda', \nu')$$

**Observation Types and Stochastic Model**

Gravity vector taken from original gravity measurement vectors  $g^{LAV} = [0, 0, -g]^T$  in the local astronomical vertical system (LAV), reduced for vertical deflections and transformed to the SCH-system referring to  $(\varphi_0, \lambda_0)$ . (3.6j)

With  $(\lambda', \nu')$  we introduce the local azimuth-coordinates referring to the SCH-pole  $(\varphi_0, \lambda_0)$ . Besides (3.6j) existing geopotential models, e.g. EGM96, are to be introduced direct as observations for the regional SCH-parameterization  $\bar{C}_{nm}, \bar{S}_{nm}$ . Eventually a datum parameterization has to be considered here. The advantage of a regional SCH-parameterization - compared to the standard of a global spherical representation - is, that for a sub-cm resolution a SCH-order of  $n=m=25$  is sufficient for an area-size of (100 km x 100 km) compared to  $n=m=7000$  for the usual global spherical harmonics parameterization with  $\varphi_0 = 90^\circ$  [34]. So the number of unknowns is to be reduced essentially. The SCH-parameters  $\bar{C}_{nm}, \bar{S}_{nm}$  (3.6j) are regarded within the DFHRS-concept (3.6a-k) only as auxiliary unknowns, while the NFEM-parameters  $p$  are the main unknowns. By the condition equations (3.6k) - introduced as pseudo observations with a high weight - the SCH-parameters  $\bar{C}_{nm}, \bar{S}_{nm}$  (3.6j) are related again to the NFEM parameters  $p$  of the DFHRS-approach, see [34].

**Functional Model**

$$0 + v_{\Delta N} = \frac{GM}{a\gamma} \sum_{n=2}^{\infty} \left(\frac{a}{r}\right)^{n+1} \sum_{m=0}^n (\delta\bar{C}_{nm} \cos m\lambda' + \delta\bar{S}_{nm} \sin m\lambda') \cdot \bar{P}_{nm}(\cos \nu') - \mathbf{f} \cdot \mathbf{p}$$

**Observation Types and Stochastic Model**

Condition equations "HRS from N(SCH) = NFEM(p)" as uncorrelated pseudo observations with small variances and high weights. (3.6k)

The approach (3.6a-k) means all in all a new method and standard (fig. 4.1, fig. 4.2), both for the over-determined boundary value problem (geoid-determination), and for the solution of a direct and online GPS/DGNSS-heighting (fig. 3.1, fig. 3. 2) by the use of DFHRS databases and the respective DFHRS correction (3.4b).

**3.3.2 DFHRS Software and Quality Control in DFHRS\_DB Computation**

The DFHRS approach (3.6a-k) has been realized in the software DFHBF©Jäger/Schneid/Schwarzer. There the mathematical model of the DFHRS approach (6a-i) is embedded in the quality control standards of a priori and a posteriori variance related tests (data snooping) and variance component estimations.

The covariance matrix of the resulting DFHRS\_DB parameters ( $\mathbf{p}, \Delta m$ ) can be used to compute and visualize the precision of the HRS and/or DFHRS correction surface (fig. 3.5).

An additional and valuable way to prove the “external accuracy” of the DFHRS\_DB is to compute a so-called “reproduction quality” and point-wise reproduction values [16], [17], [18].

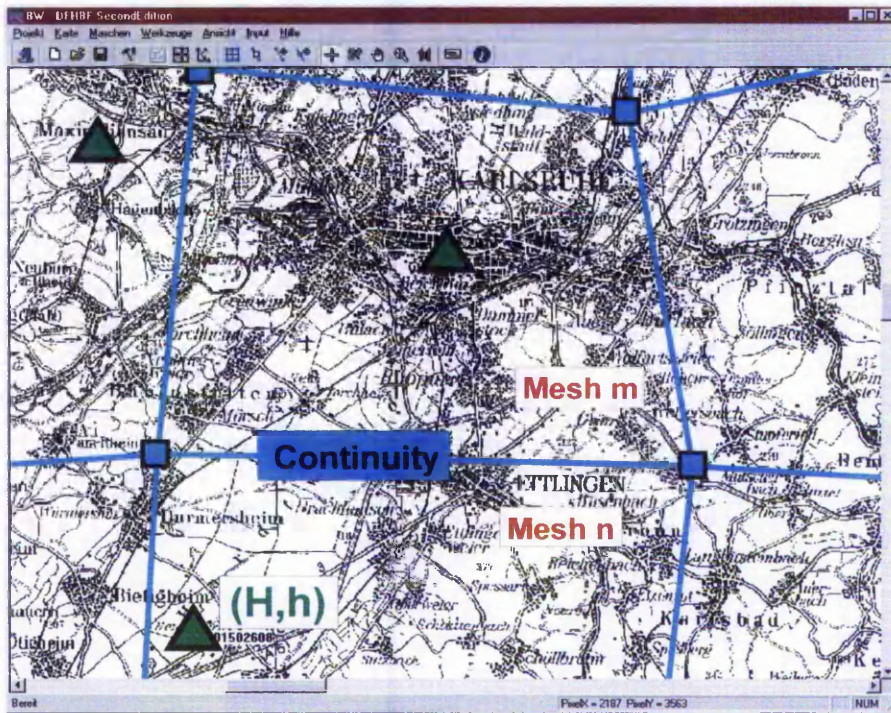


**Fig. 3.4:**

Screen shot of the DFHRS software. Continuity of the resulting HRS along the mesh borders of two general meshes  $m$  and  $n$  is provided by the continuity equations (3.6f). Identical points (3.1b) in green.

The “reproduction quality” and a number of  $n$  resulting “reproduction values  $\nabla H_i$ ” - all over the DFHRS area - are simply defined by the values of differences:

$$\nabla H_i = H_i - H_i(\text{DFHRS}_i (\hat{=} \text{without } H_i)), \text{ with} \quad (3.7a)$$

$$H_i(\text{DFHRS}_i) = h_i - \text{DFHRS}_i(\mathbf{p}, \Delta m \mid (B, L, h)_i)$$

For this quality proof no explicit “control measurements” are needed. We just have to compute successively the “DFHRS-height”  $H(B, L, h, \text{DFHRS}_i)$  of each of the  $n$  identical standard height points  $H_i$  from  $h_i$ , when using the individual data base  $\text{DFHRS}_i$ , where  $H_i$  was excluded from the respective  $\text{DFHRS\_DB}$  production (3.6a-k) (“new point”), which was then evaluated with the rest of the  $(n-1)$  points.

The “reproduction values”  $\nabla H_i$  are much more objective and informative than the pure least squares residuals  $v_i$  (3.6e). The reproduction values  $\nabla H_i$  are to be computed in the unique DFHRS production step (3.6a-k) of the DFHRS adjustment. The respective formula reads:

$$\nabla H_i = - \frac{v_{H_i}}{r_{H_i}} \quad (3.7b)$$

With  $v_{H_i}$  and  $r_{H_i}$  we describe the correction and the redundancy part of  $H_i$  in equation (3.6e).

The above reproduction values (3.7a, b) are however only directly interpretable as a quality measure, if they are applied to the part of the high accurate identical points (h,H).

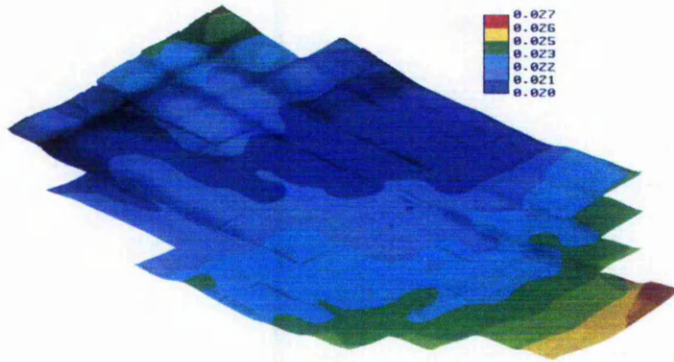


**Fig. 3.5:**

**Precision surface of the (2-3)cm DFHRS of the district Windhuk, Namibia [24], [25]**

A general measure for the precision of a DFHRS\_DB and the resulting DFHRS-correction (3.4b) is however the location-depended so-called “precision surface” (fig. 3.5), which can be evaluated from the covariance-matrix of the relevant DFHRS\_DB parameters ( $\mathbf{p}, \Delta m$ ).

### 3.4 DFHRS\_DB Contents and DB Access Software

The essential adjustment unknowns of the mathematical model (3.6a-k) and parameters of resulting DFHRS\_DB are  $\mathbf{p}$  and  $\Delta m$ . These represent the continuous model NFEM( $\mathbf{p}|x(B,L),y(B,L)$ ) of the HRS (fig. 3.1; fig. 3.2; fig. 3.7, fig. 3.8) and enable an additional scale correction  $\Delta m \cdot H$ . So these parameters provide the DFHRS correction DFHRS( $\mathbf{p}, \Delta m | B, L, h$ ) (3.4b) for an online or post-processed GNSS heighting.

Below the header (version name etc.), a DFHRS\_DB contains a second block with the mesh design (coordinates of the mesh nodal points, mesh number and topological description) and finally the block with the mesh-wise parameter sets  $\mathbf{p}$  and  $\Delta m$ .

## 3.5 Evaluation of the European HRS as part of the European Vertical Reference System (EVRS)

### 3.5.1 Preliminary Notes

An essential and very precious characteristic of the embedded FEM principle is, that any DFHRS\_DB and its reproduction quality (3.7a,b) respectively, which was achieved by using the DFHRS approach (3.6a-k) in a small area, is to be achieved - without loss of accuracy - in a corresponding large area scene, only provided that the density of the identical points ( $H, h$ ) and the quality of the geoid information  $N_G$  are kept!

So it is clear, that a 1<sup>st</sup> class of

▪ “<\_1cm\_DFHRs\_DB”

defined by a mean reproduction value  $\nabla H_i \leq 1\text{cm}$  (3.7a,b) over all precise and not rejected identical points (3.1b), (3.6a), (3.6e) and a respective “precision surface” (fig. 3.5) better than 1 cm - is to be computed by the DFHRS approach and the DFHRS software with a mesh size of 5 km, a density of about 50 identical points (H, h) per (100 km x 100 km) area, and a (30 - 40) km geoid-model “patch” size.

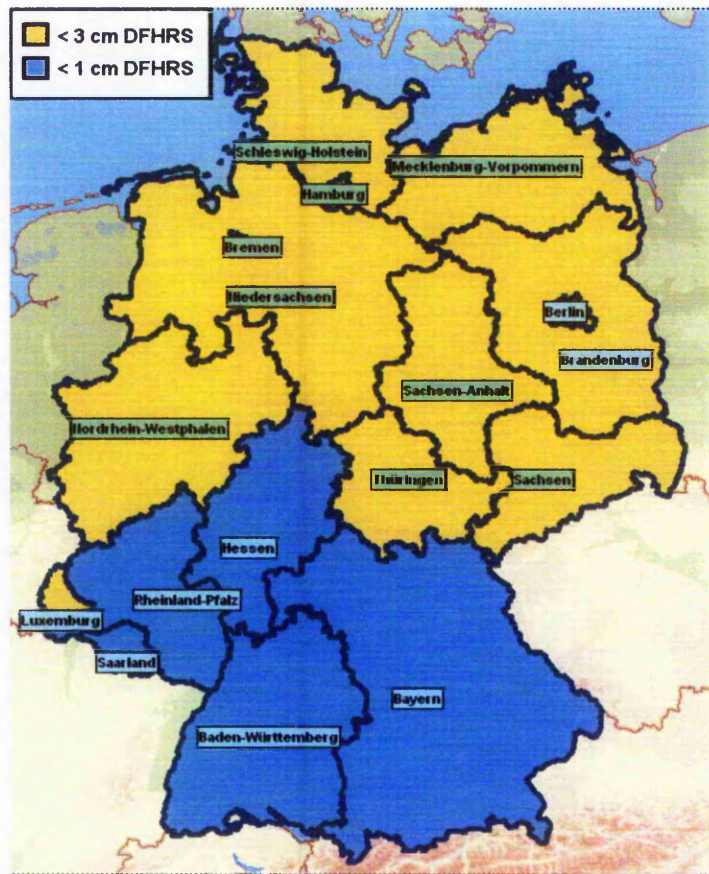


Fig. 3.6:

Blue: “<\_1cm\_DFHRs\_DB” in the German countries Saarland, Rheinland-Pfalz, Baden-Württemberg, Hessen and Bavaria. Yellow: „(1-3)\_cm\_DFHRs\_DB of Germany and Luxembourg.

Above these design parameters, the total size of the area does not play any role, so that this quality can be produced also e.g. in the European scale! Different “<\_1cm\_DFHRs\_DB”, which represent the present “high end” quality type, have already been computed [18]. They are available as official geo-data products of different German state land service departments (Saarland, Baden-Württemberg, Hessen, Rheinland-Pfalz, Bayern and Hannover district) [19], and they are used in SAPOS® and ascos® GNSS services in these parts of Germany (fig. 3.6).

Above these German countries presented in fig. 3.6, another “1\_cm\_DFHRSDB” was computed for the region of Tallinn, Estonia, and a (2-3)\_cm DFHRSDB was computed for the district of Windhoek, Namibia [24], [25] based on the EGM96 [13], (fig. 3.5).

The 2<sup>nd</sup> quality class of a

- “<\_3cm\_DFHRSDB”

is defined by mean reproduction value  $\nabla H_i \leq 3$  cm (3.7a,b) over all precise and not rejected identical points, and a respective “precision surface” (fig. 3.5) better than 3 cm. A “<\_3cm\_DFHRSDB Germany” was evaluated by a density of less than 10 identical points (H, h) per (100 km x 100 km) area, a mesh size of 10 km, and a polynomial degree n=3.

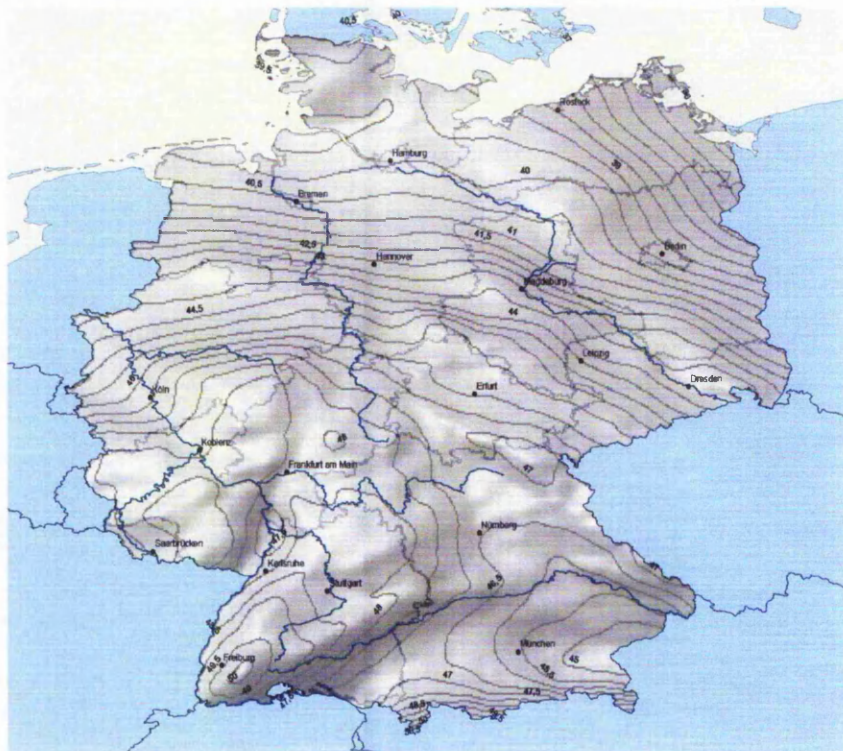


**Fig. 3.7:**

**Isolines of the HRS represented by the “3\_cm\_DFHRSDB Germany” for the European normal height system.**

The number of patches was 102 and the patch size was about 50 km. Fig. 3.7 above shows the isolines of the corresponding HRS (fig. 3.1; fig. 3.2) NFEM(p|B,L) of the “<\_3\_cm\_DFHRSDB Germany”. It is already related to the new European normal height system. For the former West Germany another “<\_3\_cm\_DFHRSDB Germany” related to the classical NN-height system was computed additionally. The “<\_3\_cm\_DFHRSDB” is applied for GNSS online and post-processing heighting by the users of SAPOS® and ascos® DGNSS services [26], [27], [28]. Above the “3\_cm\_DFHRSDB Germany” a “5\_cm\_DFHRSDB Valencia” (fig. 3.8) was computed for the district of Valencia, Spain [30]. A closed and continuous solution of a “(1-3)\_cm\_DFHRSDB Baltic States” (fig. 3.8) was computed for the Baltic States

Estonia, Latvia and Lithuania in the frame of a cooperation with the State Land Service of Latvia, Riga [29], and a “(2-3)\_cm DFHRS\_BD Windhoek” was computed for the district of Windhuk, Namibia [24], [25] based on the EGM96 [13], (fig. 3.5).

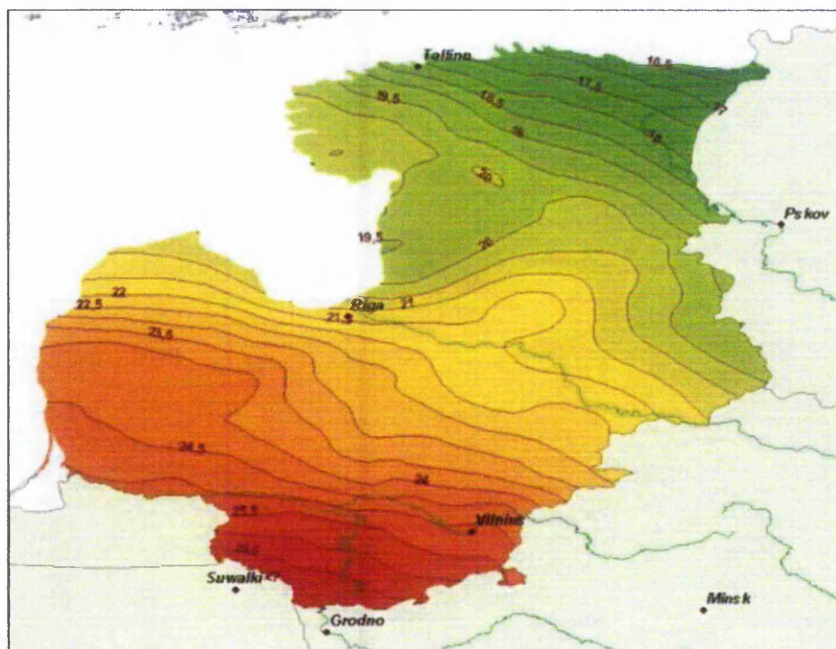


Fig. 3.8: Isolines of the HRS represented by the “(1-3)\_cm\_DFHRS\_DB Baltic States”

Figure 3.9 shows an overview on all DFHRS\_DB computed all over Europe including the different above mentioned DB for the different states.

The IAG Subcommission for Europe (EUREF) has met the decision to evaluate a continuous “<\_10\_cm European HRS”. This means an essential improvement of the HRS accuracy compared to the presently best European HRS, namely the EGG97 [1]. The EGG97 is continuous all over Europe, but it shows a high range of long-waved “weak-form” (chap. 1) deflections as shown in fig. 3.3. The respective EUREF Resolution No. 4, met on EUREF-Symposium at Dubrovnik, 2001 reads:

*The IAG Subcommission for Europe (EUREF) recognising the European Vertical GPS Reference Network (EUVN) with its GPS-derived ellipsoidal heights and levelled connections to UELN, – the definition of the European Vertical Reference System EVRS with its first realisation UELN 95/98, called EVRF2000, considering – this implicit pointwise realisation of a European geoid consistent with both ETRS89 and EVRS, – the existence of a large number of regional and local geoids in Europe, – the urgent need by the navigation community for a height reference surface, asks its Technical Working Group and the European Sub-commission of the IAG IGGC (International Gravity and Geoid Commission) to take all necessary steps to generate a European geoid model of decimetre accuracy consistent with ETRS89 and EVRS.*

The required

- “<\_1\_dm DFHRS\_DB Europe”

(fig. 3.9, green colour) was computed in a short-term project at the Karlsruhe University of Applied Sciences by using the DFHRS concept (3.6a-k) and the DFHRS software [31].

Besides the computation of DFHRS\_DB for Europe and the European states [32] a

- “< 5 cm DFHRS\_DB for Florida, USA” ,

was computed in 2005 in the frame of a master-thesis at the Karlsruhe University of Applied Sciences (fig. 3.10a,b). For further information it is referred to the DFHRS homepage [www.dfhbf.de](http://www.dfhbf.de) [27].

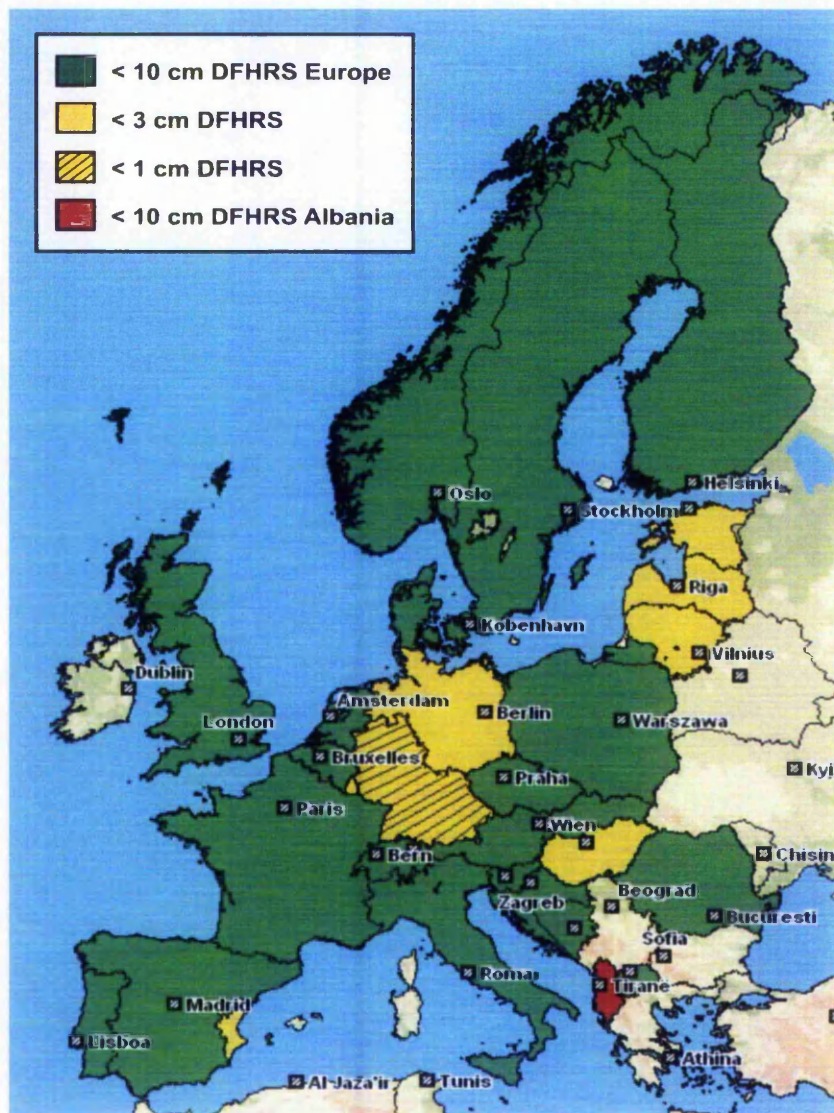


**Fig. 3.9:**

Overview on DFHRS\_DB computed all over Europe

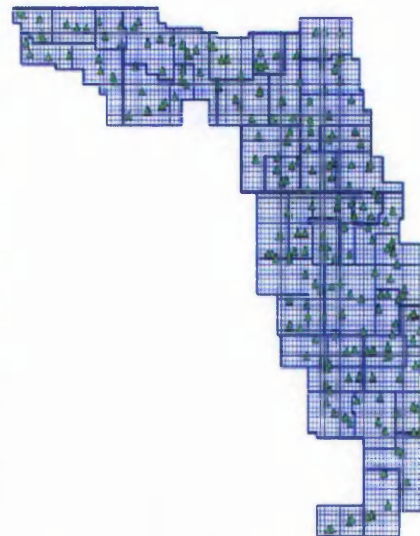


**Fig. 3.10 (a, b):**

USA map (right) and meshing (left) for the < 5 cm DHHRS DB Florida, which was computed in the frame of a master-thesis at the HS Karlsruhe.

#### 4 Standardisation of DFLBF/CoPaG and DFHRS Data Bases

For the implementation of a DFLBF/CoPaG and a DFRHS\_DB access respectively into existing software packages (fig. 4.1, fig. 4.2), DFLBF/CoPaG and DFHRS\_DB access software have been realized as DLL (Dynamics Link Library) [27], [28]. The DLL is also running in the so-called grid-factories of different GNSS-companies.



**GPS System 500. Mit V4.0 jetzt noch mehr Möglichkeiten!**

**Referenzliste und Verneuerung**  
 Nutzung von SAPORS- und ASCOS-Daten  
 Verschiedene Verneuerungslösungen  
 Vorfahrer- und ADJUSTMENTS-Liste

**Kataster- und Ingenieuranwendung**  
 Mittlungszeitpunkt ablesen oder generieren  
 Rechtsrechnerung im Feld  
 Höhenmodell „DFHRS“  
 Identifikation des nächstgelegenen Punktes

**Teach:**  
 Permanentes Integrity Monitoring der RTK-Lösung  
 RTK-Zuverlässigkeit besser als 99,99%  
 Kompatibel zu Trimble Formos (CMR/CS20)  
 Koordinatenrechner im Zeile-RECSO-Geodatenformat  
 Integrierte Höhenklärung für Gradientenlösung  
 Und viele weitere neue Features und Verbesserungen.  
 Mit der neuen Firmware V4.0 ist die System 500 einsatzbereit für jede Anwendung!

**Leica Geosystems**

**Fig. 4.1:**

DFLBF/CoPaG and DFHRS access realized in Trimble Survey Manager Software (left; [www.trimble.com](http://www.trimble.com)) and in the controller of Leica-geosystems (right; [www.leica-geosystems.com](http://www.leica-geosystems.com)).



**Fig. 4.2:**

**DFLBF/CoPaG and DFHRS access realized in the GNSS controller-software TopSURV of TOPCON ([www.topcon.de](http://www.topcon.de)) and by Thales Navigation ([www.thales-navigation.com](http://www.thales-navigation.com)).**

The growing acceptance and the different implementations of the DFLBF/CoPaG and DFHRS database standard into different GNSS equipments and software packages of the GNSS industry are shown in fig. 4.1 and fig. 4.2. That list of DFLBF/DFHBF database access-DLL implementation can be continued with respect to companies, that companies develop own surveying-software with GNSS- and totalstations-interfaces for electronic field-books, e.g. GeoSamos ([www.breining.de](http://www.breining.de)), Gart2000 ([www.allsat.de](http://www.allsat.de)). Besides the GNSS domain, the DB and DB access software is used and implemented into different GIS software packages. For details it is referred to [27] and [28].

Finally it is mentioned, that the DFHRS\_DB and DFLBF\_DB can be converted consistently and directly into the new RTCM 3.0 so- called transformation messages 1022-1028 [33].

## 5 References

- [1] Denker, H. and W. Torge (1997): The European Gravimetric Quasigeoid EGG97 – An IAG supported continental enterprise. In: Geodesy on the Move – Gravity Geoid, Geodynamics, and Antarctica. R. Forsberg, M. Feissel, R. Dietrich (eds.). IAG Symposium Proceedings Vol. 119, Springer, Berlin Heidelberg New York: 249-254.
- [2] Dinter, G. and M. Illner (2001): Höhenbestimmung mit GPS am Beispiel von Pilotprojekten aus Baden-Württemberg. DVW Schriftenreihe (41). Wittwer-Verlag. ISBN 3879192766. S. 88 - 110.
- [3] Dinter, G.; Illner, M. and R. Jäger (1997): A synergetic approach for the integration of GPS heights into standard height systems and for the quality control and refinement of geoid models. In: Veröffentlichungen der Internationalen Erdmessung der Bayerischen Akademie der Wissenschaften (57). IAG Subcommission for Europe Symposium EUREF, Ankara 1996. Beck'sche Verlagsbuchhandlung, München.
- [4] Jäger, R. (1988): Analyse und Optimierung geodätischer Netze nach spektralen Kriterien und mechanische Analogien. Deutsche Geodätische Kommission, Reihe C, No. 342, München.
- [5] Jäger, R. (1990a): Spectral Analysis of Relative and Supported Geodetic Levelling Networks due to Random and Systematic Errors. 'Precise Vertical Positioning'. Invited Paper to the Hannover Workshop of October 08-12, 1990.
- [6] Jäger, R. (1990b): Optimum Positions for GPS-points and Supporting Fix-points in Geodetic Networks. In: Ivan I. Mueller (ed.) International Association of Geodesy Symposia. Symposium No. 102:

- Global Positioning System: An Overview, Edinburgh/Scotland, Aug. 7-8, 1989. Convened and edited by Y. Bock and N. Leppard, Springer: 254-261.
- [7] Jäger, R. and H. Kaltenbach (1990): Spectral analysis and optimization of geodetic networks based on eigenvalues and eigenfunctions. *Manuscripta Geodetica* (15), Springer Verlag, S. 302-311.
- [8] Jäger, R. (1999): State of the art and present developments of a general approach for GPS-based height determination. In (M. Lilje, ed.): *Proceedings of the Symposium Geodesy and Surveying in the Future - The importances of Heights, March 15-17, 1999. Gävle/Schweden Reports in Geodesy and Geographical Informations Systems, LMV-Rapport 1999(3)*. Gävle, Schweden. ISSN 0280-5731: 161-174.
- [9] Jäger, R. und S. Kälber (2000): Konzepte und Softwareentwicklungen für aktuelle Aufgabenstellungen für GPS und Landesvermessung. DVW Mitteilungen, Landesverein Baden-Württemberg, 10/2000. ISSN 0940-2942.
- [10] Jäger, R. and S. Leinen (1992): Spectral Analysis of GPS-Networks and Processing Strategies due to Random and Systematic Errors. In: Defense Mapping Agency and Ohio State University (Eds.) *Proceedings of the Sixth International Symposium on Satellite Positioning, Columbus/Ohio (USA), 16-20 March*. Vol. (2), p. 530-539.
- [11] Jäger, R. and S. Schneid (2001a): GPS-Höhenbestimmung mittels Digitaler Finite-Elemente Höhenbezugsfläche (DFHBF) - das Online-Konzept für DGPS-Positionierungsdienste. XI. Internationale Geodätische Woche in Oberurg/Österreich, Februar 2001. *Institutsmittellungen, Heft Nr. 19, Institut für Geodäsie der Universität Innsbruck*: 195-200.
- [12] Jäger, R. and S. Schneid (2001b): Online and Postprocessed GPS-heighting based on the Concept of a Digital Height Reference Surface. *Proceedings, IAG Subcommission for Europe Symposium EUREF, Dubrovnik 2001*. Bundesamt für Kartographie und Geodäsie (BEK) (Eds.) Frankfurt.
- [13] Lemoine, F.; S. Kenyon; J. Factor; R. Trimmer; N. Pavlis; D. Chinn; M. Cox; S. Klosko; S. Luthcke; M. Torrence; Y. Wang; R. Williamson; E. Pavlis; R. Rapp and T. Olson (1998): The development of the Joint NASA GSFC and NIMA Geopotential Model EGM96. NASA Goddard Space Flight Center, Greenbelt, Maryland, 20771, USA.
- [14] Meichle, H. (2001): Digitale Finite Element Höhenbezugsfläche (DFHBF) für Baden-Württemberg. DVW Mitteilungen, Heft 2. DVW Landesverein Baden-Württemberg. ISSN 0940-2942. S. 23-31.
- [15] Schmitt, G. (1997): Spectral Analysis and Optimization of two dimensional networks. *Geomatics Research Australasia* (67): 47-64.
- [16] Schneid, S. (2002): Software Development and DFHRS computations for several countries. J. Kaminskis and R. Jäger (Eds.): *Proceedings of the 1st Common Baltic Symposium, GPS-Heighting based on the Concept of a Digital Height Reference Surface (DFHRS) and Related Topics - GPS-Heighting and Nationwide Permanent GPS Reference Systems*. Riga, June 11, 2001; Riga, Latvia.
- [17] Jäger, R. (2002): Online and Postprocessed GPS-heighting based on the Concept of a Digital Finite Element Height Reference Surface (DFHRS). J. Kaminskis and R. Jäger (Eds.): *Proceedings of the 1st Common Baltic Symposium, GPS-Heighting based on the Concept of a Digital Height Reference Surface (DFHRS) and Related Topics - GPS-Heighting and Nationwide Permanent GPS Reference Systems*. Riga, June 11, 2001; Riga, Latvia.
- [18] Jäger, R. and S. Schneid (2002): Passpunktfreie direkte Höhenbestimmung – ein Konzept für Positionierungsdienste wie SAPOS®. *Proceedings 4. SAPOS® Symposium, 21.-23. Mai 2002. Landesvermessung und Geobasisinformation Niedersachsen (LGN) (Hrsg.). LGN, Hannover*. S. 149-166.
- [19] Wirtschaftsministerium Baden-Württemberg (2002): Neue Projekte und Produkte mit Kunden- und Praxisbezug im Landesbetrieb Vermessung. Festschrift „50 Jahre Baden-Württemberg – 50 Jahre Hightech-Vermessungsland. 150 Jahre Badische Katastervermessung“. *Wirtschaftsministerium Baden-Württemberg (Hrsg.)*. S. 39-50.
- [20] Ihde, J. and W. Augath (2000): European Vertical Reference System (EVRS). In: *Veröffentlichungen der Internationalen Erdmessung der Bayerischen Akademie der Wissenschaften* (61). IAG Subcommission for Europe Symposium EUREF, Tromsø 2000. Beck'sche Verlagsbuchhandlung, München. S. 101 ff.
- [21] Jäger, R. (1998): Ein Konzept zur selektiven Höhenbestimmung für SAPOS. *Beitrag zum 1. SAPOS-Symposium. Hamburg 11./12. Mai 1998*. Arbeitsgemeinschaft der Vermessungsverwaltungen der Länder der Bundesrepublik Deutschland (Hrsg.), Amt für Geoinformation und Vermessung, Hamburg. S. 131-142.

- [22] Jäger, R. and S. Schneid (2002): Online and Postprocessed GPS-Heighting based on the Concept of a Digital Height Reference Surface. Contribution to IAG International Symposium on Vertical Reference Systems, February 2001, Cartagena, Columbia. In: H. Drewes, A.H. Dodson, L. P. Fortes, L. Sanches, P. Sandoval (Eds.). International Association of Geodesy Symposia. Symposium No. 124: 'Vertical Reference Systems', Cartagena, Colombia, February 20-23, 2001. Springer Verlag, Berlin, Heidelberg, NewYork. ISBN 3-540-43011-3. S. 203-208.
- [23] Jäger, R. und S. Schneid (2002): GNSS Online Heighting based on the Concept of a Digital Finite Element Height Reference Surface (DFHRS) and the Evaluation of the European HRS. Proceedings, GNSS 2002 Symposium. CD-ROM Publication The Nordic Institute of Navigation, Kopenhagen.
- [24] Jäger, R.; Volkman, W.E.; Niethammer, S.; Christmann, I. and A. Schick (1999): NAM97-Report – Calculation of a Zero Order ITRF based Reference Network for Namibia. Republic of Namibia, Ministry of Lands, Resettlement and Rehabilitation, Directorate of Survey and Mapping (ed.). 26 pages.
- [25] Jäger, R. (2003): Realisierung eines dreidimensionalen hochgenauen ITRF-Referenzsystems zur satelliten-gestützten GNSS-Positionierung in Namibia. (Fachhochschule Karlsruhe, Hrsg.): Forschungsberichte der Fachhochschule Karlsruhe – University of Applied Sciences.
- [26] Jäger, R., Kälber, S., Schneid, S. und S. Seiler (2003): Konzepte und Realisierungen von Datenbanken zur hochgenauen Transformation zwischen klassischen Landessystemen und ITRF/ETRS89 im aktuellen GIS- und GNSS-Anwendungsprofil. (Chesi/Weinold, Hrsg.): 12. Internationale Geodätische Woche Oberurgul, 2003 Wichmann Verlag, Heidelberg. ISBN 3-87907-401-1. S. 207-211.
- [27] Jäger, R. and S. Schneid (2002-2003): [www.dfhbf.de](http://www.dfhbf.de). DFHBF Homepage.
- [28] Seiler, S. (2000-2003): [www.ib-seiler.de](http://www.ib-seiler.de). IBS-Homepage.
- [29] Lace, L. and J. Kaminskis (2003): DGPS service / DGPS – heighting in Latvia and all Baltic States based on DFHRS. Proceedings 2<sup>nd</sup> Common Baltic Symposium “GPS-Heighting based on the Concept of a Digital Height Reference Surface (DFHRS) and Related Topics - GPS Heighting and National-wide Permanent GPS Reference Systems”, Riga 12-13 June 2003. State Land Service of Latvia, Riga.
- [30] Jäger, R., Schneid, S., Garcia Villa Major, L. Garrigues Talens, P. and L. Pascual Llorens (2003): Precise Plan Transformation of Classical National Networks to ITRF/ETRS89 and Precise Vertical Reference Surface Representation by Digital FEM Height Reference Surfaces (DFHRS) - Concepts, Databases, Present Developments and Realisation of a 5 cm DFHRS-Database District of Valencia, Spain. Symposium, IAG Subcommission for Europe, Toledo, June 2003. EUREF Publication No. 12. Verlag des Bundesamtes für Kartographie und Geodäsie, Frankfurt am Main.
- [31] Jäger, R. and S. Schneid (2004): A Decimetre Height Reference Surface (HRS) for the European Vertical Reference System (EVRS) based on the DFHRS Concept. Contribution to IAG Subcommission for Europe Symposium EUREF 2004, Bratislava, Slovakia. EUREF-Mitteilungen. Bundesamt für Kartographie und Geodäsie (BKG), Heft 14, Frankfurt. In Press.
- [32] Jäger, R.; Kälber, S.; Schneid, S.; Oelesi, G.; Nurce, B. and Cekrezi, I. (2004): Realization of CoPaG/DF-LBF and DFHRS Databases for Albania. Contribution to IAG Subcommission for Europe Symposium EUREF 2004, Bratislava, Slovakia. EUREF-Mitteilungen. Bundesamt für Kartographie und Geodäsie (BKG), Heft 14, Frankfurt. In Press.
- [33] Jäger, R. (2006): GNSS-basierte Höhen- und Lagebestimmung auf der Basis der neuen RTCM3.0-Transformationsmessage. Geomatik aktuell 2006. Seminar-Teilnehmer-Skript. Hochschule Karlsruhe – Technik und Wirtschaft, Karlsruhe.
- [34] Jäger, R. und S. Schneid (2006): DFHBF (Digitale FEM Höhenbezugsfläche) - Ein allgemeines Konzept zur Berechnung und Repräsentation hochpräziser Höhenbezugsflächen. Seminar-Teilnehmer-Skript. Hochschule Karlsruhe – Technik und Wirtschaft, Karlsruhe.
- [35] Thébault, E., J. Schott and M. Manda (2006): Revised spherical cap harmonic analysis (R-SCHA): Validation and properties, Journal of Geophysical Research (111).
- [36] Jäger, R. and S. Kälber (2003-2006): [www.geozilla.de](http://www.geozilla.de). GeoZilla Homepage.

Jäger, R.; Kälber, S.; Schneid, S; Qeleshi, G.; Nurce B. and Cekrezi, I. (2006):  
Realization of CoPaG/DFLBF and DFHRS Databases for Albania. Buletini i Shkencave  
Gjeologjike (2), 2004. Redaksia e Buletinit te Shkencave Gjeologjike. Tirana, Albania.

# Realization of CoPaG/DFLBF and DFHRS Databases for Albania<sup>1</sup>

<sup>1</sup>Reiner Jäger, <sup>2</sup>Simone Kälber, <sup>1</sup>Sascha Schneid,

<sup>3</sup>Gjergji Qeleshi, <sup>4</sup>Bilbil Nurce, <sup>5</sup>Ilir Cekrezi

<sup>1</sup> University of Applied Sciences (FH) Karlsruhe; Department of Vermessung und Geomatik and International Department of Geomatics (Msc), Moltkestrasse 30, D-76133 Karlsruhe, Germany; URL: [www.dfhbf.de](http://www.dfhbf.de). <sup>2</sup> D-76227 Karlsruhe, Germany. <sup>3</sup> Sherbimi Gjeologjik Shqiptar, Qendra Gjeofizike, Blloku Vasil Shanto, Tirana, Albania, Tel. and Fax: ++355 42 27360, Email: [qeleshi@yahoo.com](mailto:qeleshi@yahoo.com). <sup>4</sup> Universiteti Politeknik i Tiranës, Fakulteti i Inxhinjerisë së Nderimit, Departamenti i Gjeodezisë, Tirana, Albania; Tel./Fax: ++355 42 290 45, Email: [bnurce@hotmail.com](mailto:bnurce@hotmail.com). <sup>5</sup> Instituti Gjeografik Ushtarak i Shqipërisë, Tirana, Albania. Tel. and Fax: ++355 42 63427.

## 1. The Cooperation Project - Introduction and Motivation

As concerns the georeferencing of position data in modern databases, the availability of GNSS (GPS / GLONASS / GALILEO) related code- and phase-measurement DGNSS-correction data, which are provided in different ways by different GNSS positioning services in and outside for Europe, leads to the replacement of the classical geodetic reference frames by GNSS-consistent ITRF-based reference frames. So the transformation of the old plan position data  $(B, L)_{class}$ , related to the classical reference frames to the ITRF/ETRS89 datum  $(B, L)_{ITRF/ETRS89}$ , becomes urgently necessary all over Europe and the world respectively. Therefore transformation parameters  $d$  between the classical horizontal networks and position data  $(B, L)_{class}$  and the ITRF-/ETRS89-based reference frames  $(B, L)_{ITRF/ETRS89}$  become important. The transformation of  $(B, L)_{class}$  to  $(B, L)_{ITRF/ETRS89}$  is necessary to enable in future a direct horizontal positioning  $(B, L)_{ITRF/ETRS89}$  by GNSS services, and the inverse transformation  $(B, L)_{ITRF/ETRS89}$  to  $(B, L)_{class}$  is presently needed in GNSS-positioning in most states, as the classical reference frames  $(B, L)_{class}$  are still valid.

The capacity of a one-cm-positioning by GNSS services, such as SAPOS® and ascos® in Germany and others in Europe, like EUPOS in Eastern Europe, and all over the world, makes GNSS services also appropriate for a GNSS related heighting. Here the GNSS/GPS-based determination of physical (orthometric, normal, normal-orthometric) heights  $H$  requires the transformation of the ellipsoidal heights  $h_{ITRF/ETRS89}$  to the heights  $H$  of the respective physical height reference surface (HRS) set up by parameters  $p$ .

A sophisticated and general solution of these transformation problems has to include a data base concept for the provision of the corresponding transformation parameters  $d$  (plan) and  $p$  (height) for GIS, GNSS/GPS-navigation and -surveying purposes. The cooperation project between the authors of the contribution and representatives of the above institutions was concerned with the general solution concepts CoPaG/DFLBF (parameters  $d$ ) and DFHRS (parameters  $p$ ) and the computation of adequate databases for Albania. The concepts and the evaluation of the databases and the results of the computations are presented in the following.

## 2 Transformation Concepts and Databases

---

<sup>1</sup> Jäger, R.; Kälber, S.; Schneid, S.; Qeleshi, G.; Nurce, B. and Cekrezi, I. (2004): Realization of CoPaG/DFLBF and DFHRS Databases for Albania. Contribution to IAG Subcommission for Europe Symposium EUREF 2004, Bratislava, Slovakia. EUREF-Mitteilungen. Bundesamt für Kartographie und Geodäsie (BKG), Heft 14, Frankfurt. ISBN 3-89888-795-2. S: 333-339.

## 2.1 CoPaG – FEM-based Transformation Concept and Databases for Plan Positions

A sophisticated and general solution for the transformation in both directions between classical horizontal datum systems  $(B,L)_{class}$  and modern ITRF-related datum systems  $(B,L,h)$  is provided by the Finite Element Model (FEM) based so-called CoPaG-Concept (CoPaG = Continuous Patched Georeferencing). For details of the approach it is referred to *Jäger and Kälber (2000)* and *Jäger et al. (2003a,b)*. In analogy to the DFHRS concept (chap. 2.2), the whole area is subdivided into regular or irregular meshes (fig. 1, fig. 3). For each local FEM mesh the parameters  $d^i$  of a strict three-dimensional similarity transformation - namely three translations  $(u,v,w)$ , three rotations  $(\epsilon_x, \epsilon_y, \epsilon_z)$  and a scale difference  $\Delta m$  between the two concerned reference-systems - are determined by the observations of identical points within the  $i$ -th mesh in the adjustment of the CoPaG software (fig. 1, fig. 3). In this way the effect of so-called weak-shapes (*Jäger, 1988; Jäger, 1990; Jäger and Kaltenbach, 1990; Jäger and Leinen, 1992; Schmitt 1997; Jäger and Kälber 2000; Jäger et al., 2003a,b*) - which imply large quasi-systematic residuals and therefore require heuristic and more or less arbitrary interpolation methods for the case that one or few country-wide transformation parameter sets  $d^i$  are evaluated - is eliminated.

Additionally and as the second essential component of the CoPaG approach (*Jäger and Kälber, 2000; Jäger et al., 2003a,b; Jäger and Kälber 2004*) so-called "weak" continuity conditions  $C(d^k, d^l)$  are set up in the adjustment along the common borders of each pair of neighbouring meshes  $k$  and  $l$ . These continuity conditions provide that the total set of all transformation parameter sets  $d = [d^1, \dots, d^i, \dots, d^n]$  realizes a locally best-fitting, and simultaneously an all in all nation-wide continuous transformation. As classical horizontal network  $(B,L)_{class}$  are generally affected by the long-waved quasi-systematic errors of the above mentioned weak-shapes the transformation of any classical horizontal network  $(B,L)_{class}$ , to a new ITRF-datum with the CoPaG concept and databases implies automatically the geometric homogenization and improvement of the transformation result  $(B,L)_{ITRF/ETRS89}$  due to the correction of the long-waved shape-deflections, while the short-waved neighbourhood relation is preserved by the continuous similarity-transformation principle.

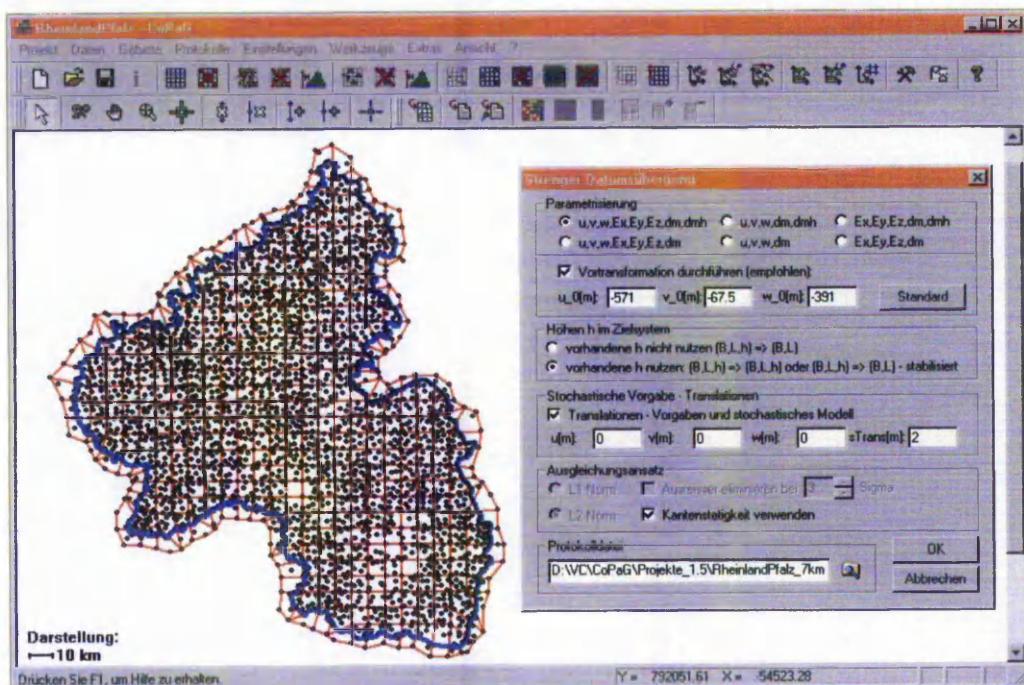


**Fig. 1:** Screenshot of the CoPaG software at the example of a CoPaG- or DFLBF-database computation of a country (accuracy  $< 1$  cm), which is subdivided into local meshes with local identical points for a best 3D fitting.

The mathematical model of the CoPaG-software is set up in such a way, that adequate precise height information for the precise identical points of a horizontal datum is obsolete and can be taken from free databases such as e.g. ETOPO. So the CoPaG approach is especially appropriate to involve also cadastral points for the determination of a locally best fitting transformation parameter set  $d$ . The continuous parameters  $d$  and the topological mesh information (fig. 1, fig. 3), as well as the remaining small residuals - which may then optionally be used for a residual interpolation based on the theory of stochastic processes - are also stored in a database.

So-called CoPaG databases are used for the strict and continuous 3D-transformation of classical plan networks to the ITRF/ETRS89 datum  $(B,L)_{ITRF/ETRS89}$  in the GIS domain, and so-called DFLBF databases are used in present GNSS/GPS-positioning, in order to transform online or in post processing ITRF/ETRS89 positions to the still existing classical plan networks  $(B,L)_{class}$ .

## 2.2 DFHRS – Concept for the FEM-based Computation of Continuous Height Reference Surfaces and DFHRS-databases for the Transformation of Ellipsoidal GNSS-heights $h$ to Physical Heights $H$

The capacity of a cm-positioning by GNSS/GPS-services, such as e.g. SAPOS® or ASCOS® in Germany (*AdV 1998-2004; Ruhrgas, 2000-2004*) and similar services in other European countries, is also appropriate for a precise GNSS/GPS based heighting. So the transition from the ellipsoidal GNSS-height  $h_{ITRF/ETRS89}$  to the height  $H = h - N$  of the relevant physical height system becomes necessary. With  $N(B,L)$  we describe the “geoid height”, or better the height of the height reference surface (HRS) over the ellipsoid at the position  $(B,L)$ .

The DFHRS (Digital-Finite-Element-Height-Reference-Surface) provides a general solution concept for the evaluation of a continuous parametric height references surface HRS by a surface  $N(p|B,L)$ , fig. 2 in any area size. The DFHRS approach was first discussed in *Jäger (1998)* and then continued as given in *Jäger and Schneid (2001; 2002a,b)*, *Jäger et al. (2003a,b)* and *Jäger and Schneid (2002-2004)*, *Jäger and Schneid (2004)*.

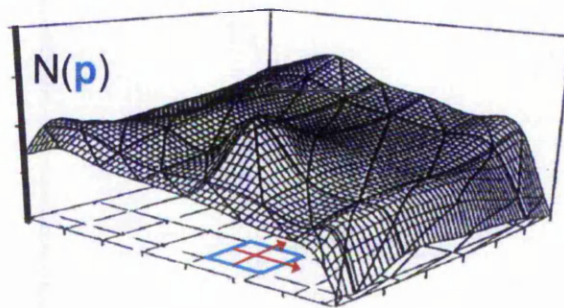


**Fig. 2:** HRS polynomials  $N(p)$  in single meshes and as part of a continuous HRS in an arbitrary large area.

Like the CoPaG concept (chap. 2.1) the DFHRS concept is also

based on the core of a FEM. Here the height reference surface (HRS) is computed and modeled as a continuous surface  $N(p|B,L)$ , which is by  $p=[p^1, \dots, p^i, \dots, p^n]$  represented by the individual polynomial parameters  $p^i$  as carrier functions over the FEM grid. In the mathematical sense, the mesh parameters  $p^i$  are to be interpreted as the coefficients of a local Taylor-series expansion of the HRS. In analogy to the CoPaG concept (chap. 2.1) the FEM meshes may cover all in all any arbitrary large area, and so-called weak continuity conditions  $C(p^k, p^l)$  are set up along the borders of neighbouring meshes  $k$  and  $l$ . This leads to the continuous parametric

model  $N(p|B,L)$  for the HRS. Due to the FEM-based approach (fig. 2) the HRS model  $N(p|B,L)$  is often called NFEM( $p|B,L$ ).

For the details of the mathematical model of DFHRS adjustment approach and the DFHRS software it is referred to *Jäger and Schneid (2002a,b)* and *Jäger and Schneid (2004)*. Heights  $N$  from existing geoid-models, vertical deflections ( $\xi, \eta$ ), gravity anomalies  $\Delta g$  and identical points ( $B, L, h; H$ ) can be used as observations in the least squares computation of the DFHRS approach to derive the DFHRS-parameters  $p$  and  $\Delta m$ . So the DFHRS concept comprises a new strict mathematical model of an over-determined "geoid-computation" with a simultaneous "geoid-fitting". Comparable and adequate to the harmonic series representation, the HRS is continuously represented by NFEM( $p|B,L$ ) over the total area (fig. 2), while the local carrier function  $p$  and the FEM concept enable a more flexible local fit. With  $\Delta m$  a regional scale difference between  $h$  and  $H$ , which is introduced in case of significance, is described. Any number of geoid height or vertical deflections models may be introduced simultaneously, and these models may be parted into different "patches" with individual datum-parameters in order to reduce the effect of existing medium- and long-waved systematic errors (*Jäger and Kälber, 2000; Jäger et al., 2003a,b*). The resulting DFHRS parameters  $p$  are set up in a so-called DFHRS database. As concerns available databases in and outside Europe it is referred to overviews given at the homepages *Jäger and Schneid (2002-2004)* and *Seiler (2000-2004)*, as well as to further individual reports such as *Lace and Kaminskis (2003)*, *Jäger (2003)* and *Jäger et al. (2003b)*.

DFHRS databases allow a GNSS height positioning by a direct online conversion of ellipsoidal - heights  $h$  into standard heights  $H$  by the so-called DFHRS-correction, which transforms by  $H=h-DFHRS(p,\Delta m|B,L,h)$  ellipsoidal GNSS heights  $h_{ITRF/ETRS89}$  into standard heights  $H$ . The DFHRS-correction  $DFHRS(p,\Delta m|B,L,h)$  consists of the above mentioned FEM-based HRS surface NFEM( $p|B,L,h$ ) - the so-called "geoid-part" as a function of ( $B,L$ ) - and an additional "scale part"  $\Delta m \cdot h$  as function of  $h$ .

### 2.3 Database Standardisation

Both the CoPaG/DFLBF and the DFHRS databases have become a standard and are broadly accepted and used by the GIS and GNSS/GPS hard- and software manufacturers and by the GIS-and GNSS/GPS-users (*Jäger and Schneid (2002-2004); Jäger and Kälber (2004); Seiler (2000-2004)*). The concepts and databases have also become official geodata products in many states and GNSS-services (*Wirtschaftsministerium Baden-Württemberg (2002)*, *Adv (1998-2004)*, *Ruhrgas 2000-2004*).

A direct access and transformation using the databases is realized by respective DLLs' (Dynamic Link Libraries), which can be implemented into any existing software environment. The databases are also appropriate for classical so-called grid-files, e.g. for a use in GNSS/GPS-controllers.

Both concepts are last not least prepared to provide transformation parameters for the new upcoming RTCM-3.0 standard. So all in all the concepts and database are in many ways open for a use in online GNSS/GPS-positioning services, such as SAPOS® or AscOS® in Germany, and in all other upcoming GNSS-services.

## 3. Albanian Reference Frames and Data for CoPaG/DFLBF and DFHRS Database Computation

The state of Albania is situated between latitude 39°38' - 42°39' North and longitude 19°16' - 42°04' East and extends over an area of 28.748 km<sup>2</sup> (land 27,398 km<sup>2</sup>; water 1,350 km<sup>2</sup>). The terrain is mostly mountainous (highest point 2753 m) and has hills with small plains along the coast. Albania is affected from natural hazards such as destructive earthquakes, tsunamis and draughts.

The present national horizontal geodetic network and datum, ALB87, is referring to the Krasowski ellipsoid and the Gauß-Krüger projection. Five common points were used to transform by a 7PT similarity transformation further 16 points  $(X, Y, Z)_{ITRF}$  from ITRF96.1998.0 to ETRS89 (Nurce, 2000). So a total number of 21 (identical points were available with respect to the horizontal datum  $(B, L)_{ALB87}$  and ITRF-based positions  $(B, L, h)_{ITRF}$  in the ITRF96.1988.0 and the ETRS89 datum, respectively (fig. 3), and for the CoPaG/DFLBF databases computation (chap. 4.1; fig. 3).

The vertical datum of Albania is referring to MSL of the Adriatic Sea, and the datum point is situated at the tide-gauge station Durresi. The 1<sup>st</sup> order levelling network of Albania consists of 4 loops with a total length of 4200 km with attached 2<sup>nd</sup> and 3<sup>rd</sup> order networks (Qeleshi, 2003-04). The type of the physical height system H are so-called normal-orthometric heights (NN-heights), where the gravity measurements along the levelling lines are replaced by the values of a normal gravity field (Qeleshi, 2003-2004). A number of 17 identical points with  $(B, L, h)_{ETRS89}$  and heights H was presently available for the DFRHS database computation (chap. 4.2; fig. 5 and fig. 6). Many of these are part of the above mentioned set of 21 identical points of the horizontal datum.

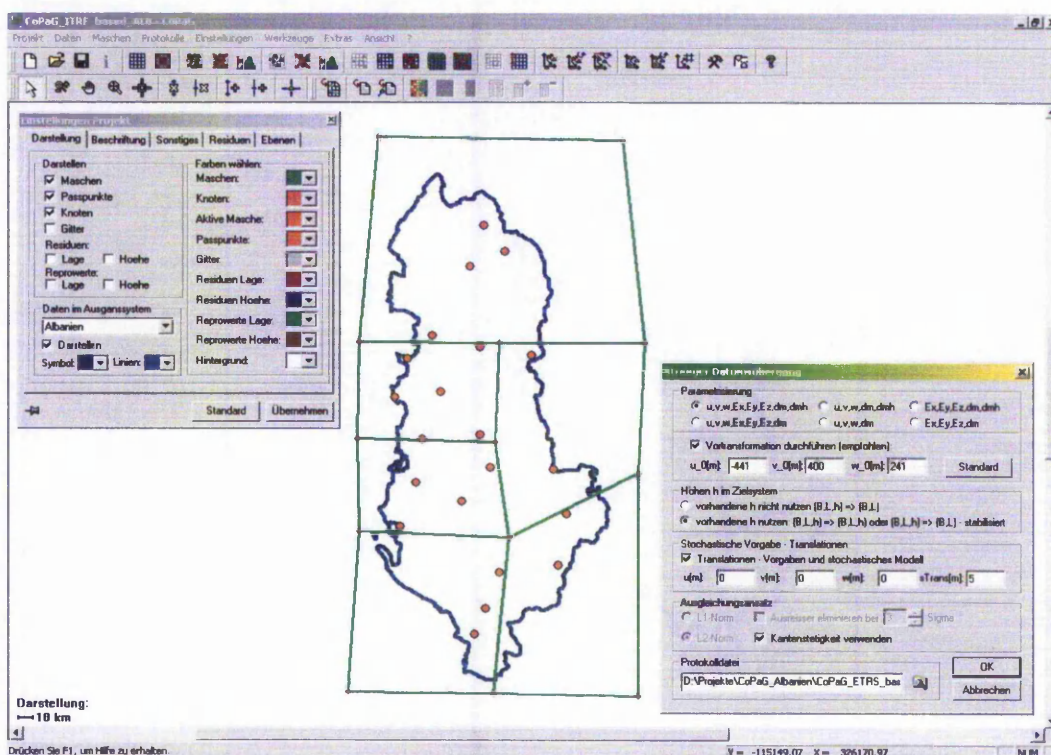


**Fig. 3:** Screenshot of the CoPaG software with the FEM meshing and the identical points used for the CoPaG database and DFLBF database computations for Albania.

## 4. Computations and Results

### 4.1 CoPaG/DFLBF Database Computations and Results for Albania

According to the presently available data (chap. 3) a total number 21 of identical points  $(B,L)_{ALB87}$  most with heights  $H$ , and  $(B,L,h)_{ITRF}$  were available as observations in the CoPaG approach (chap. 2.1) for the computation of the present CoPaG and DFLBF databases.

Two CoPaG databases and two DFLBF databases were computed. This enables both a transformation between  $ALB87 \leftrightarrow ETRS89$  by a respective first CoPaG/DFLBF database set, and a transformation between  $ALB87 \leftrightarrow ITRF96.1998.0$  by a second respective CoPaG/DFLBF database set.

The fig. 3 above shows a screenshot of the CoPaG software and gives at the same time an overview over the FEM mesh design and the identical points, which were defined and used for the computation of the above mentioned CoPaG and DFLBF databases.

Fig. 4 shows the accuracy surface, which is to be computed in dependence of the location  $(B,L)$  by means of the covariance matrix  $C_d$  resulting from the adjustment with the CoPaG software, which includes all standards of statistical testing and variance component estimation.

The adjusted transformation parameters  $d$ , which set up the present CoPaG and DFLBF databases for Albania imply an accuracy in between (2-5) cm all over the country (fig. 4).

This accuracy was confirmed independently by the transformation of one further identical point, which was not used for the computation of the CoPaG and DFLBF databases (Qeleshi, 2003-2004).

Although the accuracy of the presently computed CoPaG and DFLBF databases is already very satisfactory, the introduction of further identical points, will allow smaller meshes and a further increase of the accuracy and reliability of the database parameters  $d$ .

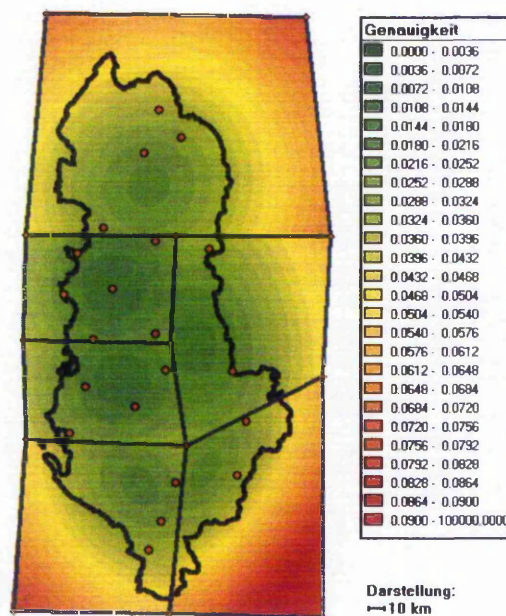


Fig. 4: Accuracy surface of the two CoPaG and the two DFLBF databases for Albania

## 4.2 DFHRS Database Computations and Results for Albania

The DFHRS database was computed with respect to a ETRS89-georeferencing using a number of 17 identical points  $((B, L, h)_{ETRS89}; H)$  as first group of observations (fig. 5; fig. 6). Additionally EGG97 Q-geoid height and vertical deflection observations were introduced. Fig. 5 shows the meshing and patching design, which was used for the computation of the DFHRS database for Albania. The meshsize (thin lines, fig. 5) of 5 km enables the representation of the continuous HRS Finite Element Model  $NFEM(p|B,L)$  with an approximation of error less than 5 mm (Jäger and Schneid, 2004). So the chosen mesh design (fig. 5) can be kept for further computations, and only the patch-design (thick lines, fig. 5) has to be modified with respect to achieve smaller patches and reduce the effect of the above mentioned "weak-shapes", which are also existing e.g. for geoid models (Jäger and Kälber, 2000), as soon further observation data becomes available.

According to the adjustment results of the DFHRS software the accuracy of the HRS as represented by the parameters ( $p$  and  $\Delta m$ ) of the computed DFHRS database for Albania is estimated to be better than 10 cm. Presently the patch-size reaches up to 80 km, so that long-waved systematic errors (weak shapes) in the Q-geoid height and vertical deflections observation groups still partly remain. An improvement to the accuracy level of a (3 - 5) cm DFHRS database can be achieved by introducing a number of at least 20 further identical points ( $(B, L, h)_{ETRS89}$ ;  $H$ ) and/or other additional data, such as e.g. gravity data  $\Delta g$  or vertical deflection data  $(\xi, \eta)$  observed e.g. with modern zenith cameras.

Fig. 6 shows the isolines of the HRS represented by the present DFHRS database for Albania.

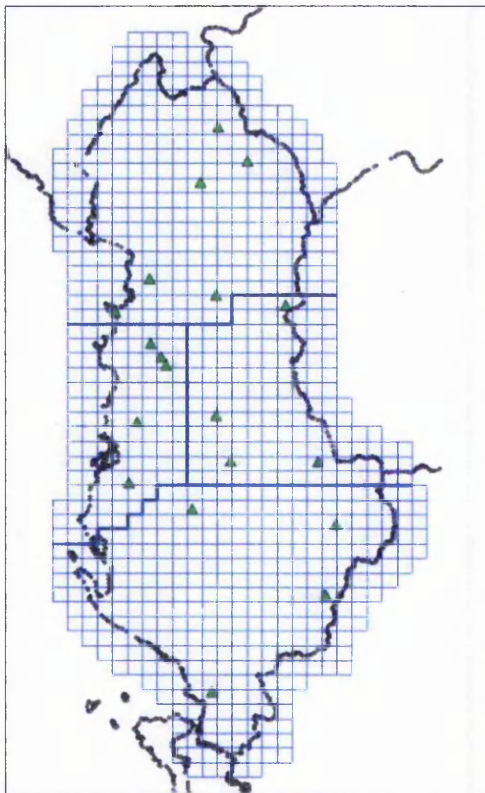


**Fig. 5:** FEM mesh-design with 10 km meshsize for the computation of the DFHRS database for Albania

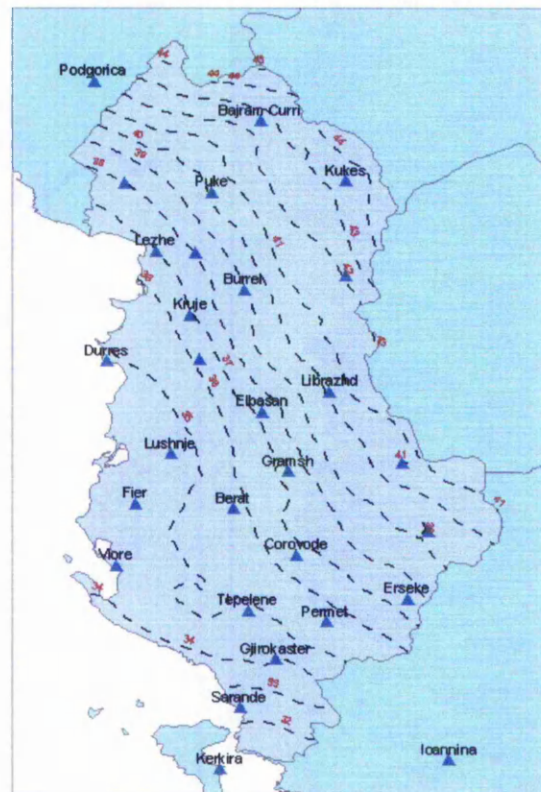


**Fig. 6:** Isoline plot of the HRS represented by the parameters  $p$  of the DFHRS database for Albania

## 5. Conclusions

The computed CoPaG databases enable the transformation of the classical ALB87 geodetic networks, cadastral databases and any ALB87 object position to ITRF96.1988.0 or to ETRS89 (the official European datum accepted by EU Commission) with a nation-wide mean accuracy of 3 cm. So the CoPaG databases can be used for setting up a new GNSS/GPS consistent and ITRF/ETRS89-related reference frame for Albania. This would enable a transformation-free absolute horizontal positioning in a respective GNSS/GPS-reference station network.

If the classical datum ALB87 is kept, the computed DFLBF databases enable the direct transformation of GNSS/GPS-positions referring to ITRF96.1988.0, or better to the EU-official datum ETRS89, to the classical datum ALB87 in an Albanian GNSS/GPS-service.

The computed DFHRS database enables a nation-wide GNSS/GPS height-positioning with an estimated accuracy of presently less than 10 cm.

The CoPaG/DFLBF and DFHRS database standard (chap. 2.3) can be used in all present GPS/GNSS equipments and they are compatible with the future RTCM-3.0 transformation parameter messages standard.

So Albania is best prepared for the installation of a Albanian GNSS/GPS positioning service with the same spectrum of applications and users like e.g. SAPOS® (AdV, 1998-2004) or ASCOS® (Ruhrgas, 2000-2004) in Germany.

## 6. References

- Jäger, R. (1988): Analyse und Optimierung geodätischer Netze nach spektralen Kriterien und mechanische Analogien. Deutsche Geodätische Kommission, Reihe C, Nr. 342, München.
- Jäger, R. (1990): Spectral Analysis of Relative and Supported Geodetic Levelling Networks due to Random and Systematic Errors. 'Precise Vertical Positioning'. Invited Paper to the Hannover Workshop of October 08-12, 1990.
- Jäger, R. and H. Kaltenbach (1990): Spectral analysis and optimization of geodetic networks based on eigenvalues and eigenfunctions. Manuscripta Geodetica (15), Springer Verlag. S. 302-311.
- Jäger, R. und S. Kälber (2000): Konzepte und Softwareentwicklungen für aktuelle Aufgabenstellungen für GPS und Landesvermessung. DVW Mitteilungen, Landesverein Baden-Württemberg. 10/2000. ISSN 0940-2942.
- Jäger, R. and S. Leinen (1992): Spectral Analysis of GPS-Networks and Processing Strategies due to Random and Systematic Errors. In: Defense Mapping Agency and Ohio State University (Eds.) Proceedings of the Sixth International Symposium on Satellite Positioning, Columbus/Ohio (USA), 16-20 March. Vol. (2), p. 530-539.
- Jäger, R. (1998): Ein Konzept zur selektiven Höhenbestimmung für SAPOS. Beitrag zum 1. SAPOS-Symposium. Hamburg 11./12. Mai 1998. Arbeitsgemeinschaft der Vermessungsverwaltungen der Länder der Bundesrepublik Deutschland (Hrsg.), Amt für Geoinformation und Vermessung, Hamburg. S. 131-142.
- Jäger, R. and S. Schneid (2001): Online and Postprocessed GPS-heighting based on the Concept of a Digital Height Reference Surface. Proceedings, IAG Subcommission for Europe Symposium EUREF, Dubrovnik 2001. Bundesamt für Kartographie und Geodäsie (BEK) (Eds.) Frankfurt.
- Jäger, R. and S. Schneid (2002a): Passpunktfreie direkte Höhenbestimmung – ein Konzept für Positionierungsdienste wie SAPOS®. Proceedings 4. SAPOS® Symposium, 21.-23. Mai 2002. Landesvermessung und Geobasisinformation Niedersachsen (LGN) (Hrsg.). LGN, Hannover. S. 149-166.
- Jäger, R. and S. Schneid (2002b): Online and Postprocessed GPS-Heighting based on the Concept of a Digital Height Reference Surface. Contribution to the IAG International Symposium on Vertical Reference Systems in Cartagena, Columbia. In: H. Drewes, A.H. Dodson, L. P. Fortes, L. Sanches, P. Sandoval (Eds.). International Association of Geodesy Symposium No. 124: 'Vertical Reference Systems', Cartagena, Colombia, February 20-23, 2001. Springer Verlag, Berlin, Heidelberg, NewYork. ISBN 3-540-43011-3. S. 203-208.
- Jäger, R. (2003): Realisierung eines dreidimensionalen hochgenauen ITRF-Referenzsystems zur satellitengestützten GNSS-Positionierung in Namibia. (Fachhochschule Karlsruhe, Hrsg.): Forschungsberichte der Fachhochschule Karlsruhe – University of Applied Sciences.
- Jäger, R., Kälber, S., Schneid, S. und S. Seiler (2003a): Konzepte und Realisierungen von Datenbanken zur hochgenauen Transformation zwischen klassischen Landessystemen und ITRF/ETRS89 im aktuellen GIS- und GNSS-Anwendungsprofil. (Chesi/Weinold, Hrsg.): 12. Internationale Geodätische Woche Obergurgl, 2003 Wichmann Verlag, Heidelberg. ISBN 3-87907-401-1. S. 207-211.

- Jäger, R., Kälber, S., Schneid, S., Villamaior, L., Talens, P. and P. Lourdes (2003b): Precise Plan Transformation of Classical National Networks to ITRF/ETRS89 and Precise Vertical Reference Surface Representation by Digital FEM Height Reference Surfaces (DFHRS) - Concepts, Databases, Present Developments and Realisation of a 5 cm DFHRS-Database for the District of Valencia, Spain. Contribution to IAG Subcommittee for Europe Symposium EUREF 2003, Toledo, Spain. EUREF-Mitteilungen. Bundesamt für Kartographie und Geodäsie (BKG), Heft 12, Frankfurt. In press.
- Jäger, R. and S. Schneid (2002-2004): DFHBF Homepage: [www.dfhbf.de](http://www.dfhbf.de).
- Jäger, R. and S. Kälber (2004): GEOZILLA-Homepage: [www.geozilla.de](http://www.geozilla.de).
- Jäger, R. and S. Schneid (2004): A decimetre Height Reference Surface (HRS) for the European Vertical Reference System (EVRS) based on the DFHRS concept. Contribution to IAG Subcommittee for Europe Symposium EUREF 2004, Bratislava, Slovakia. EUREF-Mitteilungen. Bundesamt für Kartographie und Geodäsie (BKG), Heft 13, Frankfurt. Included in this book.
- Lace, L. and J. Kaminskis (2003): DGPS service / DGPS – heighting in Latvia and all Baltic States based on DFHRS. Proceedings 2nd Common Baltic Symposium "GPS-Heighting based on the Concept of a Digital Height Reference Surface (DFHRS) and Related Topics - GPS Heighting and National-wide Permanent GPS Reference Systems", Riga 12-13 June 2003. State Land Service of Latvia, Riga.
- Nurce, B. (2000):The New Albanian Network and GPS measurement campaigns. Veröffentlichungen der Bayerischen Kommission für die Internationale Erdmessung. Heft Nr. 61, München p. 238-241.
- Qeleshi, G. (2003-2004): Scientific Communications Qeleshi-Jäger.
- RuhrGas (2002-2004): ASCOS Satellite Positioning Service Homepage of the RuhrGas AG, Essen, Germany. [www.ascos.de](http://www.ascos.de).
- AdV (1998-2004): SAPOS Satellite Positioning Service Homepage of the Arbeitsgemeinschaft der Vermessungsverwaltungen (AdV), Germany. [www.sapos.de](http://www.sapos.de).
- Schmitt, G. (1997): Spectral Analysis and Optimization of two dimensional networks. Geomatics Research Australasia (67): 47-64.
- Seiler, S. (2000-2004): IBS-Homepage: [www.ib-seiler.de](http://www.ib-seiler.de).
- Wirtschaftsministerium Baden-Württemberg (2002): Neue Projekte und Produkte mit Kunden- und Praxisbezug im Landesbetrieb Vermessung. Festschrift „50 Jahre Baden-Württemberg – 50 Jahre Hightech-Vermessungsland. 150 Jahre Badische Katastervermessung“. Wirtschaftsministerium Baden-Württemberg (Hrsg.). S. 39-50.

Jäger, R. and S. Schneid (2004):

A Decimetre Height Reference Surface (HRS) for the European Vertical Reference System (EVRS) based on the DFHRS Concept. Contribution to IAG Subcommission for Europe Symposium EUREF 2004, Bratislava, Slovakia. EUREF-Mitteilungen. Bundesamt für Kartographie und Geodäsie (BKG), Heft 14, Frankfurt. ISBN 3-89888-795-2. S. 194-202.

# **A Decimetre Height Reference Surface (HRS) for the European Vertical Reference System (EVRS) based on the DFHRS Concept**

Reiner Jäger and Sascha Schneid  
Fachhochschule Karlsruhe - University of Applied Sciences  
Department of Geoinformation  
Moltkestrasse 30, D-76133 Karlsruhe  
[www.dfhbf.de](http://www.dfhbf.de)

## **1. Introduction**

The recent developments of nation-wide DGNSS-Services (Differential Global Navigation Satellite System) in Europe (e.g. SAPOS, ascos, SwiPos, SwePos and EUPOS) enable online GNSS positioning with an accuracy in the centimetre range. In recent years, there has been great progress with the development of GNSS equipment and related technical DGNSS network standards for ambiguity fixing, virtual reference stations and area correction parameters etc., so that real-time positioning can be very productive and accurate.

For plan positioning, GNSS may be applied, as the new reference systems are realised in the ITRF/ETRS89. After transforming the old national systems to this new datum, the benefits of this modern positioning technique will be fully applicable.

In contrast to the plan transformation problem, GNSS height transformation involves a physical element. The GNSS-based ellipsoidal height,  $h$ , refers to an ITRF-based datum definition (e.g. ETRS89 in Europe) with the WGS84 or the GRS80 ellipsoid as reference surface, while the standard height,  $H$ , refers to a physically defined Height Reference Surface (HRS). Therefore, a transformation of the ellipsoidal GNSS height,  $h$ , to the standard height,  $H$ , is needed.

In theory the new European height system of normal heights refers to the quasi-geoid. However, in practice, the direct use of gravimetric quasigeoid models like the European Gravimetric Geoid 1997 (EGG97) for a precise online GNSS – levelling is however not possible in an adequate accuracy. One reason is, that gravimetric quasigeoid models have their own datum, different from ETRS89. Further, they suffer from long- and medium-waved systematic effects, so-called weak shapes.

To derive a model of a HRS, that is compatible to the high accuracy of the GNSS-based positions, classical geoid models have to be fitted (“geoid-fitting”) to the reference of precise discrete classical HRS. The HRS reference  $N=h-H$  is set up by the heights  $H$  of classical terrestrial height network points with known ITRF-positions ( $B, L, h$ ). So the first step of the establishment of the European Vertical Reference System (EVRS) consistent in the readjustment of the European geodetic height network UELN95/98 and its point-wise link ( $B, L, h$ ) to the ETRS89 datum. This point-wise discrete realisation ( $H, B, L, h$ ) of a European HRS is now to be taken as a reference for any continuous HRS model, which is derived from related observations. These are mainly gravity anomalies,  $\Delta g$ , and deflections from the vertical,  $\xi$  and  $\eta$ . Another possible type of observation are quasigeoid heights,  $N_{\text{grav}}$ , derived from regional or local gravimetric quasigeoid models.

The concept of the Digital FEM (Finite Element Method) Height Reference Surface (DFHRS) enables the strict adjustment of all available observation types related to the HRS. The

resulting DFHRS data-base provides a continuous FEM-based HRS and thereby a correction DFHRS(B, L, h) to transform a GPS-height, h, into a standard height, H, in a direct mode.

Applying the concept of the DFHRS, a European Height Reference Surface was determined by using the EVRF2000 points (H, B, L, h). Some densification points in Austria, Estonia, Germany, Latvia, Lithuania, and Switzerland, were used to proof the quality of the resulting HRS. As gravity based data, quasigeoid heights  $N_{\text{grav}}$ , as well as vertical deflections,  $\xi$  and  $\eta$ , derived from the EGG97 were introduced.

In the following sections, the concept of the Digital FEM Height Reference Surface is explained, and the computation of the DFHRS database for Europe is treated in details.

## 2. The DFHRS concept

Following the concept of the FEM (Finite Element Method), in a first step, the area of interest is subdivided into a grid of FEM meshes (Fig.1). Within each mesh, the HRS is approximated by local 2-D Taylor series, derived at the centre-point of each mesh. The accuracy of the final DFHRS depends mainly on the representation quality of the HRS by this Taylor series. Therefore, size of the meshes (length of the borders) and the degree n of the series expansion are important design parameters to determine DFHRS databases in a given quality (see table 2). For a degree  $n=3$ , the expansion of the Taylor series at the centre point  $P_0(Y_0, X_0)$  leads to the bivariate polynomial

$$\begin{aligned} N_{FEM}(X, Y) &= \sum_{i=0}^3 \left( \left( \frac{\partial}{\partial X} \Delta X + \frac{\partial}{\partial Y} \Delta Y \right)^i \cdot \frac{N_{FEM}(X, Y)}{i!} \right)_{P_0} & (2.1a) \\ &= \sum_{i=0}^3 \sum_{j=0}^{3-i} a_{ij} \cdot \Delta X^i \Delta Y^j = \mathbf{f}^T \cdot \mathbf{p} \\ &= N_{FEM}(X, Y | \mathbf{p}) \end{aligned}$$

With

$$\begin{aligned} \Delta X &= X - X_0 & (2.1b) \\ \Delta Y &= Y - Y_0; \text{ where } X = X(B, L) \text{ and } Y = Y(B, L) \\ \mathbf{f} &= [1 \quad \Delta X \quad \Delta Y \quad \Delta X^2 \quad \dots] \\ \mathbf{p}^T &= [a_{00} \quad a_{01} \quad a_{10} \quad a_{02} \quad \dots] \end{aligned}$$

Related investigations showed, that a meshsize up to 5 km x 5 km is representing the HRS in a quality of less than 5 millimetres. To produce a quality of 2-3 centimetres, which is well balanced with the positioning or heighting quality respectively, in GNSS-Networks, a mesh-size of 10 km x 10 km is appropriate (see also table 2).

To solve the unknown FEM parameters  $\mathbf{p}$ , any HRS related observation, such as identical points (h and H), deflections from the vertical ( $\xi$  and  $\eta$ ) and gravimetric (quasi-)geoid heights  $N_{\text{grav}}$  may be introduced into a statically controlled least-squares adjustment. The respective system of observation equations reads:

$$H + v = H \quad (2.2)$$

$$h + v = H + \Delta m(X, Y) \cdot h + N_{FEM}(X, Y | \mathbf{p}) \quad (2.3)$$

$$N_{grav}(X, Y)^i + v = N_{FEM}(X, Y | \mathbf{p}) + \Delta T_N(\mathbf{d}') \quad (2.4)$$

$$\xi^j + v = -\frac{\partial N_{FEM}(X, Y | \mathbf{p})}{M(B) \cdot \partial B} + \Delta T_\xi(\mathbf{d}') \quad (2.5)$$

$$\eta^j + v = -\frac{\partial N_{FEM}(X, Y | \mathbf{p})}{N(B) \cdot \cos B \cdot \partial L} + \Delta T_\eta(\mathbf{d}') \quad (2.6)$$

$$\mathbf{0} + v = C(\mathbf{p}). \quad (2.7)$$

$M(B)$  and  $N(B)$  denote the radius of meridian and normal curvature. The scale correction  $\Delta m(B, L)$  is modelled between the metrics of  $h$  and  $H$  and may, in case of significance) be interpreted as topographical correction. With the indices  $i$  and  $j$  in (1.4) and (1.5, 1.6) different groups of geoid heights  $N_{grav}$  and deflections of the vertical ( $\xi$  and  $\eta$ ) may be introduced.

Modern gravimetric geoid models, for example the EGG97, comprise both geoid heights and the deflections of the vertical. Due to the genesis of the models, the determined anomalous gravity potential,  $T$ , suffers from long-wave systematic errors,  $\Delta T$ , that mainly result from two sources. Once, from datum inconsistencies in the original gravity observations and twice from the so-called “weak-forms”. The weak forms are related to the maximum and some subsequent eigenvectors of the covariance-matrix as carrier functions and occur in extended networks. (Jäger, 1988, Jäger and Kälber, 2004).

To reduce this systematic errors, a set of datum parameters,  $\mathbf{d}$ , is modelled to remove the “local datum effect”,  $\Delta T_N$ ,  $\Delta T_\xi$  and  $\Delta T_\eta$  (2.3, 2.4, 2.5), from the respective observation, geoid height,  $N_{grav}$ , or deflection from the vertical  $(\xi, \eta)_{grav}$ , derived from the applied gravity field model. By adapting individual datum parameters,  $\mathbf{d}$ , any number of gravity field models may be introduced simultaneously. Further, each model may be subdivided into a number of so-called “geoid-patches”, each with an own set of parameters,  $\mathbf{d}$  (3 translations, 3 rotations).

The parameterisation of a simple 3-parameter datum shift, based on 3 translations reads:

$$\Delta \mathbf{T} = \mathbf{A} \cdot \mathbf{d} \quad (2.8)$$

$$= \begin{bmatrix} \Delta T_N \\ \Delta T_\xi \\ \Delta T_\eta \end{bmatrix} = \begin{bmatrix} \cos B \cos L & \cos B \sin L & \sin B \\ \cos B \cos L & \cos B \sin L & \sin B \\ \frac{M(B)}{\sin L} & \frac{M(B)}{\cos L} & \frac{M(B)}{0} \\ -\frac{\sin L}{N(B)} & -\frac{\cos L}{N(B)} & 0 \end{bmatrix} \cdot \begin{bmatrix} u \\ v \\ w \end{bmatrix}$$

In case of astrogeodetic deflections from the vertical,  $\xi$  and  $\eta$ , the parameterisation  $\Delta T_{\xi, \eta}$  is carrying a datum transition, if the observations are not related to ETRS89.

The use of a gravimetric geoid model or a geopotential model respectively is to be interpreted as substitute for the original gravity observations,  $\Delta g$ . The weak-shapes, mentioned in chapter

1, as stochastic source for  $\Delta T_N$ ,  $\Delta T_\xi$  and  $\Delta T_\eta$ , would significantly decrease, if the true co-variance matrix,  $C_{NN}$ , for the geoid heights and  $C_{\xi\xi}/C_{\eta\eta}$ , for the deflections of the vertical as well as the correlations,  $C_{N\xi}$ ,  $C_{N\eta}$  and  $C_{\xi\eta}$ , would be available. Unfortunately, the stochastic model resulting from the determination of a gravity field model is in general not available. As a substitute, synthetic co-variance matrices may be generated for the geoid heights  $N_{\text{grav}}$ , by means of an appropriate co-variance function, such as (Dinter et. al. 1997):

$$C_{N_i, N_j} = \sigma_\theta \cdot e^{-\frac{\ln(0.5)}{\beta} S_{i,j}} \quad 2.9$$

In the expression above,  $S_{i,j}$  denotes the distance between two points,  $i$  and  $j$ . The quantity,  $\beta$ , is the correlation length. According to Moritz (1980), p. 108, the remaining co-variances read:

$$C_{N_i, \xi_j} = \frac{\partial C_{N_i, N_j}}{M(B) \cdot \partial B_j} \quad (2.10)$$

$$C_{N_i, \eta_j} = \frac{\partial C_{N_i, N_j}}{N(B_j) \cos B_j \cdot \partial L_j} \quad (2.11)$$

$$C_{\xi_i, \xi_j} = \frac{\partial^2 C_{N_i, N_j}}{M(B_i) M(B_j) \partial B_i \partial B_j} \quad (2.12)$$

$$C_{\eta_i, \eta_j} = \frac{\partial^2 C_{N_i, N_j}}{N(B_i) N(B_j) \cos B_i \cos B_j \cdot \partial L_i \partial L_j} \quad (2.13)$$

$$C_{\xi_i, \eta_j} = \frac{\partial C_{N_i, N_j}^2}{M(B_i) N(B_j) \cos B_j \cdot \partial B_i \partial L_j} \quad (2.14)$$

The final stochastic model, applied in the least-squares adjustment (2.2 – 2.7) reads:

$$C_{II} = \begin{bmatrix} C_{HH} & & & & & & \\ \mathbf{0} & C_{hh} & & & & & \\ & \mathbf{0} & C_{NN} & & & & \\ & \mathbf{0} & \mathbf{0} & C_{N\xi} & & & \\ & \mathbf{0} & \mathbf{0} & C_{N\eta} & C_{\xi\xi} & & \\ & \mathbf{0} & \mathbf{0} & \mathbf{0} & C_{\xi\eta} & C_{\eta\eta} & \\ & \mathbf{0} & \mathbf{0} & \mathbf{0} & \mathbf{0} & \mathbf{0} & C_{C(p)} \end{bmatrix} \quad (2.15)$$

As known from the theory of least-squares adjustment, the estimation is unbiased with regard to the choice of the stochastic model (Jäger et. al. 2004). Therefore, the estimated FEM-parameters,  $\mathbf{p}$ , and the HRS are unbiased, even if the stochastic model in (2.15) is approximated as:

$$\tilde{\mathbf{C}}_{NN} = \sigma_{\sigma,N}^2 \cdot \mathbf{I} \quad (2.16)$$

$$\tilde{\mathbf{C}}_{\xi\xi} = \sigma_{\sigma,\xi}^2 \cdot \mathbf{I}, \quad (2.17)$$

$$\tilde{\mathbf{C}}_{\eta\eta} = \sigma_{\sigma,\eta}^2 \cdot \mathbf{I} \quad (2.18)$$

$$\tilde{\mathbf{C}}_{N\xi} = \tilde{\mathbf{C}}_{N\eta} = \tilde{\mathbf{C}}_{\xi\eta} = \mathbf{0} \quad (2.19)$$

However, due to the second theorem of Gauss, the most accurate FEM-representation of the HRS results from the proper stochastic model. So the accuracy of the HRS increases with the quality of the approximation (2.9 and 2.10-2.14).

To model additional systematic errors as well as topographic effects, a scale correction  $\Delta m(B,L)$  is introduced between the metrics of  $h$  and  $H$  (2.3). As the correction may vary location dependent,  $\Delta m(B,L)$  is modelled as 2-dimensional polynomial function:

$$\Delta m(B, L) = \Delta m_0 + \Delta m_1 \cdot X + \Delta m_2 \cdot Y. \quad (2.20)$$

To provide a continuous FEM-representation of the HRS, a number of continuous conditions is introduced as pseudo observations (2.7), at the common border of neighbouring meshes (Jäger, 1998, Schneid, 2002). To obtain a homogenous accuracy for the representation of the resulting DFHRS, the weight for (2.7) should correspond with the resulting accuracy of the DFHRS, for example one centimetre.

The FEM-parameters,  $\mathbf{p}$ , as well as the FEM-mesh topology are stored in a database. The access to this DFHRS-database is provided by a dynamic link library (DLL), that is to be implemented in any GPS-software package easily. The leading GPS-hardware companies have already realised interfaces to the DFHRS database standard (Jäger and Schneid, 2000-2004).

The DFHRS concept aims at the direct application of the classical relationship between ellipsoidal heights  $h$ , standard heights  $H$ , and DFHRS-heights  $N_{FEM}$ . So in GNSS positioning the conversion of the ellipsoidal height  $h$  to the physical height  $H$  by means of a DFHRS data base access reads:

$$\begin{aligned} H &= h - \Delta m(X, Y) \cdot h - NFEM(X, Y | \mathbf{p}) \\ &= h - DFHRS(X, Y | \Delta m, \mathbf{p}). \end{aligned} \quad (2.21)$$

The DFHRS concept, with respect to the computation of the DFHRS database parameters ( $\mathbf{p}$  and  $\Delta m$ ) (2.2-2.7), was realised in the Windows software package DFHBF©Jäger/Schneid/Schwarzer. Besides several graphical tools for a comfortable treatment of projects, the application provides a statistically quality control, including data-snooping for cross errors and variance-component estimation in the functional model (2.2-2.7).

The estimation of trend or datum parameters,  $\mathbf{d}$ , for each single observation group enables the simultaneous introduction of several geoid and deflection of the vertical models. Further, each gravity potential model or gravimetric geoid model may be subdivided into a number of patches (fig.1), each with an own set of datum parameters,  $\mathbf{d}$ . In this way, the long-wave errors may be modelled as a substitute of a rigorous two-step adjustment using the correct stochastic model.

### 3. The < 1 decimetre DFHRS of Europe

#### 3.1 FEM Design and observations

According to the DFHRS concept, the area was subdivided into a number of 7035 FEM-meshes (fig.1). The size of the meshes was chosen with 30 km border-length to represent the EVRF in a quality of less than one decimetre. To reduce the long-wave biases in the applied geoid model, in this case the EGG97 (Denker and Torge, 1997), was subdivided into a number of 34 patches, each with its own set of local datum parameters (2.8). The size of the patches is again a very important design parameter to compute precise DFHRS databases, DFHRS parameters and  $\Delta m$  respectively (see table 2). On the other hand, at least 4 identical points have to be included to solve the unknown parameters  $d$  in a controlled way. Due to the uneven distribution of the GNSS/levelling points, the patch-size varies from 100km to 800km border-length. The quasigeoid heights  $N_{\text{grav}}$  as well as the deflections of the verticals ( $\xi$  and  $\eta$ )<sub>grav</sub> of the EGG97 were used as gravity based observations in the adjustment approach (2.2-2.7).

The GNSS/levelling points from the EVRF2000 were used as group of identical points ( $h$  and  $H$ ) in the adjustment of the DFHRS Europe (fig.2). Additional densification points were available in Estonia, Germany, Latvia, Lithuania and Switzerland. In total, 355 points with known ellipsoidal and standard heights were used.

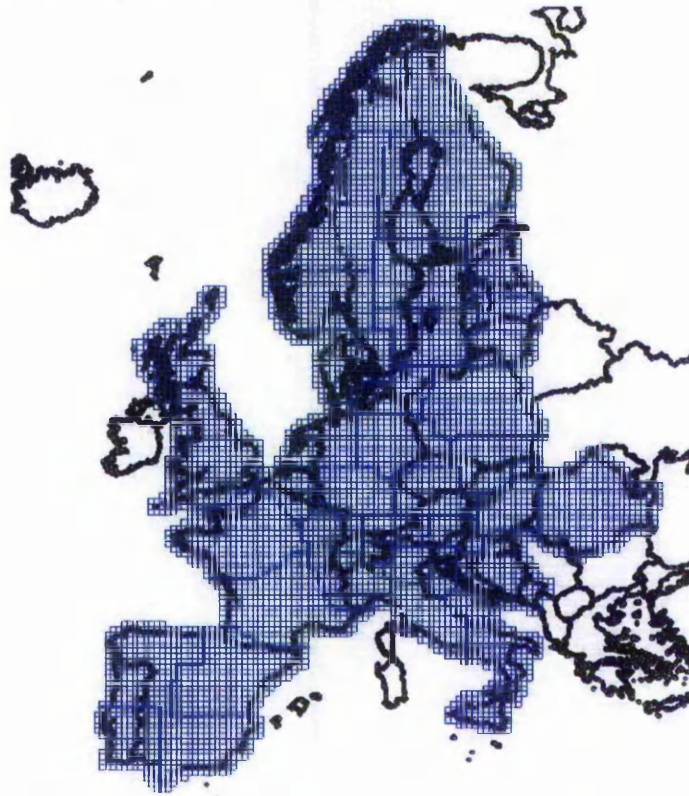


**Fig. 1:** FEM Meshes (thin lines) and patches (thick lines) in the DFHRS Europe project

### 3.2. Quality control

A first way to prove the external accuracy (“reproduction quality”) of the DFHRS data base for Europe was to compute successively the normal height  $H_{i,DFHRS}$  using an individual database  $DFHRS_i$ , where  $H_{i,EVRS}$  was excluded from the adjustment of the FEM-parameters,  $p$ . The reproduction quality  $H_i$  is then simply given by the value of the difference

$$\nabla H_i = H_{i,EVRS} - H_{i,DFHRS} \quad (3.1a)$$

The computation of all  $\nabla H_i$  can be performed by the DFHRS Production Software in the unique DFHRS production step by the division of the residual  $v_i$ , by its part of redundancy,  $r_i$ .

$$\nabla H_i = -\frac{v_i}{r_i} \quad (3.1b)$$

Another quality check was the computation of independent control points and comparison with the known normal heights. In this way, ~200 points in 6 different countries, Austria, Germany, Estonia, Latvia, Lithuania and Switzerland, have been recomputed. The results show, that the accuracy of less than one decimetre is reached. The detailed results for the single countries are compiled in table 1, below.

	Austria 	Germany 	Estonia 	Latvia 	Lithuania 	Switzerland 
<b>No. of control points</b>	9	95	21	25	46	13
<b>RMS [cm]</b>	7,5	4,2	8,8	9,2	6,8	7,0

**Table 1:** Compilation of the results for the different countries, where independent GNSS/levelling points have been re-computed.

The re-computation of the known points indicates that the external accuracy of less than one decimetre for the DFHRS for Europe is reached in every country, where control points were available (table 1).

A DFHRS data base with a surface covering proved quality of 5-10 centimetres may be computed after incorporating more observations, for example the data from the currently running densification activities.

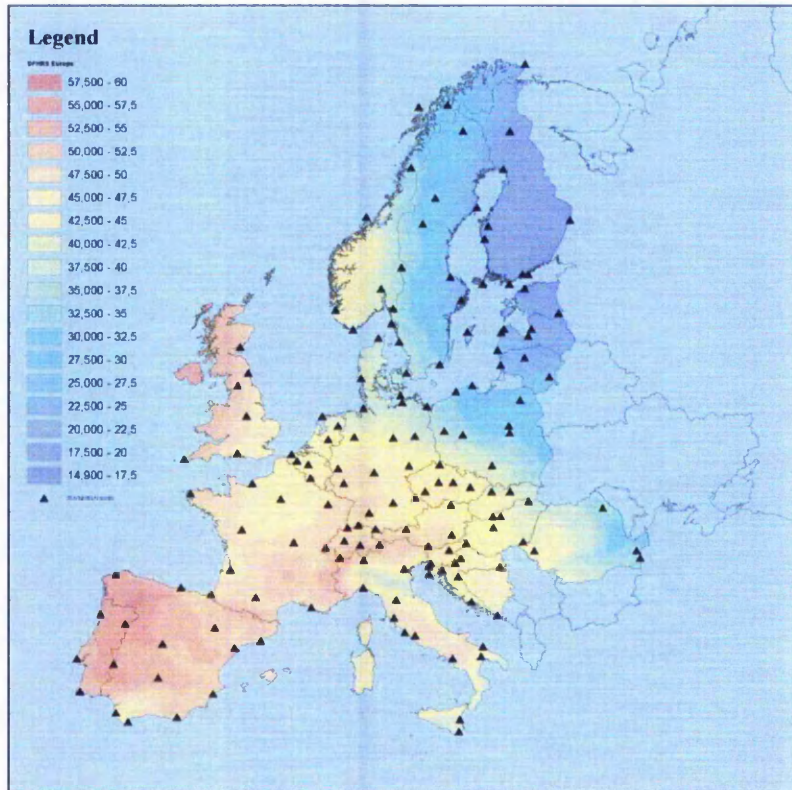


Fig.2: Visualisation of the DFHRS for Europe. The triangles mark the EVRF2000 points

## 4. Further studies and outlook on DFHRS-Concept

### 4.1 Basic Design aspects

The possibility, to produce DFHRS-Databases in different qualities was first discussed in (Jäger, 1998). The size of the FEM-meshes, the size of the geoid-patches and the number as well as the quality of the identical points (h, H) are design parameters to control the resulting accuracy of the computed DFHRS Database. The resulting accuracy is only depending on the design parameters and not depending on the size of the computed area. The rule of thumb for the design of DFHRS in different quality classes is shown in table 2 (holding for a polynomial degree  $n=3$ ).

HRS quality	Size of FEM-meshes	Size of geoid-patches	Density of fitting points
< 1 cm	5 km x 5 km	30 km – 40 km	50 points / 100 km <sup>2</sup>
1 cm – 3 cm	10 km x 10 km	50 km – 70 km	10 points / 100 km <sup>2</sup>
5 cm – 10 cm	30 km x 30 km	~ 300 km	> 3 points /100 km <sup>2</sup>

Table 2 : Design parameters as rule of thumb for a DFHRS realisation in different accuracy classes, referred to polynomial degree  $n=3$

In recent years, several DFHRS databases have been computed, to support GNSS-based height determination. Due to the different possible application requirements of DFHRS data

bases, there are different types of DFHRS databases. The “high-end product”, based on a mesh-size of 5km x 5km, with a statistically controlled accuracy of less than one centimetre was computed for six state land service departments in Germany (Baden-Württemberg, Bayern, Hessen, Nordrhein-Westfalen, Rheinland-Pfalz and Saarland) (Jäger and Schneid, 2000-2004).

The DFHRS for Germany was designed to support an online GPS-height determination in combination with the DGPS-correction services ascos and SAPOS, in a quality of less than three centimetres. (Schneid 2003, Seiler 2004). This approximation quality is reached with a mesh-size of 10km x 10km.

The same design was applied for the computation of the DFHRS data bases for the Baltic states. In a co-operation of the Latvian State Land Service, The Latvian University of Agriculture and the University of Applied Sciences in Karlsruhe 4 different data bases, for Latvia, Lithuania, Estonia and a surface covering DFHRS for the Baltic states was determined (Lace, 2004).

The DFHRS Albania (Jäger et a. 2004, included in these proceedings) was designed with 10 km mesh-size. A patch-size of >100 km led to a final accuracy of less than one decimetre.

Fig. 3 gives an overview on the different DFHRS existing all over Europe.

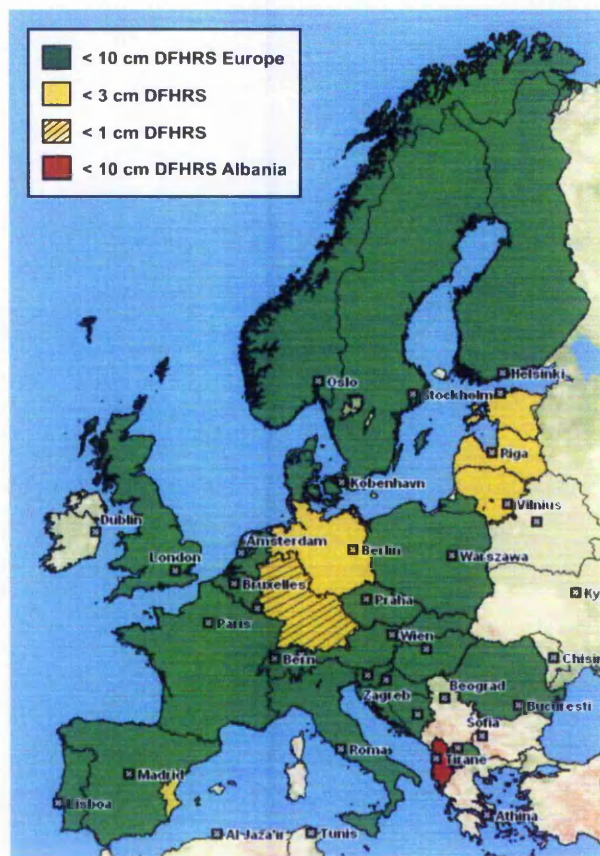


Fig. 3: Overview on DFHRS\_DB in Europe

Based on the EGM96 and 100 GNSS/levelling points DFHRS databases for Namibia, < 5 dm quality, and the capital Windhoek, 1 centimetre quality, have been computed (Tepper and Hoffmann, 2002).

#### 4.2 Quality improvement by means using a proper stochastic model

It was mathematically proved in Jäger and Schneid (2002b), that the use of geoid-heights  $N_{\text{grav}}$  as observations leads to the same results and DFHRS parameters,  $\mathbf{p}$  and  $\Delta m$ , in the DFHRS approach as the use of the original gravity data, as soon as the covariance matrix  $C_{N_{\text{grav}}}$  is introduced. It is further known from adjustment theory, that any approximation and neglect in the stochastic model of an adjustment decreases the quality of the results, namely the accuracy of the estimated DFHRS parameters.

So the use of a the correct stochastic model, e.g.  $C_{N_{\text{grav}}}$  in the context with the introduction of geoid-height observations  $N_{\text{grav}}$ , or the use of an appropriate artificial substitute (e.g. by the use of covariance functions (tab. 3) in the context with the functional model of the DFHRS adjustment (2.2 – 2.7) will provide an increase of the accuracy of the DFHRS.

If the distribution of identical points is sparse, the number of possible “geoid-patches” is limited. The quality of the HRS representation then may be improved by using a co-variance function, such as (2.9, 2.10-14) to generate an a-priori co-variance matrix,  $C_{II}$ .

In a test project, the significant increase of the resulting accuracy is demonstrated. The approximation of the HRS is carried by FEM meshes of 10 km border-length (fig.4). 46 GPS/levelling points were introduced and a 3-parameter datum shift, containing one constant offset and two rotations, was modelled to reduce long-wave errors in the applied gravimetric geoid model, here the EGG97.

In a first computation, the a-priori covariance matrix,  $C_{N_{\text{grav}}}$ , of the used geoid heights,  $N_{\text{grav}}$ , was simply approximated with (2.16). The resulting standard deviation,  $S_{\text{DFHRS}}$ , of the estimated DFHRS, was  $\pm 1,9$  cm, found by the re-computation of known points.

In a second and third computation, two different covariance functions were used to generate a better approximation for  $C_{NN}$ . The correlation length,  $\beta$ , was introduced with 100 km. A compilation of the results is given in table 3.

Covariance function for $N_{\text{grav}}$	RMS [cm]	Maximum $\Delta H$ [cm]	Minimum $\Delta H$ [cm]
Uncorrelated	1,92	4,4	-3,1
$\sigma_{\theta} \cdot e^{-\ln(\theta, S) \frac{S}{\beta}}$	0,86	2,1	-2,1
$\sigma_{\theta} \cdot \frac{\beta}{\beta + S}$	0,86	2,1	-2,0

**Table 3:** Comparison of the results, when applying different covariance functions.

The reliability of this result was proven in a second investigation. 11 GNSS/levelling points from the inner zone of the project-area were removed and not used for the adjustment of the DFHRS (Fig. 4).

Covariance function for $N_{\text{grav}}$	RMS [cm]	Maximum $\Delta H$ [cm]	Minimum $\Delta H$ [cm]
Uncorrelated	1,53	0,6	-2,7
$\sigma_\theta \cdot e^{-\ln(\theta, S) \frac{S}{\beta}}$	0,82	0,3	-1,4
$\sigma_\theta \cdot \frac{\beta}{\beta + S}$	0,84	0,3	-1,4

**Table 4:** Comparison of the results from re-computing the removed points, when applying different covariance functions.

The re-computation of the removed 11 points lead to a standard deviation,  $s_{DFHRS}$ , of  $\pm 0,82\text{cm}$ . The complete results are compiled in table 4.

The significant increase of the external accuracy may be transferred to other projects, with a similar FEM design. The use of an appropriate covariance function for the stochastic model of gravimetric geoid heights increases essentially the accuracy of the HRS, even in areas where the density of GNSS/levelling points is sparse.

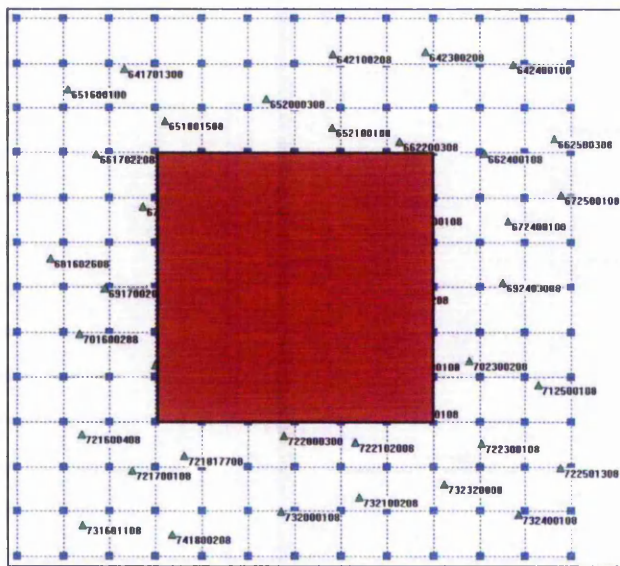


**Fig.4:** Situation of the 46 GPS/levelling points. In a second project, 11 points from the inner zone (red) have been removed.

### 4.3 Implementation of gravity observations

The use of gravimetric geoid heights  $N_{\text{grav}}$  and deflections from the vertical ( $\xi$  and  $\eta$ )<sub>grav</sub> may be interpreted as substitute for the original gravity observations,  $g$ . However, in general, new gravity observations are carried out. To make use of this additional gravity data, the integration of gravity anomalies,  $\Delta g$  and gravity disturbances,  $\delta g$ , in the DFHRS concept and software is currently running.

## 5. Conclusions

The concept of the Digital FEM Height Reference Surface, DFHRS, enables a combined least-squares adjustment of gravimetric geoid models, vertical deflections and GNSS/levelling points in one closed mathematical model. To reduce long-wave biases in gravimetric geoid models, local datum parameterisations may be applied, on dividing the total area into a number of patches. Further, any number of geoid models and vertical deflection observation groups may be introduced simultaneously in one closed least-squares adjustment. The use of appropriate co-variance functions for the applied gravimetric models is a substitute for the use of the original gravity observations.

The change of the main design parameters, the size of FEM-meshes and geoid-patches, enables the production of DFHRS databases in different qualities. According to this principle, the DFHRS concept has been applied and proven in several projects. For six federal states of Germany, a DFHRS in a statistical controlled quality of less than one centimetre have been computed. To support GPS-based online height determination in combination with DGPS-correction services, such as SAPOS, ascos or EUPOS, a DFHRS for Germany has been computed with an external accuracy of three centimetres.

The DFHRS concept was realised as a Windows-Application, that is available both, for commercial and for scientific purposes

Following the concept of the Digital FEM Height Reference Surface (DFHRS) a decimetre model of the European Vertical Reference System (EVRS) was computed. Using the GNSS/levelling points from the European Vertical Reference Network 2000 (EVRF2000) and the EGG97 Quasigeoid, an external accuracy of less than 10 centimetres was proven by means of the re-computation of known points in Austria, Estonia, Germany, Latvia, Lithuania and Switzerland.

With this, the DFHRS for Europe is the first product that fulfils the EUREF Resolution No. 4 of the EUREF Symposium 2001, Dubrovnik, where a decimetre HRS was requested.

According to the FEM principle, any accuracy may be reached by changing the corresponding design parameters, the border-length and the size of the patches. As the patch size mainly depends on the density of the GNSS/levelling points, a representation of the EVRS in a quality of less than 5 centimetres could be reached, after incorporating additional data. This data is available by identical points ( $h$  and  $H$ ), for example from the EVRF densification activities and further by national quasigeoid models and deflections from the vertical ( $\xi$  and  $\eta$ ).

## 5. Literature

BKG (2003), European Vertical Reference System EVRS, URL: <http://evrs.leipzig.ifag.de/>, Bundesamt für Kartographie und Geodäsie, Frankfurt.

Dinter, G.; Illner, M. and R. Jäger (1996): A synergetic approach for the integration of GPS heights into standard height systems and for the quality control and refinement of geoid models. In: Veröffentlichungen der Internationalen Erdmessung der Bayerischen Akademie der Wissenschaften (57). IAG Subcommission for Europe Symposium EUREF, Ankara 1996. Beck'sche Verlagsbuchhandlung, München.

Denker, H. and W. Torge (1997): The European Gravimetric Quasigeoid EGG97 – An IAG supported continental enterprise. In: Geodesy on the Move – Gravity Geoid, Geodynamics,

- and Antarctica. R. Forsberg, M. Feissel, R. Dietrich (eds.) IAG Symposium Proceedings Vol. 119, Springer, Berlin Heidelberg New York: 249-254.
- Hoffmann, A. and S. Tepper (2002): Planung, Berechnung und Qualitätsanalyse der DFHBF\_DB Namibia und Windhuk unter Einbindung zusätzlicher GPS-Messungen. Diploma thesis at Fachhochschule Karlsruhe - University of Applied Sciences, unpublished.
- Jäger, R. (1988): Analyse und Optimierung geodätischer Netze nach spektralen Kriterien und mechanische Analogien. DGK Reihe C, Nr. 342, München.
- Jäger, R. (1998): Ein Konzept zur selektiven Höhenbestimmung für SAPOS. Beitrag zum 1. SAPOS-Symposium. Hamburg 11./12. Mai 1998. AdV (Hrsg.), Amt für Geoinformation und Vermessung, Hamburg. S. 131-142
- Jäger, R. und S. Kälber (2000): Konzepte und Softwareentwicklungen für aktuelle Aufgabenstellungen für GPS und Landesvermessung. DVW Mitteilungen, Landesverein Baden-Württemberg. 10/2000. ISSN 0940-2942.
- Jäger, R. (2002): Online and Postprocessed GPS-heighting based on the Concept of a Digital Finite Element Height Reference Surface. In: J. Kaminskis and R. Jäger (Eds.): 1st Common Baltic Symposium. Riga, June 11, 2001. ISBN 9984-9507-7-5
- Jäger, R. and S. Schneid (2002a): Passpunktfreie direkte Höhenbestimmung mittels DFHBF - ein Konzept für Positionierungsdienste wie SAPOS. Landesvermessung und Geobasisinformation Niedersachsen (LGN) (Hrsg.). Hannover. S. 149-166. <http://www.sapos.de/pdf/4symposium/149-166.pdf>
- Jäger, R. and S. Schneid (2002b): Online and Postprocessed GPS-Heighting based on the Concept of a DFHRS. In : Proc IAG International Symposium 'Vertical Reference Systems', H. Drewes, A. Dodson, L.P.S. Fortes, L. Sanchez, P. Sandoval (EDS), Vol. 124, Springer Berlin, Heidelberg, New York, pp 203-208.
- Jäger, R. and S. Kälber (2004): Precise Vertical Reference Surface Representation and Precise Transformation of Classical Networks to ETRS89 / ITRF - General Concepts and Realisation of Databases for GIS, GNSS and Navigation Applications in and outside Europe. In: Proc. of the 2<sup>nd</sup> Common Baltic Symposium. Riga, 2003. in press.
- Jäger, R. and S. Schneid (2000-2004): Homepage of the DFHRS-project, [www.dfhbf.de](http://www.dfhbf.de) .
- Jäger, R., Müller, T., Saler, H. and R. Schwäble (2004): Klassische und robuste Ausgleichungsverfahren. Wichmann, Heidelberg. ISBN 3-87907-370-8.
- Lace, L. (2004): „LATVIJAS TERITORIJAS DIGITĀLĀS AUGSTUMA VIRSMAS MODELĒŠANA” - Masterthesis at the Latvian University of Agriculture, Jelgava, unpublished.
- Moritz, H. (1980): Advanced Physical Geodesy, Wichmann Verlag, Karlsruhe, 1980. ISBN 3-87907-106-3
- Schneid, S. (2002): Software Development and DFHRS computations for several countries. J. Kaminskis and R. Jäger (Eds.): 1<sup>st</sup> Common Baltic Symposium, June 11, 2001. ISBN 9984-9507-7-5
- Schneid, S. (2003): The Digital FEM-Height Reference Surface DFHRS of Gemany. In: Proc. of the 2<sup>nd</sup> Common Baltic Symposium, Riga, June 11, 2003. In press.
- Seiler, S (2004): Homepage of IB-Seiler, Lauf. <http://www.ib-seiler.de> .

Jäger, R., Kälber, S., Seiler, S. and S. Schneid (2003):

Precise Vertical Reference Surface Representation and Precise Transformation of Classical Networks to ETRS89 / ITRF - General Concepts and Realisation of Databases for GIS, GNSS and Navigation Applications in and outside Europe. Proceedings GNSS2003 – The European Navigation Conference, Graz, April 22-25, 2003. CD-ROM Publication. The Austrian Institute of Navigation, Graz.

# Precise Vertical Reference Surface Representation and Precise Transformation of Classical Networks to ETRS89 / ITRF - General Concepts and Realisation of Data- bases for GIS, GNSS and Navigation Applications in and outside Europe

<sup>1)</sup> Prof. Dr.-Ing. Reiner Jäger, <sup>2)</sup> Dipl.-Ing. (FH) Simone Kälber

<sup>1)</sup> Dipl.-Ing. (FH) Sascha Schneid und <sup>3)</sup> Dipl.-Ing. (FH) Stephan Seiler

<sup>1)</sup> Fachhochschule Karlsruhe - University of Applied Sciences  
Studiengang Vermessung und Geomatik & Internationaler Studiengang Geomatics (MSc)  
Moltkestrasse 30, D-76133 Karlsruhe

Email: reiner.jaeger@fh-karlsruhe.de. URL: [www.dfhbf.de](http://www.dfhbf.de)

<sup>2)</sup> Lamprechtstrasse 13, D-76227 Karlsruhe

<sup>3)</sup> Ingenieurbüro Seiler (IBS), Hauptstrasse 45, D-77886 Lauf, URL: [www.ib-seiler.de](http://www.ib-seiler.de)

## 1 Introduction

As concerns the georeferencing of position data in modern data bases, the availability of GNSS (GPS/GLONASS/GALILEO) related code- and phase-measurement DGNSS-correction data, which are provided in different ways and by different positioning services in and outside Europe, leads to the replacement of the classical geodetic reference systems by GNSS-consistent ITRF-based reference systems.

So the transformation of the old plan position data  $(N,E)_{class}$  related to the classical reference systems to the ITRF/ETRS89 datum  $(N,E)_{ITRS}$  becomes urgently necessary. A sophisticated and general solution of this transformation problem has to include a data base concept for the provision of the corresponding transformation parameters for GIS, GNSS and Navigation purposes. It is presented in chap. 2 in terms of the COPAG concept.

Further the capacity of a one-cm-positioning by GNSS services, such as e.g. SAPOS® and ascos® in Germany, is also appropriate for a GNSS related heighting. The GNSS-based determination of sea-level (orthometric, normal) heights  $H$  requires however the transformation of the ellipsoidal GNSS heights  $h_{ITRS}$  to the respective physically defined height reference surface (HRS). The DFHRS (Digital-Finite-Element-Height-Reference-Surface) concept presented in chap. 3 provides for GNSS positioning (GPS/GLO-NASS/GALILEO) a direct and online conversion of ellipsoidal heights  $h$  into standard heights  $H$  referring to the height reference surface (HRS) of orthometric or normal height systems.

## 2 GNSS Plan Positioning – Data Bases to transform between ETRS89/ITRS and Classical Datum Systems

### 2.1 Continuous Patched Georeferencing (COPAG) Concept

This part of the contribution deals with the homogenisation, cm-accurate and neighbourhood consistent transformation of plan coordinates between classical national reference-systems  $(N,E)_{Class}$  and the unique ITRF/ETRS89-datum  $(N,E)_{ITRF}$ .

The so-called COPAG (Continuously Patched Georeferencing) transformation concept [26] implies the improvement and homogenisation of the geometrical quality of existing classical networks (such as e.g. the German DHDN network and datum, fig. 2.1; fig. 2.2) by the developed method of an ITRF/ETRS89 related georeferencing. So the qualification of the old position data for a future utilization and the continuation of existing databases are provided. Therefore also a high economic benefit as well as signals for further innovative developments in the GIS-, GNSS- and LBS-sector are set by the COPAG concept of transforming the old classical data to the GNSS consistent ITRF/ETRS89 datum.

The COPAG concept is based on a strict three-dimensional similarity transformation between the two concerned reference-systems. The equations of this transformation are linearized under the realistic assumption of small rotation angles and the linearization point of the geographical coordinates  $(B,L,h)_1$ . This leads to the resulting part for the plan component  $(B,L)$  of the three-dimensional similarity transformation in geographical coordinates  $(B,L,h)$  reading [8], [9], [26]:

$$B_2 + v = B_1 + \partial B_1(d) = B_1 + \partial B_1(u, v, w, \varepsilon_x, \varepsilon_y, \varepsilon_z, \Delta m, \Delta a, \Delta f) \quad (2.1a)$$

$$\begin{aligned} &= B_1 + \left[ \frac{-\cos(L) \cdot \sin(B)}{M+h} \right]_1 \cdot u + \left[ \frac{-\sin(L) \cdot \sin(B)}{M+h} \right]_1 \cdot v + \left[ \frac{\cos(B)}{M+h} \right]_1 \cdot w + \\ &\quad \left[ \frac{\sin(L) \cdot \frac{h+N \cdot W^2}{M+h}}{1} \right]_1 \cdot \varepsilon_x + \left[ \frac{-\cos(L) \cdot \frac{h+N \cdot W^2}{M+h}}{1} \right]_1 \cdot \varepsilon_y + [0] \cdot \varepsilon_z + \\ &\quad \left[ \frac{-e^2 \cdot N \cdot \cos(B) \cdot \sin(B)}{M+h} \right]_1 \cdot \Delta m + \Delta B(\Delta a, \Delta f) \end{aligned} \quad (2.1b)$$

$$L_2 + v = L_1 + \partial L_1(d) = L_1 + \partial L_1(u, v, w, \varepsilon_x, \varepsilon_y, \varepsilon_z, \Delta m, \Delta a, \Delta f)$$

$$\begin{aligned} &= L_1 + \left[ \frac{-\sin(L)}{(N+h) \cdot \cos(B)} \right]_1 \cdot u + \left[ \frac{\cos(L)}{(N+h) \cdot \cos(B)} \right]_1 \cdot v + [0] \cdot w + \\ &\quad \left[ \frac{-(h+(1-e^2) \cdot N)}{(N+h) \cdot \cos(B)} \cdot \cos(L) \cdot \sin(B) \right]_1 \cdot \varepsilon_x + \left[ \frac{-(h+(1-e^2) \cdot N)}{(N+h) \cdot \cos(B)} \cdot \sin(L) \cdot \sin(B) \right]_1 \cdot \varepsilon_y + \\ &\quad + [1] \cdot \varepsilon_z + [0] \cdot \Delta m + \Delta L(\Delta a, \Delta f) \end{aligned}$$

In the above formulas the following abbreviations were introduced:

$$\Delta B(\Delta a, \Delta f) = B_1(a_1, f_1) - B_1(a_2, f_2); \quad \Delta L(\Delta a, \Delta f) = L_1(a_1, f_1) - L_1(a_2, f_2) = 0; \quad (2.1c,d)$$

$$N = \frac{a^2}{b \cdot \sqrt{1 + e^2 \cdot \cos^2 B}}; M = \frac{a^2}{b \cdot \left( \sqrt{1 + e^2 \cdot \cos^2 B} \right)^3}; W = \frac{a}{N} \quad (2.1e,f,g)$$

As transformation parameters  $d$  (2.1a,b) three translations ( $u,v,w$ ), three rotations ( $\varepsilon_x, \varepsilon_y, \varepsilon_z$ ) and the parameter of a scale difference  $\Delta m$  between the two reference systems occur in the observation equations (2a,b). The corrections  $\Delta B$  and  $\Delta L$  (2.1c,d) are due to the known changes ( $\Delta a, \Delta f$ ) in the ellipsoid dimensions  $a$  and  $f$  at the transition from reference system 1 (e.g. DHDN in Germany) to reference system 2 (e.g. ETRS89). As the transformation is concerning the plan component ( $B,L$ ), and in general no heights for the respective identical points, nor for the points to be transformed (e.g. cadastral points, buildings etc.), are available in the different databases, the height component  $h$  – taken as third observation equation – is only needed for a small number of three dimensional identical points (e.g. points of a 1<sup>st</sup> order networks). The transformation equation for the height component  $h$  reads:

$$\begin{aligned} h_2 + v &= h_1 + \partial h_1(d) = h_1 + \partial h_1(u, v, w, \varepsilon_x, \varepsilon_y, \varepsilon_z, \Delta m, \Delta a, \Delta f) & (2.1h) \\ &= h_1 + [\cos(L) \cdot \cos(B)]_1 \cdot u + [\cos(B) \cdot \sin(L)]_1 \cdot v + [\sin(B)]_1 \cdot w + \\ &\quad \left[ e^2 \cdot N \cdot \sin(B) \cdot \cos(B) \cdot \sin(L) \right]_1 \cdot \varepsilon_x + \left[ -e^2 \cdot N \cdot \sin(B) \cdot \cos(B) \cdot \cos(L) \right]_1 \cdot \varepsilon_y \\ &\quad + [0] \cdot \varepsilon_z + [h + W^2 \cdot N]_1 \cdot \Delta m + \Delta h(\Delta a, \Delta f), \end{aligned}$$

accordingly with  $\Delta h(\Delta a, \Delta f) = h_1(a_1, f_1) - h_1(a_2, f_2)$ . An advantage of the approach (2.1a-h) is that the ellipsoidal heights  $h_1$  (which are due to all classical network datum close to the standard heights  $H$ ) are only needed with a subordinate accuracy. Therefore the height information  $h_1$  can be taken from free available databases (e.g. the digital terrain model database ETOPO5 or ETOPO30).

## 2.2 COPAG and DFLBF Data Bases (DB) for Germany

Besides some solutions for different German states and city areas in Germany, two nationwide databases for Germany were computed with the COPAG software, namely the "(3-5)\_cm\_COPAG\_DB Germany" (Fig. 2.2a) and the "(3-5)\_cm\_DFLBF\_DB Germany" (fig. 2.2b) [28].

As the ETRS89 frame has one cm precision, e.g. all over Germany and the 1<sup>st</sup> Order ITRF/ETRS89 of other states all over the world, the residuals shown in fig. 2.1 left mean the deflection of the classical plan DHDN network coordinates  $\hat{x}=(B,L)_1$  from its true shape  $\tilde{x}$ . The residuals of the DHDN network of Germany West (fig. 2.1, left) reach the range of  $\pm 2.5$  m.

The shape and amount of the deflections  $\nabla x = \tilde{x} - \hat{x}$  are to be explained by the theory of so-called "natural weak-forms" [4], [5], [6], [15] and eventually a second part of so-called "stochastic weak-forms" [10]. The "natural weak-forms" of classical geodetic networks are related to the eigenvalue-problem

$$[C_{\hat{x}} - \mu_i \cdot I] \cdot m_i = 0 \quad (2.2a)$$

of the covariance matrix  $C_{\hat{x}}$  of the adjusted network coordinates  $\hat{x}$ .

The eigenvalue problem (2.2a) is part of the theory and concepts of spectral analysis and optimization of geodetic networks [4], [7]. It is shown in [4], [5], [7], [15] and [9] that the spectral components  $\nabla_i$

$$\nabla_i = \sqrt{\mu_i} \cdot m_i. \quad (2.2b)$$

are the key for the prediction (comparing e.g. the 1989 prediction results for Baden-Württemberg [6] with the real deflections for Baden-Württemberg presented 2000 in [9]) and theoretical understanding of deflections  $\nabla_{\hat{x}}$  of large networks from their true shape  $\hat{x}$ .

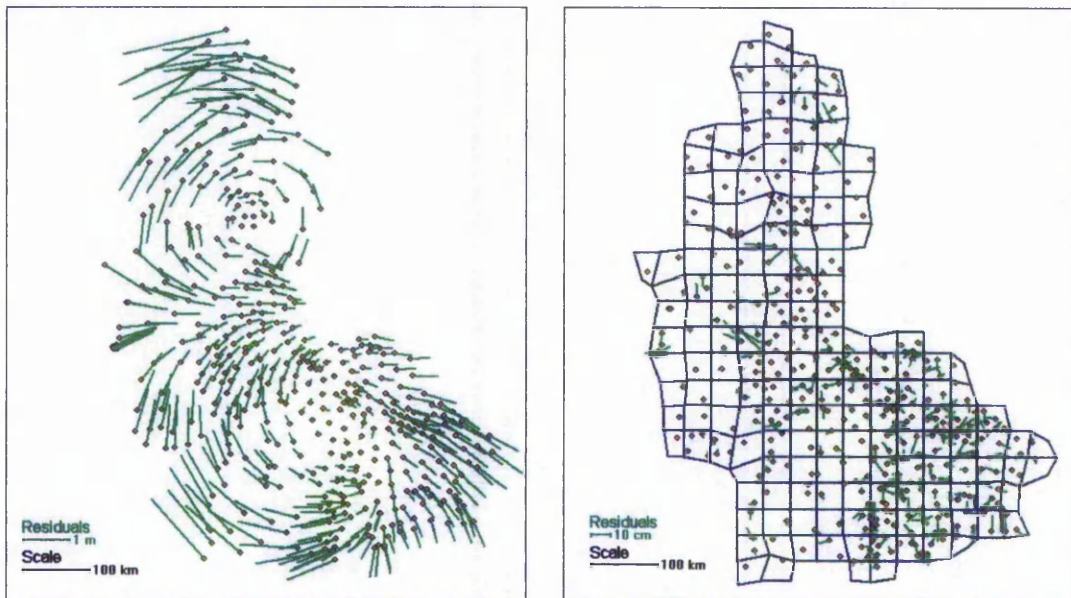


Fig. 2.1, left: Residuals up to 2.5 m for the transformation of the German DHDN plan coordinates to ETRS89 with only one nationwide set of transformation parameters  $d$ .  
 Fig. 2.1, right: Strict transformation with continuity conditions of the transformation parameters of the coordinates from German DHDN to ITRF (ETRS89) under partition in 177 patches. This leads to a drastic reduction of the residuals to less than 0.02 m in average.

In case of an occurring shape deflection  $\nabla_{\hat{x}}$  - like shown for the plan German DHDN network in fig. 2.1, left - the spectral components  $\nabla_i$  (2.2b), which are carried by the eigenvectors  $m_i$  (2.2a) and scaled by the square roots of the corresponding eigenvalues  $\mu_i$  (2.2a) give - in the descending order of the eigenvalue size  $\mu_i$  - the probability and amount of respective geometric deflection parts, which span up the total deflection shape  $\nabla_{\hat{x}}$  (fig. 2.1, left). As large geodetic networks tend to have a number of high dominant eigenvalues, the maximum spectral components (2.2b) (especially the maximum component  $\nabla_{\max} = \sqrt{\mu_{\max}} \cdot m_{\max}$ ) point out the quasi systematic shape deflection  $\nabla_{\hat{x}}$ . In case that the covariance matrix  $C_{\hat{x}}$  is regarded with respect to the assumed stochastic model of normal distributed observations, and the spectral analysis is accordingly based on (2.2a,b), the essential main spectral components  $\nabla_i = \sqrt{\mu_i} \cdot m_i$  are called the "natural weak-forms" of a geodetic network [4], [15].

Another type and an additional amount of weak-form deflections  $\nabla \hat{x}$  - namely the so-called "stochastic weak forms"  $\nabla_{i,\text{stoch}} = \sqrt{\mu_{i,\text{stoch}}} \cdot m_{i,\text{stoch}}$  already mentioned above - occur due to neglects in the stochastic model of the observations of a geodetic network adjustment [5], or a non over-determined parameter-computation  $\hat{x}$  from a respective observation set. The spectral components  $\nabla_i = \sqrt{\mu_i} \cdot m_i$  of the "stochastic weak forms" are then related to a general eigenvalue problem, which is regarded in [10].

To manage the weak-form problem with respect to the plan transformation (2.1a,b), the transformation area has to be divided into so-called patches (fig. 2.1b) with individual datum parameter sets  $d^j$  (accordingly the term COPAG = Continuously Patched Georeferencing).

In the example of applying the COPAG concept to the plan German DHDN network, the average residual was reduced from 0.33 m (only one patch and datum set  $d$  for the whole area of Germany, fig. 2.1, left) to a range of less than 0.02 m by the division of the transformation area into 177 patches with individual datum parameters  $d^j$  (fig. 2.1, right). To achieve a continuous and homogenising transformation, appropriate continuity conditions  $C(d^j, d^{j+1})$  - in analogy to these of the DFHRS concept (3.6f) - along the borders of neighbouring patches  $j$  and  $(j+1)$  have to be set up as additional condition equations concerning neighbouring parameter sets  $d^j$  and  $d^{j+1}$ , in order to complete the COPAG adjustment approach (2.1a,b,h) [26].

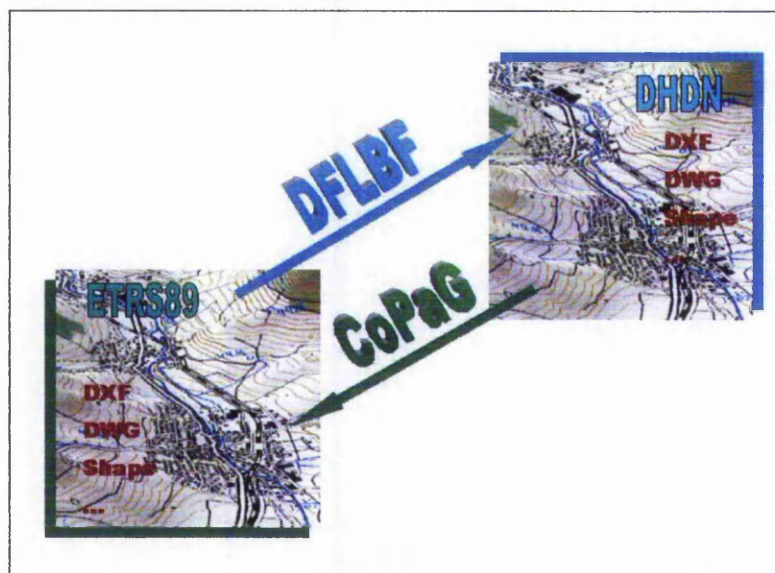


Fig. 2.2a, b:

Left: DFLBF\_DB for the transformation from ETRS89 to a classical plan reference system.

Right: COPAG\_DB for the transformation from a classical plan reference system to ETRS89.

The present COPAG\_DB and the DFLBF\_DB (Digital Finite Element Plan Reference System Transformation, in analogy to the term DFHBF, chap. 3) allow the strict and neighbourhood consistent transformation from/to the classical German reference-

systems (e.g. DHDN in Western Germany presented in fig. 2.1 and RD83 in Eastern Germany) to/from ETRS89 with a reproduction quality of (3-5) cm.

## **2.3 COPAG Software and COPAG/DFLBF\_DB Access Software**

The COPAG approach (2.1a-h) was realized in the COPAG-Software ©Jäger/Kälber, which allows the computation of transformation parameters  $d^j$  on dividing the whole transformation area into an arbitrary number of irregular patches (fig. 2.1b) and introducing the additional continuity conditions  $C(d^j, d^{j+1})$  to achieve the continuity of the total set of parameters and the homogenisation of the transformed configuration. The quality control is – in addition to standards of statistical testing – performed by regarding the quality measure of reproduction values. The two-dimensional reproduction values are evaluated in the COPAG concept and software in analogy to these of the quality control concept of DFHRS computation (see chapter 3.3.2).

As concerns software for a direct access to the COPAG\_DB and DFLBF\_DB produced with the COPAG software, as well for the DFLBF\_DB based computation of so-called LSKS-files for Leica Geosystems GNSS equipment, it is referred to [28].

## **2.4 Outlook to the COPAG Concept and COPAG/DFLBF\_DB**

The COPAG\_DB provide the direct transformation (no identical points) of the classical plan networks and related DB positions to the ETRS89 datum (fig. 2.2b), and the DFLBF\_DB (fig. 2.2a) are used vice-verse for the direct transformation (no identical points) of ETRS89 related GNSS positions in SAPOS®- and ascos® GNSS positioning to the classical plan datum systems.

The further development of the (3-5)\_cm data bases, which is directed to the computation of a "1\_cm\_COPAG\_DB/DFLBF\_DB for Germany" is merely a question of the number and density of further identical points. This is to be concluded from successful test computations for the area of Rheinland-Pfalz, Germany, where a number of 2500 identical points was used to evaluate the respective continuous transformation parameters sets  $d = (d^1, \dots, d^j, \dots, d^n)$  enabling a mean reproduction quality of 1\_cm.

The weak-form problem (fig. 2.1, left) is of general nature, and it concerns all classical networks all over Europe and the whole world respectively. So the COPAG concept can be applied generally to solve the related transformation problems and to evaluate precise and economic COPAG\_DB and DFLBF\_DB worldwide.

# **3 GNSS-Heighting - Precise Vertical Height Reference Surface Representation by the Digital FEM Height Reference Surface Concept (DFHRS) and DFHRS Data Bases**

## **3.1 Motivation and Situation**

Standard heights  $H$  are referring to different types of height reference surfaces (HRS). The common root of all three relevant HRS-types is the idea, that the HRS should be that equipotential surface of the earth's gravity field with a potential  $W_0$ , which coincides

with the normal potential  $U_0$  and the mean sea-level surface  $H=0$  (fig. 3.1, fig. 3.2)<sup>1</sup> and continues it outside the oceans. The datum of a height system is fixed by at least one point with an assigned value  $W_0$  and  $H=0$ . The height  $H_P$  of any point  $P$  on the earth's surface (ES) is then defined as the curved distance between  $P$  and the respective HRS (fig. 3.1; fig. 3.2).

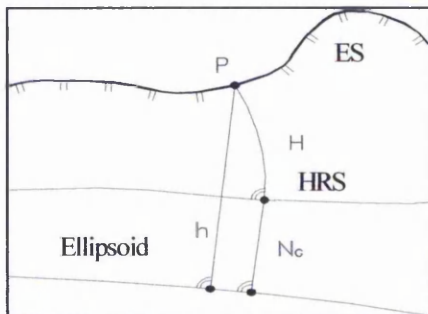
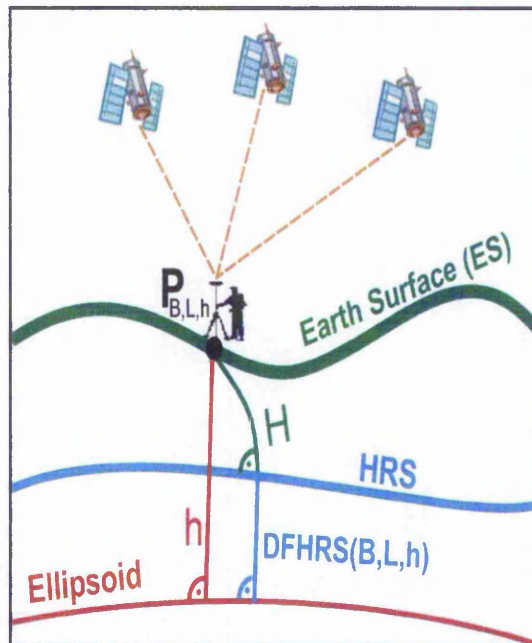


Fig. 3.1 (above): Formula ideal (1a): earth surface (ES) at position  $P(B,L)$ , ellipsoidal GPS/GNSS height  $h$ , standard height  $H$  and a two-dimensional HRS model  $N_G$ .

Fig. 3.2 (right): In real world GNSS-positioning the extended formulas (1b,c) and a three-dimensional HRS model  $N_G(B,L,h)$  however have to be taken into account.



The two modern standard HRS-types are the geoid and the so called quasi-geoid. The geoid HRS type realizes exactly the equipotential surface concept. The related so-called orthometric heights  $H_{\text{orth}} = (W_0 - W_P) / \bar{g}$  or  $H_{\text{orth}} = C_P / \bar{g}$  respectively are found, by dividing the geopotential number  $C_P$  (difference between  $W_0$  and the point  $P$  potential  $W_P$ ) by the mean gravity value  $\bar{g}$  between  $P$  and the HRS. A disadvantage of a HRS type of a geoid and a related orthometric height system  $H_{\text{orth}}$  is however due to the fact, that density assumptions for the area of  $P$  are needed to evaluate  $\bar{g}$ . The quasi-geoid HRS and the respective so-called normal heights  $H_{\text{normal}} = C_P / \bar{\gamma}$  as an alternative HRS and height systems  $H$  are found by dividing the geopotential number  $C_P$  by the mean gravity value  $\bar{\gamma}$  taken from the normal potential between  $P$  and HRS. Here the modern standard for the normal potential and  $\bar{\gamma}$  is related to the GRS80. The value  $\bar{\gamma}(B,h)$  is free from any density hypothesis. Therefore the decision for the new HRS and height type  $H$  for the European reference system EUREF was met for the quasi-geoid and normal height type respectively (EUREF symposium, Ankara 1996, resolution No. 10, see [3]).

The most precise way to determine the standard height of a point  $H_P$  of the earth's surface (ES) is based on levelling, or better levelling and gravity measurements in

<sup>1</sup> For the new Europe normal height system presently the Normaal Amsterdams Peils (NAP) [20]

higher order networks, meaning by the realization of the geopotential number  $C_P$  as  $C_P = \sum g_i \cdot \Delta n_i$ .

The recent adjustment of the normal height  $H$  related European Vertical Network - as part of new European Vertical Reference System (EVRS) - was based on  $C_P$  and is ready on the continental level [20]. The accuracy as e.g. predicted to be 5 cm on continental level [5] is kept. The short-wave precision of the adjusted height differences  $\Delta H$  of neighbouring points in the different European national networks of lower order is of course better and represented in the low sub-cm range [20].

The GNSS-based determination of standard heights  $H$  on any accuracy level however requires principally the transition of the ellipsoidal GNSS height  $h$  to the standard height  $H$ . So a GNSS-based determination of standard height  $H$  makes it necessary to subtract the height  $N_G$  of the height reference surface (HRS) from the ellipsoidal GNSS height  $h$  (fig. 3.1; fig. 3.2). Therefore the HRS must be represented relative to the ellipsoid surface in terms of a two-dimensional HRS model  $N_G(B,L)$ . The old term "geoid" and "geoid height" for the HRS model and  $N_G(B,L)$  (fig. 3.1) are getting properly replaced by "HRS" and "height of the HRS (fig. 3.2, DFHRS)", which is more convenient with respect to the above mentioned different standard HRS and height types <sup>2</sup>.

The classical gravity related geoid or quasi-geoid models  $N_G(B,L)$ , such as EGG97 [1], EGM96 [13] ) and the large number of local and regional geoid models are not fitted to the HRS. This is for the reason, that the geometrical information of the identical points ( $h,H$ ) is in general not taken into account art of a "geoid-computation" approach. A quasi-geoid for example is computed based on the Stokes formula as

$$N_G(B,L) = \frac{a}{4\pi \cdot \gamma(B)} \iint_{\sigma} \Delta g \cdot S(\psi) \cdot d\sigma \quad (3.1a)$$

(in practice of course in the so-called remove restore technique [1] and so due to a basic gravity reference e.g. EGM96 [13]). The precise information of the type

$$N_G(B,L) = (h - H)_{B,L} \quad (3.1b)$$

remains however unused in most of all geoid approaches. So the ideal formula

$$H = h - N_G(B,L) \quad (3.2)$$

fig. 3.1 does not hold for the use of standard HRS in terms of "geoid-model" in GNSS-based heighting. In spite of a however sufficient HRS shape representation in the short wave range, HRS models represented by standard geoid models (3.1a) suffer from medium and long waved systematic shape deflections. The reasons are again a big amount of both types of "weak forms" (chap. 2). Also for locally and short waved precise geoid models, e.g. the EGG97 [1], the "weak-form" deflections reach a "meter range" over large areas e.g. for Europe (fig. 3.3).

Of course the HRS represented by the standard height system  $H$  and  $h$  (3.1b) is also subjected to "weak-forms" in  $H$  and  $h$ , but their amount is much smaller. For  $H$  they reach only in a "cm" range or a "few cm" range respectively in large areas [5], [15]. For Europe and the EVRS, see [5]. Consequently "levelled heights"  $H$ , which were

<sup>2</sup> For historical reasons even some types more exist, such as e.g. the NN-type of HRS and the respective spheroidal normal heights ("NN-heights") as precursor of the normal heights.

evaluated from geopotential numbers (levelling and gravity) and the respective precise ellipsoidal heights  $h$  are representing by (3.1b) the precise and discrete control points for the long and short-wave domain of the HRS shape, while geoid-models of standard type  $N_G(B,L)$  (3.1a) (fig. 3.3) can be used only as observations concerning the HRS shape in the local short wave domain.

An additional reason why (3.2) is not valid, is because of a scale difference  $\Delta m$  occurring between the GPS/GNSS-heights  $h$  and the heights  $H$  of the standard height system ([2], [3], [18], [19]). One reason for scale inconsistency  $\Delta m$  is, that most existing standard height systems  $H$  were not evaluated by the GRS80 normal gravity field  $\gamma(B,h)$ . Other proved sources for scale effects  $\Delta m$  are occurring due to neglected (hidden) observation correlations and related stochastic weak-forms [5] and different systematic error types in levelling ([5], [10]). All these systematics tend to imply a scale error  $\Delta m$ . So, all in all, the above formula ideal (3.2) has to be modified with respect to "real world conditions". In classical approaches ([2], [3]) and software packages like HEIDI2©Dinter/Illner/Jäger [3], which use explicitly geoid models  $N_G(B,L)$  (3.1a), the relation between GNSS heights  $h$  and standards heights  $H$  reads:

$$H = h - \frac{(N_G(B,L) + \partial N(\mathbf{d}_{local}) + NFEM(p | B, L)) - \Delta m_{regional} \cdot H}{\text{Uncontinuous "3 component" HRS}} \quad (3.3a)$$

The formula (3.3a) represents the so-called "geoid-refinement approach" [3], [11], [14]. Here the geoid model heights  $N_G(B,L)$  are used both as observations and as unknowns. So the geoid-model heights  $N_G(B,L)$  become part of the HRS together with additional local datum parts  $\partial N(\mathbf{d}_{local})$ ,  $\mathbf{d}_{local}^T = [u, v, w, \varepsilon_x, \varepsilon_y, \Delta m_G]$  and an additional refinement  $NFEM(p|B,L)$  component.

The refinement part  $NFEM(p|B,L)$ , which is described theoretically in chap. 3.2, is based on the same mathematical concept of a surface representation as in the DFHRS concept. But it has a quite different meaning in the DFHRS concept than in the above classical geoid-refinement approach (3.3a). With respect to the determination of new points in the geoid-refinement approach (3.3a), the final HRS is to be considered as a compound of 3 components – the original and unimproved geoid-model  $N_G(B,L)$ , the local datum-parts  $\partial N(\mathbf{d}_{local})$  and the refinement  $NFEM(p|B,L)$ . The compound of a three component HRS would be a badly portable and heterogeneous concept for a data base in online GNSS heighting. Therefore the geoid refinement approach (3.3a) is in practice a post-processing solution. Above this, the effect of the local datum-parts  $\partial N(\mathbf{d}_{local})$  of the geoid-model(s) (3.3a) introduced in the total area (3.3a), reading explicitly [3]

$$\begin{aligned} \partial N_G(\mathbf{d}) = & [\cos(L) \cdot \cos(B)] \cdot u + [\cos(B) \cdot \sin(L)] \cdot v + [\sin(B)] \cdot w \\ & + [e^2 \cdot N(B) \cdot \sin(B) \cdot \cos(B) \cdot \sin(L)] \cdot \varepsilon_x + [-e^2 \cdot N(B) \cdot \sin(B) \cdot \cos(B) \cdot \cos(L)] \cdot \varepsilon_y \\ & + [-N_G] \cdot \Delta m_G \end{aligned} \quad (3.3b)$$

is not controlled with respect to the continuity of the 3 component HRS model at the borders of the local areas. These are some decisive disadvantages of the "geoid refinement" approach (3.3a).

In the DFHRS approach [11], [16], [17], [18], [21], [22], [23] and the computation of DFHRS\_DB [14], [26], [27], [28] for GNSS-based heighting, which are further treated as

main subject of chap. 3, however the role of the former 3-component HRS model (3.3a) is completely taken over by the 1-component HRS model of a Digital Finite Element Height Reference Surface (DFHRS). The DFHRS modelling the HRS is described continuously by the surface NFEM(p|B,L).

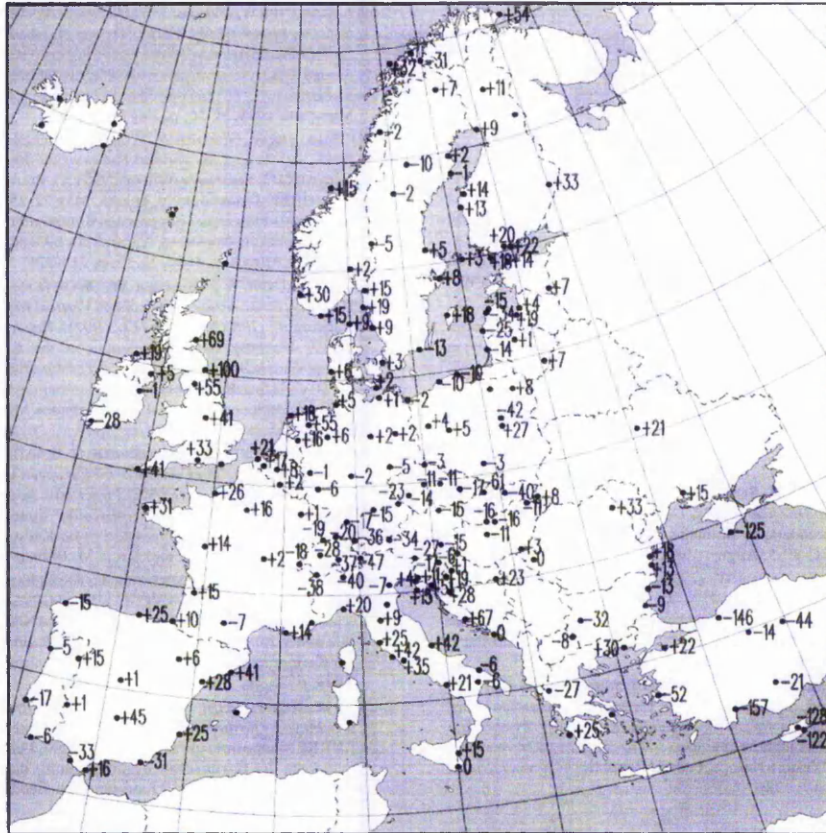


Fig. 3.3.: Long-waved deflections, to be declared as natural and stochastic "weak-forms" (chap.1), in the (dm – meter) range of the EGG97, which has above a cm-accuracy concerning the local shape quality (EUREF series)

The two-dimensional Finite Element Model (FEM) NFEM(p|B,L) (3.5a) of the HRS takes over the role of the HRS (fig. 3.1; fig. 3.2), and is represented in a continuous way by mesh-wise sets of polynomial parameters p (3.5b). So we have for the DFHRS concept the following basic relation between the ellipsoidal GNSS height h and the standard height H (fig. 3.1; fig. 3.2):

$$H = h - \underbrace{\text{NFEM}(p | B, L)}_{\text{Continuous "1 component" HRS}} - \Delta m_{\text{regional}} \cdot H \quad (3.4a)$$

In this way the continuous Finite Element Model NFEM(p|B,L) of the HRS is a two-dimensional function of the plan position (B,L), and is accordingly called the "geoid-part" of the so-called three-dimensional DFHRS correction. The part  $\Delta m \cdot h$  is accordingly

called the "scale part" of the DFHRS correction. So three-dimensional DFHRS correction DFHRS(B,L,h) (fig. 3.2), which has to be subtracted from the GNSS height h in order to receive the standard height H, reads in total:

$$H = h - \text{DFHRS}(\mathbf{p}, \Delta m | B, L, h) = h - (\text{NFEM}(\mathbf{p} | B, L) - \Delta m \cdot H) \quad (3.4b)$$

The respective DFHRS data bases (DB) contain - as essential parts for HRS representation and the scale parametrisation - the "DFHRS\_DB parameters"  $\mathbf{p}$  and  $\Delta m$ .

### 3.2 FEM representation of a Height Reference Surface (DFHRS)

The finite element representation NFEM( $\mathbf{p}|x,y$ ) is carried by the base functions of bivariate polynomials of degree N, which are set up in regular or irregular meshes. If we describe with  $\mathbf{p}^i$  the polynomial coefficients ( $a_{00}, a_{10}, a_{01}, a_{20}, a_{11}, a_{02}, \dots$ )<sup>i</sup> of the i-th mesh, we have for the height NFEM( $\mathbf{p}^i|x,y$ ) of the HRS over the ellipsoid (fig. 3.1; fig. 3.2) in the i-th mesh:

$$\text{NFEM}(\mathbf{p}^i | x, y) = \mathbf{f}(x(B,L), y(B,L)) \cdot \mathbf{p}^i ; i = 1, m; \text{ with} \quad (3.5a)$$

$$\mathbf{p}^i = (a_{00}, a_{10}, a_{01}, \dots)^i \text{ and } \mathbf{f}(x(B,L), y(B,L)) = (1, x, y, x^2, xy, y^2, \dots) \quad (3.5b), (3.5c)$$

The vector  $\mathbf{f}$  means the so called Vandermond vector and contains the different powers of the coordinates (x,y) according to the polynomial degree n. The total parameter vector  $\mathbf{p}$  consists of the coefficient sets  $\mathbf{p}^i = (a_{j,k})^i$ , ( $j=0,N; k=0,N$ ) of all m meshes. The plan position in (3.5a,c) is due to metric ellipsoidal coordinates ( $y(B,L)$ ="East" and  $x(B,L)$ ="North") introduced e.g. as Mercator or Lambert coordinates, which are in any case functions of the geographical coordinates (B,L).

To imply a continuous surface NFEM( $\mathbf{p}|x,y$ ), one set of continuity conditions of different type  $C_{0,1,2}$  has to be set up for the computation of NFEM( $\mathbf{p}|x,y$ ) for each couple of neighbouring meshes (fig. 3.4). The continuity type  $C_0$  implies the same functional values, the continuity type  $C_1$  implies the same tangential planes and the continuity type  $C_2$  the same curvature along common mesh borders of the DFHRS as represented by NFEM( $\mathbf{p}|x,y$ ) (3.5a). The continuity conditions occur as additional observation equations  $C(\mathbf{p})=0$  to be added to the parametrization of NFEM( $\mathbf{p}|x,y$ ). The condition equations  $C(\mathbf{p})=0$  are related to the polynomial sets of the coefficients ( $a_{jk}$ )<sup>m</sup> and ( $a_{jk}$ )<sup>n</sup> of each couple of neighbouring meshes m and n. To force e.g.  $C_0$ -continuity, the difference  $\Delta N_{m,n}$  in the geoid height  $N_G$  of any point S at the common border SA-SE of two meshes m and n (see fig. 3.4; fig. 3.8) has to become zero. So the basic condition equation for a polynomial representation of N-th degree reads [22]:

$$\Delta N_{m,n} = \sum_{j=0}^N \sum_{k=0}^{N-j} (a_{jk,n} - a_{jk,m}) \cdot (y_{SA} + t \cdot (y_{SA} - y_{SE}))^j \cdot (x_{SA} + t \cdot (x_{SA} - x_{SE}))^k \equiv 0 \quad (3.5d)$$

With ( $y_{SA}, x_{SA}, y_{SE}, x_{SE}$ ) we introduce the plan metric coordinates of the nodal points SA and SE of a mesh borderline. Equation (3.5d) represents a polynomial of n-th degree parametrized in the border line parameter  $t (t \in [0,1])$ . The subset of (N+1)  $C_0$ -continuity condition equations  $C(\mathbf{p})=0$  for the border between mesh m and n results in case of  $C_0$ -continuity from (3.5d) by setting all (N+1) coefficients related to t to zero ([22]).

The mesh size and mesh shape for the computation of the NFEM( $\mathbf{p}|x,y$ ) - representing the so called HRS or "geoid" part (3.3a) of the DFHRS correction and DB content - may be chosen with an arbitrary shape. The best approximation of a HRS by NFEM( $\mathbf{p}|x,y$ ) results of course by introducing small meshes, e.g. in a range of 5 km to keep a 5 mm range for any HRS shape approximation by a polynomial degree up to  $n=3$ .

A special advantage and characteristic of the NFEM( $\mathbf{p}|x(B,L), y(B,L)$ ) representation consists in the fact, that the nodal points of the FEM grid are totally independent of the location of the geodetic observations and the geoid data points. In principle any type of HRS and height related observation data can be used for the determination of the parameter vector  $\mathbf{p}$  of NFEM( $\mathbf{p}|x,y$ ), namely height observations ( $h,H,\Delta H,\Delta h$ ), the geoid-model heights  $N_G(B,L)$ , deflections of the vertical ( $\xi,\eta$ ) and gravity anomalies  $\Delta g$  (see chap. 3.3).

### 3.3 Digital FEM Height Reference Surface (DFHRS) Approach and Computation

#### 3.3.1 Mathematical Adjustment Model

The mathematical model of the so-called DFHRS data base production step reads in the system of observation equations (functional model) and the corresponding stochastic models of a least squares adjustment as follows:

##### Functional Model

$$h + v = H + h \cdot \Delta m + \mathbf{f}(x, y) \cdot \mathbf{p},$$

with NFEM( $\mathbf{p}|x,y$ ) =:  $\mathbf{f}(x,y) \cdot \mathbf{p}$

$$N_G(B, L)^j + v = \mathbf{f}(x, y) \cdot \mathbf{p} + \partial N_G(\mathbf{d}^j)$$

$$\xi + v = -\mathbf{f}_B / M(B) \cdot \mathbf{p} + \partial B(\mathbf{d}_{\xi, \eta})$$

$$\eta + v = -\mathbf{f}_L / (N(B) \cdot \cos(B)) \cdot \mathbf{p} + \partial L(\mathbf{d}_{\xi, \eta})$$

$$H + v = H$$

$$C + v = C(\mathbf{p})$$

##### Observation Types and Stochastic Models

Uncorrelated observations of ellipsoidal heights  $h$  Covariance matrix  $C_h = \text{diag}(\sigma_{h_i}^2)$ . (3.6a)

Correlated geoid height observations. With a given real covariance matrix  $C_{N,G}$  or a  $C_{N,G}$  evaluated from an artificial covariance function. (3.6b)

Observations of vertical deflections ( $\eta, \xi$ ). Pairwise correlated or uncorrelated among each other in case of astronomical observations. Correlated in case of being taken from a gravity potential model. (3.6c)

(3.6d)

Uncorrelated standard height  $H$  observations with covariance matrix (3.6e)

$$C_H = \text{diag}(\sigma_{H_i}^2).$$

Continuity condition equations (3.5d) introduced as uncorrelated so-called pseudo observations with accordingly small variances and high weights. (3.6f)

With  $\mathbf{f}_B$  and  $\mathbf{f}_L$  we introduce the partial derivatives of the Vandermonds' vector  $\mathbf{f}(x(B,L), y(B,L))$  (3.6c) with respect to the geographical coordinates  $B$  and  $L$ .  $M(B)$  and

$N(B)$  mean the radius of meridian and normal curvature at a position  $P(B,L)$  respectively. The continuity of the resulting HRS  $NFEM(p|x,y)=f(x,y) \cdot p$  is automatically provided by the continuity equations  $C(p)$  (3.6f).

A number of identical points  $(h, H)$  (3.1b) is introduced by the observation equations (3.6a) and (3.6e). In the practice of DFHRS data base evaluation, also one or a number of several geoid models  $N_G(B,L)^j$  are used as additional observations to produce DFHRS\_DB in the least squares estimation (3.6a-g). To reduce the effect of medium or long waved systematic shape deflections, namely the natural and stochastic "weak-forms" (chap. 2) of geoid models  $N_G$  (3.6b) (fig. 3.3), the geoid model heights observations  $N_G$  (3.6b) are parted to into a number of so-called "geoid-patches"  $N_G(B,L)^j$  (3.6b) (see fig. 3.8). Each patch is set up, with individual datum-parameters  $d^j$ , which are introduced by the datum part  $\partial N_G(d^j)$  (3.3b) into (3.6b). It is of course also possible to introduce by  $N_G(B,L)^j$  - and a respective parametrization  $\partial N_G(d^j)$  - (3.6b) several patched or unpatched geoid models in the same area, and of course also geoid models of a different type than the classical ones  $N_G$  (3.1a) may be used.

With  $\partial B(d_{\xi,\eta})$  and  $\partial L(d_{\xi,\eta})$  we describe the datum parts concerning observation of the type deflections of the vertical  $(\xi,\eta)$  respectively.

Observations form classical geoid models  $N_G$  (3.6b) are to be introduced instead of the original gravity observations  $\Delta g$ , which had been introduced for the computation of  $N_G$ . In this case the correlated geoid models observations  $N_G$  (3.6b) and original gravity observations  $\Delta g$  lead to identical results for the HRS by the parameters  $p$  ([22], [23]). So the use of observation type  $N_G$  (3.6b) allows a more elegant data treatment than the original gravity anomalies  $\Delta g$  (3.6g). Consequently observation equations for gravity observations  $\Delta g$

#### Functional Model

$$\frac{a}{4\pi \cdot \gamma(B)} \iint_{\sigma} \Delta g \cdot S(\psi) \cdot d\sigma + v = f(x,y) \cdot p$$

$$= NFEM(p | x,y)$$

#### Observation Types and Stochastic Model

Vector of reduced gravity anomalies  $\Delta g$  introduced with covariance matrix  $C_g$  into (3.6g) Stokes formula. The gravity anomalies  $\Delta g$  in this way determine the DFHRS with parameters  $p$  at position  $(x(B,L),y(B,L))$ .

need to be set up in the DFHRS approach (3.6a-g), only if additional gravity observations  $\Delta g$  occur, which have not yet been used for the former computation of a geoid model  $N_G$  (3.6b).

The approach (3.6a-g) means all in all a new method and standard (fig. 4.1), both for the over-determined boundary value problem (geoid-determination), and for the solution of a direct and online GPS/DGNSS-heighting (fig. 4.1) by the use of DFHRS databases and the DFHRS correction (3.4b).

### **3.3.2 DFHRS Software and Quality Control in DFHRS\_DB Computation**

The DFHRS approach (3.6a-g) has been realized in the software DFHBF©Jäger/Schneid/Schwarzer. There the mathematical model of the DFHRS approach (6a-g) is embedded in the quality control standards of a priori and a posteriori variance related tests (datasnooping) and variance component estimations.

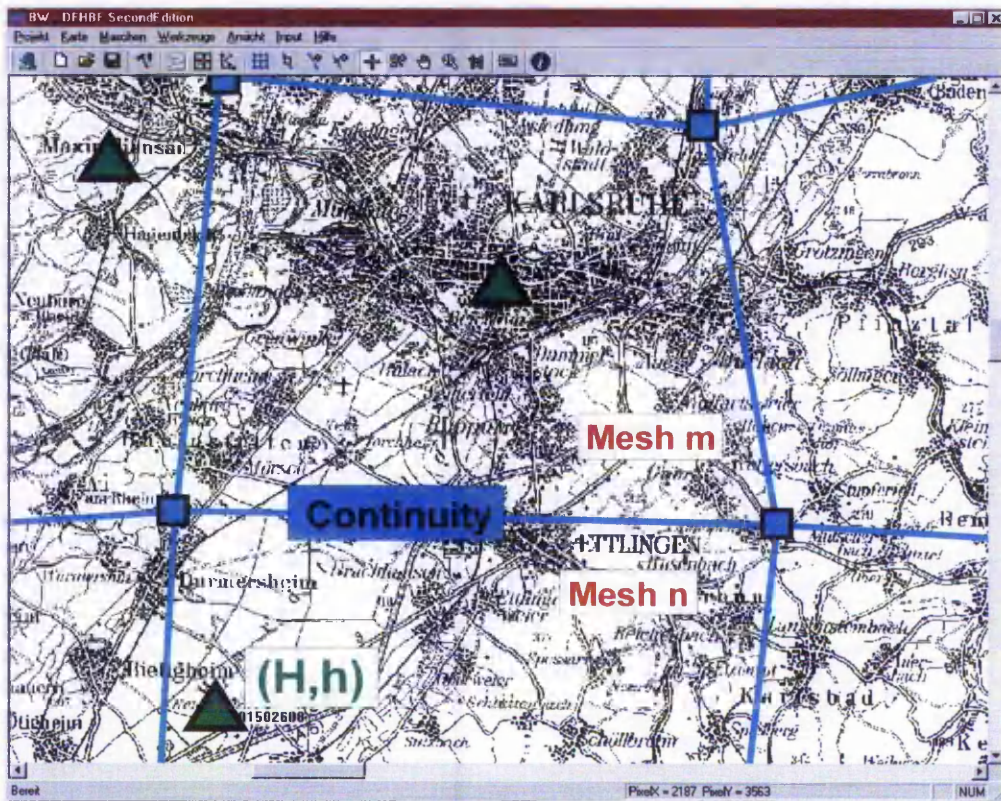


Fig. 3.4: Screen shot on the DFHRS software. Continuity of the resulting HRS along the mesh borders of two general meshes  $m$  and  $n$  is provided by the continuity equations (3.6f). Identical points (3.1b) in green.

The covariance matrix of the resulting DFHRS\_DB parameters  $(\mathbf{p}, \Delta m)$  can be used to compute and visualize the precision of the HRS and/or DFHRS correction surface (fig. 3.5).

An additional and valuable way to prove the “external accuracy” of the DFHRS\_DB is to compute a so-called to “reproduction quality” and point-wise reproduction values [16], [17], [18]. The “reproduction quality” and a number of  $n$  resulting “reproduction values  $\nabla H_i$ ” - all over the DFHRS area - are simply defined by the values of differences:

$$\nabla H_i = H_i - H_i(\text{DFHRS}_i; (= \text{without } H_i)), \text{ with} \quad (3.7a)$$

$$H_i(\text{DFHRS}_i) = h_i - \text{DFHRS}_i(\mathbf{p}, \Delta m | (B, L, h)_i)$$

For this quality proof no explicit “control measurements” are needed. We just have to compute successively the “DFHRS-height”  $H(B, L, h, \text{DFHRS})_i$  of each of the  $n$  identical standard height points  $H_i$  from  $h_i$ , when using the individual data base  $\text{DFHRS}_i$ , where  $H_i$  was excluded from the respective DFHRS\_DB production (3.6a-g) (“new point”), which was then evaluated with the rest of the  $(n-1)$  points.

The "reproduction values"  $\nabla H_i$  are much more objective and informative than the pure least squares residuals  $v_i$  (3.6e). The reproduction values  $\nabla H_i$  are to be computed in the unique DFHRS production step (3.6a-g) of the DFHRS adjustment. The respective formula reads:

$$\nabla H_i = - \frac{v_{H_i}}{r_{H_i}} \quad (3.7b)$$

With  $v_{H_i}$  and  $r_i$  we describe the correction and the redundancy part of  $H_i$  in equation (3.6e).

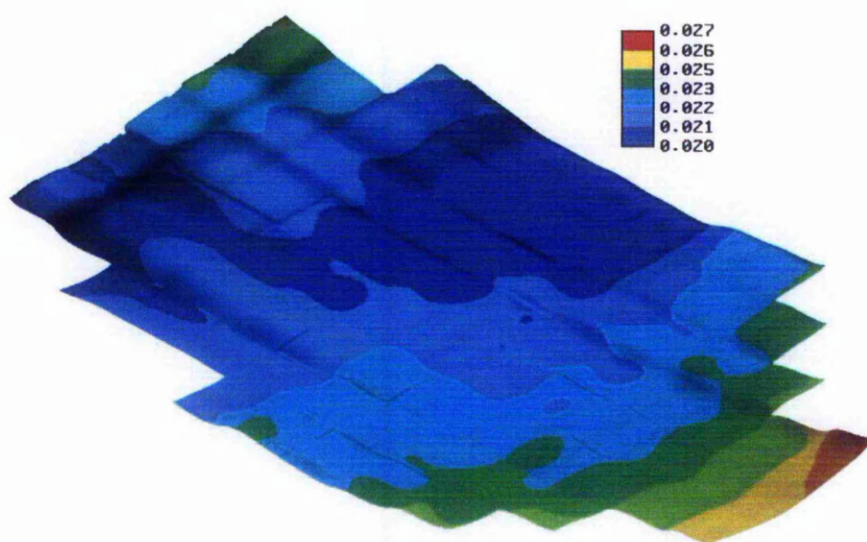


Fig. 3.5: Precision surface of the (2-3)cm DFHRS of the district Windhuk, Namibia [24], [25]

### 3.4 DFHRS\_DB Contents and DB Access Software

The essential adjustment unknowns of the mathematical model (3.6a-g) and parameters of resulting DFHRS DB are  $\mathbf{p}$  and  $\Delta_m$ . These represent the continuous model  $NFEM(\mathbf{p}|x(B,L),y(B,L))$  of the HRS (fig. 3.1; fig. 3.2; fig. 3.7) and enable an additional scale correction  $\Delta_m \cdot H$ . So these parameters provide the DFHRS correction  $DFHRS(\mathbf{p}, \Delta_m | B, L, h)$  (3.4b) for an online or post-processed GNSS heighting. So, below the header (version name etc.), a DFHRS DB contains a second block with the mesh design (coordinates of the mesh nodal points, mesh number and topological description) and finally the block with the mesh-wise parameter sets  $\mathbf{p}$  and  $\Delta_m$ .

### 3.5 Evaluation of the European HRS as part of the European Vertical Reference System (EVRS)

#### 3.5.1 Preliminary Notes

An essential and very precious characteristic of the embedded FEM principle is, that any DFHRS\_DB and its reproduction quality (3.7a,b) respectively, which was achieved by using the DFHRS approach (3.6a-g) in a small area, is to be achieved - without loss of accuracy - in a corresponding large area scene, only provided that the density of the identical points (H,h) and the quality of the geoid information  $N_G$  are kept!

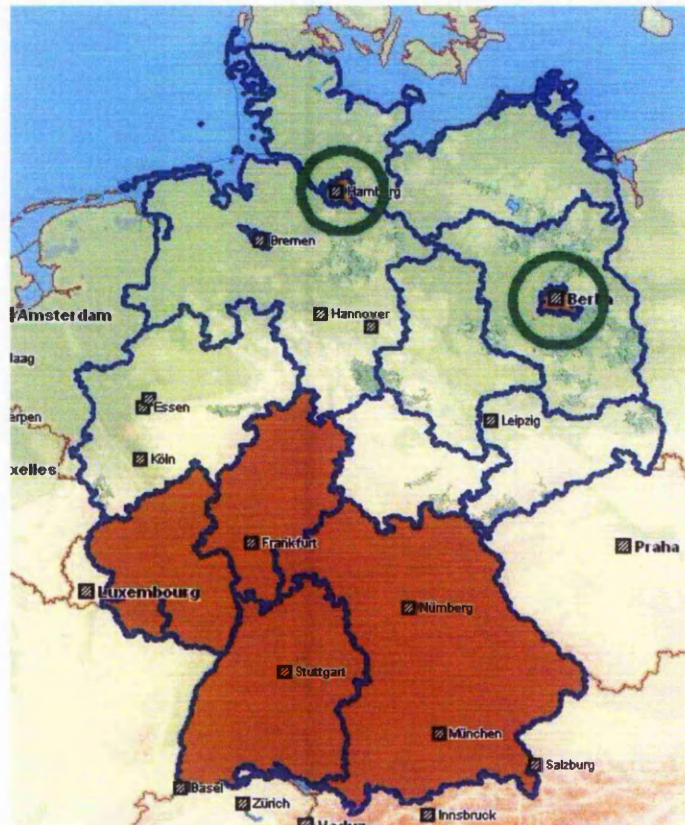


Fig. 3.6: Existing "1\_cm\_DFHRS\_DB" in the German countries Saarland, Rheinland-Pfalz, Baden-Württemberg, Hessen and Bavaria (orange) and those planned for spring 2003.

So it is clear, that a

- " $<1\text{cm\_DFHRS\_DB Europe}$ ", representing the " $1\text{cm\_EVRS}$ "

defined by a mean reproduction value  $\nabla H_i \leq 1\text{cm}$  (3.7a,b) over all statistically tested identical points (3.1b), (3.6a), (3.6e) - is to be computed by the DFHRS approach and the DFHRS software with a mesh size of 5 km, a density of about 50 identical points (H, h) per (100 km x 100 km) area, and a (30 - 40) km geoid-model "patch" size. Different " $<1\text{cm\_DFHRS\_DB}$ ", which represent the present "high end" quality type,

have already been computed [18]. They are available as official geo-data products of different German state land service departments (Saarland, Baden-Württemberg, Hessen, Rheinland-Pfalz, Bayern) [19], and they are used in SAPOS® and ascos® GNSS services in these parts of Germany (fig. 3.5).

Above these German countries presented in fig. 3.6, another “1\_cm\_DFHRs\_DB” was computed for the region of Tallinn, Estonia, and a (2-3)\_cm DFHRs\_BD was computed for the district of Windhuk, Namibia [24], [25] based on the EGM96 [13], (fig. 3.5).

The 2<sup>nd</sup> quality class of a

- “<\_3cm\_DFHRs\_DB Europe”, representing the “3cm\_EVRS”

is defined by mean reproduction value  $\nabla H_i \leq 3\text{ cm}$  (3.7a,b) over all tested identical points.

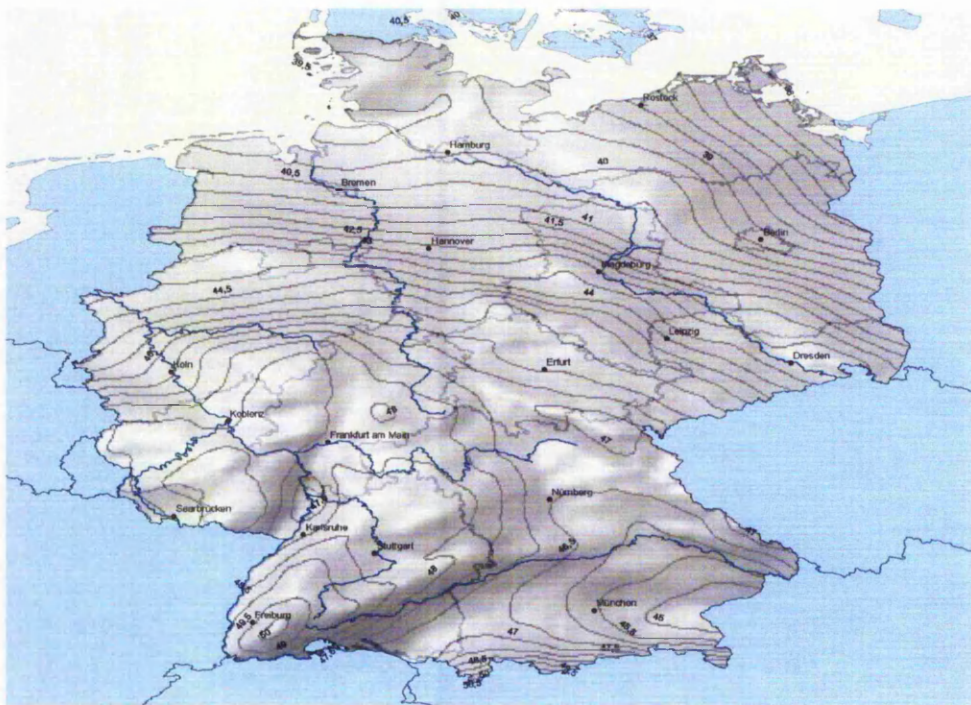


Fig. 3.7: Isolines of the HRS represented by the “3\_cm\_DFHRs\_DB Germany” for the European normal height system.

A “<\_3cm\_DFHRs\_DB Germany” was evaluated by a density of less than 10 identical points (H, h) per (100 km x 100 km) area, a mesh size of 10 km, and a polynomial degree N=3. The number of patches was 102 and the patch size was about 50 km. Fig. 3.7 shows the isolines of the corresponding HRS (fig. 3.1; fig. 3.2) NFEM(p|B,L) of the “<\_3m\_DFHRs\_DB Germany”.

It is already related to the new European normal height system. For the former West Germany another “<\_3m\_DFHRs\_DB Germany” related to the classical NN-height system was computed additionally. The “<\_3\_cm DFHRs\_DB” is applied for GNSS

online and post-processing heighting by the users of SAPOS® and ascos® DGNSS services [26], [27], [28].

### 3.5.2 EUREF requirement of a “1\_dm EVRS” – Real Data Studies and a Rapid Solution on applying the DFHRS Approach

The IAG Subcommission for Europe (EUREF) has met the decision to evaluate a continuous “<\_10\_cm European HRS”. This would mean an essential improvement of the HRS accuracy compared to the presently best European HRS, namely the EGG97 [1]. The EGG97 is continuous all over Europe, but it shows a high range of long-waved “weak-form” (chap. 1) deflections as shown in fig. 3.3. The respective EUREF Resolution No. 4, met on EUREF-Symposium at Dubrovnik, 2001 reads:

*The IAG Subcommission for Europe (EUREF) recognising the European Vertical GPS Reference Network (EUVN) with its GPS-derived ellipsoidal heights and levelled connections to UELN, – the definition of the European Vertical Reference System EVRS with its first realisation UELN 95/98, called EVRF2000, considering – this implicit pointwise realisation of a European geoid consistent with both ETRS89 and EVRS, – the existence of a large number of regional and local geoids in Europe, – the urgent need by the navigation community for a height reference surface, asks its Technical Working Group and the European Sub-commission of the IAG IGGC (International Gravity and Geoid Commission) to take all necessary steps to generate a European geoid model of decimetre accuracy consistent with ETRS89 and EVRS.*

The required

- “1\_dm DFHRS\_DB Europe” representing the “dm\_EVRS”,

may be computed in a short-term project, so to say “immediately”, by using the DFHRS concept (3.6a-g) and the DFHRS software.

Fig. 3.8 shows the design of the (25 km x 25 km) meshes (thin blue lines) and 14 patches (thick blue lines) of the designed German part of the “1\_dm\_DFHRS\_DB Europe”.

The test computations for this design German part of the “1\_dm DFHRS\_DB Europe” were performed with the DFHBF software using the 102 identical points of the 1<sup>st</sup> order German ETRS89 reference network “DREF” and geoid-model observations  $N_G$  of the EGG97. These real-data results of the DFHRS computation showed, that the design and number of the DREF identical points (h,H) (3.1b) are sufficient and provide even a mean value of 3 cm and a span-width of less than 10 cm respectively, for the reproduction values (3.7a,b) all over the German part of the “1\_dm\_EVRS”.

As 1<sup>st</sup> order ETRS89 reference networks like DREF exist all over Europe, there is no doubt, that the required “1\_dm EVRS”, is to be computed instantaneously using the DFHRS concept and software.

### 3.5.3 Conclusions and Outlook

With regard to the corresponding densities for the identical points (h, H), which are stated in 3.5.1, any quality class of a DFHRS\_DB can be achieved with the DFHRS approach (3.6a-g) in any size of area.

The DFHRS computation of the European HRS (EVRS) can be started, as soon as the EUREF community supplies the data (H, h) of the readjustment of the European Vertical Reference System EVRS [20] to the DFHRS team. The "1\_dm\_EVRS" proclaimed and required by the IAG Subcommission for Europe (EUREF) can be provided by the DFHRS concept in a short time project, based in general on the existing data (H, h) of the respective 1<sup>st</sup> Order ETRS89 networks of the European nations.

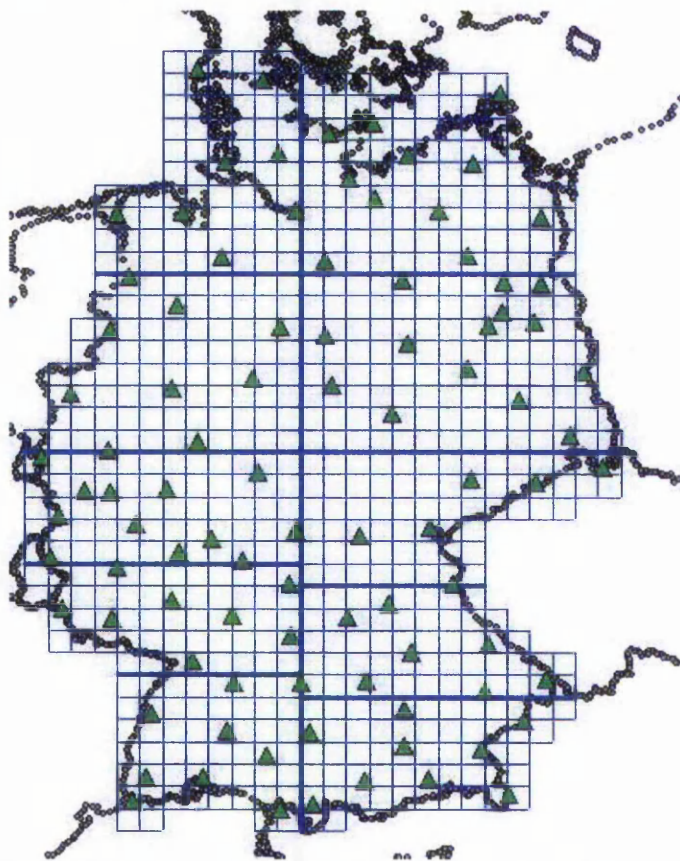


*Fig. 3.8: Design of the meshes (thin blue lines) and patches (thick blue lines) of the German part of the "1\_dm\_DFHRS\_DB Europe". The number of the 102 identical points (green) of the German 1<sup>st</sup> order ETRS89 reference network "DREF" are more than sufficient for the desired quality.*

As concerns the further development of the European EVRS, the DFHRS concept guarantees, that according to the ongoing densifications of the normal height network in the different European countries, any quality for DFHRS\_DB Europe representing the EVRS (dm  $\rightarrow$  3cm  $\rightarrow$  1cm) can be provided. The respective high end class of the DFHRS\_DB Europe can be updated and improved, respectively according to the rhythm of the EVRS densifications. The use of geoid observations  $N_G$  taken from the EGG97 [1] shows a sufficient quality for a "1\_cm HRS" quality all over in Europe. This is evident from DFHRS computations in different European countries [8], [22], [23].

Additionally the DFHRS approach (3.6a-g) contributes an effective and synergetic use and combination of the large number of existing geoid models  $N_G$  cited in the above

EUREF resolution no. 4 for the evaluation of a 1\_cm EVRS in a statistically controlled manner. So the DFHRS approach is proposed as a potential and flexible candidate for the controlled evaluation, continuation and improvement of the EVRS in the near future work to the EUREF Technical Working Group [12].

#### 4 Standardisation of DFLBF/COPAG and DFHRS Data Bases

For the implementation of a DFLBF/COPAG and a DFRHS\_DB access respectively into existing software packages (fig. 4.1), DFLBF/COPAG and DFHRS DB access software have been realized as DLL (Dynamics Link Library) [27], [28].

Company	Logo	Software	CoPaG DFLBF	DFHRS
<b>ALLSAT</b> www.allsat.de		GART2000	-	<input checked="" type="checkbox"/>
<b>GeoNav</b> www.geonav.de		DCTOOLS	<input checked="" type="checkbox"/>	<input checked="" type="checkbox"/>
<b>IBS</b> www.ib-seller.de		OLGA_PRO, USE3DIM	<input checked="" type="checkbox"/>	<input checked="" type="checkbox"/>
<b>LEICA Geosystems</b> www.leica-geosystems.com		SKI-PRO SR530 Software Controller	<input checked="" type="checkbox"/>	<input checked="" type="checkbox"/>
<b>THALES</b> www.thales-navigation.com		GART2000 OLGA_PRO	<input checked="" type="checkbox"/>	<input checked="" type="checkbox"/>
<b>TRIMBLE</b> (in prep.) www.trimble.com		Trimble Office 5700 Controller Software	<input checked="" type="checkbox"/>	<input checked="" type="checkbox"/>

Fig. 4.1: Growing acceptance and implementation of the DFHRS and DFLBF/COPAG database standard by the GNSS industry

Above these the DFLBF/COPAG and DFHRS\_DB access are implemented in the Windows/CE software USE3DIM [28].

The growing acceptance and the different implementations of the DFLBF/COPAG and DFHRS database standard into different GNSS equipments and software packages of the GNSS industry are shown in fig. 4.1. Besides the GNSS domain, the DB and DB access software is used and implemented into different GIS software packages. For details it is referred to [27] and [28].

#### 5 References

- [1] Denker, H. and W. Torge (1997): The European Gravimetric Quasigeoid EGG97 – An IAG supported continental enterprise. In: Geodesy on the Move – Gravity Geoid, Geodynamics, and Antarctica. R. Forsberg, M. Feissel, R. Dietrich (eds.). IAG Symposium Proceedings Vol. 119, Springer, Berlin Heidelberg New York: 249-254.
- [2] Dinter, G. and M. Illner (2001): Höhenbestimmung mit GPS am Beispiel von Pilotprojekten aus Baden-Württemberg. DVW Schriftenreihe (41). Wittwer-Verlag. ISBN 3879192766. S. 88 - 110.
- [3] Dinter, G.; Illner, M. and R. Jäger (1997): A synergetic approach for the integration of GPS heights into standard height systems and for the quality control and refinement of geoid models. In: Veröffentlichungen der Internationalen Erdmessung der Bayerischen Akademie der Wissenschaften (57). IAG Sub-commission for Europe Symposium EUREF, Ankara 1996. Beck'sche Verlagsbuchhandlung, München.
- [4] Jäger, R. (1988): Analyse und Optimierung geodätischer Netze nach spektralen Kriterien und mechanische Analogien. Deutsche Geodätische Kommission, Reihe C, No. 342, München.
- [5] Jäger, R. (1990a): Spectral Analysis of Relative and Supported Geodetic Levelling Networks due to Random and Systematic Errors. 'Precise Vertical Positioning'. Invited Paper to the Hannover Workshop of October 08-12, 1990.
- [6] Jäger, R. (1990b): Optimum Positions for GPS-points and Supporting Fix-points in Geodetic Networks. In: Ivan I. Mueller (ed.) International Association of Geodesy Symposia. Symposium No. 102: Global Positioning System: An Overview, Edinburgh/Scotland, Aug. 7-8, 1989. Convened and edited by Y. Bock and N. Leppard, Springer: 254-261.
- [7] Jäger, R. and H. Kaltenbach (1990): Spectral analysis and optimization of geodetic networks based on eigenvalues and eigenfunctions. Manuscripta Geodetica (15), Springer Verlag. S. 302-311.
- [8] Jäger, R. (1999): State of the art and present developments of a general approach for GPS-based height determination. In (M. Lilje, ed.): Proceedings of the Symposium Geodesy and Surveying in the Future - The importance of Heights, March 15-17, 1999. Gävle/Schweden Reports in Geodesy and Geographical Informations Systems, LMV-Rapport 1999(3). Gävle, Schweden. ISSN 0280-5731: 161-174.
- [9] Jäger, R. und S. Kälber (2000): Konzepte und Softwareentwicklungen für aktuelle Aufgabenstellungen für GPS und Landesvermessung. DVW Mitteilungen, Landesverein Baden-Württemberg. 10/2000. ISSN 0940-2942.
- [10] Jäger, R. and S. Leinen (1992): Spectral Analysis of GPS-Networks and Processing Strategies due to Random and Systematic Errors. In: Defense Mapping Agency and Ohio State University (Eds.) Proceedings of the Sixth International Symposium on Satellite Positioning, Columbus/Ohio (USA), 16-20 March. Vol. (2), p. 530-539.

- [11] Jäger, R. and S. Schneid (2001a): GPS-Höhenbestimmung mittels Digitaler Finite-Elemente Höhenbezugsfläche (DFHBF) - das Online-Konzept für DGPS-Positionierungsdienste. XI. Internationale Geodätische Woche in Oberurg/Österreich, Februar 2001. Institutsmittellungen, Heft Nr. 19, Institut für Geodäsie der Universität Innsbruck: 195-200.
- [12] Jäger, R. and S. Schneid (2001b): Online and Postprocessed GPS-heighting based on the Concept of a Digital Height Reference Surface. Proceedings, IAG Subcommission for Europe Symposium EUREF, Dubrovnik 2001. Bundesamt für Kartographie und Geodäsie (BEK) (Eds.) Frankfurt.
- [13] Lemoine, F.; S. Kenyon; J. Factor; R. Trimmer, N. Pavlis; D. Chinn; M. Cox; S. Klosko; S. Luthcke; M. Torrence; Y. Wang; R. Williamson; E. Pavlis; R. Rapp and T. Olson (1998): The development of the Joint NASA GSFC and NIMA Geopotential Model EGM96. NASA Goddard Space Flight Center, Greenbelt, Maryland, 20771, USA.
- [14] Meichle, H. (2001): Digitale Finite Element Höhenbezugsfläche (DFHBF) für Baden-Württemberg. DVW Mitteilungen, Heft 2. DVW Landesverein Baden-Württemberg. ISSN 0940-2942. S. 23-31.
- [15] Schmitt, G. (1997): Spectral Analysis and Optimization of two dimensional networks. Geomatics Research Australasia (67): 47-64.
- [16] Schneid, S. (2002): Software Development and DFHRS computations for several countries. J. Kaminskis and R. Jäger (Eds.): Proceedings of the 1st Common Baltic Symposium, GPS-Heighting based on the Concept of a Digital Height Reference Surface (DFHRS) and Related Topics - GPS-Heighting and Nationwide Permanent GPS Reference Systems. Riga, June 11, 2001; Riga, Latvia.
- [17] Jäger, R. (2002): Online and Postprocessed GPS-heighting based on the Concept of a Digital Finite Element Height Reference Surface (DFHRS). J. Kaminskis and R. Jäger (Eds.): Proceedings of the 1st Common Baltic Symposium, GPS-Heighting based on the Concept of a Digital Height Reference Surface (DFHRS) and Related Topics - GPS-Heighting and Nationwide Permanent GPS Reference Systems. Riga, June 11, 2001; Riga, Latvia.
- [18] Jäger, R. and S. Schneid (2002): Passpunktfreie direkte Höhenbestimmung – ein Konzept für Positionierungsdienste wie SAPOS®. Proceedings 4. SAPOS® Symposium, 21.-23. Mai 2002. Landesvermessung und Geobasisinformation Niedersachsen (LGN) (Hrsg.). LGN, Hannover. S. 149-166.
- [19] Wirtschaftsministerium Baden-Württemberg (2002): Neue Projekte und Produkte mit Kunden- und Praxisbezug im Landesbetrieb Vermessung. Festschrift „50 Jahre Baden-Württemberg – 50 Jahre Hightech-Vermessungsland. 150 Jahre Badische Katastervermessung“. Wirtschaftsministerium Baden-Württemberg (Hrsg.). S. 39-50.
- [20] Ihde, J. and W. Augath (2000): European Vertical Reference System (EVRS). In: Veröffentlichungen der Internationalen Erdmessung der Bayerischen Akademie der Wissenschaften (61). IAG Subcommission for Europe Symposium EUREF,

Schneid, S.(2003):

The Digital FEM-Height Reference Surface DFHRS of Germany. In: Proc. of the 2<sup>nd</sup> Common Baltic Symposium, GPS-Heighting based on the Concept of a Digital Height Reference Surface (DFHRS) and Related Topics - GPS-Heighting and Nationwide Permanent GPS Reference Systems. Riga, June 11, 2003.

# The Digital FEM Height Reference Surface (DFHRS) of Germany.

Sascha Schneid

Karlsruhe University of Applied Sciences  
Institut für Angewandte Forschung (IAF)

Moltkestraße 30  
76133 Karlsruhe

Email: [Schneid@fh-karlsruhe.de](mailto:Schneid@fh-karlsruhe.de)

Homepage: [www.dfhbf.de](http://www.dfhbf.de)

## Summary

The recent developments of nation-wide DGPS-Services (Differential Global Positioning System) in Europe (e.g. SAPOS, ascos, SwiPos, SwePos) enable online GNSS/GPS positioning with accuracy in the centimetre range. In recent years, there has been great progress with the development of GPS equipment and related technical DGPS network standards for ambiguity fixing, virtual reference stations and area correction parameters etc., so that real-time positioning can be very productive and accurate.

In contrast to the plan transformation problem, GPS height transformation involves a physical element. GPS-based height,  $h$ , refers to the World Geodetic System 1984 (WGS84) ellipsoid, while standard height,  $H$ , refers to a physically defined Height Reference Surface (HRS). Therefore, a transformation of the ellipsoidal GPS height,  $h$ , to the standard height  $H$  is needed. In theory, i.e. the new German height system of normal heights refers to the quasi-geoid. However, in practice, the direct use of quasigeoid models like the European Gravimetric Geoid 1997 (EGG97) or Earth Gravity Model (EGM96) is not possible. One reason is, that (quasi-)geoid models have their own datum (especially when they were developed without using identical points ( $h,H$ )) and suffer from long- and medium-waved systematic effects. Besides this, scale terms occur between the height systems.

A better way to transform ellipsoidal GPS-heights,  $h$ , into standard heights,  $H$ , is the use of a direct model of the Height Reference Surface (HRS) and a respective correction.

The concept of the Digital FEM (Finite Element Method) Height Reference Surface (DFHRS) enables the strict adjustment of available observation types related to the HRS. These are heights at identical points ( $h,H$ ), gravity anomalies  $\Delta g$ , deflections of the vertical ( $\xi, \eta$ ) as well as existing geoid models.

The resulting DFHRS data-base provides a correction  $DFHRS(B,L,h)$  to transform a GPS-height  $h$  into a standard height  $H$  in a direct mode.

In this paper, the new Digital FEM Height Reference Surface for Germany is presented. Further a mesh- or patching-design study is outlined for a so-called "light" dm solution for the European Vertical Reference System – EVRS.

## 1. Objectives of the DFHRS Computation for Germany

In recent years, the development of two DGNSS-Referencestation networks, namely SAPOS and ASCOS took place in Germany. Both services provide a positioning quality in cm range in an online mode. Parallel a big progress took place in the sector of the GPS equipments and the related technical DGPS network standards (ambiguity fixing, virtual reference station or area

correction parameters concept), so that real-time positioning has the capacity to be very accurate and economic.

In relation to the high technical state of the art however, the number of DGPS-Service users still is very small in total. A main reason is due to the fact, that in Germany a general ETRS89-georeferencing has not been realized. So uneconomical transformations related to identical points and field-calibration procedures are still a standard in DGPS applications. Meanwhile approaches for the transformation of the old DHDN-Datum to ETRF89 are [Jäger,R., et al 2003a], implemented into respective software and tested out successfully. Data bases for the transformation of DHDN to ETRS89 and ETRS89 to DHDN have recently been evaluated.

In opposite to the plan transformation problem, the GPS-height transformation has a physical nature, because GPS-based heights  $h$  refer to the ellipsoid, while standard heights  $H$  refer to physically defined Height Reference Surfaces (HRS). Hence a transformation of the ellipsoidal GPS-height  $h$  is needed (fig.1).

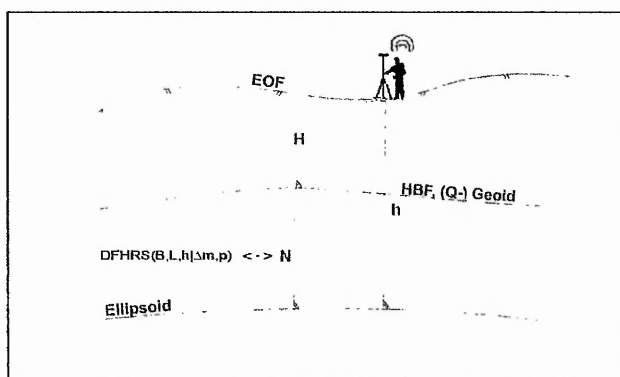


Fig.1: Scheme of the GNSS-Height using DFHRS Databases

The DFHRS is modelled as a continuous HRS in arbitrary large areas by bivariate polynomials over an irregular grid of Finite Element meshes (FEM) (Fig.2). (Quasi-)Geoid height information  $N_G$ , deflections of the vertical  $(\xi, \eta)$ , gravity observations  $(\Delta g)$  and identical points  $(h, H)$  are to be used as observations in a least squares DFHRS adjustment concerning the DFHRS parameters  $\mathbf{p}$ . Several geoid models may be introduced simultaneously and geoid models may be parted into different "geoid-patches" [Jäger, R. und S. Kälber (2000)], to reduce the influence of their long-waved systematic errors on the DFHRS result.

The resulting DFHRS parameters  $\mathbf{p}$  represent the HRS and provide the DFHRS correction  $DFHRS(B, L, h | \Delta m, \mathbf{p})$  to transform by

$$H = h - DFHRS(B, L, h | \Delta m, \mathbf{p}) \quad (1.1)$$

$$= h + \Delta m \cdot h - NFEM(B, L | \mathbf{p}) \quad (1.2)$$

ellipsoidal GNSS heights  $h$  into standard heights  $H$ . The correction  $DFHRS(B, L, h | \Delta m, \mathbf{p})$  consists of the FEM surface of the HRS ("geoid-part"  $NFEM(B, L | \mathbf{p})$ ) as function of  $(B, L)$ , and an additional "scale part"  $\Delta m \cdot h$ , to provide a completely 3D correction (1.1 – 1.2).

The resulting accuracies of the DFHRS or the correction  $DFHRS(B, L, h | \Delta m, \mathbf{p})$  respectively, may be tuned by changing the meshsize. Related investigation showed, that a meshsize up to

5 km x 5 km is representing the HRS in a quality of < 5 mm. To produce a quality <2-3cm, which is well balanced with the positioning or heighting quality respectively, in GNSS-Networks, a meshsize of 10 km x 10 km is appropriate. Hence, different standards of quality for a DFHRS\_DB may be defined, the so called <\_1\_cm\_DFHRS\_DB and the <\_3\_cm\_DFHRS\_DB. The precise version of <1cm quality has been realized for several federal states of Germany, e.g. Baden-Württemberg, Bayern, Hessen, Rheinland-Pfalz and Saarland (Jäger, R. and S. Schneid (2001a)). In cooperation with the respective state land service departments the DFHRS Databases have been computed and are already used as new geo-data products in practice. Several GNSS-Receiver-Hardware producers (i.e. Trimble, Leica, Topcon and Thales) already implented interfaces to the DFHRS\_DB.

The DFHRS concept also allows computations of updates, i.e. when new identical points (h, H) are available. These updates may also be computed by the state land service departments with their own DFHRS production software.

The new DFHRS\_DB for Germany was realized in a < 3cm quality. This accuracy is appropriate for online positioning in DGNSS-Networks. In the following chapters, the evaluation and quality control of the Digital FEM Height Reference Surface is described and approaches to produce national and international Databases in a 1cm up to a <10cm quality are discussed.

## **2. The Digital FEM Height Reference Surface for Germany**

### **Computation of the DFHRS DB**

Due to the different types of the german height-systems, spheroidal-normal heights in Western Germany and normal heights in Easter Germany three different version were produced. One for Western Germany, one for Easter Germany and a third one related to the new system of normal heights which has been derived on a continental European level (EVRS).

The necessary identical points (h, H) for the computation of the DFHRS\_DB Germany were provided by the external DFHRS-project cooperation partner (IB Seiler, Lauf, Germany, see [www.ib-seiler.de](http://www.ib-seiler.de)). Another observation group were quasigeoid-heights  $N_G$ , derived from the EGG97-quasigeoid.

The whole area was subdivided into a grid of regular FEM-meshes with 10km x 10km meshsize. To reduce the datum-problems as well as the long- and mediumwaved systematics a number of geoid-patches (i.e. 102 patches for whole Germany, see fig.2) were introduced, each with its own set of datum-parameters (1 shift, 2 rotations).

For the DFHRS\_DB Germany a number of 51923 unknowns in total had to be solved in a least-squares adjustment. These were:

- 822 standard heights H (from identical points) in cm quality
- 1 scale correction  $\Delta m$  between the heights h and H
- 520 datum parameters (1 Shift, 2 Rotations) in 102 patches
- 50590 FEM – parameters (10 for each mesh)

The system of observation equations for the used observation groups reads [Jäger, R. (2001)]:

$$H + v = H \quad (2.1)$$

$$h + v = H - h \cdot \Delta m + NFEM(B, L | \mathbf{p}) \quad (2.2)$$

$$N_G(B, L)^j + v = NFEM(B, L | \mathbf{p}) + \partial N(\mathbf{d}^j) \quad (2.3)$$

$$C + v = C(\mathbf{p}) \quad (2.4)$$

With  $\partial N(\mathbf{d}^j)$  (2.3) the datum part of the geoid heights in the  $j$ -th geoid-patch is introduced. In (2.4) a set of C-continuity conditions is introduced as observations at common borders of neighbouring FEM meshes. The derivation of these continuity conditions is treated in [Schneid, S. (2001)].

The observations (2.1-2.4) were set up in a common least-squares adjustment with the usual standards of quality control, data-snooping to detect cross errors and variance component estimation. The resulting DFHRS (Fig.3) is stored in a comprimized database and may be placed on a usual GNSS-Receiver for an online GNSS-Heighting using (1.1) or (1.2) respectively. The needed disk-storage is 552 KB.

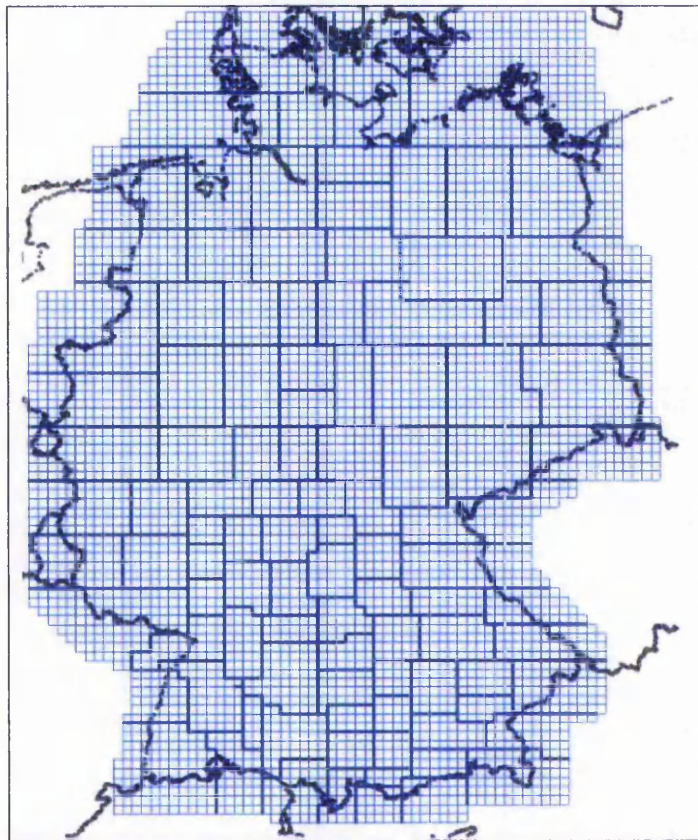


Fig.2 FEM-meshing with 102 geoid-patches of the DFHRS-Germany.

### Quality control

The DFHRS production includes a statistical quality control. Besides the standards of data-snooping to detect cross errors and variance component estimation, another very simple, but effective control is the computation of the so-called reproduction- or "Repro-value" of each identical point  $i$

$$\nabla H_i = H_{i,known} - H_{i,DFHRS} \quad (2.5)$$

$$= -\frac{v_i}{r_i} \quad (2.6)$$

where  $v_i$  and  $r_i$  mean the residual and the part of redundancy respectively.

This value  $\nabla H_i$  gives a measure for the change in the resulting DFHRS if the point  $H_{i,known}$  would not have been used in the adjustment. In case of a not significant test statistic, a big *Repro-Value*  $\nabla H_i$  at the same time with a big part of redundancy ( $r_i > 30\%$ ) indicates either inaccurate identical points or a wrong modelling of the DFHRS (i.e. meshsize too big). In case of a not significant test statistic, a big *Repro-Value*  $\nabla H_i$ , together with a small part of redundancy ( $r_i < 30\%$ ) points to a too small number of identical points in this area. The target in the computation of the DFHRS Germany, was to keep the *Repro-Value* in the range of less than 5cm.

In addition to a DFHRS correction  $DFHRS(B, L, h | \Delta m, p)$  the standard-deviation  $S_{DFHRS(B, L, h | C_{\Delta m, p})}$  is provided by the co-variance matrix of the DFHRS parameters for further analysis.

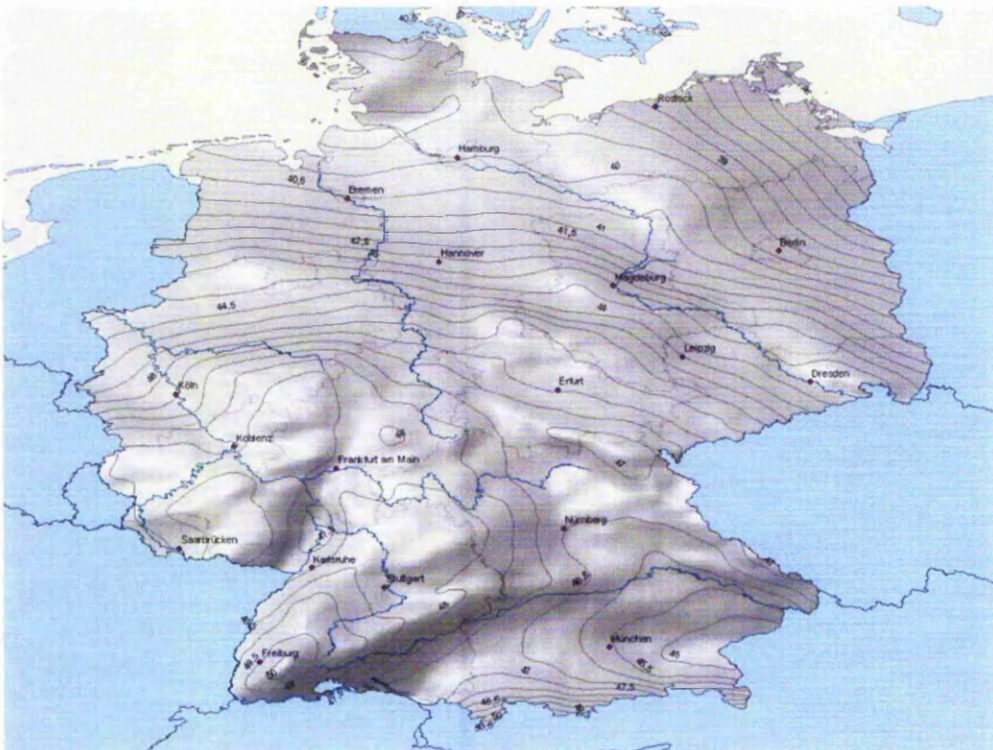


**Fig.3** Visualisation of the Digital FEM Height Reference Surface for Germany

The best and most independent control of a database of course would be measurements at any point of the related area. To simulate this at least in some places or regions (south-western Germany) respectively, available points from the database of the University of Applied Sciences Karlsruhe were used to test the external quality of the computed Databases. These points were not used in the computation of the database. They had a quality of 3 cm. So this control points have been recomputed using the DFHRS Database of Western Germany in the old system of normal-orthometric heights (“NN-Heights”).

In Fig.4 the differences between the known “NN-Heights”  $H_{known}$  and the Heights  $H_{DFHRS}$

resulting from the transformation by means of the DFHRS\_correction  $DFHRS(B, L, h | \Delta m, p)$ , are shown as a histogram. It documents, that only at 16 points of 3243 (maximum standard deviation  $\sigma_H = 3\text{cm}$ ), thus only about 0.5 %, showed a difference of more than 5 cm.

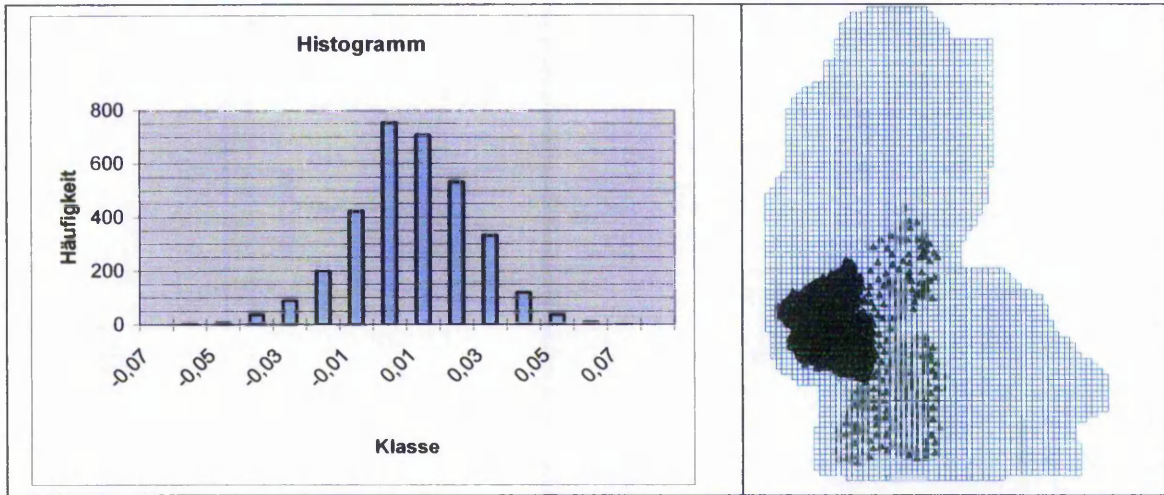


**Fig.4:** left: Histogram of the differences between known control points  $H_{\text{known}}$  which were recomputed by means of the  $<_3\text{cm\_DFHRS\_DB}$ . right: Distribution of the treated 3243 control points.

The differences (2.5) between the known height  $H$  and the heights  $H_{DFHRS}$  transformed by means of the  $DFHRS\_DB$

$$\nabla H_i = H_{i,\text{known}} - (h_i - DFHRS(B, L, h | \Delta m, p)). \quad (2.7)$$

From (2.7) a standard deviation of  $s_{H,DFHRS} = \pm 1,8 \text{ cm}$  can be evaluated using the 3243 control points. This value is representing the accuracy of the resulting heights  $H_{DFHRS}$ . Hence the standard deviation of the DFHRS correction  $DFHRS(B, L, h | \Delta m, p)$   $s_{DFHRS} < 1,8\text{cm}$  and can be approximated with

$$s_{DFHRS} = \sqrt{s_{H,DFHRS}^2 + s_{H,\text{known}}^2 + s_h^2}. \quad (2.8)$$

In Fig.5, left the estimated co-variance matrix  $C_{DFHRS}$  of Western Germany is visualised as a surface plot. It shows an accuracy of  $< 2,0 \text{ cm}$  in most parts of the surface, which is in accordance with the estimation (2.8) using the control points.

The quality control of the DFHRS germany showed, that the principle aim of the project, to compute a database in a quality of  $< 3 \text{ cm}$  has been reached and has been surpassed. In this accuracy the database is a well balanced tool for an online heighting in GNSS-networks. It can be improved by updating the computation, when new observations, i.e. identical points  $(h, H)$ , are available.

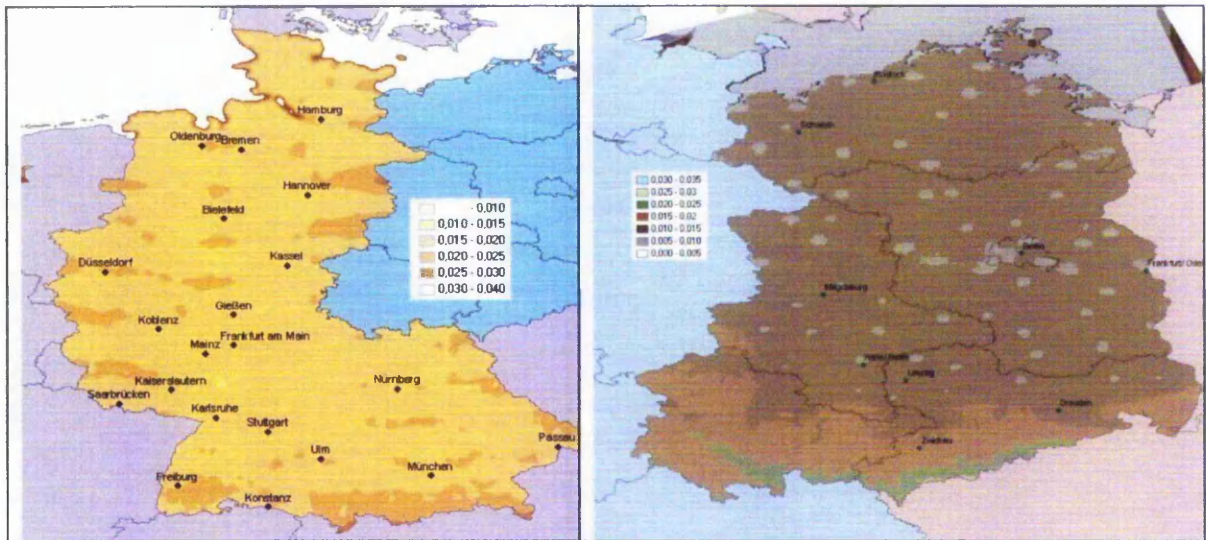


Fig.5: Visualisation of the estimated accuracy of the DFHRS western (left) as well as eastern (right) Germany.

### 3. Theoretical aspects and further development

#### Using a (quasi-) geoidmodel instead of gravity observations $\Delta g$

The identity of using a correlated (quasi-) geoidmodel  $N_G$  instead of the original gravity values  $\Delta g$  was first derived in [Jäger, R. (2001)]. So the DFHRS concept realizes a rigorous 2-step least-squares adjustment with respect to original gravity observation  $\Delta g$ .

If a a priori co-variance matrix  $C_{NG}$  is available, ie. an estimation resulting from an adjustment or an appropriate co-variance function, the (quasi-)geoid heights  $N_G$  are set up in a least-squares adjustment, together with any other height related observation  $l_o$ , with its co-variance matrix  $C_o$ . The FEM parameters  $p$  are estimated as:

$$\hat{p} = (A^T C^{-1} A)^{-1} A^T C^{-1} l = F \cdot l, \text{ and} \quad (3.3)$$

$$C_{\hat{p}} = (A^T C^{-1} A)^{-1} \quad (3.4)$$

where

$$A = \begin{bmatrix} A_{NG} \\ A_o \end{bmatrix}, C = \begin{bmatrix} C_{NG} & \\ & C_o \end{bmatrix} \text{ and } l = \begin{bmatrix} N_G \\ l_o \end{bmatrix}.$$

As often an a priori co-variance matrix  $C_{NG}$  for (quasi-)geoidheights  $N_G$  is not available, a neglect of  $\Delta C_{NG}$  in stochastic model is made. In this way the stochastic model

$$\bar{C}_{NG} = C_{NG} - \Delta C_{NG} \text{ i.e. } \bar{C}_{NG} = \sigma^2 I \quad (3.5)$$

is used instead of the correct co-variance matrix  $C_{NG}$ . The respective estimation reads:

$$\bar{\mathbf{p}} = (\mathbf{A}^T \bar{\mathbf{C}}^{-1} \mathbf{A})^{-1} \mathbf{A}^T \bar{\mathbf{C}}^{-1} \mathbf{l} = \bar{\mathbf{F}} \cdot \mathbf{l}, \text{ and} \quad (3.6)$$

$$\mathbf{C}_{\bar{\mathbf{p}}} = (\mathbf{A}^T \bar{\mathbf{C}}^{-1} \mathbf{A})^{-1} \quad (3.7)$$

where

$$\mathbf{A} = \begin{vmatrix} \mathbf{A}_{NG} \\ \mathbf{A}_o \end{vmatrix}, \bar{\mathbf{C}} = \begin{bmatrix} \bar{\mathbf{C}}_{NG} & \mathbf{0} \\ \mathbf{0} & \mathbf{C}_o \end{bmatrix} \text{ and } \mathbf{l} = \begin{vmatrix} \mathbf{N}_G \\ \mathbf{l}_o \end{vmatrix}.$$

But nevertheless the result  $\bar{\mathbf{p}}$  is also an unbiased estimation. This can be proved in the following way (Jäger, R, et. al. 2003):

$$\mathbf{E}(\bar{\mathbf{p}}) = \mathbf{E}(\bar{\mathbf{F}} \cdot \mathbf{l}) = \bar{\mathbf{F}} \cdot \mathbf{E}(\mathbf{l}) = \bar{\mathbf{F}} \cdot \mathbf{A} \cdot \tilde{\mathbf{p}} = \tilde{\mathbf{p}} \equiv \mathbf{E}(\hat{\mathbf{p}}) = \mathbf{F} \cdot \mathbf{E}(\mathbf{l}) = \mathbf{F} \cdot \mathbf{A} \cdot \tilde{\mathbf{p}} = \tilde{\mathbf{p}} \quad (3.8)$$

with  $\tilde{\mathbf{p}}$  = true parameters,  $\mathbf{F}$  see (3.3) and  $\bar{\mathbf{F}}$  see (3.6).

So in spite of the neglect in (3.5), the adjusted DFHRS is representing the Height Reference Surface.

So an imprecise stochastic model  $\bar{\mathbf{C}}_{NG}$  in the least-squares adjustment only imply an decrease in the resulting stochastic model  $\mathbf{C}_{\bar{\mathbf{p}}}$  (Jäger,R. et.al. 2003). But this suboptimality should be small, because the neglect  $\bar{\mathbf{C}}_{NG} = \sigma^2 \mathbf{I}$  is only due to the off-diagonal elements. To improve the accuracy of the results, the neglect  $\Delta \mathbf{C}_{NG}$  should be minimized. Related investigations with appropriate correlation functions are currently running at Fachhochschule Karlsruhe University of Applied Sciences.

In the quality control of the DFHRS DB for Germany by a number of 3243 recomputed independent control points, the standard deviation  $s_{DFHRS}$  was approximated as <1,8 cm (chapter 2). This large number of points (see Fig. 4) should be representative. For comparison with this external accuray, the surface of accuracies, derived from the co-variance is printed in Fig.5. The accuracies provided by the co-variance matrix indicate a standard deviation of <2,0 cm for most parts of the area.

### Deflections of the vertical as additional observation group

The DFHRS concept of the representation of the HRS by its Taylor-series, derived as a bivariate polynomial in each mesh links to any kind of height- or HRS- related observation. One group of observation that is available, but still unused for online GNSS heighting are deflection of the vertical ( $\xi, \eta$ ). They may either result from astronomical observations or may just be taken from gravity potential models (EGM96, EGG97). The observation group  $\Delta g$  could be the transformed to vertical deflections using the Venning-Meinesz formula

$$\begin{Bmatrix} \xi \\ \eta \end{Bmatrix} = \frac{1}{4 \cdot \pi \cdot \gamma_m} \iint_{\sigma} \frac{dS(\psi)}{d(\psi)} \Delta g \cdot \begin{Bmatrix} \cos(\alpha) \\ \sin(\alpha) \end{Bmatrix} \cdot d\sigma. \quad (3.9)$$

Starting with the FEM representation  $NFEM(B,L|\mathbf{p})$  is first written as inner product

$$NFEM(B,L|\mathbf{p}) = F(B,L) \cdot \mathbf{p} \quad (3.10)$$

$$\xi = -\frac{\partial N}{\partial_{SB}} = \frac{-\partial NFEM}{\partial B} \cdot \frac{\partial B}{\partial_{SB}} = -\mathbf{F}(B, L)_B \cdot \mathbf{p} \cdot \frac{\partial B}{\partial_{SB}} \quad (3.11)$$

$$\eta = -\frac{\partial N}{\partial_{SL}} = \frac{-\partial NFEM}{\partial L} \cdot \frac{\partial L}{\partial_{SL}} = -\mathbf{F}(B, L)_L \cdot \mathbf{p} \cdot \frac{\partial L}{\partial_{SL}} \quad (3.12)$$

With the partial derivatives  $F_B$  and  $F_L$  in latitude and longitude and the standard formulars for the differential way increment  $ds$  on the ellipsoid

$$\frac{\partial_{SB}}{\partial B} = M(B) \text{ and } \frac{\partial_{SL}}{\partial L} = N(B) \cdot \cos(B)$$

we get the following observation equation for the deflections  $\xi$  and  $\eta$

$$\xi + v = -\mathbf{F}_B / M(B) \cdot \mathbf{p} + \partial_{\xi}(\mathbf{d}_{\xi, \eta}) \quad (3.13)$$

$$\eta + v = -\mathbf{F}_L / (N(B) \cdot \cos(B)) \cdot \mathbf{p} + \partial_{\eta}(\mathbf{d}_{\xi, \eta}) \quad (3.14)$$

$M(B)$  and  $N(B)$  mean the meridian and normal radius of curvature respectively. With  $\partial_{\xi}$  and  $\partial_{\eta}$  a set of datum parameters  $\mathbf{d}_{\xi, \eta}$  is introduced with

$$\begin{aligned} \partial_{\xi}(\mathbf{d}) = & \left[ \frac{-\cos(L) \cdot \sin(B)}{M+h} \right] \cdot u + \left[ \frac{-\sin(L) \cdot (\sin(B))}{M+h} \right] \cdot v + \left[ \frac{\cos(B)}{M+h} \right] \cdot w \\ & + \left[ \sin(L) \frac{h+N \cdot W^2}{M+h} \right] \cdot \varepsilon_x + \left[ -\cos(L) \frac{h+N \cdot W^2}{M+h} \right] \cdot \varepsilon_y + [0] \varepsilon_z \\ & + \left[ \frac{-e^2 \cdot N \cdot \cos(B) \cdot \sin(B)}{M+h} \right] \cdot \Delta m + \Delta B(\Delta a, \Delta f) \end{aligned} \quad (3.15)$$

and

$$\partial_{\eta}(\mathbf{d}) = \left[ \begin{array}{l} \left[ \frac{-\sin(L)}{(N+h) \cdot \cos(B)} \right] \cdot u + \left[ \frac{\cos(L)}{(N+h) \cdot \cos(B)} \right] \cdot v + [0] \cdot w \\ + \left[ \frac{-(h+(1-e^2) \cdot N)}{(N+h) \cdot \cos(B)} \cdot \cos(L) \cdot \sin(B) \right] \cdot \varepsilon_x \\ + \left[ \frac{-(h+(1-e^2) \cdot N)}{(N+h) \cdot \cos(B)} \cdot \sin(L) \cdot \sin(B) \right] \cdot \varepsilon_y \\ + [1] \cdot \varepsilon_z \end{array} \right] \cdot \cos(B) \quad (3.16)$$

It is evident, that using the additional observations (3.13) and (3.14) will increase the accuracy and reliability of DFHRS databases.

#### 4. Design of a < 10 cm DFHRS i.e. for Europe

The possibility, to produce DFHRS-Databases in different qualities was first discussed in [Jäger, R. (1998)]. Editing the meshsize, the size of the geoid-patches as well as the number and quality of the identical points ( $h$ ,  $H$ ) are design parameters to control the resulting

accuracy of the computed DFHRS Database. The resulting accuracy is only depending on the design parameters and not depending on the size of the computed area.

## **EUREF Symposium 2001, 16-18 May, Dubrovnik Resolution No. 4**

The IAG Subcommission for Europe (EUREF)

*Recognising* – the European Vertical GPS Reference Network (EUVN) with its GPS-derived ellipsoidal heights and levelled connections to UELN, – the definition of the European Vertical Reference System EVRS with its first realisation UELN 95/98, called EVRF2000,

*Considering* – this implicit pointwise realisation of a European geoid consistent with both ETRS89 and EVRS, – the existence of a large number of regional and local geoids in Europe, – the urgent need by the navigation community for a height reference surface,

*asks* its Technical Working Group and the European Sub-commission of the IAG IGGC (International Gravity and Geoid Commission) to take all necessary steps to generate a European geoid model of decimetre accuracy consistent with ETRS89 and EVRS.

So one way to fulfill the EUREF Resolution Nr. 4 / 2001 (see quotation above), to produce a european Height Reference Surface in decimetre accuracy consistent with ETRS89 and EVRS, would be the computation of a DFHRS\_Europe. In an example project, based on a FEM – Meshing for Europe in a size of i.e. 35 km x 35 km meshsize (fig.6, left) the resulting DFHRS\_DB provides a respective correction in an accuracy  $< 1$  dm.

Representative for the DFHRS Europe design studies were performed in the area of Germany was computed with this meshsize. A small number of 31 identical points (see fig.6, right) allowed the definition of 6 patches. This number of identical points is representative all over europe. In addition to the points from the EVRS campaign only 10 more identical points (h, H) have been introduced to the adjustment together with geoidheights  $N_G$ , derived from the EGG97 quasigeoid. For quality control, a number of 177 known control points, that were not used as identical point in the DFHRS computation and are distributed all over Germany (fig.7, left), were recomputed. The resulting differences are shown in the histogram in fig.7. The recomputation led to a standard deviation of the recomputed heights  $H_{DFHRS}$  of  $\pm 4,1$ cm.

In another control, the differences of the DFHRS corrections  $DFHRS(B, L, h | \Delta m, p)$  all over Germany, using the DFHRS\_DB with 35km x 35km meshsize and the  $< 3$  cm DFHRS\_DB for Germany, were computed. The accuracy of  $< 3$ cm of the DFHRS Germany is shown in a statistical quality control as well as in measurements (chapter 3), so it is used as a reference for the  $< 10$ cm DFHRS\_DB.

The large number of scanned points  $\sim 20.000$  and the derived differences respectively, led to an standard deviation of  $\pm 4,6$  cm. The differences between the DFHRS\_correction of both DFHRS\_DB is visualized as a surface plot in fig. 8. It shows, that differences of more than 10 cm are only reached in mountainous areas. Hence the borderlength of a mesh in this areas should not be more than  $\sim 20$  km to guarantee a HRS-representation of less than 10 cm [Jäger, R. et al. 2003b].

In contrast to a DFHRS based on 10km x 10 km meshsize (or even 5km x 5km) the short-waved accuracies may generally be represented with a 35km borderlength for the FEM meshing.

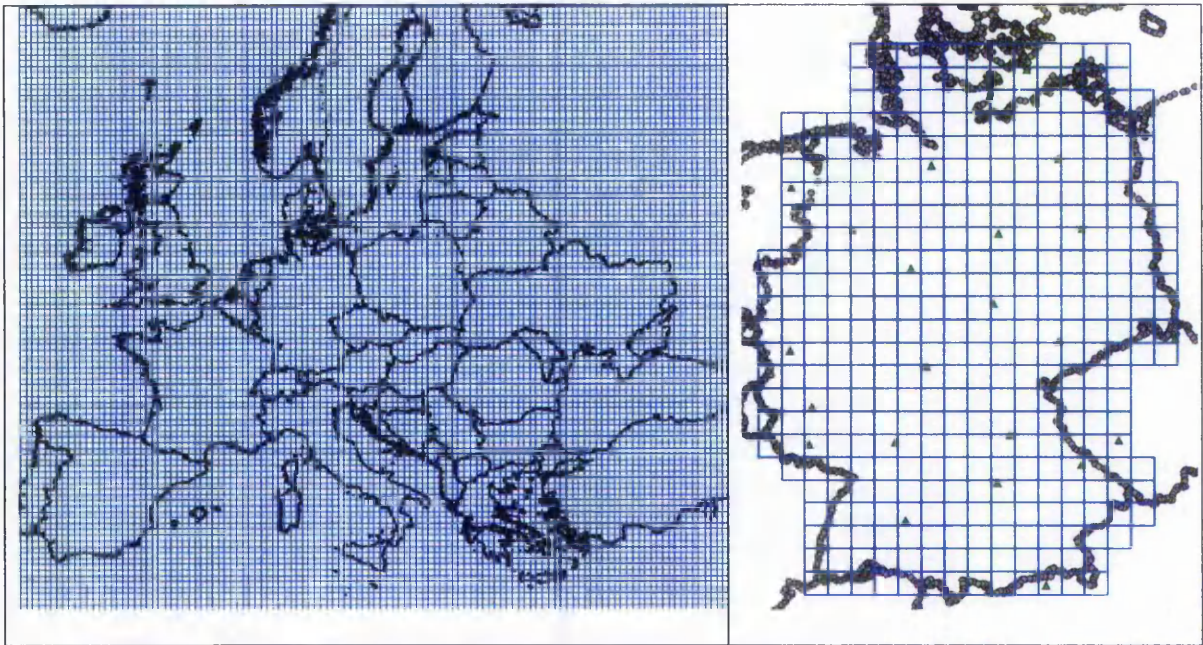


**Fig.6: left:** Scheme of a 35km x 35km FEM Meshing for Europe. **Right:** 35km x 35km FEM meshing for Germany with 31 identical points (h, H) for the computation of a  $\ll 10$  cm DFHRS.

A  $\ll 10$  cm DFHRS\_DM based on 35km meshes is appropriate i.e. for the use in GIS or navigation, as the resulting database only needs a small storage of less than 1 MB.

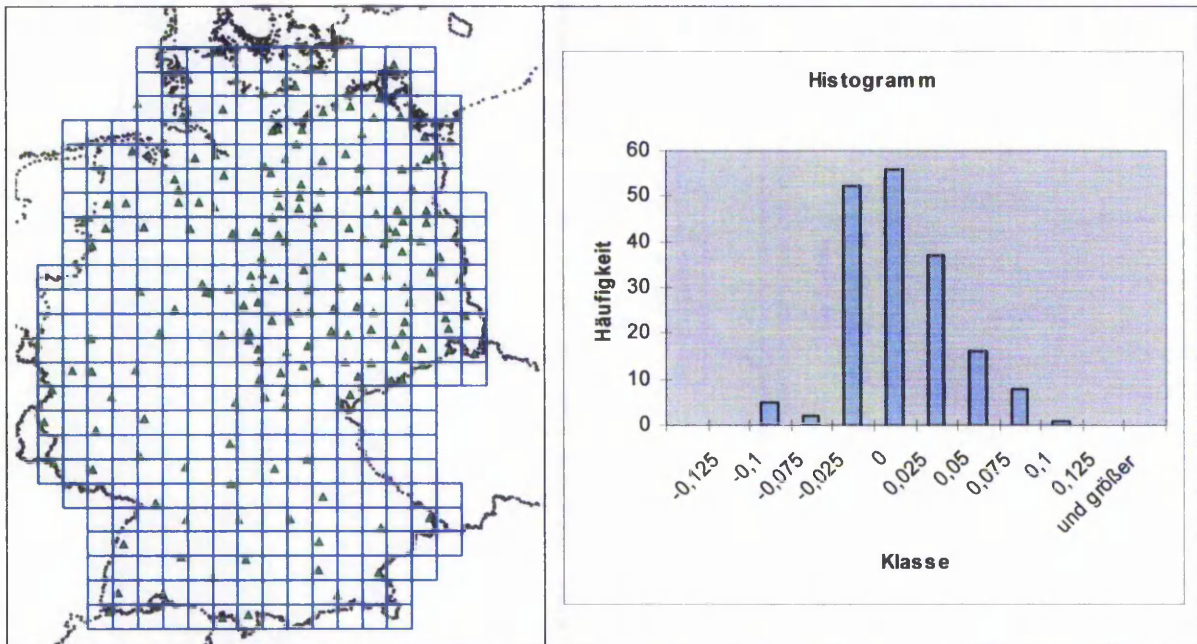


**Fig.6.** Distribution of the 177 points used for control (left) and differences between known heights H and height derived by means of the DFHRS-correction.

## 5. Conclusions

DGNSS-networks like SAPOS or ascos in Germany, provide RTK-corrections that enable an online positioning in an accuracy of cm-range. But in spite of these developments, the number

of users still is very small in total, because a ETRS/EVRS based reference system has not yet been introduced.

The DFHRS\_DB for Germany provides a correction  $DFHRS(B,L,h|\Delta m,p)$  that enables a direct conversion of ellipsoidal height  $h$  into standard heights  $H$ , without any uneconomical measurements on identical points ( $h, H$ ). The DFHRS\_DB for Germany in the realized quality of  $\ll 3\text{cm}$  is a well balanced tool for online GNSS based heighting using DGNSS-services like SAPOS or ascos. The quality of  $\ll 3\text{cm}$  has been proved in a statistical quality control as well as with independent measurements. The results show a indicate a quality of  $\ll 3\text{cm}$  all over Germany. (Measurments in Western Germany led to a quality of  $< 1,8\text{ cm}$ ).

The DFHRS concept allows the production of DFHRS databases in different qualities and according to the FEM theory in different sizes. So it has the capacity to fulfill the EUREF Resolution to produce a HRS in a dm-quality. Hence, an example a  $< 10\text{cm}$  DFHRS for Germany has been computed vicarious for whole Europe with a meshsize of  $35\text{km} \times 35\text{km}$ . An accuracy of  $\sim 5\text{ cm}$  has been reached using 31 identical points ( $h, H$ ).

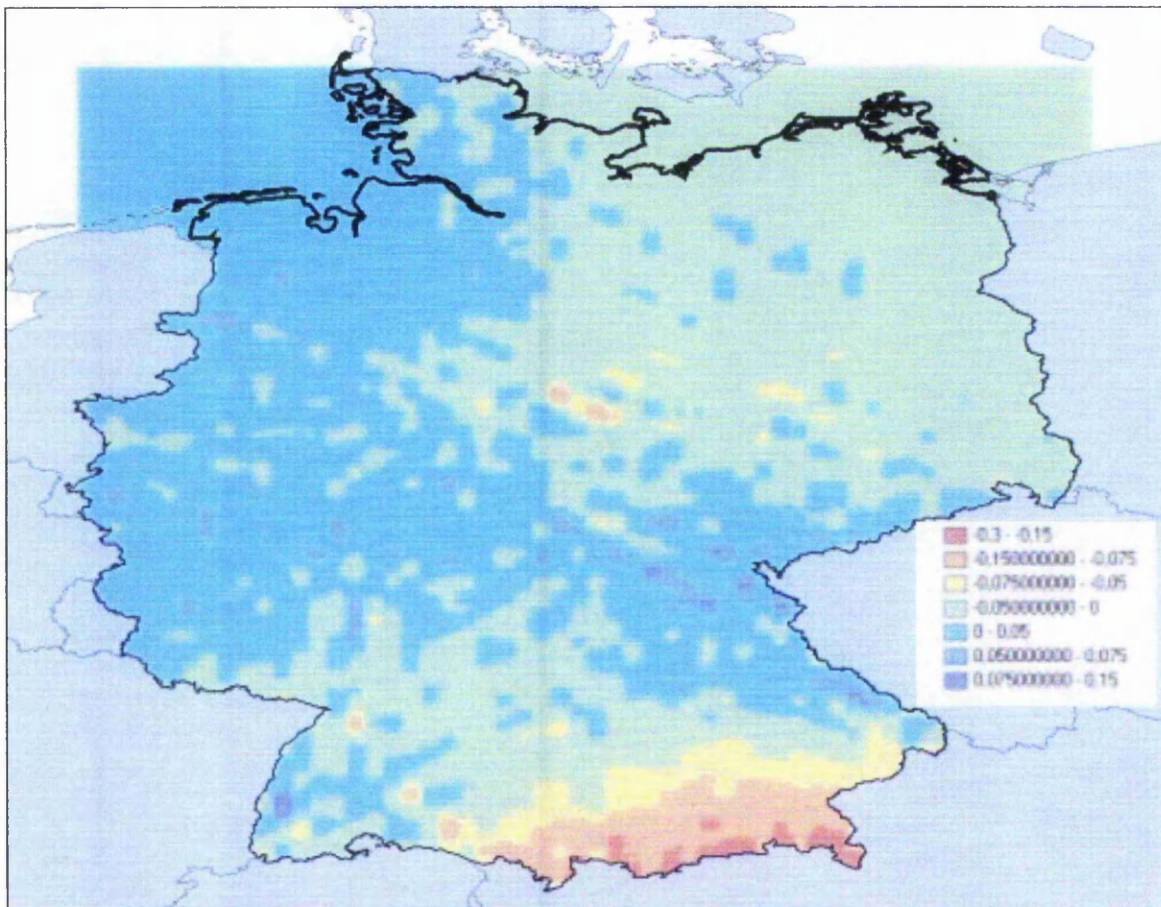


**Fig.8** .: Differece between the DFHRS\_DB based on 35 km meshes and the  $< 3\text{ cm}$  DFHBF\_DE. An average accuracy of  $< 5\text{cm}$  has been reached in total. To guarantee differences  $< 10\text{ cm}$  in mountainous areas, a meshsize  $\sim 20\text{km}$  is to be used finally [Jäger,R. et al. 2003b].

Many GNSS receiver manufactors (e.g. Leica, Trimble, Topcon, Thales) have already implemented an interface to the DFHRS\_DB in their software-products. In all propability, the availability of the DFHRS\_DB will increase the number of users of DGNSS services.

## Literature

- Denker, H. and W. Torge (1997): The European Gravimetric Quasigeoid EGG97 – An IAG supported continental enterprise. In: *Geodesy on the Move – Gravity Geoid, Geodynamics, and Antarctica*. R. Forsberg, M. Feissel, R. Dietrich (eds.) IAG Symposium Proceedings Vol. 119, Springer, Berlin Heidelberg New York: 249-254.
- Jäger, R. (1998): Ein Konzept zur selektiven Höhenbestimmung für SAPOS. Beitrag zum 1. SAPOS-Symposium. Hamburg 11./12. Mai 1998. Arbeitsgemeinschaft der Vermessungsverwaltungen der Länder der Bundesrepublik Deutschland (Hrsg.), Amt für Geoinformation und Vermessung, Hamburg. S. 131-142.
- Jäger, R. (2001): Online and Postprocessed GPS-heighting based on the Concept of a Digital Finite Element Height Reference Surface. In: J. Kaminskis and R. Jäger (Eds.): 1st Common Baltic Symposium, GPS-Heighting based on the Concept of a Digital Height Reference Surface (DFHRS) and Related Topics - GPS-Heighting and Nation-wide Permanent GPS Reference Systems Riga, June 11, 2001. p.15-24. ISBN 9984-9508-7-5
- Jäger, R. und S. Kälber (2000): Konzepte und Softwareentwicklungen für aktuelle Aufgabenstellungen für GPS und Landesvermessung. DVW Mitteilungen, Landesverein Baden-Württemberg. 10/2000. ISSN 0940-2942.
- Jäger, R. and S. Schneid (2001a): DFHRS-Homepage: [www.DFHBF.de](http://www.DFHBF.de) .
- Jäger, R. and S. Schneid (2001b): Online and Postprocessed GPS-Heighting based on the Concept of a Digital Height Reference Surface. Contribution to IAG International Symposium on Vertical Reference Systems, February 2001, Cartagena, Columbia. In press.
- Jäger, R. and S. Schneid (2001c): Online and Postprocessed GPS-heighting based on the Concept of a Digital Height Reference Surface. In: *Veröffentlichungen der Internationalen Erdmessung der Bayerischen Akademie der Wissenschaften* (62). IAG Subcommittee for Europe Symposium EUREF, Dubrovnik 2001. Beck'sche Verlagsbuchhandlung, München. In press.
- Jäger, R. and S. Schneid (2002): GNSS Online Heighting based on the Concept of a Digital Finite Element Height Reference Surface (DFHRS) and the Evaluation of the European HRS. Proceedings, ENC - GNSS 2002 Symposium, European Navigation Conference. Kopenhagen. In press.
- Jäger, R., Müller, T., Saler, H. and R. Schwäble (2003): Klassische und robuste Ausgleichungsverfahren. Herbert Wichmann Verlag, Heidelberg. ISBN 3-87907-370-8, in press.
- Jäger, R., Kälber, S., Schneid, S. und S. Seiler (2003a): Konzepte und Realisierungen von Datenbanken zur hochgenauen Transformation zwischen klassischen Landessystemen und ITRF / ETRS89 im aktuellen GIS- und GNSS - Anwendungsprofil. (Chesi/Weinold, Hrsg.): 12. Internationale Geodätische Woche Obergurgl 2003. Wichmann Verlag, Heidelberg. ISBN 3-87907-401-1. S. 207-211.
- Jäger, R., Kälber, S., Schneid, S. und S. Seiler (2003b): Precise Vertical Reference Surface Representation and Precise Transformation of Classical Networks to ETRS89 / ITRF - General Concepts and Realisation of Databases for GIS, GNSS and Navigation Applications in and outside Europe. Proceedings GNSS2003 – The European Navigation Conference, Graz, April 22-25, 2003. In press.
- Schneid, S. (2001): Software Development and DFHRS computations for several countries. In: J. Kaminskis and R. Jäger (Eds.): 1st Common Baltic Symposium, GPS-Heighting based on the Concept of a Digital Height Reference Surface (DFHRS) and Related Topics - GPS-Heighting and Nation-wide Permanent GPS Reference Systems Riga, June 11, 2001. p.25-25. ISBN 9984-9508-7

Schneid, S. (2002):

Software Development and DFHRS computations for several countries. J. Kaminskis and R. Jäger (Eds.): 1<sup>st</sup> Common Baltic Symposium, GPS-Heighting based on the Concept of a Digital Height Reference Surface (DFHRS) and Related Topics - GPS-Heighting and Nationwide Permanent GPS Reference Systems Riga, June 11, 2001. ISBN 9984-9507-7-5

# Software Development and DFHRS computations for several countries

Sascha Schneid

Institut für Innovation und Transfer (IIT)

Fachhochschule Karlsruhe – University of Applied Sciences, Moltkestr. 30, D-76133 Karlsruhe

Email : [schneid@fh-karlsruhe.de](mailto:schneid@fh-karlsruhe.de)

## Summary

Online GPS-heighting with the concept of a Digital Finite Element Height Reference Surface (DFHRS) is based on the representation of the Height Reference Surface (HRS) by bivariate polynomials over an irregular grid in arbitrary large areas. Geoid information (geoid heights  $N$ , deflections of the vertical  $(\xi, \eta)$ ), gravity anomalies  $(\Delta g)$ , if necessary, and identical points  $(h, H)$  as observations in a least squares adjustment enable the statistically controlled DFHRS computation in the right datum of the HRS. After this so called production step, the resulting DFHRS database may be used for the direct conversion of ellipsoidal heights  $h$ , resulting from DGPS measurements, into standard heights  $H$ .

To compute DFHRS databases and for their application in online GPS-heighting several software packages have been developed at Fachhochschule Karlsruhe - University of Applied Sciences. Besides some useful graphical and visualization tools a powerful least squares adjustment including a statistically quality control and assurance is implemented into the so-called DFHRS production software. The application of DFHRS databases enable by means of the so-called DFHRS correction  $DFHBF(\mathbf{p}, \Delta m | B, L, h)$  the direct conversion of the ellipsoidal GPS height  $h$  to the standard height  $H$  by  $H = h - DFHBF(\mathbf{p}, \Delta m | B, L, h)$ . With  $\mathbf{p}$  and  $\Delta m$  we describe the DFHRS polynomial parameters and the scale parameter(s)  $\Delta m$  between ellipsoid heights  $H$  and standard heights  $H$ , respectively. The DFHRS data base access is realised twice. Once by means of a Dynamic Link Library (DLL), which can be easily implemented into any standard RTK-software and once as a Windows application, that is also able to handle the covariance matrix of the DFHRS, resulting from the least squares adjustment.

The practicability of the DFHRS concept is shown in two examples, namely Saarland and Baden-Württemberg (federal states of Germany), which installed the DFHRS and the respective use of DFHRS data bases as official Height Reference Surface for a direct GPS-heighting without identical points and field calibration in DGPS networks like SAPOS ®. The mean accuracy of 1 cm for the DFHRS correction  $DFHBF(\mathbf{p}, \Delta m | B, L, h)$  is statistically assured and proved, and it has been demonstrated in practical control measurements.

## 1. Computation and Application of DFHRS databases

### 1.1 DFHRS Production

In this step the DFHRS is modelled as a continuous Height Reference Surface (HRS) over an arbitrary large area. The HRS is carried over an irregular grid of finite elements by the base function of bivariate polynomials. In this way the DFHRS concept provides - by the subdivision of the whole area of any size into finite elements with a continuous transition in between neighbouring meshes - a continuous HRS in the total area. Presently geoid information (height  $N$  and deflections of the vertical  $(\xi, \eta)$ ) are introduced to a common adjustment with identical points, giving the information of the ellipsoidal height  $h$  and the information of the standard height system  $H$ .

The mathematical model for the introduction of additional gravity observations, and the mathematical proof that the use of the correlated geoid height information  $N_G(B, L)$  in (1.2) is equivalent to the use of the original gravity information are given in [Jäger, 2001, these proceedings].

The respective system of observation equations reads:

$$h + v = H - h \cdot \Delta m + \mathbf{f}(x, y) \cdot \mathbf{p} \quad (1.1)$$

$$N_G(B, L)^j + v = \mathbf{f}(x, y) \cdot \mathbf{p} + \partial N(\mathbf{d}^j) \quad (1.2)$$

$$\xi + v = -\mathbf{f}_B / M(B) \cdot \mathbf{p} + \partial B(\mathbf{d}_{\xi, \eta}) \quad (1.3)$$

$$\eta + v = -\mathbf{f}_L / (N(B) \cdot \cos(B)) \cdot \mathbf{p} + \partial L(\mathbf{d}_{\xi, \eta}) \quad (1.4)$$

$$H + v = H \quad (1.5)$$

$$C + v = C(\mathbf{p}) \quad (1.6)$$

With  $\partial N(\mathbf{d}^j)$  (1.2) and with  $\partial B(\mathbf{d}_{\xi, \eta})$  and  $\partial L(\mathbf{d}_{\xi, \eta})$  (1.3, 1.4) we introduce the datum part of the geoid height of any geoid model or of single "geoid patches" (fig.3, left) and the datum parts of the deflections of the vertical ( $\xi, \eta$ ) respectively (JÄGER, 1999). With  $\mathbf{f}_B$  and  $\mathbf{f}_L$  we introduce the partial derivatives of the Vandermonds' vector  $\mathbf{f}(x, y) = (1, x, y, x^2, xy, y^2, \dots)$  with respect to the geographical coordinates B and L.  $M(B)$  and  $N(B)$  mean the radius of meridian and normal curvature at a point P(B, L) respectively. The parameters of bivariate polynomial are introduced as  $\mathbf{p}^T = (a_{00}, a_{10}, a_{01}, a_{20}, a_{11}, a_{02}, \dots)$ . The expression  $\mathbf{f}(x, y) \cdot \mathbf{p}$  means the finite element model (FEM) of the Height Reference Surface over the ellipsoid (the so called "geoid part" N). It is equivalent to the usual representation of a bivariate polynomial as a double indexed sum as written explicitly by formula (3.1). In the following the formula  $\mathbf{f}(x, y) \cdot \mathbf{p}$  will be replaced by the abbreviation NFEM ( $\mathbf{p} \mid x, y$ ).

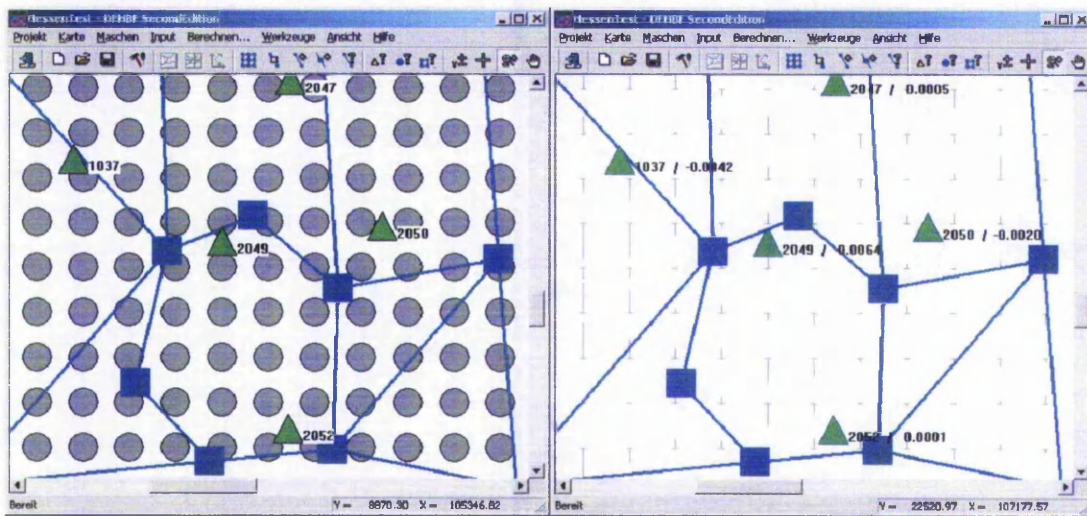


Fig.1: Left: Visualisation of meshes (blue), identical points (green) and geoid information (grey). Right : Optional displaying of residuals

Besides several tools to visualize the observation types and the residuals, the DFHRS production software offers an automatic meshing with respect to a square grid. The grid can be edited and modified afterwards manually. In this context the shape of the meshes is not restricted to a square and each polygon shape is allowed.

To choose the right mesh-size, some pre-analysis with the real data is generally to be recommended. Experiences up to now show that a size of 5 km x 5 km enables the representation of any geoid surface by bivariate polynomial of 2<sup>nd</sup> degree in a mean accuracy about 5 mm. The mesh-size may be chosen bigger in areas of less geoid roughness. Another condition of the mesh-size is that in case of using polynomials of 2<sup>nd</sup> degree 6 unknowns need to be solved. So for an adjustment at least 7 observations (e.g. geoid heights  $N_G(B, L)$  (1.2)) are needed in one mesh.

The adjusted polynomials are representing the HRS for each mesh in a sufficient accuracy, e.g. with a 5 mm accuracy as mentioned above. But the quality of the whole DFHBF is also depending on the continuity at the transition between neighbouring meshes (fig.1). For that reason, the system of observation equations is enlarged by continuity conditions (1.6). So the quality assurance in this case becomes an additive part of the functional model. The derivation of the condition equations (1.6) is described in chapter 3.

## 1.2 DFHRS Application

The application of DFHRS databases is realised twice. For the use in a direct online GPS-heighting without identical points and field calibration, the DFHRS data base access is done by a Dynamic Link Library (DLL). The DLL can easily be implemented in any usual RTK software. Concerning companies, which already supply the DFHRS interface, we refer to the DFHRS-homepage ([www.dfhbf.de](http://www.dfhbf.de)). For the use in postprocessing applications a standard Windows software is provided. Besides the direct transformation of GPS heights  $h$  into standard heights  $H$ , this version enables the access to the covariance matrix of the polynomial parameters, and in this way the computation of the final accuracy of the transformed height  $H$ .

The three dimensional DFHRS-correction  $DFHRS(\mathbf{p}, \Delta m \mid B, L, h)$ , that converts an ellipsoidal GPS height  $h$  to the standard height  $H$  is - with regard to (1.1) - depending both on to the plan position  $(B, L)$  and the ellipsoidal height  $h$  itself, and we get:

$$\begin{aligned} H &= h - DFHBF(\mathbf{p}, \Delta m \mid B, L, h) \\ &= h - NFEM(\mathbf{p} \mid B, L) - \Delta m \cdot h \end{aligned} \quad (1.7)$$

The 3-dimensional correction  $DFHRS(\mathbf{p}, \Delta m \mid B, L, h)$  is composed by the 2D "geoid part", namely  $NFEM(\mathbf{p} \mid B, L)$  and a 1D "scale part"  $\Delta m \cdot h$ . The "geoid-part"  $NFEM(\mathbf{p} \mid B, L)$  computed from (1.1)-(1.6) is high accurate and above this already provided in the correct datum (a first condition for a direct height conversion), and it is above this equivalent to the usual (2D) "geoid-grid". The "scale part"  $\Delta m \cdot h$  resulting from (1.1)-(1.6) is modelling the (mostly highly) significant scale between the GPS-heights  $h$  and the standard heights  $H$ . Thus the DFHRS-correction  $DFHRS(\mathbf{p}, \Delta m \mid B, L, h)$  is all in all a 3-dimensional quantity, as it is basically necessary for the problem of a GPS-height integration (Dinter et al., 1997). With respect to the fact, that the scale difference  $\Delta m$  may reach a size of  $10^{-4}$  (1cm per 100 m height  $h$ ) the DFHRS concept and DFHRS data bases respectively are the only ones to solve the basic 3D problem of GPS-heighting, and can provide directly a "1cm" height  $H$  or better.

## 2. Quality control during the DFHRS computation

The DFHRS production software also provides a statistically quality control. A basic quantity in statistical testing, reliability of tests and variance component estimation is the so-called redundancy matrix  $R$ , which carries the individual redundancy parts of the observations  $r_i$  on its diagonal and reads:

$$R = Q_{vv} \cdot P \quad (2.1)$$

With  $Q_{vv}$  and  $P$  we describe the cofactor matrix of the residuals and the weight matrix of the observations respectively. To analyse and compare each observation group with respect to the common a priori variance factor  $s_0^2$  the so called variance component of any observation group  $j$  is computed as:

$$s_j^2 = \frac{(v^T P v)_j}{\left(\sum r_i\right)_j} = \frac{\Omega_j}{\left(\sum r_i\right)_j} \quad (2.2)$$

With  $\mathbf{v}_j$  and  $\mathbf{P}_j$  we describe the vector of observation corrections of the  $j$ -th observations group and the weight matrix of the respective observation group and with  $\Omega_j$  the residual sum of squares belonging to this group. The a-priori variance related single observations test  $NV_i$ , known also as Baarda's data snooping, is realised in the DFHRS production software once for uncorrelated single observations (e.g. the height observations  $H$  or  $h$ ) reading

$$T_{\text{priori}} = NV_i = \frac{|v_i|}{\sigma_{ii} \cdot \sqrt{r_i}} \sim N(0,1) \quad , \text{uncorrelated observation} \quad (2.3)$$

and for the second for correlated single observations (e.g. GPS baselines  $\Delta h$  correlated within as session adjustment, or respective correlated absolute GPS heights  $h$  or correlated geoid height observations  $N_G(B,L)$ ) and reads

$$T_{\text{Priori}} = NV_i = \frac{[\mathbf{Pv}]_i}{\sigma \cdot \sqrt{[\mathbf{PQvvP}]_{ii}}} \sim N(0,1) \quad , \text{ correlated observation} \quad (2.4)$$

The a-posteriori variance related so called Student t-test holding for single observations reads for uncorrelated observations

$$T_{\text{Post}} = \frac{|\mathbf{v}_i|}{s' \sqrt{q_{ii}} \cdot \sqrt{r_i}} \sim F_{1,r-1} = t_{r-1} \quad , \quad s'^2 = \frac{\mathbf{v}^T \mathbf{Pv} - \frac{v_i^2}{q_{ii}}}{r-1} \quad , \text{ uncorrelated observations} \quad (2.5)$$

and for correlated observations

$$T_{\text{Post}} = \frac{[\mathbf{Pv}]_{ii}}{s'^2 \cdot \sqrt{[\mathbf{PQvvP}]_{ii}}} \sim F_{1,r-1} = t_{r-1} \quad , \quad s'^2 = \frac{\mathbf{v}^T \mathbf{Pv} - \frac{[\mathbf{P} \cdot \mathbf{v}]_i^2}{[\mathbf{PQ}_{vv} \mathbf{P}]_{ii}}}{r-1} \quad , \text{ correlated observations} \quad (2.6)$$

The above tests (2.3 - 2.6) are performed as a sophisticated standard in the DFHRS production with respect to detection of gross errors. In case of a significance test, the quantity of the respective gross error is estimated and the influence on the relative and absolute network quality is computed. For the respective quantities and formulas see (Illner and Jäger, 1993) .

To prove the so called "reproduction quality" of the DFHRS database parameters ( $\mathbf{p}$ ,  $\Delta m$ ) we compute the DFHRS height  $H_i(\text{DFHRS}, h_i)$  of each identical point  $(H, h)_i$  successively for the case that the respective database DFHRS<sub>i</sub> was produced in (1.1-1.6) under exclusion of  $(H, h)_i$  and we compare  $H_i(\text{DFHRS}, h_i)$  to the independently known height  $H_i$ . The reproduction quality measure  $\nabla H_i$  is then simply given by the value of difference

$$\nabla H_i = H_i - H_i(\text{DFHRS}, h_i) \quad (2.7)$$

It can be shown, that for the identical points  $(H, h)_i$  , where  $H_i$  is introduced as stochastic point observation, the above "reproduction quality"  $\nabla H_i$  can be evaluated as

$$\nabla H_i = -\frac{v_i}{r_i} \quad , \quad (2.8)$$

in the final DFHRS production step, where all identical points  $(H, h)_i$  are used.

### 3. Modelling the continuity conditions of the DFHRS

Like mentioned above, a bivariate polynomial is able to represent the surface of any geoid, or better the Height Reference Surface HRS in the small area of a mesh (fig. 1), for the reason (in the mathematical sense), that the bivariate polynomial is to be assumed as a local Taylor series expansion of the HRS in the small mesh area. In practice a mesh extension of few kilometers keeps a HRS approximation quality of few millimetres. The quality of a the complete Height Reference Surface, based on this concept of polynomials in an irregular grid is however to be kept additionally by requiring a continuous transition of the HRS between neighbouring meshes. Because of the principal accuracy of "few mm", these continuity conditions do not need to be "strong". Therefore they are formulated as observations with an a-priori variance of again "few mm" (1.6) implying a respective weight in the

common adjustment of DFHRS production given by the observation equations (1.1 - 1.6).

The modelling of the continuity conditions for  $C_0$ -continuity means same functional value at the common border straight line and is described in the following. With  $x^I$  and  $x^{II}$  we describe two independent point positions of a HRS point, situated in mesh I and in mesh II respectively, and we get:

$$x^I = \begin{bmatrix} x \\ y \\ N^I(x,y) \end{bmatrix} = \begin{bmatrix} x \\ y \\ \sum_{i=0}^n \sum_{k=0}^{n-i} a_{i,k}^I \cdot x^i y^k \end{bmatrix} \quad \text{and} \quad x^{II} = \begin{bmatrix} x \\ y \\ N^{II}(x,y) \end{bmatrix} = \begin{bmatrix} x \\ y \\ \sum_{i=0}^n \sum_{k=0}^{n-i} a_{i,k}^{II} \cdot x^i y^k \end{bmatrix} \quad (3.1)$$

According to the DFHRS concept the "z-component" is replaced by the polynomial function  $N(x,y)$  of the bivariate polynomial  $a_{ik}$  as a function of the plan position  $(x,y)$ . Both independent surface points introduced by (3.1) are now restricted to run along the common border straight line AE (fig. 2) of both meshes.

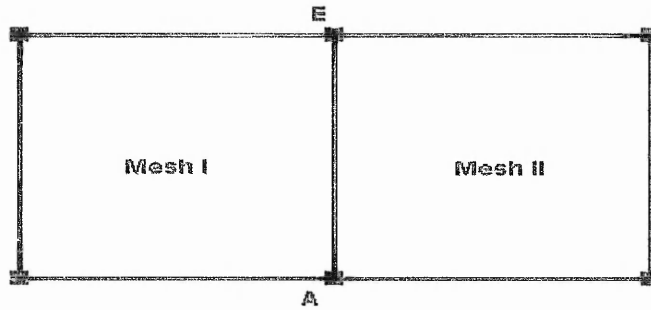


Fig.2: Scheme of two neighbouring meshes I and II, where a continuous transition at the common border straight line AE has to be forced

For this reason, the next step requires to describe the straight line AE in its parametric expression for both meshes I and II and we get

$$x^I = \begin{bmatrix} x_a + t(x_e - x_a) \\ y_a + t(y_e - y_a) \\ \sum_{i=0}^n \sum_{k=0}^{n-i} a_{i,k}^I \cdot (x_a + t(x_e - x_a))^i (y_a + t(y_e - y_a))^k \end{bmatrix} \quad (3.2a)$$

and

$$x^{II} = \begin{bmatrix} x_a + t(x_e - x_a) \\ y_a + t(y_e - y_a) \\ \sum_{i=0}^n \sum_{k=0}^{n-i} a_{i,k}^{II} \cdot (x_a + t(x_e - x_a))^i (y_a + t(y_e - y_a))^k \end{bmatrix} \quad (3.2b)$$

with

$x_e, y_e$  = plan coordinates of point E,

$x_a, y_a$  = plan coordinates of point A

$t \in [0,1]$  = parameter of straight line position within AE

It is easy to see that both vectors  $x^I$  and  $x^{II}$  can only differ with respect to the space and degrees of freedom supplied by the number of the two sets different polynomial coefficients  $a_{ik}^I$  and  $a_{ik}^{II}$  respectively. So both surfaces are  $C_0$  - continuous, only if the functions  $N^I(x,y,a_{ik}^I)$  and  $N^{II}(x,y,a_{ik}^{II})$  are restricted to the same values along the border AE, meaning that the functions difference becomes zero. With the abbreviations

$$da_{ik} = a_{ik}^I - a_{ik}^{II}, \quad dx = x_e - x_a, \quad dy = y_e - y_a \quad (3.3a)$$

we get for the difference vector

$$\Delta x_I^{II} = \begin{bmatrix} 0 \\ 0 \\ \Delta N(t) \end{bmatrix} = \begin{bmatrix} 0 \\ 0 \\ \sum_{i=0}^n \sum_{k=0}^{n-i} da_{i,k} \cdot (x_a + t(dx))^i (y_a + t(dy))^k \end{bmatrix} \equiv \begin{bmatrix} 0 \\ 0 \\ 0 \end{bmatrix} \quad (3.3b)$$

While the difference in the plan position components (x,y) becomes automatically zero by the restriction to the common straight line AE, the difference

$$\Delta N(t) = N^I(x,y,a_{ik}^I,t) - N^{II}(x,y,a_{ik}^{II},t) \quad (3.3c)$$

leads to an univariate polynomial in t of  $n^{\text{th}}$  degree. Requiring the difference  $\Delta N(t)$  to become zero is equivalent to the requirement of a so called  $C_0$ -continuity (in the FEM terminology), meaning the same DFHS functional values along the common border.

With e.g.  $n=2$  and setting the corresponding difference  $\Delta N(t)$  (3.3b) to zero, we get a polynomial in t of 2<sup>nd</sup> degree. After a separation with respect to the different powers of the free parameter t we get the following structure and coefficients A,B,C for the polynomial in t:

$$A(a_{ik}^I, a_{ik}^{II}, x_e, x_a, y_e, y_a) \cdot t^2 + B(a_{ik}^I, a_{ik}^{II}, x_e, x_a, y_e, y_a) \cdot t + C(a_{ik}^I, a_{ik}^{II}, x_e, x_a, y_e, y_a) \equiv 0 \quad (3.4)$$

The constant coefficients A,B and C are depending on the polynomial coefficients and the nodal point position A and E. As (3.4) has to be valid for all  $t \in [0,1]$  to force  $C_0$ -continuity, we have to require

$$A(a_{ik}^I, a_{ik}^{II}, x_e, x_a, y_e, y_a) \equiv 0, \quad B(a_{ik}^I, a_{ik}^{II}, x_e, x_a, y_e, y_a) \equiv 0, \quad C(a_{ik}^I, a_{ik}^{II}, x_e, x_a, y_e, y_a) \equiv 0 \quad (3.5)$$

We finally get in details for  $n=2$  the following  $C_0$ -continuity restrictions

$$A = da_{0,2} dy^2 + da_{1,1} dx dy + da_{2,0} dx^2 = 0 \quad (3.6a)$$

$$B = da_{0,1} dy + 2da_{0,2} y_a dy + da_{1,0} dx + da_{1,1} x_a dy + da_{1,1} dx y_a + 2da_{2,0} x_a dx = 0 \quad (3.6b)$$

$$C = da_{0,0} + da_{0,1} y_a + da_{0,1} y_a^2 + da_{1,0} x_a + da_{1,1} x_a y_a + da_{2,0} x_a^2 = 0 \quad (3.6c)$$

which are set up in the DFHS production adjustment (1.1)-(1.6) with respect to each common border line AE of the mesh grid (fig.2) as pseudo-observations C(p) as given in (1.6).

## 4. Examples

After demonstrating the practical suitability of the DFHRS concept in pilot-projects (e.g. Tallinn/Estonia), several computation of DFHRS databases have been performed or are presently running respectively. The first DFHRS databases that were installed as official Height Reference Surfaces by the respective State Land Service Department, e.g. for a SAPOS®-based direct online GPS-heighting, were those of Saarland and Baden-Württemberg (federal states of Germany). The computational designs of these DFHRS network and the results of the quality control are shown in this chapter.

### 4.1 DFHRS of Baden-Württemberg

To compute the Digital Finite Element Height Reference Surface 130 so called BWRef points (precise identical points  $h, H$  in the ETRS89 datum) where provided by the State Land Service Department. Additional identical points were provided by the neighbouring states, so there was a complete number of 192 identical points taking part in the DFHRS data base production, namely the adjustment represented by (1.1) - (1.6).

As a first base for the computation a regular grid of 7 km x 7 km mesh-size was generated by the respective tool of the DFHRS software, which was slightly modified during different computation designs (fig. 3 left). To reduce the well known long-waved systematic errors, the surface of the used EGG97 (quasi geoid) (DENKER and TORGE, 1997) was subdivided into 28 "geoid-patches", each with its own set of datum parameters  $\partial N(\mathbf{d}^j)$  (1.2).

The basic and essential result was the fact, that the aspired mean " $< 1\text{cm}$ -DFHRS" database was achieved, as the average reproduction value (2.7), (2.8) was 9,7 mm (JÄGER et al. 2001, MEICHLE, 2001).

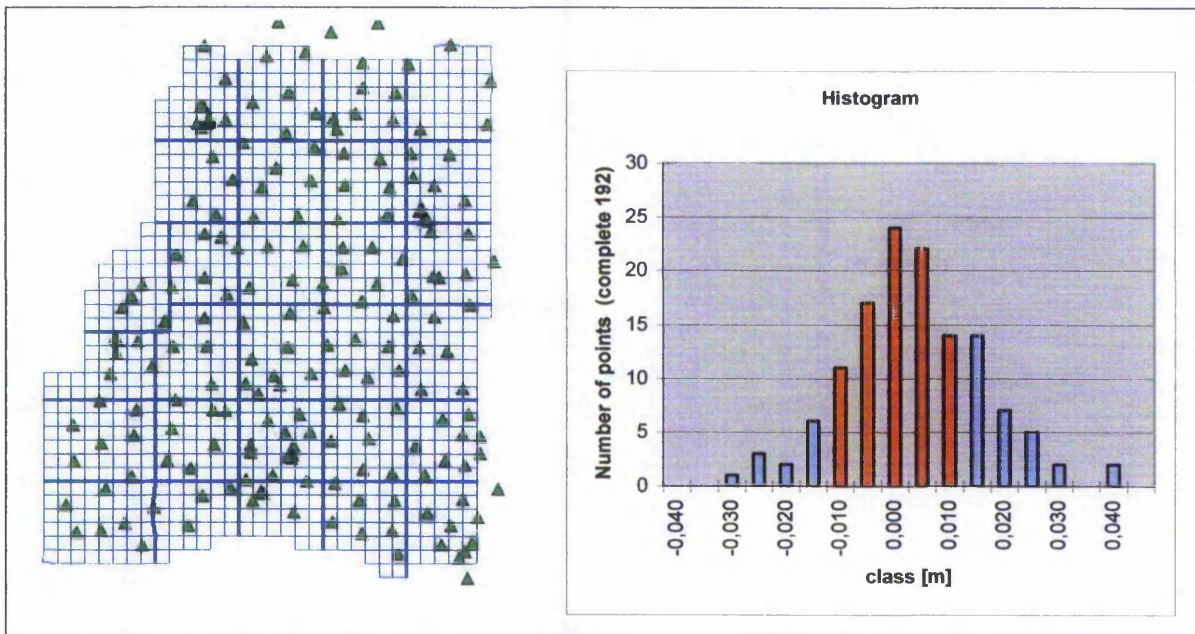


Fig. 3: left.: DFHRS meshing (blue), "geoid patching" (thick blue) and the 192 identical points (green) of Baden-Württemberg. Right: Histogram of the "reproduction-values" (2.7), (2.8)

According to the theory of the Gauss normal distribution (being demonstrated again) 68 % (88 of the 130 BWRef points) were within "one sigma", meaning that they had a reproduction value less than 1 cm. The scale parameter  $\Delta m$  was  $-11 \cdot 10^{-5}$  - meaning 1,1 cm / 100 m. This shows, that the "scale correction part"  $\Delta m \cdot h$  (1.7) is - besides the pure "geoid-part"  $NFEM(\mathbf{p}|B,L)$  and a generally not sufficient standard formula  $H = h - N$  - absolutely necessary for a direct online GPS-heighting.

## 4.2 DFHRS of Saarland

The basic mesh design for the computation of the DFHRS database in Saarland was a 5 km x 5 km mesh size. The total area was subdivided in 6 "patches" to reduce the long-waved geoid model errors. The EGG97 as a set of (2 x 2) km geoid grid observations (1.2) and a rather big number of 474 identical points (h, H) were used as observations.

The quality control was done in the described way and the reproduction quality (2.7), (2.8) for an aspired "< 1 cm-DFHRS" data base was to be verified by the respective mean reproduction value of 9.3 mm, which was for the 474 identical points again smaller than 1 cm.

Both, the DFHRS database of Saarland as well as the DFHRS database of Baden-Württemberg are already used in practice for online GPS-heighting in the SAPOS® network. So the suitability of the DFHRS concept is no more theory.

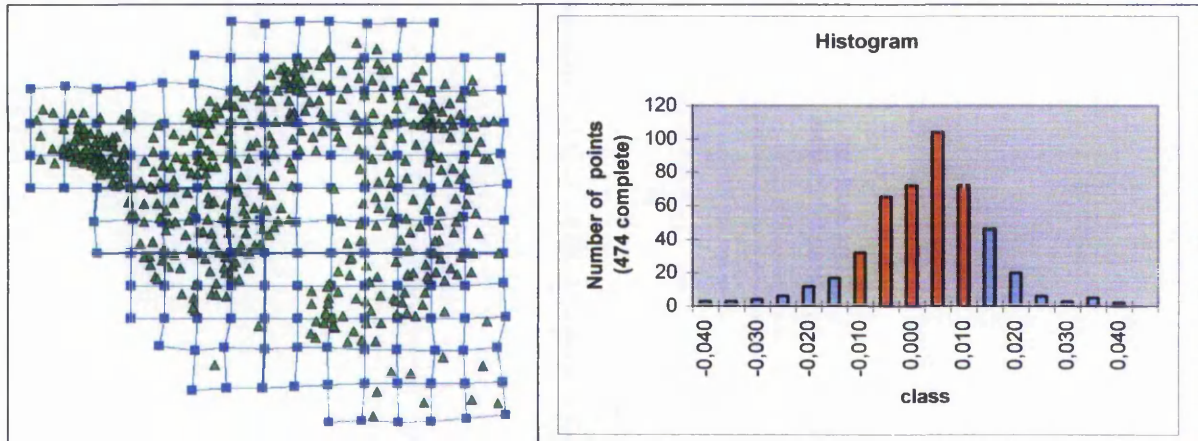


Fig 4.: left: DFHRS meshing and the 474 identical points in Saarland.  
Right : Histogram of the "reproduction values" (2.7), (2.8)

## 5. Conclusions

The suitability of the DFHRS concept in online GPS-heighting e.g. by SAPOS®, is shown by the examples of Baden-Württemberg and Saarland, both federal states of Germany. The mean accuracy of both DFHRS databases was proved to be better than 1 cm by the concept of quality assurance based on the computation of the so called "reproduction values". Both DFHRS databases are meanwhile installed as official Digital Height Reference Surfaces (DFHRS) by the respective State Land Service Departments.

The concept consists of the common adjustment of geoid information (height N and deflections of the vertical  $(\xi, \eta)$  and identical points (h, H)). The DFHRS approach allows the common adjustment of several geoid models as well as the subdividing of any geoid model into single so called "geoid patches" with own sets of datum parameters, to reduce the influence of long-waved systematic errors in geoid models.

So by the use of the concept, there are no limits to introduce the available national geoid models into a common adjustment of any Digital Finite Element Height Reference Surface (DFHRS) together with international geoid models (e.g. EGG97, EGM96).

The DFHRS software development at the Fachhochschule Karlsruhe – University of Applied sciences is continued and the flexibility and power of the DFHRS software is accordingly growing. Presently the DFHRS data bases production for 3 other states of the Federal Republic of Germany is running, namely Bavaria, Hessen and Niedersachsen. The focus of the DFHRS project is set on the realisation of the adjustment (1.1 - 1.6) and a respective quality control and assurance, as well as the introduction of a innovative standard for a "1 cm" online GPS-heighting. So DFHRS data bases enable a respective conversion of the GPS height h to the standard height H by the so called DFHRS-correction, which reads in total  $H = h - \text{NFEM}(\mathbf{p} | \mathbf{B}, \mathbf{L}) - \Delta m \cdot h$ . It is clearly proved that a 2D correction referring purely to the "geoid-part"  $\text{NFEM}(\mathbf{p} | \mathbf{B}, \mathbf{L})$  (or generally any datum adapted or fitted "2D geoid grid") is not sufficient for this accuracy level, and the additional "scale correction part"  $\Delta m \cdot h$  provided the DFHRS-correction is necessary.

The DFHRS data base software interface is realised as a Dynamic Link Library (DLL) and has already been implemented into usual RTK software equipments (for the present state, see [www.dfhbf.de](http://www.dfhbf.de)).

## References

- DENKER, H. and W. TORGE (1997): The European Gravimetric Quasigeoid EGG97 – An IAG supported continental enterprise. In: *Geodesy on the Move – Gravity Geoid, Geodynamics, and Antarctica*. R. Forsberg, M. Feissel, R. Dietrich (eds) IAG Symposium Proceedings Vol. 119, Springer, Berlin Heidelberg New York: 249-254.
- DINTER, G.; ILLNER, M. and R. JÄGER (1997): A synergetic approach for the integration of GPS heights into standard height systems and for the quality control and refinement of geoid models. In: *Veröffentlichungen der Internationalen Erdmessung der Bayerischen Akademie der Wissenschaften (57)*. IAG Subcommission for Europe Symposium EUREF, Ankara 1996. Beck'sche Verlagsbuchhandlung, München.
- ILLNER, M and R. JÄGER (1993): Ein Konzept zur Integration von GPS in Verdichtungsnetze – Modellbildung und Ableitung von zugehörigen Genauigkeits- und Zuverlässigkeitsmaßen, *ZfV* 118, Nr 11: S. 552-574
- JÄGER, R. (1990): Optimum Positions for GPS-points and Supporting Fix-points in Geodetic Networks. In: Ivan I. Mueller (ed.) *International Association of Geodesy Symposia. Symposium No. 102: Global Positioning System: An Overview*, Edinburgh/Scotland, Aug. 7-8, 1989. Convened and edited by Y. Bock and N. Leppard, Springer: 254-261.
- JÄGER, R. (1999): State of the art and present developments of a general approach for GPS-based height determination. In (M. Lilje, ed.): *Proceedings of the Symposium Geodesy and Surveying in the Future - The importance of Heights*, March 15-17, 1999. Gävle/Schweden Reports in Geodesy and Geographical Informations Systems, LMV-Rapport 1999(3). Gävle, Schweden. ISSN 0280-5731: 161-174.
- JÄGER, R. and S. KÄLBER (2000): Konzepte und Softwareentwicklungen für aktuelle Aufgabenstellungen für GPS und Landesvermessung. DVW Mitteilungen, Landesverein Baden-Württemberg. 10/2000. ISSN 0940-2942.
- JÄGER, R. and S. SCHNEID (2001a): GPS-Höhenbestimmung mittels Digitaler Finite-Elemente Höhenbezugsfläche (DFHBF) - das Online-Konzept für DGPS-Positionierungsdienste. XI. Internationale Geodätische Woche in Obergurgl/Österreich, Februar 2001. Institutsmittellungen, Heft Nr. 19, Institut für Geodäsie der Universität Innsbruck: 195-200.
- JÄGER, R. and S. SCHNEID (2001b): DFHRS-Homepage: [www.DFHBF.de](http://www.DFHBF.de) .
- JÄGER, R. and S. SCHNEID (2001c): Online and Postprocessed GPS-heighting based on the Concept of a Digital Height Reference Surface. Contribution to IAG International Symposium on Vertical Reference Systems, February 2001, Cartagena, Columbia. In press.
- JÄGER, R. and S. SCHNEID (2001d): Online and Postprocessed GPS-heighting based on the Concept of a Digital Height Reference Surface. In: *Veröffentlichungen der Internationalen Erdmessung der Bayerischen Akademie der Wissenschaften (62)*. IAG Subcommission for Europe Symposium EUREF, Dubrovnik 2001. Beck'sche Verlagsbuchhandlung, München. In press.
- JÄGER, R.; SCHNEID, S. and S. SEILER (2001): Berechnung der Digitalen Finite Element Höhenbezugsfläche (DFHBF) für Baden-Württemberg. Abschlußbericht, Landesvermessungsamt Baden-Württemberg, unpublished.
- MEICHLE, H. (2001): Digitale Finite Element Höhenbezugsfläche (DFHBF) für Baden-Württemberg. DVW Mitteilungen, Landesverein Baden-Württemberg. 10/2001. ISSN 0940-2942.
- SCHWARZER, F. (2000): Entwicklung grafikfähiger C-Software zur Berechnung Digitaler Finite Element Höhenbezugsflächen und DFHBF-Implementierung in GPS-Kommunikationssoftware. Diplomarbeit, Studiengang Vermessung und Geomatik, Fachhochschule Karlsruhe – University of Applied Sciences, unpublished
- WERNY, E. (2001) : Berechnung und Qualitätsanalyse einer hochgenauen Digitalen Finite Element Höhenbezugsfläche für das Saaland sowie Untersuchungen verschiedener Hard- und Softwarekonfigurationen zur GPS-basierten Lage- und Höhenbestimmung im SAPOS-Netz Saarland. Diplomarbeit, Studiengang Vermessung und Geomatik, Fachhochschule Karlsruhe – University of Applied Sciences, unpublished

Jäger, R. and Schneid (2002):

Passpunktfreie direkte Höhenbestimmung mittels DFHBF – ein Konzept für Positionierungsdienste wie SAPOS. Landesvermessung und Geobasisinformation Niedersachsen (LGN) (Editor). Hannover. p. 149-166.

# Passpunktfreie direkte Höhenbestimmung mittels Digitaler Finite Elemente Höhenbezugsfläche (DFHBF) - ein Konzept für Positionierungsdienste wie SAPOS® -

Prof. Dr.-Ing. Reiner Jäger <sup>1),2)</sup> und Dipl.-Ing. (FH) Sascha Schneid <sup>2)</sup>

<sup>1)</sup> Studiengang Vermessung und Geomatik

<sup>2)</sup> Institut für Innovation und Transfer

Fachhochschule Karlsruhe - University of Applied Sciences

Moltkestrasse 30, D-76133 Karlsruhe

E-mail: dfhbf@fh-karlsruhe.de; URL: www.dfhbf.de

## Summary

The contribution discusses the state of the art, aspects and present developments in a GNSS-based (Global Navigation Satellite Systems, e.g. GPS, GLONASS, GALILEO, etc.) height determination. Introductory an overview is given on classical GNSS-based height determination approaches, which are both used in field-calibration procedures and in post-processing. These require both identical points in the application step and geoid information. In the classical case the geoid information is poorly unexploited, namely only at the discrete identical and the new points, and remains above also uncontrolled with respect to the determination of new points. The target and the main part of this article is dealing with a direct online GNSS height-determination, meaning that no identical points are needed in the application step. The concept and realization of the so-called Digitale Finite-Elemente Höhen-Bezugs-Fläche (DFHBF) - Digital Finite Element Height Reference Surface (DFHRS) in English - provides in GNSS the direct online conversion of ellipsoidal heights  $h$  into standard heights  $H$  referring to the height reference surface (HRS), of orthometric, normal-orthometric or normal height systems. The DFHRS is modelled as a continuous HRS in arbitrary large areas by bivariate polynomials with parameters  $p$  over an irregular grid of the respective Finite Element Model (FEM) meshes. Geoid information (geoid heights  $N_G$ , vertical deflections  $\xi, \eta$ ), gravity anomalies  $\Delta g$  and identical points ( $h, H$ ) are to be used as observations in a least squares DFHRS computation. It is shown that the correlated geoid heights  $N_G$  of a geoid model (e.g. EGM96, EGG97) provide the same DFHRS parameters, than the introduction of the original gravity anomalies  $\Delta g$  used for the evaluation of  $N_G$ . Several geoid models may be introduced simultaneously, and geoid models may be parted into different "geoid-patches" with individual datum-parameters to reduce the effect of different long-waved systematic errors. Additionally a scale  $\Delta m$  between the height systems  $h$  and  $H$  is part of DFHRS parameter estimation. So the resulting DFHRS represents the HRS in the correct datum, and provides by the 3-dimensional DFHRS-correction  $DFHRS(p, \Delta m | B, L, h)$  - which depends both on plan position ( $B, L$ ) and the height  $h$  - the direct transformation of an ellipsoidal GNSS height  $h$  into the standard height  $H$ . The complete 3D DFHRS-correction consists of two different parts. The first correction is the FEM of the HRS, described as a 2D function of the plan position ( $B, L$ ) by the formula abbreviation  $N_{FEM}(p | B, L)$ . This correction is accordingly called "geoid-part". The second correction, described as a 1D function of the height  $h$ , and appearing as  $\Delta m \cdot h$ , is accordingly called "scale-part". Proceeding scientific work and examples have been presented on symposia of FIG Commission 5, IAG and IAG Subcommission for Europe (EUREF). The DFHRS concept has also been proposed as a potential and flexible candidate for the evaluation of the DFHRS for Europe (EU\_DFHRS) for the GNSS user community. Meanwhile DFHRS data bases have become official products in different countries and the DFHRS data base access is provided by different receiver manufacturers. The accuracy of the DFHRS is controlled by the mesh size, and a one-cm accuracy for the online correction  $DFHRS(p, \Delta m | B, L, h)$  is a proved standard, e.g. for SAPOS® DGPS, while also dm ("rapid/light") DFHRS are requested by e.g. GIS/Navigation users. The basic ideas and the mathematical model of DFHRS computation and quality controls are discussed theoretically and finally referred to some DFHRS project examples.

## 1. Einführung und allgemeine Betrachtungen

Der Einzug neuer Sensorik, Mess- und Navigationstechniken und die mit Ausbau des satelliten- und referenzstationsnetz gestützten International Terrestrial Reference Frame (ITRF) einsetzende Globalisierung des Raumbezugs wirken als essentieller Motor für die wirtschaftlichen Wachstumsfelder der kommenden Jahre. GNSS (Global Navigation Satellite Systems) - wie GPS, GLONASS, GALILEO u. a. - leisten eine Positionsbestimmung, Standortinformation und Richtungsempfehlung mit einheitlichem ITRF-Bezug und gelten als wichtiger Taktgeber für innovative Wirtschaftsbereiche in den Sektoren Dienstleistungen, LBS, Fahrzeugindustrie und Mobilitätskommunikation. Im weiteren wird im

Kontext mit Satellitenvermessung bzw.- Navigation und der Systemvielfalt gleich der allgemeine Begriff "GNSS" anstelle des speziellen Systems "GPS" verwendet.

In Verbindung mit dem weltweit zu beobachtenden Trend, die alten derzeit noch präsenten klassischen nationalen Datumssysteme (z.B. DHDN in Deutschland) zugunsten ITRF-basierter Datumssysteme (z.B. ETRS89) und entsprechender GNSS-Referenzstationsnetze wie *SAPOS*® zu ersetzen, wird das Datumproblem in Bezug auf die Lagekomponente (B,L) zugunsten einer damit passpunkt-freien online GNSS-Lagepositionierung nach und nach keine Rolle mehr spielen. Dagegen erfordert die GNSS-basierte Höhenbestimmung aus physikalischen Gründen stets eine Bezugsflächentransformation der ellipsoidischen GNSS-Höhen  $h$  in Landeshöhen  $H$ , da sich letztere auf eine in Definition und Realisierung potentialtheoretisch fundierte Höhenbezugsfläche (HBF) - NN-Fläche (NN-Höhen), Quasigeoid (Normalhöhen) oder Geoid (orthometrische Höhen) - beziehen (Abb. 1). Die gerade auch im Kontext mit der GNSS-basierten Höhenbestimmung und der entsprechenden Nutzung von Geoidmodellen wie das EGG97 (Denker and Torge, 1997) oder das EGM96 (Lemoine et al., 1998) lehrbuchmäßig angeführte und in Abb.1 dargestellte Standardformel

$$H = h - N_G(B,L) \quad , \quad (1a)$$

erweist sich im Hinblick auf praktische Anwendungen als nicht ausreichend modelliertes Ideal. Als erster Grund dafür ist anzuführen, dass Geoidmodellen  $N_G$  zum einen ein eigenes lokales bzw. regionales Datum zu unterstellen ist (Dinter et. al., 1997; Dinter and Illner, 2001), und dass sie darüber hinaus mit mittel- und langwelligigen systematischen Formabweichungen sog. Schwachformen (Jäger, 1988; Jäger and Kaltenbach, 1990; Schmitt, 1997) behaftet sind. Auch die per "Nivellement und Schwere" realisierten Höhenbezugsflächen (HBF) bzw. die Höhensysteme  $H$  weisen, wenn auch in geringerer Ausprägung, mittel- und langwellige geometrische Defizite in Form von Schwachformen auf (Jäger 1990a,b; Jäger and Leinen, 1992; Jäger und Kälber, 2000).

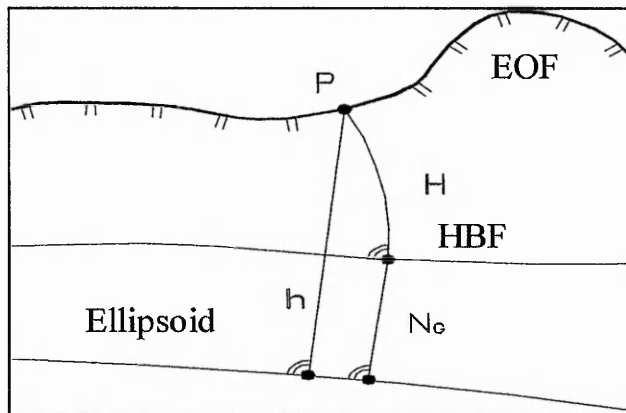


**Abb. 1:** Darstellung der Formelideals(1a): Erdoberfläche (EOF) am Ort  $P(B,L,h)$ , ellipsoidische GNSS-Höhe  $h$ , Landeshöhe  $H$  und Höhenbezugsfläche (HBF) im Kontext mit dem ideal eines Geoidmodells  $N_G$ . Unter "Real World Conditions" ist davon abweichend jedoch die Beziehung (1b) maßgeblich.

Beide o.g. Formabweichungen bzw. die damit bestehende Flächendiskrepanz kann im Sinne einer simultanen Flächenanpassung mit einem dem sog. Datumsanteil  $\partial N(d)$  (2e) modelliert und getilgt werden. Ein dritter Anteil von Inkonsistenzen bei (1a) beruht in der Maßstabdifferenz  $\Delta m$  zwischen den ellipsoidischen GNSS-Höhen  $h$  und den Höhen  $H$  des Landessystems (Dinter et al., 1997; Dinter and Illner, 2001; Schneid, 2001), wobei ein separater Maßstab des Geoidmodells bereits im Anteil der Datumparameter  $d$  (2e) zu berücksichtigen ist (Jäger, 1999c). Die Ursachen für die Maßstabdifferenz  $\Delta m$  sind vielschichtig. Zu nennen wären die mit dem topographischen Profil gehenden Maßstabeffekte infolge vernachlässigter zufälliger und systematischer Fehleranteile beim Nivellement (Jäger, 1990a) sowie die Inkonsistenzen der Georeferenzierung des Normalschwerefeldes klassischer Höhennetze bzw. Geoidmodelle gegenüber dem WGS84-Niveuellipsoid. Daher ist das obige Formelideal (1a) in Bezug auf "Real World Conditions" entsprechend zu modifizieren und lautet schließlich:

$$H = h - \underbrace{(N_G(B,L) + \partial N(d))}_{NFEM(p|B,L)} + \Delta m \cdot h \quad . \quad (1b)$$

In dem diesem Beitrag schwerpunktmäßig gegenständlichen DFHBF Konzept, wird die Rolle der in Bezug auf das GNSS-Datum (z.B. ETRS89) angepaßten und von systematischen Fehlern befreite Digitale Finite Elemente Höhenbezugsfläche (DFHBF) vom 2D Finite Element Modell (FEM) der HBF übernommen. Diese wird in (1b) entsprechend als NFEM( $\mathbf{p}|B,L$ ) - auch "Geoid-Anteil", -genannt. Das mathematische Modell des DFHBF-Ansatzes zur Berechnung von sogenannten DFHBF-Datenbanken findet sich in (4a) -(4g).

## 2. Datumsübergang und klassische Ansätze zur GNSS-Höhenintegration

Das mathematische Modell des umfassenden derzeitigen Standard Postprocessing Ansatzes zur GNSS-Höhenintegration wurde bereits vor einigen Jahren entwickelt und im Softwarepaket HEIDI2© Dinter/Illner/Jäger implementiert (Dinter et al., 1997). Dieser sogenannte "Geoidverfeinerungsansatz" stellt sich im System der Verbesserungsgleichungen wie folgt dar:

$$h + v = m \cdot H + N_G \quad (2a)$$

$$N_G(B,L) + v = N_G + \partial N_G(\mathbf{d}) + \text{NFEM}(\mathbf{p} | x, y) \quad (2b)$$

$$H + v = H \quad (2c)$$

$$C(\mathbf{p}) = 0 \quad (2d)$$

Mit  $N_G(B,L)$  werden die aus einer entsprechenden Geoidmodell-Datenbank entnommenen Geoidhöhen bezeichnet. Die Parametrisierung des Datumsübergangs  $\partial N_G(\mathbf{d})$  für das betreffende Geoidmodell lautet (Jäger, 1999c):

$$\begin{aligned} \partial N_G(\mathbf{d}) = & [\cos(L) \cdot \cos(B)] \cdot u + [\cos(B) \cdot \sin(L)] \cdot v + [\sin(B)] \cdot w \\ & + [e^2 \cdot N(B) \cdot \sin(B) \cdot \cos(B) \cdot \sin(L)] \cdot \varepsilon_x + [-e^2 \cdot N(B) \cdot \sin(B) \cdot \cos(B) \cdot \cos(L)] \cdot \varepsilon_y + [-N_G] \cdot \Delta m_G . \end{aligned} \quad (2e)$$

Zusätzlich können gemäß (2b) die Höhen  $N_G(B,L)$  des Geoidmodells durch ein sogenanntes Finites Element Model NFEM( $\mathbf{p}|x,y$ ) verfeinert werden, welches im Detail in Kap. 3 beschrieben wird. Im o.g. "Geoidverfeinerungsansatz" (2a-d) wirkt das Modell NFEM( $\mathbf{p}|x,y$ ) so als zusätzliches "Overlay" (als "Fließspachtel") einer im mittel- und langwelligen Bereich angesiedelten Formverbesserung des Geoidmodells  $N_G(B,L)$ . Ein Finite Elemente Modell NFEM( $\mathbf{p}|x,y$ ) kann ebenso auch zur kompletten Repräsentation der Höhenbezugsfläche HBF in Ansatz gebracht werden. Auf diese Idee und der damit verbundenen Behandlung von Geoidinformation  $N_G(B,L)$  beruht das diesem Beitrag schwerpunktmäßig gegenständliche DFHBF-Konzept (Kap. 4). Mit  $N(B)$  (2e) wird der Normalkrümmungsradius des Bezugsellipsoids am Ort  $P(B,L)$  bezeichnet. Die Datumsparameter  $\mathbf{d}$  umfassen drei Translationen ( $u,v,w$ ), zwei Rotationen ( $\varepsilon_x, \varepsilon_y$ ) und eine Maßstabsdifferenz  $\Delta m_G$  in der Geoidhöhe  $N_G$ .

Was weitere Einzelheiten zum Datumsproblem bzw. Datumsübergang (2b,e) und zur Verfeinerung NFEM( $\mathbf{p}|x,y$ ) sowie die Diskussion und Behandlung der Sonderfälle des o.g. klassischen Standardansatzes der GNSS-Höhenintegration - nämlich dem "Reinen Geoid-Ansatz" und dem "Reinen FEM-Ansatz" - anbelangt, so wird auf Dinter et al. (1997) and Jäger (1999c) verwiesen. Die mathematischen Grundlagen des mächtigen Tools des Finite Element Modells NFEM( $\mathbf{p}|x,y$ ), zugleich auch der zentrale Kern des DFHBF-Konzeptes, werden in Kap. 3 behandelt.

Als Nachteil des obigen Standardansatzes (2a-d) gilt, dass es sich in seinem vollen Umfang um einen typischen Postprocessingansatz handelt. Da identische Punkte ( $H, h$ ) benötigt werden, bedeutet der Ansatz ein zu unwirtschaftliches (zeitaufwendige sog. Fieldcalibration sowie Kosten für Passpunkte) Verfahren zur online GNSS-Höhenbestimmung in GNSS-Referenzstationsnetzen (Abb. 3). Aufgrund der Tatsache, dass Geoidmodelle  $N_G(B,L)$  über einen Datumsanteil  $\partial N(\mathbf{d})$  immer nur regional einpassbar sind (siehe auch "Patching", Kap. 5; Ab.4), wäre zwar ein landesweites Vorhalten regional ermittelter Datumsparameter  $\mathbf{d}$  auf einer Datenbank denkbar, nachteilig wäre bei diesem Vorgehen aber, dass auf diese Weise keine Stetigkeit von Region zu Region besteht. Darüber hinaus bliebe die mit einem Geoidmodell eigentlich zur Verfügung stehende Information nahezu vollkommen unausgeschöpft, da die Geoidhöheninformation mit  $N_G(B,L)$  im Ansatz (2a-d) nur am diskreten Ort ( $B,L$ ) der mit GNSS bestimmten Punkte einfließt. Der übrige Informationsgehalt des Geoidmodells bzw. der Geoiddatenbank bleiben ungenutzt bzw. im weiteren auch geometrisch unverbessert. Auch die seitens Geoidmodellen zur Verfügung stehende Lotabweichungsinformation ( $\xi, \eta$ ) sowie Schwere-

anomalien  $\Delta g$  finden keinen Eingang im Standardansatz (2a-d). Schließlich erfordert seine Anwendung im Postprocessing- bzw. auch im Onlinemodus der Fieldcalibration immer noch geodätisches Expertenwissen, so dass der Ansatz (2a-d) nicht für das breite Spektrum der GNSS-Anwender für eine online GNSS-Höhenbestimmung geeignet ist. Aufgrund der o.g. Nachteile ist der klassische Standardansatz (2a-d) suboptimal im Vergleich zum modernen und umfassenden DFHBF-Konzept einer online oder postprocessing-basierten GNSS-Höhenbestimmung (Kap. 3-6).

An dieser Stelle sei angemerkt, dass die fachliche Grundsteinlegung bzw. Premiere des DFHBF-Konzeptes und auch Vorbereitung der Fachwelt bereits auf dem 1. *SAPPOS*<sup>®</sup>-Symposium in 1998 (Jäger, 1998) sowie unmittelbar danach in internationalen FIG/IAG Symposien stattfand (Jäger, 1999c). Die theoretischen Erweiterungen und Realisierungsschritte, die nach der Entwicklung der DFHBF-Basissoftware (Schwarzer, 2000) im Rahmen des gleichnamigen vom Bundesministerium für Bildung, Wissenschaft und Technologie unterstützten Forschungs- und Entwicklungsprojektes zu DFHBF als neuem wissenschaftlich-technologischen Standard beitragen haben, wurden in großem Maße auch durch die Mitwirkung der unmittelbaren Projektpartner, dem Landesvermessungsamt Baden-Württemberg und IBS ([www.ib-seiler.de](http://www.ib-seiler.de)) sowie darüber hinaus dem Hessischen Landesvermessung und der Firma Leica Geosystems getragen.

### 3. Finite Elemente Modell (FEM) Repräsentation von Höhenbezugsflächen (HBF)

Ein mächtiges Tool, welches bereits im Rahmen des Standardansatzes (2a-d) der GNSS-basierten Bestimmung von Landeshöhen Einsatz findet und zugleich das zentrale Tool des DFHBF-Ansatzes (Kap. 4) ist, besteht in der Höhenbezugsflächen-Repräsentation durch ein sogenanntes Digitales Finite Element Modell NFEM( $\mathbf{p}|x,y$ ). Als Trägerfunktionen für das Modell NFEM( $\mathbf{p}|x,y$ ) der Höhenbezugsfläche (HBF) werden bivariate Polynome verwendet, welche über den Maschen eines regelmäßigen oder unregelmäßigen Finite Elemente Maschennetzes (Abb. 2, Abb. 5) in Ansatz gebracht werden. Mit  $\mathbf{p}^i$  werden die der  $i$ -ten Masche zugeordneten Polynomkoeffizienten ( $a_{00}, a_{10}, a_{01}, a_{20}, a_{11}, a_{02}, \dots$ )<sup>i</sup> bezeichnet. Unter der Prämisse der Beschreibung der kompletten HBF bzw. des "Geoids"  $N_G$  (Abb. 1) als Finites Elemente Modell (FEM) stellt sich "N<sub>G</sub>-FEM" - im weiteren entsprechend mit NFEM( $\mathbf{p}^i|x,y$ ) bezeichnet - innerhalb der  $i$ -ten Masche wie folgt dar:

$$\text{NFEM}(\mathbf{p}^i | x, y) = f(x(B,L), y(B,L)) \cdot \mathbf{p}^i ; i = 1, m; \text{ mit} \quad (3a)$$

$$\mathbf{p}^i = (a_{00}, a_{10}, a_{01}, \dots)^i \text{ and } f(x(B,L), y(B,L)) = (1, x, y, x^2, xy, y^2, \dots) \quad (3b), (3c)$$

Mit  $\mathbf{f}$  wird der sogenannte Vandermond'sche Vektor bezeichnet, der dem Polynomgrad  $n$  entsprechend die verschiedenen bivariaten Terme und Potenzen der Lagekoordinaten  $(x,y)$  enthält. Der Parametervektor  $\mathbf{p}$  besteht insgesamt aus den Sätzen der Maschenkoeffizienten  $\mathbf{p}^i = (a_{j,k})^i$ , ( $j=0,n; k=0,n$ ) aller  $m$  Maschen. Mit  $y(B,L)$ ="East" und  $x(B,L)$ ="North" werden in (3a,c) die kartesischen Lagekoordinaten z.B. in Form von UTM-, Mercator oder Lambertkoordinaten, jeweils Funktionen der geographischen Koordinaten  $(B,L)$ , eingeführt.

Um die Stetigkeit der Finiten Element Modell NFEM( $\mathbf{p}|x,y$ ) beschriebenen HBF zu erreichen, ist dem mathematischen Modell zur Berechnung von NFEM( $\mathbf{p}|x,y$ ) darüber hinaus ein Satz von Stetigkeitsbedingungen (siehe (4f)) unterschiedlichen Typs  $C_{0,1,2}$  für jede Kante von benachbarten Maschen (Abb. 2) hinzuzufügen. Stetigkeitsbedingungen vom Typ  $C_0$  implizieren die selben Funktionswerte,  $C_1$  - Stetigkeiten die selben Tangentialeben und  $C_2$ -Stetigkeiten die selbe Krümmung entlang der Kanten benachbarter Maschen der in (4a) insgesamt stetig repräsentierten Höhenbezugsfläche NFEM( $\mathbf{p}|x,y$ ). Die Stetigkeitsbedingungen treten als Bedingungsgleichungen  $C(\mathbf{p})=0$  zur Parametrisierung NFEM( $\mathbf{p}|x,y$ ) hinzu, und beziehen sich satzweise auf die Koeffizienten  $(a_{jk})^m$  and  $(a_{jk})^n$  von Nachbar-maschen  $m$  and  $n$ .

Die Bedingungsgleichungen können gemäß (4f) auch als fingierte Bedingungsgleichungen mit variablen Gewicht eingeführt werden. Um z. B.  $C_0$ -Stetigkeit an beliebiger Stelle entlang der Kante SA-SE zweier Maschen  $m$  and  $n$  (siehe Abb.2) zu erzielen, muss die Differenz  $\Delta N_{m,n}$  der "Geoidhöhe"  $N_G$  - besser der Höhe der HBF-Repräsentation NFEM( $\mathbf{p}|x,y$ ) - entlang der kompletten Kante SA-SE Null werden. Für das bivariate Polynom  $n$ -ten Gerade lautet die Ausgangsbeziehung für  $C_0$ -Stetigkeit entsprechend (Schneid 2001):

$$\Delta N_{m,n}(t) = \sum_{j=0}^n \sum_{k=0}^{n-j} (a_{jk,n} - a_{jk,m}) \cdot (y_{SA} + t \cdot (y_{SA} - y_{SE}))^j \cdot (x_{SA} + t \cdot (x_{SA} - x_{SE}))^k \quad (3d)$$

$$\equiv 0$$

Mit  $(y_{SA}, x_{SA}, y_{SE}, x_{SE})$  werden die Lagekoordinaten der Knotenpunkte SA und SE (Abb. 2) eingeführt, für den Geradenparameter  $t$  zur Kante SA-SE gilt als Wertebereich das geschlossene Intervall  $(t \in [0,1])$ . Die Untermenge der  $(n+1)$   $C_0$ -Stetigkeitsbedingungen  $C(p)=0$  zur allgemeinen Kante SA-SE der Maschen  $m$  und  $n$  (Abb. 2) geht im Fall der mit (3d) gefordertern  $C_0$ -Stetigkeit schließlich hervor, indem dort alle  $(n+1)$  auf die Variable  $t$  bezogenen Polynomkoeffizienten einzeln zu Null gesetzt werden.

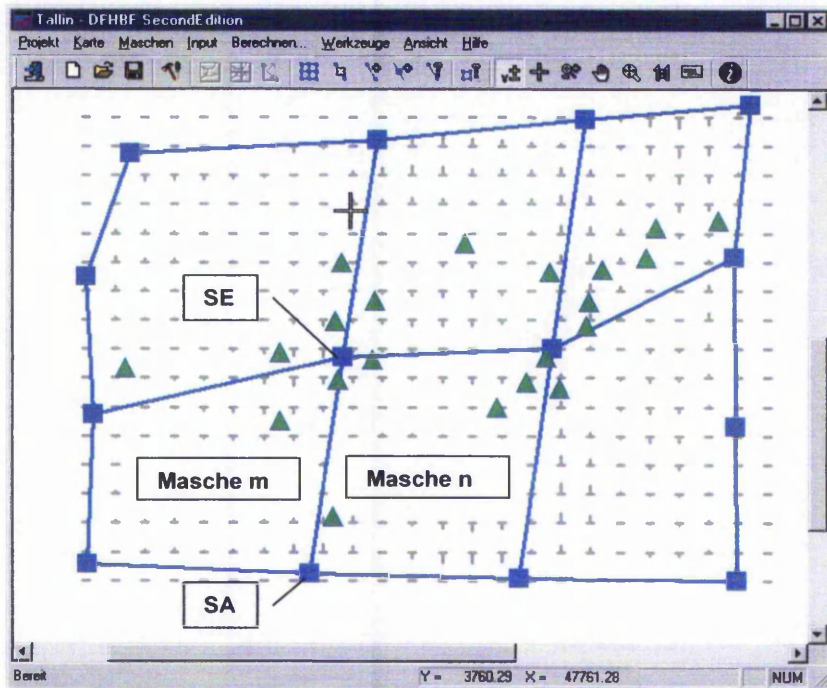


**Abb. 2:** Screenshot auf DFHBF-Produktionssoftware. Unregelmäßiges FEM-Maschennetz und verschiedene Beobachtungstypen: Geoiddatenraster dargestellt als graue Horizontalstriche mit Residuen; identische Punkte (H,h) dargestellt als Dreiecke. Beispiel zur Berechnung der DFHBF\_DB Tallinn, Estland im Normalhöhenystem.

Die Maschengröße und die Maschenform zur Berechnung der HBF-Repräsentation  $NFEM(p|x,y)$  - im Kontext mit dem DFHBF-Konzept (Kap. 3-6) und der entsprechenden DFHBF-Datenbanken auch als "Geoid-Anteil" (7c) bezeichnet - sind gerade auch, was deren Erzeugung und Gestaltung in der DFHBF-Produktionssoftware (Schwarzer, 2000; Schneid, 2001) beliebig (Abb. 2, Abb. 5). Die Approximationsqualität einer Höhenbezugsfläche durch das Modell  $NFEM(p|x,y)$  hängt hinsichtlich der Auflösung von Kleinformen sowohl von der Maschengröße als auch dem Polynomgrad ab. Aus verschiedenen Untersuchungen gilt als Richtwert für eine HBF-Auflösung besser als 5 mm eine Vierecksmaschengröße von 5 km bei einem Polynomgrad  $n=3$ .

Ein spezieller Vorteil und Charakteristik der Finite Element Repräsentation  $NFEM(p|x,y)$  besteht im Vergleich zu anderen Ansätzen (z.B. sonstigen Standards wie der Vermaschung, Berechnung und Repräsentation von topographischen Höhenmodelle) darin, dass die Knotenpunkte des unregelmäßigen FEM-Netzes (Abb. 2) von der Lage und Topologie der in die  $NFEM(p|x,y)$ -Berechnung einfließenden geodätischen Beobachtungen bzw. dem geodätischen Netzdesign (z.B. gerade auch von der Lage "Passpunkte" (H,h) ) vollkommen entkoppelt sind. De facto kann so jeder beliebige HBF-bezogene Beobachtungstyp an jedem Ort in die Bestimmung der Parameter  $p$  des  $NFEM(p|x,y)$  Modells sowie zusätzlicher Maßstabsparameter  $\Delta m$  in die überbestimmte und damit kontrollierte Berechnung von DFHBF\_DB einfließen (4a-g). Zu nennen wären als Beobachtungstypen zur DFHBF\_DB-Berechnung absolute und relative ellipsoidische bzw. Landeshöheninformation  $(h, H, \Delta H, \Delta h)$ , satellitengeodäti-

sche bzw. gravimetrische Geoidhöhen  $N_G(B,L)$  und Lotabweichungsinformation  $(\xi,\eta)$  aus entsprechenden Datenbanken oder aus astrogeodätischen Messungen sowie Schwereanomalien  $\Delta g$ .

#### 4. Konzept der Digitalen Finite Elemente Höhenbezugsfläche (DFHBF)

Das DFHBF Konzept zielt auf eine direkte passpunktfreie GNSS-basierte Höhenbestimmung ab, wobei im ersten Schritt, der sogenannten DFHBF-Produktion (4a-g), eine überstimmte statistisch kontrollierte Berechnung der Parameter einer sogenannten DFHBF-Datenbank, kurz DFHBF\_DB, bei optimaler und maximal effizienter Ausschöpfung aller verfügbaren Datenquellen erfolgt. Damit stellt sich das alle theoretischen und praxisrelevanten Optimalitätskriterien auf sich vereinigende DFHBF-Konzept im Profil der passpunktfreien GNSS-basierten online oder im Postprocessing erfolgenden Bestimmung von Landeshöhen  $H$  - d.h. im Schritt der DFHBF\_DB Nutzung - wie folgt dar:

Im Zugriff auf die DFHBF-DB soll die am Ort  $(B,L,h)$  bestimmte ellipsoidische GNSS Höhe  $h$  in Form einer von der Position  $(B,L,h)$  abhängigen sogenannten DFHBF-Korrektur  $DFHBF(p,\Delta m|B,L,h)$  (7a-c) direkt in die Landeshöhe  $H$  zu konvertieren sein.

Der Schritt der DFHBF\_DB-Nutzung ist, insbesondere mit Blick auf eine passpunktfreie GNSS-basierte online Höhenbestimmung bei GNSS-Referenzstations- bzw. Korrekturdatendiensten wie SAPOS® (Abb. 3) auf zweierlei Art denkbar: Zum einen kann die DFHBF-Korrektur bei unidirektionaler Verbindung im Referenzstationensnetz im Zugriff auf die im Feld mitgeführte DFHBF\_DB ermittelt werden. Vorteilhaft ist hier der, verglichen mit klassischen "Geoid"-Datenbanken, geringe Speicherbedarf für DFHBF\_DB, z.B. nur ca. 90KB für die "1 cm DFHBF\_DB Baden-Württemberg" (Kap. 6). Zum zweiten könnte die DFHBF-Korrektur bei bidirektionaler Kommunikation (wie im Fall virtueller Referenzstationen), z.B. als Bestandteil der RTCM-Korrektur (z.B. in Message 59), durch den GNSS-Korrekturdatendienst versendet werden.

##### 4.1 DFHBF\_DB Produktion

Das mathematische Modell zur DFHBF\_DB Produktion stellt sich im System der Verbesserungsgleichungen der verschiedenen Beobachtungstypen (funktionales Modell) und der entsprechenden stochastischen Modell einer Kleinsten-Quadrate-Ausgleichung wie folgt dar:

###### Funktional Modelle

$$h + v = H + h \cdot \Delta m + f(x, y) \cdot p,$$

$$\text{mit NFEM}(p | x, y) =: f(x, y) \cdot p$$

$$N_G(B, L)^j + v = f(x, y) \cdot p + \partial N_G(d^j)$$

$$\xi + v = -f_B / M(B) \cdot p + \partial B(d_{\xi, \eta})$$

$$\eta + v = -f_L / (N(B) \cdot \cos(B)) \cdot p + \partial L(d_{\xi, \eta})$$

$$H + v = H$$

$$C + v = C(p)$$

###### Beobachtungstypen und Stochastische Modelle

Korrelierte oder unkorrelierte ellipsoidische Höhen  $h$ . Kovarianzmatrix  $C_h$  (4a)

Korrelierte Geoidhöhenbeobachtungen  $N_G$ . Gegebene reale oder einer aus geeigneter Kovarianzfunktion entwickelte synthetische Kovarianzmatrix  $C_{N,G}$ . (4b)

Lotabweichungsbeobachtungen  $(\eta, \xi)$ . Korreliert für den Fall (4c)

der Entnahme aus Schwerpotential basierten Datenbank. Korreliert oder unkorreliert im Fall astrogeodätischer Beobachtungen. Kovarianzmatrix  $C_{\xi, \eta}$ . (4d)

Unkorrelierte Landeshöhen  $H$ . Kovarianzmatrix (4e)

$$C_H = \text{diag}(\sigma_{H_i}^2)$$

Stetigkeitsbedingungen (3d) eingeführt als unkorrelierte Pseudobeobachtungen mit entsprechend kleinen Varianzen und (4f)

hohen Gewichten  $C_C = \text{diag}(\sigma_{C_i}^2)$

Mit  $\partial N_G(d^j)$  (4b) wird der in (2e) formelmäßig dargestellten Datumsübergänge der "Geoid"-Höhen  $N_G$  des dem HBF-Typ entsprechenden  $j$ -ten Geoid- oder Quasigeoidmodells bzw. auch das Datum des einzelnen  $j$ -ten sogenannten Geoid-"Patches" ("Patching", siehe Kap. 5) bezeichnet. Mit  $\partial B(d_{\xi, \eta})$  bzw.  $\partial L(d_{\xi, \eta})$  (4c,d) werden die Datumsübergänge einer Lotabweichungsgruppe  $(\xi, \eta)$  eingeführt. Explizite Formeln für  $\partial B(d_{\xi, \eta})$  und  $\partial L(d_{\xi, \eta})$  finden sich in Jäger and Schneid (2001a). Mit  $f_B$  und  $f_L$  (4c,d) werden die partiellen Ableitungen des Vandermondschen Vectors  $f(x(B,L), y(B,L))$  (3c) nach den geogra-

phischen Koordinaten B und L bezeichnet. M(B) und N(B) bedeuten in diesem Kontext den Meridian- bzw. Normalhalbmesser des Bezugsellipsoids an der Stelle (B,L). Prinzipiell wäre analog zu (2b) auch in (4b) ein zusätzlicher FEM-basierter Verfeinerungsterm für das Geoidmodell  $N_G^j$  in (4b) in Ansatz zu bringen. Schwereanomalien  $\Delta g$  sind im DFHBF-Konzept als zusätzliche Beobachtungsgruppe über das Theorem von Stokes einzuführen. Es gilt damit:

**Funktionales Modell**

$$\frac{a}{4\pi\gamma(B)} \iint_{\sigma} \Delta g \cdot S(\psi) \cdot d\sigma + v = \mathbf{f}(x, y) \cdot \mathbf{p}$$

$$= \text{NFEM}(\mathbf{p} | x, y)$$

**Beobachtungstyp und Stochastisches Modell**

Vektor der reduzierten Schwereanomalien  $\Delta g$ , einzuführen mit (4g) der Kovarianzmatrix  $C_g$  via Theorem von Stokes. Damit besteht die Beziehung zwischen den Beobachtungen  $\Delta g$  und dem FEM-Modell  $\text{NFEM}(\mathbf{p}|B,L)$  der HBF .

Die Berechnung von DFHBF\_DB erfolgt im Standard über identische Punkte (H, h) bzw. Höhenunterschiede ( $\Delta H, \Delta h$ ) als Mindestanforderung, und darüber hinaus über ein oder mehrere als Beobachtungen in die Kleinste-Quadrate-Ausgleichung (4a-g) einzuführende Geoidmodelle  $N_G(B,L)^j$ . Die rasterartig eingeführten Geoidhöhenbeobachtungen (Abb. 2) der Geoidmodelle  $N_G(B,L)^j$  werden so unter optimal suffizienter Ausschöpfung deren geometrischer Information in das zweidimensionale und mit (4f) explizit stetige Finite Element Modell  $\text{NFEM}(\mathbf{p}|x,y)$  der HBF abgebildet ("Geoid-Mapping"). Dabei werden die Datumsanteile  $\partial N_G(\mathbf{d}^j)$  entfernt und regionale Maßstabsdifferenzen  $\Delta m$  berücksichtigt. Im Zuge des "Geoid-Patching" - der Flickenteppich-artigen Aufteilung der Geoidmodelle (Kap. 5) - werden zur Tilgung regionaler systematischer Fehler von Geoidmodellen auch entsprechend regionale Datumsanteile  $\partial N_G(\mathbf{d}^j)$  bzw. Datumparameter  $\mathbf{d}^j$  vergeben.

Die zur Konvertierung von h nach H nach (7a-c) im Zugriff auf die DFHBF\_DB zu ermittelnden DFHBF-Korrektur  $\text{DFHBF}(\mathbf{p}, \Delta m | B, L, h)$  erfolgt im DFHBF\_DB-Produktionsschritt (4a-g) unter Einbettung in die Qualitätskontrollstandards sowie weiterer spezifischer Qualitätsmaße (Kap. 4.3) einer Kleinsten Quadrate Ausgleichung (Schwarzer, 2000; Schneid, 2001).

Bei Einführung eines Geoidmodells  $N_G$  (4b) anstelle der erneuten Einführung der dessen Berechnung verwendeten originären Schwereanomalien  $\Delta g$  (4g) liefert der DFHBF-Ansatz (4a-g) ein dazu äquivalentes Ergebnis im Sinne einer strengen zweistufigen Ausgleichung. Der DFHBF-Ansatz leistet damit zugleich eine formverbessernde und datumsanpassende Neuberechnung von Geoidmodellen  $N_G$  (4b), die sich im Beitrag ihrer entsprechenden Teilinformation dann in Gestalt des neuen Produkts des Finite Elemente Modells  $\text{NFEM}(\mathbf{p}|x,y)$  der Höhenbezugsfläche HBF (zugleich der 2D "Geoidanteil" der 3D DFHBF-Korrektur (7a-c)) wiederfinden. Dem o.g. Äquivalenzaspekt und dessem mathematischen Beweis widmet sich das nachfolgende Kap. 4.2.

**4.2 Äquivalenz von "Geoidmodell  $N_G$ " und "originären Schwereanomalien  $\Delta g$ "**

Der klassische Ansatz der gravimetrischen Geoidbestimmung (4g) läßt sich in äquivalenter Form auch dem funktionalen Modell einer Kleinste Quadrate Ausgleichung zuordnen, die o.B.d.A. nicht überbestimmte wie überbestimmte Berechnung einschließt (so wie z.B. die Berechnung eines einfachen nichtlinearen Bogenschnitts auch als linearisierte Ausgleichungsaufgabe erfolgen kann). Wir erhalten vor diesem Hintergrund bzgl. (4g) formal den folgenden Ansatz:

- **Klassische gravimetrische "Geoid"-Bestimmung  $N_G$  als Ausgleichungsansatz**

**Funktionales Modell**

$$E(\Delta g_{St}) = A_G \cdot N_G$$

**Beobachtungstyp und Stochastisches Modell**

Mit  $\Delta g_{St}$  wird der "schwerbezogene Beobachtungstyp" wie er z.B. nach Stokes (4g) als (5a)

$$\Delta g_{St} =: \frac{a}{4\pi\gamma(B)} \iint_{\sigma} \Delta g \cdot S(\psi) \cdot d\sigma$$

zur Bestimmung der "Geoid"-Höhe  $N_G$  eingeführt wird. Mit  $A_g$  und  $C_g$  werden die zugehörige Designmatrix ( $A_g = I$  inbegriffen) und Kovarianzmatrizen bezeichnet.

**Ergebnis der Kleinste Quadrate Ausgleichung**

$$N_G = (A_G^T \cdot C_g^{-1} \cdot A_G)^{-1} \cdot A_G^T \cdot C_g^{-1} \cdot \Delta g_{St} \quad \text{und} \quad C_{N,G} = (A_G^T \cdot C_g^{-1} \cdot A_G)^{-1} \quad (5b)$$

Wir gehen nun zurück zum DFHBF-Ansatz (4a-g). Wir führen die dort nun die Geoidhöhen  $N_G$  (5b) zusammen mit ihrer Kovarianzmatrix  $C_{N,G}$  (5b) ein, und wir subsumieren mit "I" alle übrigen Beobachtungen, mit Ausnahme eben der in die Berechnung von  $N_G$  bereits eingeflossenen Schwereanomalien  $\Delta g$  (4g). Auf diese Weise erhalten wir das mathematische Modell (5c,d). Daraus gehen die Parameter  $\mathbf{p}$  des - vorteilhaft im DFHBF-Ansatz berechneten - neuen Geoidmodells nun in Gestalt des Finite Elemente Modells NFEM( $\mathbf{p}|x,y$ ) der Höhenbezugsfläche HBF nach (5e) hervor.

• **Üblicher DFHBF Ansatz: Geoidbeobachtungen  $N_G$  anstelle von Schwereanomalien  $\Delta g$**

**Funktionales Modell**

**Beobachtungstypen und stochastisches Modell**

$E(N_G) = A_N \cdot \mathbf{p}$  (entsprechend 4a reduziert, auf Parameter  $\mathbf{p}$ )      Kovarianzmatrix (5b)  $C_{N,G} = (A_G^T \cdot C_g^{-1} \cdot A_G)^{-1}$       (5c)

$E(l) = A_l \cdot \mathbf{p}$       Restliche Beobachtungen l, Ausnahme  $\Delta g$ . Kovarianzmatrix  $C_l$       (5d)

**Ergebnis der Kleinste-Quadrate-Schätzung der Geoidparameter  $\mathbf{p}$**

$\mathbf{p} = (A_N^T \cdot C_N^{-1} \cdot A_N + A_l^T \cdot C_l^{-1} \cdot A_l)^{-1} \cdot (A_N^T \cdot C_N^{-1} \cdot N_G + A_l^T \cdot C_l^{-1} \cdot l)$       (5e)

Wir gehen nun wieder zurück zum DFHBF-Ausgangsansatz (4a-g). Nun führen wir dort die originären Schwereanomalien  $\Delta g$  und ihre Kovarianzmatrix  $C_g$  ein, die nach (5a,b) zur Berechnung des ursprünglichen Geoidmodells  $N_G$  (4b) verwendet wurden. Wir subsumieren wieder die übrigen Beobachtungen, nun mit Ausnahme des Geoidmodells  $N_G$ , im Vektor "I". Mit Bezug zu (4a) und (5c) verifizieren wir die Parametertransformation  $N_G = A_N \cdot \mathbf{p}$ , mit  $f(x,y) = A_N$ , zwischen Geoidhöhen  $N_G$  und den DFHBF-bezogenen Geoidparametern  $\mathbf{p}$ . Auf diese Weise erhalten wir das mathematische Modell (5f-h). Im DFHBF-Ansatz (4a-g) und der entsprechenden Kleinste Quadrate Ausgleichung gehen hieraus die NFEM- bzw. "Geoid"-Parameter  $\mathbf{p}$  nach (5h) hervor. Durch Einführung der Beziehungen (5b) und (5f) in (5h) erhalten wir schließlich (5i).

• **Alternative DFHBF-Lösung: Originäre Schweranomalie  $\Delta g$  anstelle der Geoidhöhen  $N_G$**

**Funktionales Modell**

**Beobachtungstypen und Stochastische Modelle**

$E(\Delta g_{St}) = A_G \cdot N_G$       Originäre Schwereanomalien  $\Delta g_{St}$  (5a), originäre Kovarianzmatrix  $C_g$ . Designmatrix bzgl. Geoidhöhen  $N_G$       (5f)

(5c)  $N_G = A_N \cdot \mathbf{p}$        $\Updownarrow$       Parametertransformation zwischen den Geoidhöhen  $N_G$  und den DFHBF-Parametern  $\mathbf{p}$

$E(\Delta g_{St}) = A_G \cdot A_N \cdot \mathbf{p}$

$E(l) = A_l \cdot \mathbf{p}$       Restliche Beobachtungen, Ausnahme der Geoidmodellhöhen  $N_G$ , mit Kovarianzmatrix  $C_l$       (5g)

**Ergebnis der Kleinste-Quadrate-Schätzung der Geoidparameter  $\mathbf{p}$**

$\mathbf{p} = (A_N^T \cdot \underbrace{A_G^T \cdot C_g^{-1} \cdot A_G}_{C_{N,G}^{-1}, \text{ siehe (5b)}} \cdot A_N + A_l^T \cdot C_l^{-1} \cdot A_l)^{-1} \cdot (A_N^T \cdot \underbrace{A_G^T \cdot C_g^{-1} \cdot \Delta g_{St}}_{C_{N,G}^{-1} \cdot N_G, \text{ mit } \Delta g_{St} = A_G \cdot N_G \text{ (5f)}} + A_l^T \cdot C_l^{-1} \cdot l)$       (5h)

$\Rightarrow \mathbf{p} = (A_N^T \cdot C_N^{-1} \cdot A_N + A_l^T \cdot C_l^{-1} \cdot A_l)^{-1} \cdot (A_N^T \cdot C_N^{-1} \cdot N_G + A_l^T \cdot C_l^{-1} \cdot l) \equiv \mathbf{p}$  (5e)      (5i)   
 q.e.d

Das Ergebnis (5i) beweist, dass die Parameter  $\mathbf{p}$  des in Gestalt des neuen Produkts Finite Elemente Modells NFEM( $\mathbf{p}|x,y$ ) der Höhenbezugsfläche HBF mit entsprechendem Beitrag auftretenden Geoidmodelle im DFHBF-Ansatz (4a-g) in äquivalenter Form wahlweise entweder mit den originären Schwereanomalien  $\Delta g$  (4g) oder mit dem entsprechend daraus vorausgehend zustande gekommenen

"alten" Geoidmodells  $N_G$  (2b) berechnet werden können. Für die Praxis der DFHBF\_DB-Berechnung bedeutet diese Äquivalenz, dass der Geoidmodell-Input in der Form  $N_G$  (4b) insofern und o.B.d.A. bevorzugt wird, als dass dieser - ohne Verlust an Information und geometrischer Qualität - eine einfachere und kompaktere Datenbehandlung als die originären Schwereanomalien  $\Delta g$  (4g) erlaubt. Entsprechend sind die Verbesserungsgleichungen für Schwereanomalien  $\Delta g$  (4g) im DFHBF-Konzept (4a-g) nur dann in Ansatz zur bringen, wenn zusätzliche Schwereanomalien  $\Delta g$  vorliegen, die (noch) nicht in die Berechnung des/der vorliegenden Geoidmodelle  $N_G$  (4b) eingeflossen waren. Die Betrachtungen bzw. der Beweis (5a-i) zeigen, dass das DFHBF-Konzept und der Ansatz (4a-g) ein

- strenges zweistufige Ausgleichungsverfahren zur
- optimalen Verbesserung der Geometrie klassischer Geoidmodelle  $N_G$ , (hiernach anteilmäßig repräsentiert im Finite Elemente Modell NFEM( $p|B,L$ ) (4a) der HBF) und damit zur
- Reduktion der geometrischer Defekte in Form mittel- und langwelliger Geoidmodell-Schwachformen, zu deren
- gleichzeitiger Anpassung an die gegebene HBF-Geometrie und schließlich zur
- erforderlichen Schätzung der regionalen Maßstabsdifferenzen  $\Delta m$  (4a)

beinhalten. Auf diese Weise definiert ich mit dem DFHBF-Ansatz (4a-g) insgesamt eine neue Methode bzw. ein neuer Standard sowohl zur Lösung des überbestimmten RWP der Geoidbestimmung als auch zur Lösung des Problems einer direkten GNSS-basierten Landeshöhenbestimmung im online (z.B. SAPOS®-HEPS) oder im Postprocessing Modus unter Einsatz entsprechender DFHBF-Datenbanken und der daraus hervorgehenden 3D DFHBF-Korrekturen DFHBF( $p,\Delta m|B,L,h$ ) (7a-c).

### 4.3 Qualitätskontrolle bei der Produktion von DFHBF\_DB

Über die bei DFHBF\_DB-Berechnungen im DFHBF-Ansatz (4a-g) und den in der DFHBF-Software realisierten Qualitätssicherungsstandards (Datennooping, Varianzkomponentenschätzung etc.) der Netzausgleichung (Schwarzer, 2000; Schneid, 2001) hinaus, wurde als aussagekräftiges Maß zur Qualitätsbemessung der DFHBF-Korrektur DFHBF( $p,\Delta m|B,L,h$ ) (7a-c) der sogenannte Reproduktionswert, kurz "Repro-Wert", entwickelt und implementiert. Der für jeden in die Berechnung einer DFHBF\_DB nach (4a-g) einfließendes Paßpunktepaar  $(h,H)_i$  zu ermittelnden Repro-Wert definiert sich über als Differenz  $\nabla H_i$

$$\nabla H_i = H_i - H_i(h_i, DFHBF(p,\Delta|B,L,h)_{n-1}) = H_i - H_{i,n-1} \quad (7a, b, c). \quad (6a)$$

aus dessen vorliegender Landeshöhe  $H_i$  und der aus  $h_i$  über die DFHBF-Korrektur DFHBF( $p,\Delta m|B,L,h$ )<sub>n-1</sub> zu ermittelnde Landeshöhe  $H_{i,n-1}$ . Dabei soll der betreffenden DFHBF-Korrektur DFHBF( $p,\Delta m|B,L,h$ )<sub>n-1</sub> jeweils jene  $i$ -te individuelle DFHBF\_DB zugrunde liegen, an deren Berechnung (4a-g) der betreffende identische Punkt  $(h,H)_i$  ausgeschlossen war. Die Repro-Werte  $\nabla H_i$  aus der Klasse "genauer" Paßpunkte  $(h,H)_i$  liefern so eine - unmittelbar auf die DFHBF\_DB bzw. einer daraus zu erhaltenen DFHBF-Korrektur beziehbare - objektive globale wie auch landesweit lokal anzugebende Qualität des DFHBF\_DB-Produktes. Es lässt sich zeigen, dass die Repro-Werte  $\nabla H_i$  (6a) im Zuge der DFHBF\_DB Berechnung nach (4a-g) auch in einem Guss, nämlich in der Form

$$\nabla H_i = - \frac{v_{H_i}}{r_{H_i}} \quad (6b)$$

zu ermitteln sind. Mit  $v_{H_i}$  und  $r_{H_i}$  werden die Verbesserung bzw. der Redundanzanteil der in die DFHBF\_DB nach (4e) eingehenden Landeshöhe  $H_i$  bezeichnet.

### 4.4 DFHBF\_DB in der Anwendungspraxis

Die Ausgangsbeziehung zur Berechnung der dreidimensionalen DFHBF-Korrektur (siehe auch Jäger, 1998) geht bereits unmittelbar aus der Verbesserungsgleichung (4a) der DFHBF\_DB Produktion hervor. Unter direkter Umstellung dieser berechnet sich die 3-dimensionale DFHBF-Korrektur DFHBF( $p,\Delta m|B,L,h$ ) und das Ergebnis  $H$  der positionsabhängigen Konvertierung der ellipsoidischen Höhe  $h$  in die Landeshöhe  $H$  sofort als:

$$H = h - DFHBF(\mathbf{p}, \Delta m | B, L, h) \quad (7a)$$

$$= h - \mathbf{f}(x(B, L), y(B, L)) \cdot \mathbf{p} - h \cdot \Delta m \quad (7b)$$

$$= h - NFEM(\mathbf{p} | x(B, L), y(B, L)) - h \cdot \Delta m. \quad (7c)$$

Dabei hängt die DFHBF-Korrektur  $DFHBF(\mathbf{p}, \Delta m | B, L, h)$  (7a) sowohl von der Lage  $(B, L)$  als auch der ellipsoidischen Höhe  $h$  ab. Der zweidimensionale von der Lage  $(B, L)$  abhängige Korrekturanteil  $NFEM(\mathbf{p} | B, L)$  wird in seiner Eigenschaft als Finite Elemente Modell  $NFEM(\mathbf{p} | x, y)$  der Höhenbezugsfläche HBF (Abb. 3, links) auch als "Geoid-Anteil" bezeichnet. Der eindimensionale zusätzliche Korrekturanteil  $\Delta m \cdot h$  wird geometrischen Bedeutung entsprechend als "Maßstabs-Anteil" bezeichnet. Gemäß dem Korrekturschema (7a-c) umfassen  $DFHBF\_DB$  neben den Angaben zur Topologie der FEM-Vermaischung (Abb. 2) die Polynomkoeffizienten  $\mathbf{p}$  und die zugehörigen Maßstabsterme  $\Delta m$ . Die Abb. 3 zeigt die Anwendung einer  $DFHBF\_DB$  bei der online GNSS-basierten Bestimmung von Landeshöhen in Referenzstationsnetzen wie *SAPPOS*<sup>®</sup>.

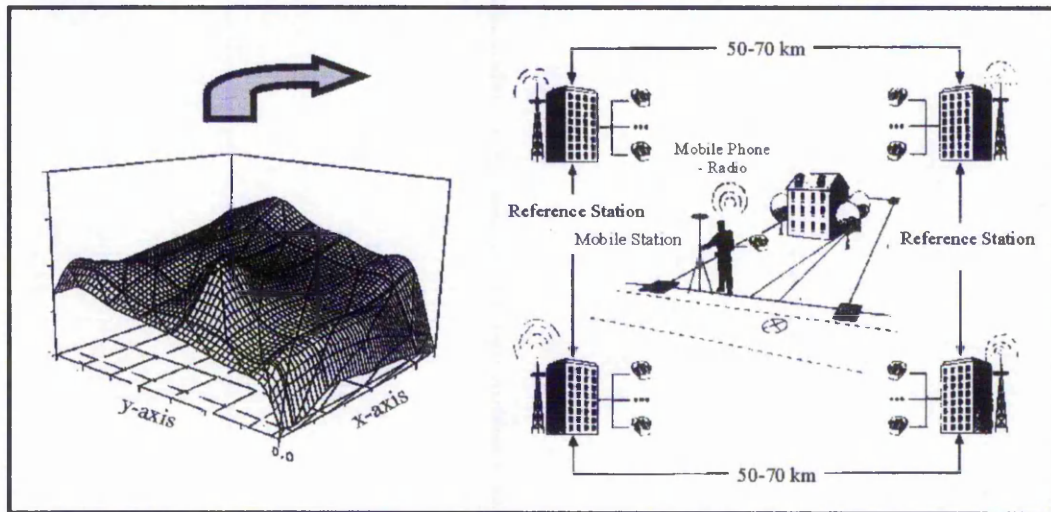


**Abb. 3:**  $DFHBF\_DB$  symbolisiert durch den "Geoid"-Anteil  $NFEM(\mathbf{p} | B, L)$  des Finite Element Modells der HBF (links) und Anwendungsszene der online GNSS-Höhenbestimmung z.B. mit *SAPPOS*<sup>®</sup> (rechts).

Für große Gebiete bzw. kompakte  $DFHRS\_DB$ , welche sich über mehrere Länder erstrecken, ist im Zuge der  $DFHBF$ -Berechnung (4a-g) die Schätzung mehrerer regionaler Maßstabsfaktoren  $\Delta m$  in (4a) vorzusehen. Bei den bisherigen  $DFHBF\_DB$  Berechnungen (Kap. 6) hat sich gezeigt, dass auch Länder in der Größe von Baden-Württemberg (Abb. 5) mitunter mit einem Maßstabsfaktor  $\Delta m$  auskommen. Das  $DFHBF$ -Korrekturschema (7a,b,c) erfüllt alle für das Anforderungsprofil einer direkten online oder Postprocessing-basierten maßgeblichen Erfordernisse (1b).

## 5 Spezielle Anforderungen und Techniken zum Mathematischen Modell des $DFHBF$ Konzeptes

Wie in Kap. 4.2 gezeigt, leistet der  $DHBF$ -Ansatz (4a-g) bei Einführung eines Geoidmodells  $N_G$  mit originären Kovarianzmatrix oder eines adäquaten Ersatzes  $C_{N,G}$  (5b) prinzipiell eine strenge zwei-stufige Ausgleichung und sichert so die Äquivalenz zur wiederholten Einführung der originären Schwereanomalien  $\Delta g$ , welche zur Berechnung des Geoidmodells  $N_G$  beigetragen haben. Die durch den Anteil der bekannten zufälligen Beobachtungsfehler  $C_g$  der Schwereanomalien  $\Delta g$  (5a) induzierten und als geometrische Formabweichungen auftretenden natürlichen Schwachformen (Jäger, 1990a,b; Jäger and Leinen 1992; Schmitt, 1997) der Geoidmodelle  $N_G$  (Dinter et al., 1997) werden auf diese Weise durch die geometrischen Information aller zusätzlichen Beobachtungstypen - z.B. die der identischen Punkte  $(h, H)$  - im Ergebnis der  $DFHBF$ -Berechnung (4a-d) reduziert. Analog dazu sind auch den Höhennetzen  $H$  und  $h$  entsprechende Schwachformen zu unterstellen, die jedoch im Vergleich zu den Schwachformen der Geoidmodelle  $N_G$  (Jäger, 1999c; Dinter et al., 1997) von geringerem Umfang sind. In Bezug auf Untersuchungen und Quantifizierungen der Schwachformen von Höhennetzen  $H$ , z.B. auch zum europäischen Höhennetz, wird auf Jäger (1990a) verwiesen.

Ein zweiter mittel- und langwelliger Schwachformenanteil, der sowohl die Geoidform  $N_G$  (wie analog wenn auch in geringerem Umfang durch die Form der mit den Höhen  $H$  repräsentierten HBF), entsteht durch zusätzliche Anteile von korrelierten Beobachtungsfehlern in  $\Delta g$ . Auch dieser Typ tritt in Höhennetzen  $H$  und  $h$  auf und führt hier zu entsprechenden Aufbiegungen, wenn auch geringeren Umfangs. Schließlich kommt ein dritter Typ und Anteil mittel- und langwelliger Schwachformen durch unterschiedliche Typen latent systematischer Fehler zustande. Die Theorie und Beispiele für alle drei der o.g. Klassen von Beobachtungsfehlern und den entsprechend induzierten Schwachformen finden sich für Landes- und GPS-Höhennetze in Jäger (1990a,b) sowie Jäger und Leinen (1992).

Den im Vergleich gering ausfallenden Schwachformen der Höhennetze  $H$  und  $h$  sowie dem negativen Einfluß der beiden letztgenannten Typen der Schwachformen bei Geoidmodellen  $N_G$  auf das DFHBF\_DB Ergebnis wird bei der Berechnung von DFHBF\_DB konzeptionell durch die spezielle Technik des "Geoid-Patching" entgegengewirkt. Die nachfolgend zu beschreibende Technik des Geoid-Patching ist auch für die natürlichen Schwachformen von Geoidmodellen  $N_G$  infolge zufälliger Fehleranteile dann relevant, wenn die Geoidbeobachtungen  $N_G$  (4b) - abweichend von  $C_{N,G}$  (4b) - als unkorrelierte Beobachtungen behandelt werden.

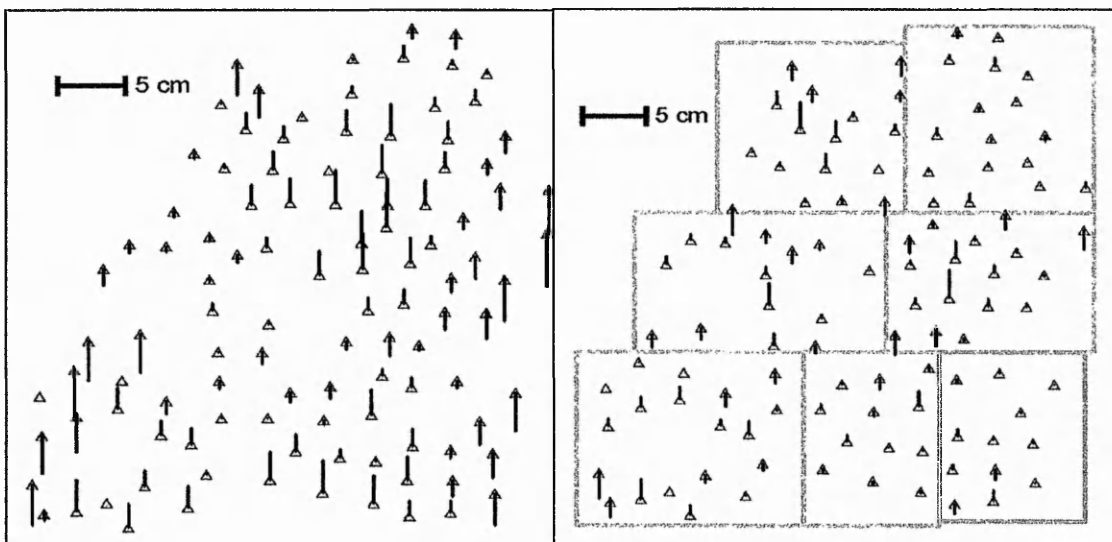


**Abb. 4:** Effekt des "Patching" am Beispiel Baden-Württemberg: Große Residuen in den identischen Punkten und damit in der DFHBF bei nur einen Satz von Datumparametern (links), weitaus kleinere Residuen bei exemplarisch 7 Patches mit individuellen Datumanteilen  $\partial N_G(\mathbf{d}^j)$  (rechts).

Das "Patching" wird als Maßnahme eingeführt, um über die o.g. strenge stochastische Modellwahl hinaus einer negativen Einflußnahme der o.g. mittel- bzw. langwelligigen systematischen Schwachformen auf die Qualität der DFHBF entgegenzuwirken. Es definiert sich in Verbindung mit dem DFHBF-Ansatz (4a-g) bzw. der DFHBF-Software über die Möglichkeit, das FEM-Maschennetz (Abb. 2) bzw. die einzelnen Geoidmodelle  $N_G$  in eine Anzahl sogenannter "Patches" (Abb. 4, Abb. 5) aufzuteilen, für welche jeweils ein individueller Satz von Datumparametern  $\mathbf{d}^j$  über  $\partial N_G(\mathbf{d}^j)$  (4b) eingeführt werden kann (Jäger und Kälber, 2000; Schneid, 2001). Die Stetigkeit des mit "Patching" signifikant zu verbessernden DFHBF\_DB-Resultats bleibt wegen (4f) durch das "Patching" unberührt.

Die Abb. 4 zeigt die Residuen bzw. mittel- und langwelligen systematischen Fehleranteile in den identischen Punkten  $H$  für unterschiedliche DFHBF-Testrechnungen mit dem EGG97 für Baden-Württemberg. Abb. 4, links zeigt die verbleibenden mittel- und langwelligen systematischen Fehleranteile für den Fall, dass Datumparametersatz  $\mathbf{d}$  für das Gesamtgebiet eingeführt wird. Wie Abb. 4, rechts am Beispiel von 7 Patches mit individuellen Datumparametern  $\mathbf{d}^j$  zeigt, leistet das "Patching" eine deutliche Reduktion der in der resultierenden DFHBF verbleibenden systematischen Fehleranteile.

## 6. DFHBF-Softwareprofil und DFHBF\_DB Standards und Beispiele

Zur Berechnung von DFHBF\_DB (Datenbanken Digitaler Finite Element Höhenbezugsflächen wurde in der Programmiersprache C++ die DFHBF-Produktionssoftware entwickelt (Schwarzer, 2000; Schneid,

2001). Neben verschiedenen Features zur Visualisierung (Datentypen, Kartenhintergrund, Residuen, Vermaschung, siehe Abb. 2) und Werkzeugen zur automatischen und manuellen Vermaschung wurde das mathematische Modell (4a-g) als Kleinste-Quadrate-Ausgleichung mit allen Standards der statistischer Qualitätssicherung implementiert. Die DFHBF-Produktionssoftware leistet darüber hinaus die Erstellung der DFHBF\_DB in einem komprimierten Format und ermöglicht zur gleichen Zeit die Implementierung eines auf die DFHBF\_DB-Zugriffssoftware abgestimmten Kopier- und Datenzugriffsschutzes.

Der Dateninhalt der DFHBF\_DB besteht aus einem ersten Datenblock zur Topologie der Vermaschung (Abb. 2, Abb. 5), einem zweiten Block mit den DFHBF-Parametern  $p$  and  $\Delta m$  (7a-c) und optional einem dritten Datenblock mit deren Kovarianzmatrix. Die DFHBF\_DB-Zugriffssoftware steht in Form einer Dynamic Link Library (DLL) zur Implementierung in GNSS Onlinesoftware (Abb. 3) oder auch Postprocessing Software zur Verfügung.

Eine erste DFHBF\_DB wurde für das (40 x 40) km Gebiet von Tallinn, Estland berechnet (Abb. 2) (Jäger, 1999c; Schwarzer, 2000; Jäger and Schneid, 2001a). Dabei wurden das EGG97 Quasigeoidmodell  $N_G$  (Denker and Torge, 1997) und 23 identische Punkte (H,h) verwendet. Der durchschnittliche bzw. maximale Repro-Wert (6a, b) und die Qualität der DFHBF-Korrektur (7a-c) liegen hier bei 4 mm bzw. bei 10 mm.

Auch im Fall der das Landesgebiet von (250 x 350) km umfassenden DFHBF\_DB Baden-Württemberg (Abb. 5) konnte ein durchschnittlicher Repro-Wert  $\overline{VH}_i$  (6a,b) unter 1 cm erreicht werden (siehe auch Meichle, 2001). Die Charakteristika des Berechnungsdesigns zur "<\_1\_cm\_DFHBF\_DB Baden-Württemberg" sind 1013 Maschen mit Kantenlänge von ca. 7 km, 192 identische Punkte (H,h) und 28 Patches (Schneid, 2001).

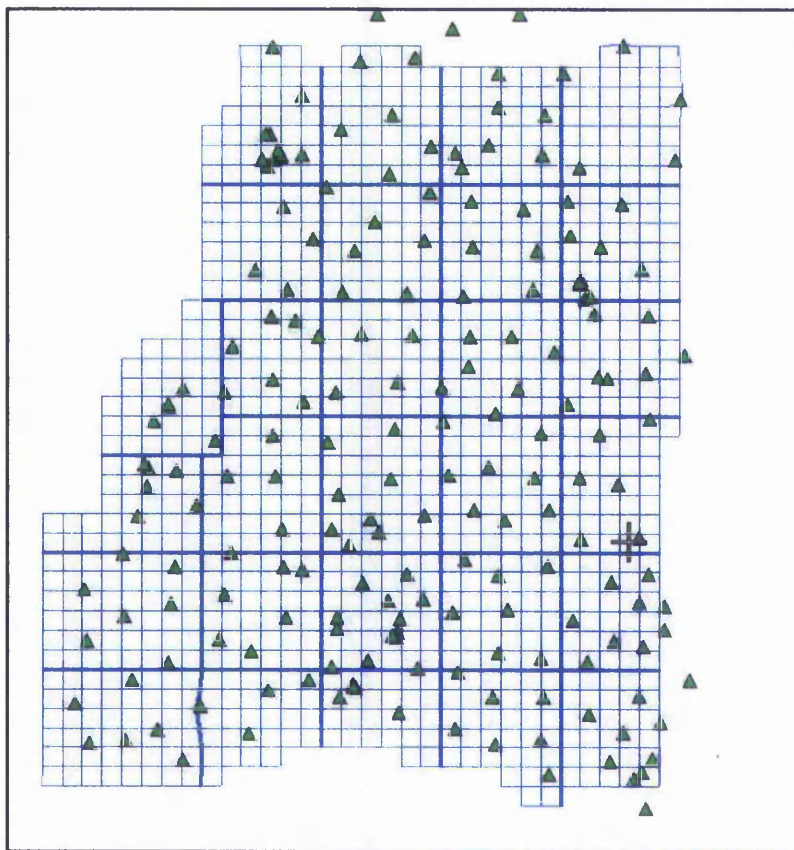


**Abb. 5:** DFHBF\_DB Produktion für das Land Baden-Württemberg, Gebietsgröße 250 km x 350 km. Nahezu regelmäßige Vierecksmaschen mit durchschnittlicher Kantenlänge 7 km, 28 Patches, 1013 Maschen und 192 identischen Punkten (h,H).

Das DFHBF-Konzept ist mit der Berechnung landesweiter "<1cm DFHBF\_DB" als derzeitiges "High-End" Produkt der passpunktfreien Höhenbestimmung - auch schon allein im Hinblick auf den Geoid-Anteil NFEM(p|B,L) (7c) - unerreicht.

Die gegenwärtig High-End Klasse der "<1cm DFHBF\_DB" ist durch einen

- mittleren Repro-Wert  $\overline{VH}_i$  (6a,b) bzw. eine entsprechend Qualität in der äußeren Genauigkeit der DFHBF-Korrektur DFHBF(p,Δm|B,L,h) (7a-c) von weniger als 1 cm und eine
- landesweite Spannweite der Repro-Werte im Intervall [- 3 cm, +3 cm]

charakterisiert.

Die "<1cm\_DFHBF\_DB" der Länder decken das gesamte SAPOS<sup>®</sup> Spektrum ab und werden mittelfristig im Aufgabenfeld des klassischen Nivellements Einzug halten. Hierfür bietet das DFHBF-Konzept die Möglichkeit der Fortführung mit der o.g. DFHBF-Produktionssoftware und eignet sich so zur stetigen Verbesserung der HBF-Repräsentation durch Einführung neuer Daten in den betreffenden Ländern.

Für die zuletzt im Auftrag des Hessischen Landesvermessungsamtes berechnete DFHBF\_DB für Hessen wurde die o.g. Qualitätscharakterista einer "<1cm\_DFHBF\_DB Hessen" bereits vorab vertraglich zugesichert und auch erreicht. Die Abb. 6 zeigt das Histogramm der Reprowerte der insgesamt 67 im Landesgebiet von Hessen gelegenen HREF-Punkte sowie weiterer 6, im Rahmen der mit der Berechnung der "<1\_cm\_DFHBF\_DB Hessen" befassten Diplomarbeit (Ludwig, 2002) bestimmten, identischen Punkte (H,h).

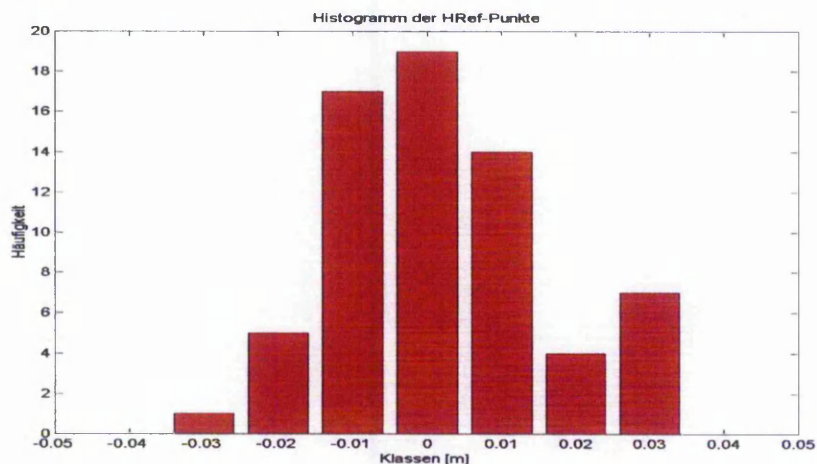


**Abb. 6:** Histogramm der Reprowerte  $\overline{VH}_i$  der "<1cm\_DFHBF\_DB Hessen" mit absoluten Häufigkeiten. Mittlerer Repro-Wert bzw. Qualität der DFHBF-Korrektur unter 1cm. Spannweite der Repro-Werte [-3cm, +3 cm].

Seitens des DFHBF-Teams Karlsruhe wird darüber hinaus vorgeschlagen bzw. die entsprechende Bereitschaft signalisiert, eine bundesweite "<1\_cm\_DFHBF\_DB Deutschland" (NN-Höhen oder Normalhöhen) unter Zusammenschluss und Vervollständigung der bisherigen "<\_1\_cm" Länderlösungen zu bearbeiten.

Die Möglichkeit, durch eine weniger enge Vermaschung bzw. weniger Paßpunkte gezielt und flexibel verschiedene DFHBF-Leistungsstandards zu schaffen, wurde auf der fachlichen Premiere des DFHBF-Konzeptes, dem SAPOS<sup>®</sup>-Symposium 1998 inhaltlich dargelegt (Jäger, 1998). Nach vollständiger Vernetzung der SAPOS<sup>®</sup> - Stationen wird der HEPS - Dienst erwartungsgemäß Genauigkeiten von 1 bis 2 cm in der Lage und 2 bis 4 cm in der Höhe bereitstellen. Die in Bearbeitung befindliche "<\_3\_cm\_DFHBF-DB Deutschland" wird durch einen

- mittleren Repro-Wert  $\overline{VH}_i$  (6a,b) bzw. eine entsprechend Qualität in der äußeren Genauigkeit der DFHBF-Korrektur DFHBF(p,Δm|B,L,h) (7a-c) von weniger als 3 cm und eine
- landesweite Spannweite der Repro-Werte im Intervall [-5 cm, + 5 cm]

charakterisiert. Sie erschließt den Bedarf einer dieser Genauigkeitsklasse entsprechenden passpunktfreien online GNSS-basierte Bestimmung von Landeshöhen. Es ist ferner zu erwarten, dass die "<\_3cm\_DFHBF\_Deutschland" die Nutzung des SAPOS® - Dienstes weiter ankurbeln wird. Die Koexistenz der "<1cm\_DFHBF\_DB" der Länder und der "< 3cm\_DFHBF\_DB Deutschland" stellen vor den o.g. Hintergründen somit eine Bereicherung in der passpunktfreien online Höhenpositionierung dar.

Deutschland	
Baden-Württemberg	Hessen
Saarland	Bayern (in Entwicklung)
Rheinland-Pfalz (in Entwicklung)	
Europäische Länder	
Letland (ausgeschrieben)	Estland (geplant)
Afrika	
Bezirk Windhuk	
USA	
California (geplant)	

**Tab. 1:** Verfügbare sowie geplante "< 1cm\_DFHBF\_DB". Stand März 2002

Die Berechnung der "<\_3cm\_DFHBF\_DB\_Deutschland" (Abb. 6) erfolgt im Auftrag des Ingenieurbüros Seiler (IBS), Lauf ([www.ib-seiler.de](http://www.ib-seiler.de)).

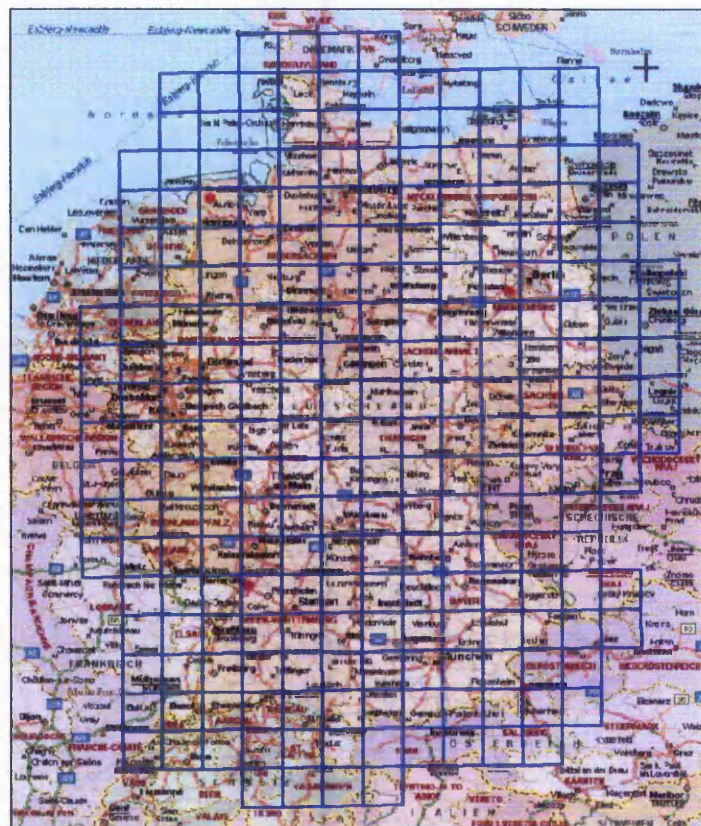


**Abb. 7:** Vermaschungsschema der "<3cm\_DFHBF\_DB\_Deutschland" (konkrete Maschengröße ist 10 km).

Neben der den komplett bzw. zu verschiedenen Testzwecken bisher bereits erfolgten bzw. anlaufenden Berechnungen von DFHBF-DB für verschiedene europäische (Deutschland, Baltische Staaten, N.N.) und außereuropäische Staaten (Namibia, Venezuela, N.N.) strebt das DFHBF\_Team Karlsruhe mittelfristig die Berechnung der "<1\_dm\_DFHBF\_DB\_Europa" im Sinne der Resolution No. 4, EUREF-Symposium 2001, Dubrovnik an (siehe [www.dfhb.de](http://www.dfhb.de)) an.

Firma		Software
IBS (www.ib-seiler.de)		OLGA_PRO
ALLSAT (www.allsat.de)		GART2000
GeoNav (www.geonav.de)		DCTOOLS
LEICA Geosystems (www.leica-geosystems.com)		SKI-PRO SR530 Controller Software
TRIMBLE (in preparation) (www.trimble.com).		Trimble Office 5700 Controller Software

**Tab. 2:** Firmen und Software mit DFHBF\_DB Schnittstelle. Stand März 2002

Tab. 2 zeigt mit Blick auf Firmen und die entsprechenden Softwareprodukte, welche bereits den Zugriff auf DFHBF\_DB leisten, dass das DFHBF-Konzept und das Produkt entsprechender DFHBF\_DB gegenwärtig zu einem internationalen Standard im GNSS-Technologiebereich avanciert.

## 7. Literatur

- Denker, H. and W. Torge (1997): The European Gravimetric Quasigeoid EGG97 – An IAG supported continental enterprise. In: Geodesy on the Move – Gravity Geoid, Geodynamics, and Antarctica. R. Forsberg, M. Feissel, R. Dietrich (eds.) IAG Symposium Proceedings Vol. 119, Springer, Berlin Heidelberg New York: 249-254.
- Dinter, G. and M. Illner (2001): Höhenbestimmung mit GPS am Beispiel von Pilotprojekten aus Baden-Württemberg. DVW Schriftenreihe (41). Wittwer-Verlag. ISBN 3879192766. S. 88 - 110.
- Dinter, G.; Illner, M. and R. Jäger (1997): A synergetic approach for the integration of GPS heights into standard height systems and for the quality control and refinement of geoid models. In: Veröffentlichungen der Internationalen Erdmessung der Bayerischen Akademie der Wissenschaften (57). IAG Subcommittee for Europe Symposium EUREF, Ankara 1996. Beck'sche Verlagsbuchhandlung, München.
- Jäger, R. (1988): Analyse und Optimierung geodätischer Netze nach spektralen Kriterien und mechanische Analogien. Deutsche Geodätische Kommission, Reihe C, No. 342, München.
- Jäger, R. (1998): Ein Konzept zur selektiven Höhenbestimmung für SAPOS. Beitrag zum 1. SAPOS-Symposium. Hamburg 11./12. Mai 1998. Arbeitsgemeinschaft der Vermessungsverwaltungen der Länder der Bundesrepublik Deutschland (Hrsg.), Amt für Geoinformation und Vermessung, Hamburg. S. 131-142.
- Jäger, R. (1990a): Spectral Analysis of Relative and Supported Geodetic Levelling Networks due to Random and Systematic Errors. 'Precise Vertical Positioning'. Invited Paper to the Hannover Workshop of October 08-12, 1990.
- Jäger, R. (1990b): Optimum Positions for GPS-points and Supporting Fix-points in Geodetic Networks. In: Ivan I. Mueller (ed.) International Association of Geodesy Symposia. Symposium No. 102: Global Positioning System: An Overview, Edinburgh/Scotland, Aug. 7-8, 1989. Convened and edited by Y. Bock and N. Leppard, Springer: 254-261.
- Jäger, R. (1999c): State of the art and present developments of a general approach for GPS-based height determination. In (M. Lilje, ed.): Proceedings of the Symposium Geodesy and Surveying in the Future - The importance of Heights, March 15-17, 1999. Gävle/Schweden Reports in Geodesy and Geographical Information Systems, LMV-Rapport 1999(3). Gävle, Schweden. ISSN 0280-5731: 161-174.

- Jäger, R. (2001): Online and Postprocessed GPS-heighting based on the Concept of a Digital Finite Element Height Reference Surface. In: J. Kaminskis and R. Jäger (Eds.): 1st Common Baltic Symposium, GPS-Heighting based on the Concept of a Digital Height Reference Surface (DFHRS) and Related Topics - GPS-Heighting and Nation-wide Permanent GPS Reference Systems Riga, June 11, 2001. In press.
- Jäger, R. and H. Kaltenbach (1990): Spectral analysis and optimization of geodetic networks based on eigenvalues and eigenfunctions. *Manuscripta Geodetica* (15), Springer Verlag. S. 302-311.
- Jäger, R. und S. Kälber (2000): Konzepte und Softwareentwicklungen für aktuelle Aufgabenstellungen für GPS und Landesvermessung. DVW Mitteilungen, Landesverein Baden-Württemberg. 10/2000. ISSN 0940-2942.
- Jäger, R. and S. Leinen (1992): Spectral Analysis of GPS-Networks and Processing Strategies due to Random and Systematic Errors. In: Defense Mapping Agency and Ohio State University (Eds.) Proceedings of the Sixth International Symposium on Satellite Positioning, Columbus/Ohio (USA), 16-20 March. Vol. (2), p. 530-539.
- Jäger, R. and S. Schneid (2001a): GPS-Höhenbestimmung mittels Digitaler Finite-Elemente Höhenbezugsfläche (DFHBF) - das Online-Konzept für DGPS-Positionierungsdienste. XI. Internationale Geodätische Woche in Obergurgl/Österreich, Februar 2001. Institutsmitteilungen, Heft Nr. 19, Institut für Geodäsie der Universität Innsbruck: 195-200.
- Jäger, R. and S. Schneid (2001b): DFHRS-Homepage: [www.DFHBF.de](http://www.DFHBF.de) .
- Jäger, R. and S. Schneid (2001c): Online and Postprocessed GPS-Heighting based on the Concept of a Digital Height Reference Surface. Contribution to IAG International Symposium on Vertical Reference Systems, February 2001, Cartagena, Columbia. In press.
- Jäger, R. and S. Schneid (2001d): Online and Postprocessed GPS-heighting based on the Concept of a Digital Height Reference Surface. In: Veröffentlichungen der Internationalen Erdmessung der Bayerischen Akademie der Wissenschaften (62). IAG Subcommittee for Europe Symposium EUREF, Dubrovnik 2001. Beck'sche Verlagsbuchhandlung, München. In press.
- Lemoine, F.; S. Kenyon; J. Factor; R. Trimmer, N. Pavlis; D. Chinn; M. Cox; S. Klosko; S. Lutcke; M. Torrence; Y. Wang; R. Williamson; E. Pavlis; R. Rapp and T. Olson (1998): The development of the Joint NASA GSFC and NIMA Geopotential Model EGM96. NASA Goddard Space Flight Center, Greenbelt, Maryland, 20771, USA.
- Ludwig, M. (2002): Erprobung der 1. Stufe der Digitalen Finite-Elemente Höhenbezugsfläche (DFHBF) für Hessen. Diplomarbeit am Fachbereich Vermessungswesen der FH Frankfurt (in Zusammenarbeit mit DFHBF\_Team der FH Karlsruhe). Unveröffentlicht.
- Meichle, H. (2001): Digitale Finite Element Höhenbezugsfläche (DFHBF) für Baden-Württemberg. DVW Mitteilungen , Heft 2. DVW Landesverein Baden-Württemberg. ISSN 0940-2942. S. 23-31.
- Schmitt, G. (1997): Spectral Analysis and Optimization of two dimensional networks. *Geomatics Research Australasia* (67): 47-64.
- Schneid, S. (2001): Software Development and DFHRS computations for several countries. J. Kaminskis and R. Jäger (Eds.): 1st Common Baltic Symposium, GPS-Heighting based on the Concept of a Digital Height Reference Surface (DFHRS) and Related Topics - GPS-Heighting and Nation-wide Permanent GPS Reference Systems Riga, June 11, 2001.
- Schwarzer, F. (2000): Entwicklung grafikfähiger C-Software zur Berechnung Digitaler Finite Element Höhenbezugsflächen (DFHBF) und DFHBF-Implementierung in GPS-Kommunikationssoftware. Diplomarbeit am Studiengang Vermessungswesen, Fachhochschule Karlsruhe, unveröffentlicht.

Jäger, R. and S. Schneid (2002):

Online and Postprocessed GPS-Heighting based on the Concept of a Digital Height Reference Surface. In : Proc IAG International Symposium 'Vertical Reference Systems', H. Drewes, A. Dodson, L.P.S. Fortes, L. Sanchez, P. Sandoval (EDS), Vol. 124, Springer Berlin, Heidelberg New York, pp 203-208.

# Online and Postprocessed GPS-heighting based on the Concept of a Digital Height Reference Surface (DFHRS)

Reiner Jäger and Sascha Schneid

Department of Surveying and Geomatics, Fachhochschule Karlsruhe-University of Applied Sciences  
Moltkestraße 30, D-76133 Karlsruhe, Germany. Email: dfhbf@fh-karlsruhe.de

**Abstract.** The DFHRS (Digital-Finite-Element-Height-Reference-Surface) project aims at the conversion of ellipsoidal GPS-heights  $h$  into heights  $H$  of a standard height system (e.g. orthometric or normal height system) in an online or postprocessed GPS-heighting. The DFHRS is modeled as a continuous surface called NFEM( $\mathbf{p},x,y$ ) in an arbitrary large area by bivariate polynomials over an irregular finite element mesh grid. With  $\mathbf{p}$  we describe the total set of all polynomial coefficients in the meshes, and with  $x=x(B,L)$  and  $y=y(B,L)$  the metric plan position on the ellipsoid. The continuity of the DFHRS namely its Finite Element Model NFEM( $\mathbf{p},x,y$ ) along the borders of neighbouring meshes is provided by condition equations  $C(\mathbf{p})$ . In opposite to e.g. digital terrain models, the nodes of the finite element mesh of NFEM( $\mathbf{p},x,y$ ) may differ from the position of the observation data used for the determination of  $\mathbf{p}$ . The parameters  $\mathbf{p}$  of the DFHRS are computed in an adjustment procedure based on the observations of geoid heights  $N_G$ , deflections of the vertical ( $\xi,\eta$ ), terrestrial heights  $H$  or height differences  $\Delta H$ , and ellipsoidal GPS heights  $h$  or height differences  $\Delta h$ . Geoid models are adapted by datum parameters  $\mathbf{d}$  to the DFHRS ("geoid mapping") and above this they may be subdivided into different parts with individual datum parameters ("geoid patching"), in order to reduce their typical long-waved systematic errors. The computed DFHRS data base is to be set up in a direct GPS-based online heighting in DGPS networks. No identical points or further transformations are needed. The DFHRS data base provides directly a correction  $\Delta=\Delta(B,L,h)$  to convert the GPS-height  $h$  into the standard height  $H$ . Examples for computation and use of DFHRS data-bases in DGPS-networks (e.g. SAPOS, Germany) are presented.

**Keywords.** GPS online heighting, digital height reference surface, geoid datum, geoid mapping, geoid patching.

## 1. Introduction

With the trend towards replacing the former still present national datum systems in favour of ITRF-related datum systems and respective DGPS reference station systems (like e.g. SAPOS in Germany), the datum problem for the plan position component (B,L) in DGPS-based positioning applications will vanish by and by. For the reason of a physically different height reference surface HRS for the standard heights  $H$  (fig. 1) however, which are defined by geopotential numbers, the problem of a transition of the ellipsoidal GPS-heights  $h$  to the standard heights  $H$  referring to a HRS (geoid for an orthometric height system, quasi-geoid for a normal height system) will remain. Using directly geoid models such as EGG97 (Denker and Torge, 1997) or EGM96 (Lemoine et al., 1998) the ideal formula

$$H = h - N_G(B, L) \quad (1)$$

as represented in fig.1, does not hold. The reason is, that geoid models have their own datum and suffer from at least long-waved systematic effects (Dinter et al., 1997; Jäger 1999, 2000; Jäger and Kälber, 2000). Besides this the precision of the standard height  $H$  resulting from a GPS height is mostly restricted additionally by a poor short-waved accuracy of geoid models. The observation equation for the powerful standard approach for GPS-height integration, which was developed and implemented in the software package HEIDI2 some years ago (Dinter et al., 1997) and has meanwhile been applied by many DGPS users. The so called "geoid refinement approach" reads in the system of observation equations:

$$h + v = m \cdot H + N_G \quad (2a)$$

$$N_G(B, L) + v = N_G + \partial N(\mathbf{d}) + NFEM(\mathbf{p}, x, y) \quad (2b)$$

$$H + v = H \quad (2c)$$

$$C(\mathbf{p}) = 0 \quad (2d)$$

The standard approach (2a-d) holds, if geoid heights  $N_G(B,L)$  from a respective geoid model are available. The parametrization of a datum change  $\partial N(\mathbf{d})$  reads (Jäger 1999, 2000):

$$\begin{aligned} \partial N(\mathbf{d}) = & [\cos(L) \cdot \cos(B)] \cdot u + [\cos(B) \cdot \sin(L)] \\ & \cdot v + [\sin(B)] \cdot w + [e^2 \cdot N(B) \cdot \sin(B) \cdot \\ & \cos(B) \cdot \sin(L)] \cdot \varepsilon_x + [-e^2 \cdot N(B) \cdot \\ & \sin(B) \cdot \cos(B) \cdot \cos(L)] \cdot \varepsilon_y \\ & + [-N_G] \cdot \Delta m_G \end{aligned} \quad (2e)$$

In (2a-d) the height  $N_G(B,L)$  of a geoid model is refined by a so called Finite Element Model NFEM( $\mathbf{p},x,y$ ).  $N(B)$  means the radius of normal curvature of the ellipsoid at a point  $P(B,L)$ . The datum parameters  $\mathbf{d}$  comprise three translations ( $u,v,w$ ), two rotations ( $\varepsilon_x, \varepsilon_y$ ) and the scale change  $\Delta m_G$  of the geoid height  $N_G$ . The NFEM( $\mathbf{p},x,y$ ) acts as an additional overlay for a middle- and short-waved shape improvement of the geoid heights  $N_G(B,L)$ .

For more details concerning the datum transition problem (2b,e) and the refinement NFEM( $\mathbf{p},x,y$ ), as well as for the discussion of the special cases of the standard approach - namely the "pure geoid-approach" and the "pure FEM-approach" - it is referred to Dinter et al. (1997) and Jäger (1999, 2000). The mathematical background of the powerful tool of the Finite Element Model NFEM( $x,y,\mathbf{p}$ ), which will become also the central core of the DFHRS concept, is treated in chap. 2.

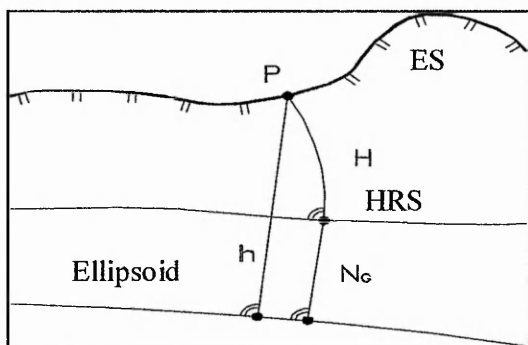


Fig. 1: Ellipsoidal GPS height  $h$ , standerd height  $H$ , height reference surface HRS, its ellipsoidal height  $N_G$  and earth surface ES at a point  $P(B,L)$

A disadvantage of the above standard approach (2a-d) is, that it is in its full power a typical post-processing application. As identical points ( $H,h$ ) are needed, the approach is not very economical for an on-line GPS heighting in DGPS networks (fig.3). Furtheron the geoid model heights  $N_G(B,L)$  are only used at discrete points and so the complete geoid height information  $N_G(B,L)$  is neglected. Besides this also the vertical deflection information ( $\xi,\eta$ ), e.g. available from geoid models, remains totally

unused. The application of the standard approach (2a-d) requires experts knowledge, so that it is not adequate for "any" DGPS user. Because of all above mentioned reasons the standard approach (2a-d) remains suboptimal compared to the new DFHRS-concept presented in chap. 3.

## 2. FEM Representation of Height Reference Surfaces

A powerful tool used already within the standard GPS height integration approach (chap. 2) and a central tool of the DFHRS approach (chap. 3) as well, consists in the representation of the height reference surface HRS or its additional refinement by a finite element surface called NFEM( $\mathbf{p},x,y$ ). NFEM( $\mathbf{p},x,y$ ) is carried by the base functions of bi-variate polynomials which are set up in the meshes. If we describe with  $\mathbf{p}^i$  the polynomial coefficients ( $a_{00}, a_{10}, a_{01}, a_{20}, a_{11}, a_{02}, \dots$ )<sup>i</sup> of the  $i$ -th mesh, we have for the height NFEM( $\mathbf{p}^i, x, y$ ) of the HRS over the ellipsoid (fig. 1) in the  $i$ -th mesh:

$$\text{NFEM}(\mathbf{p}^i, x, y) = \mathbf{f}(x(B,L), y(B,L)) \cdot \mathbf{p}^i \quad (3a)$$

$$i = 1, m$$

$$\mathbf{p}^i = (a_{00}, a_{10}, a_{01}, \dots)^i \quad (3b)$$

$$\mathbf{f}(x(B,L), y(B,L)) = (1, x, y, x^2, xy, y^2, \dots) \quad (3c)$$

The vector  $\mathbf{f}$  means the so called Vandermond vector and contains the different powers of the coordinates ( $x,y$ ) according to the polynomial degree  $n$ . The total parameter vector  $\mathbf{p}$  consists of the coefficient sets  $\mathbf{p}^i = (a_{j,k})^i$ , ( $j=0,n; k=0,n$ ), of all  $m$  meshes. The plan position in (3a,c) is due to the metric ellipsoidal coordinates ( $y(B,L)$ ="East" and  $x(B,L)$ ="North") introduced e.g. as UTM or Lambert coordinates, which are functions of the geographical coordinates ( $B,L$ ).

To imply a continuous surface NFEM( $\mathbf{p},x,y$ ) one set of continuity conditions of different type  $C_{0,1,2}$  has to be set up in the computation of NFEM( $\mathbf{p},x,y$ ) for each couple of neighbouring meshes. The continuity type  $C_0$  implies the same functional values, the continuity type  $C_1$  implies the same tangential planes and the continuity type  $C_2$  the same curvature along common mesh borders of the DFHRS NFEM( $\mathbf{p},x,y$ ). The continuity conditions occur as additional observation equations  $C(\mathbf{p})=0$  to be added to the parametrization of NFEM( $\mathbf{p},x,y$ ). The condition equations  $C(\mathbf{p})=0$  are related to the polynomial sets of the coefficients ( $a_{jk})^m$  and ( $a_{jk})^n$  of each couple of neighbouring meshes  $m$  and  $n$ . To force e.g.  $C_0$ -continuity, the difference  $\Delta N_{m,n}$  in the geoid height  $N_G$  of any point

S at the common border SA-SE of two meshes m and n (fig.2) has to become zero. So the basic condition equation for a polynomial representation of n-th degree reads (Dinter et. al., 1997)

$$\Delta N_{m,n}(t) = \sum_{j=0}^n \sum_{k=0}^{n-j} ((a_{jk,n} - a_{jk,m}) \cdot (y_{SA} + t(y_{SA} - y_{SE}))^j \cdot (x_{SA} + t \cdot (x_{SA} - x_{SE}))^k) \equiv 0 \quad (3d)$$

With  $(y_{SA}, x_{SA}, y_{SE}, x_{SE})$  we introduce the plan metric coordinates of the nodal points SA and SE (fig. 2). Equation (3d) represents a polynomial of n-th degree parametrized in the border line parameter  $t(t \in (0,1))$ . The subset of  $(n+1)$   $C_0$ -continuity condition equations  $C(p)=0$  for the border between mesh m and n results in case of  $C_0$ -continuity from (3d) by setting all  $(n+1)$  coefficients related to  $t$  to zero.

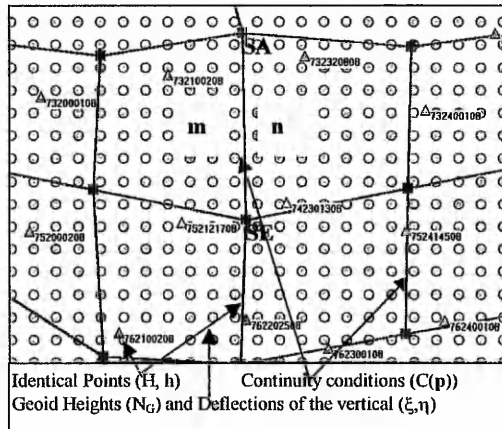


Fig. 2: DFHRS mesh grid and different observation types

The mesh size and shape for the computation of the DFHRS NFEM( $p, x, y$ ) may be chosen arbitrary (fig. 2). The best approximation of a HRS by NFEM( $p, x, y$ ) results of course by introducing small meshes, e.g.  $(5 \times 5)$  km in order to keep a 5mm range for any HRS shape approximation by a polynomial degree up to  $n=3$ . A special advantage and characteristic of the NFEM( $p, x, y$ ) representation consists in the fact, that the nodal points of the FEM grid are totally independent of the geodetic network and data points. Observation data which are presently used for the determination of the parameter vector  $p$  of NFEM( $p, x, y$ ) are height observations  $(h, H, \Delta H, \Delta h)$ , the geoid height ob-

servations  $N_G(B, L)$  and the deflections of the vertical observations  $(\xi, \eta)$ .

### 3. Digital Finite Element Height Reference Surface (DFHRS)

#### 3.1. Basic Ideas of the DFHRS Concept

The DFHRS concept aims at a direct online or post-processed GPS heighting with an optimum and simultaneous use of all available data sources. Within this aim the profile of an online (or also postprocessed) GPS-heighting is easy to formulate: An ellipsoidal GPS-height  $h$ , determined at a plan position  $x(B, L)$  and  $y(B, L)$  is to be made convertible directly to the height  $H$  of the standard height system. The converted height  $H$  should result online on applying a respective correction to  $h$ , and the resulting  $H$  should not suffer with a quality-decrease compared to the heights  $H$  resulting from a postprocessed GPS height integration.

In the following the general so called DFHRS concept is presented, which fulfils all above requests and shows besides this even some more positive aspects. The concept is to produce in a first step in a controlled way a new kind of data base product. This step is called the DFHRS data base production step.

The second step is to make this data base accessible for an online DGPS-heighting. This is called the application step. The use of the DFHRS in a postprocessing mode (e.g. in GIS) is of course included in the concept. In the application step either the DGPS user has the DFHRS at his disposal on his field equipment or the DGPS service exclusively uses the DFHRS for the evaluation of a correction  $\Delta = \Delta(B, L, h)$  to convert a GPS height  $h$  into the height  $H$  of the standard height system (principle, see fig. 3).

#### 3.2. DFHRS Data Base Production Step

The DFHRS data base production step reads in the system of observation equations as follows:

$$h + v = H - h \cdot \Delta m + f(x, y) \cdot p \quad (4a)$$

$$N_G(B, L)^j + v = f(x, y) \cdot p + \partial N(d^j) \quad (4b)$$

$$\xi + v = -f_B / M(B) \cdot p + \partial B(d_{\xi, \eta}) \quad (4c)$$

$$\eta + v = -f_L / (N(B) \cdot \cos(B)) \cdot p + \partial L(d_{\xi, \eta}) \quad (4d)$$

$$H + v = H \quad (4e)$$

$$C + v = C(p) \quad (4f)$$

With  $\partial N(\mathbf{d}')$  (2d) and with  $\partial B(\mathbf{d}_{\xi,\eta})$  and  $\partial L(\mathbf{d}_{\xi,\eta})$  we introduce the datum part of the geoid heights of any geoid model or of single "geoid patches" (see chap. 3.3) and the datum parts of the deflections of the vertical  $(\xi,\eta)$  respectively. Explicit formulas for  $\partial B(\mathbf{d}_{\xi,\eta})$  and  $\partial L(\mathbf{d}_{\xi,\eta})$  are given in Jäger (2000). With  $\mathbf{f}_B$  and  $\mathbf{f}_L$  we introduce the partial derivatives of the Vandermonds' vector  $\mathbf{f}(x(B,L),y(B,L))$  (3d) with respect to the geographical coordinates B and L.  $M(B)$  and  $N(B)$  mean the radius of meridian and normal curvature at a point P(B,L) respectively.

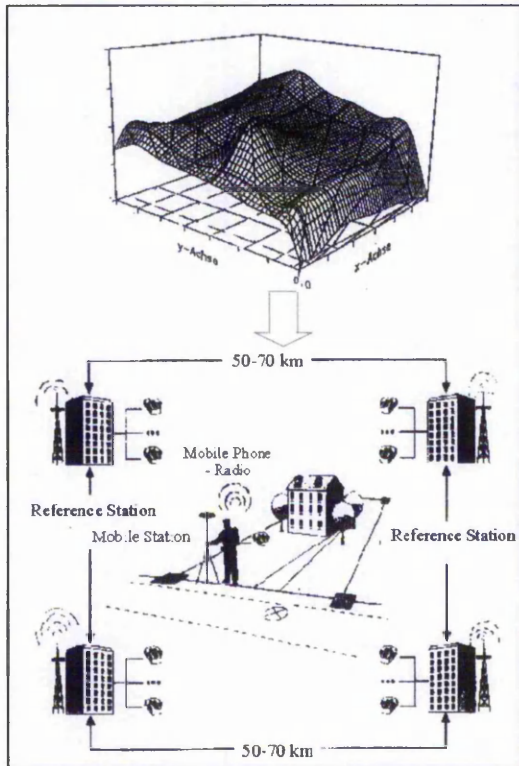


Fig. 3 : DFHRS data base application for an online GPS-heighting

Identical points  $(H, h)$  and if available, one or a number of geoid models  $N_G(B,L)$  are used as observations to produce the DFHRS by a least squares estimation related to (4a-f). The DFHRS on the right side is, except of the scale part  $\Delta m \cdot h$  (4a), represented completely by the finite element model  $NFEM(\mathbf{p},x,y)=\mathbf{f}(x,y) \cdot \mathbf{p}$ , while the continuity is provided by the continuity equations  $C(\mathbf{p})$  (4f) below.

This means that the geoid model input of any geoid model  $N_G(B,L)$  or "geoid patch" is "mapped" to the DFHRS by removing the datum part  $\partial N(\mathbf{d}')$ .

An additional NFEM-refinement term may be set up in (4b). The production step of the DFHRS (4a-f) is embedded in a statistical quality control concept of a least squares estimation, so that any observation component - including the input of "mapped" and datum-adapted geoid-model - is well controlled (Jäger and Schneid, 2001a).

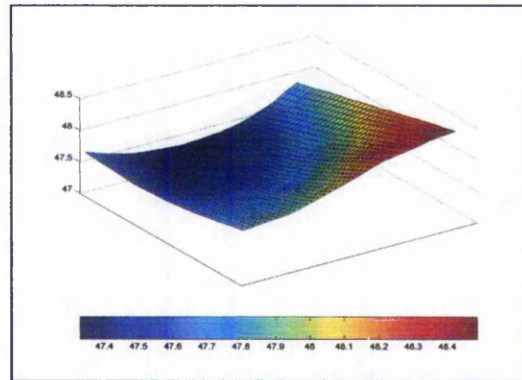


Fig. 4: Visualisation of a DFHRS represented by NFEM(p,x,y) for Baden-Württemberg (Germany) about 150x150km.

### 3.3. DFHRS Application Step

The decisive components and formula parts of the production step, which are afterwards needed in the application step - namely in an online GPS-heighting - are contained in (4a). Equation (4a) leads to the following correction scheme, which has to be applied to the GPS height  $h$  in an online application of the DFHRS data base with respect to convert  $h$  into the standard height  $H$ :

$$H = h + \Delta(B, L, h) = h + corr1 + corr2 \quad (5a)$$

$$= h - \mathbf{f}(x(B, L), y(B, L)) \cdot \mathbf{p} + h \cdot \Delta m \quad (5b)$$

$$= h - NFEM(\mathbf{p}, x(B, L), y(B, L)) + h \cdot \Delta m. \quad (5c)$$

The first correction part "corr1=corr1(B,L)" is due to the Finite Element Model part  $NFEM(\mathbf{p},x(B,L),y(B,L))$  of the DFHRS data base ("geoid correction"), and the second "corr2 = corr2(h)" is due to the scale  $\Delta m$  between the GPS heights  $h$  and those of the standard height system  $H$  ("scale correction").

### 3.4. Special Requests and Advantages

To reduce the effect of long-waved systematic errors of geoid models as well as those of the standard HRS (Dinter et al., 1997; Jäger, 1990) the mathematical model of the DFHRS-concept (4a-f) and the

DFHRS software respectively allow to subdivide any given geoid height model  $N_G(B,L)$  into a number of so called "geoid-patches" (fig. 5), each with an own set of datum-parameters  $\partial N(\mathbf{d}^j)$ . Fig. 5 shows the residuals of two different DFHRS adjustments for the country of Baden-Württemberg (Germany). Fig. 5. (left) shows long-waved systematic errors, which occur on introducing only one datum parameter set  $\mathbf{d}$  for the whole area, meaning without "patching". The result of the "geoid-patching" on the right shows the benefit of the patching with respect to reduce the influence of systematic errors by the subdivision of the geoid model into a number of different patches with individual datum parameters  $\mathbf{d}^j$  (Jäger and Kälber, 2000). Patching also improves the resulting DFHRS significantly.

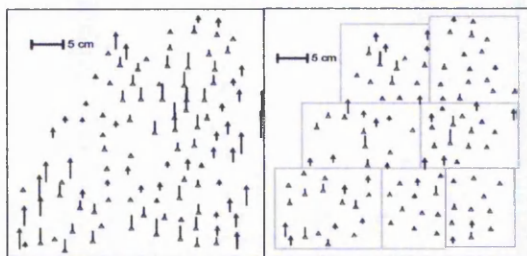


Fig. 5: Effect of a "geoid-patching" at the example of Baden-Württemberg. Only one set of datum parameters (left) and 7 patches with individual datum sets (right).

The continuity equations (4f) are introduced as additional observation equations with variable weights. So the dimension of the normal equation matrix is not blown up due to the conditions  $C(\mathbf{p})$  and the approach is kept very flexible: The continuity conditions can be introduced "hard" or "soft", according to a prescribed weight, and they can also be statistically tested.

#### 4. DFHRS Software and Examples

To compute Digital-Finite-Element Height Reference Surfaces, a special C++ software ("DFHRS-production software") was developed at FH Karlsruhe - University of Applied Sciences (Schwarzer, 2000). Several functions for visualisation and utilities for an automatic and a manual meshing and a powerful least-squares adjustment have been implemented into the DFHRS production software. It enables the mathematical model (4a-f) including gross error detection and variance component estimation for all observations and observation groups respectively, and it sets up the DFHRS data base in a compressed format. The data base consists of a block of

meshgrid information, a block with the DFHRS parameters  $\mathbf{p}$  and  $\Delta m$  and optionally a third block with the covariance matrix of the DFHRS parameters.

A simple but very effective way to test the external accuracy ("reproduction quality") of the resulting DFHRS data base is to compute known standard heights  $H$  of some representative identical points ( $h,H$ ), which were not introduced into the DFHRS production (4a-f).

In a first pilot project a DFHRS was computed for the (40 x 40) km area of Tallinn/Estonia with a mesh size of 5 km (Jäger and Schneid, 2001b). Using the EGG97 geoid model (Denker and Torge,1997) and 23 identical points, the average reproduction quality of the standard heights  $H$  evaluated from GPS heights  $h$  was in the range of 4 mm (max. 10 mm). The "reproduction quality" of the (100 x 100) km of the Saarland (part of Germany) DFHRS produced recently using identical points, EGG97 and a mesh size of 5 km was better than 1cm in the average (2.5 cm max.).

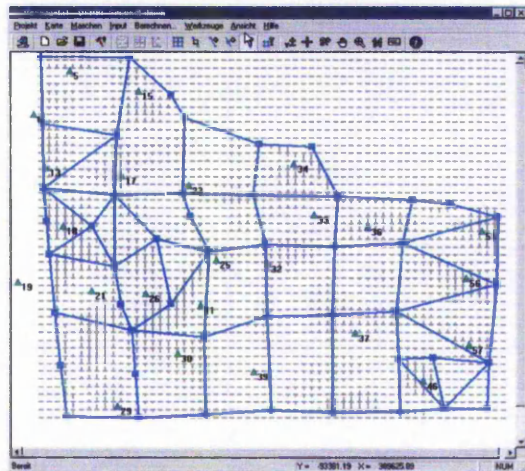


Fig. 6 : DFHRS-meshgrid and residuals in Venezuela (500 x 700) km area

This DFHRS data base is already used as standard in the practice of DGPS heighting in the SAPOS® DGPS network of Saarland.

A third series of test computations was performed for a (500 x 700) km area in Venezuela, which was meshed according to fig. 6. Only 22 identical points and geoid heights  $N_G$  from the EGM96 were used for the DFHRS production. Even the large size of meshes (about 70-80km) and the less accurate EGM96 provided a DFHRS with an average reproduction quality of 15 cm for the standard heights  $H$ .

## 5. Conclusions

The DFHRS (Digital Finite Element Height Reference Surface) concept provides a new standard for an online GPS heighting in DGPS networks. The approach is based on the representation of the Height Reference Surface (HRS) by the base functions of bivariate polynomials. These are set up in the area over a grid of arbitrary shaped finite element meshes. To imply a continuous HRS, a set of continuity conditions is introduced for each border of neighbouring meshes. The DFHRS data base, computed in the DFHRS production step, provides any DGPS user in the DFHRS application step with a correction  $\Delta = \Delta(B, L, h)$ , which converts the ellipsoidal height  $h$  directly to the standard height  $H$ . Identical points and transformations are not needed any more in the application step. So geodetic expert knowledge is needed only in the production step, while GPS heighting becomes as simple and economic as it can be.

The production step allows to use all above observation type simultaneously. The whole geometrical information, namely identical points and height differences ( $h, \Delta h, H, \Delta H$ ) as well as geoid model heights  $N_G$  and deflections of the vertical ( $\xi, \eta$ ) are set up in a strict least squares adjustment, which becomes most efficient in this way with respect to the resulting DFHRS. The extension of the DFHRS approach (4a-f) with respect to gravity observations is intended. The production step simultaneously enables the statistical quality control of the DFHRS. In the sense of a two step adjustment the other observation groups enable the control and improvement of the geoid model input, which is simultaneously "mapped" to the new DFHRS product. To reduce the influence of long-waved systematic errors, geoid models may be divided into continuous "geoid-patches". The resulting data base is stored together with its covariance matrix and may be implemented by a DFHRS Dynamic Link Library (DLL) in any GPS-RTK-software for online GPS-heighting or in postprocessing software.

The DFHRS-concept has been tested in several pilot-projects and is already used in practice. The results indicate accuracies less than 1cm for the reproduction of standard heights  $H$  from ellipsoidal heights  $h$ .

## References

- Denker, H. and W. Torge (1997): The European Gravimetric Quasigeoid EGG97 – An IAG supported continental enterprise. In: *Geodesy on the Move – Gravity Geoid, Geodynamics, and Antarctica*. R. Forsberg, M. Feissel, R. Dietrich (eds) IAG Symposium Proceedings Vol. 119, Springer, Berlin Heidelberg New York, pp 249-254.
- Dinter, G.; Illner, M. and R. Jäger (1997): A synergetic approach for the integration of GPS heights into standard height systems and for the quality control and refinement of geoid models. In: *Veröffentlichungen der Internationalen Erdmessung der Bayerischen Akademie der Wissenschaften (57)*. Bayerische Akademie der Wissenschaften (ed) IAG Subcommission for Europe Symposium EUREF, Ankara 1996. Beck'sche Verlagsbuchhandlung, München.
- Jäger, R. (1990): Optimum Positions for GPS-points and Supporting Fix-points in Geodetic Networks. In: Ivan I. Mueller (ed.) International Association of Geodesy Symposia. Symposium No. 102: *Global Positioning System: An Overview*, Edinburgh/Scotland, Aug. 7-8, 1989. Convened and edited by Y. Bock and N. Leppard, Springer Verlag pp 254-261.
- Jäger, R. (1999): State of the art and present developments of a general approach for GPS-based height determination. In (M. Lilje, ed.), *Proceedings of the Symposium Geodesy and Surveying in the Future – The importance of Heights*, March 15-17, 1999. Gävle/Schweden Reports in Geodesy and Geographical Informations Systems, LMV-Rapport 1999(3). Gävle, Schweden. ISSN 0280-5731: 161-174.
- Jäger, R. (2000): State of the Art and Present Developments of a General Concept for GPS-based Height determination. *Proceedings of the First Workshop on GPS and Mathematical Geodesy in Tanzania (Kilimanjaro Expedition 1999)*. October 4, 1999, University College of Lands and Architectural Studies (UCLAS), Dar Es Salaam. URL (download): <http://www.dfhb.de>.
- Jäger, R. und S. Kälber (2000): Konzepte und Software-entwicklungen für aktuelle Aufgabenstellungen für GPS und Landesvermessung. *DVW Mitteilungen*, Landesverein Baden-Württemberg. 10/2000. ISSN 0940-2942.
- Jäger, R. und S. Schneid (2001a): GPS-Höhenbestimmung mittels Digitaler Finite-Elemente Höhenbezugsfläche (DFHBF) - das Online-Konzept für DGPS-Positionierungsdienste. *XI. Internationale Geodätische Woche in Obergurgl/Österreich*, Februar 2001. Institutsmittellungen, Heft Nr. 19, Institut für Geodäsie der Universität Innsbruck. pp 195-200.
- Jäger, R. und S. Schneid (2001b): DFHRS-Homepage: [www.DFHBF.de](http://www.DFHBF.de)
- Lemoine, F.; S. Kenyon; J. Factor; R. Trimmer, N. Pavlis; D. Chinn; M. Cox; S. Klosko; S. Luthcke; M. Torrence; Y. Wang; R. Williamson; E. Pavlis; R. Rapp and T. Olson (1998): The development of the Joint NASA GSFC and NIMA Geopotential Model EGM96. *NASA Goddard Space Flight Center*, Greenbelt, Maryland, 20771, USA.
- Schwarzer, F. (2000): Entwicklung graphikfähiger C-Software zur Berechnung Digitaler Finite Element Höhenbezugsflächen (DFHBF) und DFHBF-Implementierung in GPS-Kommunikationssoftware. *Diplomathesis*, Studiengang Vermessung und Geomatik, FH Karlsruhe, unpublished.

Jäger, R. and S. Schneid (2001):

Online and Postprocessed GPS-heighting based on the Concept of a Digital Height Reference Surface (DFHRS). Report on the Symposium of the IAG subcommision for Europe (EUREF) held in Dubrovnik, May 2001. Veröffentlichungen der bayerischen Kommission für die internationale Erdmessung der Bayerischen Akademie der Wissenschaften.

# Online and Postprocessed GPS-heighting based on the Concept of a Digital Height Reference Surface (DFHRS)

R. JÄGER, S. SCHNEID<sup>1</sup>

## Summary

The DFHRS (Digital-Finite-Element-Height-Reference-Surface) research and development project is funded by the German Ministry of Education and Research. It aims at the conversion of ellipsoidal GPS-heights  $h$  in an online or postprocessed GPS-heighting into the standard heights  $H$ , which refer to the height reference surface (HRS) of an orthometric, NN- or normal standard height system. The DFHRS is modelled as a continuous HRS in arbitrary large areas by bivariate polynomials over an irregular grid. Geoid information (geoid heights  $N$ , deflections of the vertical  $\xi, \eta$ ) provided with a HRS datum adoption parametrization and identical points ( $h, H$ ) as observations in a least squares procedure enable the statistically controlled DFHRS computation. Several geoid models may be introduced simultaneously and any geoid model may be splitted into different "geoid-patches" with individual datum-parameters and continuity requirements along the patch borders. The resulting DFHRS data-base provides a correction  $\Delta = \Delta(B, L, h)$  to transform an ellipsoidal GPS-height  $h$  directly and online into a standard height  $H$ . Examples for the computation and use of DFHRS data-bases in DGPS-networks (e.g. SAPOS, Germany) are presented for different countries.

## 1 Introduction

With the trend towards replacing the former still present national datum systems in favour of ITRF-related datum systems and respective DGPS reference station systems (like e.g. SAPOS in Germany), the datum problem for the plan position component ( $B, L$ ) in DGPS-based positioning applications will vanish by and by. For the reason of a physically different height reference surface HRS for the standard heights  $H$  (fig. 1) however, which are defined by geopotential numbers, the problem of a transition of the ellipsoidal GPS-heights  $h$  to the standard heights  $H$  referring to a HRS (geoid for an orthometric height system, quasi-geoid for a normal height system) will remain. Using directly geoid models such as EGG97 (Denker and Torge, 1997) or EGM96 (LEMOINE et al., 1998) the ideal formula

$$H = h - N_G(B, L) \quad (1)$$

represented in fig.1, does not hold. The reason is, that geoid models have their own datum and additionally suffer from at least long-waved systematic effects

(DINTER et al., 1997; JÄGER 1999, 2000; JÄGER and KÄLBER, 2000). Besides this the precision of the standard height  $H$  resulting from a GPS height is mostly restricted additionally by a poor short-waved accuracy of geoid models. The observation equation for the powerful standard approach for GPS-height integration, which was developed and implemented in the software package HEIDI2 some years ago (DINTER et al., 1997) and has meanwhile been applied by many DGPS users. The so called "geoid refinement approach" reads in the system of observation equations:

$$h + v = m \cdot H + N_G \quad (2a)$$

$$N_G(B, L) + v = N_G + \partial N_G(\mathbf{d}) \quad (2b)$$

$$+ \text{NFEM}(\mathbf{p}, x, y)$$

$$H + v = H \quad (2c)$$

$$C(\mathbf{p}) = 0 \quad (2d)$$

The standard approach (2a-d) holds, if geoid heights  $N_G(B, L)$  from a respective geoid model are available. The parametrization of a datum change  $\partial N_G(\mathbf{d})$  reads (JÄGER, 1999, 2000):

$$\begin{aligned} \partial N_G(\mathbf{d}) = & [\cos(L) \cdot \cos(B)] \cdot u + [\cos(B) \cdot \sin(L)] \cdot v \\ & + [\sin(B)] \cdot w \\ & + [e^2 \cdot N(B) \cdot \sin(B) \cdot \cos(B) \cdot \sin(L)] \cdot \varepsilon_x \\ & + [-e^2 \cdot N(B) \cdot \sin(B) \cdot \cos(B) \cdot \cos(L)] \cdot \varepsilon_y \\ & + [-N_G] \cdot \Delta m_G \end{aligned} \quad (2e)$$

In (2a-d) the height  $N_G(B, L)$  of a geoid model is refined by a so called Finite Element Model  $\text{NFEM}(\mathbf{p}, x, y)$  described in chap. 2. In (2e)  $N(B)$  means the radius of normal curvature of the ellipsoid at a point  $P(B, L)$ . The datum parameters  $\mathbf{d}$  comprise three translations ( $u, v, w$ ), two rotations ( $\varepsilon_x, \varepsilon_y$ ) and the scale change  $\Delta m_G$  of the geoid height  $N_G$ . The  $\text{NFEM}(\mathbf{p}, x, y)$  acts as an additional overlay for a middle- and short-waved shape improvement of the geoid heights  $N_G(B, L)$ .

For more details concerning the datum transition problem (2b,e) and the refinement  $\text{NFEM}(\mathbf{p}, x, y)$ , as well as for the discussion of the special cases of the standard approach - namely the "pure geoid-approach" and the "pure FEM-approach" - it is referred to DINTER et al.

<sup>1</sup> Reiner Jäger, Sascha Schneid: Fachhochschule Karlsruhe - University of Applied Sciences, Moltkestrasse 30, D-76133 Karlsruhe, Germany. Tel: ++49 721 9252620, Fax: ++49 721 9252591. Email: dfhbf@fh-karlsruhe.de . URL: www.dfhbf.de .

(1997) and JÄGER (1999, 2000). The mathematical background of the powerful tool of the Finite Element Model NFEM(x,y,p), which will become also the central core of the DFHRS concept, is treated in chap. 2.

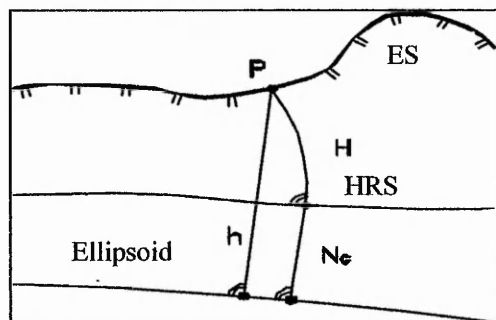


Fig. 1: Ellipsoidal GPS height  $h$ , standard height  $H$ , height reference surface HRS, its ellipsoidal height  $N_G$  and earth surface ES at a point  $P(B,L)$

A disadvantage of the above standard approach (2a-d) is, that it is in its full power a typical post-processing application. As identical points  $(H,h)$  are needed, the approach is not very economical for an online GPS heighting in DGPS networks (fig.3). Furtheron the geoid model heights  $N_G(B,L)$  are only used at discrete points (as "direct observations") and so the complete geoid height information  $N_G(B,L)$  is neglected and remains unused. Besides this also the vertical deflection information  $(\xi,\eta)$ , e.g. available from geoid models, remains totally unused. The application of the standard approach (2a-d) still requires experts knowledge, so that it is not adequate for "any" DGPS user. Because of the above mentioned disadvantages the standard approach (2a-d) remains suboptimal compared to the new DFHRS-concept presented in chap. 3.

## 2 FEM Representation of Height Reference Surfaces

A powerful tool used already within the standard GPS height integration approach (chap. 1) and a central tool of the DFHRS approach (chap. 3) as well, consists in the representation of the height reference surface HRS or its additional refinement by a finite element surface called NFEM(p,x,y). NFEM(p,x,y) is carried by the base functions of bivariate polynomials which are set up in regular or irregular meshes (fig. 2, fig. 5). If we describe with  $\mathbf{p}^i$  the polynomial coefficients  $(a_{00}, a_{10}, a_{01}, a_{20}, a_{11}, a_{02}, \dots)^i$  of the  $i$ -th mesh, we have for the height NFEM( $\mathbf{p}^i, x, y$ ) of the HRS over the ellipsoid (fig. 1) in the  $i$ -th mesh:

$$\text{NFEM}(\mathbf{p}^i, x, y) = \quad (3a)$$

$$\mathbf{f}(x(B,L), y(B,L)) \cdot \mathbf{p}^i; i=1, m$$

$$\mathbf{p}^i = (a_{00}, a_{10}, a_{01}, \dots)^i \quad (3b)$$

$$\mathbf{f}(x(B,L), y(B,L)) = (1, x, y, x^2, xy, y^2, \dots) \quad (3c)$$

The vector  $\mathbf{f}$  means the so called Vandermond vector and contains the different powers of the coordinates  $(x,y)$  according to the polynomial degree  $n$ . The total parameter vector  $\mathbf{p}$  consists of the coefficient sets  $\mathbf{p}^i = (a_{jk})^i$ , ( $j=0,n; k=0,n$ ), of all  $m$  meshes. The plan position in (3a,c) is due to the metric ellipsoidal coordinates  $(y(B,L) = \text{"East"} \text{ and } x(B,L) = \text{"North"})$  introduced e.g. as UTM or Lambert coordinates, which are functions of the geographical coordinates  $(B,L)$ .

To imply a continuous surface NFEM(p,x,y) one set of continuity conditions of different type  $C_{0,1,2}$  has to be set up in the computation of NFEM(p,x,y) for each couple of neighbouring meshes. The continuity type  $C_0$  implies the same functional values, the continuity type  $C_1$  implies the same tangential planes and the continuity type  $C_2$  the same curvature along common mesh borders of the DFHRS as represented by NFEM(p,x,y) (4a). The continuity conditions occur as additional observation equations  $C(\mathbf{p})=0$  to be added to the parametrization of NFEM(p,x,y). The condition equations  $C(\mathbf{p})=0$  are related to the polynomial sets of the coefficients  $(a_{jk})^m$  and  $(a_{jk})^n$  of each couple of neighbouring meshes  $m$  and  $n$ . To force e.g.  $C_0$ -continuity, the difference  $\Delta N_{m,n}$  in the geoid height  $N_G$  of any point  $S$  at the common border SA-SE of two meshes  $m$  and  $n$  (see fig.2) has to become zero. So the basic condition equation for a polynomial representation of  $n$ -th degree reads (DINTER et al., 1997) :

$$\begin{aligned} \Delta N_{m,n}(t) = & \sum_{j=0}^n \sum_{k=0}^{n-j} (a_{jk,n} - a_{jk,m}) \cdot \\ & (y_{SA} + t \cdot (y_{SA} - y_{SE}))^j \cdot \\ & (x_{SA} + t \cdot (x_{SA} - x_{SE}))^k \\ & \equiv 0 \end{aligned} \quad (3d)$$

With  $(y_{SA}, x_{SA}, y_{SE}, x_{SE})$  we introduce the plan metric coordinates of the nodal points SA and SE (fig. 2). Equation (3d) represents a polynomial of  $n$ -th degree parametrized in the border line parameter  $t(t \in (0,1))$ .

The subset of  $(n+1)$   $C_0$ -continuity condition equations  $C(\mathbf{p})=0$  for the border between mesh  $m$  and  $n$  results in case of  $C_0$ -continuity from (3d) by setting all  $(n+1)$  coefficients related to  $t$  to zero.

The mesh size and shape for the computation of the NFEM(p,x,y) representing the so called "geoid part" (see 5a,b,c) of the DFHRS data base by may be chosen arbitrary (fig. 2, fig. 5). The best approximation of a HRS by NFEM(p,x,y) results of course by introducing small meshes, e.g. in the range of 5 km in order to keep a 5 mm range for any HRS shape approximation by a polynomial degree up to  $n=3$ .

A special advantage and characteristic of the NFEM(p,x,y) representation consists in the fact, that the nodal points of the FEM grid are totally independent of the location of the geodetic observations and the geoid data points. Observation data which are presently used for the determination of the parameter vector  $\mathbf{p}$  of NFEM(p,x,y) are height observations  $(h, H, \Delta h, \Delta H)$ ,

the geoid height observations  $N_G(B,L)$  and the deflections of the vertical observations  $(\xi,\eta)$ .

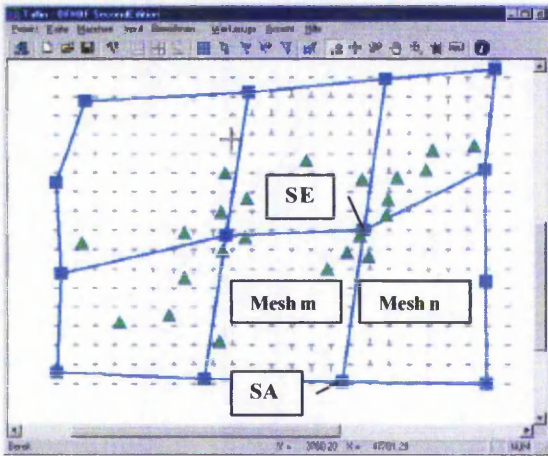


Fig. 2: Irregular mesh grid and different observation types (geoid data grid; triangles meaning identical points (H,h)). Example of DFHRS data base computation of Tallinn, Estonia with DFHRS production software.

### 3 Digital Finite Element Height Reference Surface (DFHRS) - Basic Ideas of the Concept

The DFHRS concept aims at a direct online or postprocessed GPS heighting with an optimum and simultaneous use of all available data sources. Within this aim the profile of a GPS-heighting is easy to formulate: An ellipsoidal GPS-height  $h$ , determined at a plan position  $x(B,L)$  and  $y(B,L)$  is to be made convertible directly to the height  $H$  of the standard height system. The converted height  $H$  should result online on applying a respective correction to  $h$ , and the resulting  $H$  should not suffer with a quality-decrease compared to the heights  $H$  resulting from a postprocessed GPS height integration.

In the following the general so called DFHRS concept is presented, which fulfils all above requests and shows besides this even some more positive aspects. The concept is to produce in a first step in a controlled way a new kind of data base product. This step is called the DFHRS data base production step.

The second step is to make this data base accessible for an online DGPS-heighting. This is called the application step. The use of the DFHRS in a postprocessing mode (e.g. in GIS) is of course included in the concept. In the application step either the DGPS user has the DFHRS at his disposal on his field equipment or the DGPS service exclusively uses the DFHRS for the evaluation of a correction  $\Delta = \Delta(B,L,h)$  to convert a GPS height  $h$  into the height  $H$  of the standard height system (principle, see fig. 3).

#### 3.1 DFHRS Data Base Production

The DFHRS data base production step reads in the system of observation equations as follows:

$$h + v = H + h \cdot \Delta m + \mathbf{f}(x,y) \cdot \mathbf{p}, \quad (4a)$$

$$\text{with NFEM}(\mathbf{p}, x, y) =: \mathbf{f}(x, y) \cdot \mathbf{p}$$

$$N_G(B,L)^j + v = \mathbf{f}(x,y) \cdot \mathbf{p} + \partial N_G(\mathbf{d}^j) \quad (4b)$$

$$\xi + v = -\mathbf{f}_B / M(B) \cdot \mathbf{p} + \partial B(\mathbf{d}_{\xi,\eta}) \quad (4c)$$

$$\eta + v = -\mathbf{f}_L / (N(B) \cdot \cos(B)) \cdot \mathbf{p} + \partial L(\mathbf{d}_{\xi,\eta}) \quad (4d)$$

$$H + v = H \quad (4e)$$

$$C + v = C(\mathbf{p}) \quad (4f)$$

With  $\partial N_G(\mathbf{d}^j)$  (2d) and with  $\partial B(\mathbf{d}_{\xi,\eta})$  and  $\partial L(\mathbf{d}_{\xi,\eta})$  we introduce the datum part of the geoid heights of any geoid model or of single "geoid patches" (see chap. 4) and the datum parts of the deflections of the vertical  $(\xi,\eta)$  respectively. Explicit formulas for  $\partial B(\mathbf{d}_{\xi,\eta})$  and  $\partial L(\mathbf{d}_{\xi,\eta})$  are given in JÄGER (2000). With  $\mathbf{f}_B$  and  $\mathbf{f}_L$  we introduce the partial derivatives of the Vandermonds' vector  $\mathbf{f}(x(B,L),y(B,L))$  (3c) with respect to the geographical coordinates  $B$  and  $L$ .  $M(B)$  and  $N(B)$  mean the radius of meridian and normal curvature at a point  $P(B,L)$  respectively.

Identical points  $(H, h)$  and if available, one or a number of geoid models  $N_G(B,L)^j$  are used as observations to produce the DFHRS by a least squares estimation related to (4a-f). The DFHRS on the right side is, except of the scale part  $\Delta m \cdot h$  (4a), represented completely by the finite element model  $\text{NFEM}(\mathbf{p},x,y) = \mathbf{f}(x,y) \cdot \mathbf{p}$ , and the continuity is provided by the continuity equations  $C(\mathbf{p})$  (4f) below.

This means that the geoid model input of any geoid model  $N_G(B,L)^j$  or "geoid patch" is "mapped" to the DFHRS by removing the datum part  $\partial N_G(\mathbf{d}^j)$ . An additional NFEM-refinement term may be set up in (4b). The production step of the DFHRS (4a-f) is embedded in a statistical quality control concept of a least squares estimation, so that any observation component - including the input of "mapped" and datum-adapted geoid-model - is well controlled (JÄGER and SCHNEID, 2001a). With respect to geoid models  $N_G^j$  (4b) the DFHRS approach is to be regarded as the second step of a two step adjustment, which improves geoid models  $N_G^j$  in terms of the new product  $\text{NFEM}(\mathbf{p},x,y)$  representing the "geoid part" (see 5a) of the DFHRS.

The most valuable way to check the external accuracy ("reproduction quality") of the DFHRS data base parameters  $(\mathbf{p}, \Delta m)$  (4a-f) is to compute successively the DFHRS-height  $H_{i,DFHRS}$  of each identical point  $H_i$  from  $h_i$  when using the individual data base  $DFHRS_i$ , where  $H_i$  was excluded from the respective production (4a-f). The reproduction quality measure  $\nabla H_i$  is then simply given by the value of the difference

$$\begin{aligned} \nabla H_i &= H_i - H(B,L,h, DFHRS)_i \\ &= H_i - H_i(5a, b, c) \end{aligned} \quad (4g)$$

The computation of all  $\nabla H_i$  can be performed however in the unique production step, where all identical

points  $(H_i, h_i)$  are used. The respective formula reads:

$$\nabla H_i = - \frac{v_{H_i}}{r_{H_i}} \quad (4h)$$

With  $v_{H_i}$  and  $r_{H_i}$  we describe the correction and the redundancy part of the observation  $H_i$  in equation (4e).

### 3.2 DFHRS Data Base Application

The decisive components and formula parts of the production step, which are afterwards needed in the application step – namely in an online GPS-heighting – are contained in (4a).

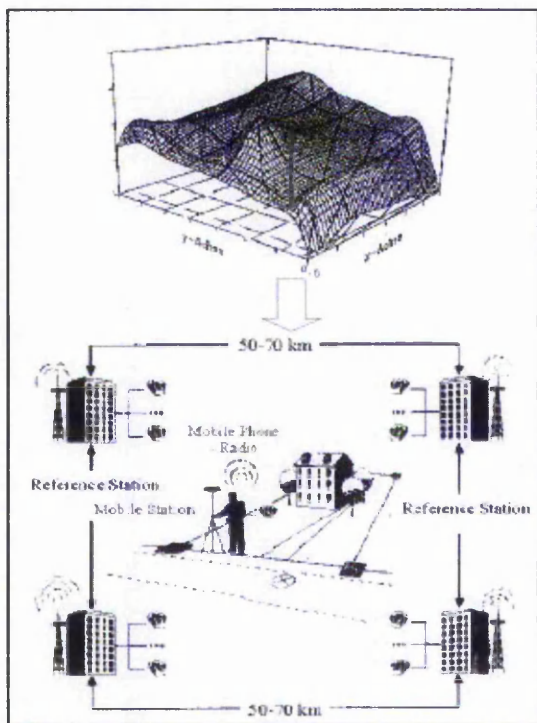


Fig. 3 : DFHRS data base symbolized by the Finite Element Model NFEM(p) of the HRS (above) and "application scenery" of an online GPS-heighting (below).

Equation (4a) leads to the following correction scheme, which has to be applied to the GPS height  $h$  in an online (or postprocessing) use of the DFHRS data base in order to convert  $h$  into the standard height  $H$ :

$$H = h - \Delta(B, L, h) = h - \text{corr1} - \text{corr2} \quad (5a)$$

$$= h - f(x(B, L)y(B, L)) \cdot p - h \cdot \Delta m \quad (5b)$$

$$= h - \text{NFEM}(p, x(B, L), y(B, L)) - h \cdot \Delta m. \quad (5c)$$

In opposite to the limitations concerning the use of conventional geoid models  $N_G$  by formula (1), the "DFHRS-correction"  $\Delta(B, L, h)$  in the corresponding formula (5a) holds. The first correction part "corr1=corr1(B, L)" is due to the FEM part  $\text{NFEM}(p, x(B, L), y(B, L))$  (fig. 3, above) of the DFHRS data base ("geoid correction").

The second correction "corr2 = corr2(h)" is due to the scale  $\Delta m$  between the GPS heights  $h$  and those of the standard height system  $H$  ("scale correction").

### 4 Special Requests and Advantages

To reduce the effect of long-waved systematic errors of geoid models as well as those of the standard HRS (DINTER et al., 1997; JÄGER, 1990) the mathematical model of the DFHRS-concept (4a-f), and the DFHRS software respectively, allow to subdivide any given geoid height model  $N_G(B, L)$  into a number of so called "geoid-patches" (fig. 5), each with an own set of datum-parameters  $d$  by  $\partial N_G(d)$  (4b). Fig. 4 shows the residuals of two different DFHRS adjustments for the country of Baden-Württemberg, Germany (see also fig. 5). Fig. 4 (left) shows long-waved systematic errors, which occur on introducing only one datum parameter set  $d$  for the whole area, meaning without "patching". The result of the "geoid-patching" on the right shows the benefit of the patching with respect to reduce the influence of systematic errors by the subdivision of the geoid model  $N_G(B, L)$  into a number of different patches with individual datum parameters  $d$  (JÄGER and KÄLBER, 2000). Geoid-patching significantly improves the accuracy of the resulting DFHRS.

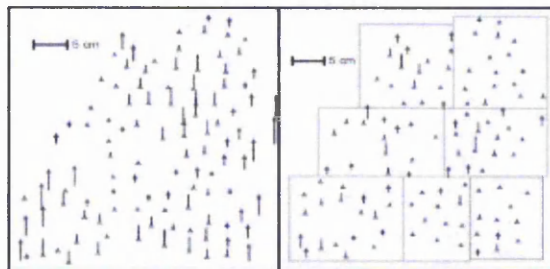


Fig. 4: Effect of a "geoid-patching" at the example of Baden-Württemberg: Large residuals in identical points with only one set of datum parameters (left) and much smaller residuals with 7 patches with individual datum sets  $\partial N_G(d)$  (right).

It is of course also possible to introduce by  $N_G(B, L)^j$  (4b) different (patched or unpatched) geoid models, even concerning the same area.

The continuity equations (4f) are introduced as additional observation equations with variable weights. So the dimension of the normal equation matrix is not blown up due to the conditions  $C(p)$  and the approach is kept very flexible: The continuity conditions can be introduced "hard" or "soft", according to a prescribed weight, and they can also be statistically tested.

### 5 DFHRS Software and Examples

For the computation of Digital-Finite-Element Height Reference Surfaces a special C++ software ("DFHRS-production software") has been developed at FH Karlsruhe - University of Applied Sciences within the running research and development project DFHRS (URL: [www.dfhbf.de](http://www.dfhbf.de)). Several functions for visualisation and utilities for an automatic and a manual meshing and a

powerful least-squares adjustment have been implemented. The DFHRS production software enables the mathematical model (4a-f) including gross error detection and variance component estimation for all observations and observation groups respectively, and it sets up the DFHRS data base in a compressed format, enabling at the same time a copy protection key. The DFHRS data base consists of a block of mesh-grid information, a block with the DFHRS parameters  $\mathbf{p}$  and  $\Delta m$ , and optionally a third block with their covariance matrix. The DFHRS data base access software is available as Dynamic Link Library (DLL) for an implementation in any DGPS online software.

A first DFHRS data base was computed for the (40 x 40) km area of Tallinn/Estonia (fig. 2) (JÄGER and SCHNEID, 2001b,c). Using the EGG97 geoid model (DENKER and TORGE, 1997) and 23 identical points, the average reproduction quality (4g,h) of the standard heights  $H$  evaluated from GPS heights  $h$  was in the range of 4 mm (max. 10 mm). The reproduction quality of the (250 x 350) km of DFHRS Baden-Württemberg (fig. 5) was also better than 1 cm using 192 identical points, 1013 meshes with a mesh size of 7 km, and 28 EGG97 patches.

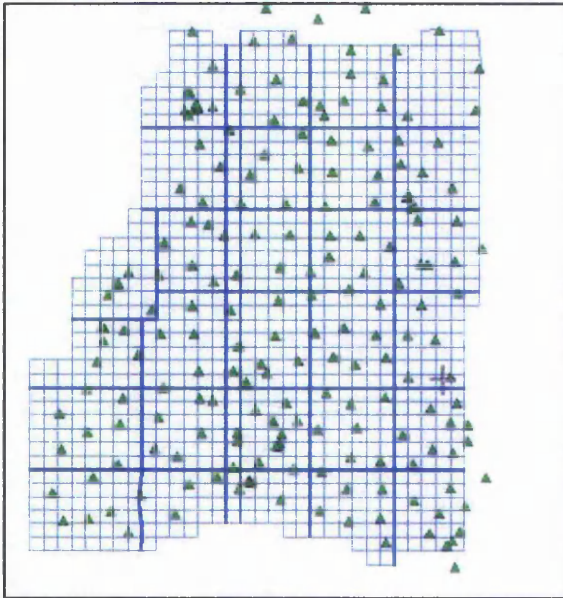


**Fig. 5:** DFHRS production for the country of Baden-Württemberg, Germany. Area size 250 km x 350 km. Almost regular meshes with an average size of 7 km, 28 geoid-patches, 1013 meshes and 192 identical points.

DFHRS data bases are already available and used respectively as standard in the practice of DGPS heighting in the SAPOS® DGPS networks of Saarland, Hessen, Baden-Württemberg and Bavaria.

A third series of test computations was performed for a (500 x 700) km area in Venezuela (JÄGER and SCHNEID, 2001c). Only 22 identical points and geoid heights  $N_G$  from the EGM96 were used for the DFHRS production. Even the large size of meshes (about 70-80 km) and the less accurate EGM96 provided a DFHRS

with an average reproduction quality of 15 cm for the standard heights  $H$ .

## 6 Conclusions

The DFHRS (Digital Finite Element Height Reference Surface) concept provides a new standard for an online GPS heighting in DGPS networks. The approach is based on the representation of the Height Reference Surface (HRS) by the base functions of bivariate polynomials. These are set up in the area over a grid of arbitrary shaped finite element meshes. To imply a continuous HRS, a set of continuity conditions is introduced for each border of neighbouring meshes. With respect to geoid models  $N_G^j$  the DFHRS approach is to be regarded as second step of a two step adjustment, which improves any geoid model  $N_G^j$  in terms of the resulting DFHRS. The DFHRS data base, computed in the DFHRS production step, provides any DGPS user in the DFHRS application step with a correction  $\Delta = \Delta(B, L, h)$ , which converts the ellipsoidal height  $h$  directly to the standard height  $H$ . Identical points and transformations are not needed any more in the application step. So geodetic expert knowledge is reduced to the production step, while GPS heighting becomes as simple and economic as it can be.

The production step allows to use all above observation type simultaneously. The whole geometrical information, namely identical points and height differences ( $h$ ,  $\Delta h$ ,  $H$ ,  $\Delta H$ ) as well as geoid model heights  $N_G$  and deflections of the vertical ( $\xi, \eta$ ) are set up in a strict least squares adjustment, which becomes most efficient in this way with respect to the resulting DFHRS. The extension of the DFHRS approach (4a-f) with respect to gravity observations is intended. The production step simultaneously enables the statistical quality control of the DFHRS. In the sense of a two step adjustment the other observation groups enable the control and improvement of the geoid model input, which is simultaneously "mapped" to the new DFHRS product. To reduce the influence of long-waved systematic errors, geoid models may be divided into continuous "geoid-patches". The resulting DFHRS data base is stored optionally together with its covariance matrix. The DFHRS data base access software is ready to be implemented as a DFHRS Dynamic Link Library (DLL) in any GPS-RTK-software for online GPS-heighting or in postprocessing software, e.g. for GIS.

## 7 Evaluation of the European Height Reference Surface (E\_HRS)

The DFHRS concept has successfully been introduced in practice. DFHRS data bases have become an official sales product of state land survey agencies and also private companies in different countries. The approach (4a-f) is presently also used for the evaluation of the Height Reference Surfaces (HRS) of large scale areas such as Venezuela (JÄGER and SCHNEID, 2001c) and Germany. The results of DFHRS computations (see chap. 5) prove accuracies better than 1 cm. Another topic of interest and external requests is directed to the production

of DFHRS data bases for "GIS and navigation" on a (5-50) cm accuracy level. Such "rapid" or "light" DFHRS data bases are easy to compute, simply by enlarging the mesh size without a need of change in the data blocks. So the DFHRS concept is all in all best prepared both for producing different accuracy levels of DFHRS data bases, as well as for using different data sources (e.g. several geoid models). The detection and reduction of systematic errors in big networks is enabled, and the DFHRS approach (4a-f) is implemented in a powerful software with graphic tools. So the authors offer the DFHRS concept and software as potential and flexible candidate for the controlled evaluation of the HRS of Europe (E\_HRS) in the near future work of EUREF TWG.

## 8 References

- DENKER, H. and W. TORGE (1997): The European Gravimetric Quasigeoid EGG97 – An IAG supported continental enterprise. In: *Geodesy on the Move – Gravity Geoid, Geodynamics, and Antarctica*. R. Forsberg, M. Feissel, R. Dietrich (eds) IAG Symposium Proceedings Vol. 119, Springer, Berlin Heidelberg New York: 249-254.
- DINTER, G.; ILLNER, M. and R. JÄGER (1997): A synergetic approach for the integration of GPS heights into standard height systems and for the quality control and refinement of geoid models. In: *Veröffentlichungen der Internationalen Erdmessung der Bayerischen Akademie der Wissenschaften (57)*. IAG Subcommission for Europe Symposium EUREF, Ankara 1996. Beck'sche Verlagsbuchhandlung, München.
- JÄGER, R. (1990): Optimum Positions for GPS-points and Supporting Fix-points in Geodetic Networks. In: Ivan I. Mueller (ed.) *International Association of Geodesy Symposia. Symposium No. 102: Global Positioning System: An Overview*, Edinburgh/Scotland, Aug. 7-8, 1989. Convened and edited by Y. Bock and N. Leppard, Springer: 254-261.
- JÄGER, R. (1999): State of the art and present developments of a general approach for GPS-based height determination. In (M. Lilje, ed.): *Proceedings of the Symposium Geodesy and Surveying in the Future – The importance of Heights*, March 15-17, 1999. Gävle/Schweden Reports in Geodesy and Geographical Informations Systems, LMV-Rapport 1999(3). Gävle, Schweden. ISSN 0280-5731: 161-174.
- JÄGER, R. (2000): State of the Art and Present Developments of a General Concept for GPS-based Height determination. *Proceedings of the First Workshop on GPS and Mathematical Geodesy in Tanzania (Kilimanjaro Expedition 1999)*. October 4, 1999, University College of Lands and Architectural Studies (UC-LAS), Dar Es Salaam. URL (download): <http://www.dfhbf.de>.
- JÄGER, R. und S. KÄLBER (2000): *Konzepte und Softwareentwicklungen für aktuelle Aufgabenstellungen für GPS und Landesvermessung*. DVW Mitteilungen, Landesverein Baden-Württemberg. 10/2000. ISSN 0940-2942.
- JÄGER, R. und S. SCHNEID (2001a): GPS-Höhenbestimmung mittels Digitaler Finite-Elemente Höhenbezugsfläche (DFHBF) - das Online-Konzept für DGPS-Positionierungsdienste. XI. Internationale Geodätische Woche in Obergurgl/Österreich, Februar 2001. *Institutsmitteilungen*, Heft Nr. 19, Institut für Geodäsie der Universität Innsbruck: 195-200.
- JÄGER, R. und S. SCHNEID (2001b): DFHRS-Homepage: [www.DFHBF.de](http://www.DFHBF.de).
- JÄGER, R. and S. SCHNEID (2001c): Online and Postprocessed GPS-Heighting based on the Concept of a Digital Height Reference Surface. Contribution to IAG International Symposium on Vertical Reference Systems, February 2001, Cartagena, Columbia. In press.
- JÄGER, R.; SCHNEID, S. and S. SEILER (2001): Berechnung der Digitalen Finite Element Höhenbezugsfläche (DFHBF) für Baden-Württemberg. Abschlussbericht, Landesvermessungsamt Baden-Württemberg, unpublished.
- LEMOINE, F.; S. KENYON; J. FACTOR; R. TRIMMER, N. PAVLIS; D. CHINN; M. COX; S. KLOSKO; S. LUTHCKE; M. TORREENCE; Y. WANG; R. WILLIAMSON; E. PAVLIS; R. RAPP and T. OLSON (1998): The development of the Joint NASA GSFC and NIMA Geopotential Model EGM96. NASA Goddard Space Flight Center, Greenbelt, Maryland, 20771, USA.